USE OF SOLID-PHASE MICROEXTRACTION IN ANALYSIS OF PESTICIDES IN SOIL

Helena Prosen, Lucija Zupančič-Kralj

Faculty of Chemistry and Chemical Technology, University of Ljubljana, Aškerčceva 5, SLO-1000 Ljubljana, Slovenia

ABSTRACT

Residues of pesticides and their degradation products in soil present a serious problem for crops, soil organisms and humans. For isolation of this type of compounds solid-phase microextraction (SPME) could be used in combination with conventional extraction method. This modern separation method was optimized for extraction of organochlorine and triazine pesticides from soil samples. Analytes were desorbed from the fiber in the injector of a gas chromatograph and determined by either electron capture or mass spectrometric detection. Linearity and limits of detection were tested in the 0.1 – 20.0 ng/g range for organochlorines and 10 – 100 ng/g range for triazines. The method presented could be used for screening of pesticides in contaminated soil samples and offers a simple alternative to established methods of pesticide analysis in soil.

INTRODUCTION

Pesticide analysis in soil represents a problem mainly because of the high level of interfering compounds such as humic and fulvic acids. Moreover, pesticide residues tend to adsorb to soil particles very strongly [1], which poses the question of the

reliability of spikes used as a means of evaluating the recovery of a pesticide from soil by the chosen extraction technique.

The pesticides chosen for this study were the ones most commonly present in soil samples from our area, that is triazines, which are widely applied herbicides, and a group of chlorinated insecticides, banned years ago, the residues of which are still found in environmental samples. The most common method for isolation of these compounds from the soil is extraction with organic solvents [2], followed by extensive clean-up procedures in order to remove interferences prior to analysis. Better recoveries are obtained by use of the Soxhlet apparatus or sonication. Analysis is usually accomplished by gas chromatography - GC [3-8] or by high performance liquid chromatography - HPLC for the triazines [9-10].

However, these extraction methods are becoming increasingly unpopular for two reasons: the time-consuming clean-up procedures with great chances of analyte loses and the high consumption of high purity, expensive organic solvents, which pose a burden to the environment thus offsetting the benefits of pesticide residue analysis [11]. Therefore, new extraction methods are being introduced to this branch of analysis, the most applied of which are supercritical fluid extraction [12], and extraction with organic solvents combined with solid-phase extraction [9-10, 13-16]. These techniques are certainly a great improvement, but in our opinion, the emphasis should be on minimization of the consumption of the organic solvent, if adequate detection limits can be reached [10, 14-16].

Recently a new, completely solventless extraction method called solid-phase microextraction (SPME) has been introduced by Pawliszyn and co-workers [17], using a fused silica fiber coated with various stationary phases, similar to those in GC capillary columns, as an extraction medium. Analytes are subsequently thermally desorbed from the fiber in the GC injector.

Both types of pesticides discussed in the present paper were already found to be amenable to SPME. Organochlorine insecticides have been extracted from different water samples [3-5, 18], as well as triazine herbicides [5-8, 19-20]. The conditions of extraction were found to be important for the best performance of SPME: extraction

time, fiber type, ionic strength of the sample, etc. However, to our knowledge no attempt was made to extract these compounds from soil samples, except a single experiment [8]. In this case, the soil sample was suspended in water and the suspension extracted with an SPME fiber.

In the present work, a combination of classical extraction of soil by an organic solvent and solid-phase microextraction was applied for isolation of pesticides from soil. Subsequent analysis was accomplished by gas chromatography with either electron capture (ECD) or mass spectrometric detection (MSD) in electron impact mode (EI). Possibilities of screening tests and quantitative analysis were assessed and are discussed in the present paper.

EXPERIMENTAL

1. Materials

Triazine standards of 98-99% purity were obtained from Riedel - de Haën (Seelze, Germany). Organochlorine insecticide standards were obtained from Supelco (Bellefonte, USA) in the form of a standard pesticide mix of 16 compounds. Stock standard solutions were prepared in acetonitrile at concentrations of 500 mg/l for triazines and in hexane at concentrations of 0.2 - 1.2 mg/l for organochlorines. They were kept in a refrigerator and were found to be stable for several months. Acetonitrile was "gradient grade", hexane "for trace organic analysis grade" and acetone "p.a. grade", all three from Merck (Darmstadt, Germany). LC-grade water was obtained by purifying distilled water with a Milli-Q water purification system (Millipore, Bedford, USA). Sodium chloride was p.a. grade from Kemika (Zagreb, Croatia).

A manual holder for solid-phase microextraction was obtained from Supelco (Bellefonte, USA). SPME fibers for the manual holder were 100 μm polydimethylsiloxane or 85 μm polyacrylate from Supelco.

Capillary columns for gas chromatography were HP-1 12 m x 0.2 mm i.d. x 0.33 μm (GC-ECD) or HP-1 25 m x 0.2 mm i.d. x 0.11 μm (GC-MS) from Hewlett-Packard (Palo Alto, USA).

2. Chromatographic conditions

The gas chromatograph was an HP 6890 equipped with an electron capture detector (ECD) from Hewlett-Packard (Palo Alto, USA). The injection port temperatures were 280°C for triazine or 250°C for organochlorine analysis, and the detector temperature was 320°C. The oven temperature program for triazine analysis was as follows: 70°C hold for 4 min, then ramp at 25°C/min to 140°C, then ramp at 3°C/min to 190°C, then ramp at 10°C/min to 220°C and hold for 10 min. The oven temperature program for organochlorine analysis was as follows: 120°C hold for 3 min, then ramp at 30°C/min to 180°C, then ramp at 3°C/min to 220°C and hold for 2 min. Carrier gas was H_2 at a flow rate of 1 ml/min, make-up gas for ECD was N_2 at a flow rate of 30 ml/min. Injection was in the splitless mode, purge was set on after 4 min (triazines) or 3 min (organochlorines) and purge flow was 15 ml/min. Chromatograms were recorded with an HP 3395 computing integrator (Hewlett-Packard).

For GC-MS analysis, the gas chromatograph was an HP 5890 coupled to an HP 5989A mass spectrometer MS Engine (Hewlett-Packard). The injection port and GC-MS interface temperatures were 220°C and 200°C, respectively. Temperatures of the ion source compartment and quadrupole mass analyzer compartment were 250°C and 100°C. The GC oven temperature program for triazine analysis was the same as above, but the carrier gas was He at a flow rate of 0.7 ml/min. Injection conditions were the same as above.

The ionization mode was electron impact at an electron energy of 70 eV. In the scan mode, spectra were recorded in the m/z range 35-400 amu. In the single ion monitoring (SIM) mode, different m/z ion groups were monitored at different time ranges (see Tables 1 and 2). For quantification, areas of the base peaks (indicated in Table 2) were measured in both scan and SIM modes.

TABLE 1:
Ion groups for single ion monitoring (SIM) of triazines.

time range / min	ions monitored (m/z / amu)
4.0 - 12.9	145, 158, 172, 173, 186, 187, 201
12.9 - 17.0	173,186, 200, 201, 214, 215, 229
17.0 - 30.0	198, 212, 225, 240

TABLE 2:
Ions (m/z) monitored in SIM for different triazines. Those printed in italic were used for comparative quantitation in the scan mode.

compound	ions monitored (m/z / amu)	MW
desisopropylatrazine (DPA)	145, 158, *173*	173.6
desethylatrazine (DEA)	145, *172*, 187	187.6
desethylterbutylazine (DET)	145, *186*, 201	201.7
simazine (SZ)	173, 186, *201*	201.7
atrazine (AZ)	173, *200*, 215	215.7
terbutylazine (TZ)	173, *214*, 229	229.7
cyanazine (CZ)	198, 212, *225*, 240	240.7

3. Soil spiking procedure

Soil samples were partially provided by the Agricultural Institute in Ljubljana and partially collected by us at different contaminated and uncontaminated sites. All samples were air-dried, finely ground and homogenized.

Uncontaminated soil was suspended in an acetone solution of an appropriate amount of pesticides. The suspension was thoroughly stirred, then allowed to air-dry for ca. 24 h. Samples for time-dependent experiments were left in a sunny site to allow weathering of the residues.

4. Solvent extraction procedure

A soil sample (7 g) was weighed into the extraction vessel, 15 ml of acetone was added and the suspension was shaken in an ultrasonic bath for 30 min. The suspension was centrifuged at 3000 rpm for 7 min, the clear supernatant separated and evaporated on a

water bath (approx. 50°C) under a stream of N$_2$. The dry residue was reconstituted in either 100 μl of acetone for direct injection into the GC or in 3.5 ml (triazines) or 7 ml (organochlorines) of water for subsequent solid-phase microextraction.

5. Solid-phase microextraction procedure

Procedure for SPME was optimized using water spiked with known amount of pesticides. The conditions optimized were:

- type of the SPME fiber: 100 μm polydimethylsiloxane versus 85 μm polyacrylate

- extraction time

- effect of agitation with a magnetic stirrer

- effect of neutral salt addition.

The following SPME conditions were found to be the most efficient for the extraction of organochlorine insecticides from aqueous solution: 100 μm polydimethylsiloxane fiber, extraction time 15 min at a stirring rate of 250 rpm and no addition of salt. For extraction of triazines, the optimal SPME conditions were an 85 μm polyacrylate fiber, extraction time 30 min at a stirring rate of 150 rpm, and the aqueous solution saturated with NaCl prior to extraction. Desorption temperatures are listed under chromatographic conditions.

RESULTS AND DISCUSSION

1. Results of SPME procedure optimization

The solid-phase microextraction procedure was optimized for aqueous solutions of pesticides, separately for both groups.

Firstly, a suitable SPME coating had to be chosen. Polydimethylsiloxane (PDMS) and polyacrylate (PA) stationary phases were tested. The PA coating was more efficient in extracting the more polar triazine herbicides (see Figure 1). The difference between the coatings was even more pronounced for desalkylated triazine degradation products,

which are more polar than their parent compounds. The PDMS coating was better for extraction of organochlorine insecticides, which are less polar compared to triazines.
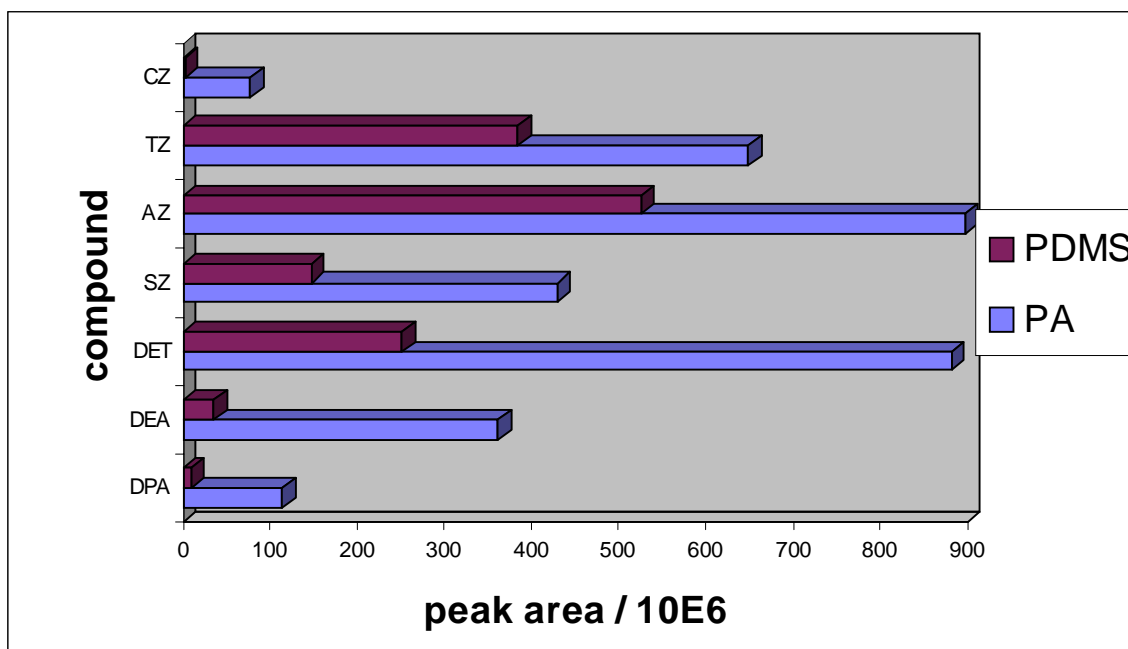

Figure 1: Comparison of polydimethylsiloxane - PDMS (100 µm) and polyacrylate - PA (85 µm) fiber coating for extraction of triazines from aqueous solution, concentration 50 ng/ml. For extraction conditions, see Experimental section. GC-MS detection. Abbrev.: DPA - desisopropylatrazine, DEA - desethylatrazine, DET - desethylterbutylazine, SZ - simazine, AZ - atrazine, TZ - terbutylazine, CZ - cyanazine.

After the initial choice of stationary phase, the effect of extraction time was assayed. This is usually recommended to be as near as possible to the equilibration time, which is much shorter if the sample is agitated. For agitated samples (magnetic stirrer at 100-250 rpm), the dependence of amount of analyte extracted by the fiber on the extraction time is shown in Figure 2. The minimum equilibration time for triazines was reported to be 60-90 min [7] or even up to 120 min [8]. In our experiments, similar results were obtained; however, an extraction time of 30 min was chosen for further work as a compromise between time and detection limits of the method.
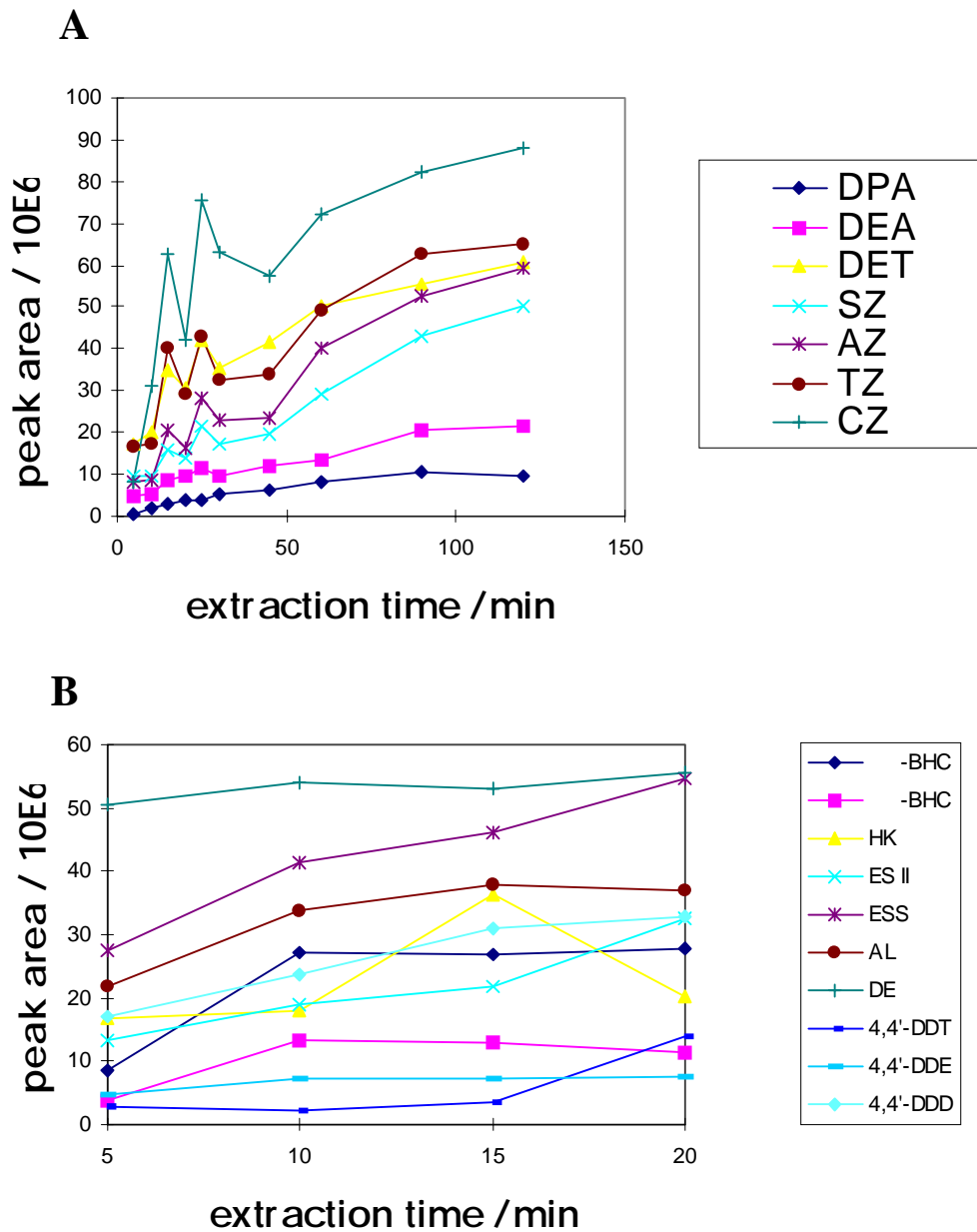
A

B

<u>Figure 2</u>: SPME extraction time - response (peak area) diagram for:
A - triazines, 85 μm PA fiber, 100 ng/ml in aqueous solution; for abbreviations, see Figure 1;
B - organochlorines, 100 μm PDMS fiber, 0.2-1.2 ng/ml in aqueous solution. Abbrev.: α-BHC - α-"benzenehexachloride", γ-BHC - lindane, HC - heptachlor, ES II - endosulfan II, ESS - endosulfan sulfate, AL - aldrin, DE - dieldrin.

Organochlorines are much less soluble in water, which means faster adsorption onto the fiber. Equilibration times were reported to range between 15 and 180 min, depending on the chemical structure of the compound, the fastest being for BHC isomers [18]. As is

evident from Figure 2, in our experiments no particular differences were seen between BHC isomers and other organochlorine insecticides analyzed, and therefore 15 min extraction time was chosen as suitable for extraction of these compounds.

Mixing of the sample has an effect on equilibration time and usually also a certain influence on the repeatability of the SPME extraction results. The latter is much less pronounced when using an autosampler, but in manual SPME, the fiber is not likely to be placed in the same position regarding the magnetic stirrer bar in repeated extractions. Thus, the fiber is exposed to different turbulences, resulting in a rather high RSD of the results. The repeatability of SPME for some organochlorines under mixed and non-mixed conditions are shown in Table 3. Except for lindane, the RSD is lower when the sample was not agitated, but the differences are not great enough to justify extraction from unagitated samples as this would mean more time-consuming procedure.

TABLE 3:
Comparison of detector response and RSD (3 extr.) for some organochlorines extracted from aqueous solution - concentration 80 ng/ml with SPME (100 μm polydimethylsiloxane fiber, 15 min) under mixed (magnetic stirrer, 250 rpm) and non-mixed conditions.

	non-mixed conditions		mixed conditions	
compound	peak area / 10^6	RSD	peak area / 10^6	RSD
lindane	1.8 ± 0.6	$\pm 33\%$	5.1 ± 0.8	$\pm 16\%$
heptachlor	0.5 ± 0.1	$\pm 21\%$	5.1 ± 1.6	$\pm 31\%$
4,4'-DDE	7.8 ± 1.4	$\pm 18\%$	8.7 ± 1.6	$\pm 19\%$
endrin	5.9 ± 0.9	$\pm 16\%$	9.6 ± 2.1	$\pm 22\%$
dieldrin	3.3 ± 0.6	$\pm 18\%$	7.1 ± 1.3	$\pm 19\%$

The effect of sodium chloride addition to the sample prior to extraction was also tested. As reported before, triazines are better adsorbed onto the fiber in saturated salt solution [19]. Our experiments were conducted on samples with no NaCl added or in saturated solution, and better results were obtained under the later conditions for triazines. For organochlorines, which are strongly hydrophobic compounds, no such effect was observed, and therefore further experiments were made without salt addition. Desorption conditions were chosen from the literature and were not optimized. As no cryofocusing

was available in our gas chromatograph, the desorption time was chosen to be short: 4 min at 220°C for triazines and 3 min at 250°C for organochlorines, while the head of the column was kept at 70°C for triazines and at 120°C for organochlorines. No additional peak broadening was observed under these conditions compared to direct injection and also no carry-over from the fiber. Nevertheless, the fiber was left in the GC injector after opening the purge valve for a further 5-10 min to ensure complete desorption of other contaminants from the fibre.

2. Soil extraction procedure evaluation

Extraction of pesticides from soil by SPME was reported to be successful for screening purposes, if performed from a soil suspension in water [8]. We tried to repeat the experiment with spiked soil, but found the amount of pesticides adsorbed onto the fiber too low for our detection limits, if only 0.5 g of soil were suspended in 5 ml of water. When a thicker suspension was prepared, a new problem arose: the coating of the fiber was brushed off during agitation of the sample which was necessary to maintain the suspension. As the compounds analyzed are not sufficiently volatile to be extracted from the headspace, another approach had to be chosen.

A two-step extraction procedure was designed: first, extraction of pesticides from soil by conventional means, that is, with an organic solvent; second, the solid-phase microextraction of the extraction residue in aqueous solution.

Acetone was chosen for the extraction in the first step, as it was reported before to be efficient [10, 15, 16], as well as because of its rather high volatility and low toxicity. The amount of sample analyzed had to be minimized to reduce solvent consumption. A suitable amount was found to be 7 g of air-dried soil.

The procedure was evaluated by extracting a series of prepared spiked soil samples. In Table 4, extraction recoveries for a group of organochlorines are given separately for the SPME process and the overall recovery of the method. Though the percentage of the analyte extracted by the fiber is extremely small in comparison to other extraction

methods where quantitative extraction is usually achieved, the amount of analyte on the fiber is sufficient to achieve adequate limits of detection.

TABLE 4:
Extraction recoveries (η) for organochlorine pesticides: separately for SPME only and for overall extraction procedure from soil spiked with 2 - 12 ng/g of pesticide. For extraction conditions, see Experimental section.

Compound	η (SPME)	η (overall)	compound	η (SPME)	η (overall)
α-BHC	7.3 %	0.9 %	ES sulfate	8.4 %	0.3 %
β-BHC	4.0 %	0.2 %	aldrin	4.6 %	0.1 %
γ-BHC	5.9 %	0.9 %	endrin	3.3 %	0.1 %
δ-BHC	7.4 %	0.5 %	EN aldehyde	1.6 %	0.04 %
heptachlor	5.1 %	0.2 %	dieldrin	3.6 %	0.1 %
HC epoxide	3.7 %	0.3 %	4,4'-DDT	2.0 %	0.1 %
endosulfan I	5.1 %	0.2 %	4,4'-DDE	0.9 %	0.03 %
endosulfan II	5.6 %	0.2 %	4,4'-DDD	1.5 %	0.03 %

The same soil extract in aqueous solution could be extracted by SPME over five times with good repeatability (3-10%) for triazines, but only twice for organochlorines. In the third extraction, the amount of pesticide extracted was 8-60% of the amount in the previous extractions, depending on the compound.

Another interesting, yet not surprising feature was noticed during our work. It was often observed before that spikes are not equivalent to the native analytes in soil regarding binding to soil particles and thus amenability to extraction. In our case, this was easily confirmed. Figure 3 depicts a comparison of results for triazine herbicides after the complete extraction procedure. Results are compared for soil a few days after spiking with a standard mixture and a few weeks later, after soil was left in a sunny, open site and thus partial "weathering" of the added pesticides was achieved. Though it might be possible that part of analytes could have evaporated from the sample during standing, triazines are not very volatile compounds and it seems much more likely that on weathering, they were adsorbed to soil more strongly or they even formed complexes with some soil components – e.g. humic acids [1], causing poorer extraction recoveries.
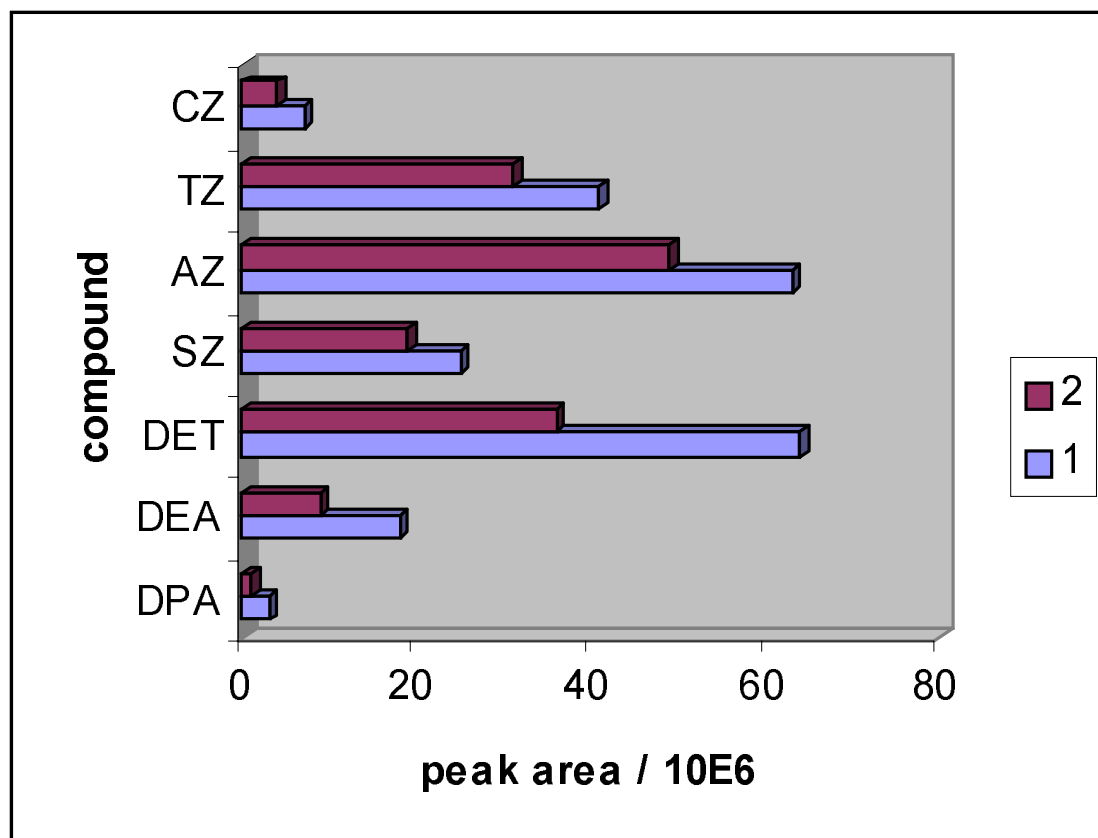
Figure 3: Comparison of peak areas (GC-MS detection) after extraction of triazine herbicides from soil spiked at 30 ng/g level. Extraction a few days after spiking (**1**) and one month after spiking (**2**). For abbreviations, see Figure 1.

3. Discussion of pesticide identification in soil

In Figure 4, ECD chromatograms of organochlorine and triazine pesticides extracted from spiked soil by the proposed method are depicted. Notice the great difference in the spiking level for the two pesticide groups at approximately the same signal / noise level. As expected, organochlorines were very well detected on an electron capture detector; whereas triazines, which were all chloro-triazines, showed a rather poor response. It was thus concluded that the EC detector is not suitable for triazine detection, while for organochlorines, retention times were repeatable enough to allow for identification of individual compounds, though this is not a completely reliable means.

Figure available in printed version only

Figure 4: Chromatograms of SPME soil extracts recorded with electron capture detector. **A** - soil spiked with organochlorines at 1 ng/g level, integrator attenuation 9. **B** - soil spiked with triazines at 50 ng/g level, integrator atten. 10. For abbreviations, see Figures 1 and 2, except: EN - endrin, ENA - endrin aldehyde

Triazine herbicides were detected using a mass spectrometer in the scan mode. Figure 5 depicts a comparison of GC-MS generated chromatograms after injecting an acetone solution of a soil extract and after extracting the same soil extract in water with an SPME fiber. Though the signals in chromatogram are lower in the second case, the chromatogram is much cleaner and the spectra obtained for the analyzed compounds were free of interferences and amenable to computer identification down to the level of approximately 20 ng of pesticide/g of soil.

Figure available in printed version only

Figure 5: Chromatograms of soil extracts recorded with MS in scan mode. Soil spiking level for triazines: 50 ng/g. **A** - soil extract after solvent extraction only, reconstituted in acetone. **B** - soil extract reconstituted in water after extraction with SPME. For abbreviations, see Figure 1.

4. Discussion of pesticide quantification in soil

As said before, part of the investigated compounds is strongly bonded in the soil and cannot be extracted. Thus, the method presented could be used only for the non-bonded part of the pesticides in soil. Some data are presented here regarding the linearity and detection limits. To our knowledge, there are no standard materials for analysis of pesticides in soil, so recoveries, linearity, and detection limits were tested using only spiked samples.

Organochlorines were spiked at the 0.1-20.0 ng/g level. Linearity was quite good (r > 0.98 for most compounds), while limits of detection calculated after the method of Winefordner and Long [21] ranged from 0.6 - 5.2 ng/g of soil, except for the analytes showing a poorer response on the ECD (4,4'-DDD, 4,4'-DDT, endosulfan sulfate, endrin aldehyde), which also had to be spiked at a higher level. Some real-life samples were analyzed, including a heavily contaminated field sample containing 30 ± 10 ng/g of DDT.

For triazine analysis, quantification was achieved using single ion monitoring (SIM) mass spectrometric detection. Soil was spiked at the 10-100 ng/g level. The linearity of the method was good (r > 0.99), and the limits of detection calculated after the method of Winefordner and Long [21] were 10-15 ng/g, which is acceptable for the level of these compounds usually found in field samples.

Some field samples were analyzed, but levels of triazines were below detection limits except in one case, when a triazine degradation product was found (Figure 6), but was not quantified because of the lack of a suitable standard compound.

Figure available in printed version only

<u>Figure 6</u>: GC-MS (scan mode) generated chromatogram of a real-life soil sample after extraction procedure. A triazine degradation product (marked **X**) was detected (spectrum shown below).

CONCLUSIONS

The method presented offers a simple alternative to established methods of pesticide analysis in soil. In this case SPME is used after transfer of pesticides from soil to aqueous solution, so time-consuming clean-up techniques for organic extracts are eliminated. Though the recoveries cannot be compared to conventional methods, the results show the suitability of the method in terms of identification and quantification of the analytes. These are analyzed by GC with either ECD or MSD. The former is very suitable for organochlorines, while the latter was used to detect triazines, where identification of compounds through mass spectra was possible. To achieve satisfactory limits of detection of target compounds, the SIM mode had to be used. Due to its simplicity and short time of analysis, the described method could be used for quick screening for pesticides in the contaminated soil in GC-MS scan mode.

REFERENCES

[1] A. Heintz, G.A. Reinhardt, *Chemie und Umwelt*, 4th ed., Vieweg Lehrbuch, Germany, 1996, pp. 228.

[2] H.-P. Thier, H. Zeumer, *Manual of pesticide residue analysis* Vol. I, DFG-VCH Publishers, Weinheim, Germany, 1987, pp.265-295.

[3] R. Young, V. Lopez-Avila, and W.F. Beckert, *J. High Resol. Chromatogr.* **1996**, *19*, 247-256.

[4] R.E. Shirey, *J. High Resol. Chromatogr.* **1995**, *18*, 495-499.

[5] A.A. Boyd-Boland, S. Magdic, and J.B. Pawliszyn, *Analyst* **1996,** *121*, 929-937.

[6] R. Eisert, K. Levsen, *J. Am. Soc. Mass Spectrom.* **1995**, *6*, 1119-1130.

[7] R. Eisert, K. Levsen, *Fresenius' J. Anal. Chem.* **1995**, *351*, 555-562.

[8] A.A. Boyd-Boland, J.B. Pawliszyn, *J. Chromatogr. A* **1995**, *704*, 163-172.

[9] R. Schewes, F.X. Maidl, G. Fischbeck, J. Lepschy von Gleissenthall, A. Süss, *J. Chromatogr.* **1993**, *641*, 89-93.

[10] H. Prosen, L. Zupancic-Kralj, J. Marsel, *J. Chromatogr. A* **1995**, *704*, 121-130.

[11] H. Steinwandter, *Fresenius' J. Anal. Chem.* **1992**, *343*, 604-606.

[12] E.G. van der Velde, M. Dietvorst, C.P. Swart, M.R. Ramlal, P.R. Kootstra, *J. Chromatogr. A* **1994**, *683*, 167-174.

[13] H. Weil, K. Haberer, *Fresenius' J. Anal. Chem.* **1991**, *339*, 405-408.

[14] M.S. Mills, E.M. Thurman, *Anal. Chem.* **1992**, *64*, 1985-1990.

[15] M..J. Redondo, M.J. Ruiz, R. Boluda, G. Font, *Chromatographia* **1993**, *36*, 187-190.

[16] M.J. Redondo, M.J. Ruiz, R. Boluda, G. Font, *J. Chromatogr. A* **1996**, *719*, 69-76.

[17] Zh. Zhang, M.J. Yang, J. Pawliszyn, *Anal. Chem.* **1994**, *66*, 844A-853A.

[18] S. Magdic, J.B. Pawliszyn, *J. Chromatogr. A* **1996**, *723*, 111-122.

[19] T.K. Choudhury, K.O. Gerhardt, T.P. Mawhinney, *Environ. Sci. Technol.* **1996**, *30*, 3259-3265.

[20] I.J. Barnabas, J.R. Dean, I.A. Fowlis, S.P. Owen, *J. Chromatogr. A* **1995**, *705*, 305-312.

[21] G.L. Long, J.D.Winefordner, *Anal. Chem.* **1983**, *55*, 713A-724A.

Preostanki pesticidov in njihovih razgradnih produktov v prsti predstavljajo resen problem za posevke, organizme v prsti in ljudi. Za izolacijo te vrste spojin lahko uporabimo mikroekstrakcijo na trdni fazi (solid-phase microextraction – SPME) v kombinaciji z običajno ekstrakcijsko metodo. To moderno separacijsko metodo smo optimizirali za ekstrakcijo kloriranih in triazinskih pesticidov iz vzorcev prsti. Analizirane spojine smo desorbirali z vlakna v injektorju plinskega kromatografa in določili z detektorjem na zajetje elektronov (electron capture detector – ECD) ali z masnim spektrometrom (MS). Linearnost in meje detekcije smo testirali v območju 0.1–20.0 ng/g za klorirane insekticide in v območju 10–100 ng/g za triazine. Predstavljeno metodo lahko uporabimo za pregledno analizo (screening) na pesticide v onesnaženih vzorcih prsti. Omogoča preprostejši pristop k analizi pesticidov v prsti kot že uveljavljene metode.

SUBSTRATE SPECIFICITY OF 17β-HYDROXYSTEROID
DEHYDROGENASE FROM *PLEUROTUS OSTREATUS*

M. Pogačar, M. Zorko and M. Žakelj-Mavrič

Institute of Biochemistry, Medical Faculty, Ljubljana, Slovenia

ABSTRACT

We present evidence which suggests that *Pleurotus ostreatus* 17β-HSD is a pluripotent enzyme which can oxidize 17β-hydroxysteroids and even more so hydroquinone in the presence of NAD^+. The study of the reverse reaction indicates that the carbonyl reductase activity prevails over the hydroxysteroid dehydrogenase activity. Kinetic studies also reveal the presence of a separate acetoacetyl CoA reductase / β-hydroxybutyryl CoA dehydrogenase activity in *Pleurotus ostreatus*.

INTRODUCTION

The metabolism of xenobiotics and steroids has been intensively studied from the point of view of their oxidation by different cytochromes P-450. Recently, the reduction of these compounds by carbonyl reducing enzymes has attracted more attention. A group of enzymes, classified either as hydroxysteroid dehydrogenases (HSDs) or carbonyl reductases, was found to exhibit specificity towards both groups of compounds (1). 17β-hydroxysteroid dehydrogenases (17β-HSDs) can be taken as representatives of this group of enzymes since several 17β-HSDs from mammalian peripheral as well as steroidogenic tissues have been found to posses carbonyl reductase activity in addition to

hydroxysteroid dehydrogenase activity (2-7). In fungi the pluripotency has been established only for 17β-HSD from the filamentous *Cochliobolus lunatus* (8). The white-rot fungus *Pleurotus ostreatus* has so far been found to metabolize polycyclic aromatic hydrocarbons (9) as well as to oxidize androgens and estrogens (10). Since recently a preliminary study suggested several differences in the characteristics between 17β-HSDs from both fungi, we studied *Pleurotus ostreatus* 17β-HSD in greater detail.

EXPERIMENTAL

1) Fungal species

Pleurotus ostreatus G7 was obtained from the Microbial Culture Collection of the Chemical Institute , MZKIBK Ljubljana.

2) Growth conditions

Ten-day-old cultures on agar slants (2% agar in 6^0 Blg malt extract) were used to inoculate 100 ml of liquid media composed of 0.5% cornstep liquor, 1% oatmeal, 1% glucose, 4% tomato paste, 10ml/l mineral solution, pH 7 (mineral solution: 1g/l $FeSO_4$ x $7H_2O$, 1g/l $MnSO_4$ x0 H_2O, 0.2 g/l $ZnSO_4$ x $7H_2O$, 0.1 g/l $CaCl_2$ x $2H_2O$, 0.056 g/l H_3BO_3, 0.0025 g/l $CuCO_3$, 0.019 g/l $(NH_4)_6Mo_7O_{24}$ x $4H_2O$). Cultivation was performed in 500 ml Erlenmeyer flasks for six days at 25^0 C on a rotary shaker at 110 rpm.

3) Enzyme preparation

After six days of growth the mycelium of *Pleurotus ostreatus* was filtered and frozen by liquid nitrogen. The enzyme preparation used for kinetic measurements was prepared in 50 mM Tris/HCl, pH 9, 20% glycerol, as described previously (11).

4) Enzyme assays

a) Chromatographic method

During the partial purification procedure the enzyme activity was tested as described (11).

b) Spectrophotometric method

For the kinetic measurements a similar procedure was used as already described (8).

Measurements were performed against blanks without the substrate in the reaction mixture, or without the enzyme in the case of quinone. Reaction rates were expressed as relative enzyme activities (%) with different substrates oxidized or reduced by 100μl of the enzyme preparation. The enzyme activities with 100 μM testosterone and 100 μM NAD$^+$ in 50 mM Tris/HCl, pH 8.5 with 20 % glycerol for the oxidation or 100 μM androstenedione and 100 μM NADH in 50 mM Tris/HCl, pH 7.0 with 20 % glycerol for the reduction reaction were taken as 100 %.

5) Competition between different substrates

Competition between the most effective substrates was studied for the oxidation reaction because of more comparable relative activities of selected substrates and because of higher initial velocities of testosterone oxidation in comparison to androstenedione reduction. It was tested by following the activity of 17β-HSD in the presence of each individual substrate and in the presence of two substrates simultaneously; the concentration of one substrate varied (testosterone from zero to 250 μM, β-hydroxybutyryl CoA from zero to 200μM, and hydroquinone from zero to 400 μM) while the concentration of the other was kept constant (testosterone 100μM, hydroquinone 150 μM and β-hydroxybutyryl CoA 75μM), and *vice versa.* The concentration of the enzyme was constant in all experiments. From the Michaelis-Menten curves fitted to the experimental results obtained in the presence of each individual substrate, we determined the apparent K_m and V_{max} for each individual substrate in the presence of 20 μM NAD$^+$. These parameters were then used for the calculation of the curves valid for the competition between two substrates for the same enzyme or/and for the parallel action of two different enzymes on two substrates (12).

RESULTS

A range of hydroxylated steroid and non-steroid compounds was used to investigate the substrate specificity of the 17β-HSD enzyme preparation. Table 1 shows that it has a broad specificity for hydroxylated substrates with NAD$^+$ required as a coenzyme.

Table 1. Relative oxidative activities of 17β-HSD enzyme preparation in the presence of different substrates and 100 μM coenzymes. The activities are normalized to the activity in the presence of 100 μM testosterone and 100 μM NAD^+, considered to be 100%.

SUBSTRATE	CONC.	COENZYME	RELATIVE ACTIVITIES (%)
testosterone	100μM	NAD^+	100
		$NADP^+$	0
estradiol	100μM	NAD^+	80
		$NADP^+$	0
hydroquinone	100μM	NAD^+	116
		$NADP^+$	0
DL-β-hydroxybutyryl CoA	100μM	NAD^+	506
		$NADP^+$	0
L-β-hydroxybutyrate	1mM	NAD^+	13
		$NADP^+$	0
p-nitrobenzyl alcohol	1mM	NAD^+	69
		$NADP^+$	0
L-malate	1mM	NAD^+	40
		$NADP^+$	0

0 = no detectable activity

β-Hydroxybutyryl CoA was found to be the best substrate while hydroquinone, testosterone, and estradiol were also readily oxidized. The relative activities for β-hydroxybutyrate, malate and p-nitrobenzyl alcohol were much smaller than for testosterone (100%). No enzyme activity could be detected in the presence of $NADP^+$.

In addition carbonyl compounds, including steroids, quinones, aromatic aldehyde and aliphatic ketones were tested as substrates for the reductase activity of 17β-HSD enzyme preparation (Table 2). Both nicotinamide nucleotides could serve as electron donors. Acetoacetyl CoA and benzoquinone were reduced at much higher relative activities than androstenedione in the presence of NADH (100%). No activity could be detected in the presence of the other tested compounds.

Table 2. Relative reductive activities of 17β-HSD enzyme preparation in the presence of different substrates and 100 μM coenzymes. The activities are normalized to the activity of 100 μM androstenedione and 100 μM NADH which was taken as 100%.

SUBSTRATE	CONC.	COENZYME	RELATIVE ACTIVITIES (%)
androstenedione	100μM	NADH	100
		NADPH	31.3
estrone	100μM	NADH	0
		NADPH	0
benzoquinone	100μM	NADH	3103
		NADPH	3737
acetoacetyl CoA	100μM	NADH	3108
		NADPH	728
acetoacetate	1mM	NADH	0
		NADPH	0
p-nitrobenzaldehyde	1mM	NADH	0
		NADPH	0

0 = no detectable activity

As the above mentioned results suggested that at least some of the reactions could be catalyzed by 17β-HSD, competition experiments between the most effective substrates testosterone, hydroquinone, and β-hydroxybutyryl CoA were performed. Testosterone was found to compete with hydroquinone for the active centre of 17β-HSD (Fig.1A). On the other hand, the results on Fig.1B suggest parallel oxidations of testosterone and β-hydroxybutyryl CoA catalyzed by two different enzymes. These results were confirmed by experimental data suggesting parallel oxidations also for hydroquinone and β-hydroxybutyryl CoA (data not shown).
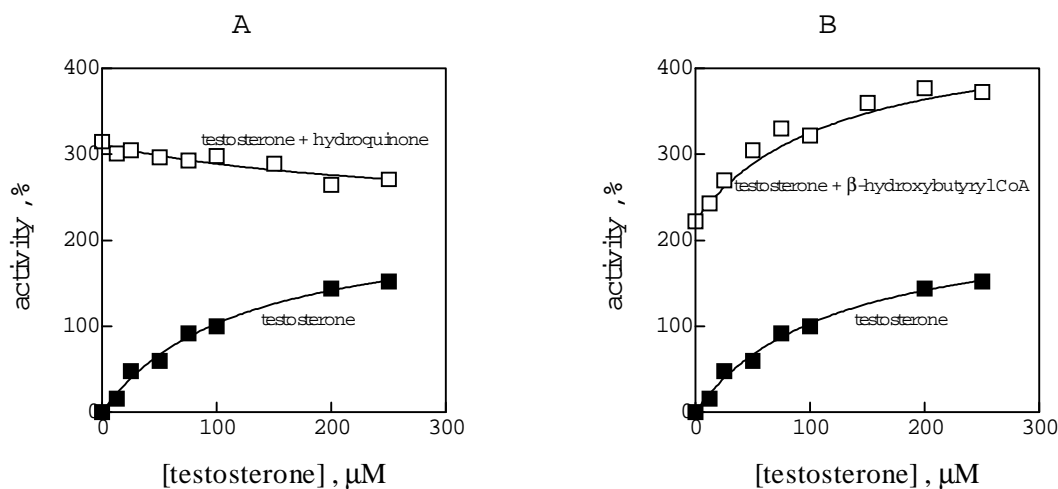
Fig.1.
A: Competition between substrates testosterone (variable concentration) and hydroquinone (150 µM) for the active centre of 17β-HSD.
B: Parallel oxidation of testosterone (variable concentration) and β-hydroxybutyrylCoA (75 µM) catalyzed by two different enzymes.
Points were obtained experimentally but the curves were calculated as described in Experimental, section 5.

CONCLUSIONS

While the important role of 17β-HSD in mammalian organisms is well established (13) the question about the role of these enzymes in primitive eukaryotes is not yet clear. It represents a challenge to those interested in fungal metabolism *per se* as well as the evolution of HSD and steroid hormone signalling system. In this sense, further characterization of fungal 17β-HSD seems desirable.

In the present study, the *Pleurotus osteratus* 17β-HSD enzyme preparation was found to have a broad substrate specificity catalyzing efficiently the oxidation of the steroid hormones testosterone and estradiol as well as the non-steroidal compounds hydroquinone and β-hydroxybutyryl CoA . NAD^+ is required as an electron donor. The results of the reverse reaction revealed the prevailing carbonyl reductase and acetoacetyl

reductase activity over 17β-HSD (reductase) activity. The competition experiments between the most effective substrates of 17β-HSD enzyme preparation suggested the presence of two separate enzymes, 17β-HSD and β-hydroxybutyryl CoA dehydrogenase / acetoacetyl CoA reductase. *Pleurotus osteratus* 17β-HSD was found to be pluripotent enzyme capable of testosterone and hydroquinone oxidation. It thus joins pluripotent HSDs whose role in detoxification of xenobiotic carbonyl compounds in addition to their role in the metabolism of endogenous steroids and quinones is only suspected (14).

ACKNOWLEDGMENTS

REFERENCES

(1) E. Maser, *Biochem.Pharmacol.* **1995**, 49, 421-440.
(2) R. Jarabak et al., *Arch.Biochem.Biophys.* **1996**, 327, 174-180.
(3) Y. Deyashiki et al., *J.Biol.Chem.* **1995**, 270, 10461-10467.
(4) T.Nishinaka et al., *Enzyme* **1992**, 46, 221-228.
(5) J.Klein et al., *Eur.J.Biochem.* **1992**, 205, 1155-1162.
(6) A.Hara et al., *Arch.Biochem.Biophys.* **1986**, 249, 225-236.
(7) H.Sawada et al., *Biochem.Pharmacol.* **1988**, 37, 453-458.
(8) T. Lanišnik Rižner et al., in Enzymology and Molecular Biology of Carbonyl Metabolism 6, ed.by Weiner et al., Plenum Press, New York, 1996, pp.569-577.
(9) L. Bezalel et al., *Appl.Environ.Microbiol.* **1996**, 62, 292-295.
(10) T. Lanišnik et al., *FEMS Microbiol.Lett.* **1992**, 99, 49 -52.
(11) T. Lanišnik Rižner et al., *J.Steroid Biochem.Molec.Biol.* **1996**, 59, 205-214.
(12) A. Cornish-Bowden, *Fundamentals of Enzyme Kinetics,* Portland Press, London, 1995, pp 108-109.
(13) T.M. Penning, *Endocrine Reviews* **1997**, 18, 281-305.
(14) N. Iwata et al., *J.Biochem.* **1989**, 105, 556-564.

POVZETEK

Na osnovi kinetičnih študij, prikazanih v članku, lahko sklepamo, da je 17β-HSD iz glive *Pleurotus ostreatus* pluripotenten encim, ki lahko oksidira 17β-hidroksisteroide in hidrokinon v prisotnosti NAD$^+$. V smeri redukcije prevladuje karbonil-reduktazna aktivnost nad hidroksisteroidno reduktazno aktivnostjo. Rezultati kažejo, da je v glivi *Pleurotus ostreatus* prisotna tudi neodvisna acetoacetil CoA reduktaza / β-hidroksibutiril CoA dehidrogenaza.

STRUCTURAL FEATURES OF AMPHIPATHIC PEPTIDES
REQUIRED FOR THE ACTIVATION OF G-PROTEINS

Aljoša BAVEC[1], Ursel SOOMETS[2], Ülo LANGEL[2] and Matjaž ZORKO[1]

[1]Institute of Biochemistry, Medical Faculty, University of Ljubljana, Ljubljana, Slovenia

[2]Dept. Neurochem. Neurotox., Stockholm University, Stockholm, Sweden

ABSTRACT

Eight different amphipathic peptides were tested as modulators of GTPase activity of G-proteins from rat brain cortex membranes: mastoparan and melittin (components of wasp and bee venom, respectively), MAS17 (inactive mastoparan analog), M252 and M256 (peptides derived from nerve growth factor receptor), PD$_1$ (synthetic peptide detergent), M366 (peptide derived from β-amyloid protein) and cys-pAntp (homeodomain part of *Drosophila* antennapedia protein). Four of the peptides (mastoparan, melittin, PD$_1$ and M366) increased GTPase activity, other peptides showed no effect. Correlation of these data with peptide sequences, their predicted secondary structure and residue solvent accessibility pointed to two types of activators. First type (melittin and PD1) is characterised by longer (24-26 amino acids) fully amphipathic helical structure with separated charges at both ends of the sequence. Second type of activators (mastoparan and M366) is a shorter helix (11-14 amino acids) and contains a motif consisted of lysine in position 4, followed by 5 to 6 amino acids with the residues of low solvent accessibility.

INTRODUCTION

It is well known that several amphipathic peptides activate G-proteins. It was suggested that mastoparan, a component of wasp venom, and some of its analogs increase GTPase activity of G-proteins by binding to the C-terminus of G_i/G_o α-subunit, mimicking in this

way the action of G-protein coupled receptors [1]. However, it has not yet been clarified which structural elements of amphipathic peptides are crucial for their activity. In order to shed some light on this problem we have tested eight different amphipathic peptides as potential modulators of GTPase activity of G-proteins and correlated the obtained results with the peptide sequences, their predicted secondary structures and calculated solvent accessibility. The following amphipathic peptides were studied: mastoparan, MAS17 (inactive mastoparan analog) [1], melittin (a component of bee venom) [2], M252 and M256 (sequences (272-291) and (370-383) from the intracellular loop of p75 nerve growth factor receptor) [3], PD₁ (synthetic peptide detergent-peptitergent) [4], M366 (β-amyloid protein (25-35)) [5], and cys-pAntp (*Drosophila* homeoprotein Antennapedia (43-58)) [6] .

METHODS

Peptide synthesis: Peptides were synthesised by solid phase synthesis using *t*-Boc-chemistry . Peptides were synthesised in a stepwise manner on a 0.1 mmol scale using an Applied Biosystem Model 431A peptide synthesiser as described earlier [7].

Plasma membranes preparation: Wistar rats were sacrificed, brain was removed and sliced, brain cortex separated and quickly frozen in liquid nitrogen. Membranes were prepared according to the protocol of McKenzie [8], with minor modifications. The protein concentration in the obtained preparation was determined by the method of Lowry [9]. Membranes were then diluted in TRIS-EDTA buffer pH 7.5 and were used in the final protein concentration of 2.21 mg/ml.

GTPase assay: The determination of GTPase enzymatic activity was performed radiometrically according to Cassel and Selinger [10], with the modifications suggested by McKenzie [8]. The total concentration of GTP was 0.5 µM with trace amounts of γ[^{32}P]GTP to give 50.000 - 100.000 cpm in an aliquot of the reaction cocktail in which plasma membranes diluted in Tris-EDTA buffer pH 7.5 were added. Background low-affinity hydrolysis of γ[^{32}P]GTP was assessed by incubating parallel tubes in the presence of 100 µM GTP. Blank values were determined by the replacement of rat brain cortex

membrane solution with assay buffer. The GTPase reaction was started by transferring the reaction mixtures to a 25°C water bath for 10 minutes. Subsequently, free [^{32}P$_i$] was separated from the unhydrolysed γ[^{32}P]GTP in 5% suspension of activated charcoal in 20 mM H_3PO_4. The amount of the yielding radioactive phosphate was determined in a LKB 1214 Rackbeta liquid scintillation counter. Basal GTPase activity of rat brain cortex plasma membranes was 0.52 pmol/min/mg protein.

Secondary structure prediction: Secondary structure prediction of the peptides and prediction of residue solvent accessibility were performed by using two PHD methods (**P**rofile fed neural network systems from **H**ei**D**elberg), PHDsec (secondary structure) and PHDacc (solvent accessibility) [11-14]. Internet accessible (http//www.embl-heidelberg.de/ predictprotein) programs installed in Heidelberg University, FRG, were used. PRISM (GraphPad Software, USA) computer program was used for the fitting of the curves and other calculations, as well as for the graphical presentation of the results.

Chemicals: [γ-^{32}P]GTP was from NEN, UK; *tert*-butyloxycarbonyl amino acids were from Chemimpex, USA; all other chemicals were from Sigma, USA.

RESULTS AND DISCUSSION

It is seen from Fig. 1 and Table 1 that four out of eight tested amphipathic peptides (mastoparan, melittin, PD$_1$ and M366) were able to increase GTPase activity of G-proteins. The activation with mastoparan and melittin was in accordance with a bi-phasic dose-response curve with maximally 221% and 148% of basal GTPase activity, respectively. Maximal activation of M366 and PD$_1$ was 211% and 194% of the basal and a single-step dose-response curve could be used. The other four peptides showed no effect within the error limits (Table 1) up to the concentration as high as 100 μM.

Comparison of the effect of the peptides on GTPase activity with the peptide sequences, predicted secondary structure and predicted residue solvent accessibility (Figs. 2 and 3) has revealed two types of GTPase activators among studied peptides. First type

represent longer peptides, PD$_1$ and melittin (Fig. 2), with the following features: a) complete α-helical structure in which the hydrophilic amino acids regularly alternate
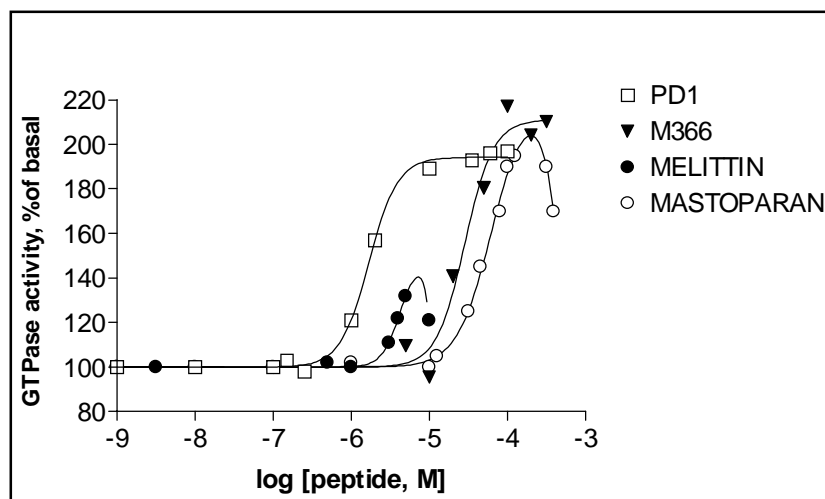

Fig. 1: Activation of GTPase by different amphipathic peptides. Standard deviation of the points was 5 - 12 % and is not shown for clarity.

Table 1: Kinetic parameters calculated from the effect of amphipathic peptides on GTPase activity of G-proteins. EC$_{50}$ represents the concentration of the peptide with 50% effect and n$_H$ is the Hill coefficient. For mastoparan and melittin only parameters for the ascending phase of the dose-response curves are shown.

peptide name and sequence	max. effect (% of basal)	EC$_{50}$ (μM)	n$_H$
CONTROL **(NO PEPTIDE ADDED)**	**100 ± 10**	**-**	**-**
MASTOPARAN **I N L K A L A A L A K K I L**	**221 ± 19**	**62 ± 10**	**2.0 ± 0.3**
M366 (β-amyloid protein (25-35)) **G S N K G A I I G L M**	**211 ± 7**	**28 ± 5**	**2.4 ± 0.8**
PD$_1$ (peptitergent) **E E L L K Q A L Q Q A Q Q L L Q Q A Q E L A K K**	**194 ± 5**	**1.7 ± 0.2**	**2.3 ± 0.3**
MELITTIN **G I G A V L K V L T T G L P A L I S W I K R K R G G**	**148 ± 22**	**4.2 ± 2.2**	**3.8 ± 2.7**
M252 (p75 nerve growth factor receptor (272-291)) **A F K R W N S C K Q N K Q G A N S R P V**	**109 ± 8**	_	_
M256 (p75 nerve growth factor receptor (370-383)) **L D A L A A L R R I Q R A**	**107 ± 3**	_	_
MAS17 (inactive analog of mastoparan) **I N L K A K A A L A K K L L**	**102 ± 10**	_	_
cys-pAntp (*Drosophila* Anntenapedia (43-58)) **C R Q I K I W F Q N R R M K W K K**	**101 ± 10**	_	_

with hydrophobic ones, forming thus two well separated hydrophobic/hydrophilic surfaces throughout the whole length of the peptide; and b) separation of charges located at the terminal parts of the molecule. The peptides M252 and cys-pAntp (Fig. 2) are similar in alternating hydrophilic and hydrophobic amino acids, but they do not contain a complete α-helical structure and the charges are not separated within molecule; this seems to prevent them to function as GTPase activators. The results of structure prediction of PD_1 and melittin are in full accordance with the structure of these two peptides obtained by X-ray diffraction and NMR studies [2, 4]. Additional common feature of PD_1 and melittin is their strong tendency to form aggregates, mostly tetrameres [2, 4].

The second type of GTPase activators (mastoparan and M366) bears a shorter α-helix and is characterised by a specific motif consisting of positively charged lysine near N-terminus, followed by 5-6 hydrophobic amino acids (Fig. 3). In other tested short peptides which are not GTPase activators this motif is not present or is incomplete. In e. g. MAS17 an additional charged lysine occurs within the hydrophobic region (Fig. 3) and M256 includes a negatively charged residue (aspartic acid) in the vicinity of the N-terminus (Fig. 3). Both these peptides seem to be in α-helical structure (Fig. 3), but this is obviously a feature not sufficient for the activation of GTPase.

Our data are in accordance with the findings of Higashijima et al [15], who claimed that amphiphilicity of the GTPase activating peptides is of the primary importance, but the charged residues defining the amphiphilic character of the peptide may also play important role. Detert and co-workers [16] suggest that charge is not necessary for the GTPase activation, however, their results were not obtained with peptides but rather with substituted histamines, which might have different mechanism of enzyme activation. This rises also the questions such as: on which type of G-proteins the peptides act, how many interaction sites are important for the activation and where on the surface of G-proteins are these sites. It was suggested for mastoparan that it activates G-proteins by binding to C-terminal helix of G_i/G_o alpha subunit [1]. Similar structure and effect of
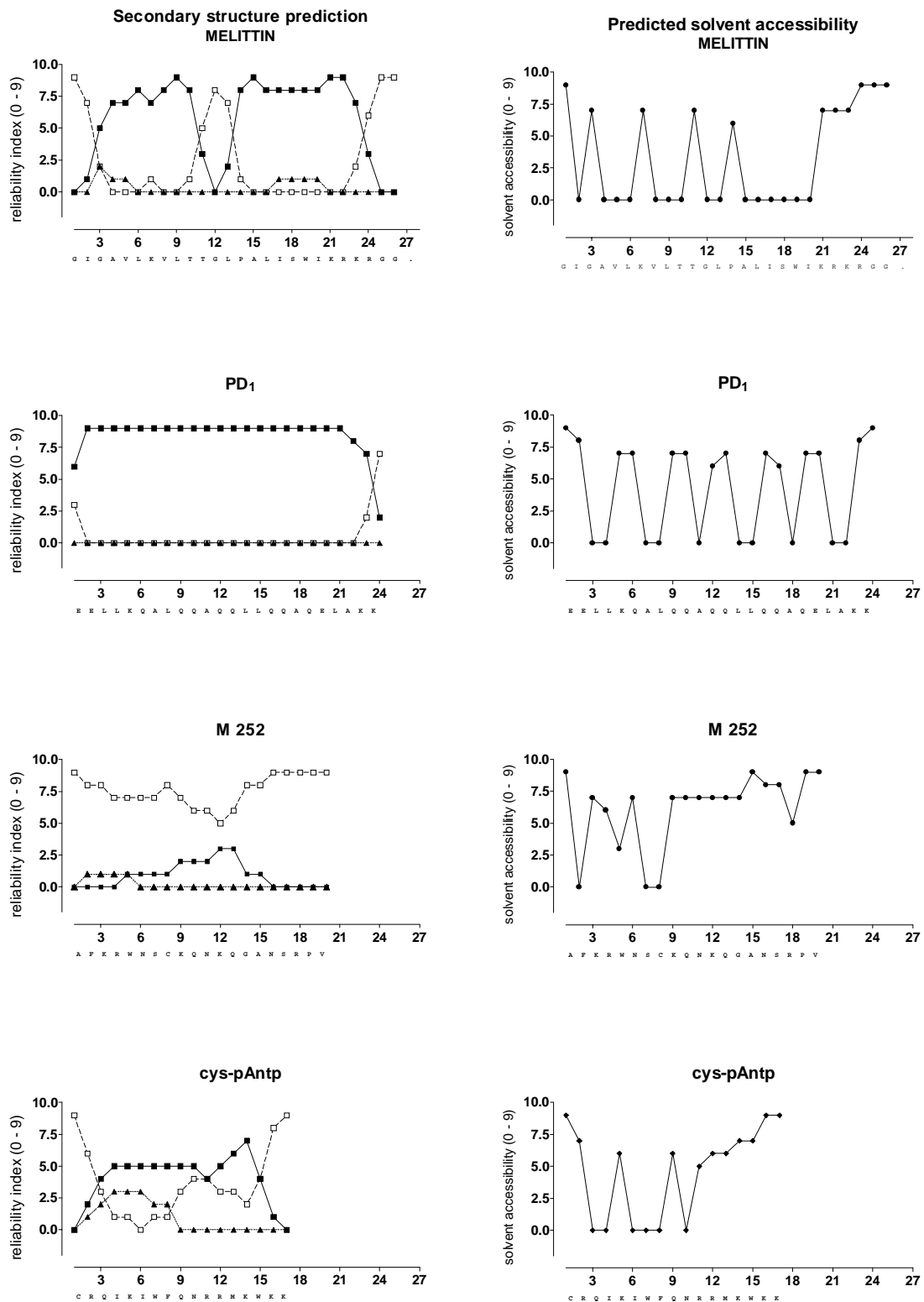
Fig. 2: Predicted secondary structure and predicted solvent accessibility of long (17-26 amino acids) amphipathic peptides. Symbols: ′, α-helix; π, β-structure; ≤, loop.
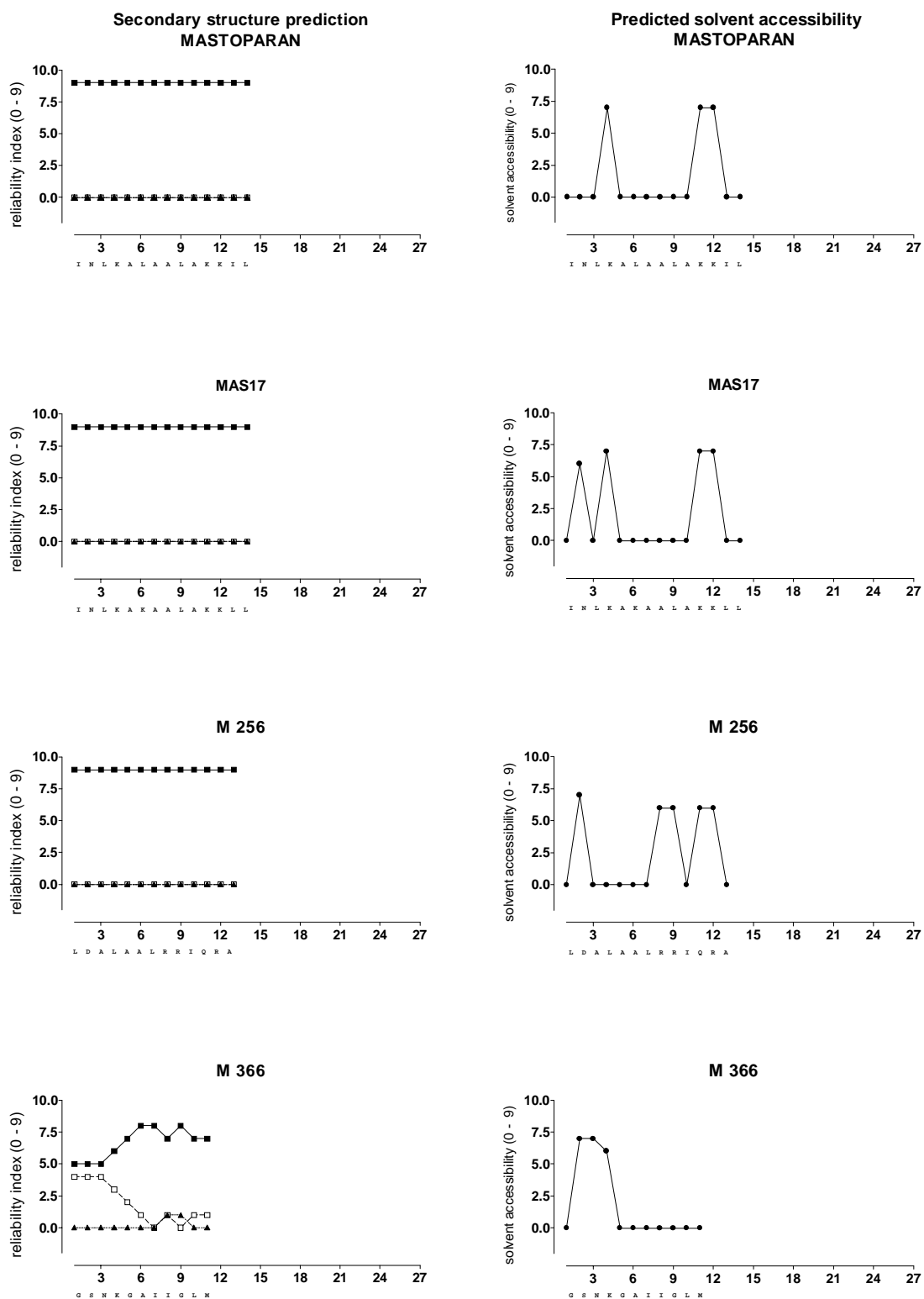
Fig. 3: Secondary structure prediction and predicted solvent accessibility of short (11-14 amino acids) amphipathic peptides. Symbols: ′, α-helix; π, β-structure; ≤, loop.

M366 and mastoparan, revealed in our study, allow us to speculate that these two peptides activate GTPase by binding to the same binding site. This is additionally corroborated by the similarity of their EC_{50} values (Table 1). Melittin and PD_1, which are structurally different from M366 and mastoparan, activate GTPase with EC_{50} which is for one order of magnitude lower than that for M366 and mastoparan. This suggests the possibility that melittin and PD_1 act on G-proteins by binding to site(s) different from that of M366 and mastoparan. Besides, the values of Hill coefficients significantly larger than 1, obtained for all GTPase activating peptides (Table 1), suggest multiple binding of the peptides to G-proteins.

REFERENCES

[1]   T. Higashijima et al., *J. Biol. Chem.* **1988**, *263*, 6491-6494.
[2]   A. Okada, et al., *Biochemistry* **1994**, *33*, 9438-9446.
[3]   D. L. Feinstein and D. Larhammar, *FEBS Lett.* **1990**, *272*, 7-11.
[4]   C. E. Schafmeister et al., *Science* **1993**, *262*, 734-738.
[5]   J. Hardy, *TINS*, **1997**, *20*, 154-159
[6]   D. Derossi et al., *J. Biol. Chem.*, **1994**, *269*, 10444-10450
[7]   Ü. Langel et al., *Int. J. Pept. Protein Res.* **1992,** *39*, 516-522.
[8]   F. R. McKenzie, *in: Signal Transduction (Milligan, E., ed.)*, Oxford Un. Press, **1992**, p. 31.
[9]   O. H. Lowry et al., *J. Biol. Chem.* **1951**, *193*, 265-275.
[10] D. Cassel and Z. Selinger, *Biochim. Biophys. Acta* **1976***, 452*, 538-551.
[11] B. Rost and C. Sander, *J.Mol. Biol.* **1993**, *232*, 584-599.
[12] B. Rost and C. Sander, *Proteins* **1994**, *19*, 55-72.
[13] B. Rost et al., *Prot. Science* **1995,** *4*, 521-533.
[14] B. Rost and C. Sander, *PNAS* **1993**, *90*, 7558-7562.
[15] T. Higashijima et al., *J. Biol. Chem.* **1990**, *265*, 14176-14186.
[16] H. Detert et al., *Eur. J. Med. Chem.* **1996**, *31*, 397-405.

POVZETEK

Osem različnih amfipatičnih peptidov smo testirali kot modulatorje GTPazne aktivnosti G-proteinov v membranah iz korteksa podganjih možganov: mastoparan in melittin (komponenti osjega in čebeljega strupa), MAS17 (neaktivni mastoparanov analog), M252 and M256 (peptida izvedena iz receptorja za živčni rastni faktor), PD_1 (sintetični peptidni detergent-peptitergent), M366 (peptid izveden iz β-amyloidnega protein) in cys-pAntp (homeodomenski del antennapedia proteina iz *Drosophile*). Štirje peptidi (mastoparan, melittin, PD_1 in M366) so povečali aktivnost GTPaze, ostali pa niso imeli nobenega vpliva. Primerjava teh podatkov s sekvenco peptidov, njihovo napovedano sekundarno strukturo in izračunano topnostjo posameznih aminokislinskih ostankov, je pokazala na dva tipa aktivatorjev. Za prvi tip (melittin in PD_1) je značilen daljši, v celoti amfipatični a-heliks (24-26 aminokislin), z ločenimi naboji na obeh koncih peptida. Drugi tip (mastoparan in M366) predstavlja krajši a-heliks (11-14 aminokislin) in kaže značilen motiv, ki ga sestavlja lizin na mestu 4 ter 5 do 6 aminokislin z radikali, ki imajo majhno sposobnost raztapljanja v vodi.

AChE mRNA STABILITY IN MAMMALIAN SKELETAL MUSCLE, STUDIED
IN VITRO

K. Zajc Kreft, S. Kreft, and Z. Grubič

Institute of Pathophysiology, Medical Faculty, Ljubljana, Slovenia

Acetylcholinesterase (AChE) mRNA in fast rat skeletal muscle is downregulated by both, electromechanical activity and denervation. One candidate mechanism that could explain decreased level of AChE mRNA in the denervated muscle is increased rate of its degradation. In order to test this possibility, total deproteinated RNA was isolated from rat m. SM and exposed to subcellular muscular fractions prepared from contralateral m.SM. After selected time intervals, we determined remaining AChE mRNA by nonradioactive Northern blot analysis.

AChE mRNA remained at the same level during first 5 hours after denervation and abruptly fell after subsequent 13h. Further decrease in the transcript level proceeded at much slower rate. Longer transcript (3.5 kb) was more affected than the shorter (2.3 kb) one. The level of α-actin mRNA was also decreased in the denervated muscle, and the rate of its disappearance was similar to that of AChE mRNA, suggesting that AChE mRNA is not specifically affected under such conditions. Degradation of AChE mRNA was observed in all subcellular fractions studied. Postmitochondrial and postpolysomal fractions exibited higher rate than polysomal fraction. We find experimental approach demonstrated here suitable for studies of degradation capacities of the specific mRNAs in the adult skeletal muscles. Our preliminary results suggest, that fall of AChE mRNA after denervation at least partly results from increased degradation of transcripts under such conditions.

INTRODUCTION

Most skeletal muscle genes are expressed at similar levels in electrically active, innervated muscle, and in electrically inactive, denervated muscle (1). However, expression of a small number of genes becomes altered after denervation. Some of them, including genes for acetylcholine receptor subunits, N-CAM, and myogenin, are expressed at significantly higher levels under such conditions, while the opposite was observed for some other genes like that of acetylcholinesterase (AChE; EC 3.1.1.7) (2,3,4) and α-actin (5) genes.

Decreased expression of AChE in the denervated and therefore inactive muscle is especially puzzling, since it is downregulated by both, electromechanical activity and denervation (2,6). It could be hypothesized, that electromechanical activity downregulates AChE in a specific manner and through the same mechanisms, responsible for downregulation of acetylcholine receptor subunits. On the other hand, denervation decreases AChE and its mRNA through some other events, which are obviously strong enough to override upregulating effect of electromechanical inactivity. One possible mechanism that could explain decreased level of AChE mRNA in the denervated muscle is increased rate of its degradation.

Expression of AChE in the mammalian skeletal muscle was already reported to be importantly controlled at the mRNA stability level (7). However, this report is based on the observations on the cultured mouse muscle cell line during fusion and could therefore not be simply extrapolated to the adult denervated muscle. The aim of our research is to investigate, whether decreased AChE mRNA level in the denervated muscle reflects higher capacity of AChE mRNA degradation under such conditions. Following specific questions were addressed: 1) What is the time course of AChE mRNA decrease after mechanical interruption of the motor nerve; this information is essential for understanding of the mechanisms underlying the observed AChE mRNA fall. In order to answer this question, we determined AChE mRNA levels 5 h, 18 h, 2

days, 5 days, and 8 days following denervation of rat SM muscle; 2) How is the capacity of AChE mRNA degradation distributed among muscle subcellular fractions? AChE mRNA degradation rate was determined in the postmitochondrial and polysomal fractions and in the postpolysomal supernatant of adult rat muscle; 3) What is the role of the divergent 3' untranslated region of AChE mRNA in the stabilization of mRNA against degradation in muscle subcellular compartments. Namely, AChE gene has two polyadenylation signals. Their alternate usage gives rise to two transcripts, 2.3 and 3.5 kb long. It has been reported, that additional sequence of the long transcript contains ARE elements (7). These sequences were suggested to be responsible for the control of AChE expression at the level of mRNA stability (15); 4) How specific is AChE mRNA degradation in the muscle subcellular compartments. Degradation rate of AChE mRNA was compared to the degradation rates of ribosomal RNA and of α - actin mRNA.

EXPERIMENTAL PROCEDURES

Treatment of animals and muscle preparation

Female Wistar strain albino rats, weighting about 190 g, were used. Sternomastoideus muscles (m. SM) were unilaterally denervated by the excision of a few millimeters of motor nerve close to its entry to the muscle. After 5 and 18 hours, 2, 5 and 8 days muscles were isolated. Prior the isolation rats were anesthetized with the i.p. injection of anaesthetic containing Ketanest[®] /Park-Davis; 100 mg/kg) and Rompun[®] (Bayer; 15 mg/kg). SM muscle were quickly isolated, frozen in liquid nitrogen and stored at -80 $^{\circ}$C until used for RNA isolation. For the preparation of total RNA, used as substrate in *in vitro* degradation systems, untreated m. SM were isolated as described. Muscle subcellular fractions were prepared from fresh SM muscle.

RNA isolation and Northern blot analyses

Total RNA was isolated from the frozen SM muscles by guanidinium thiocianate procedure (8). We added two more precipitation steps and phenol extraction. Final RNA had A_{260}/A_{280} around 1.8 and A_{260}/A_{230} from 2.3-2.8.

40 μg of total RNA (from denervated muscles) or RNA recovered from degradation reactions were fractionated on the 1% denaturing formaldehyde-agarose gels, transferred to the nylon membrane (Boehringer Mannheim) and UV fixated. RNA loading was controlled by ethidium bromide staining.

Blots were prehybridized for 2-3 hours at 58^oC with DIG Easy Hyb (Boehringer Mannheim), 50 μg/ml denatured herring sperm DNA and then hybridized for 18 hours at 58^oC with AChE RNA probe 20-50 ng/ml (DIG Easy Hyb; 25 μg/ml denatured herring sperm DNA). The AChE RNA probe was synthesized with Riboprobe$^®$ Combination Systems (Promega) and DIG RNA Labeling Mix (Boehringer Mannheim) according to manufacturer's instructions. The synthesized RNA corresponds to nt. 370-706, part of second exon of AChE gene. Membrane was successively washed: once for 15 minutes in 2 X SSC with 0.1% SDS, 0.5 X SSC with 0.1 % SDS and 0.2 X SSC with 0.1 % SDS at room temperature and for 15 minutes at 58^oC in 0.1 X SSC with 0.1 % SDS. Detection of DIG labeled probe was carried out with DIG Nucleic Acid Detection Kit, according to manufacturer's instructions, with CDP-*Star*^{TM} as chemiluminescent substrate for alkaline phosphatase. After stripping with boiled 0.1% SDS the membrane was hybridized with human β-actin probe (Boehringer Mannheim), 10 ng of probe per ml of DIG Easy Hyb and 25 μg/ml denatured herring sperm DNA, at 58^oC for 18 hours. Washing of membrane and detection of labeled probe was the same as for AChE RNA probe.

Northern blot luminographs were densitometrically analyzed by image analyzer (hardware: Imaging Research Inc., Brooke University, Ontario, Canada; software: Micro Computer Imaging Device) according to Masters et al. (9).

Preparation of muscle subcellular fractions

Fresh SM muscle was quickly homogenized (1g/ 30 ml) (20 seconds at maximal speed) with Ultra-Turrax T25 (Janke & Kunkel Labortechnik) in chilled buffer A (250 mM potassium acetate, 10 mM magnesium acetate, 2 mM dithiothreitol, 10 mM Tris-acetate, pH 7.6 (10,11,12). The homogenate was centrifuged at 15000 x *g* for 10 minutes. A part of the supernatant (postmitochondrial fraction) was quickly frozen and stored at -80^oC. Centrifugation of the remaining postmitochondrial fraction at 100000 x

g for 1 hour yielded a supernatant fraction (postpolysomal fraction) and a pellet used as polysomes. Both were quickly frozen and stored at -80°C.

Analysis of RNA stability *in vitro*

Each subcellular fraction, obtained as described, was combined with total deproteinated RNA from SM muscle and incubated at 37°C. We used 60 µg of total RNA per reaction and a selected volume of subcellular fraction (see Figures). The concentrations of ions were adjusted so that the final reaction conditions were: 100 mM potasium acetate, 2 mM magnesium acetate, 2 mM dithiothreitol, 10 mM Tris-acetate, pH 7.6 (12). The degradation reactions with a certain subcellular fraction were carried out in a single tube, and 60 µl aliquots were removed at various time points. The reaction was terminated by transferring the aliquot to 500 µl of chilled guanidinium thiocianate solution. This solution was frozen and later processed as described by Chomczynsky and Sacchi (8). The RNA obtained was used for Northern blot analysis.

RESULTS AND DISCUSION

We found that AChE mRNA level remains the same during first 5h after denervation and that it abruptly falls after subsequent 13 hours. Much slower decrease rate was observed after this period of time (Fig. 1). Densitometric analyses of three independent Northern blots revealed that the longer transcript was more affected than the shorter one. The level of α-actin mRNA was also decreased in the denervated muscle and the rate of its disappearance was similar to that of AChE mRNA, suggesting that AChE mRNA is not specifically affected under such conditions. The mechanism underlying reduction in AChE mRNA level seems to be fully developed in less than one day after denervation, but needs more than 5 hours to start acting. Therefore, electromechanical activity due to the fibrillations observed occasionally in the denervated muscle could not be responsible for the observed decrease in AChE mRNA, since these fibrillations were reported to occur 3 days after denervation.
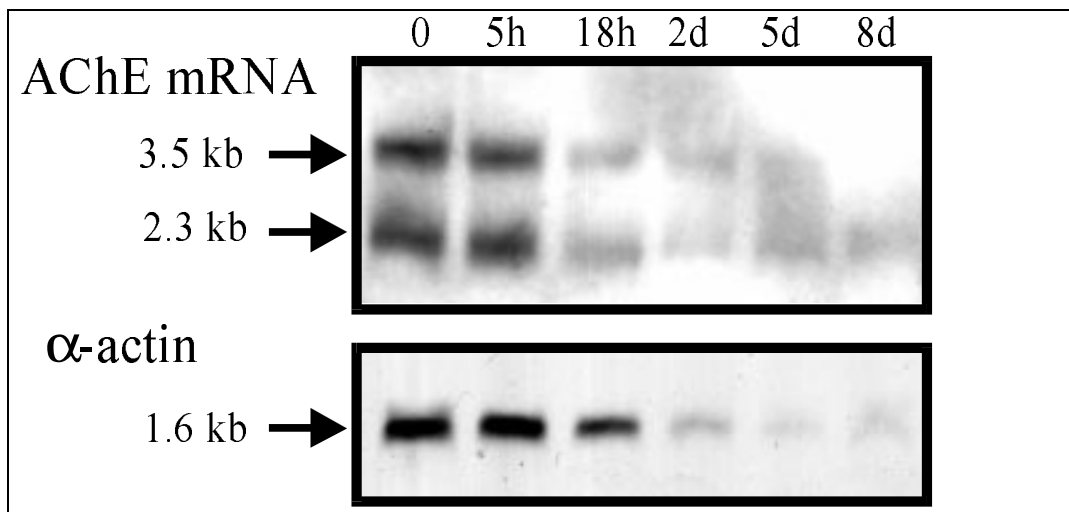
Figure 1: Northern blot analysis of AChE mRNA and α-actin mRNA from SM muscles, isolated at different times after denervation (h=hours; d=days). Equal amounts of total RNA (40 µg) were loaded (ethidium bromide staining).

Degradation of AChE mRNA was observed in *in vitro* degradation systems with all three subcellular fractions. The degradation rate was higher in postmitochondrial (Fig. 2) and postpolysomal fractions (Fig. 4) than in polysomal fraction (Fig. 3).

With a probe corresponding to nt. 370 - 706 in the second exon of AChE gene, three degradation products of approximately 1700, 1100 and 600 bases were detected (Fig. 2,3,4). Additional degradation products, not corresponding to our probe and therefore not detected, could not be excluded.

Longer transcript (3.5 kb) appeared more sensitive to degradation than the shorter one (2.3 kb). No difference in this sensitivity could be observed among subcellular fractions studied. Results from the higher degradation rate of the longer transcript leads to the conclusion that altered 3.5/2.3 ratio, observed after denervation, results from higher degradation rate of longer transcript and not its decreased transcription. Two transcripts differ in their 3'UTR, suggesting that this region, by some yet unknown mechanism mediates different stability. It has been reported that stability of many mRNA species is indeed controlled by the nucleotide sequences at their 3'UTR (13,14). In particular, the AU- rich region in this part of the molecule, demonstrated also in case of AChE mRNA (7), was found to destabilize mRNA (15).

Complete figure available in printed version

AChE mRNA

3.5 kb →

2.3 kb →

degradation
intermediate →

min   0   15   30   60

α-actin

1.6 kb →

min   0   15   30   60

Et-Br stained gel

28 S rRNA →

18 S rRNA →
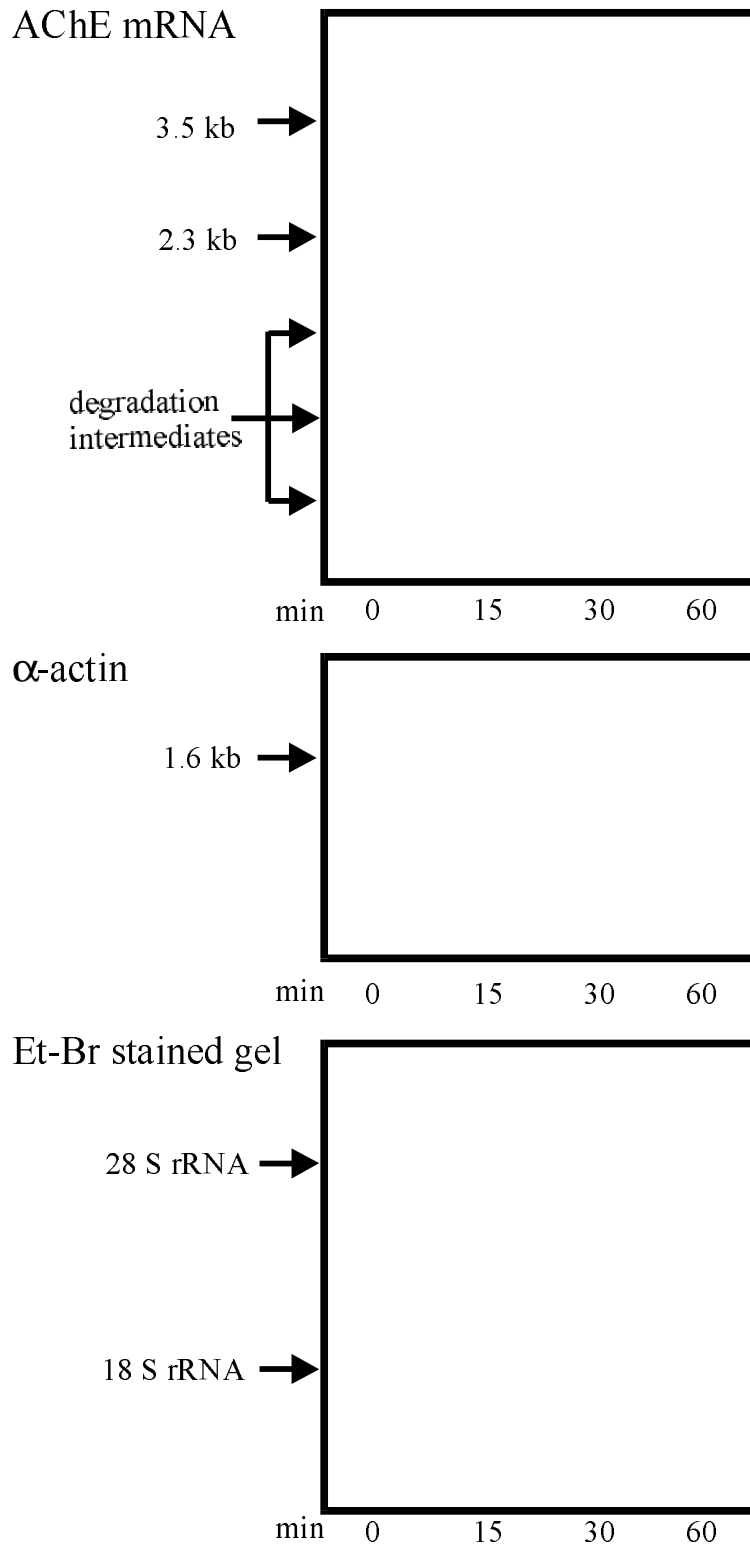
min   0   15   30   60
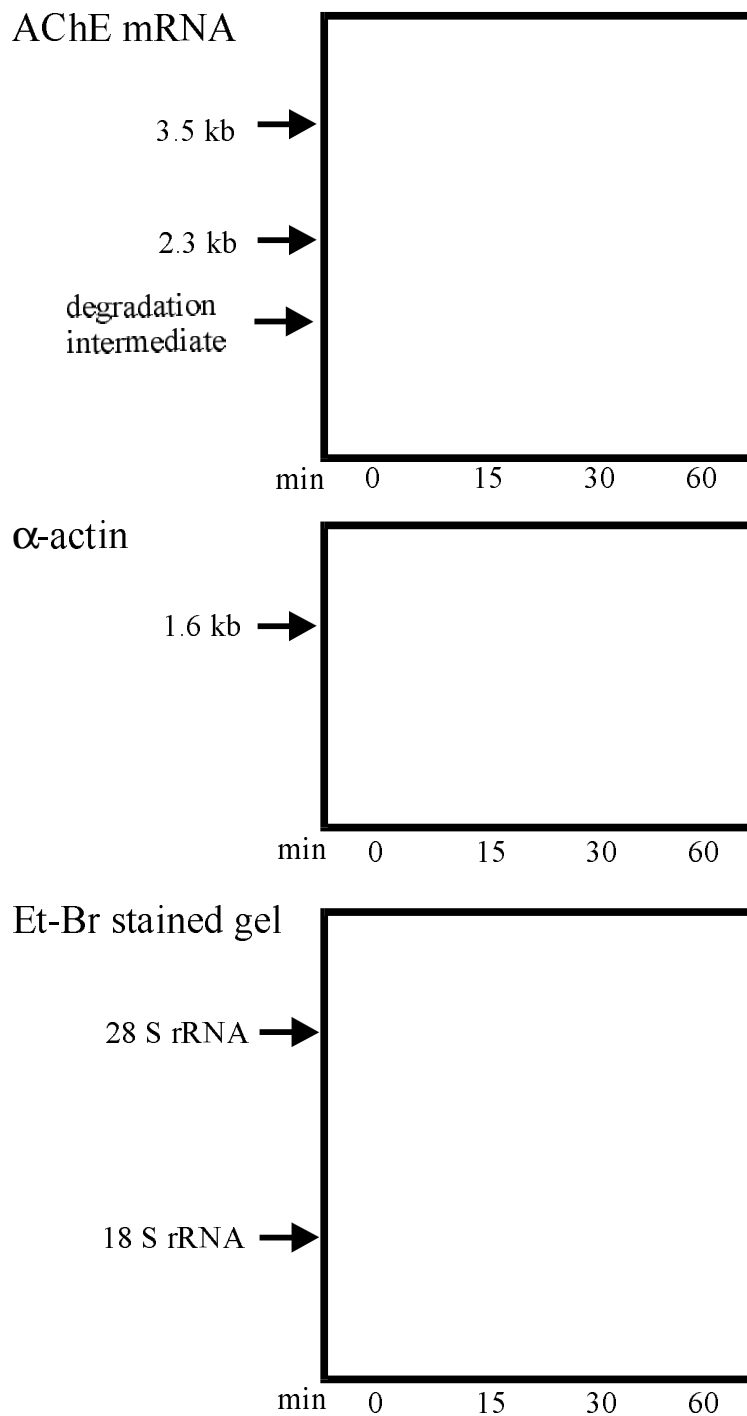
Figure 2: **Degradation with postmitochondrial fraction:** Northern blot analysis of AChE mRNA and α-actin mRNA remaining intact after selected time intervals in *in vitro* system with postmitochondrial fraction (per degradation reaction 1/200 of volume of postmitochondrial fraction obtained from one muscle). After prolonged washing following hybridization we detected 3 intermediates as in Fig.3 and 4.

Complete figure available in printed version

AChE mRNA

3.5 kb →

2.3 kb →

degradation intermediates →

min   0   30   60   130

α-actin

1.6 kb →

min   0   30   60   130

Et-Br stained gel

28 S rRNA →

18 S rRNA →

min   0   30   60   130
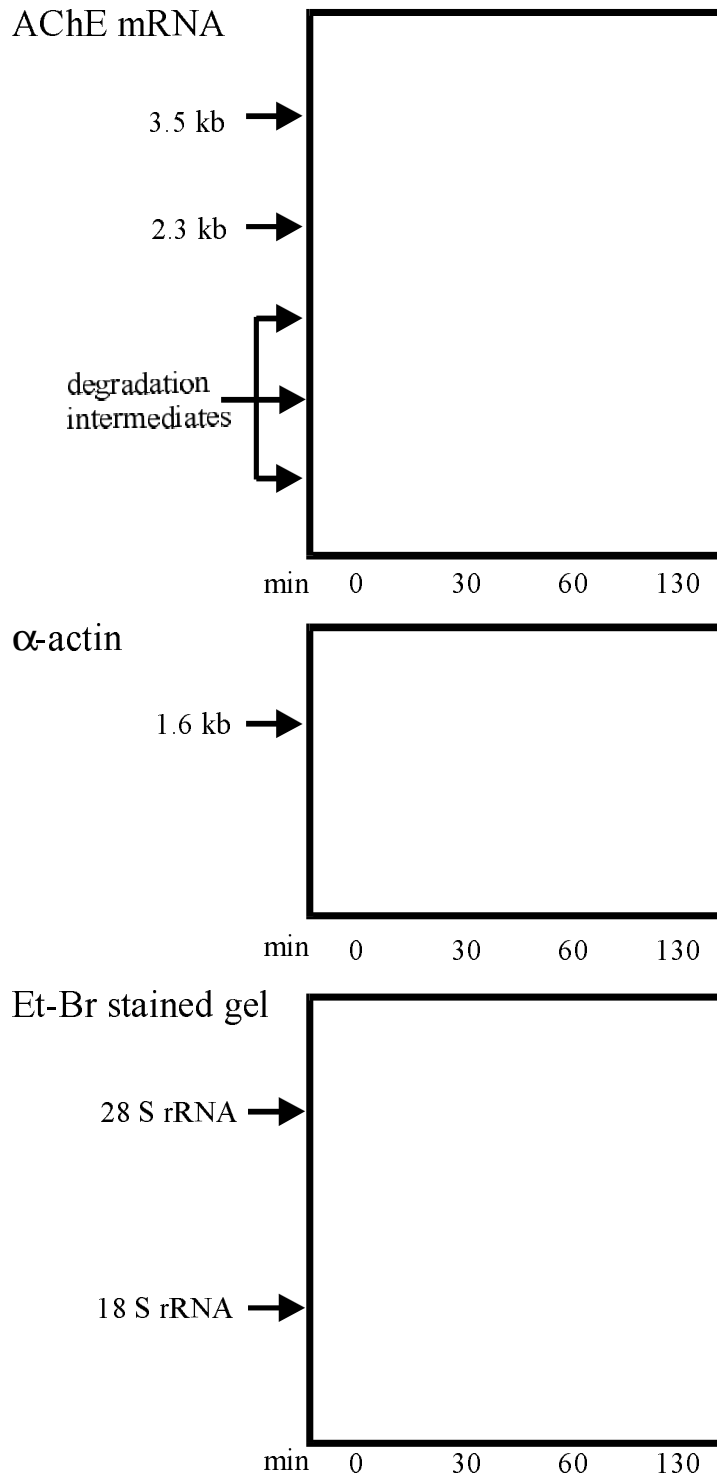
Figure 3: **Degradation with polysomal fraction:** Northern blot analysis of AChE mRNA and α-actin mRNA remaining intact after selected time intervals in *in vitro* system with polysomal fraction (per degradation reaction 1/200 of volume of polysomal fraction obtained from one SM muscle).

Complete figure available in printed version

AChE mRNA

3.5 kb →

2.3 kb →

→
degradation →
intermediates →

min   0   15   30   60

α-actin

1.6 kb →

min   0   15   30   60

Et-Br stained gel

28 S rRNA →

18 S rRNA →

min   0   15   30   60

Figure 4: **Degradation with postpolysomal fraction:** Northern blot analysis of AChE mRNA and α-actin mRNA remaining intact after selected time intervals in *in vitro* system with postpolysomal fraction (per degradation reaction 1/1000 of volume of postpolysomal fraction obtained from one muscle).

The experimental approach demonstrated here, could be applied to the studies of degradation capacities of the specific mRNAs in the adult skeletal muscles. Our preliminary results suggest, that postdenervational fall of AChE transcripts is at least partly due to increased degradation susceptibility of AChE mRNA.

REFERENCES

[1] X. Zhu, J.E. Yeadon, S.J. Burden, *Mol. Cell. Biol.* **1994**, 14, 8051-8062.
[2] B.J. Jasmin, R.K. Lee, R.l. Rotundo, *Neuron* **1993**, 11, 467-477.
[3] B. Črešnar, N. Črne-Finderle, K. Breskvar, J. Sketelj, *J. Neurosci. Res.* **1994**, 38, 294-299.
[4] M. Brank, K. Zajc Kreft, S. Kreft, R. Komel, Z. Grubič, *Eur. J. Biochem.* **1998**, 251, 374-381.
[5] N.S. Schimizu, S. Kamel-Reid, R. Zak, *Dev. Biol.* **1988**, 128, 435-440.
[6] Z. Grubič, R. Komel, W.F. Walker, A.F. Miranda, *Neuron* **1995**, 14, 317-327.
[7] M.E. Fuentes, P. Taylor, *Neuron* **1993**, 10, 679-687.
[8] P. Chomczynsky, N. Sacchi, *Anal.Biochem.* **1987**, 162, 156-159.
[9] D.B. Masters, C.T. Griggis, C.B. Berde, *Biotechniques* **1992**, 12, 902-908.
[10] S.C. Chen, V.R. Young, *Biochem. J.* **1968**, 106, 61-67.
[11] S.M. Heywood, R.M. Dowben, A. Rich, *Proc.Nat. Acad. Sci.Wash.* **1967**, 57, 1002-1011.
[12] G. Brewer, J. Ross, *Methods in Enzymology* **1990**, 181, 202-210.
[13] S. Miyamoto, J.A. Chiorini, E. Urcelay, B. Safer, *Biochem. J.* **1996**, 315, 791-801.
[14] M.C. d'Hooghe, S. Galiegue-Zouitina, D. Szymiczek, D. Lantoine, S. Quief, M.-H.. Loucheux-Lefebvre, J.-P. Kerckaert, *Leukemia* **1993**, 7, 1777-1787.
[15] G. Shaw, Kamen R., *Cell* **1986**, 46, 659-667.

POVZETEK

Tako elektromehanska aktivnost kot tudi denervacija povzročita padec ravni acetilholinesterazne (AChE) mRNA v hitri podganji skeletni mišici. Povečana hitrost razgradnje je eden od možnih mehanizmov za zmanjšanje ravni AChE mRNA v denervirani mišici. Da bi to preverili, smo iz podganje m. SM izolirali deproteinizirano RNA in jo izpostavili delovanju mišičnih subceličnih frakcij, pripravljenih iz kontralateralne m. SM. Po določenih časovnih intervalih, smo z neradioaktivno Northern blot analizo določili količino nerazgrajene AChE mRNA.

Vsebnost AChE mRNA v mišici ostane nespremenjena tekom prvih 5 ur po denervaciji, potem pa strmo pade v naslednjih 13 urah. Nadaljnje padanje je veliko počasnejše. Daljši transkript (3,5 kb) je manj stabilen kot krajši (2,3 kb).V denervirani mišici se je znižala tudi vsebnost α-aktinske mRNA, in to s podobno hitrostjo kot AChE mRNA, kar nakazuje, da AChE mRNA v takih razmerah ni prizadeta specifično. AChE mRNA se je razgrajevala z vsemi testiranimi subceličnimi frakcijami. Postmitohondrijska in postpolisomalna frakcija sta imeli večjo kapaciteto razgradnje kot polisomalna frakcija.

Ugotovili smo, da je uporabljen pristop primeren za proučevanje kapacitete razgradnje specifičnih mRNA v odrasli skeletni mišici. Naši preliminarni rezultati kažejo, da je za padec AChE mRNA po denervaciji vsaj deloma odgovorna povečana nagnjenost k razgradnji te molekule.

ENZYMES WITH A LOW MOLECULAR WEIGHT

Michael Mattey[1], Davina Simoes[2], Angela Brown[1] and Xiaolian Fan[1]

[1]Department of Bioscience and Biotechnology, University of Strathclyde, Todd Centre, 31, Taylor Street, Glasgow, G4 0NR, Scotland.
[2]University of Sunderland, School of Health Sciences, Chester Road, Sunderland SR1 35D, UK.

Abstract.

Two esterase enzymes have been isolated, one from *Candida lipolytica* and one from *Bacillus stearothermophilus*, which are characterised by an unusually small molecular weight. The *Candida* enzyme is 5.7 kDa, with 56 amino acid residues and the *Bacillus* enzyme is 1.57 kDa, with only 17 residues (1).

In both cases the catalytic activity appears to depend on a bound metal ion, as shown by dialysis against chelating agents, ion replacement and inhibition by metal complexing agents. Specific activities are similar to reported esterase activities.

The *Candida* esterase has a temperature optimum of 28^0 , as might be expected from a mesophilic organism, but it has a half-life of 2 hours at 50^0 . The esterase from *B.stearothermophilus* is thermophilic, but whereas the optimum growth temperature is 55^0 the enzyme optimum is about 120^0.

Both enzymes exhibit some substrate specificity. The *Bacillus* enzyme has no particular specificity towards the chain length of the substrate, but shows a marked activity towards the 2-position of triglycerides. The *Candida* enzyme shows both chain length specificity (optimum at butyl esters), as well as specificity towards the 1-position.

Introduction

The size of enzymes has been the subject of debate for many years; the question is often posed in the form "Why are enzymes large?" The text-book answer is usually given in terms of bond energies; biological systems operate with two broad classes of chemical bond, firstly "weak" bonds, such as van der Waals Forces (1 kcal/mole), hydrogen bonds (3 - 7 kcal/mole), ionic bonds (5 kcal/mole) and hydrophobic

interactions (-1 to -3 kcal/mole) and secondly "strong" covalent bonds (~20 kcal/mole) .

The weak bonds are responsible for virtually all the higher orders of biochemical structure, as well as most biochemical interactions that demand a high degree of stereochemical specificity. As these bonds are no more than an order of magnitude greater than the thermal energy of the environment such weak interactions are readily disrupted by the kinetic energy present in living systems. Covalent bonds, on the other hand, are not readily broken at physiological temperatures, enzyme - catalysed reactions are required for such bonds to be rapidly made and ruptured. The rate at which an enzyme catalyses a chemical reaction is probably dependent on the rapidity of a reversible conformational change induced by interaction with a substrate; such conformational changes involve breaking and forming many weak bonds throughout the protein, with the result that a covalent bond is cleaved.

Because weak bonds can be broken by the kinetic energy released during the binding of substrates and modulators to enzymes so they can be broken by the addition of kinetic energy in, for example, the increase in environmental temperature. These changes may reduce the catalytic function, or the different tertiary and quaternary structures at the new temperature might have a enhanced functional properties. Thus size, function and thermostability are closely linked in proteins.

As the enzyme molecule becomes smaller the number of hydrogen bonds etc. falls, so that less catalytic activity but more stability might be expected.

The purpose of this paper is to establish that the size range of naturally occurring proteins with catalytic activity is greater than hitherto thought, secondly that such enzymes exhibit thermal properties that are both consistent with their size and are adapted to the rigorous extracellular environment, and thirdly that their mechanism of action results in substrate and product specificity.

There have been a few reports in the literature in which an enzyme activity has been attributed to proteins with a molecular weight of less than 10 kDa ("microenzymes")(2). A lipase from bovine milk slime with an apparent molecular weight of 7 kDa was reported by Chandan & Shahani (3). The molecular weight was

determined by sedimentation velocity and osmotic pressure methods, and the activity exhibited a pH optimum of 9.2 and 37^0.

A rennin from an unidentified thermophilic actinomycete, isolated from soil near Beer Sheva, was found to have a molecular weight of 10.5 kDa, based on analytical ultra-centrifugation and SDS electrophoresis (4). The amino acid composition was determined and the protein was found to have 78 residues, of which 9 were proline, giving a molecular weight of 9.7 kDa. The temperature optimum was 75^0, and it required calcium ions for activity. Limited proteolytic activity against insulin was noted.

Another small proteolytic enzyme was reported by Steele et al. (5) isolated from a novel spiral bacterium, *Kurthia spiroforme*. This gram-positive bacterium grew at neutral pH in a thermal spring, but exhibited a wide range of growth temperatures and pH values, ranging from 4^0 to 47^0 and a pH range from 7 to 11.5 with an optimum of 30^0 and pH 10.5. The extracellular protease was alkaline-stable and had an optimum temperature of 60^0 and optimum pH of 11.

An amylase from *Bacillus caldolyticus* (6) was shown to have active subunits of less than 10 Kda, which associate in the presence of calcium ions to give the classic thermophilic amylase active at 70^0. The subunits of the thermophilic amylase exist when calcium is absent or low in concentration and are not thermophilic but are still thermostable, showing activity up to 40^0, but are stable up to 60^0, as shown by the recovery of activity when the temperature is reduced, or when calcium is added at a higher temperature.

We have described two extracellular peptides with esterase activity, one produced by a strain of *Candida lipolytica* (CMI 92,743) (7) and one from *Bacillus stearothermophilus* (1). The esterase from the *Candida* species had a molecular weight of 5 kDa ± 500 as determined by both Sephadex G-100 gel filtration and SDS-polyacrylamide electrophoresis. The enzyme contained 56 amino acid residues, 13 of which were proline, giving a molecular weight of 5717 kDa. The *Bacillus* esterase was much smaller, with 15 amino acid residues, none of which was proline, giving a molecular weight of 1556 kDa. The composition of the two esterases is shown in Table 1.

One feature of the Candida esterase is the high percentage of proline, a feature also noted with the rennin from a thermophilic actinomycete, although at 23.7 mole%

Amino acid	*Candida*	*Bacillus*
Ala	5	1
Asp	3	3
Arg	1	1
Cys	1	-
Glu	8	1
Gly	8	2
His	3	2
Ileu	1	-
Leu	3	-
Lys	1	-
Pro	13	-
Phe	1	-
Ser	1	4
Thr	2	1
Tyr	1	-
Val	4	-
Total	56	15

Table 1   Amino acid composition of the extracellular esterases from *Candida lipolytica* and *Bacillus stearothermophilus*. Amino acid analysis was carried out on an Applied Biosystems 420H Amino acid Analyser using phenylthiocarbamyl derivitisation. Calibration used an internal standard of norleucine.

the esterase has twice the proline content.

Proline has been associated with increased protein thermostability (8, 9) on the basis of the different thermostability of five *Bacillus* oligo-1,6- glucosidases. Comparisons were made of aminoacid composition and structural parameters and from the analysis, in conjunction with the strong site specificity of proline residues for β-turns (10, 11, 12) it was proposed that enhanced stability could be gained by increasing the frequency of proline occurrence at β-turns and the total number of hydrophobic residues (8) This appeared to be given support by Matthews *et al* (13) where the thermostability of bacteriophage lysozyme was increased by replacing alanine with

proline at position 82 of a β-turn so as to decrease the backbone entropy of unfolding. Other results have correlated increased proline with increase thermostability with different enzymes (14, 15, 16) The correlation with both pullulanases and oligo-1.6-glucosidases between proline percentage and T_m (the temperature at which the enzyme was half inactivated in 10 minutes at pH6.8) was linear between 3% and 9% proline and 45^0 to 98^0. The *Candida* esterase does not fall on that line, although its T_m, at 70^0 is higher than expected for a mesophilic organism. The rennin (3) similarly does not coincide with the *Bacillus* data, but its stability (T_m 75 ^{0}) is greater than the optimum growth temperature (52 ^{0}).

Mode of Action:

The two esterases show different behaviour towards a range of inhibitors (Table 2)

Addition	*Candida lipolytica*	*Bacillus stearothermophilus*
None	100	100
NaN$_3$	35	90
KCN	29	85
p-chloro-mercuribenzoate	29	79
CuSO$_4$	100	0
FeSO$_4$	100	80
1,10 phenanthroline	20	113
EDTA	30	89

Table 2. The effect of inhibitors on the activity of the esterases from *Candida lipolytica* and *Bacillus stearothermophilus*.The additions were made at 5mM.

The *Candida* esterase shows a pattern of inhibition consistent with iron chelation, with the cytochrome oxidase inhibitor azide, p-chloro-mercuribenzoate and 1,10 phenanthroline being potent inhibitors, and general metal chelators such as EDTA

also effective. The *Bacillus* esterase shows slight inhibition with some of these inhibitors, but with 1,10 phenanthroline shows slight activation. The most striking inhibitor of the *Bacillus* enzyme was copper sulphate which had an effect considerably greater than other inorganic salts, for example ferrous sulphate. Inorganic salts are known to weaken electrostatic forces within the protein molecule (17), but the complete inhibition could not be attributed to this. Cu^{2+} is known to form complexes with amino and amide groups, as in the classic Biuret test for proteins.

If the enzymes are dialysed against EDTA then a loss of activity is observed in both cases (Fig 1). The rate of activity loss is similar in both cases although the temperature at which the *Candida* enzyme (28^0) and the *Bacillus* enzyme (70^0) were treated was different.
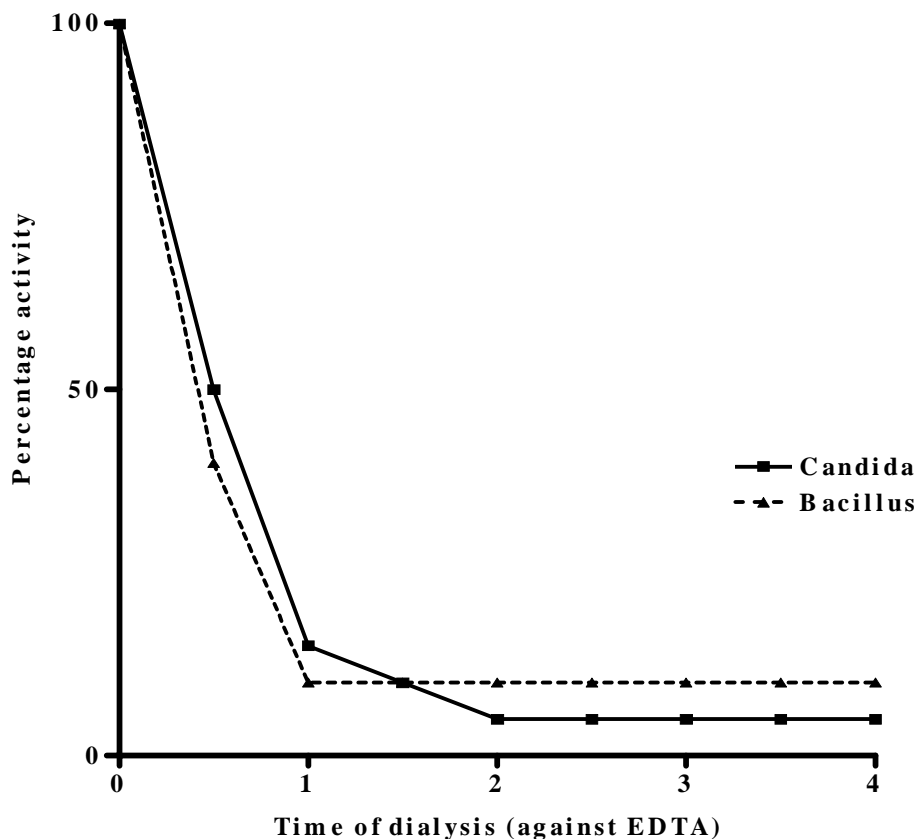
Figure 1. The effect of dialysis on esterase activity. The enzyme preparations were dialysed against 1mM EDTA at 70^0 in the case of *Bacillus* and 28^0 in the case of *Candida* for four hours. The results are expressed as a percentage of the starting

activity as determined by fluorometric assay using fluorescein dibutyrate at $10^{-7}M$ as substrate.

Attempts to restore the activity were made with a number of cations, added at 5 mM to the dialysed solution. For the esterase from *Candida lipolytica* 90% of the original activity was restored by ferric ions, other ions such as zinc, ferrous ions, nickel and copper restored about 20%, while monovalent ions, calcium and magnesium either did not have any effect or further reduced the residual activity.

For the *Bacillus* esterase the only ion found with any significant effect was Fe^{3+}, but only 40% activity was restored. When dialysis was carried out against water instead of EDTA the activity was lost more slowly, but 80% of the activity could be restored by mixing the dialysed enzyme with the dialysis solution, unlike ferric ions where again 40% activity was restored.

Effect of pH.

The two esterases showed quite distinct pH profiles, the *Candida* esterase showed a flat profile until pH values below 2, while the *Bacillus* enzyme showed an optimum at pH 9.0 which is above the growth optimum for the organism (pH 6 to 8).
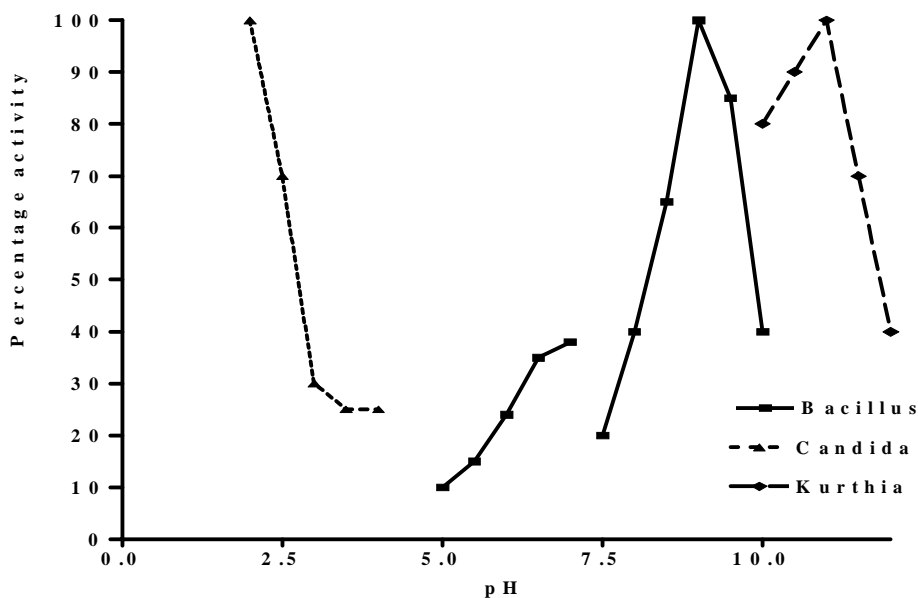
Figure 2.   The effect of pH on esterase activity. In the range 2 to 4 acetate buffer was used, phosphate buffer from 5 to 7.5 and tris-HCl from 7.5 to 11. All buffer concentrations were 0.1M; activity was determined using flurorescein dibutyrate with a blank control at the same pH and buffer condition.

The enzymes were stable to a range of pH values from 5 to 10 for several hours.

Effect of Temperature.

The effect of temperature on esterase activity is shown in Fig. 3. The two esterases show very different temperature optima as would be expected from a mesophilic and a thermophilic organism. In the case of the mesophilic enzyme the growth temperature and the enzyme optimum are the same at 28 ^{0}, but in the case of *B. stearothermophilus* the growth optimum is 55 ^{0} , but the temperature optimum is 120^0.
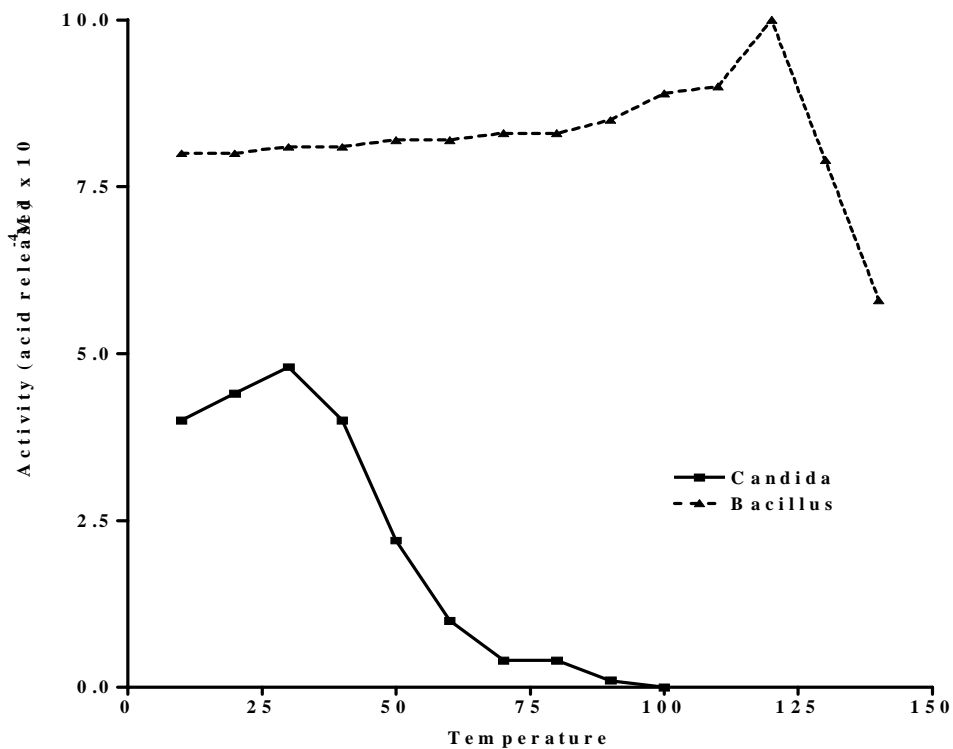
Figure 3. The effect of temperature on the activity of the esterases from *C. lipolytica* and *B. stearothermophilus*.

For the *Candida* esterase the optimum temperature was determined at pH 6.0 using a flurimetric assay, the sample was equilibrated for one minute before activity

measurements were made. The optimum for the *Bacillus* enzyme was determined by hydrolysis of tributyrin in a sealed tube for two hours, followed by titration of the acid liberated, using a control without enzyme to correct for thermal hydrolysis at elevated temperatures.

The optimum temperature of 120^0 is exceptionally high,and compares with that of the extreme thermophile *Sulpholobus solfataricus* (18) where 5'methylthio-adenosine-phosphorylase had an optimum of 120^0 and *Pyrococcus furiosus* protease at 115^0.

The Arrhenius plot (Fig 4.) was discontinuous and concave upwards, a feature unusual in enzyme-catalysed reactions, although at temperatures above 120^0 rapid inactivation occurs .
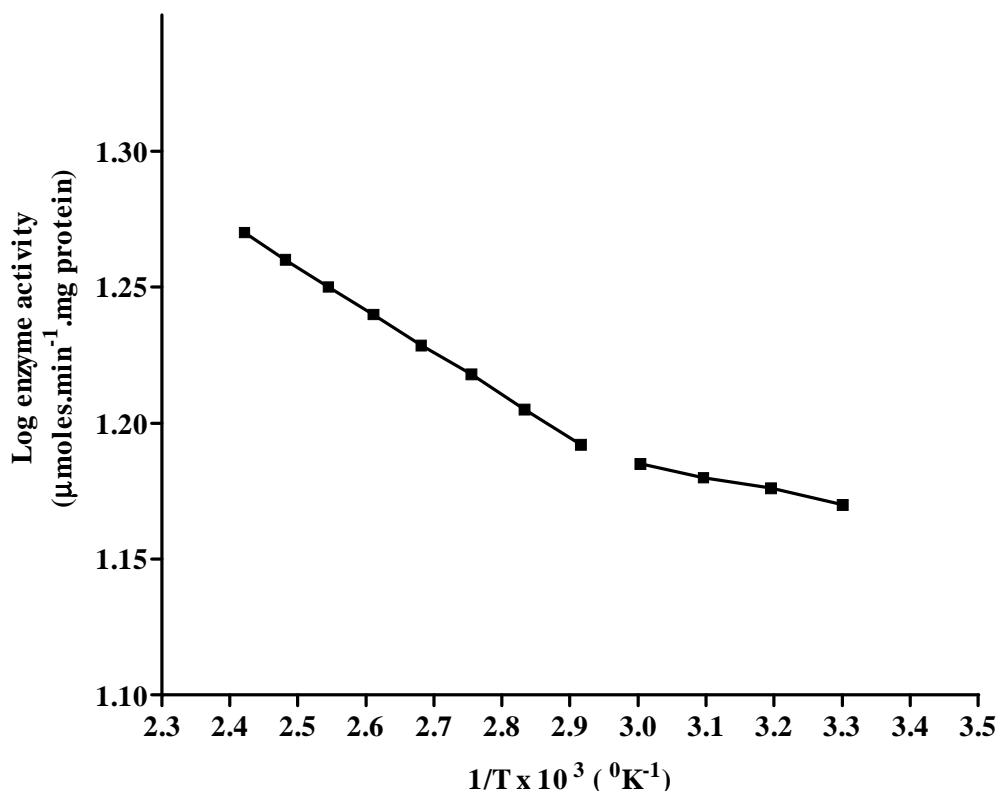
Figure 4. Arrhenius plot for *B. stearothermophilus* esterase.

Such plots are observed when a reaction system consists of two parallel reactions with different efficiencies, where the activation energies are such that one dominates at a higher temperature and the other at a lower temperature (19).

The energy of activation (E_a) from 30^0 to 70^0 was 355 cal mole^{-1} and from 80^0 to 120^0 was 948 cal mole $^{-1}$.

The thermostability of these small esterases is high, although the thermophilic enzyme is more stable, as might be expected

Figure 5 shows the stability over a 100 hour period, with the *Candida* esterase having a half life of 2 hours at 50^0, very stable for a mesophilic organism, and the *Bacillus* esterase retained 95% of its activity at 70^0 at 100 hours. Even at 90^0 the enzyme had a half life of 12 hours.

Increased thermostability is the sort of property that might be useful in the extracellular environment. Robust enzymes which persist will maximise the substrate returns on the investment in extracellular proteins. From the economic viewpoint a small thermostable extracellular enzyme is efficient providing its activity is similar to that of large enzymes.
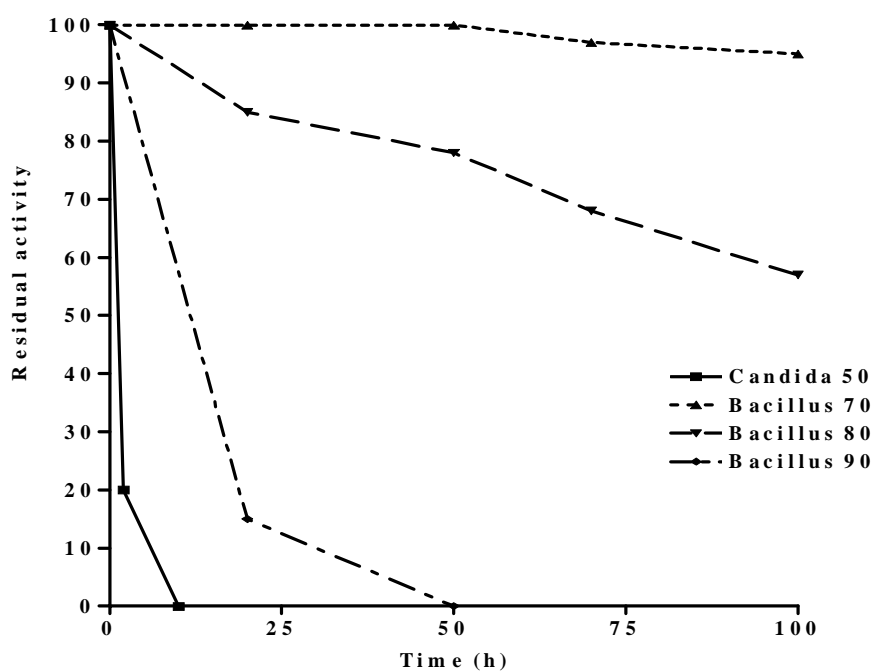
Figure 5 Thermostability of the esterases.

Specificity.

The two esterases differ both in their specificity towards triglycerides and towards the chain length of the fatty acid chains.

Figure 5 shows that the *Candida* esterase shows a preference for shorter chain lengths, with a peak at butyric although it is still effective against palmitic acid side chains with about 20% of the relative activity shown towards butyrate esters. This preference is seen both with fluorescein diesters and glycerol esters.

Products of the hydrolysis of triglycerides were separated by HPLC on a Lichrosorb Si60 column with a mass detector (Sedex 55) using a mobile phase of toluene-hexane (1:1) (solvent A) and toluene-ethyl acetate (3:1) plus 1.2% formic acid (solvent B). A gradient of 1 - 50% B over 10 minutes and 50 - 100% B from 10 to 15 minutes, with 100% B from 15 to 40 minutes was used.

The *Candida* esterase showed a peak of 2,3 diglyceride in the early stages of hydrolysis , with 1,3 diglyceride in small quantities appearing after all triglyceride was hydrolysed.

The *Bacillus* esterase on the other hand showed 1, 3 diglyceride only.

In both cases the diglyceride was slowly hydrolysed further to monoglyceride and butryric acid .
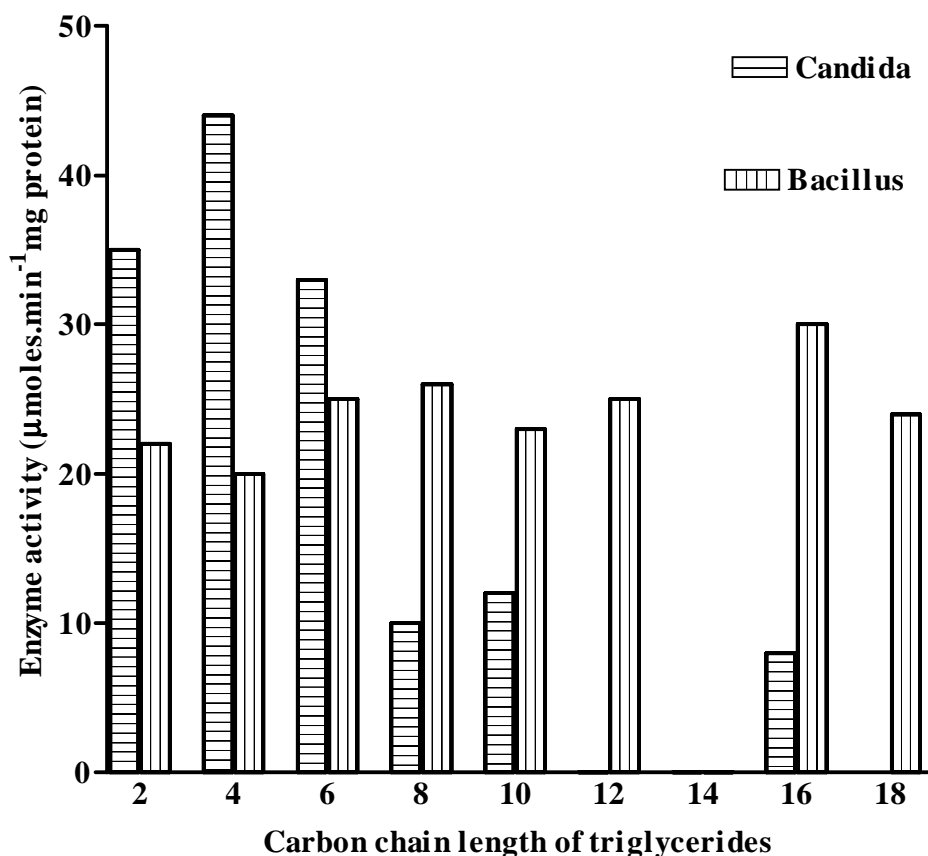
Figure 6 Esterase specificity

Conclusions.

It is apparent that the lower limit on the size of naturally occurring enzymes is well below 10 kDa, the *Bacillus* esterase described here is only 1.57 kDa and is little more than a peptide.

The range of activities so far seen is limited to simple hydrolysis, which is not unexpected given the small size; the scope for the binding of substrates with recognition between similar groups must be limited. Esterases, lipases and proteases have been described, but so far not carbohydrate or nucleic acid degrading activities.

Despite the limited substrate binding possibilities both esterases show specificity towards triglycerides, and these enzymes, with their considerable thermostability and reasonable activity, are of interest in industrial processes. Stability can be further enhanced by immobilisation which retains activity.

It is not known how widespread such enzymes are but preliminary screens show many thermophiles have enzyme activities in the micorenzyme size range.

It is noteworthy that the two esterases described appear to have different mechanisms of activity. The larger esterase from *C.lipolytica* has an ferric iron active site, where the metal catalyses an acid hydrolysis of the substrate. This is demonstrated by the pH dependence and the effect of dialysis.

The *Bacillus* esterase appears to use the metal ion to maintain the conformation of the peptide, but the pH optimum is not consistent with metal catalysis, nor is the effect of dialysis consistent with an active site metal ion, although the effect of chelators such as EDTA is consistent with the involvement of metal ions in an important functional role.

The active site sequences for a number of esterases show great similarity with the sequence Gly-Glu-Ser*-Ala-Gly being conserved and Glu/Asp -Ser being very common in the next two positions. The amino acid composition of the microenzyme from B stearothermophilus contains the seven amino acids found in the active site

sequence although the sequence is not known. The peptide is N terminal blocked, possibly by a formyl group. If this hypothesis is substantiated the mechanism whereby a confomrational change in such a small protein could cleave the ester bond will be of interest. The possible number of hydrogen bonds etc. is small but the role of metal ions in stabilisation may be significant.

References

[1]   D de C. M. Simoes, D. McNeill, B. Kristiansen, M. Mattey, *Biotech. Lett*. **1995**, 17, 9, 953 - 958.

[2]   R. U. Schenk, J. Bjorksten, *Finska Kemists. Medd.* **1973**, 82, 26 - 46.

[3]   R. C. Chandan, K. M. Shahani, *J. Dairy Sci.*   **1963**, 46, 275 - 283.

[4]   S. H. Laxer, A. Pinsky, B. Bartoov, *Biotech. Bioeng.* **1981**, 23, 2483 - 2492.

[5]   D. B. Steele, M. J. Fiske, B. P. Steele, V. C. Kelley,   *Enz. Microb. Tech.* **1992** , 14, 5, 358 - 360

[6]   W. Heinen, A. M. Lauwere,   *Proc. Int. Symp. Enzymes and Proteins from Thermophilic Microorganisms Zurich* **1975** 78 - 89 (Birkauser Verlag, Basel und Stuttgart)

[7]   G. Adoga, M. Mattey, *FEMS Microbiol. Lett*. **1979**, 6, 61 - 63.

[8]   Y. Susuki, K. Oishi, H. Nakano, T. Nagayama,   *Appl. Microbiol. Biotechnol*., **1987**, 26, 546 - 551.

[9]   Y. Susuki, *Proc. Jpn. Acad. Ser. B*. **1977**,   65, 146 - 148.

[10]   P. Y. Chou, G. D. Fasman, *J. Mol.Biol.* **1977**,   115, 135 - 175.

[11]   P.N. Lewis, F.A. Momany, H.A. Scheraga,   *Biochem. Biophys. Acta* **1973** , 303, 211 - 229.

[12]   M. Levitt, *Biochemistry* **1978** , 17,   4277 - 4285.

[13]   B. W. Mathews, H. Nicholson, W. J. Becktel,   *Proc. Natl. Acad. Sci USA* **1987**,   84, 6663 - 6667.

[14]   H. S. Tesfay, R. E. Amelunxen, I. D. Goldberg, *Gene* **1989**, 82 , 237 - 248.

[15]   U. Karst, H. Schutte, H. Baydoun, H. Tsai, *J.Gen Microbiol.* **1989**, 135, 1305 - 1313.

[16]   Y. Suzuki, K. Hatagaki, H. Oda,   *Appl. Microbiol. Biotechno.l* **1991**, 34, 707 - 714.

[17]   M. P. Brosnan, C. T. Kelly, M. W. Forgaty, *Eur. J. Biochem.* **1992**, 203, 225 - 231.

[18]   G. Cacciapuoti, M. Porcelli, C. Bertoldo, M. Rosa, V. Zappia, *J. Biol. Chem.* **1994** , 269, 24762 - 24769.

[19]   M. H. Han, *J. Theor. Biol.* **1972**,   35 , 543 - 568.

ALTERED GENE EXPRESSION IN THE FOETAL RAT TESTIS FOLLOWING THE OESTROGEN EXPOSURE

*Gregor Majdic, #Philippa TK Saunders
*Faculty of veterinary medicine, Gerbiceva 60, 1000 Ljubljana, Slovenia
#MRC - Reproductive Biology Unit, 37 Chalmers street, Edinburgh EH3 9EW, Scotland

Abstract

Several reports in recent years have shown evidence for increasing incidence of male reproductive problems as cryptorchidism, hypospadias and testicular cancer. In addition, several reports have published evidence for decrease in sperm counts in many western countries, which might be as high as 50% in the last 50 years. One hypothesis have linked this problems to increased exposure to oestrogenic chemicals during foetal development. Aim of our studies was to establish whether environmental oestrogens could affect testicular development in rats. Time-mated pregnant rats were treated subcutaneously with either diethylstilbestrol (DES, potent synthetic oestrogen), octylphenol (OP, environmental oestrogen) or oil alone as control on days 11.5 and 15.5 p.c. Animals were sacrificed on day 17.5 p.c. Testes were dissected from their foetuses and either fixed in Bouin's solution, used for RNA extraction or used directly for measuring P450c17 enzyme activity. Lower activity and expression of steroidogenic enzyme P450c17 has been detected in the testes from foetuses whose mothers received either DES or OP. In addition, reduced expression of recently discovered transcription factor Steroidogenic factor-1 (SF-1) has been detected.

Introduction

Sexual differentiation of the male is not just the process of establishing the normal male phenotype but it is also a period when the foundations for fertility in adulthood are laid down. Sexual differentiation and especially development of the male gonads and male phenotype are hormonally regulated and therefore any disturbances of the hormone action in this sensitive period could have far reaching consequences. Recent reports about falling sperm counts and increasing incidence of testicular cancer and other

disorders of development of the male reproductive tract have been hypothetically linked to increased exposure to environmental chemicals which are either oestrogenic or anti-androgenic hormonal mimics. In the present article, the evidence for importance of foetal/neonatal period for functioning of adult reproductive system and some date about the effects of oestrogenic chemicals will be discussed.

Development of the testis and male phenotype

The first morphological event in the development of the testis is appearance of Sertoli cells within the testicular cords (1). Thereafter, these cells control and co-ordinate all the processes relating to testicular development and masculinisation. Sertoli cells secrete antimullerian hormone (AMH), responsible for regression of female reproductive ducts in the male foetus. Via the unknown factors, the Sertoli cells also regulate the regulation and multiplication of early germ cells and also the differentiation and function of Leydig cells, which produce testosterone, hormone responsible for the masculinisation of the whole foetus (1). Simultaneously with their differentiation, Sertoli cells start to proliferate and this continues for the rest of the foetal life and short period unto postnatal life. However, soon after birth, in rats around day 18 p.n. while in humans it is thought to continue at a slow rate until beginning of the puberty, the proliferation of Sertoli cells cease and their numbers remain constant for the rest of the life (2). Therefore the increase of Sertoli cells in the foetal/neonatal period is crucial as the number of Sertoli cells determines the final adult testis size and the capacity for sperm production. This has been clearly shown in studies in animals, when the window of Sertoli cells proliferation has been changed therefore increasing or decreasing their numbers. The regulation of Sertoli cells multiplication is not known yet, however, several hormones are thought to be involved in these processes. This include FSH, which stimulates proliferation of Sertoli cells and thyroid hormones T3 and T4, which seems to be involved in determining the cessation of Sertoli cells proliferation. Experiments in rats have shown that hypothyroidism will prolong the time of Sertoli cells proliferation and therefore result in higher number of Sertoli cells, bigger testis and higher sperm output in adult life. In contrast, hyperthyroidism cause premature cease of Sertoli cells proliferation and finally results in lower testis size and lower sperm production (2, 3, 4).

The proper function of Leydig cells is equally important for normal functioning of reproductive system. Testosterone, main product of the Leydig cells is main factor responsible for masculinisation of the foetus and any interference with its action will have deleterious effects in the male foetus (1). The importance of testosterone is clearly shown in pathological condition called androgen insensitivity syndrome. In this syndrome, the testosterone cannot act due to a mutation in the gene encoding androgen receptor. Subsequently, such foetuses develop female phenotype (or in some cases various degrees of intersex phenotype), despite the presence of the testosterone producing testis in the abdominal cavity (5). Descensus of the testis in the neonatal life into the scrotum is also thought to be regulated by testosterone and cryptorhidism is thought to be a result of improper action of testosterone in the time when descensus should occur (1).

Male reproductive problems

In recent years, several reports have been published about increase in male reproductive problems in western world. These include increased incidence of developmental defects cryptorhidism and hypospadias and increase in incidence of testicular cancer (6). In addition, several reports have shown decline in average sperm counts in western males in last 50 years, which might be as high as 50% (6, 7). While the data about lower sperm counts are still highly debated and will be difficult to prove, the data about increased incidence of cryptorhidism, hypospadias and testicular cancer is most likely to be real. All three conditions are unlikely to be undetected and in several countries, including Slovenia, there exist reliable medial records about their incidence (6).

The cause of these problems is not yet known. Similar problems have been observed in the offspring from mothers, who were treated with potent synthetic oestrogen diethylstilbestrol (DES) during their pregnancies. Namely, in 1950 and 60's, several millions women in Europe and USA were treated with DES as a prevention of miscarriage. Unfortunately, later studies have shown that DES had a very deleterious effects on the development of reproductive system of their offspring. In male offspring of these mothers, very high incidence of cryptorhidism, hypospadias, testicular cancer as well as smaller testis and lower sperm production were detected (8). Similarities between these problems have suggested potential link. Sharpe and Skakkebaek (9) have

reviewed the possible sources of oestrogenic exposure and have suggested that changes in diet, increases in body fat and obesity, together with increases in exposure to environmental pollutants with oestrogenic activity could all contribute to increased exposure to oestrogenic chemicals in present time. The diet of the individuals in many developed countries has radically changed over the last 50 years with an increase in the consumption of milk and dairy products. These may contain oestrogens due to intensive farming with milking occurring during pregnancy. A large increase in use of soya (soya is very rich in phytooestrogens) could also have contributed to an increased exposure to oestrogens in every day life. Furthermore, it is likely that we are all exposed to many oestrogens or chemicals mimicking oestrogen action due to environmental pollution. It has been speculated that usage of contraceptive pills containing synthetic oestrogens, the use of anabolic oestrogens in animal farming and widespread use of chemical agents that exhibit oestrogenic activity by industry may all have contributed to an increasing exposure to oestrogens (9).

Environmental oestrogens

This term is applied to phytoestrogens and man-made chemicals which are released into environment and which have oestrogenic activity either in vivo or in vitro (10). It is known for some time that some PCB isomers and DDT and its metabolites have such activity. However, more worrying, similar action has been shown for several other chemicals including alkylphenols, bisphenol-A and phtalates. The majority of these chemicals have a different chemical structure to endogenous oestrogens and at present it is not therefore possible to assess whether a compound is likely to have oestrogenic activity based on the knowledge of its chemical structure (10). In many instances the oestrogenic activity of these chemicals was discovered accidentally. For example, the observation that oestrogenic substances were released from laboratory plastic ware led to the identification of alkylphenols, in particularly nonylphenol and bisphenol-A as a chemicals with oestrogenic activity (11, 12). In addition, oestrogenic activity has also been shown for phthalate esters, another group of chemicals that are ubiquitously found in the environment (13).

Alkylphenol polyethoxylates were introduced in the 1940s and are widely used in detergents, paints, herbicides, pesticides and many other products (14). Studies by White et al. (15) have shown oestrogenic activity of nonylphenol and octylphenol (OP) *in vitro* and *in vivo* and in addition studies by Sharpe et al. (16) have shown the effects of octylphenol exposure in utero and postnatally on the adult testis size in rats. In this studies, female rats were treated with DES or OP via drinking water during pregnancy and postnatally untill weaning in the doses 100 and 1000μg/L of OP and 10 and 100μg/L of DES, doses probably comparable to human exposure. Their male offspring where sacrificed on day 90 and their testis size and daily sperm production (DSP) assesed. In animals treated either with DES or OP, small but significant reduction in both testis size and daily sperm production were observed therefore showing that exposure to even small doses of these chemicals in fetal and neonatal life could have deleterious effects on developing testis.

Effect of oestrogenic chemicals

In our experiments, time mated female rats were treated on day 11.5 p.c. (just prior to start of gonadal development) and on day 15.5 p.c. (at the start of testosterone production) subcutaneously with 100 or 500μg/Kg of DES in oil, 100 or 600 mg/Kg of OP in oil or oil alone as a control group. Animals were sacrificed on day 17.5 p.c., when the production of testosterone in the foetal testes is at its highest level, and the testes from their foetuses either fixed in Bouins', used for total RNA isolation or used directly for enzyme activity measurements. Administration of either OP or DES resulted in a massive reduction in immunostaining for P450c17 when this was assessed (17) and a parallel reduction in enzyme activity was also found when the testis were removed and homogenised (Fig. 1). The effect of oestrogenic chemicals appear to be at the level of mRNA as in situ hybridisation studies have shown reduced expression of CYP51 gene (17). This decrease could be a consequence of reduced Leydig cell number and/or a decrease in the level of enzyme in the cells. In this instance it appears to be the later, as the immunostaining for 3β-hydroxysteroid dehydrogenase, another Leydig cell steroidogenic enzyme, was comparable in control, OP- and DES-treated animals (17).
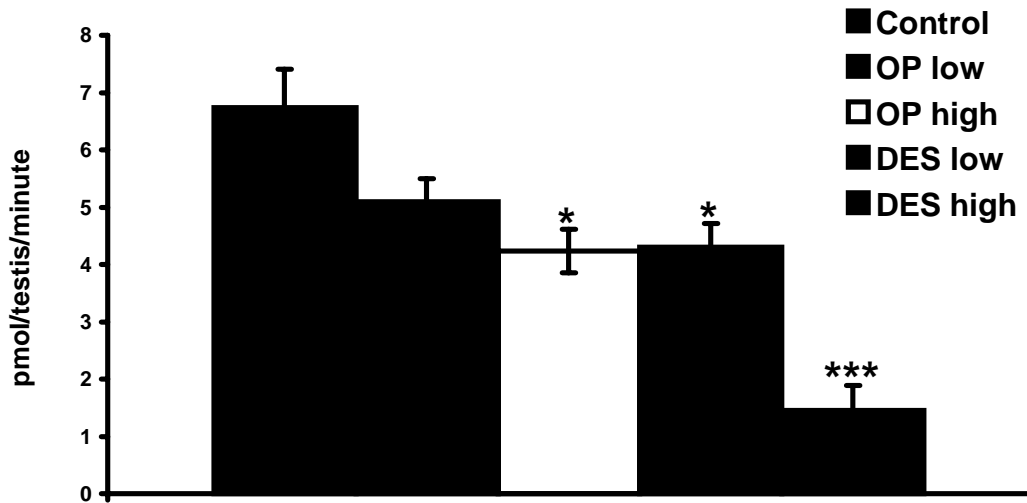
Fig. 1: P450c17 enzyme activity in the foetal testis isolated on day 17.5 p.c. from mothers treated with: Control - oil alone, OP low - 100mg/Kg, OP high - 600mg/Kg, DES low - 100µg/Kg, DES high - 500µg/Kg (* $p<0.05$, *** $p<0.001$).

In additional experiments, the expression of Steroidogenic factor-1 (SF-1) was also assessed. SF-1 is a transcription factor with important function in the development of reproductive tract. Transgenic mice, lacking functional SF-1 gene do not develop either gonads or adrenal glands, have disorganised hypothalamus and unfunctional pituitary gonadotroph cells. The exact function of this factor is not known yet, however, several studies have shown that it regulates expression of several genes with important functions in development of reproductive axis. These include AMH, α-GSU, LH-β subunit, oxytocytine and several cytochromes P450s including P450c17 (18). In our studies, reduced expression of SF-1 was found at both protein and mRNA level (19). Immunostaining showed severely reduced immunoexpression of SF-1 protein and RNAse protection studies have shown similar decrease in gene expression (Fig. 2).

The consequences of both these findings are unknown yet. However, reduced expression of P450c17 is certainly expected to result in reduced testosterone production, which could have deleterious effects on masculinisation of the foetus which is occurring at that time. The possible consequences of reduced SF-1 expression could be even more

severe, bearing in mind the importance of SF-1 for development of reproductive system, but further studies will be needed to establish this.
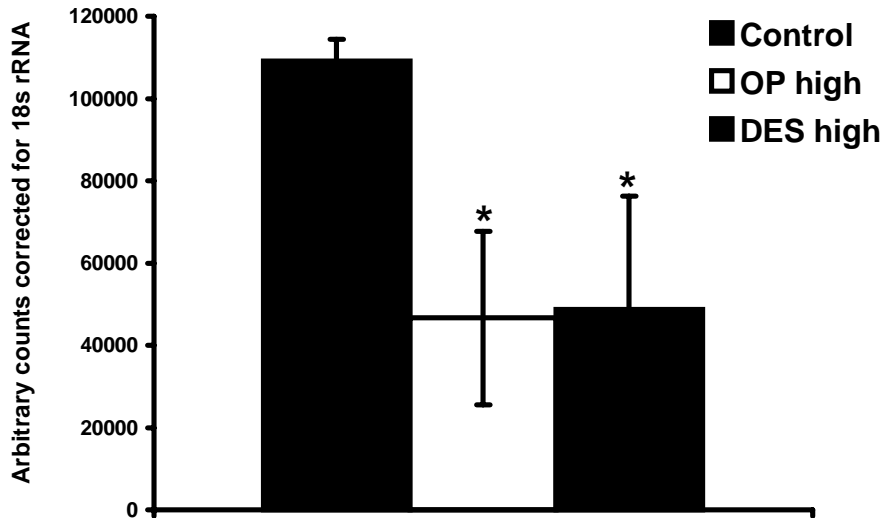
Fig. 2: SF-1 mRNA levels in testes from fetuses of OP and DES treated mothers. Control - oil alone, OP high - 600mg/Kg, DES high - 500μg/Kg (* $p<0.05$).

Conclusion

The available data for man and animals demonstrate clearly that early development of the testis, beginning at the time of sexual differentiation and extending out into early postnatal life, is critical in determining the function of reproductive tract in adult life. This is a very sensitive period and any interference with these processes is likely to have far reaching dire effects. Exposure to exogenous hormones or to chemicals with hormone-like activity thus has the potential to interfere with these processes, an effect which is likely to be irreversible because of the relatively narrow time-window within which these changes occur. The present and other studies (16, 17, 19) demonstrate that indirect exposure of the foetal/neonatal male rat to environmental oestrogenic chemicals administered to the mother, can significantly perturb these early processes by affecting the capacity of Leydig cells to secrete testosterone or reduce the testis size and sperm production (most likely due to reduced Sertoli cell number). It remains to be shown whether these changes actually affect fertility or reproductive function (e.g. behaviour) in

adulthood. The relevance to man of these findings is also unknown and will depend mainly on the level of human exposure to these chemicals. Therefore, it remains the matter of speculation whether these findings are connected with reported increase in male reproductive problems and fallen sperm counts. However, the mechanisms for deleterious action of oestrogenic chemicals on developing foetus exist and further studies will be needed to asses the potential danger for human population.

Povzetek

Več člankov je v zadnjih letih objavilo ugotovitve, da pri ljudeh narašča pojavnost problemov na moških spolnih organih kot so kriptorhizem, hipospadije in rak na modih, objavljenih pa je bilo tudi več poročil, ki kažejo na to da se je povprečno število semenčic v ejakulatu pri moškem v zadnjih petdesetih letih zmanjšalo kar za polovico. Eden od možnih vzrokov za povečanje pojavnosti teh problemov je povečana izpostavljenosti snovem z estrogenim delovanjem. Namen naših raziskav je bil ugotoviti možen vpliv teh kemikalij na razvoj moda pri podgani. Breje podgane so prejele podkožno Dietilstilboestrol (DES), onesnaževalec okolja Oktilfenol ali samo olje (kontrolna skupina) na dan 11.5 in 15.5 brejosti. Podgane so bile žrtvovane na dan 17.5 ter iz njihovih zarodkov izolirana moda, ki so bila fiksirana v Bouinovi raztopini, uporabljena za izoliranje RNK ali pa uporabljena neposredno za merjenje encimske aktivnosti. V modih podgan, katerih matere so bile tretirane z omenjenima estrogenima snovema je bila ugotovljena zmanjšana aktivnost encima P450c17 ter tudi zmanjšana izraženost gena, ki kodira ta encim, vendar pa to ni bilo na račun manjšega števila Lejdigovih celic saj imunohistokemično barvanje z uporabo protiteles proti encimu 3β-hidroksisteroidna dehidrogenaza (3β-HSD) ni pokazalo očitnih razlik v številu teh celic med tretiranimi in kontrolnimi živalmi. Poleg zmanjšane izraženosti gena CYP17 pa je bila ugotovljena tudi zmanjšana izraženost gena SF-1, ki kodira jedrni hormonski receptor Steroidogeni faktor-1.

References

[1] F.W. George and J.D. Wilson, The Physiology of Reproduction, Raven Press, New York, 1994, pp 3-28.
[2] R.M. Sharpe, The Physiology of Reproduction, Raven Press, New York, 1994, pp 1363-1434.
[3] R.A. Hess, P.S. Cooke, D. Bunick and J.D. Kirby, *Endocrinology*, **1993,** 132, 2607-2613.
[4] L.H. Van Haster, F.H. de Jong, R. Docter and D.G. de Rooij, *Endocrinology*, **1993**, 133, 755-760.
[5] C. Quigley, A. De Bellis, K. Marschke, M. El-Awady, E. Wilson and F. French, *Endo. Rev.*, **1995**, 16, 271-321.
[6] A. Giwercman, *Hum. Rep.*, **1995**, 10, 158-164.
[7] E. Carlsen, A. Giwercman, N. Keiding and N.E. Skakkebaek, *B. Med. J.*, **1992**, 305, 609-613.
[8] R.J. Stillman, *Am. J. Obst. Gynae.*, **1982**, 142, 905-921.
[9] R.M. Sharpe and N.E. Skakkebaek, *Lancet*, **1993**, 341, 125-126.
[10] R.M. Sharpe, *Curr. Opinion in Urol.*, **1994**, 4, 295-304.
[11] A.V. Krishnan, P. Stathis, S.F. Permuth, L Tokes and D Feldman, *Endocrinology*, **1993**, 132, 2279-2286 .
[12] A.M. Soto, H. Justicia, J.W. Wray and C. Sonnenschein, *Environ. Health Perspec.*, **1991**, 92, 167-173.
[13] S. Jobling, T. Reynolds, R. White, M.G. Parker and J.P. Sumpter, *Environ. Health Perspec.*, **1995**, 103, 582-586.
[14] G.C. Naylor, J.P. Mierure, J. Weeks, F.J. Castaldi and R.R. Romano, *J. Am. Oil Chemists Soc.*, **1992**, 69, 695-703.
[15] R. White, S. Jobling, S.A. Hoare, J.P. Sumpter and M.G. Parker, *Endocrinology*, **1994**, 135, 175-182.

[16]   R.M. Sharpe, J. Fisher, M.R. Millar, S. Jobling and J.S. Sumpter, *Environ. Health Perspec.*, **1995**, 103, 1136-1143.

[17]   G. Majdic, R.M. Sharpe, P.J. O'Shaughnessy and P.T.K. Saunders, *Endocrinology*, **1996**, 137, 1063-1070.

[18]   K.L. Parker, BP Schimmer, *Endo. rev.*, **1997**, 18, 361-377.

[19]   G. Majdic, R.M. Sharpe and P.T.K. Saunders, *Mol. Cell. Endocrinol.*; **1997**, 127, 91-98.

THE TEMPERATURE DEPENDENCE OF DYNAMIC VISCOSITY FOR SOME VEGETABLE OILS

H. Abramovič and C. Klofutar*

Department of Food Technology, Biotechnical Faculty, University of Ljubljana,

1000 Ljubljana, Jamnikarjeva 101, Slovenia

ABSTRACT

Dynamic viscosities for a number of vegetable oils (unrefined sunflower oil, refined sunflower oil, olive oil, refined corn oil, unrefined pumpkin oil, a mixture of refined vegetable oil and unrefined pumpkin oil) were determined at temperatures from 298.15 K to 328.15 K. Some empirical relations that describe the temperature dependence of dynamic viscosity were fitted to the experimental data and the correlation constants for the best fit are presented.

INTRODUCTION

In the food industry, viscosity is one of the most important parameters required in the design of technological process. On the other side, viscosity is also an important factor that determines the overall quality and stability of a food system. From the physicochemical point of view, viscosity means the resistance of one part of the fluid to move relative to another one. Therefore, viscosity must be closely correlated with the

* To whom correspondence should be addressed

structural parameters of the fluid particles. On the basis of published data [1] concerning flow properties of oils, the oil viscosity has a direct relationship with some chemical characteristics of the lipids, such as the degree of unsaturation and the chain length of the fatty acids that constitute the triacylglycerols. The viscosity slightly decreases with increased degree of unsaturation and rapidly increases with polymerisation.

In the present study we determined the viscosities of some edible oils from vegetable sources in the temperature range from 298.15K to 328.15K. Applicable empirical relations which describe the variation of dynamic viscosity with temperature were fitted to the experimental data and the correlation constants for the best fit are presented. The criteria used for model selection were the magnitude of the determination coefficient, r^2, and the deviation of viscosity, calculated according to a particular theoretical model from the experimentally determined value.

EXPERIMENTAL

Oil samples

The vegetable oils utilised in this work where supplied by the GEA Oil Factory, Slovenska Bistrica. In our investigation we used the following samples of edible oils or oil mixtures: refined sunflower oil, unrefined sunflower oil, refined corn germ oil, olive oil, unrefined pumpkin oil and salad oil (a mixture of refined vegetable oil and unrefined pumpkin oil)

For the samples the results of the determination of some chemical characteristics i.e. the acid value (A.V.), the saponification value (S.V.), the iodine value (I.V.) and the peroxide value (P.V.) are given in [2]. Table 1 presents the manufacturers' data [3] for the fatty acid composition of the investigated oil samples.

Viscosity determination

The dynamic viscosity, η (cP), of the oil samples was determined with an Ubbelohde viscometer at temperatures ranging from 298.15K to 328.15K at 10.0K intervals. The dynamic viscosity was estimated by means of the following equation [4]:

$$\eta = C \cdot t \cdot d - \frac{E \cdot d}{t^2} \qquad (1),$$

where t is the measured flow time, C and E are instrumental constants and d is the density of the oil sample. The constants C and E were evaluated according to [4] by a sucrose solution. The temperature of the bath was controlled to 0.05 K. The densities of oil samples were measured in a previous investigation [2]. The estimated error in viscosity determination was 0.4%.

Table 1. The fatty acid composition of the oils investigated

Oil	% composition		
	saturated fatty acid	monounsaturated fatty acid	polyunsaturated fatty acid
unrefined sunflower oil	10	20	70
refined sunflower oil	10	20	70
refined corn oil	12	31	57
olive oil	15	75	10
unrefined pumpkin oil	10	30	60
salad oil	10 - 15	20 - 30	55 - 65

RESULTS AND DISCUSSION

It is known that certain properties of fatty acid residues in the molecule of triacylglycerol have significant effects on the fluidity of the oil [5]. Most of the bonds in the hydrocarbon chains of fatty acids are single bonds. This linear " zig-zag " organisation enables the chains to be lined up close to each other and intermolecular

interactions such as Van der Waals interactions can take place. This system inhibits flow of the fluid, resulting in the relatively high viscosity of the oils. The presence of double bonds, which in fatty acid residues exist in *cis* configurational form, produces "kinks" in the geometry of the molecules. This prevents the chains coming close together to form intermolecular contacts, resulting in an increased capability of the fluid to flow.

If we compare some chemical characteristics and viscosities of the investigated oils we can observe from the results given in Table 2 that the highest values for viscosity were found in the case of olive oil where the concentration of monosaturated fatty acid is 75%.

Table 2.   Experimental data for the dynamic viscosity of vegetable oils as a function of temperature.

	η / (cP)			
T / (K)	298.15	308.15	318.15	328.15
Oil				
unrefined sunflower oil	49.14	33.45	23.92	17.71
refined sunflower oil	48.98	33.33	23.79	17.63
refined corn oil	51.44	34.77	24.79	18.25
olive oil	63.28	41.67	28.99	21.03
unrefined pumpkin oil	54.82	36.93	26.04	19.11
salad oil	50.80	34.48	24.62	18.33

As we can see in Table 1 olive oil has a very low content of polyunsaturated fatty acids (10%). Unrefined sunflower oil, has the lowest viscosities compared to the other oil samples, and as presented in Table 1, quite an appreciable amount of polyunsaturated fatty acids (70%). The viscosities at 298.15 K for the investigated oils are plotted on Figure 1 as a function of the iodine value [2] which indicates the degree of unsaturation. From this figure we can see that the viscosity almost linearly decreases as the iodine value increases. On the other hand, no correlation was found for the dependence of

viscosity on saponification value, which characterises the chain length of fatty acids. It is possible that the influence of the degree of polymerisation of fatty acid residues on oil viscosity is completely diminished with other effects existing in the oil system.
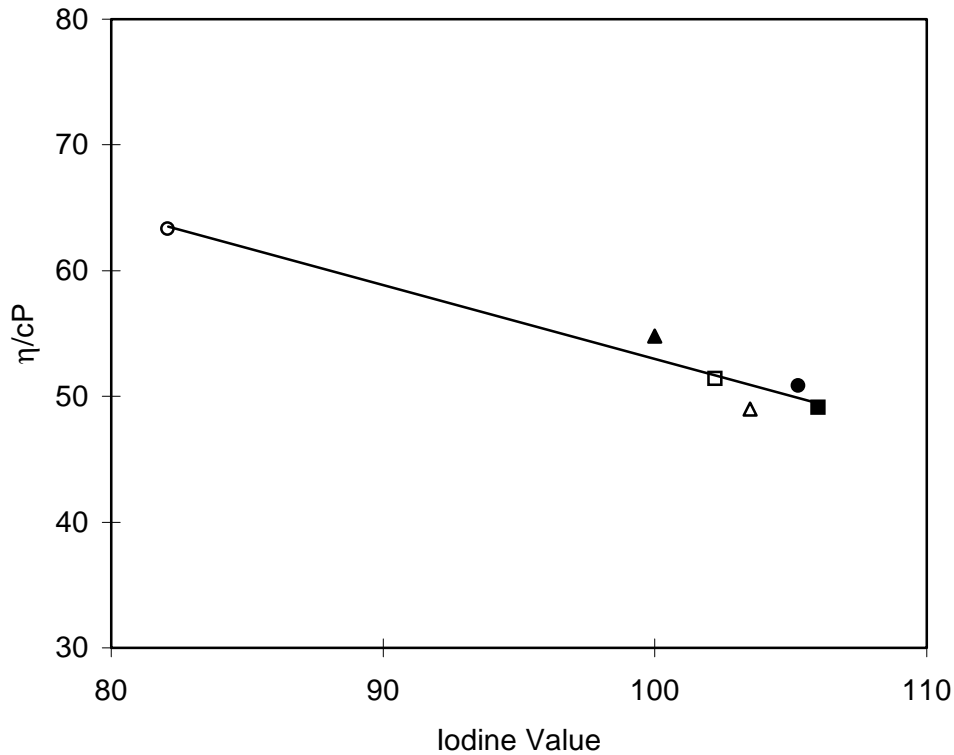
Figure1. Viscosities of investigated oils at 298.15K as a function of iodine value; ■, unrefined sunflower oil; Δ, refined sunflower oil; □, refined corn oil; o, olive oil; ▲, unrefined pumpkin oil; ●, salad oil.

Some investigators [6] tried to find a relationship that describes the variation of viscosity with some structural characteristics (degree of unsaturation i.e. iodine value, I.V. and chain length of the fatty acids i.e. saponification value, S.V.) and proposed the following relation:

$$\ln\eta = -4.7965 + 2525.92962 \, (1/T) + 1.6144 \, (SV)^2 / (T)^2$$
$$- 101.06 \cdot 10^{-7} \, (IV)^2 \tag{2},$$

where $\ln\eta$ is the natural logarithm of the viscosity. For our samples the proposed equation could not be considered appropriate since it gives values of η which are substantially higher (about 50%) than those obtained by experiment.

In Figure 2 typical viscosity behaviour of oil samples as a function of temperature is shown, where the viscosity rapidly decreases when temperature is increased.
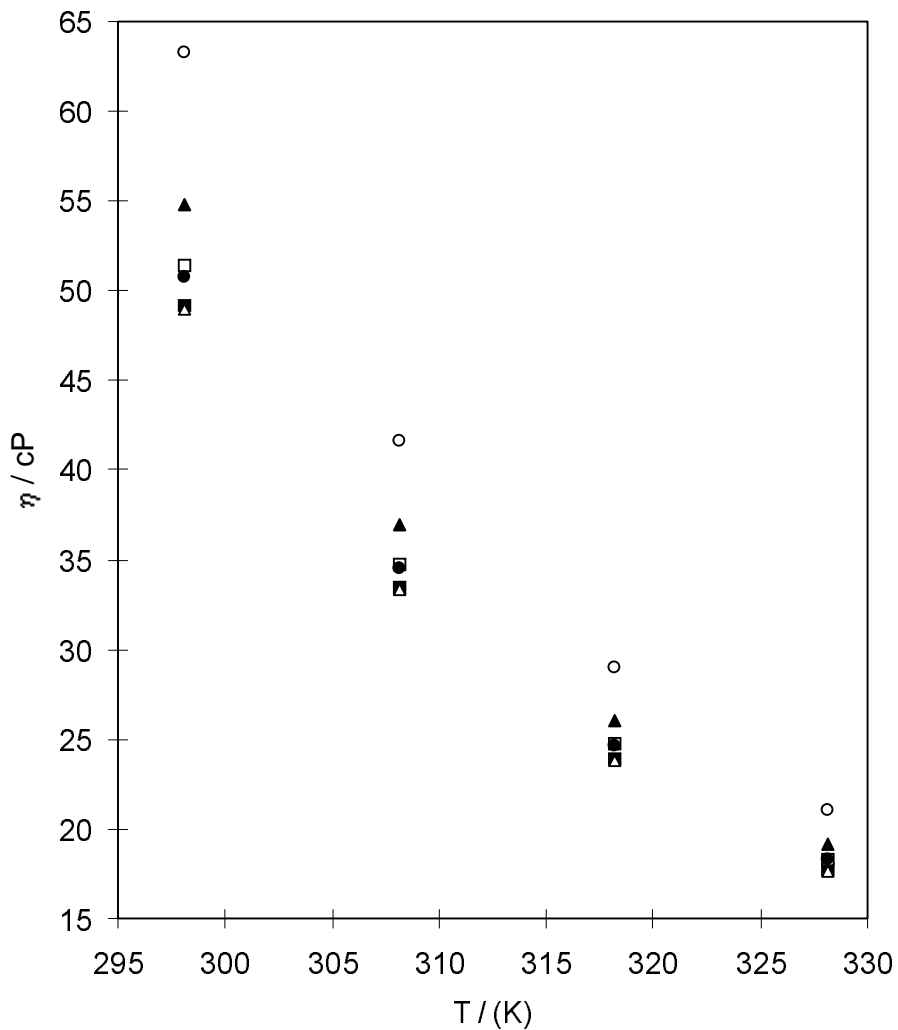
Figure 2.   The viscosities of investigated oils as a function of temperature; ■, unrefined sunflower oil; Δ, refined sunflower oil; □, refined corn oil; o, olive oil; ▲, unrefined pumpkin oil; ●, salad oil.

With the aim of predicting this dependence many empirical relations have been proposed. We used modified versions of the Andrade equation [7] represented by equations (3) and (4):

$$\ln\eta = A + \frac{B}{T} + \frac{C}{T^2} \tag{3}$$

and

$$\ln\eta = A + \frac{B}{T} + C.T \tag{4}$$

To describe the effect of temperature on η the relations (5), (6), (7) and (8) were also used:

$$\log\eta = \frac{A}{T} - B \tag{5}$$

$$\eta = A - B . \log t \tag{6}$$

$$\eta . v^{1/2} = A . e^{B/T} \tag{7}$$

and

$$\eta = \frac{A}{v - B} \tag{8}$$

where v means the specific volume of the oil, t is the temperature in degrees Celsius and A, B and C in the equations (3) to (8) are correlation constants. The results of regression analyses to these relations are presented in Table 3.

Table 3. Values of parameters of the theoretical models described by equations (3), (4), (5), (6), (7) and (8) and the standard error of regression analysis, sd.

	eq. (3)				eq. (4)			
Oil	A	$B.10^{-3}$	$C.10^{-5}$	sd	A	B	C	sd
unrefined sunflower oil	2.6572	2.8827	9.6889	0.1	-27.33	6454.75	0.03	0.01
refined sunflower oil	3.0044	3.1068	10.0457	0.6	-28.09	6575.60	0.03	0.01
refined corn oil	2.7691	2.9769	9.9107	0.7	-27.89	6572.41	0.03	0.01
olive oil	4.3806	4.0938	11.9926	0.5	-32.72	7462.27	0.04	0.01
unrefined pumpkin oil	2.9791	3.1323	10.2448	0.1	-28.75	6744.09	0.03	0.01
salad oil	4.8140	4.2094	11.7573	0.3	-31.56	7120.03	0.04	0.01

	eq. (5)			eq. (6)		
Oil	A	B	sd	A	B	sd
unrefined sunflower oil	1443.3	3.157	0.006	177.2	92.3	1.5
refined sunflower oil	1445.3	3.165	0.006	176.8	92.1	1.5
refined corn oil	1464.1	3.207	0.006	186.6	97.4	1.6
olive oil	1558.2	3.433	0.008	235.4	124.1	2.3
unrefined pumpkin oil	1489.6	3.265	0.007	200.4	104.9	1.7
salad oil	1442.5	3.141	0.008	183.2	95.4	1.6

	eq. (7)			eq. (8)		
Oil	A	B	sd	A	B	sd
unrefined sunflower oil	0.0008	3288.9	0.02	0.648	1.079	0.001
refined sunflower oil	0.0008	3292.5	0.02	0.661	1.079	0.002
refined corn oil	0.0007	3335.6	0.02	0.684	1.079	0.002
olive oil	0.0004	3552.4	0.02	0.763	1.089	0.002
unrefined pumpkin oil	0.0006	3394.5	0.02	0.708	1.082	0.002
salad oil	0.0008	3287.2	0.02	0.671	1.080	0.002

From Table 3 we can see that the empirical relations which give the best prediction in the present study for the temperature dependence of oil viscosity are described by the equations (3) and (4), where the determination coefficient value is almost 1.000. The viscosity calculated through eq. (3) deviates from the experimental one by less than 0.1%. The relationships (5) and (7) could be also treated as useful approaches with the determination coefficient greater than 0.999. On the other hand the relations (6) and (8) are less suitable for description of the temperature dependence of oil viscosity, while the determination coefficient value being less than 0.992, and the deviation of calculated viscosity from the experimental one is appreciable and amounts to more than 2%.

REFERENCES

[1] N. V.   K. Dutt, D. H. L. Prasad, *J. Am. Oil Chem. Soc.* **1989,** *66,* 701-705.

[2] C. Klofutar, D. Rudan-Tasič and K. Romih, Densities and thermal expansion coefficients of some vegetable oils; *Acta Chim. Slov.* **1997,** *44,* 45-55.

[3] D. Pokorn, Olje in zdravje - priloga, Medicinska fakulteta v Ljubljani, Tovarna olja GEA, D.D. Slovenska Bistrica, Ljubljana, 1995, p.5.

[4] M. R. Cannon, R. E. Manning, J. D. Bell, Viscosity measurement. *Anal .Chem.* **1960,** *32,* 355-358.

[5] H. Lawson, Food, *Oils and Fats,* Chapman & Hall, New York 1995, p.35.

[6] J. F. Toro-Vazquez and R. Infante-Guerrero, *J. Am. Oil Chem. Soc.* **1993,** *70,* 1115-1119.

[7] E. N. da C. Andrade, *Nature,* **1930,** *125,* 309-318.

Nekaterim vzorcem jedilnega olja (nerafinirano sončnično olje, rafinirano sončnično olje, olivno olje, rafinirano olje koruznih kalčkov, nerafinirano bučno olje, mešanica rafiniranega rastlinskega in nerafiniranega bučnega olja) smo določili dinamično viskoznost v temperaturnem območju od 298.15 K do 328.15 K. Preizkusili smo nekaj empiričnih relacij, ki opisujejo odvisnost dinamične viskoznosti od temperature.

THE INFLUENCE OF THE PROTEINASE INHIBITOR EP475 ON SOME MORPHOLOGICAL CHARACTERISTICS OF POTATO PLANTS (*Solanum tuberosum* L. cv. Desirée)

Maruša Pompe[1], Borut Štrukelj[2], Maja Ravnikar[1]

[1]National Institute of Biology, Večna pot 111, Ljubljana, Slovenia

[2]Jožef Stefan Institute, Jamova 39, Ljubljana, Slovenia

Abstract

EP475 is a synthetic cysteine proteinase inhibitor. The potato plants *Solanum tuberosum* L. cv. Desirée grew in node culture in controlled conditions. We added 10μM or 50μM of EP475 to the media to investigate its influence on some morphological and biochemical characteristics. The medium without EP475 was used as a control.

The number of nodes of the major shoot increased significantly under the influence of 10μM EP475, but the plants shortened under the influence of 50μM EP475. With the increase of EP475 concentration in the media the primary roots shortened. The number of secondary roots on a single primary root decreased significantly by 50μM EP475. Application of EP475 also resulted in an increased number of lateral shoots and in a significant decrease of leaf areas.

The ratio between dry and fresh weights significantly increased in roots, stems and leaves under the influence of EP475. Thus, EP475 decreased the amount of water in plants.

Decreased growth and biosynthesis due to EP475 were probably a consequence of decreased activity of endogenous proteinases.

Introduction

Proteinases and proteinase inhibitors are proteins that are ubiquitous in nature. The majority of work was done on cereals, legumes, the tomato, potato and tobacco

plants (1). Proteinase inhibitors specifically inhibit each of the four known classes of endopeptidases: serine, cysteine, aspartic and metalloproteinases. Among them, cysteine proteinases and their inhibitors are the best characterised in plants.

Proteinases and proteinase inhibitors were isolated and indentified from different plant organs but mostly they were studied in seeds. In leaves, proteinases and proteinase inhibitors are involved in degradation processes that take place in a neutral environment of cytosol, the acidic environment of lysosomes and the alkaline environment of chloroplasts (1). The ubiquitin-dependent proteolytic pathway that has an integral role in the turnover of many intracellular proteins in plants was identified in cytosol (9). Cell walls and intracellular space also exhibit proteolytic activities, mainly from the serine class (1). There is not much known about proteinases and their inhibitors in roots.

The functional role of these inhibitor proteins appears to be either to protect tissues or fluids from proteolysis by foreign proteases or to regulate the levels of proteases that are metabolically active in the tissues or fluids that they are associated with (8). Proteinases and their inhibitors are involved in senescence proceses (2) and in plant responses on stress (9), pathogens and wounding (3).

Much work has been done on cDNA cloning (2, 3, 4, 5, 10) and on the structure and molecular characteristics of proteinases and their inhibitors.

EP475 is synthetic cysteine proteinase inhibitor with a molecular weight of 370 g/mol. In preliminary experiments it was found that EP475 is transported from media into the plant and along the plant itself. To examine the influence of EP475 on growth and development of potato plants and eventual interactions with endogenous proteinases, EP457 was added into the growth media.

Materials and methods

Single-node cuttings of potato plants (*Solanum tuberosum* L. cv. Desirée) were grown *in vitro* on modified Murashige-Skoog medium (6) without EP475 or with a supplement of 10 µM or 50 µM EP475. The plants were kept at a temparature 21±2°C, the light was 50 $\mu Mm^{-2}s^{-1}$ (Osram L18W 20 lamps), with a photoperiod of 16 h.

In 3 and 5-week-old stem node cultures the length of axillary shoots was measured and stem nodes were counted. After 3 weeks the number of primary roots per plant and the number of secondary roots per primary root were determined and the length of primary roots was measured. After 5 weeks lateral shoots were counted and leaf areas were measured with a ΔT areameter.

To determine the fresh weight of plants, the leaves, stems and roots were separated and weighed. After drying at 45°C to a constant weight they were reweighed to determine the dry weight.

Results and discusion

The plants grown on media supplemented with 50 µM EP475 were significantly smaller than the controls. The number of stem nodes increased significantly on medium supplemented with 10 µM EP475 as compared to control.

PARAMETER	AGE (weeks)	CONTROL	10 µM EP475	50 µM EP475
shoot height (mm)	3	30.44 ± 0.52	33.44 ± 0.57	18.52 ± 0.44
shoot height (mm)	5	57.00 ± 1.10	70.32 ± 1.87	46. ± 1.11
number of nodes	3	8.24 ± 0.05	9.48 ± 0.08	8.32 ± 0.10
number of nodes	5	11.72 ± 0.08	14.2 ± 0.12	13.32 ± 0.12
primary root length (mm)	3	30.33 ± 1.04	22.66 ± 0.77	15.49 ± 0.55
number of secondary roots	3	3.21 ± 0.31	2.04 ± 0.21	0.65 ± 0.11
number of lateral shoots	5	0.04 ± 0.02	0.48 ± 0.07	0.88 ± 0.11
leaf area (cm^2)	6	7.95 ±0.86	3.76 ± 0.71	1.62 ± 0.09
fresh weight of plant (mg)	6	261.53 ± 15.18	207.57 ± 14.48	124.52 ± 8.69
dry weight of plant (mg)	6	19.96 ± 0.85	18.66 ± 0.89	13.23 ± 0.64
dry/fresh weight of plant	6	0.0771± 0.0018	0.0912± 0.0023	0.1076± 0.0026

Table 1: Various parameters of plants grown on control medium, on medium supplemented with 10 µM EP475 and on medium supplemented with 50 µM EP475. The average ± standard error is shown.
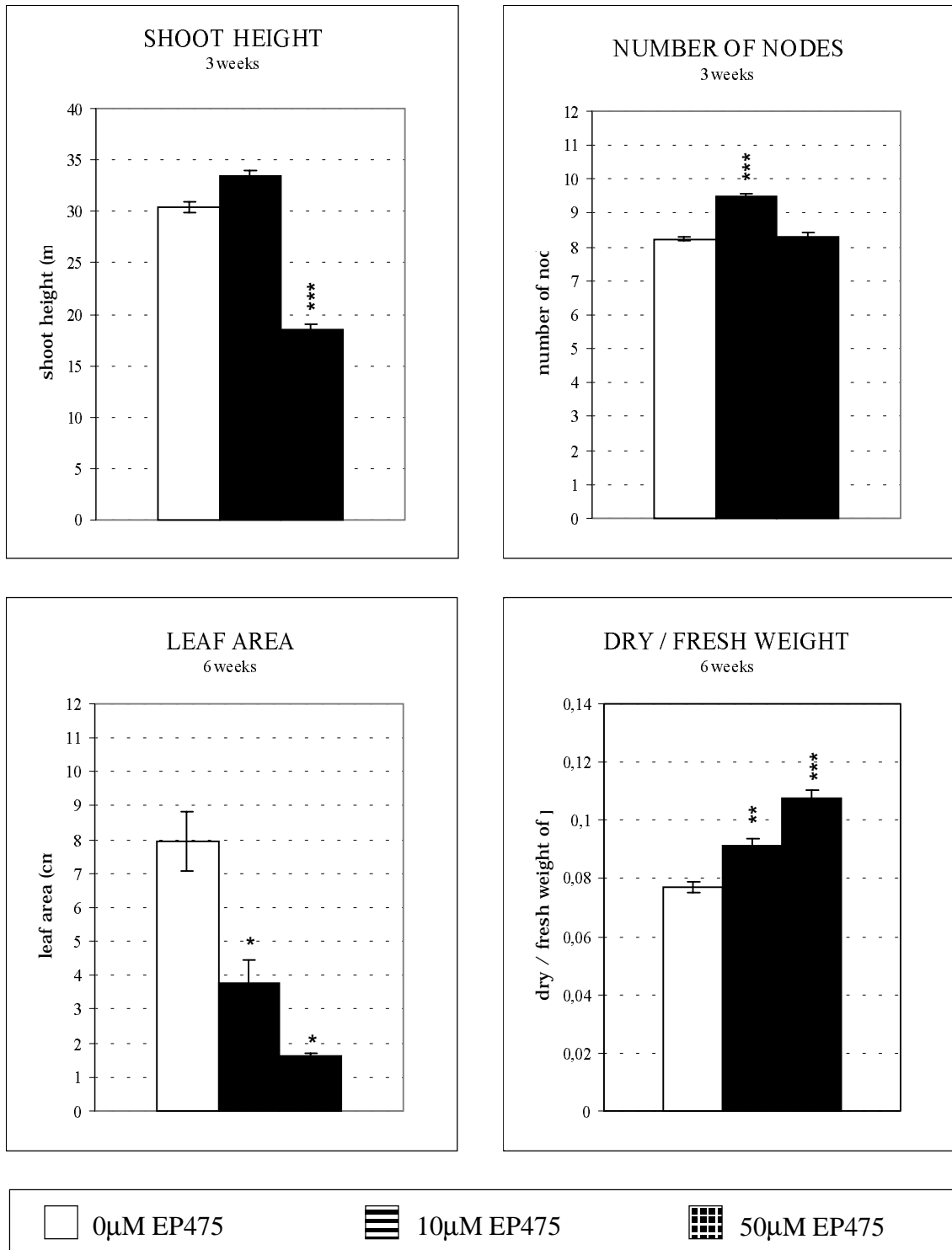
Figure 1: Average shoot height, number of nodes, leaf area per plant and the ratio between dry and fresh weight of plants on control medium without EP475 and on media with 10μM or 50μM of EP475. Statistical comparison is made between plants on media with 10μM of EP475 and plants on control medium and between plants on media with 50μM of EP475 and plants on control medium. Two times the standard error is shown.

With the increase of EP475 concentration in the media were primary roots significantly shorter. The number of secondary roots on a single primary root was significantly reduced under the influence of 50 μM EP475. Application of EP475 also resulted in an increased number of lateral shoots.

The leaf areas of plants grown on medium supplemented with 10 μM EP475 decreased significantly as compared to controls and the leaf areas of those grown on medium supplemented with 50 μM EP475 were still smaller.

Application of EP475 also resulted in significantly decreased fresh and dry weights of roots and leaves. The fresh weights of stem tended to increase under the influence of 10μM EP475, but decreased significanly with 50 μM EP475. The stem dry weights also increased under the influence of 10 μM EP475. With the increase of EP475 concentration, the fresh weight of whole plants decreased and also the dry weight of whole plants grown on medium with 50 μM EP475 decreased as compared to the controls. The ratio between dry and fresh weights significantly increased in roots, stems, and leaves under the influence of 10 μM EP475 and even more under the influence of 50 μM EP475.

Thus, the decreased size of plants due to EP475 is probably at least in part a result of the decreased amount of plant water and in part a consequence of the decreased activity of endogenous proteinases (T. Popovič, personal communication), though the cell divisions are stimulated as the larger number of nodes and lateral shoots develop.

Following these results, we continue to investigate eventual differences between endogenous activity of proteinases in untreated plants and plants treated with EP475. We are also investigating the immunolocalization of proteinases in tissues of plants grown on medium supplemented with EP475 and on control medium.

References

1. J. Brzin, M. Kidrič, *Biotechnology and Genetic Engeneering Rewiews* **1995**, 13, 421-467
2. R. Drake et all., *Plant Molecular Biology* **1996**, 30, 755-767
3. J. M. Hubb et all., *Plant Molecular Biology* **1993**, 21, 685-694
4. J. M. Hubb Linthorst et all., *Plant Physiol.* **1993**, 101, 705-706
5. A. J. Lidgett et all., *Plant Molecular Biology* **1995**, 29, 379-384
6. Murashige, F. Skoog, *Physiol. Plant.* **1962**, 15, 473
7. C. A. Ryan, *The Biochemistry of Plants* **1981**, 6, 351-370
8. C. A. Ryan, **1988**, 223-233

9. R. D. Vierstra, *Annu. Rev. Plant Physiol. Plant Mol. Biol.* **1993**, 44, 385-410
10. H. Watanable et all., *The Journal of Biological Chemistry* **1991**, 266, 16897-16902

Povzetek

EP475 je sintetični proteinazni inhibitor. Rastline krompirja *Solanum tuberosum* cv. Desirée smo gojili v nodijski kulturi v kontroliranih pogojih. V MS gojišče smo dodali 10µM ali 50µM EP475 in opazovali vpliv na nekatere morfološke značilnosti. Gojišče brez EP475 smo uporabili kot kontrolno gojišče.

Število nodijev glavnega poganjka se je pod vplivom 10µM EP475 statistično značilno povečalo, pri koncentraciji 50µM EP475 pa so bile rastline značilno nižje. Z večanjem koncentracije EP475 se je manjšala dolžina primarnih korenin. Število sekundarnih korenin na posamezni primarni korenini se je statistično značilno zmanjšalo pri rastlinah na gojišču s 50µM EP475. Z dodajanjem EP475 v gojišče se je značilno povečalo tudi število stranskih poganjkov, listna površina pa se je statistično značilno zmanjšala.

Razmerje med suho in svežo težo se je z večanjem koncentracije EP475 v gojišču statistično značilno zvečalo tako v koreninah kot tudi v steblih in listih; EP475 torej vpliva na zmanjšanje količine vode v rastlini. Zmanjšana rast in biosinteza pri 50µM EP475 sta verjetno posledica zmanjšane aktivnosti endogenih proteinaz.

DIFFERENT DISSOLUTION PROCEDURES FOR ANALYSIS OF TITANIUM(IV) OXIDE WHITE PIGMENT

Nineta Majcen

Cinkarna Celje d.d., Kidričeva 26, SI-3000 Celje, Slovenia

ABSTRACT

Various ways of sample preparation for subsequent analysis of titanium(IV) oxide white pigment are represented. Three different procedures: digestion in various mediums, lithium metaborate fusion and pressure dissolution with hydrofluoric acid are precisely represented and considering accuracy, precision, blank values, time of analysis and general procedure's simplicity, the last procedure is undoubtedly the most appropriate one.

INTRODUCTION

In spite of the fact that titanium(IV) oxide white pigment is indispensable in our everyday life, very few procedures for its analysis are described in literature [1-14]. Among the most common approaches of sample dissolution described in these articles are either treating the pigment with different mixtures of various chemicals and subsequent extraction or slurry introduction accompanied by electrothermal or flame atomic absorption spectrometry. The main imperfections of the before mentioned dissolution procedures are long duration time of the sample preparation for the first procedure and poor precision for the second one. Nowadays, some information about pressure dissolution in conventional and microwave ovens using various acids and about solid sampling following by electrothermal atomisation are also available.

While neither of the already described dissolution procedures are suitable for our purposes, we decided to try finding another simple and rapid dissolution procedure which would give accurate and precise results for concentration of trace metals in titanium(IV) oxide white pigment. After detailed study of the literature data about the already known dissolution procedures which enables the determination of trace elements in oxides of refractory elements, three different ways of sample preparation were experimentally performed [15-48]. First, digestion of samples with various acids followed by spectrophotometric determination of iron were investigated. Due to some considerate imperfections which this procedure has, it was replaced first by lithium metaborate fusion and finally, the pressure dissolution with hydrofluoric acid took place.

EXPERIMENTAL

Apparatus

For spectrophotometric determination of iron concentration with o-phenantroline Iskra spectrophotometer model HPV210 was used. Absorbances were measured at 510 nm.

A Perkin-Elmer model 4000 flame atomic absorption spectrophotometer with conventional and high performance nebuliser (HPN) and Perkin-Elmer model 2280 with HGA 400 AAS were used. For atomic absorption measurements, standard instrumental parameters were applied using background correction.

Results obtained by X-ray fluorescence spectrometric method were achieved on a Philips PW 1404 instrument interfaced to a Philips P 2723-302 computer for automatic control and data processing at standard conditions; a Cr anode X-ray tube was used throughout.

For pressure dissolution of samples four 25 ml and four 30 ml teflon vessels made by two different producers were used.

Reagents

All reagents used were of analytical reagent grade.

Digestion

1.0000g of pigment was treated with 50 ml of various acids or their mixtures. After heating for some hours, suspensions were filtered and absorbances were measured. Regarding the results of these preliminary experiments, five different samples of titanium(IV) oxide were digested in 6 M hydrochloric acid for three hours. Each sample was analysed in at least three replicates. For the determination of the element's concentration standard addition technique was used.

Lithium Metaborat Fusion Procedure

The detailed description of this sample dissolution procedure is explained in already published article [13].

Hydrofluoric Acid Decomposition Method

Before the decomposition procedure was developed, several reagents, their mixtures and different experimental conditions (time, temperature), at which quantitatively dissolution takes place, were examined.

1.0000 g of sample was transferred to PTFE vessels. 5 ml of HF was added and pressure dissolution was took place at 150°C for two hours. After cooling the PTFE vessels, the solutions were quantitatively transferred to 25 ml polypropylene volumetric flasks. Three different volumes of standard solutions were added and absorbances were measured. Blank solution was prepared for each experiment separately.

In the above described way achieved results were statistically treated and compared to results obtained by X-ray fluorescence spectrometry, which is used as every day analytical method for the determination of traces of elements in titanium dioxide white pigment samples [49-51].

RESULTS AND DISCUSSION

Digestion

As already mentioned , digestion of the same sample with different reagents, represented in Table 1, was studied first.

Table 1. Reagents and their mixtures used for digestion of titanium(IV) oxide white pigment samples

Acid	Mixtures						
	A	B	C	D	E	F	G
HCl	1M	6M	1M	1M	1M	3M	
HNO$_3$			5M	1M	3M	1M	
HClO$_4$							1M

On the basis of measured absorbances and other procedures' characteristics, 6M HCl was chosen for all succeeding experiments. Obtained results and results achieved by XRF technique, are shown in Table 2.

Table 2. Results obtained by the digestion procedure followed by AAS technique and by XRF method

Sample	$c(Fe)_{AAS}$ mg/kg	$s_{rel.}$ %	$c(Fe)_{XRF}$ mg/kg
A	45	6	38
B	55	25	28
I	32	14	19
J	26	4	32
K	12	-	10
L	12	-	16
M	25	22	42
U	30	7	37
Z	32	10	29

Statistical comparison of the results obtained by the digestion procedure followed by AAS technique and by XRF method showed, that these two methods do not give statistically different results at 95 % confidence level. Such at a first sight surprisingly statistical conclusion is a consequence of a high imprecision of the results obtained by AAS technique which is due to very low measured absorbances. In order to avoid this problem, the procedure for quantitatively sample dissolution with lithium metaborate followed by hydrochloric melt dissolution was developed.

Lithium metaborate fusion

Since detailed description of given procedure has already been published [13] only the main ascertainments will be discussed here. First, different experimental conditions i.e. the ratio of masses of $LiBO_2$ and K_2CO_3 and concentration and volume of HCl were examined. As optimal procedure for quantitative dissolution of pigment and subsequent determination of concentration of the elements in the solution, a procedure where a melt, obtained by fusing 0.2000 g of sample with 1.0 g of $LiBO_2$ and 4.0 g of K_2CO_3 in platinum crucible at 1000°C was quenched in 150 ml of hot HCl acid. Concentration of HCl depends on the further treating of the solution. If the iron concentration was determined spectrophotometrically and extraction was used as a separation step, 6 M HCl was used, while in all other cases, where the concentrations of elements (Al, Cu, Cr, Fe, Sb, V) was determined either by flame or electrothermal atomic spectroscopy, 3M HCl was used [52]. The main imperfection of the above described sample dissolution procedure is high absorbances of blank solutions, which disable the determination of elements which are present in lower concentration i.e. few ppm. In Table 3 results for spectrophotometric determination of iron are shown.

Table 3. Experimental results for spectrophotometric determination of iron in titanium(IV) oxide white pigment by o-phenantroline

Determinations	Absorbances	
	Blank	Sample
1	0.006	0.028
2	0.008	0.026
3	0.019	0.025
4	0.026	0.026
5	0.058	0.059
6	0.025	0.028
7	0.014	0.019
8	0.035	0.055
9	0.021	0.028
10	0.021	0.021

The detailed further investigations showed that the high blank values are caused by leaching of elements from platinum crucibles [53, 54]. The experiments showed that the most important component in this process is the amount of K_2CO_3 and that after each fusion the platinum crucible is lighter for about 20 mg. Considering described important deficiency of this sample dissolution procedure which is suitable only for quantitative determination of elements in higher concentration range, another procedure for titanium(IV) oxide white pigment dissolution was developed. In Table 4 results obtained by the above described procedure for the concentration determination of antimony are shown and compared with results achieved by XRF method.

Table 4. Results for antimony in titanium(IV) oxide white pigment samples obtained by flame AAS and XRF method

Sample	Concentration (%)	
	AAS	XRF
VA	0.02	0.02
VB	0.04	0.02
VC	0.13	0.12
VD	0.04	0.03

Pressure pigment dissolution

It is already well known that among various acid and their mixtures only hydrofluoric acid quantitatively dissolute the titanium(IV) oxide white pigment, but its aggressive nature against glass should be appropriately overcome. For that purpose, boric acid was frequently mentioned, but according to our experience, it is very unsuitable for quantitative trace elements determination. Nowadays, the problem could be easily overcome if all accompanied equipment is made from appropriate material, in that case from polypropylene (PP). The procedure where 1.0000g of titanium(IV) oxide white pigment sample and 5 ml of hydrofluoric acid is heated to 250°C for two hours was used for different types of titanium(IV) oxide white pigment's samples. The subsequent determination of elements' concentration could be easily performed, obtaining precise results. Considering this and the fact that no insurmountable troubles during performing

these analyses were observed, this dissolution procedure is proposed as the most suitable one for the subsequent trace element determination in titanium(IV) oxide white pigment.

CONCLUSION

From represented results is evident that the pressure dissolution of titanium(IV) oxide white pigment with hydrofluoric acid is undoubtedly the most suitable way of quantitative dissolution of this kind of samples. While the imperfections of the digestion method and the lithium metaborate fusion procedure could be eliminated, the only accompanied trouble with this procedure i.e. the aggressive nature of hydrofluoric acid, could easily be overcome by using the equipment from appropriate material. The precision of the pressure dissolution procedure followed by AAS method for elements' concentration determination is also acceptable and the time required for complete quantitative determination of seven elements do not exceed four hours and is therefore highly recommended as regularly used analytical procedure for trace element determination in titanium(IV) oxide white pigment samples. Moreover, it can also serve as an alternative method to routine XRF method and particularly for analysing standards for the later method.

REFERENCES

[1]   *Pigment Handbook*; John Wiley &Sons, 1988.
[2]   *Industrial Inorganic Pigment*; VCH, 1993.
[3]   Z. Šulcek, P. Povondra, *Methods of Decomposition in Inorganic Analysis*, CRC Press, 1989.
[4]   J.C. Meranger, E. Somers, *Analyst* **1968**, *93*, 799.
[5]   W. Jackson, T.S. West, *Anal. Chem.* **1973**, *45(2)*, 249.
[6]   C.W. Fuller, *Analyst* **1976**, *101*, 961.
[7]   C.W. Fuller, *Prog. Analyt. Atom. Spectrosc.* **1978**, *1*, 255.
[8]   A. Dorneman, H. Kleist, *Farbe+Lack* **1984**, *90(9)*, 750.
[9]   J.D. Norris, *Polymers Paint Colour Journal* **1988**, *178*, 816.
[10] N. Chakraborty, S.K. Roy, *Transactions of the Indian Ceramic Society* **1990**, *49(2)*, 26.
[11] I.L. Garcia, M.J.V. Martinez, M.H. Cordoba, *J. Anal. At. Spectrom.* **1991**, *6(8)*, 627.
[12] J.D. Norris, B. Preston, L.M. Ross, *Analyst* **1992**, *117*, 3.
[13] N. Majcen, *Acta Chimica Slovenica* **1993**, *40(1)*, 19.
[14] M. Tramšek, *Diploma thesis*, University of Ljubljana, 1993.
[15] *Introduction to Microwave Sample Preparation*, ACS, 1988.
[16] H.K. Worner, N. Standish, *Analyst* **1989**, *114*, 115.
[17] L.L. Jackson, T.L. Fries, J.M. Grossman, B.S.W. King, P.J. Lamothe, *Anal. Chem.* **1991**,

63,33R.

[18]   U. Bagschik, D. Quack, M. Stoeppler, *Fresenius J. Anal. Chem.* **1990**, *338*, 386.

[19]   W. Hennig, H. Berndt, G. Schaldach, *Fresenius J. Anal. Chem.* **1990**, *33*, 275.

[20]   D.C. Baxter, W. Frech, *Fresenius J. Anal. Chem.* **1990**, *337*, 253.

[21]   K.D. Ohls, *Fresenius J. Anal. Chem.* **1990**, *337*, 280.

[22]   R.E. Sturgeon, *Fresenius J. Anal. Chem.* **1990**, *337*, 538.

[23]   P. Tittarelli, C. Biffi, *Journal of Analytical Atomic Spectrometry* **1992**, *7*, 409.

[24]   J.A.C. Broekaert, *Analytical Proceedings* **1990**, *27*, 336.

[25]   A.H. van den Akker, H. van den Heuvel, *Atomic Spectroscopy* **1992**, *13(2)*, 72.

[26]   N.J. Miller-Ihli, *Atomic Spectroscopy* **1992**, *13(1)*, 1.

[27]   K.W. Jackson, *Anal. Chem* **1992**, *64*, 50R.

[28]   E. Jackwerth, S. Gomišček, *Pure&Applied Chemistry* **1984**, *56(4)*, 479.

[29]   L.L. Jackson, D.M. McKown, J.E. Taggart, Jr., P.J. Lamothe, F.E. Lichte, *Anal. Chem* **1989**, *61*, 109R.

[30]   W.T. Westbrook, R.H. Jefferson, *J. Microwave Power* **1986**, *25*.

[31]   P. Esser, *Fresenius J. Anal. Chem.* **1987**, *328*, 410.

[32]   J.R. Castillo, J. M. Mir, M.C. Martinez, T. Gomez, *Atomic Spectroscopy* **1988**, *9(1)*, 9.

[33]   N. Carrion, Z.A. de Benzo, B. Moreno, A. Fernandez, E.J. Eljuri, D. Flores, *Journal of Analytical Atomic Spectrometry* **1988**, *3*, 479.

[34]   N.J. Miller-Ihli, *Fresenius J. Anal. Chem.* **1990**, *337*, 271.

[35]   G.R. Carnrick, G. Daley, A. Fotinopoulos, *Atomic Spectroscopy* **1989**, *10(6)*, 170.

[36]   A. Morales, F. Pomares, M. de la Guardia, A. Salvador, *Journal of Analytical Atomic Spectrometry* **1989**, *4*, 329.

[37]   J.H. Trefry, S. Metz, *Anal. Chem.* **1984**, *56*, 745.

[38]   M.C. Williams, E.A. Stallings, T.M. Foreman, E.S. Glaney, *Atomic Spectroscopy* **1988**, *9(4)*, 110.

[39]   R.A. Nadkarni, *Anal. Chem.* **1984**, *56*, 2233.

[40]   C.O. Ingamells, *Anal. Chim. Acta* **1974**, *69*, 19.

[41]   N.T. Bailey, S.J. Wood, *Anal. Chim. Acta* **1974**, *69*, 19.

[42]   B. Bernas, *Anal. Chem.* **1968**, *40(11)*, 1682.

[43]   D.C. Bartenfelder, A.D. Karathanasis, *Commun. in Soil Sci. Plant Anal.* **1988**, *19(4)*, 471.

[44]   C. Feldman, *Anal. Chem.* **1983**, *55*, 2451.

[45]   C.O. Ingamells, *Anal. Chem.* **1966**, *38(9)*, 1228.

[46]   N.H. Suhr, C.O. Ingamells, *Anal. Chem.* **1966**, *38(6)*, 729.

[47]   P.L.Boar, L.K. Ingram, *Analyst* **1970**, *95*, 124.

[48]   C.W. Sill, *National Bureau of Standards Special Publication* **1976**, *422*, 463.

[49]   J.C. Miller, J.N. Miller, *Statistics for Analytical Chemistry*, Ellis Horwood Limited, Chichester, 1988.

[50]   P.C. Meier, R.E. Zund, *Statistical Methods in Analytical Chemistry*, John Wiley&Sons, 1993.

[51]   D.L. Massart, B.G.M. Vandeginste, S.N. Deming, Y. Michotte, L. Kaufman, *Chemometrics: A Textbook*, Elsevier Science Publishers, 1990.

[52]   A.I. Vogel, *A Text-book of Quantitative Inorganic Analysis*, Longmans, 1961.

[53]   B.G. Russel, J.D. Spangenberg, T.W. Steele, *Talanta* **1969**, *16*, 487.

[54]   M. Zief, J.W. Mitchell, *Contamination Control in Trace Element Analysis*, John Wiley&Sons, 1976.

POVZETEK

V članku so opisani različni postopki raztapljanja belega pigmenta titanovega(IV) oksida. Izmed izluževanja v različnih medijih, raztapljanja taline z litijevim metaboratom v klorovodikovi kislini in raztapljanja vzorca pod tlakom s fluorovodikovo kislino, se je slednji postopek izkazal kot najprimernejši, upoštevajoč pravilnost in natančnost postopka, slepe vrednosti in čas analize.

USING NETWORK INFORMATION RESOURCES IN CHEMISTRY

Primož Škulj and Peter Krajnc

Laboratory for Organic and Bioorganic Chemistry, Faculty of Chemistry and Chemical Technology, University of Ljubljana, Aškerèeva 5, Ljubljana, Slovenia

Abstract: Retrieving chemical information from local and global networks was studied. The advances in computers and their interconnections have enabled various services based on client-server approach. The possibilities of specialised information services like the Scientific and Technical Information Network providing databases as Chemical Abstracts On-line and local services were compared to global and general server platforms on World Wide Web. Fast development is obvious and hints are given for successful conduct of searches or browsing primary and secondary literature.

Introduction

Informatics has thoroughly influenced the way everyday's activities are conducted. Computers have been used for calculation, later to increase personal productivity use, for presentation and finally, communication.

Because the search for scientific literature and data is of great importance for a research worker and not much has been said about the new methods of information retrieval which have emerged, we here present some of network accessible resources for study and research work.

Chemists were amongst the earliest users of computers for generating, acquiring or searching data what could not have been done without access to remote computers i. e. networking. [1-3] The most known network is certainly the Internet, but it is merely a network which connects many WANs (Wide Area Network) and

LANs (Local Area Network). The physical connections are made by different technologies, though the core is protocol TCP/IP which packs all transmitted data into packets and routes them to the addressee. The most known tasks on the network are electronic mail, transfer of files, access to Web servers. WANs and specially the whole Internet give the possibility of accessing information on machines anywhere. [4] Today the client-server technology prevails and its widest implementation is the World Wide Web developed at CERN. [5] Different network tasks are accomplished using various protocols - language by which machines communicate. Information on the Web are retrieved by Hypertext Transfer Protocol (`http`)[6], files are sent over using File Transfer Protocol (`ftp`)[6], on most UNIX platforms the mail is routed using Simple Mail Transfer Protocol (`smtp`)[6]. URL[6] (Universal Resource Locator) for instance: `http://pubs.acs.org/hotartcl/index.html` means that the computer named `pubs.acs.org` is accesed with protocol `http` and that the requested file `index.html` can be found in directory `/hotartcl/` on that computer. Every computer on the Internet has its own IP address that correspond to its name and the task of finding it is done by the nearest Domain Name Server (DNS) – a server specially for that purpose.

The computer being rather a communication tool than a typewriter substitute, enables access to information services and databases. Information is either public and (free of charge or per-pay) available to all as the Web and Scientific and Technical Information Network (STN) or some service run locally like Intranets or services providing access to University Library databases. The mass of available information is overwhelming so strategies were devised to make them manageable. More or less complete pieces of information about one subject are either made accessible using special software (for example STN providing CA online) or by publishing it on the Web. The advantage of on-line search is clearly evident from the possibility to combine or limit searches to achieve a manageable number of hits, which one can list and browse.

We present the following network accesible services: Current Contents Service, Scientific and Technical Information Network and chemical recources and chemical journals available on the Web[7].

Current Contents Service [8]

The profusion of original papers is so great that the publications that merely list the titles and abstracts of current papers find much use. One of those is the Current Contents Physical, Chemical and Earth Sciences, which has been released weekly since 1967 and has provided data and abstracts on articles published in more than 4000 journals for exactly one year back and is available also on-line. There exist various user interfaces to browse Current Contents. With the example search for textword `fibre` we retrieved more then 700 hits and for textword `polymer*` (here is `*` used as a truncation sign so program looks for all words with the same root, for example polymeric, polymerase, polymerised,...) hits counted to few thousand, but the combination of search terms would display only articles which contain both two matches. Further limitation to *latest update*, or *list of journals* would result in perhaps ten hits, which can be displayed with title, author(s), address of the author, number and year of publication, its page and abstract.

Scientific and Technical Information Network [9]

Databases in chemistry are available from several organisations, but by far the most important one is STN International (The Scientific & Technical Information Network), a service operated jointly by CAS in North America, by the Japan Science and Technology Corporation (JST) in Asia, and by Fachinformation Zentrum (FIZ) - Karlsruhe in Germany for users in Europe. STN charges for each use, depending on databases searched, for how long and what kind of information is retrieved.

Chemical Abstracts and other databases on-line

CA On-line is counterparting the printed Chemical Abstracts. It covers all areas of chemistry, biochemistry and chemical engineering. Sources include journals, patents, technical reports, books, conference proceedings, and dissertations. Bibliographic terms, indexing terms, and CAS Registry Numbers are searchable. Over 87% of the records also contain CA abstracts, the text of which is searchable. Unfortunately database is complete only from 1967 to present, nevertheless has many advantages.

Not only is it a great deal faster, but one can do kinds of searches online that are simply not possible using only the printed volumes. Furthermore, online files are regularly updated so one finds information well past the appearance of the latest semi-annual indexes, even before the library has received the last issue of CA. Nevertheless, CA File is just one of the many databases provided by STN; they have established a comprehensive supply of databases in science and technology. For references prior to 1967 there is a file CAOLD, which contains 695.000 records for the period from 1957-1966. Other important databases include: BEILSTEIN, which contains organic chemical structures, preparation and reaction information, and numeric property data. The source for the BEILSTEIN database is the Beilstein Handbook of Organic Chemistry; REGISTRY File is a chemical structure and dictionary database that contains unique substance records identified by the Chemical Abstracts Service (CAS) Registry System. Each record contains the CAS Registry Number, CA index name, commonly used synonyms, a structure diagram, and a molecular formula, all of which are searchable. Substances containing rings may be retrieved using ring system data; alloys may be retrieved using alloy composition information; and protein and nucleic acid sequences may be retrieved using codes for the amino acids or nucleotides; CASREACT contains information on reactions of organic substances, including organometallics and biomolecules, it also contains single and multi-step reaction information for reactants, products, reagents, solvents, and catalysts. The source for CASREACT is the Chemical Abstracts Organic Sections (21-34). [2,9,10]

A Messenger - common command language is used in all databases, though its major disadvantage is that it is almost fully command line oriented and allows no intuitive user interface. Free access to some of online learning databases is available on `telnet://a45.fiz-karlsruhe.de:4050`. It is limited to fifteen minutes and maximally 5 simultaneous users but allows one to learn basic commands and search strategies. Once connected to STN and with selected database one is presented with a command prompt to enter the query. With the command `SEARCH BENZENE` in learning database LBEILSTEIN we have got the answer:

```
L1 1678 BENZENE
```

The L1 means that this is line 1, the 1678 means that system has 1678 abstracts that contain word benzene. The word may be in the title, an index entry or a keyword. Compounds can be also searched for by using the Registry number. To display the first three matches for benzene one enters the command

```
DISPLAY L1 1-3
```

It is possible to specify the output format (bibliographical data, text of the abstract, abstract number only...).

The real power of online searching is its ability to combine and filter different queries. Operators of Boolean algebra (AND, NOT, OR) provide useful mean to extract the information needed. Instead of querying many words with single root, one can truncate the search term and get all the matches at once. There is no need to search several annual and monthly volumes because databases are unity as a whole. On the other hand it is possible to limit the search only to specific area, time period, journal, etc.

An alternative to terminal accessed STN International is STN Easy which provides point-and-click access to STN International. STN Easy operates through World Wide Web[9] and has two modes of searching; Basic Search - the easiest way to locate relevant answers by simple keyword searching and Advanced Search with greater flexibility in setting search criteria for author searches, Boolean operators, index browsing, etc.

World Wide Web

More than ten years ago an idea was persuived at CERN laboratories, Switzerland, to establish a common mean of accessing data on different computers running different software platforms [5]. Such tasks are usually achieved using server-client technologies, meaning that users retrieving information run client software on their machines and computer they are accessing is running server software. A client is equipped with what is needed to process and display data received from the server. Such system has many advantages; it lowers the burden (the needed bandwidth) on network connection and also on the server, because server processor power is not used for the displaying and formatting.. `Http` protocol [6] is the basis for WWW (World

Wide Web); a network of servers which can be all accessed from any computer. With WWW there is no need for specialised client software, a Web browser is sufficient. Fast development of the Internet can be illustrated by the number of computers, connected to Internet, which exceeded the 10.000 mark in 1987, 100.000 in 1989 and 1.000.000 in 1992.[11] While in January 1996 over 1000 servers, dealing with chemistry, existed[3], over 277.000 sites were found in January 1998 using the AltaVista search engine. This information clearly shows the rapid increase in the use of Internet as an information source for a scientific worker. As the number is huge we reviewed some of them and summarised the ones for which we think are most resourceful. In *Table 1* we list their URLs. Due to the numerous links they offer one can explore further on the Web to find the sites and topics of specific interest. Sites accessed frequently can be bookmarked [12] easily by most browsers.

Table 1: URLs of chemical sites on the Internet

• **University of Hertfordshire**	`http://www.herts.ac.uk/lrc/subjects/natsci/chem/chemweb/`
• **American Chemical Society**	`http://www.acs.org/`
• **Royal Society of Chemistry**	`http://www.rsc.org/`
• **University of Sheffield**	`http://www.shef.ac.uk/chemistry/chemdex/`
• **Chemcenter**	`http://www.chemcenter.org/`
• **Tennessee State University**	`http://acad.tnstate.edu/~chemnet/www.html`
• **Department of Chemistry, Imperial College of Science, Technology and Medicine, London**	`http://www.ch.ic.ac.uk/`
• **Faculty of Chemistry and Chemical Technology, University of Ljubljana**	`http://www.uni-lj.si/www/kem/`
• **Faculty of Chemistry and Chemical Engineering, University of Maribor**	`http://www.uni-mb.si/new/fkkt/okv_an.htm`
• **Slovenian Chemical Society**	`http://www.kemijsko-drustvo.ki.si/`
• **Slovenian National Institute of Chemistry**	`http://www.ki.si/`

Chemical journals on the Web [13]

Staying in touch with the latest developments in the field of research is of great importance for a scientific worker. Libraries have thus always been a special place for a scientist. However, with a growing number of journals on line [14], classical libraries are losing a bit of magical atmosphere since the computers are winning the battle of access speed and, even more important, most publishers now offer their own search engines to facilitate efficient or specific information retrieval. An article, dealing with one's topics of interest, can therefore quickly be located and viewed. Typical time of access to a bookmarked journal would be less than a minute provided the local net and server are not very crowded. In *Table 2* URLs of some renowned chemical journals are summarised.

Table 2: URL's of some chemical journals

• **Journals published by the Am. Chem. Soc.** (J. Org. Chem., J. Am. Chem. Soc., Chem. Rev., …)	`http://pubs.acs.org/`
• **Chemical Communications**	`http://www.rsc.org/is/journals/current/ chemcomm/cccpub.htm`
• **Tetrahedron Information System** (Tetrahedron, Tetrahedron Lett., …)	`http://oxford.elsevier.com/tis/`

To access most of them, a username and a password are required, while some are at the moment still free of charge. Most of the journals offer their articles as both: HTML (Hypertext Markup Language) and PDF (Portable Document Format) [15], of which the later enables the viewer [16] to view on the monitor and print the pages exactly as they appear in the printed form of journal, which is of course important for schemes, tables and figures. In February 98, 387 chemical journals were found available on line [17], some of them complete, while others only with abstracts of articles. At `http://www.chemconnect.com/library/journals.shtml` there are links to probably all chemical journals on line. Advantage of following journals on-line can be clearly demonstrated by ASAP (As Soon as Publishable) service of American Chemical Society publishing peer-reviewed journal articles 2-11 weeks

before they appear in the print journal. Recently some journals emerged, published only on-line, without the printed version.[18]

Conclusion

Scientists have always stridden for an immediate access to scientific literature. The technological advances have enabled steady improvements and the advent of World Wide Web has rekindled popular interest in those issues. Traditionally the information retrieval was a task for professional librarians, who conducted the searches and reported results to querying scientists. The rise of the Internet has made most of the mediators obsolete and access to databases is enabled to a wider audience. Today the state of technology allows users to interact effectively with information distributed across the network. Network information systems in various forms support search and retrieval of items from organised collections. In their historical evolution, the mechanisms for retrieval of scientific literature have been particularly important. With move from syntactic to semantic and searching concepts rather then words the utilisation of network resources is becoming more pertinent and user friendly.

References and notes

[1]   B. R. Schatz, *Science* **1997**, *275*, 327-334
[2]   D.D. Ridley, *Online Searching: A Scientist's Perspective*; John Wiley and Sons, New York, **1996**
[3]   P. Murray-Rust, H. S. Rzepa, B. J. Whitaker. *Chem. Soc. Rev.* **1997.** *26*, 1-10
[4]   O. Kirch, *Linux Network Administrator's Guide,* **1996**, *http://www.linux.org*
[5] B. Segal, *http://wwwcn.cern.ch/pdp/ns/ben/TCPHIST.html*
[6]   Used terms are defined in request for comments (RFC) documents which are accessible at
      ftp://ftp.arnes.si/standards/ftp
      http - Hypertext Transfer Protocol (RFC 2068, RFC 1945), ftp - File Transfer Protocol (RFC 430),
      smtp Simple Mail Transfer Protocol (RFC 876), url - Universal Resource Locator (RFC 1738)
[7]   Popularity and simplicity of the Web are resulting in more and more services becoming reachable
      and searchable by an Web browser.
[8]   Institute for Scientific Information *http://www.isinet.com*
[9]   Fachinformationzentrum Karlsruhe *http://www.fiz-karlsruhe.de/*
[10] J. March, *Advanced Organic Chemistry*; John Wiley and Sons, New York, **1992**
[11] S. M. Bachrach (Ed.), *The Internet: A Guide For Chemists*, American Chemical Society, **1995**
[12] To *bookmark* a site is to store its URL adress on your computer's harddisk so you can later access
      this site without typing its URL adress.
[13] *Web* and *Internet* are both mistakenly often used to describe only the World Wide Web.
[14] On-line journals is an accepted phrase for journals appearing in an electronic form accesible via the
      Internet.

[15] PDF is a format developed to create and edit cross-platform documents by Adobe Systems Incorporated *http://www.adobe.com/*

[16] The word *viewer* instead of *reader* was used to distinguish between reading a printed article and article appearing on the computer screen.

[17] *http://www.chemconnect.com/library/journals.shtml*

[18] *http://www.ijc.com/*

Povzetek: Vzpostavitev računalniških omrežij je omogočila dostop do različnih novih ali spremenjenih virov informacij. Predstavila sva informacijske servise, namenjene prvenstveno kemikom. Informacijski viri, dostopni raziskovalcem, so bodisi lokani ali globalni. Pregledala sva njihove lastnosti in uporabo ter podala nekaj napotkov za uspešno iskanje infromacij iz omrežnih virov.

^{31}P-NMR CHARACTERIZATION OF CHAIN ENDS IN POLYMERS AND COPOLYMERS PREPARED USING LUCIRIN TPO AS A PHOTOINITIATOR

Robert E. Medsker, Manuel Chumacero, Everett R. Santee,

Anton Sebenik[†] and H. James Harwood[*]

Maurice Morton Institute and Department of Polymer Science

The University of Akron, Akron, Ohio 44325-3909

Abstract: ^{31}P-NMR spectra of polymers and copolymers prepared from styrene, substituted styrenes, methyl methacrylate and methyl acrylate using diphenyl(2,4,6-trimethylbenzoyl)phosphine oxide (Lucirin TPO) as a photoinitiator are interpreted and analyzed. The spectra provide information about the structures and configurations of phosphorus-containing end groups. The relative amounts of various chain ends present in TPO-initiated copolymers correspond well with the relative amounts of monomers employed in copolymerizations, indicating that photogenerated diphenylphosphine oxide radicals are nonselective in reactions toward the monomers investigated. This result is consistent with the high reactivity reported previously for diphenylphosphine oxide radicals but is not in agreement with the results of time-resolved ESR measurements, which indicate that the diphenylphosphinyl radical is more reactive toward methyl methacrylate than toward styrene by a factor of 1.45.

INTRODUCTION

Acylphosphine oxides and acylphosphonate esters are very effective photoinitiators for vinyl monomer polymerizations, [1-4] but little is known about the chemoselectivity, regioselectivity or stereoselectivity of phosphorus-centered radicals that are de-

---

rived from them. Information of this sort can be obtained from the ^{31}P-NMR spectra of polymers and copolymers that are derived from such radicals, in much the same way that ^{13}C-NMR studies on polymers and copolymers derived from ^{13}C-enriched initiators have provided such information. [5-7] In this paper, the ^{31}P-NMR spectra of polymers and copolymers that were prepared using diphenyl(2,4,6-trimethylbenzoyl)phosphine oxide (Lucirin TPO) **1** as a photoinitiator are reported and analyzed. This initiator generates a diphenylphosphine oxide radical and a 2,4,6-trimethylbenzoyl radical when irradiated with visible light (Equation 1). Both radicals can initiate polymerization, but based on the

$$\phi_2\overset{O}{\overset{\|}{P}} - \overset{O}{\overset{\|}{C}} - \langle\bigcirc\rangle\overset{CH_3}{\underset{CH_3}{}} - CH_3 \xrightarrow{h\nu} \phi_2\overset{O}{\overset{\|}{P}}\cdot + \cdot\overset{O}{\overset{\|}{C}} - \langle\bigcirc\rangle\overset{CH_3}{\underset{CH_3}{}} - CH_3 \qquad (1)$$

$$\mathbf{1}$$
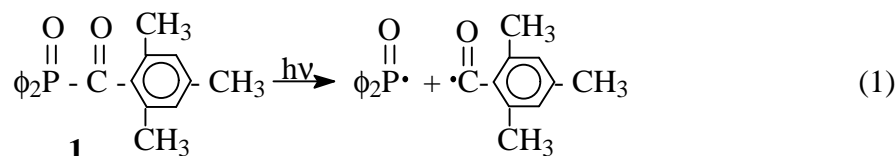
extremely high reactivity of phosphorus-centered radicals, [2,3] compared to carbon-centered radicals, a large proportion of the polymers can be expected to contain diphenylphosphine oxide groups at their chain ends.

If a monomer can be represented by the general structure **2**, many possible chain end structures can be considered. Initiation of polymerization by addition of the unsubstituted or substituted (Equations 2 and 3) ends of the monomer double bond can result in several structures for each mode of addition, if account is taken of the configuration of the monomer-monomer placement that follows the initiation step.

$$\phi_2\overset{O}{\overset{\|}{P}}\cdot + CH_2 = \overset{A}{\underset{B}{C}} \longrightarrow \phi_2\overset{O}{\overset{\|}{P}} - CH_2 - \overset{A}{\underset{B}{C}} - CH_2 - \overset{A}{\underset{B}{\underset{m}{C}}} \text{\scriptsize www} \qquad (2)$$

$$\mathbf{2}$$

$$\text{or}$$

$$\phi_2\overset{O}{\overset{\|}{P}} - CH_2 - \overset{A}{\underset{B}{C}} - CH_2 - \overset{B}{\underset{A}{\underset{r}{C}}} \text{\scriptsize www}$$

$$\phi_2\overset{\overset{\displaystyle O}{\|}}{P}\cdot \;+\; CH_2 = \underset{\underset{B}{}}{\overset{\overset{A}{}}{C}} \longrightarrow \phi_2\overset{\overset{\displaystyle O}{\|}}{P} - \underset{\underset{B}{|}}{\overset{\overset{A}{|}}{C}} - CH_2 - CH_2 - \underset{\underset{B}{|}}{\overset{\overset{A}{|}}{\underset{m}{C}}} \text{\scriptsize www} \tag{3}$$

$$\text{or}$$

$$\phi_2\overset{\overset{\displaystyle O}{\|}}{P} - \underset{\underset{B}{|}}{\overset{\overset{A}{|}}{C}} - CH_2 - CH_2 - \underset{\underset{A}{|}}{\overset{\overset{B}{|}}{\underset{r}{C}}} \text{\scriptsize www}$$
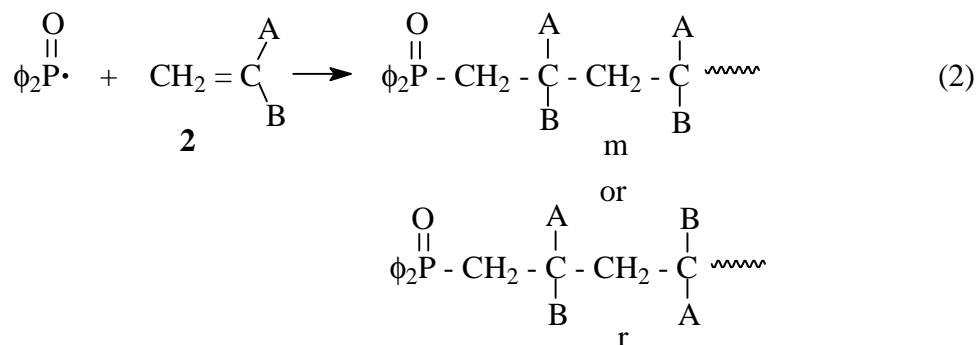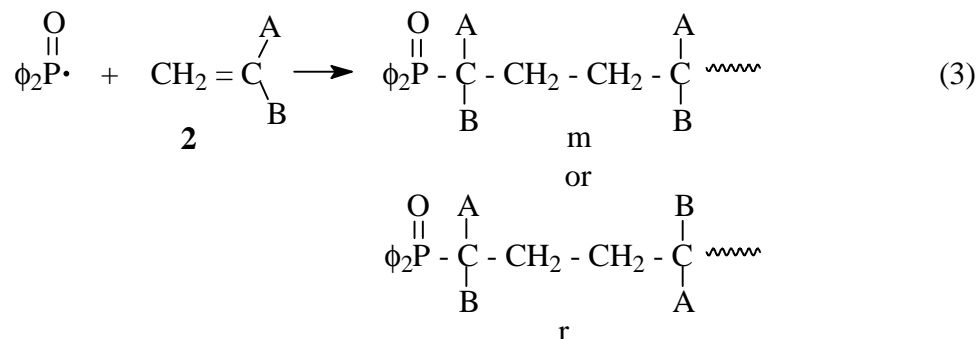
These various configurations will be termed meso (m) and racemic (r), just as they would be if they occurred in the center of the polymer chain. It should be noted that the second monomer placement in such structures is considered to have resulted from addition of a propagating monomer radical to the unsubstituted end of the second monomer, which is the predominant if not almost exclusive mode of propagation when vinyl monomers are polymerized.

In addition, propagating polymer radicals can be terminated by reaction with the diphenylphosphine oxide radical (primary radical termination) (Equation 4) or perhaps by chain transfer with initiator (induced decomposition of initiator) (Equation 5) to yield other chain ends, as shown below.

$$\phi_2\overset{\overset{\displaystyle O}{\|}}{P}\cdot \;+\; \cdot\underset{\underset{B}{|}}{\overset{\overset{A}{|}}{C}} - CH_2 \text{\scriptsize www} \longrightarrow \phi_2\overset{\overset{\displaystyle O}{\|}}{P} - \underset{\underset{B}{|}}{\overset{\overset{A}{|}}{C}} - CH_2 - \underset{\underset{\underset{m}{B}}{|}}{\overset{\overset{A}{|}}{C}} - CH_2 \text{\scriptsize www} \tag{4}$$

$$\text{or}$$

$$\phi_2\overset{\overset{\displaystyle O}{\|}}{P} - \underset{\underset{B}{|}}{\overset{\overset{A}{|}}{C}} - CH_2 - \underset{\underset{\underset{r}{A}}{|}}{\overset{\overset{B}{|}}{C}} - CH_2 \text{\scriptsize www}$$

$$\phi_2\overset{\overset{\displaystyle O}{\|}}{P}\text{-}\overset{\overset{\displaystyle O}{\|}}{C}\text{-}\underset{CH_3}{\overset{CH_3}{\langle\bigcirc\rangle}}\text{-}CH_3 + \cdot\underset{\underset{B}{|}}{\overset{\overset{A}{|}}{C}}\text{-}CH_2 \text{\scriptsize www} \longrightarrow \phi_2\overset{\overset{\displaystyle O}{\|}}{P}\text{-}\overset{\overset{A}{|}}{C}\text{-}CH_2\text{-}\underset{\underset{m}{B}}{\overset{\overset{A}{|}}{C}} CH_2 \text{\scriptsize www} + \cdot\overset{\overset{\displaystyle O}{\|}}{C}\text{-}\underset{CH_3}{\overset{CH_3}{\langle\bigcirc\rangle}}\text{-}CH_3 \tag{5}$$

$$\text{or}$$

$$\phi_2\overset{\overset{\displaystyle O}{\|}}{P}\text{-}\overset{\overset{A}{|}}{C}\text{-}CH_2\text{-}\underset{\underset{r}{A}}{\overset{\overset{B}{|}}{C}} CH_2 \text{\scriptsize www} + \cdot\overset{\overset{\displaystyle O}{\|}}{C}\text{-}\underset{CH_3}{\overset{CH_3}{\langle\bigcirc\rangle}}\text{-}CH_3$$
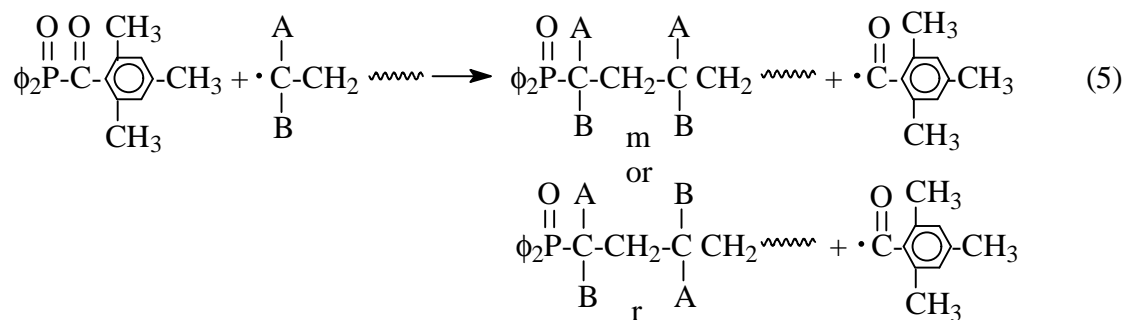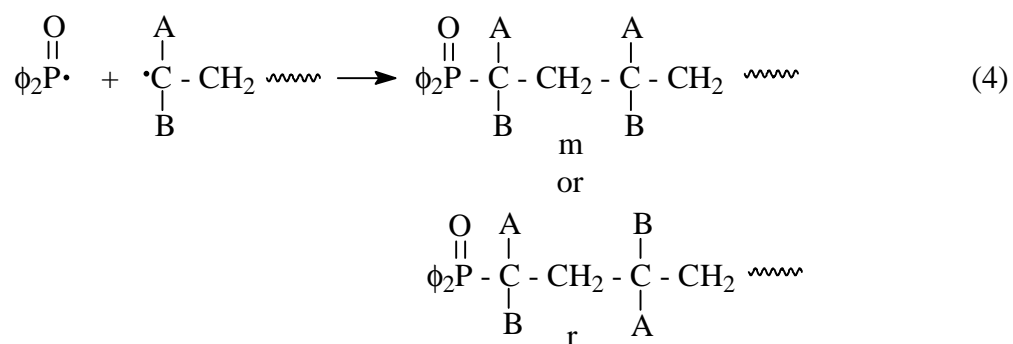
It should be noted that the structures of the chain ends that result from Equations 4 and 5 are different than those that result from Equation 3.

When the ^{31}P-NMR spectra of copolymers prepared from TPO-initiated polymerizations are considered, end group structures such as are outlined above must be considered for each monomer. In addition structures involving the two monomers that constitute the terminal monomer-monomer dyad must also be considered. Many different types of phosphorus-containing chain ends may thus be present in polymers and copolymers prepared by TPO-initiated polymerization. The purpose of this paper is to demonstrate that the resonances of many such chain ends can be distinguished by high field ^{31}P-NMR spectroscopy and that useful chemical information can be obtained from their relative intensities.

EXPERIMENTAL

Monomers were obtained from commercial sources and were purified by a two-fold washing with equal volumes of 1 N NaOH followed by a two-fold washing with equal volumes of distilled water. They were then dried over calcium hydride, distilled under reduced pressure and stored in a refrigerator. Prior to use, monomers were tested for the presence of polymer by adding a portion to an excess of a precipitant for the polymer. Only polymer-free monomer was used for polymerization experiments.

Diphenyl(2,4,6-trimethylbenzoyl)phosphine oxide, (Lucirin TPO) was generously supplied by the BASF Corporation and used as received.

TPO-initiated polymerizations and copolymerizations were conducted in bulk in clear one-ounce bottles under nitrogen. Each polymerization mixture contained 3.5 mole percent TPO. The bottles were sealed with rubber septa and were irradiated with light from a tungsten lamp. The lamp was placed sufficiently far from the bottles that the polymerization mixtures did not exceed 30ºC. Homopolymerizations were allowed to proceed to high conversion (~ 3 hr.) but copolymerizations were limited to below 5 percent conversion. The polymerization mixtures were poured into a large volume of methanol to precipitate the polymers. These were then reprecipitated three times from THF solution into methanol. All polymers were then dried at 60º in vacuo.

Polymerization of MMA by Group Transfer Polymerization and Termination with Di-
phenylphosphinic Chloride

A mixture containing freshly dried (12 hr. @ 260ºC) zinc chloride (5.5 g), dry tolu-
ene (15 ml) and methyl methacrylate was allowed to stir for fifteen minutes and then
treated with methyl trimethylsilyl dimethylketene acetal. After being allowed to stir for
45 minutes, a portion of the reaction mixture was added to an excess of diphenylphos-
phinic chloride. The reaction mixture was poured into methanol to precipitate the poly-
mer. It was then reprecipitated twice from THF solution into methanol. The Mn of this
polymer, as measured by GPC, was 18,000 and it contained 0.67 weight percent phos-
phorus.

Polymerization of MMA Initiated by the Lithium Salt of Diphenylphosphine Oxide

Diphenylphosphine oxide (0.5 g, 0.0025 moles) was treated with a stoichiometric
amount (1.5 ml) of a 1.6 M solution of n-butyl lithium in hexane under a nitrogen blan-
ket. [8] The reaction mixture was vigorously stirred at room temperature and a yellow
solid rapidly formed. A solution of methyl methacrylate (0.5 g) in dry THF was then
added dropwise into the reaction mixture. After 45 minutes, the solution was concen-
trated by evaporation in vacuo and poured into methanol to precipitate the polymer. The
crude polymer (0.27 g, 54% yield) was precipitated twice from THF solution into
methanol and then dried at 45ºC in a vacuum oven overnight. Gel permeation chroma-
tography indicated the polymer to have a number average molecular weight of 30,000.
The polymer contained 1.14 weight percent phosphorus.

Reaction of Polystyryllithium with Diphenylphosphinic Chloride

A solution of polystyryllithium in benzene (3% v/v, 100 ml), kindly provided by Dr.
Thomas J. Lynch, was gradually treated with diphenylphosphinic chloride until the
characteristic orange color of the lithiated polymer disappeared. The solution was
evaporated to dryness using a rotatory evaporator and the residue was dissolved in THF.
The solution was added to methanol to precipitate the polymer, which was then repre-
cipitated twice from THF solution into methanol and dried in a vacuum oven overnight at
40ºC.

Reaction of Polystyrene with Diphenylphosphinic Chloride

A mixture of polystyrene (0.2 g, 0.0019 moles of repeat groups), diphenylphosphinic chloride (0.34 g, 0.0026 moles), aluminum chloride (1.0 g, 0.0077 moles) and carbon tetrachloride was stirred at 75ºC for one hour under nitrogen. It was then poured into 40 ml methanol to precipitate the polymer. This was dried overnight in a vacuum oven at room temperature.

Phosphorus NMR Spectroscopy

Phosphorus NMR measurements were performed on samples in $CDCl_3$ using a Varian XL-400 spectrometer operating at a resonance frequency of 161.91 MHz. A 90º pulse, a 0.3 second acquisition time, 30012 data points and a 2 second delay between acquisitions were employed with 15,000 – 20,000 transients being acquired for each spectrum. Polymer solution concentrations were 10 – 15% (w/v). Each sample contained 3 mg of Lucirin TPO which was employed as an internal standard. The chemical shift of Lucirin TPO, relative to 85% ortho phosphoric acid was 11.0 ppm.

Elemental Analyses

Phosphorus analyses were performed by Galbraith Microanalytical Laboratories, Knoxville, Tennessee.

RESULTS AND DISCUSSION

TPO-Initiated Poly(Methyl Methacrylate)

Figure 1A shows the ^{31}P-NMR spectrum of a PMMA sample that was prepared by TPO-initiated polymerization. This sample had a Mn of 102,000 as measured by gel permeation chromatography and a phosphorus content of 0.029 weight percent. These values indicate that there is an average of almost exactly one phosphorus-containing chain end group per chain. The spectrum contains two signals having relative intensities of 0.30 and 0.70 in order of increasing field. There is much evidence to indicate that these signals are due to chain ends that result from initiation and not termination processes. For example, this same spectrum is observed for a PMMA sample prepared by TPO-initiated polymerization in the presence of a large amount (10 mole percent) of 1-octylmercaptan. Under such conditions, propagating PMMA radicals can be expected to

terminate almost entirely by chain transfer. There should be almost no opportunity for them to terminate by combining with a diphenylphosphine oxide radical. Similarly, PMMA prepared by AIBN-initiated polymerization in the presence of diphenylphosphine oxide, a powerful transfer agent that is a source of diphenylphosphine oxide radicals, exhibits the same ^{31}P-NMR spectrum as the polymer prepared by TPO-initiated polymerization. In addition, polyMMA prepared anionically using the lithium salt of diphenylphosphine oxide as initiator also exhibits resonances that have the same chemical shift as those in the spectra of the polymers prepared by radical polymerization. However, as can be seen in Figure 1B, the relative intensities of the resonances are different for polymers initiated by diphenylphosphine oxide radicals or anions. Finally, the ^{31}P-NMR spectrum of PMMA prepared by group transfer polymerization and terminated by reaction with diphenylphosphinic chloride (Figure 1C) contained a single resonance at 26.6 ppm, considerably downfield from the resonances (24.3 and 25.0 ppm) of PMMA initiated by diphenylphosphine oxide radicals or anions. Collectively, these results strongly indicate that the resonances at 24.3 and 25.0 ppm are attributable to chain ends that resulted from reaction 2 (A = -CH$_3$, B = -COOCH$_3$). Due to the substantial steric hindrance associated with their formation, chain ends that would result from reaction 3 are not considered likely.
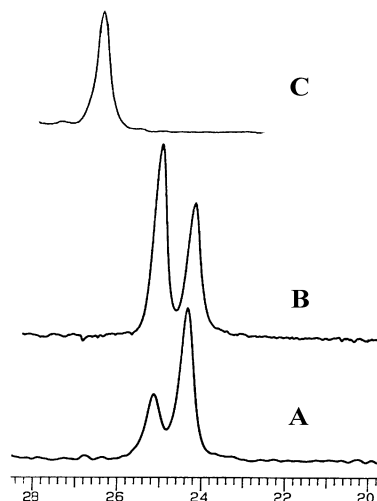
Figure 1. ^{31}P-NMR Spectra of PolyMMA Samples Prepared by TPO-Initiated Polymerization (A), by φ$_2$P(0)Li-Initiated Polymerization (B), and by Group Transfer Polymerization Followed by Termination with φ$_2$P(0)Cl (C).

It seems reasonable to attribute the lower field ^{31}P resonance (25.0 ppm) to ϕ_2P(0)-ends that are connected to MMA units that, in turn, are bound by meso placements to adjacent MMA units. Similarly, the upper field resonance (24.3 ppm) can be attributed to ϕ_2P(0)-ends that are connected to racemic MMA-MMA dyads. These assignments are made because of the similarity of the relative intensities of the resonances to the relative amounts of meso and racemic enchainments in the polymers, as estimated in the classical way [9] from the methyl proton or methyl carbon resonances of the polymers. For example, in the spectra of the ϕ_2P(0)• radical initiated samples, the lower field ^{31}P-resonance accounts for 0.30 of the total ^{31}P-resonance and the meso content of the polymers, as estimated from their methyl proton resonance pattern, is 0.22. In the spectrum of the ϕ_2P(0)Li initiated polymer, the lower field ^{31}P-resonance accounts for 0.55 of the total and the meso content of the polymer, as measured by ^{1}H-NMR is 0.58.

TPO-Initiated Polystyrene

Figure 2A shows the ^{31}P-NMR spectrum of TPO-initiated polystyrene. It contains two major (27.6 and 28.0 ppm) and two minor (30.3 and 30.9 ppm) resonances. The resonance at 27.6 ppm corresponds well with the resonance observed in the spectrum (Figure 2B) of the polymer obtained by terminating polystyryllithium with diphenylphosphinic chloride as shown by Equation (6). This suggests that it can be attributed to chain ends that contain the ϕ_2P(0)-group attached to the head of a styrene unit (resulting from reactions 3, 4 or 5 with A = H and B = C_6H_5). Since the relative intensity of the resonance is the same in Figure 2A as in the spectrum (Figure 2C) of polystyrene prepared using diphenylphosphine oxide as a chain transfer agent, this resonance is attributed to chain ends that resulted from initiation reactions (Equation 3). Resonance at 28.0 ppm is attributed to chain ends that resulted from addition of diphenylphosphinyl radicals to the unsubstituted carbon of styrene (Equation 1, A = H, B = C_6H_5). These assignments are supported by results obtained in a 3D – H,C,P-NMR study of polystyrene prepared using diphenylphosphine oxide as a chain transfer agent. [10]

$$\text{Bu-(CH}_2\text{CH)}_n\text{CH}_2\text{CHCH}_2\text{CHLi} \ + \ \phi_2\overset{\overset{\text{O}}{\|}}{\text{P}}\text{Cl} \longrightarrow \text{Bu-(CH}_2\text{CH)-CH}_2\text{CHCH}_2\text{CHP}\overset{\overset{\text{O}}{\|}}{\phi_2} \qquad (6)$$
$$\phi \qquad \phi \qquad \phi \qquad\qquad\qquad \phi \qquad \phi \qquad \phi$$
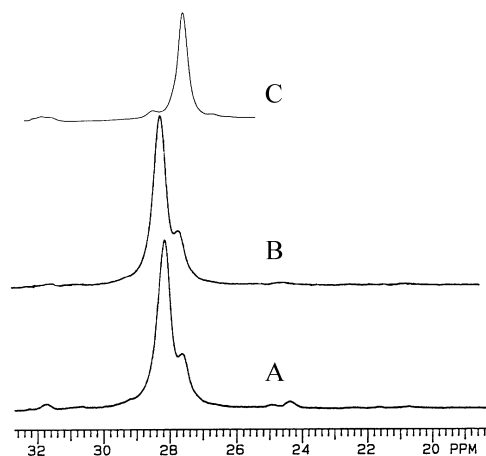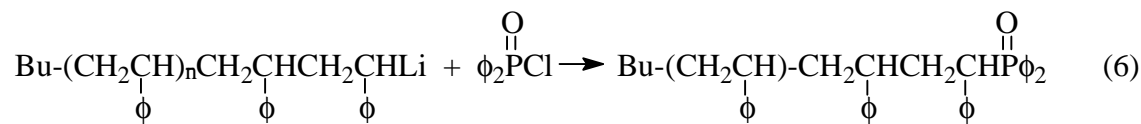
Figure 2. ^{31}P-NMR Spectra of Polystyrene Samples Prepared by TPO-Initiated Polymerization (A), by Using ϕ_2P(0)H as a Chain Transfer Agent (B), and by BuLi-Initiated Polymerization followed by Termination with ϕ_2P(0)Cl (C).

Two of the minor resonances (30.4 and 31.7 ppm) observed in Figure 2A are attributed to ϕ_2P(0)-groups attached to aromatic rings of styrene units, since polystyrene that was diphenylphosphinylated by reaction with diphenylphosphinic chloride and aluminum chloride (Equation 7) also exhibits resonances in those regions. Resonance at 30.4 ppm is attributed to m-substituted rings and that at 31.7 is attributed to p-substituted ones.

$$\sim\!\!\sim\!\!\sim \text{CH}_2\text{CH}\sim\!\!\sim\!\!\sim \xrightarrow[\text{AlCl}_3]{\phi_2\text{P(0)Cl}} \sim\!\!\sim\!\!\sim \text{CH}_2\text{CH}\sim\!\!\sim\!\!\sim \qquad (7)$$
$$\phi \text{ - } \overset{\phi}{\underset{\phi}{\text{P}}} = 0$$
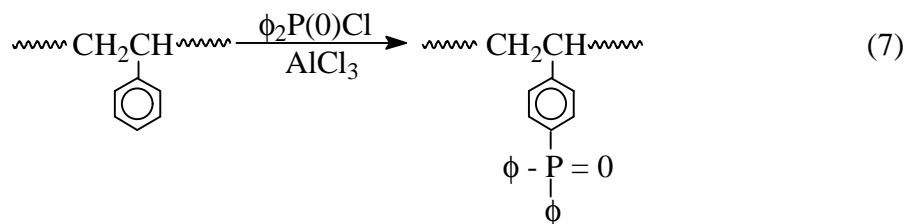
Based on the relative intensities of these resonances, it is estimated that diphenyl-phosphinyl radicals add to the unsubstituted and substituted ends of styrene 85- and 15-percent of the time, respectively. In addition, instead of initiating polymerization, approximately 5 percent of the radicals attack the aromatic rings of styrene or of styrene units. These values are to be compared to results of Solomon et al [11] who reported a 13:1 preference of the benzyloxy radical to add to the tail end of styrene and a relatively strong tendency of this radical to attack the aromatic rings of styrene or styrene units.

The lower selectivity of the diphenylphosphinyl radical compared to the benzyloxy radical with respect to the mode of addition to styrene may reflect the greater reactivity of the former. The ^{31}P-NMR spectra of TPO-initiated poly(p-methoxystyrene) end of poly(p-chlorostyrene) were very similar to that of TPO-initiated polystyrene. These spectra, along with the spectra of TPO-initiated poly(methyl acrylate) are shown in Figures 3, 4 and 5 along with spectra of their copolymers with MMA.
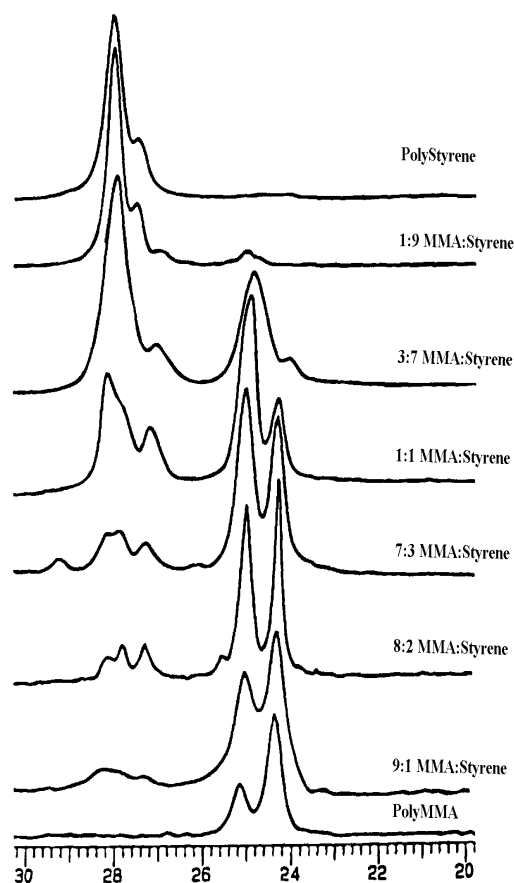
Figure 3. ^{31}P-NMR Spectra of MMA-Styrene Copolymers Prepared by TPO-Initiated Polymerization.

TPO-Initiated Copolymers

Since the chemical shifts of $\phi_2P(0)$-groups attached to styrene, substituted styrene or methyl acrylate units (26.4 – 29.0 ppm) and MMA units (23.5 – 26.2 ppm) are appreciably different, it is possible to measure the relative amounts of $\phi_2P(0)$-groups attached to styrene, substituted styrene or methyl acrylate and MMA units in copolymers initiated

by diphenylphosphinyl radicals. This will be discussed in detail for copolymers of styrene and MMA.

Figure 3 shows the ^{31}P-NMR spectra of polystyrene, polyMMA and a series of styrene-MMA copolymers that was prepared by TPO-initiated polymerization. The resonance between 26.5 and 29.0 ppm, decreases in relative proportion as the styrene content of the copolymers decreases and is taken as a measure of the ϕ_2P(0)-groups attached to styrene ends. The resonance between 23.5 and 26.0 ppm increases as the MMA content of the copolymers increases and is taken as a measure of the ϕ_2P(0)-groups attached to MMA ends. Taking A_S and A_{MMA} as the relative proportions of resonance observed at 26.5 – 29.0 and 23.5 – 26.0 ppm, respectively, the A_S/A_{MMA} ratio can be related to the relative reactivity of styrene and MMA toward the ϕ_2P(0)• radical, k_S/k_{MMA}, and the molar ratio of styrene to MMA in the copolymerization mixture, [S]/[MMA], as follows:

$$A_S/A_{MMA} = (k_S/k_{MMA}) \bullet [S]/[MMA] \tag{8}$$

According to this relationship, a plot of A_S/A_{MMA} versus [S]/[MMA] should be a straight line having a slope equal to k_S/k_{MMA}. Figure 4 shows such a plot. The slope of the plot is 1.0, indicating that the ϕ_2P(0)• radical shows the same reactivity for styrene and MMA. Similar results were obtained in studies on copolymers of MMA with p-chlorostyrene, p-methoxystyrene and methyl acrylate that were initiated by TPO. The ^{31}P-NMR spectra of the copolymers are shown in Figures 5-7 and the percentages of ϕ_2P(0)-MMA ends in the copolymers are compared with the percentages of MMA in the polymerization mixtures in Table 1. In all cases, there is excellent correspondence between the two percentages, indicating that the ϕ_2P(0)• radical is completely unselective in its reactions with MMA, methyl acrylate and substituted styrenes. This is believed to be a consequence of its high reactivity.
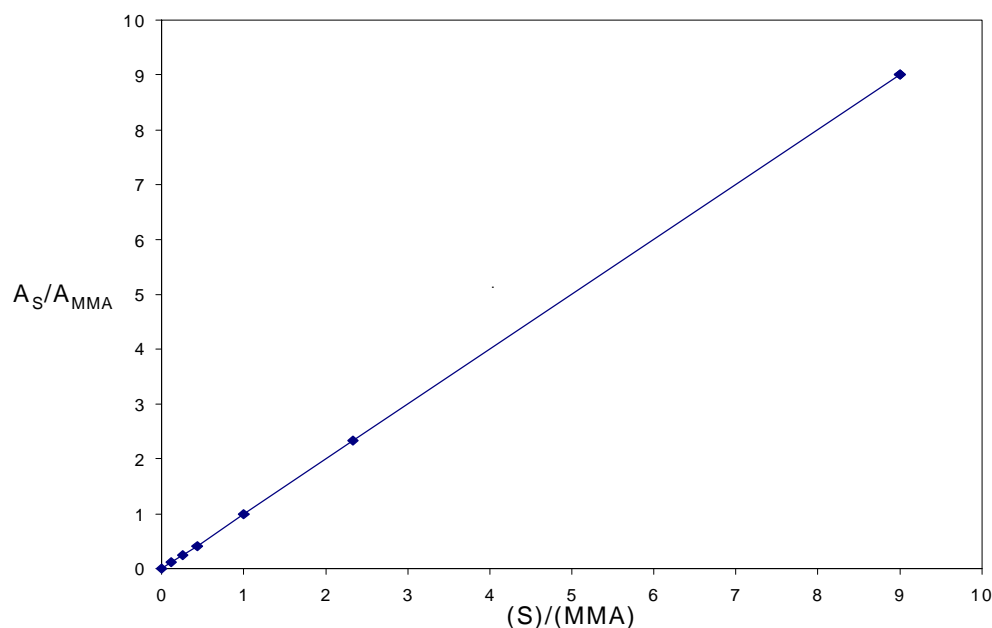
Figure 4. Plot of A_S/A_{MMA} versus $(S)/(MMA)$.

Table 1: Percentage of $\phi_2P(0)$-MMA End Groups in Copolymers Derived from Lucirin TPO-Initiated Polymerizations

Mole % MMA in Monomer Mixture	Mole % $\phi_2P(0)$-MMA End Groups			
	Styrene[a]	4-Chlorostyrene[a]	4-Methoxystyrene[a]	Methyl Acrylate[a]
90	90	90	90	91
80	80	---	80	79
70	71	70	70	69
50	50	50	50	---
30	30	30	30	32
10	10	10	11	---

[a]Comonomer, conversions below 5% in all cases.

Referring back to Figure 3, the resonance of $\phi_2P(0)\bullet$ groups attached to MMA ends (23.5 – 26.0 ppm) consists of two general areas that vary in relative intensity as the MMA content of the copolymers changes. The resonance observed between 24.7 and 26.0 ppm in the spectrum of the MMA homopolymer can be attributed to $\phi_2P(0)$-MMA-

MMA chain ends having meso configurations, as was explained earlier. However, this resonance area increases in intensity relative to that of the resonance observed from 23.5 – 24.7 ppm, as the proportion of styrene in the copolymer increases. In fact, it is the
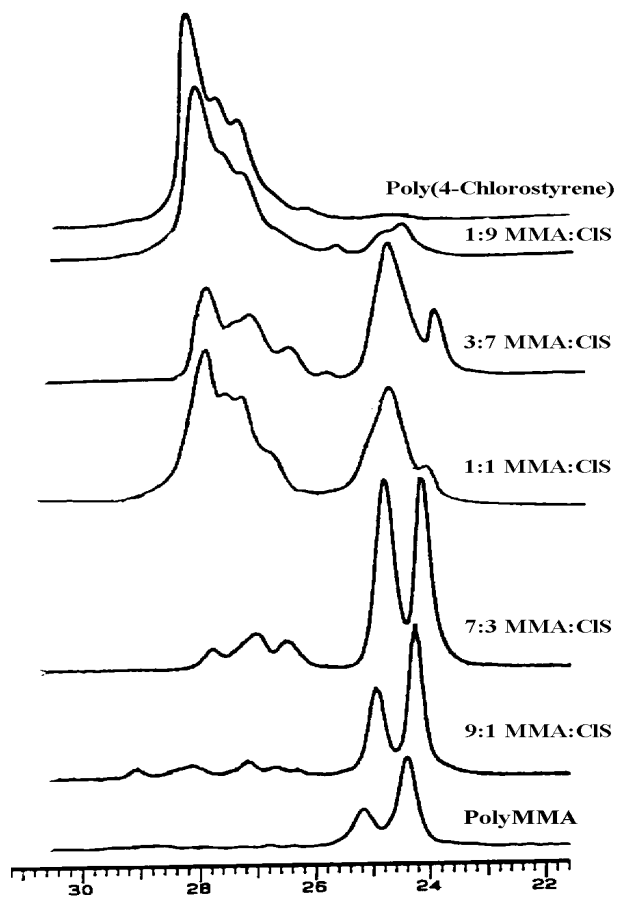
Figure 5. ^{31}P-NMR Spectra of MMA-4-Chlorostyrene Copolymers Prepared by TPO-Initiated Polymerization.

nly resonance observed from 23.5 – 26.0 ppm in the spectrum of the copolymer prepared from a 90/10 – styrene/MMA mixture. It can be calculated from the reactivity ratio for MMA in the styrene/MMA copolymerization system that 94 percent of the $\phi_2P(0)$-MMA chain ends in such a copolymer will be connected to styrene units. On this basis, it was determined that the resonance in the 24.7 – 26.0 region contained contributions from all $\phi_2P(0)$-MMA-styrene chain ends, irrespective of stereochemical considerations as well as from $\phi_2P(0)$-MMA-MMA chain ends with meso MMA-MMA dyads. Accordingly, the resonance observed in the 23.0 – 26.0 ppm region can be assigned and their relative areas can be calculated as shown in Table 2, where σ is the probability that a MMA-

MMA placement has a meso configuration and P(S/M) is the probability that a styrene unit follows a MMA unit in the copolymer. P(S/M) can be easily calculated by Equation 9, where r_M is the reactivity ratio for MMA in the S/MMA copolymerization system [12] and (M)/(S) is the ratio of monomers in the copolymerization system.

$$P(S/M) = 1/(1 + r_M(M)/(S)) \tag{9}$$

Table 2:   Assignment of Structures Contributing to ϕ_2P(0)-MMA Resonances in the Spectra of the TPO-Initiated MMA/Styrene Copolymers
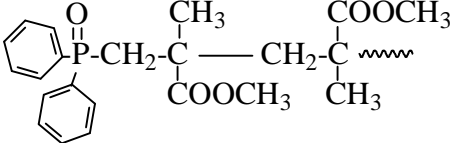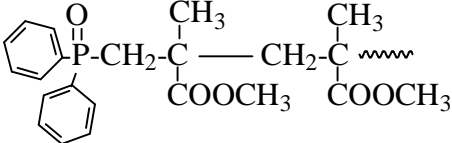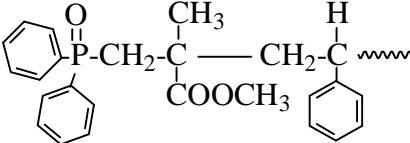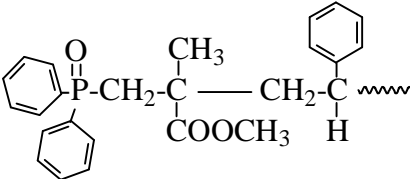
CHEMICAL SHIFT	CONTRIBUTING STRUCTURE	RELATIVE PROBABILITY
23.0-24.7 ppm	Racemic	$(1-\sigma_m)(1-P(S/M))$
24.7-26.0 ppm	Meso	$\sigma_m(1-P(S/M))$
	Meso Racemic	P(S/M)

Table 3 compares the relative areas of the resonances observed at 23.0-24.7 ppm in the copolymer spectra with values calculated using the relative probability expressions given in Table 2, a σ value of 0.27 and an r_M of 0.46. The agreement is quite good, indicating

the validity of the assignments given in Table 2. It should be noted that the value
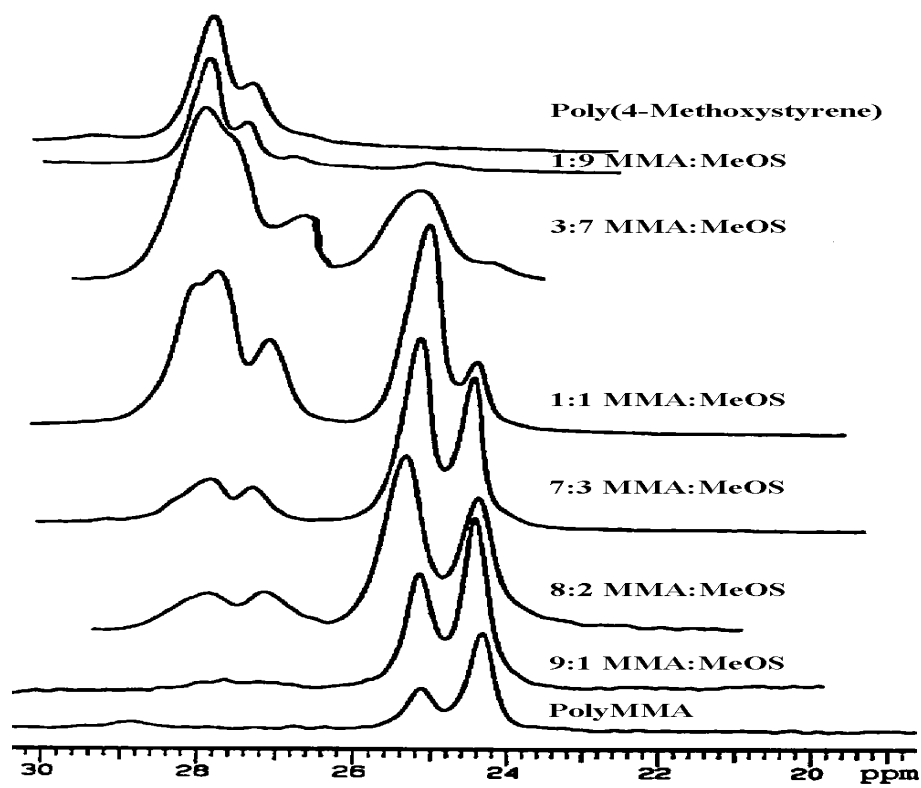
Figure 6. ^{31}P-NMR Spectra of MMA-4-Methoxystyrene Copolymers
Prepared by TPO-Initiated Polymerization.

of r_M that was used for these calculations is the same as that that applies for enchainments throughout the polymer chain and that the value of σ, which is based on the homopolymer spectrum is nearly the same as the value (0.23) that prevails for MMA-MMA placements in the main polymer backbone as measured by NMR. The probabilities for the first pair of monomers in the copolymers are apparently very nearly the same as those for monomer pairs more remote from the chain end.

Table 3 compares the relative areas of resonances observed in the 23.0 – 24.7 ppm region for copolymers of MMA with p-chlorostyrene, p-methoxystyrene and methyl acrylate with those calculated as described above for MMA-styrene copolymers. These calculations are based on σ values of 0.27 for all the copolymers and on r_M values of 0.42, 0.29 and 2.15, respectively, for MMA-p-chlorostyrene, [13] MMA-p-methoxystyrene [14] and MMA-methyl acrylate [15] copolymerizations. The agreement between observed and calculated resonance areas is also very good, indicating that these resonances

can be assigned in the same manner as the resonances of MMA-styrene copolymers. The validity of this general interpretation is strengthened by the fact that the r_M values employed from the calculations varied over a wide range.

Table 3: Percentages of ϕ_2P(0)-MMA Resonance Observed in 24.3 ppm Signal for Copolymers of MMA with Various Monomers

Mole % MMA in Polymerization Mixture	Percentage of Resonance at 24.3 ppm							
	Styrene[*]		4-Chlorostyrene[*]		4-Methoxystyrene[*]		Methyl Acrylate[*]	
	Obs'd	Calc[a]	Obs'd	Calc[b]	Obs'd	Calc[c]	Obs'd	Calc[d]
90	0.61	0.60	0.59	0.59	0.55	0.53	0.72	0.69
80	0.50	0.49	0.37	0.36	0.40	0.39	0.67	0.65
70	0.41	0.39	0.22	0.21	0.29	0.29	-----	-----
60	-----	-----	-----	-----	-----	-----	0.54	0.55
50	0.27	0.25	-----	-----	0.17	0.16	-----	-----
30	0.14	0.13	0.11	0.11	0.10	0.08	0.36	0.35

[*] Comonomer, conversions below 5% in all cases.

[a] $\sigma = 0.27$, $r_M = 0.5$; [b] $\sigma = 0.27$, $r_M = 0.42$; [c] $\sigma = 0.27$, $r_M = 0.29$; [d] $\sigma = 0.27$, $r_M = 2.15$

Fine structure that varies with copolymer composition is also evident in the resonance observed in the 26.0 – 29.0 ppm range in the spectra of the copolymers of MMA and styrene or substituted styrenes. This has not been assigned at present. Undoubtedly these resonance patterns contain information about monomer sequences and stereosequences at the chain ends also.
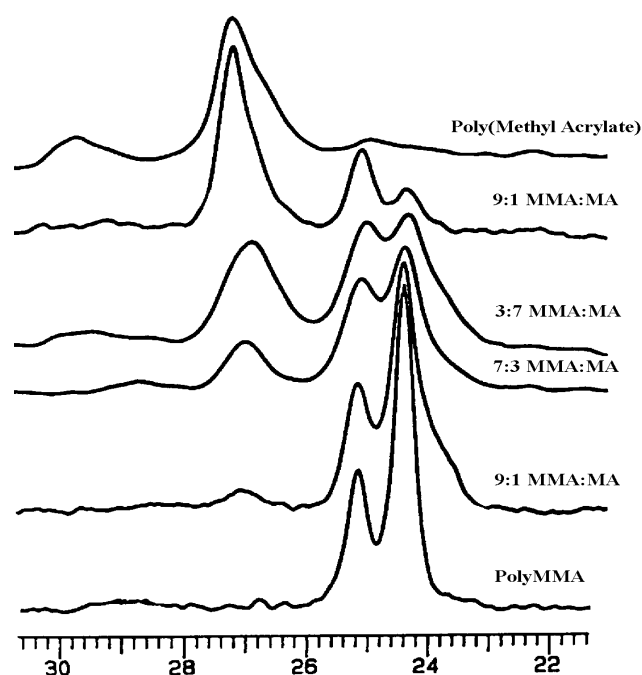
Figure 7. ^{31}P-NMR Spectra of MMA-Methyl Acrylate Copolymers Prepared by TPO-Initiated Polymerization.

CONCLUSIONS

The ^{31}P-NMR spectra of several copolymers prepared by TPO-initiated polymerizations can provide information about the structures of their chain ends. The diphenylphosphinyl radical shows no selectivity in its reactions toward MMA, styrene, p-chlorostyrene, p-methoxystyrene or methyl acrylate. This appears to be a consequence of its very high reactivity. This finding is in conflict with results obtained in time resolved ESR studies, which report a range of rate constants for the reactions of $\phi_2P(0)\bullet$ radicals with vinyl monomers. [2,3] An explanation for this discrepancy cannot be offered at this time and it needs to be investigated.

ACKNOWLEDGEMENTS

REFERENCES

[1] J. Baxter, R.S. Davidson, *Polymer* **1988**, *29*, 1569.

[2] T. Sumiyoshi, W. Schnabel, *Makromol. Chem.* **1985**, *186*, 1811.

[3] A. Kajiwara, Y. Konishi, Y. Morishima, W. Schnabel, K. Kirwata, M. Kamachi, *Macromolecules* **1993**, *26*, 1656.

[4] U. Kolczak, G. Rist, K. Dietliker, J. Wirz, *J. Am. Chem. Soc.* **1996**, *118*, 6477.

[5] J.C. Bevington, *Trends Polym. Sci.* **1993**, *1*, 68.

[6] G. Moad, D.H. Solomon, *The Chemistry of Free Radical Polymerization*; Elsevier Science, Inc., Tarrytown, N.Y., 1996, p. 126-127 and references cited therein.

[7] J.C. Bevington, *Makromol. Chem., Macromol. Symp.* **1988**, *20/21*, 59.

[8] T. Emoto, H. Gomi, T.N. Yoshifuji, *Bull. Chem. Soc. Japan* **1974**, *47*, 2449.

[9] F.A. Bovey, *High Resolution NMR of Macromolecules*; Academic Press, New York, N.Y., 1972, Chapter III.

[10] T. Saito, R.E. Medsker, H.J. Harwood, P.L. Rinaldi, *J. Magn. Resonance A* **1996**, *120*, 125.

[11] D.H. Solomon, P. Cacioli, G. Moad, *Pure Appl. Chem.* **1985**, *57*, 985.

[12] F.M. Lewis, F.R. Mayo, W.F. Hulse, *J. Am. Chem. Soc.* **1945**, *67*, 1701.

[13] C.S. Marvel, G.L. Schertz, *J. Am. Chem. Soc.* **1943**, *65*, 2054.

[14] E.P. Bonsall, L. Valentine, H.W. Melville, *Trans. Farad. Soc.* **1952**, *48*, 763.

[15] V.P. Zubov, L.J. Valnev, V.A. Kabanov, V.A. Kargin, *J. Polym. Sci., A1* **1971**, *9*, 833.

Povzetek

Analizirali in interpretirali smo ^{31}P NMR spektre polimerov in kopolimerov, ki smo jih pripravili iz stirena, substituiranih stirenov, metil metakrilata in metil akrilata z uporabo difenil-(2,4,6-trimetilbenzoil)fosfin oksida (Lucirin TPO) kot fotoiniciatorja.. Iz spektroskopskih podatkov smo izlušèili podatke o strukturi in konfiguraciji fosfor vsebujoèih konènih skupin. Relativna kolièina razliènih konènih skupin ustreza razmerjem uporabljenih kolièin monomerov pri kopolimerizaciji, katalizirani s TPO. To dokazuje neselektivnost fotogeneriranega difenilfosfin oksidnega radikala za promocijo polimerizacije razliènih monomerov. Naši rezultati se ujemajo z že opisano veliko reaktivnostjo difenilfosfin oksidnega radikala, ne pa tudi z rezultati EPR meritev. Le-te kažejo na za faktor 1.45 veèjo reaktivnost omenjenega iniciatorja z metil metakrilatom kot s stirenom.

OPTIMIZATION OF THE REACTION OF PHTHALIC ANHYDRIDE
WITH P_4S_{10}

M. Huskić[1], D. Vanderzande[2], J. Gelan[2],

[1] National Institute of Chemistry, Hajdrihova 19, 1000 Ljubljana, Slovenia.
[2] Institute for Material Research, Division Chemistry, Limburgs Universitair Centrum, Universitaire Campus, Gebouw D, B-3590 Diepenbeek, Belgium.

Abstract

Polyisothianaphthene can be synthesized by reaction of phthalic anhydride with P_4S_{10}. To make the reaction economically, as well as ecologically acceptable it was necesary to increase the yield of PITN. Therefore, the influence of reaction parameters such as reaction time, quantity of xylene and catalyst were investigated. Changing these parameters a yield of 85% was achieved what is almost double the value achieved in previous experiments.

Introduction

In the field of conjugated electroconductive polymers there is a special group of so-called low band gap polymers. The first polymer of this group was poly(isothianaphthene) (PITN) which have drawn great attention by its much higher conductivity in the neutral state than other conjugated polymers, its high contrast and reversible color change from blue in the neutral state to greenish-yellow in the doped state as well as nonlinear optical properties. [1,2,3] Later other low band gap polymers were synthesized but PITN remains the most studied. [4,5,6]

Several synthetic pathways to PITN are described in literature. It can be prepared by electrochemical polymerization of isothianaphthene (ITN) [1], or disilyl derivatives of

ITN [7] to obtain films deposited on the electrode surface. Chemically it can be synthesized by oxidation of dihydroisothianaphthene with FeCl$_3$ [4], N-chlorosuccinimide [8] or O$_2$ [9] to obtain powdery products.

PITN can also be prepared via a precursor route by dehydrogenation of poly(dihydroisothianaphthene) (PDHITN) with dehydrogenation agents such as SOCl$_2$ [10] or tert-butyl hypochlorite. [11] This method is especially interesting because it leads to a stable PITN solution, so that the films can be prepared by casting.

Recently a novel synthetic route to PITN based on the reaction of phthalic anhydride, phthalic acid or phtalide with phosphorus pentasulphide was discovered. [12,13] The major advantages of this route are availability, chemical stability and low cost of the starting materials as well as the synthetic simplicity of the reaction. Using phthalide as the starting material in xylene the yield of PITN was 80-90 %, while with using phthalic ahydride the yield was only 45%. Xylene appears to be the best solvent for this reaction. When using solvents with lower boiling points like toluene or THF, only thio- compounds and traces of PITN were formed. Using solvents with higher boiling points, like mesitylene or dichlorobenzene, increased the yield but changed the structure of PITN due to the side reactions and chain defects. As a consequence of defects in structure the conductivity of PITN was lower.

Since phthalic anhydride is much cheaper than phthalide we decided to reexamine this reaction and find the optimal conditions for the synthesis of PITN making it more profitable from the financial as well as ecological point of view.

Experimental

All syntheses were performed in a nitrogen atmosphere. Commercially available products were used without further purification.

A mixture of phthalic anhydride and P$_4$S$_{10}$ in xylene was heated to reflux and stirred with a magnetic stirrer. The reactant ratio, quantity of xylene, catalyst concentration and time of reaction were varied as described below. The reaction was stopped by cooling to room temperature. The suspension was filtered and the solid dispersed in 50 ml of

methanol and heated to reflux for one hour. After filtration the black solid was transferred to a Soxhlet extractor and continuously extracted with methanol, THF and CHCl3. Each extraction was carried out for 20 hours. The products were dried in vacuum at 80°C.

Results and disscusion

The influence of the ratio of reactants

Mechanistic studies of PITN formation from phthalic anhydride have pointed out that trithiophthalic anhydride might be the essential intermediate in the synthesis of PITN, although its isolation was not possible due to its high reactivity. Experiments showed that once the trithiophthalic anhydride is formed the thionating reagent is not a necessity in the polymerization reaction itself. [13,14]
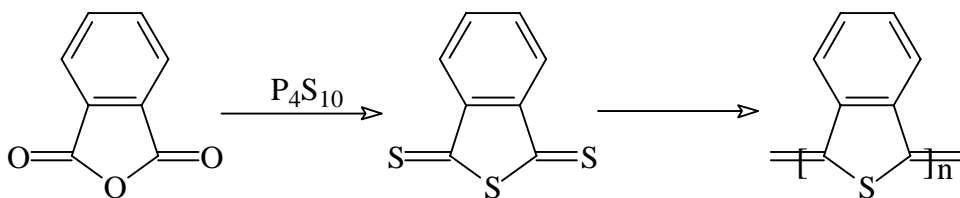
Scheme 1: Synthesis of PITN from phthalic anhydride and P_4S_{10}.

Therefore, theoretically 0.3 mol P_4S_{10} is needed for one mol of phthalic anhydride. All previous research was done with a large excess of P_4S_{10} (0.6-0.7 mol P_4S_{10}).

Using the same reaction conditions as in literature [12] (reactant ratio 1:0.7 mol; 6.2g (0.042 mol) phthalic anhydride, 13.3 g (0.03 mol) P_4S_{10}, 50 ml of xylene, 20 h reaction time) the yield of PITN was 44%. Lowering the amount of P_4S_{10} to 6.2g (0.014 mol) (reactant ratio 1:0.32), the yield dropped to 42%. All the other reactions were made with this reactant ratio since a 2% decrease in PITN yield was acceptable in light of the significant reduction in P_4S_{10} use. In addition, these results confirm the observation that a thionating reagent is not a necessity for the polymerization itself.

The influence of the reaction time

The reaction of phthalic anhydride with P_4S_{10} is slow and after 3 h no PITN was isolated. The product was a mixture of unreacted phthalic anhydride, thiophthalic anhydride, dithiophthalic anhydride, and their dimers. Prolonging the reaction time to 17 and 20 h increased the yield to 40 and 45% respectively. [13]

According to the result above the reactant ratio 1:0.32 was used and the reaction time was varied from 20 to 48 hours. The yield of PITN changed almost linearly with time and yields up to 75% were achieved. The results are shown in Table 1.

Table 1: Yield of PITN in dependence on the reaction time.

Reaction time (h)	Yield of PITN (%)
20	42
30	53
40	66
48	75

The influence of the quantity of xylene

Phthalic anhydride and P_4S_{10} are only partially soluble in xylene. The reaction seems to be heterogenus and the role of xylene is mostly to insure the mixing of reagents and to dissipate the heat that developps during the reaction. Nevertheless, lowering the quantity of xylene from 50 to 40 ml increased the yield of PITN from 42% to 55%. This can be explained by the increase of the contact area between particles of phthalic anhydride, PITN and P_4S_{10}. In the second experiment the reaction time was prolonged to 48 hours. The yield of PITN was 80%, which is only 5% higher compared to the reaction with 50 ml of xylene. Further lowering of xylene quantity was not possible because good stirring could not be assured.

Catalysis of the reaction with p-toluenesulfonic acid

A mechanism for the formation of PITN from phthalic anhydride and P_4S_{10}, based on a sequence of substitution (thionation), isomerization, and polymerization reactions has already been proposed. [13] The first step is a substitution reaction by which a carbonyl is converted to a thiocarbonyl group. The product readily isomerizes to the more stable thiophthalic anhydride, which is thionated to yield dithiophthalic anhydride. This dimerizes to the dithio- dimer or reacts with P_4S_{10} to trithiophthalic anhydride. According to the proposed mechanism, the rate of reaction could be increased by protonating C=O groups. To achieve this *p*-toluenesulfonic acid (p-TSA) was chosen as a protonating agent because it is also a well known dopant for some conductive polymers. Through its use we wished to increase the yield as well as dope PITN in one step. In fact, adding 0.06g p-TSA (1 wt.% *vs.* phthalic anhydride) to the reaction mixture increased the yield of PITN to 51%. Further increase of p-TSA up to 10% gave a yield of PITN of 52-58%, but the results were scattered and no correlations were found between p-TSA concentration and yield of PITN. Scattering can be explained by different granulation of phthalic anhydride, although the yield was reproducible if no or 1% of p-TSA was used. From the relatively low increase in yield when 2-10% p-TSA was added, compared to 1%, we can assume that the p-TSA catalysed only the first reaction and had no influence on the next steps. Since the conductivity of this PITN was even slightly lower (but still in the range of 10^{-1}-10^{-2} S/cm) we believe that adding 1% of p-TSA is an optimum value.

Final optimization of PITN synthesis.

On the basis of these results the final experiment was made in which 6.2g phthalic anhydride, 0.06g p-TSA and 6.2 g P_4S_{10} in 40 ml xylene were used and the time of reaction was 48 hours. The yield of PITN was 85%, which is almost double the value from the previous experiments.

Conclusion

The reaction of phthalic anhydride with P_4S_{10} is relatively slow and high yields can only be achieved if long reaction time is used. A reduction of the quantity of xylene used increased the yield but under the experimental conditions 40 ml was the lower limit. Using a mechanical stirrer, a lower quantity of xylene could probably be used. The role of p-TSA is not clearly understood but it is evident that it acts as a catalyst.

Acknowledgements

References

[1]   F. Wudl, M. Kobayashi, A. J. Heeger, *J.Org. Chem.*, **1984**, *49*, 3382-3384.

[2] M. Kobayashi, N. Colaneri, M. Boysel, F. Wudl, A. J. Heeger, *J. Chem. Phys.,* **1985**, *82*, 5717-5723.

[3] M. Onoda, S. Morita, H. Nakayama, K. Yoshino, *JPN. J. Appl. Phys.,* **1993**, *32*, 3534-3539.

[4] M. Pomerantz, B. Chaloner-Gill, L. O. Harding, J. J. Tseng, W. J. Pomerantz, *Synth. Met.,* **1993**, *55-57*, 960-965.

[5] M. Hanack, K.-M. Mangold, U. Röhrig, C. M.-Mössmer, *Synth. Met.* **1993**, *60*, 199-210.

[6] J. P. Ferraris, T. L. Lambert, *J. Chem. Soc. Chem. Commun.* **1991**, *11*, 752-754.

[7] M. Lapkowski, R. Kiebooms, J. Gelan, D. Vanderzande, A. Pron, T. P. Nguyen, G. Louarn, S. Lefrant, *J. Mater. Chem.* **1997**, *7*, 873-876.

[8] I. Hoogmartens, D. Vanderzande, H. Martens, J. Gelan, *Synth. Met.* 1992, *47*, 367-371.

[9] K-Y. Jen, R. Elsenbaumer, *Synth. Met.,* **1986**, *16*, 379-380.

[10]T. L. Rose, M. C. Liberto, *Synth. Met.* **1989**, *31*, 395-398.

[11]S. A. Chen, C. C. Lee, *Synth. Met.* **1995**, *75*, 187-189.

[12]R. Van Asselt, I. Hoogmartens, D. Vanderzande, J. Gelan, P. E. Froehling, M. Aussems, O. Aagaard, R. Schellekens, *Synth. Met.,* **1995**, *74*, 65-70.

[13]R. Van Asselt, D. Vanderzande, J. Gelan, P. E. Froehling, O. Aagaard, *J. of Polym. Sci.Part A: Polym. Chem.,* **1996**, *34*, 1553-1560.

[14]H. Paulussen, B. Ottenbourgs, D. Vanderzande, P. Adriaensens, J. Gelan, *Polymer,* **1997**, 38, 5221-5225.

Povzetek

Reakcija med ftalanhidridom in P_4S_{10} vodi do nastanka poliizotianaftena. Da pa bi bila sinteza tako ekonomsko, kot tudi ekološko sprejemljiva, je bilo potrebno povečati izkoristek reakcije. S spreminjanjem časa reakcije, količine ksilena in dodatkom para toluensulfonske kisline kot katalizatorja, smo uspeli izkoristek reakcije povečati na 85%, kar je skoraj dvakrat toliko kot v prejšnjih raziskavah.

SYNTHESIS AND RELEVANT RHEOLOGICAL PROPERTIES OF LATEXES

Damjan Končnik[1], Janvit Golob[1], Marko Likon[2], Janez Stražišar[3] and Nevenka Leskovšek[4]

[1]*University of Ljubljana, Faculty of Chemistry and Chemical Technology, Ljubljana, Slovenia*
[2]*Polisinteza, Dekani, Slovenia*
[3]*University of Ljubljana, Department of Geotechnology and Mining, Slovenia*
[4]*Color Medvode, Paint Factory, Medvode, Slovenia*

Dedicated to the memory of Professor Anton Šebenik

ABSTRACT

The emulsion polymerisation of styrene/2-ethylhexylacrilate/acrylic acid polymer particles with narrow particle size distribution is described. By syntheses, the weight ratio between styrene and 2-ethylhexylacrilate was varied in order to obtain particles with different viscous and viscoelastic properties. These parameters were measured with Carry - med S.L.C. rheometer 500. The results show that particles containing more 2-ethylhexylacrilate exhibit a higher viscosity level and higher storage and loss moduli than particles containing more styrene.

INTRODUCTION

Emulsion polymerisation is a technologically and commercially important reaction used to produce synthetic polymers and latexes for a wide range of applications including water-borne coatings, adhesives, sealants, synthetic rubbers and many others [1]. Emulsion polymerisation is a method of producing latexes with desired particle size and its distribution, molecular weight and its distribution, composition, morphology, film-

forming properties etc. [2]. One of the most important characteristics of latexes from the theoretical and practical point of view are their rheological properties. Rheological measurements often give important information about the structure of latexes. By rheological measurements the sample is subjected to shear stress which causes deformation of polymer particles. The extent of deformation depends on the stress and chemical structure of particles. In our case, particles containing more 2-ethylhexylacrilate (2-EHA) are softer and consequently more deformable than particles containing more styrene (S). That is the reason why latexes exhibit viscoelastic properties. This term is used to define the liquids that behave as ideal liquids but under low stress conditions they behave like solids exhibiting elastic recovery. Given sufficient stress, the sample undergoes irreversible deformation and flows. Our work was focused on the rheological behaviour of latexes as a function of their chemical composition, reflected by oscillation measurements.

EXPERIMENTAL

1. Synthesis of latex

A 1.5-litre, 3-neck glass reactor with condenser, peristaltic pump and flow-variable pump was used. The reactor was dipped into a temperature controlled water bath at 80^0C. The procedure used for the "in situ" seeded emulsion was as follows: 2 g of emulsifier was dissolved in 260 g of water at 60^0C. Then 0.4 g ammonium persulfate (APS) was added and the reactor was heated to 80^0C. 20 g of preemulsion was added with the composition shown in Table 1. After 10 minutes of reaction at 80^0C the remaining preemulsion and 100 g of 1-% solution of APS were simultaneously and continuously pumped for 4 hours. After that the latex was neutralised with a 25 % solution of ammonia to achieve pH 8.0 ± 0.1 and then cooled down to room temperature.

The variable in our experiments was the weight ratio between styrene and 2-EHA. The measured characteristics are presented in Table 2.

Table 1. Composition of preemulsion.

Component	Mass (g)
Water	200
Emulsifier	20
Acrylic acid	15
Styrene	242, 297, 352, 407
2-EHA	308, 253, 198, 143

Figure available in printed version only
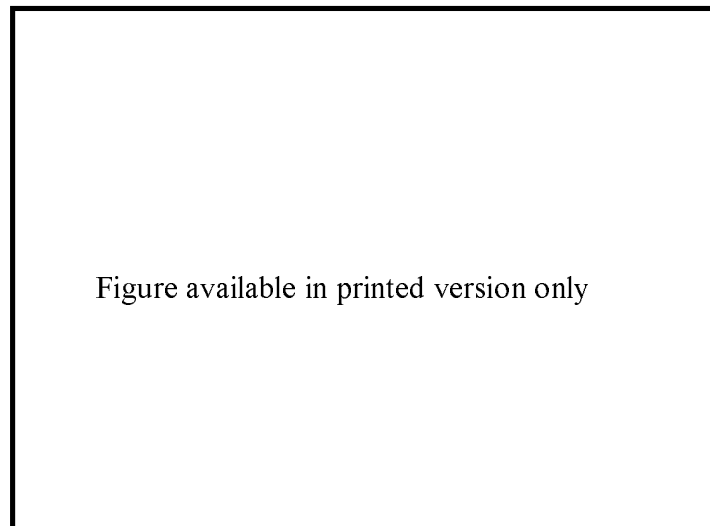
Figure 1. Scanning electron micrograph of latex particles 4.

2. Properties of latexes

a. Particle size

The particle size was measured using the Malvern Autosizer IIC. The size range of the apparatus is in a region from 3 nm to 3 μm. The instrument produces a He-Ne laser wave

of wavelength 633 nm. The scattering angle is fixed at 90^0. The pictures of samples were made by electronic microscope Jeol 300.

b. Glass transition temperature (T_g)

The values of glass transition temperature were obtained using Perkin Elmer DCS 7. The heating rate was 20 ^{0}C/min and second heating was considered. The weight of samples was 20 mg. Before measurement samples were dried at 1 hour 105 ^{0}C.

Table 2. Properties of latexes.

Characteristic	Latex			
	1	2	3	4
Weight ratio S/2-EHA	44/56	54/46	64/36	74/26
Particle size (μm)	0.22	0.22	0.23	0.23
Glass transition temperature(^{0}C)	-3	11	33.7	52.8
Polydispersity	1.06	1.05	1.03	1.04
Storage modulus, G' (Pa)	240	162	122	73
Loss modulus, G'' (Pa)	28	20	15	8
Phase angle (^{0})	7	7	7	6

b. Rheological properties

Latexes exhibit various degrees of elasticity and viscosity [3-6]. Viscoelasticity is used to describe the rheological properties expressing characteristics from viscous fluids to elastic solids. For a viscoelastic material, shear stress and shear strain are not in phase, but, rather, displaced by a certain phase angle δ. From the knowledge of shear stress τ, deformation γ and phase angle δ, it is possible to completely describe the viscoelastic behaviour of a material by the two mechanical dynamic functions, the storage shear modulus, G', and the loss shear modulus, G''.

The storage modulus G' is given as

$$G^{'} = \frac{\tau_0}{\gamma_0}\cos\delta$$

(1)

where τ_0 and γ_0 are shear stress strain amplitudes, respectively. This quantity represents a measure for the strain energy recoverably stored in the substance. Thus it characterizes the elastic behaviour of the sample.

The loss modulus G'' is given as

$$G^{''} = \frac{\tau_0}{\gamma_0}\sin\delta$$

(2)

This quantity represents a measure for the energy dissipated as heat and thus lost. It therefore characterises the viscous behaviour of the viscoelastic material.

The loss factor is defined as:

$$\tan\delta = \frac{G^{''}}{G^{'}}$$

(3)

The quantity is proportional to the ratio between the amount of the dissipated and stored energy and hence also between the viscous and the elastic portion of the sample.

From these measurements the dynamic viscosity, η', can be determined in the following manner:

$$\eta^{'} = \frac{G^{''}}{\omega}$$

(4)

Where $\omega = 2\pi\nu$ and ν is the frequency.

The strain amplitudes must be low enough in order not to destroy the structure of the examined sample. To determine the linear viscoelastic region, stress sweep tests are used. The strain amplitudes to which G' and G'' are constant are the maximum permissible

amplitudes for the structure to remain undamaged. After that the frequency sweep test is carried out in the region of linear viscoelasticity.

RESULTS AND DISCUSSION

Flow curves, stress sweep and frequency sweep measurements were carried out by Carri - med S.L.C. rheometer 500, using cone and plate geometry (6 cm/2^0) at 20^0C. The flow curves of all latexes show slightly pseudoplastic behaviour and latex 1 also shows the slightly thixotropic behaviour. Latexes containing more 2-EHA exhibit a higher yield value. The flow curves are shown in Figure 1.
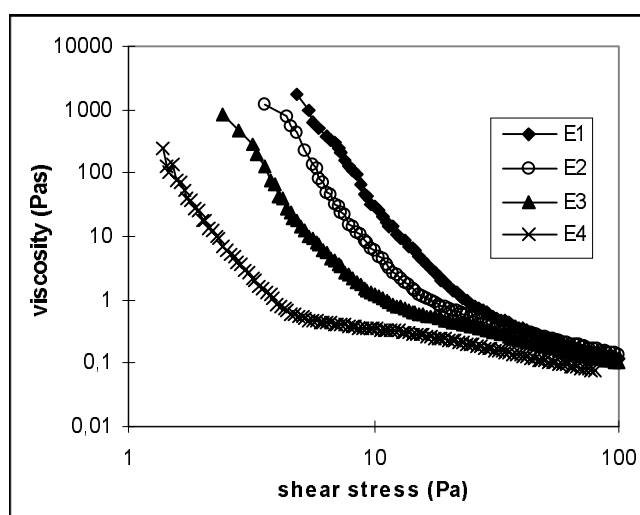
Figure 1. Flow curves of latexes.

Stress sweep measurements

Stress sweep tests were carried out at a constant frequency of 1 Hz. From Figures 2 and 3 it can be seen that the linear viscoelastic region extends from the stress of 2 Pa to the stress of 3 Pa (in this region G', G'' and phase angle δ are constant). The phase angle value in this region is for all samples about 7^0. The latex particles 1 and 2 are soft and elastic (T_g is -3^0C and $+11^0$C, respectively) and latex particles 3 and 4 are hard and stiff (T_g is $+33.7^0$C and $+52.8^0$C, respectively). Shear stress deforms polymer particles so that they take the shape of an ellipsoid. The deformation depends on the chemical

composition: the more 2-EHA the particles contain, the greater is their deformation. This structure change is reflected in the storage modulus, G', which increases with increasing amount of 2-EHA in the particles. The particles of latex 1, containing 56% of 2-EHA, have G' of 240 Pa in the linear viscoelastic region, but the particles containing 26% of 2-EHA. On the other hand, exhibit in the linear viscoelastic region G' only of 73 Pa.
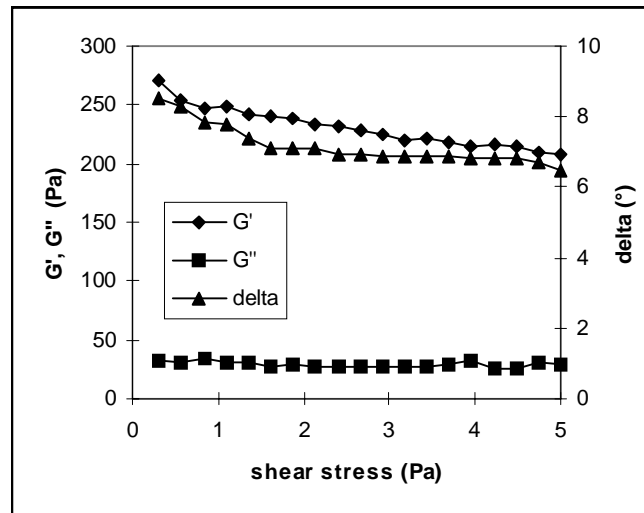
Figure 2. Stress sweep test for latex 1.
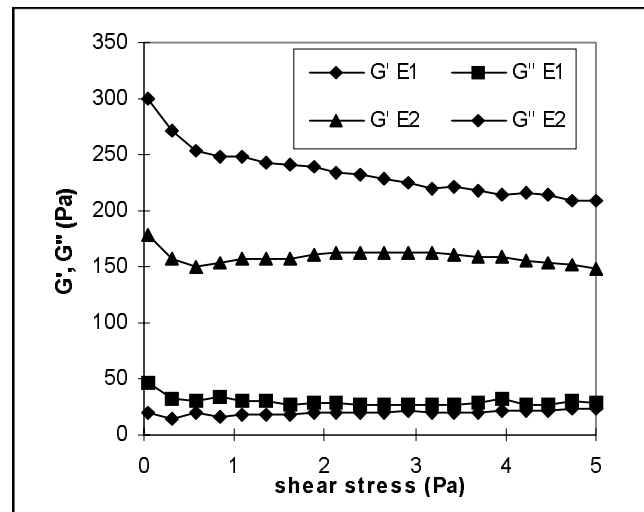
Figure 3. Storage modulus and loss modulus as a function of shear stress for latexes 1 and 2.
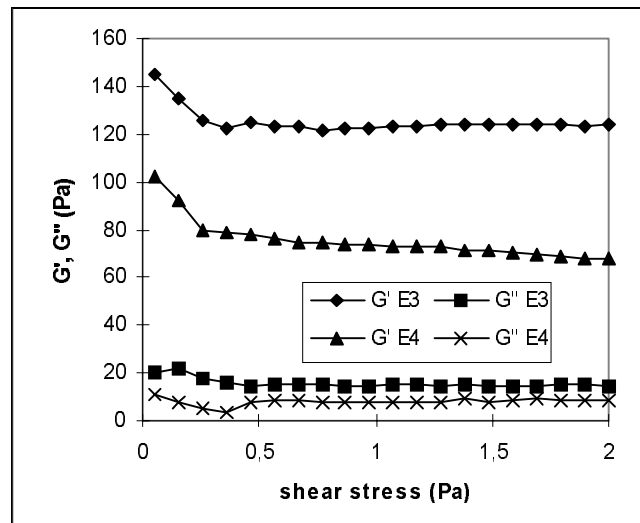
Figure 4. Storage modulus and loss modulus as a function of shear stress for latexes 3 and 4.

Latexes 2 and 3 have the storage moduli of 152 Pa and 120 Pa, respectively (see Figures 3 and 4 for this region). The loss modulus, G'' also increases with the increasing amount of 2-EHA in particles. These results show that the soft particles are able to convert more energy into heat than the hard ones. The phase angle of all latexes is in the range from 6^0 to 7^0.

Frequency sweep measurements
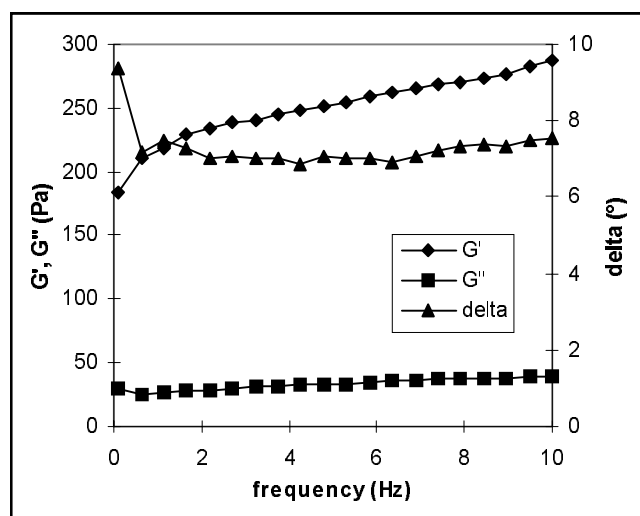
Figure 5. Frequency sweep test of latex 1.

The frequency sweep tests were made in the region of 0.1 to 10 Hz at constant shear strain amplitude of 0.015. G' and G" increase slightly with increasing frequency, but the phase angle remains constant in a wide range of frequencies. Its increase is observed only in latex 4, where the phase angle increases up to 14^0. The measurements are shown in Figures 5, 6 and 7.
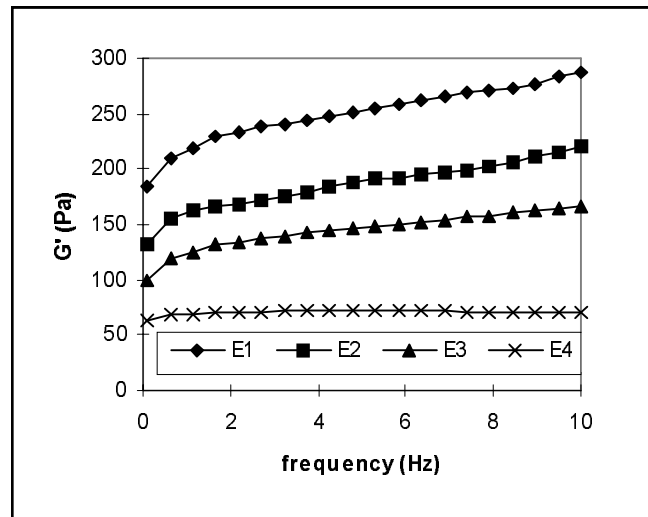
Figure 6. Storage modulus as a function of frequency.
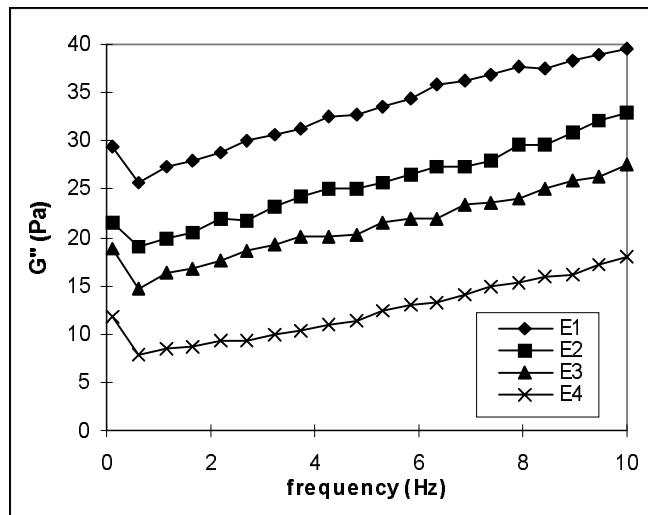
Figure 7. Loss modulus as a function of frequency.

CONCLUSION

Latexes are colloids of elastic polymer particles possessing a very complex structure especially under deformation by shear stresses. Under these conditions elastic particles are deformed and these deformations may be observed by rheological measurement. The rheological behaviour of latex particles strongly depends on their composition. Latex particles containing more styrene are harder and stiffer than particles containing more 2-ehtylhexylacrilate. With increasing stiffness of particles, the storage modulus G' as well as the loss modulus G" decrease, but their ratio remains constant between 8 and 9. These values might be acceptable for commercial latexes. The fraction of styrene in particles that is appropriate for application is up to 55-weight %. Above this concentration, the film-forming properties of films are poor unless coalescing aids are added.

REFERENCES:

1. P. A. Lovell and M. S El-Aasser, *Emulsion Polymerisation and Emulsion Polymers*, John Wiley and Sons, Chichester, 1997
2. R. G. Gilbert, *Emulsion Polymerisation A Mechanistic Approach*, Academic Press, London, 1995,
3. H.A Barnes, *Colloids and Surfaces A* **1994**, *9*, 89.
4. P. Sholz, D. Froelich, and R. Muller, *J. Rheol.* **1989**, *33*, 481.
5. D. Graebling, D. Froelich and R. Muller, *J. Rheol.* **1989**, *33*, 1283.
6. M. Osterhold, W. Shubert, and W. Schlesing; *J. Rheol.* **1992**, *36*, 245.

POVZETEK

Opisali smo postopek za polimerizacijo stirena in 2-etilheksilakrilata v emulziji. Pri polimerizaciji smo dobili delce z ozko porazdelitvijo delcev. Pri sintezah smo spreminjali razmerje stirena proti 2-etilheksilakrilatu. Na ta način smo dobili delce z različnimi viskoznimi in viskoelastičnimi lastnostmi. Te parametre smo izmerili z reometrom Carry - med S. L. C. 500. Rezultati so pokazali, da delci, ki vsebujejo več 2-etilheksilakrilata izkazujejo višjo viskoznost in tudi višjo vrednost akumulacijskega modula in modula izgub.

VISCOELASTIC PROPERTIES OF WELAN SYSTEMS - PRACTICAL APPLICATIONS

Andreja Zupanèiè

University of Ljubljana, Faculty of Chemistry and Chemical Technology, Aškerèeva 5,
1001 Ljubljana, Slovenia

Abstract

A detailed rheological characterization of aqueous welan systems was performed in the concentration range from 0.1 to 0.5 %w/w of the polymer. In order to illustrate the practical application of aqueous welan systems, the rheological investigations were extended to alumina dispersions in aqueous welan matrices where the polymer concentrations in the disperse medium were of the same range (0.1-0.5 %w/w). The dependence of the viscoelastic properties of aqueous welan systems and alumina-welan dispersions on polymer concentration was examined and discussed in the light of fractional constitutive equations and in the view of practical applications. The experimental data of aqueous welan systems, as well as the results of modeling were compared with those obtained for alumina-welan dispersions.

1. INTRODUCTION

Aqueous polymer solutions, especially those of natural biopolymers, are very important material source in various industrial branches because they exhibit a high stability level and good compatibilty and because they are biodegradable. In recent years, the production and the application of such enviromentally friendly materials has increased. Industrial uses of polysaccharide systems centre on their ability to increase their weight in the water by several times when it thickens or structures, thus controlling the rheology of hydrated systems. The solution properties of these carbohydrates are of

considerable interest for a number of practical commercial applications such as thickening, suspending and gelling agents[1]. Such properties can be profitably exploited for many industrial applications, in particular in the food, pharmaceutical and ceramic industries.

Hydrophilic polymers and their aqueous dispersions exhibit some specific rheological properties. The structural conditions of these systems, which are influenced by various environmental conditions and polymer concentration, can be determined from detailed rheological examination. Rheological characterization of aqueous polysaccharide systems deals with a wide range of mechanical responses, from pure liquids to elastic solids. These systems in general exhibit the rheological behavior characteristic for polymers or polymer solutions, but under certain circumstances also some specific rheological properties. The transport properties and, specifically, the rheological behavior of real and complex materials such as aqueous polysaccharide systems can be significantly affected by several factors, mainly related to molecular and supermolecular features. Most of these factors are common to all polymeric systems, others are peculiar to carbohydrate polymers. Since the mechanical properties of aqueous polysaccharide dispersions depend on their physical and chemical conditions, their network structural formations depend on polymer concentration, ionic strengths, presence of organic solvents, pH, temperature, etc. In general, hydrophilic polymers are able to form three-dimensional network structures or gel structure already at very low polymer concentrations. The gel structure exhibits elastic solid behavior under the conditions of small deformations. Through a rheological study it is possible to evaluate not only the time evolution of the macroscopic properties of a given system, but also its structural and /or molecular characteristics.

The structural conditions of aqueous polysaccharide dispersions can be classified as: dilute polymer solutions, weak gels, micro gels and strong gels. Above the critical polymer concentration, overlapping and associations of polymer molecules result in the formation of extended junction zones, or in other words, in the formation of a continuous three-dimensional network, where the junction zones play the part of point crosslinks in covalent gels[2]. Strong gel behavior can be observed when the polymer association is strong. Under small deformation conditions the mechanical spectra of strong gels closely approximate solid-like behavior. When subjected to large deformation or continuous flow conditions, the gel network ruptures into small gel regions. The flow conditions then become heterogeneous. This is not the case for weak gels, which may flow homogeneously, even under continuous shear conditions. They exhibit marked non-

Newtonian properties, strictly connected to the progressive disruption of the network into smaller flow units as the shear rate increases. Also weak gels exhibit elastic solid behavior under the conditions of small deformations, but the elastic contribution to the viscoelastic response in this case is not so predominant as for strong gels. When polymer aggregation is favored, segregation into two phases may take place or interchain association may be restricted to small microgel clusters dispersed in a macromolecular solution[2]. The rheological behavior of the microgels depends on the polymer concentration. At a high concentration of the aggregates they exhibit solid like behavior at low stresses and their rheological properties cannot be easily distinguished from those of weak gels. Correlation of rheological data and modeling constitutes a complementary step, necessary for the exploitation of the experimental results.

Several industrial products and biomaterials are composed of solid particles dispersed in polymeric gel matrices. The rheological properties of filled gels are strictly governed by those of the polymeric matrix. The influence of particle addition can become very important, depending on the effective volume concentration of the disperse phase and the type and extent of particle-gel matrix interactions. Weak gel matrices are frequently preferred for many practical purposes, particularly when remarkable concentration levels of the disperse phase must be reached in the filled gel, since their viscous and elastic properties are favorably combined to ensure easy manipulation and transportation, as well as good stability. Among several polysaccharides giving rise to more or less weakly structured systems when dissolved in water under proper conditions, welan can be considered a good candidate to form weak gel matrices, since the sol/gel transition can be attained at low polymer concentrations and their gel properties are only slightly dependent on environmental conditions. Welan gum is produced by Alcaligenes spp. ATCC 31555 and has the same basic backbone repeating units as gellan gum, another microbial polysaccharide of widespread industrial use, but with a single a-L-rhamnose or a-L-mannose as side groups in the ratio of 2:1 per repeating unit[2]. Even if the primary structure of these two bacterial polysaccharides differ basically only for the side chains, significant differences can be noted in their viscoelastic properties in aqueous media. Thus, whereas gellan can form stable gels in salt aqueous solutions, welan systems often behave as weak gels, so standing between solutions and chemical gels, and their thermal stability represents an important characteristic for oilfield applications.

The present paper reports the results of experimental studies carried out on aqueous welan systems under small and large deformation conditions. Furthermore, the paper deals with the problems related to the preparation of concentrated aqueous

dispersions of ceramic powders in welan matrices. High purity alumina powder is selected in order to prepare ceramic dispersion in gel matrices. The specific objective of this work is to examine the influence of welan concentration on the structural conditions of aqueous alumina-welan systems.

2. EXPERIMENTAL

The materials used for the preparation of polysaccharide matrices, alumina suspensions, and alumina dispersions in welan matrices were: welan K1A96 (Monsanto) high purity alumina powder A16 SG (Alcoa) (d50 = 0.5 mm), distilled water and anionic dispersant Duramax D3021 (modified polyacrylic acid, Mw 5000 Rohm&Haas).

The powdered polymer (welan) was dissolved at different concentrations (0.1 - 1 %w/w) in distilled water by mechanical stirring at ambient temperature and stored for two days in order to ensure a complete wetting of the polymer. Alumina-welan dispersions were prepared in two steps. Highly concentrated aqueous alumina suspensions were used as a source of particle addition in the gel matrices. Alumina suspensions were prepared at the same solid volume fraction of 0.55 by dispersing the alumina powder in aqueous - dispersant solution. The dispersant concentration was 0.3 %w/w as calculated on the alumina powder, solid dry weight basis. The suspensions were prepared by ball milling in 0.5 litre polypropylene jars filled with 500 g of Si_3N_4 milling balls for 16 hours at a speed of 70 rpm. The two components (alumina suspensions and welan systems) were blended together in proper quantities by hand mixing. For all the systems the final solid volume fractions were, 0.38 and 0.48 with welan concentration ranging from 0 to 0.5 %w/w. The rheological characterization was carried out two days after the preparation.

The rheological tests were performed under steady and oscillatory shear conditions at 20, 25 and 30°C using mainly the controlled stress rheometer Haake, RheoStress RS 150, equipped with a double cone sensor system (DC 6/4). Some additional tests were done by a controlled rate rheometer Haake CV100, equipped with coaxial cylinder sensor system ZB15. The rheological properties were studied under small and large deformations, as well as in flow conditions, by applying different procedures: stress and frequency sweeps, stress ramps and multistep sequences.

3. RESULTS AND DISCUSSION

Flow curves - large deformation conditions

The rheological behavior of aqueous welan systems strongly depends on the polymer concentration. At 0.1 wt % of welan the linear and non-linear properties are quite similar to those of polymer solutions. Shear thinning behavior and negligible time dependent effects are observed in continuous shear. With increasing polymer concentration, above 0.2 wt % of welan, more pronounced shear thinning behavior and detectable thixotropic time dependent effects are observed. The rheological properties in this case resemble those peculiar for structured liquids or weak gels. Figure 1. demonstrates the influence of welan concentration on the flow properties of aqueous welan systems.

The rheological investigation is extended to examination of alumina dispersions in aqueous welan matrices where the solid volume fraction (Φ) of alumina powder is 0.38. The most significant changes in the flow properties of the dispersions are observed already at the lowest polymer concentration (0.1 %w/w of welan) in the disperse medium. At higher welan concentrations the shape of the flow curves, as well as the viscosity level, become similar to those of aqueous welan matrices.
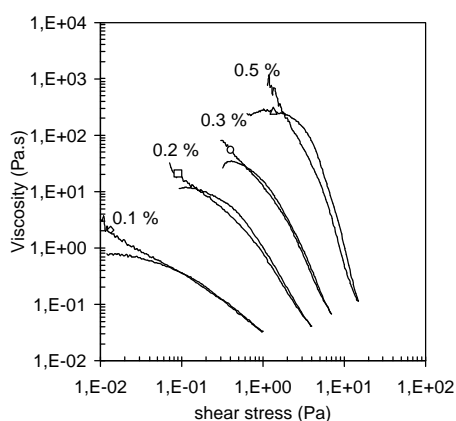
Fig.1: Flow curves of aqueous welan systems at different welan concentrations
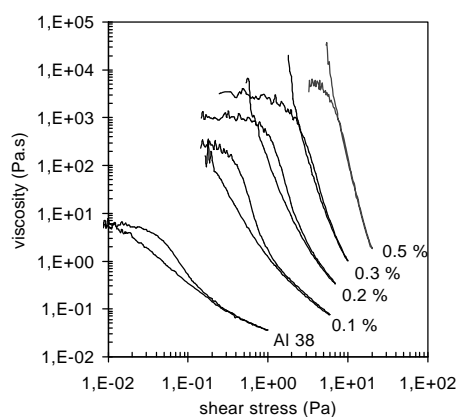
Fig.2: Flow curves of alumina-welan dispersions at $\Phi = 0.38$ and different welan concentrations

Viscoelastic properties - small deformation conditions

The results obtained from stress sweeps at a frequency of 1 Hz show that the critical strain for the linear viscoelastic regime decreases with increasing polymer concentration. Figure 3 illustrates such peculiar features for some aqueous welan systems

at different polymer concentrations. The limit of linear viscoelastic response of all aqueous welan systems ranged up to 10% of strain amplitude, whereas the critical strain amplitude of alumina-welan dispersions is shifted toward lower values of strain amplitude (between 0.7 and 2%) as shown in Figure 4. The numbers beside the symbols in Figures 3 and 4 indicate welan concentrations in %w/w.

Some preliminary tests were performed to check the influence of environmental conditions on the rheological properties of aqueous welan systems. The effects of pH by addition of HCl or NH_4OH, temperature (8 - 45°C) and the presence of dispersant were
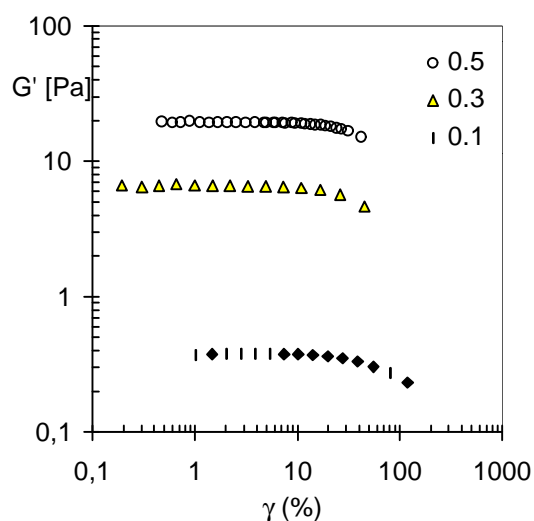
Fig. 3: Stress sweep tests: aqueous welan systems at different welan concentrations
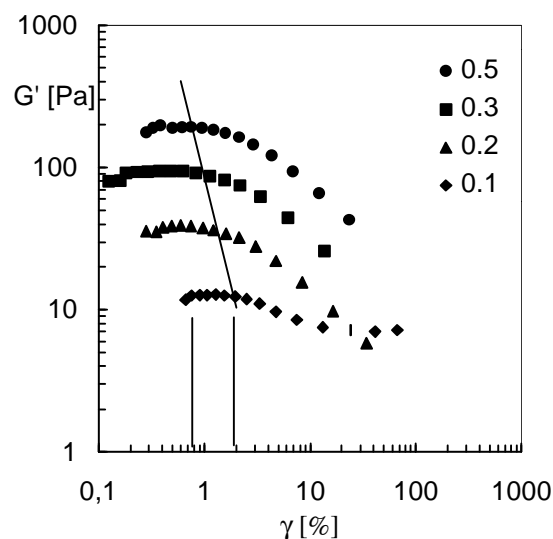
Fig. 4: Stress sweep tests: alumina-welan dispersions at $\Phi = 0.38$ and different welan concentrations

checked in the range of polymer concentration between 0.3 and 1 %w/w of welan. It was found that the systems were almost insensible to the investigated environmental conditions. This is confirmed in Figure 5 which illustrates the mechanical spectra of aqueous welan systems at different pH (2 – 9.5) and the same polymer concentration of 0.5 %w/w.

The mechanical spectra of aqueous welan systems at different polymer concentrations (at 25 °C) are reported in Figure 6. For the lowest polymer concentration (0.1 %w/w) the viscous component exceeds the elastic one under low amplitudes of oscillatory shear strains, below i.e. 10%. At >0.2 %w/w of welan the elastic component becomes predominant and both moduli are less sensitive to the applied frequency. When polymer concentration exceeds 0.1%, a net change is observed in the profiles of both moduli, suggesting the appearance of a sol/gel transition.
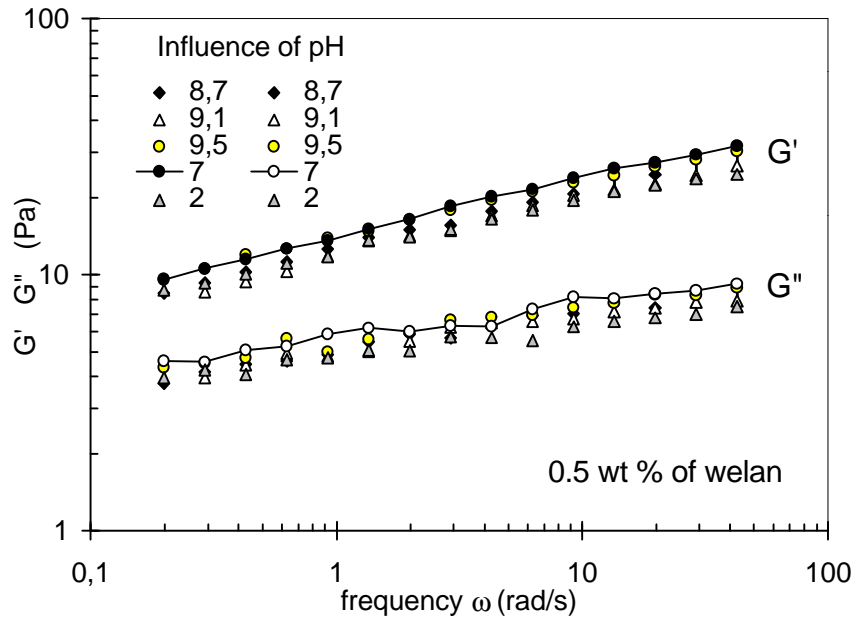
Fig. 5: The influence of pH on the mechanical spectra of aqueous welan systems

At above 0.1 % of welan the increase of polymer concentration (*C*), G' and G''
scale as *C* $^{1.9-2.3}$ and *C* $^{1.7-1.95}$, respectively (both exponents increase with decreasing
frequency). A *C* ^{2} dependence of the storage modulus (G') is often observed for gelling
systems, in accordance with theoretical models proposed for biopolymers with high
functionality[3].

Let us now consider the effects of welan concentration on viscoelastic properties
of alumina-welan dispersions at a solid volume fraction of 0.38. The mechanical spectra
of alumina-welan dispersions at different polymer concentrations in the disperse medium
are shown in Figure 7. As already mentioned, the most significant changes in the
rheological properties are observed for the systems containing 0.1 %w/w of welan.
Under linear oscillatory shear conditions the elastic component appreciably predominates
over the viscous one for all alumina-welan systems and both moduli strongly increase in
the presence of polymer in the disperse medium. When polymer concentration exceeds
0.1%, the dispersions behave like structured liquids or weak gels. With increasing
polymer concentration (> 0.2 %w/w) in the disperse medium the traces of G'(ω) and
G''(ω) become parallel to each other and G' is at least one order of magnitude higher
than G''. Such a condition corresponds to an apparent sol/gel transition according to the
criterion suggested by Winter and Chambon [4].
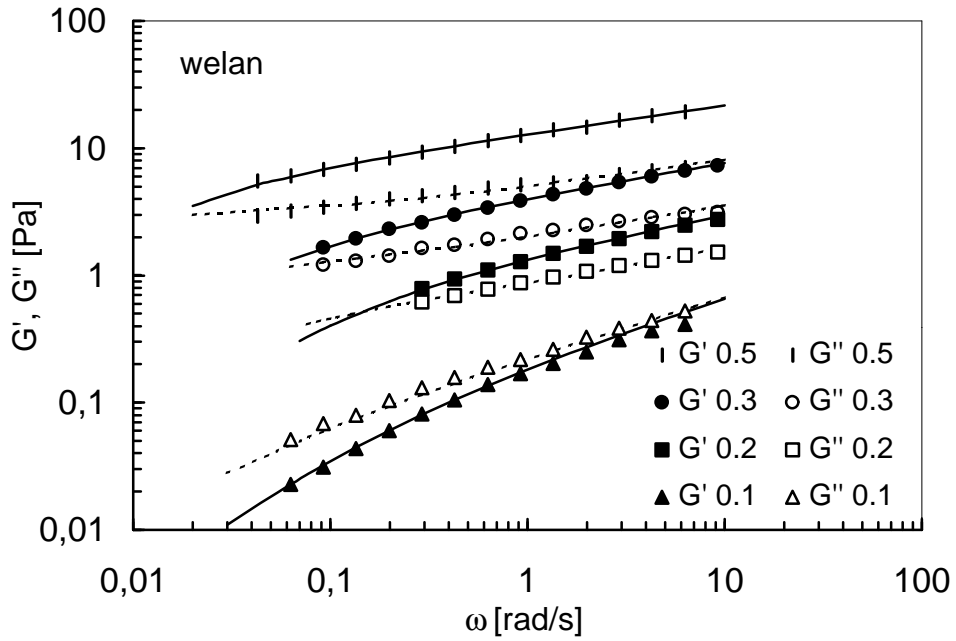
Fig. 6: Frequency dependence of G' and G'' for aqueous welan systems, numbers beside the symbols indicate welan concentrations in %w/w and curves calculated from the Friedrich model.
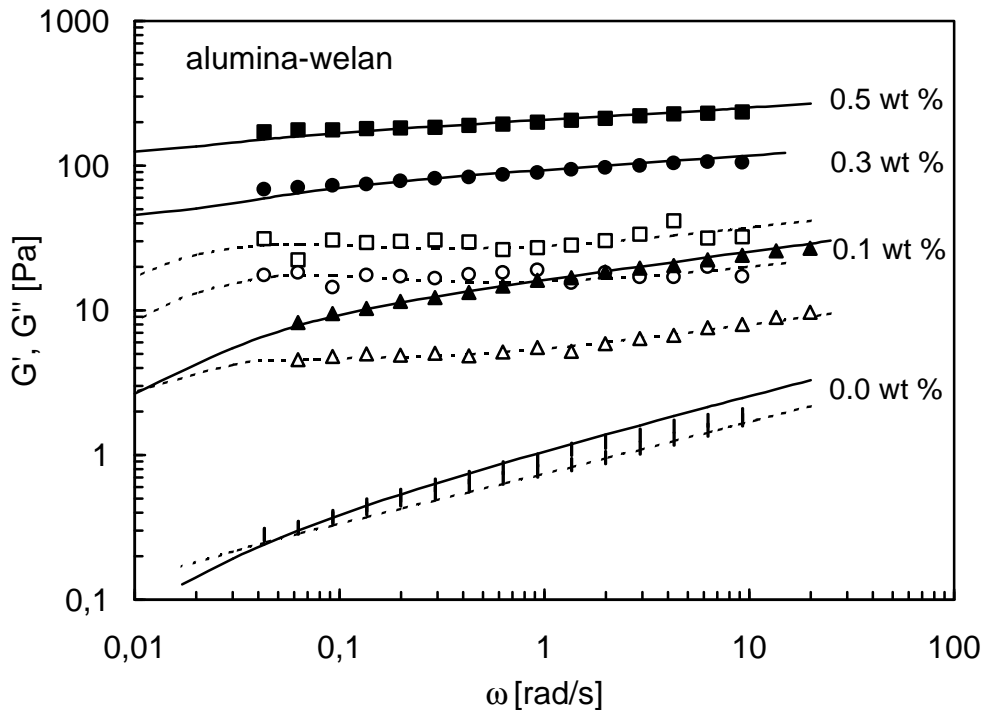
Fig. 7: Frequency dependence of G' (filled symbols) and G'' (open symbols) for alumina-welan dispersions with Φ=0.38 at 25°C, and curves calculated from the Friedrich model

In the case of such structured fluids the analysis of experimental data must necessarily be performed by resorting to phenomenological models instead of molecular approaches, particularly when we aim to describe effects of polymer concentration or sol/gel transitions. Satisfactory data fitting of mechanical spectra is provided by the fractional derivative (per time) Maxwell model suggested by Friedrich and Braun [5].

$$\overline{\overline{t}} + D^c\left[\overline{\overline{t}}\right] = G_\infty\left\{D^0\left[\overline{\overline{g}}\right] + D^c\left[\overline{\overline{g}}\right]\right\} + \Delta G\, D^d\left[\overline{\overline{g}}\right] \qquad (1)$$

where $\overline{\overline{\tau}}$ and $\overline{\overline{g}}$ are the stress and strain tensors, respectively, and c and d are the derivation orders. When c = d = 1, the equation corresponds to the 'solid model' for $G_\infty > 0$, whereas the canonical Maxwell 'liquid model' is obtained for $G_\infty = 0$. The fractional derivative model was selected because it is able to describe a wide range of viscoelastic responses, from viscous liquid to elastic solid, by a limited number of parameters. Under oscillatory shear conditions the linear viscoelastic response can be expressed by the following equations:

$$G'(\boldsymbol{w}) = G_\infty + \Delta G\; \frac{(\boldsymbol{l}\boldsymbol{w})^d\left[\cos(d\,\frac{\boldsymbol{p}}{2}) + (\boldsymbol{l}\boldsymbol{w})^c\cos((d-c)\frac{\boldsymbol{p}}{2})\right]}{1 + 2(\boldsymbol{l}\boldsymbol{w})^c\cos(c\,\frac{\boldsymbol{p}}{2}) + (\boldsymbol{l}\boldsymbol{w})^{2c}} \qquad (2)$$

$$G''(\boldsymbol{w}) = \Delta G\; \frac{(\boldsymbol{l}\boldsymbol{w})^d\left[\sin(d\,\frac{\boldsymbol{p}}{2}) + (\boldsymbol{l}\boldsymbol{w})^c\sin((d-c)\frac{\boldsymbol{p}}{2})\right]}{1 + 2(\boldsymbol{l}\boldsymbol{w})^c\cos(c\,\frac{\boldsymbol{p}}{2}) + (\boldsymbol{l}\boldsymbol{w})^{2c}} \qquad (3)$$

where $G_\yen$ represents the equilibrium modulus when the frequency tends to zero, and hence the model describes liquid-like responses if $G_\yen = 0$. Parameter $\boldsymbol{l}_0$ is a characteristic time of a material which determines the role of the relative contribution of elastic and viscous components in the viscoelastic response. Figures 6 and 7 report a comparison between experimental data and the curves calculated from equations (2) and (3). Apparently, the model provides an adequate correlation of loss and storage moduli as the function of frequency in the whole range of polymer concentration for both aqueous welan systems and alumina-welan dispersions. In order to obtain reasonable values of the parameters in equations (2) and (3), the yielding conditions: $0 < c \leq d \leq 1$ and $G_\yen \geq 0$ should be satisfied. As an objective function in the minimization procedure the mean square relative deviation was used. Evaluation of the model parameters by applying the fitting procedure simultaneously for both G'(ω) and G''(ω) showed that for almost all studied systems exponent d converged to the limiting conditions $d = 1$. Consequently, the influence of polymer concentration on the frequency dependence of the dynamic moduli

is described through the variation of only four parameters: $G_{\yen}$, DG, l_0 and c. The variation of relaxation time l_0 and exponent c with increasing welan concentration in aqueous welan systems and alumina-welan dispersions is shown in Figure 8. Increase of l_0 with polymer concentration in aqueous welan systems indicates that the elastic contribution becomes more important. The value of l_0 evaluated for the reference aqueous alumina suspension is quite different from those of the alumina-welan dispersions (Figure 8). Noticeable increase of exponent c is observed only at low polymer concentrations. At higher welan concentrations c values ranges around 0.8 for both welan and alumina-welan systems. The most significant differences in parameter ΔG, which control the level of the dynamic moduli, is observed between 0.1 and 0.2 %w/w, where sol-gel transition can be expected for aqueous welan systems, whereas ΔG exhibits a strong increase as soon as welan is present in the alumina-welan dispersions (Figure 9). The differences in structural conditions between aqueous welan systems and alumina-welan dispersions are indicated also with the appearance of G_∞, (G_e in Figure 9) for the alumina-welan dispersions. For aqueous welan systems the values of G_∞ converge to limit conditions, $G_\infty = 0$. When sol-gel transition is observed for the aqueous systems, alumina dispersions exhibit 'solid like' response under non-destructive conditions of small deformations.
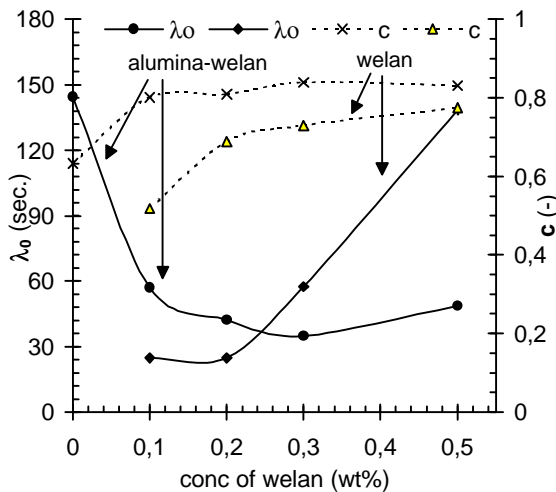
Fig. 8: Parameters l_0 and c of the Friedrich model vs. welan concentration for aqueous systems and alumina-welan dispersions at 25°C
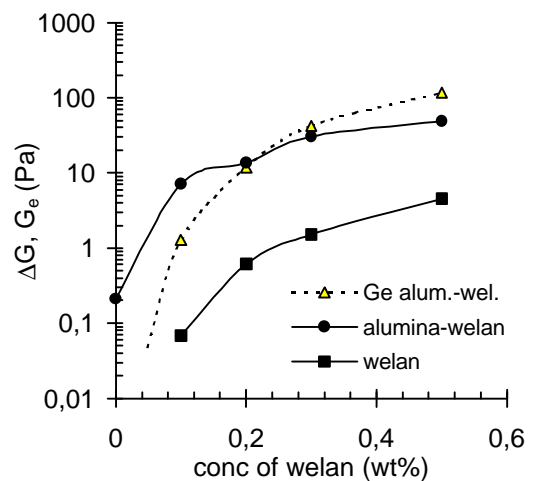
Fig. 9: Parameters DG and G_∞ of the Friedrich model vs. welan concentration for aqueous systems and alumina-welan dispersions
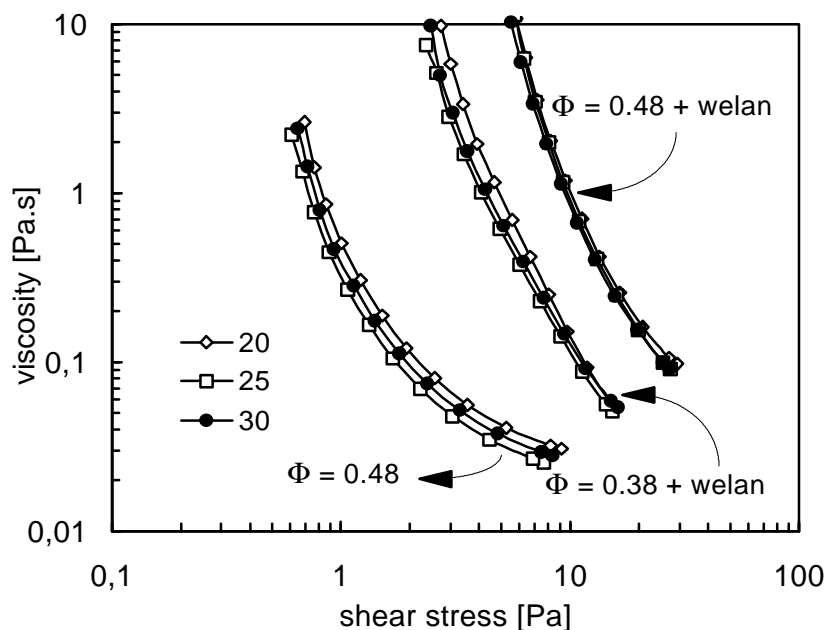
Fig. 10: Flow curves of aqueous alumina suspension ($\Phi = 0.48$) and alimina welan dispersions ($\Phi = 0.38$ and 0.48) at 20 °C, 25 °C and 30 °C.

CONCLUSIONS

Aqueous welan systems exhibit weak gel properties even at low polymer concentration and their behavior does not change appreciably when pH and other environmental conditions are changed. At 0.1 %w/w of welan the rheological properties are similar to those of polymer solution, whereas at higher polymer concentrations the systems exhibit behavior characteristic for structured systems or weak gels. Such rheological properties of aqueous welan systems enable different practical applications under wide range of environmental conditions.

Experimental tests performed with alumina-welan dispersions showed that even a small addition of welan to the disperse medium produces significant changes in the rheological properties of aqueous alumina suspensions. As soon as welan is present in the disperse medium, the rheological properties of alumina-welan dispersions changes significantly. Such systems exhibit the behavior of structured systems. At above 0.1 %w/w of welan in the disperse phase the rheological properies of alumina-welan systems are governed by welan concentration (weak gel behavior). The biopolymer under such conditions provides an essential contribution to particle stabilisation.

The experimental results demonstrate that welan can be used in ceramics as matrices for particle dispersions also in the case when high solid content should be

achieved. We need some additional tests to support these perspectives. Only for illustration, alumina-welan dispersions are possible to prepare at least to the solid volume fractions of 0.48. The effects of temperature (20 - 30 °C) on steady shear viscosity, evaluated from sequential shear rate steps, are studied for aqueous alumina suspensions at $\Phi = 0.48$ and alumina - welan (0.25 %w/w) dispersions at $\Phi = 0.38$ and 0.48. Figure 10 shows that the presence of welan in the disperse medium reduces the temperature effects.

REFERENCES

[1] P. A. Sandford, I. W. Cottrell, D. J. Pettitt, *Pure & Appl. Chem.* **1984**, *56 (7)*, 879 - 892.

[2] R. Lapasin and S. Pricl, "*Rheology of industrial polysaccharides, Theory and Applications*" Chapman&Hall, Blackie Academic & Professional, London, **1995,** Chapter. 1.

[3] R. Lapasin, A. Martorana, M. Grassi, S. Pricl, Proc. of 5th European Rheology Conference, Ed. I. Emri, Portorož , Slovenia **1998**, 579 -580.

[4] H. H. Winter, F. Chambon, *J. Rheol.* **1987**, *31*, 683 - 697.

[5] Chr. Friedrich, H. Braun., *Rheol. Acta* **1992**, *31*, 309 - 322.

POVZETEK

Obširna reološka karakterizacija vodnih gelskih sistemov velana je bila izvedena v območju koncentracij 0.1 do 0.5 utežnih % polimera v vodi. Da bi prikazala praktièno uporabo vodnih sistemov velana, sem raziskave razširila na disperzije glinice v vodnih gelskih matricah velana, pri katerih je bila koncentracija polimera v disperznem mediju v enakem obmoèju kot pri vodnih sistemih velana. Odvisnost viskoelastiènih lastnosti vodnih gelskih struktur velana in vodnih disperzij glinice v velanu od koncentracije polimera sem v predstavljenem delu analizirala z uporabo delnih odvodov konstitutivnih enaèb. Primerjava eksperimentalnih podatkov in rezultatov modeliranja, pridobljenih na vodnih sistemih velana, z rezultati doloèenimi za vodne disperzije glinice v gelskih matricah velana omogoèa predvideti pomen vodnih sistemov velana v tudi razliènih drugih aplikacijah.

INFLUENCE OF TEMPERATURE AND POLYMER CONCENTRATION ON RHEOLOGICAL PROPERTIES OF RHAMSAN

Urška Florjanèiè and Miha Žumer

Faculty of Chemistry and Chemical Technology,
Department of Chemical Engineering,
University of Ljubljana, Aškerèeva 5, SI 1001 Ljubljana,
Slovenia

Abstract. Microbial polysaccharide rhamsan imparts high solution viscosity at very low polysaccharide concentration and forms weak gels. The rheological behaviour, in particular the viscoelastic properties of aqueous rhamsan systems were investigated by using controlled stress rheometer HAAKE RS150, equipped with two sensor systems: cone-plate and double cone. The effects of temperature and polymer concentration on the rheological properties of rhamsan systems were examined under steady shear and oscillatory conditions. Variation in polymer concentration and environmental conditions results in changes of the consistency and the elastic response, which is very important for practical use. The viscoelastic data were described by applying the generalized Maxwell model.

Introduction

Microbial polysaccharides obtained from microbial fermentations can be produced under controlled conditions so that problems of property variations can be avoided [1]. They also present high structural regularity and offer a wide spectrum of rheological characteristics and potentially useful biological, chemical and physical properties. Biopolymers are widely employed in medicine, in agricultural, food, paint, ceramics, cosmetics, pharmaceutical, and textile industry, and for many others applications. They are used commercially as thickeners, film formers, gelling agents, suspending agents, stabilizers, flocculants, binders, lubricants, friction reducers, and as matrices [2].

Rhamsan gum is an anionic extracellular microbial polysaccharide produced by a strain of bacteria Alcaligenes spp. ATCC 31961 under aerobic fermentation conditions. Rhamsan greatly enhances the viscosity of aqueous media, leading with increasing polymer concentration to thermally stable systems with peculiar rheological properties [3]. Even at low polymer concentrations sol-gel transition can be attained.

We studied the rheological behaviour of aqueous rhamsan systems at different concentrations of polymer and examined the influence of temperature on the rheological properties of the investigated systems.

Experimental

Material: Rhamsan (R) produced by Monsanto company was dissolved in distilled water at polymer concentrations in the range of 0.1 - 1.0 wt.%. The measurements were carried out at three different temperatures in the range of 8°C - 45°C.

Instrument: The rheological behaviour of aqueous rhamsan systems was investigated by using the rotational controlled stress rheometer HAAKE RS150, equipped with cone and plate (6 cm, 2°) and double cone (6 cm, 4°) sensor systems.

Temperature was controlled by circulator HAAKE DC5-K20.

Procedure: Prepared rhamsan systems were investigated under continuous and oscillatory shear conditions.

Under destructive shear conditions the flow curves were determined from the shear stress ramps in the stress range of 0.03 Pa - 20 Pa, depending on the polymer concentration. Each sample was left at rest for 10 minutes before the shear stress ramp was carried out in order to ensure the same starting conditions for all the systems examined. After that, the stepwise procedure with sequential changes of shear stress was applied to examine the flow behaviour under equilibrium shear conditions.

The stress sweep tests at a frequency of 1 Hz were carried out in order to determine the range of linear viscoelastic response (the stress range of 0.005 Pa - 17 Pa, depending on the polymer concentration) under oscillatory shear conditions. The frequency sweep measurements under conditions of linear viscoelastic response were performed at a constant stress or constant strain amplitude in the range of 0.02 Hz - 10 Hz.

Analysis of viscoelastic data: The mechanical spectra obtained from the frequency sweep measurements were described by the generalized Maxwell model.

The relaxation spectra were derived on the basis of viscoelastic data analysis.

Results and discussion

Continuous shear conditions

The investigated aqueous rhamsan systems exhibit detectable reversible time dependent behaviour of thixotropic type. The appearance of Newtonian plateau in the low shear stress (or shear rate) range is observed for all samples (Fig. 1).
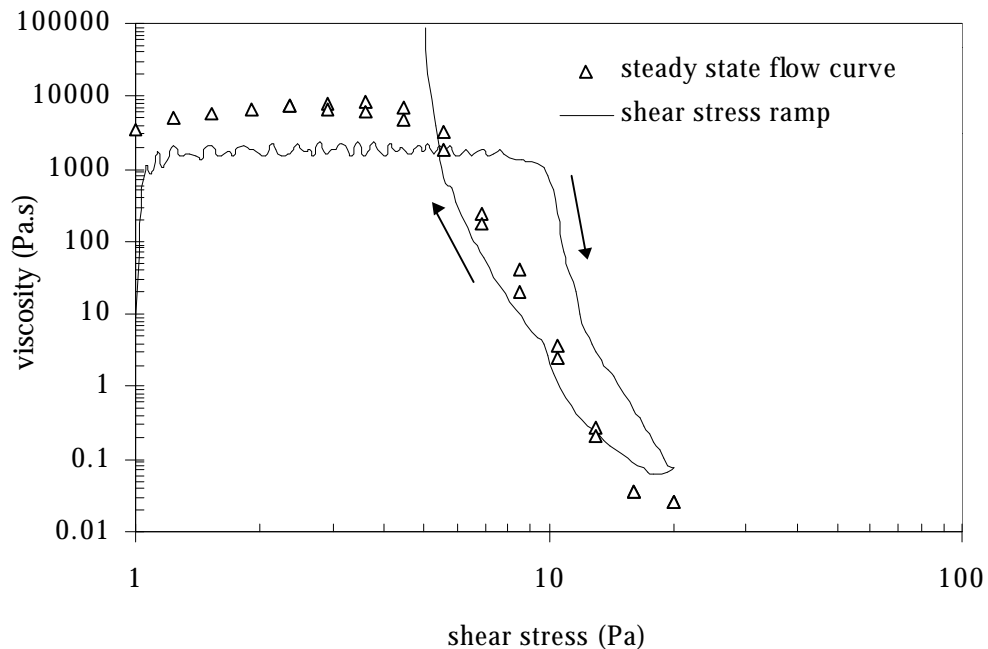
Figure 1. The comparison of the experimental data obtained from the steady shear flow and the shear stress ramp: 1 wt.% of rhamsan in distilled water at 25°C.

In the range of higher shear stresses the viscosity values obtained by using the stepwise procedure are comparable with the viscosity values arising from down curves of the shear stress ramps, whereas in the low shear stress range the down curves exhibit an asymptotic increase of viscosity, characteristic for plastic behaviour.

The shear dependent behaviour of the examined systems is strongly influenced by polymer concentration (Fig. 2). The most significant difference in the flow curves appears between the samples with 0.1 and 0.3 wt.% of rhamsan in distilled water.
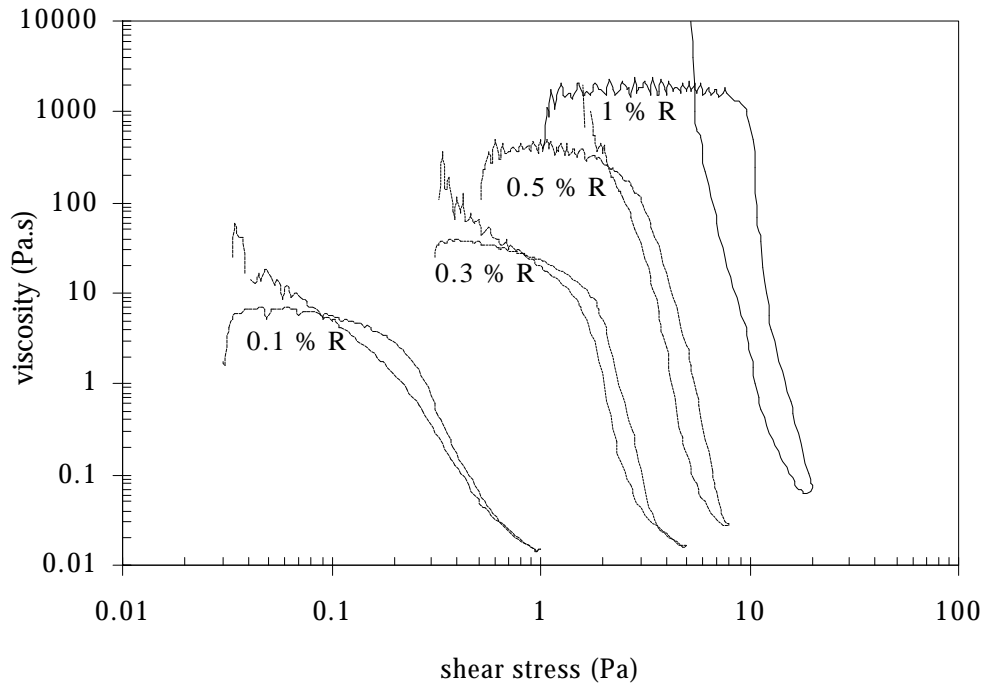
Figure 2. The effect of polymer concentration on the viscosity profiles at 25°C.

In the temperature range examined, the rheological properties of the samples prepared in distilled water are not influenced by the temperature (Fig. 3).
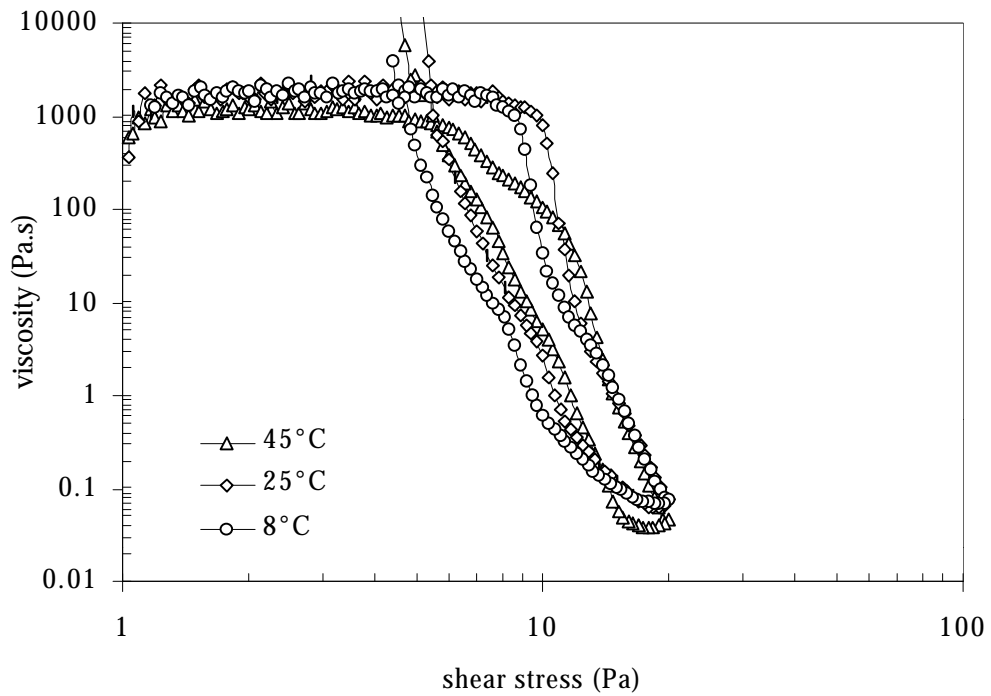
Figure 3. The effect of temperature on the viscosity profiles: 1 wt.% of rhamsan.

Detective difference is observed only for the samples of 0.1 wt.% of rhamsan in distilled water (Fig. 4).
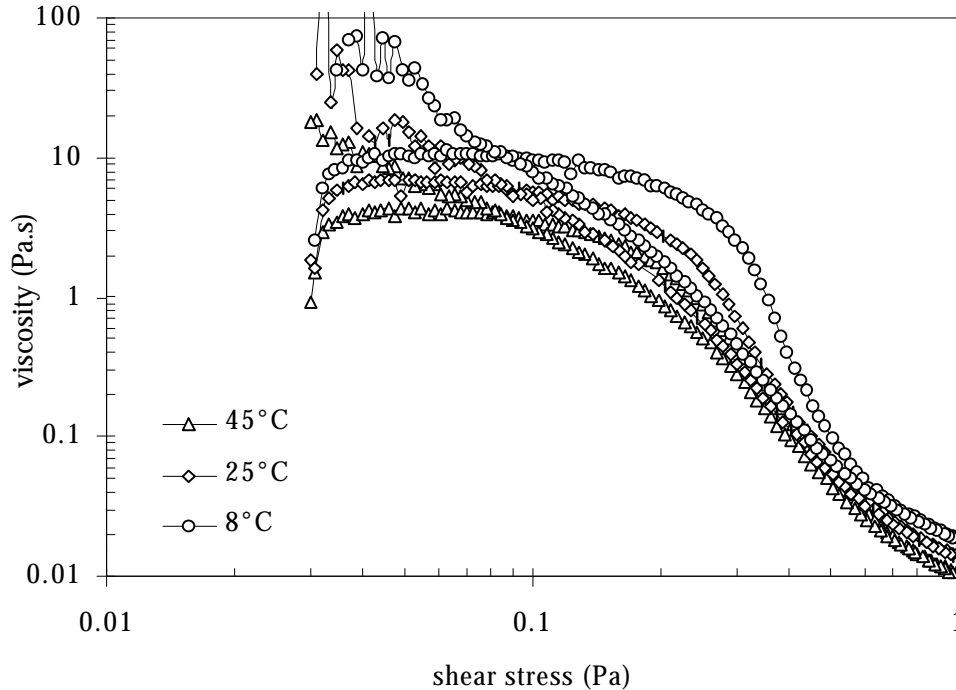
Figure 4. The effect of temperature on the viscosity profiles: 0.1 wt.% of rhamsan.

Oscillatory shear conditions

Under oscillatory shear conditions, stress sweep tests and frequency sweep experiments were performed in order to study the viscoelastic behaviour of the examined systems. All observations resulting from the continuous shear tests are confirmed with the results of oscillatory measurements.

The results of the stress sweep tests show an increase of the loss modulus, G', followed by a sharp decrease when the system passes from linear to non-linear viscoelastic regime (Fig. 5). The storage modulus, G', starts to decrease continuously at slightly higher stresses or strain amplitudes than those where the loss modulus starts to change. When polymer concentration increases, such overshoot of the loss modulus becomes more pronounced.
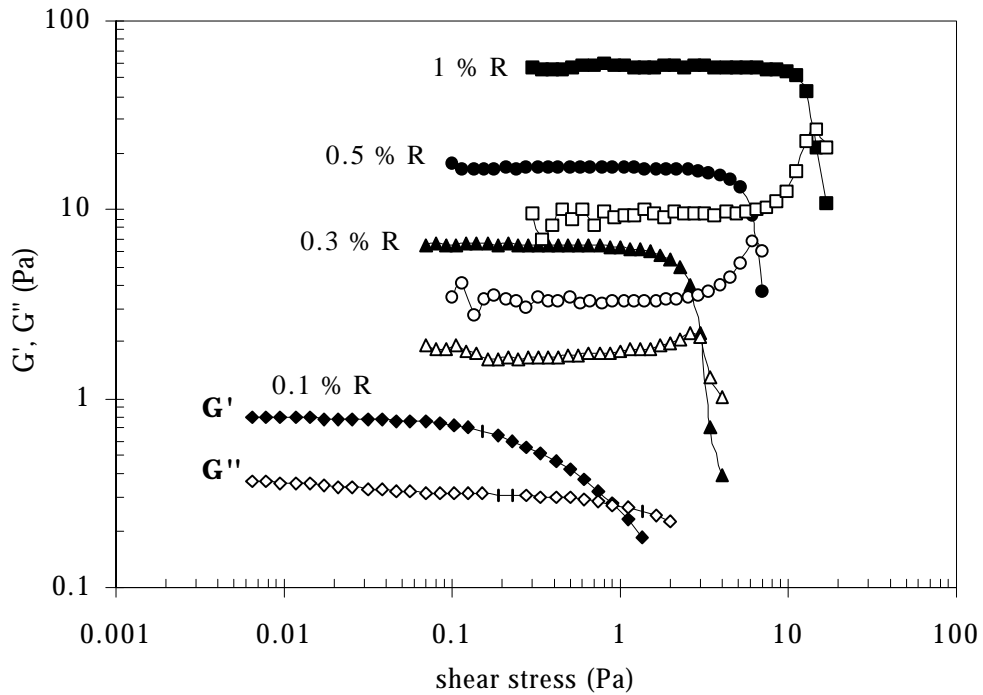
Figure 5. The effect of polymer concentration on dynamic functions G' and G'' obtained from the stress sweep tests at a frequency of 1 Hz and temperature of 25°C.

The critical strain characterizing the limit of the linear viscoelastic regime is around 10 % and is not strongly dependent on the polymer concentration (Fig. 6).
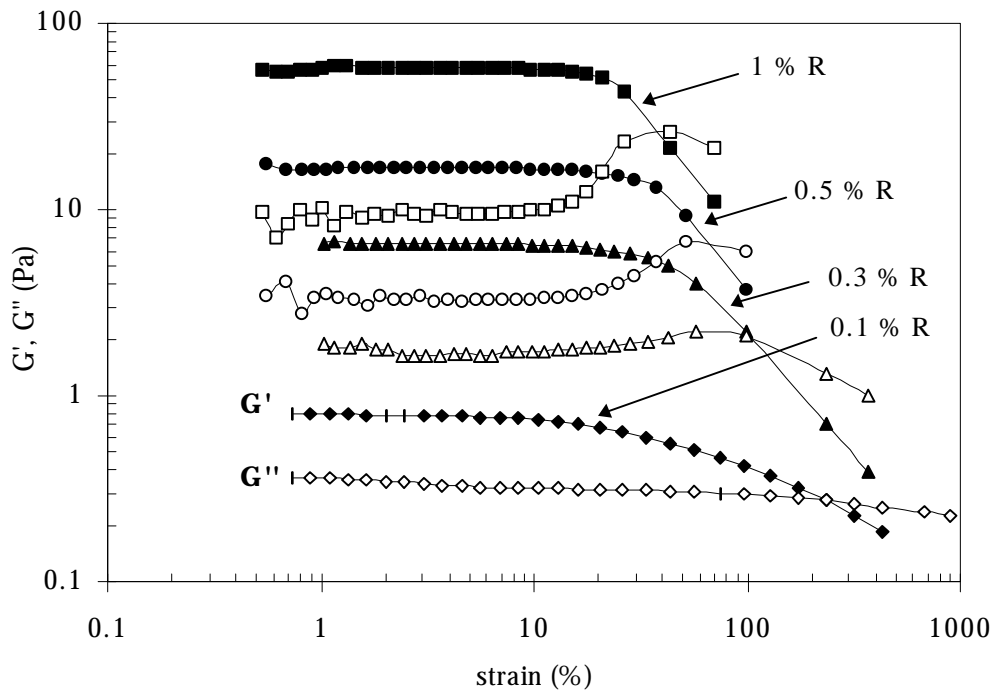
Figure 6. The effect of polymer concentration on G', G'', and the critical strain obtained from the stress sweep tests at a frequency of 1 Hz and temperature of 25°C.

The examination of temperature influence on dynamic functions shows that only at the lowest polymer concentration G' slightly decreases with increasing temperature, but G'' remains the same (Fig. 7 and Fig. 8).
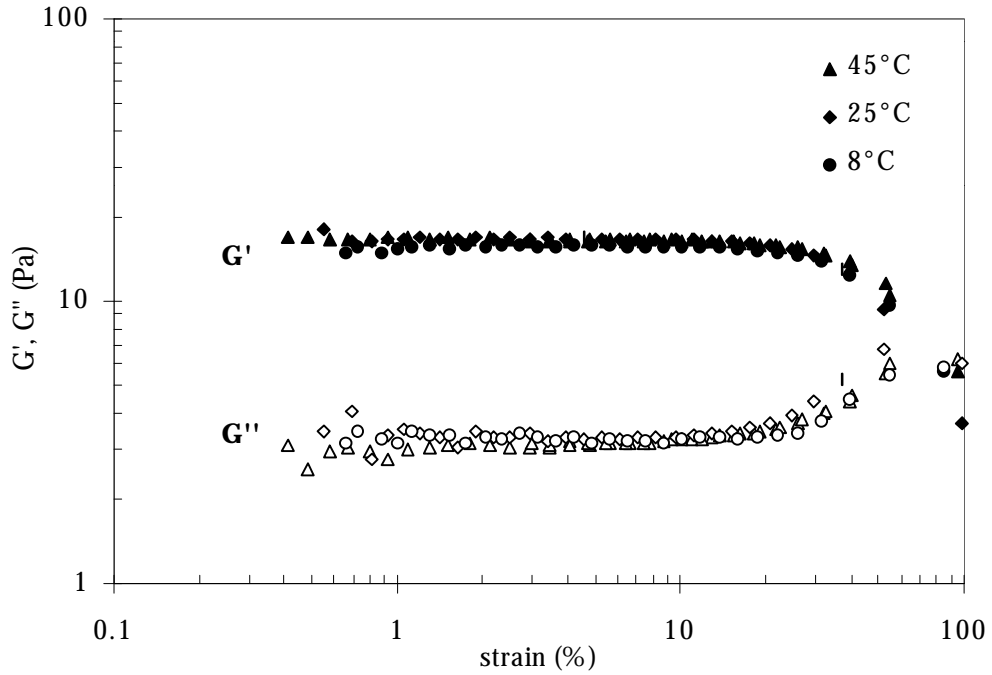
Figure 7. The effect of temperature on dynamic functions G' and G'' obtained from the stress sweep tests at a frequency of 1 Hz: 0.5 wt.% of rhamsan in distilled water.
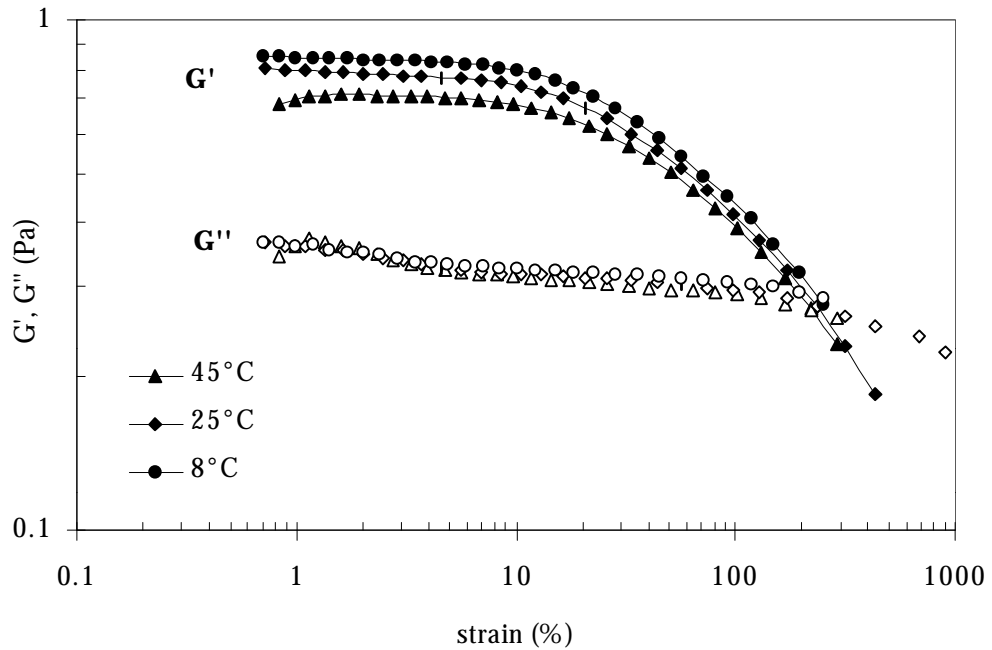
Figure 8. The effect of temperature on dynamic functions G' and G'' obtained from the stress sweep tests at a frequency of 1 Hz: 0.1 wt.% of rhamsan in distilled water.

In the frequency range examined, the elastic component is predominant for all samples. With increasing rhamsan concentration both dynamic functions becomes less sensitive to the applied frequency (Fig. 9). Such viscoelastic behaviour is usually found for structured systems and weak gels.
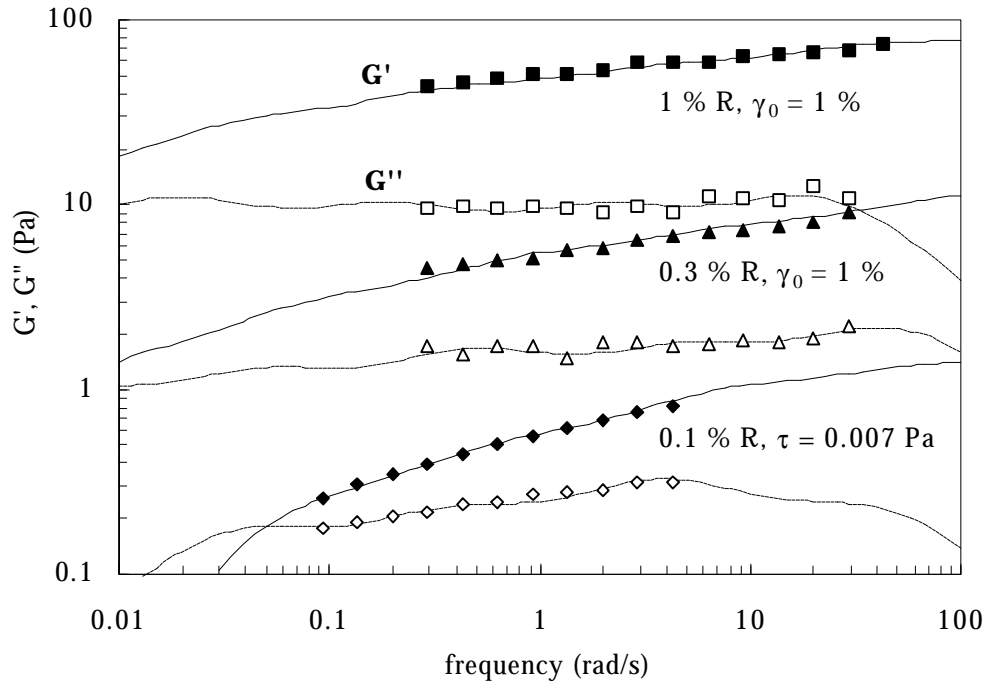
Figure 9. The comparison of experimental data from frequency sweep tests at 25°C with calculated values (curves) by using the generalized Maxwell model.

On the basis of viscoelastic data analysis by the generalized Maxwell model [1]:

$$G'(w) = \sum \frac{g_i \cdot l_i^2 \cdot w^2}{\left(1 + l_i^2 \cdot w^2\right)},$$

$$G''(w) = \sum \frac{g_i \cdot l_i \cdot w}{\left(1 + l_i^2 \cdot w^2\right)},$$

where ω is frequency, λ_i is the relaxation time of the ith Maxwell element and g_i is the elastic modulus, the discrete relaxation time spectra are derived.

The comparison of the oscillatory and the continuous shear behaviour (Fig. 10) shows a failure of the Cox-Merz rule [1]. The empirical Cox-Merz rule states that the magnitudes of the complex viscosity η^* and the steady shear viscosity η must be equal at

equal values of frequency and shear rate. Parallel dependencies of viscosity on shear rate and complex viscosity on frequency are obtained, with the values of complex viscosity higher than the viscosity values from continuous shear ramps. The rheological properties of the investigated systems differ from those of the polymer solutions and are more similar to those of the structured systems. Therefore the structural conditions of these systems can be described as a dispersion of gel micro domains in the polymer solution matrix.
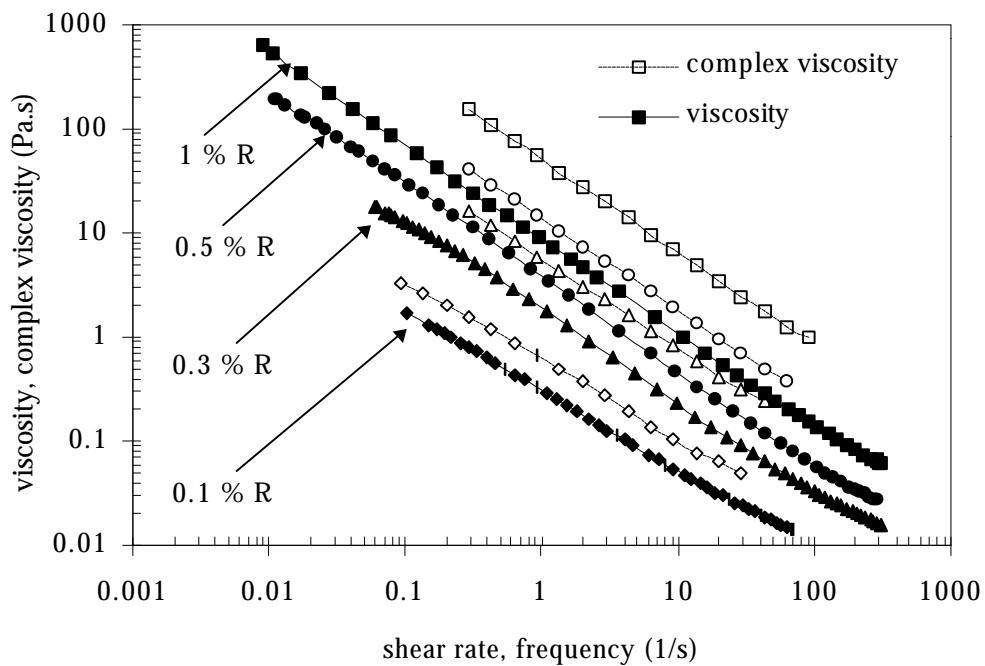
Figure 10. The comparison of the oscillatory and the continuous shear behaviour for samples with different polymer concentration at 25°C.

Conclusions

All investigated samples exhibit detectable reversible time-dependent behaviour of thixotropic type. The examined aqueous rhamsan systems are almost insensitive to temperature in the range of 8°C - 45°C. The most significant changes in the rheological behaviour appear between the samples with 0.1 and 0.3 wt.% of rhamsan. The storage modulus exceeds the loss modulus in the whole frequency range examined.

From the rheological characterisation it can be concluded that the investigated aqueous rhamsan systems behave as structured systems where gel micro domains are

dispersed in the polymer solution matrix. Such weak gel matrices can be used for preparation of a highly concentrated stable suspension containing well dispersed solid particles, e.g. in ceramic processing.

References

[1] R. Lapasin, S. Pricl, *Rheology of Industrial Polysaccharides: Theory and Applications*; Blackie Academic&Professional, An Imprint of Chapman&Hall, Glasgow, 1995.
[2] P. A. Sandford et al., *Pure & Appl. Chem.* **1984**, 56(7), 879-892.
[3] A. Cesaro et al., *Polymer* **1992**, 33(19), 4001-4008.

Povzetek. Ramzan je biopolimer, ki ga proizvaja bakterija Alcaligenes spp. ATCC 31961. Po kemijski zgradbi spada med polisaharide. Že nizke koncentracije biopolimera zadoščajo, da viskoznost raztopin močno naraste in nastanejo šibki geli. Reološko obnašanje v vodi raztopljenega ramzana smo proučevali z rotacijskim reometrom z nastavljivo strižno napetostjo HAAKE RS150, pri čemer smo uporabili senzorska sistema stožec-plošča ter dvojni stožec. Vpliv temperature in koncentracije biopolimera na reološke lastnosti proučevanih sistemov smo raziskovali pri stacionarnih in dinamičnih strižnih pogojih. Viskoelastično obnašanje vzorcev smo opisali s splošnim Maxwellovim modelom.

POLYMERS AS REAGENTS AND CATALYSTS. 39. INTRODUCTION OF PHENYLAMIDO AND PHENYLHYDRAZIDO GROUPS INTO A CROSSLINKED STYRENE-ACRYLATE MATRIX*

Marko Zupan, Peter Krajnc, and Stojan Stavber
Laboratory for Organic and Bioorganic Chemistry, Faculty of Chemistry and Chemical Technology and "J. Stefan" Institute, University of Ljubljana, Aškerčeva 5, Ljubljana, Slovenia

Abstract

Crosslinked copoly(styrene-p-nitrophenylacrylate) (**1**) was hydrolyzed to copoly(styrene-acrylic acid) (**2**) while further transformation with thionyl chloride gave copoly(styrene-acryloyl chloride) (**3**). Room temperature reaction of copoly(styrene-acryloyl chloride) (**3**) in acetonitrile with aromatic amines (aniline, pentafluoroaniline) and aromatic hydrazines (phenylhydrazine, pentafluorophenylhydrazine) gave the corresponding amides (**4**, **5**) and hydrazides (**6**, **7**). The swelling abilities of these amides and hydrazides depended on the type of functional group (amido, hydrazido), aromatic moiety (phenyl ring, pentafluorophenyl ring) and solvent polarity (chloroform, dimethylformamide, perfluorodecaline, perfluorooctane, perfluorocyclic ethers $C_8F_{16}O$). No significant enhancement in swelling capacity in perfluoro carbonated solvents was achieved by substitution of the phenyl ring by fluorosubstituted rings.

Introduction

Polymer supported reagents and catalysts play an important role in many fields of chemistry [1-9] and chemical technology [10-16], as well as in medicine [17-20] and chemistry related technologies [21-24]. Immobilisation of a reagent on an insoluble crosslinked polymer matrix is usually reflected

---

*Dedicated to the memory of Prof. Dr. Anton Šebenik.

in a much easier handling reagent, though reactivity can be changed. The required functionalization of a polymer reagent can be achieved through polymerisation of appropriately functionalized monomers or through further functionalization of polymer resins. Chemical modification of polymer resins therefore represents an important technique for preparation of new reagents, catalysts, separation media, etc. Recently much work in organic synthesis has been devoted to the use of polymer supported reagents, especially with respect to combinatorial chemistry [25-32].

By far the most studied polymer carrier is crosslinked polystyrene, and a number of reports have appeared dealing with additional crosslinking during the introduction of various functional groups into the polymer backbone, and the swelling behaviour of polystyrene based resins. Crosslinked polystyrene has a limited range of solvent compatibility due to its poor swelling capacity in polar solvents. It has, however, been demonstrated that substitution of some styrene units by acrylic esters and amides can substantively change the swelling behaviour [33]. It is known that the swelling ability of a crosslinked resin is an important factor in the selection of reaction conditions and the supported reagent itself. Since most of the reaction sites are positioned inside the crosslinked polymer particle, the accessibility of reactants is hindered in the case of poor swelling.

Perfluoro carbonated solvents have become increasingly important and the subject of many studies dealing with their applications in organic synthesis; this is due to some of their unique properties, such as inertness and non-toxicity [34,35]. Some new approaches, such as the fluorous biphasing concept were developed [36-40] and the advantages of such methods were proven, amongst other, by oxidations [41-43] and reductions [44,45]. The use of perfluoro carbonated solvents has also been reported in the context of soluble fluorocarbon polymers with reactive sites that can bind reagents and render them soluble in the fluorous phase [46]. We were interested in the effect of introduction of perfluorophenyl rings into the polymer matrix of

crosslinked copoly(styrene-acrylate) on the swelling abilities of perfluorophenyl derivatives in perfluoro carbonated solvents.

In the present paper we report the preparation of perfluorophenylamido, perflurophenylhydrazido, anilido and phenylhydrazido derivatives from copoly(styrene-p-nitrophenylacrylate) (**1**) and of the effect of the polymer structure changes on the swelling abilities of these resins in the perfluoro carbonated solvents perfluorooctane (Fluorinert FC-77), perfluorodecaline and perfluoro cyclic ethers (Fluorinert FC-75), as well as in chloroform and dimethylformamide.

Results and discussion

Several advantages of the crosslinked polystyrene-acrylate matrix for preparation of reagents and catalysts have already been presented [47,48]. We have demonstrated that p-nitrophenolate is a convenient leaving group for functionalization of crosslinked poly(styrene-acrylate) resin [49-52], and thus effectively substituting for 2,4,5-trichlorophenolate which was used in earlier investigations [47,48]. Crosslinked copoly(styrene-p-nitrophenylacrylate) (**1**) readily reacted with primary amines; however additional crosslinking of the polymer matrix was observed with some primary amines [49], bifunctional amines [50] and hydrazines [51]. On the other hand, under similar conditions functionalizations with less basic aromatic amines failed. For the above mentioned reasons we decided to test another synthetic strategy for preparation of anilido and phenylhydrazido derivatives, namely conversion of **1** to the acrylic acid derivative **2** and further transformation to the acid chloride derivative **3** (*Scheme*).

SCHEME
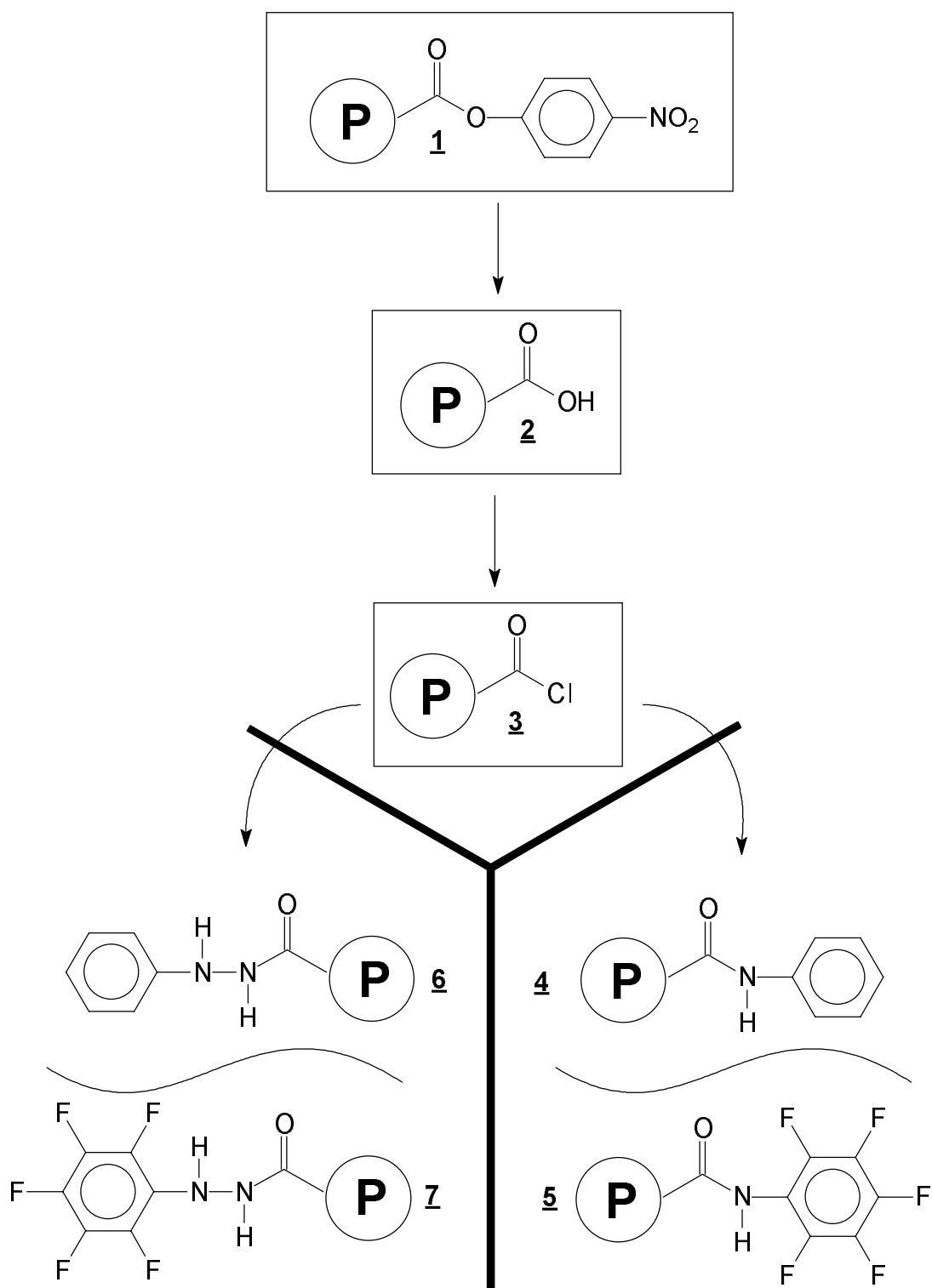
First we studied the reaction conditions for the hydrolysis of crosslinked copoly(styrene-p-nitrophenylacrylate) (**1**). Reaction with a 1.5 M aqueous solution of NaOH gave almost no desired product as the polymer beads sustained their chemical structure even after 10 hours reaction under reflux. We suspected the inertness of the beads was due to their poor swelling in water and thus performed the reaction in the presence of tetrahydrofurane since the swelling capacity of copoly(styrene-p-nitrophenylacrylate) (**1**) in tetrahydrofurane is 6.1 ml/g. The reaction was monitored by FTIR spectroscopy and after 2 hours of stirring under reflux the complete disappearance of nitro peak at 1345 cm^{-1} was observed, as well as the C=O double bond shift from 1760 cm^{-1} to 1650 cm^{-1}. The sodium salt of copoly(styrene-acrylic acid) was converted to acid (**2**) with HCl (C=O double bond shift to 1705 cm^{-1}). The resin was also analysed by combustion elemental analysis, proving complete substitution of p-nitrophenyl groups by hydroxy groups. Further reaction of copoly(styrene-acrylic acid) (**2**) with thionyl chloride in acetonitrile at room temperature resulted in a polymer resin with 13.7% of chlorine which represents more than 80% functionalization. FTIR spectroscopy showed the shift of the C=O double bond peak from 1705 cm^{-1} to 1785 cm^{-1} (*Figure 1*).

It is known that the chemical reactivity of acid chlorides strongly depends on their structure, the nucleophile and reaction conditions, and for this reason we decided to investigate the reactivity of the polymer supported acid chloride. Reactions of crosslinked copoly(styrene-acryloyl chloride) (**3**) with aniline or pentafluoroaniline in acetonitrile at 50°C in the presence of triethylamine as a base gave amides **4** or **5** , respectively, with 3.6 or 2.5 mequiv of amido group per gram (calculated for **4** 3.2 mequiv, calculated for **5** 2.5 mequiv of amido groups per gram). (*Scheme*). Under similar conditions reactions with phenylhydrazine or pentafluorophenylhydrazine resulted in resins **6** or **7**, respectively, with 2.8 mequiv or 2.5 mequiv of hydrazido groups per gram (calculated for **6** 3.0 mequiv, calculated for **7** 2.4 mequiv of hydrazido groups per gram). No additional crosslinking of the polymer matrix was observed during the nucleophile addition-substitution process. The reactions were easily monitored by FTIR spectroscopy (*Figure 1*) and
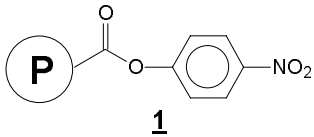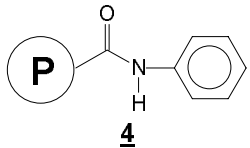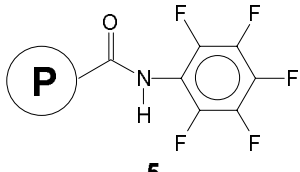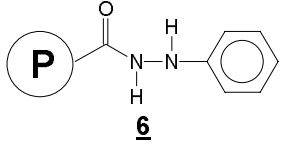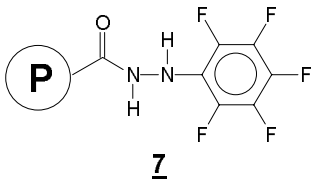
Figure 1: FTIR spectra of polymer resins

Wavenumber (cm^{-1})
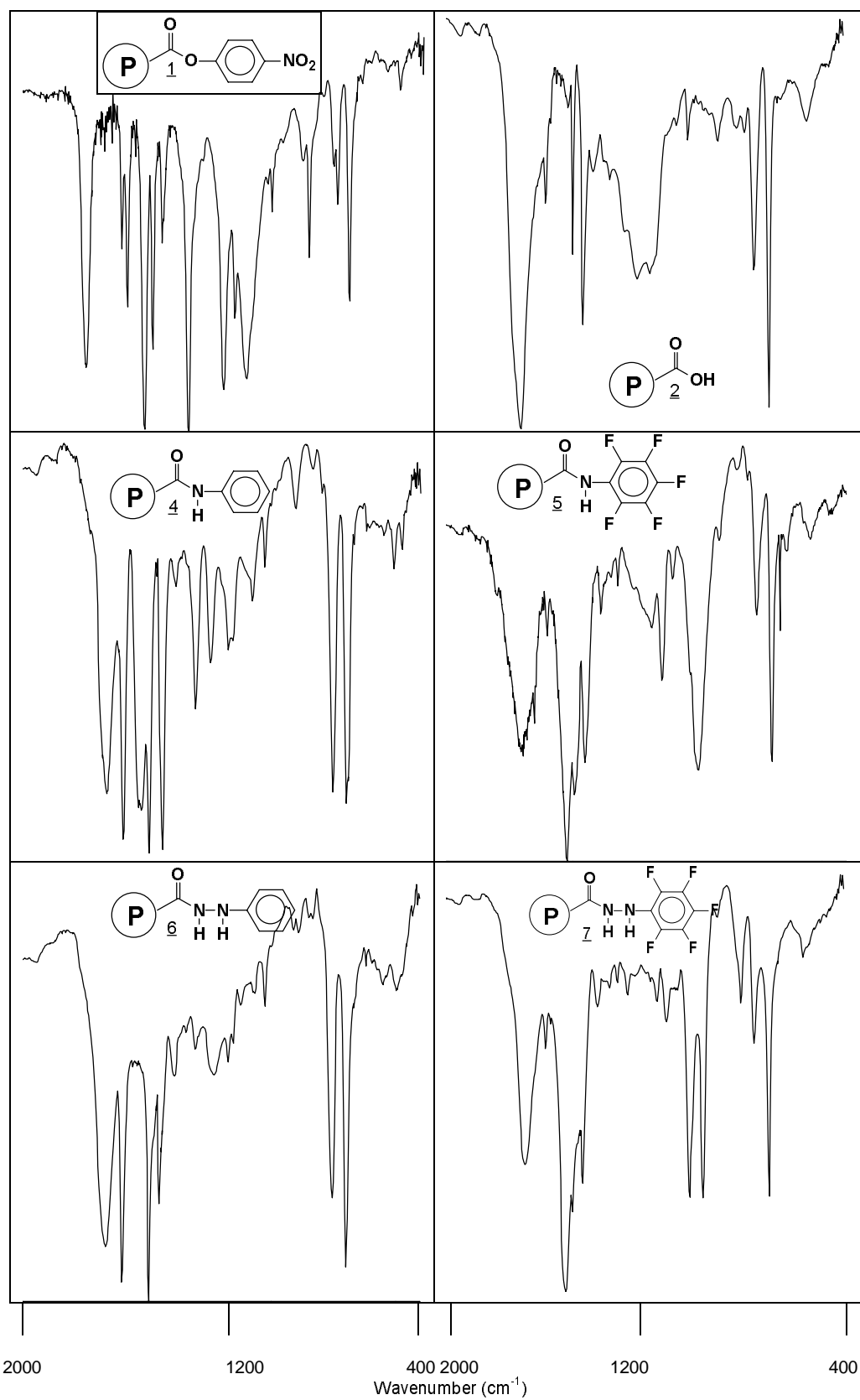
elemental analysis, showing nitrogen was again introduced into the molecules.

As crosslinked polymer beads are usually insoluble in all solvents, it is of vital importance for the polymer beads to swell in the solvent in use so that access of the soluble substrates to polymer supported reagents or catalysts is enabled. The swelling properties of the polymer in question is therefore one of its most important characteristics and can depend on the chemical structure of the backbone and the groups attached, the degree of crosslinking and its physical structure on one hand, and the properties of the solvent on the other. We tested the swelling abilities of resins **4**, **5**, **6** and **7** in dimethylformamide, chloroform and in the perfluorocarbonated solvents perfluorooctane (Fluorinert FC-77), perfluorodecaline and perfluoro cyclic ethers (Fluorinert FC-75). The results are presented in the *Table* and in *Figure 2*. Copoly(styrene-p-nitrophenylacrylate) (**1**) showed no swelling in fluoro solvents but high solvent capacity in dimethylformamide and chloroform. Substitution of the paranitrophenyl moiety in the polymer matrix with hydrazido or anilido groups did not cause significant changes in swelling capacity of the resins in chloroform; however, larger differences were observed in dimethylformamide where a higher decrease in swelling was observed for phenylhydrazido beads (**6**) than for anilido (**4**). Only slight enhancement of swelling was observed in perfluoro carbonated solvents for amido and hydrazido polymers in comparison to ester (**1**). Substitution of the phenyl ring by the pentafluorophenyl group in the polymer matrix enhanced swelling in dimethylformamide (the largest effect), chloroform and Fluorinert FC-75, while the opposite effect was observed in perfluorodecaline. On the other hand, substitution by a pentafluorophenyl group in amido resins diminished swelling in dimethylformamide (the largest effect) and chloroform, while enhancing swelling capacity in all perfluoro carbonated solvents.

The established effect of ester group substitution with amido or hydrazido functional group on swelling capacity of polymer resins (**4**-**7**) on the one hand, and the unpredictability of the effect of phenyl group substitution with pentafluoro analogues on the other, confirmed again how difficult is to foresee the physical properties of new polymeric systems and their behaviour in various solvents.

Table : Effect of polymer structure on swelling in various solvents[a]

		SOLVENT				
POLYMER	mL/g[b]	CHCl₃	FC-77	PFD	FC-75	DMF
1 (P–C(=O)–O–C₆H₄–NO₂)	1.9	4.8	1.9	1.9	1.9	7.5
4 (P–C(=O)–NH–C₆H₅)	1.7	5.0	2.3	1.9	2.2	6.5
5 (P–C(=O)–NH–C₆F₅)	2.0	4.8	2.5	2.4	2.5	5.9
6 (P–C(=O)–NH–NH–C₆H₅)	1.8	5.1	2.4	2.5	1.9	4.8
7 (P–C(=O)–NH–NH–C₆F₅)	2.0	5.7	2.4	2.2	2.4	5.6

[a] Swelling capacity in mL of swollen beads/g of air-dry resin.
[b] Volume of 1g air-dry resin.
FC-75: trade name for perfluoro carbonated solvent, consisting mainly of perfluorocyclic ethers $C_8F_{16}O$
FC-77: trade name for perfluoro carbonated solvent, consisting mainly of perfluorooctane
PFD: perfluorodecaline
DMF: dimethylformamide

Figure 2: *Effect of solvent and polymer structure on swelling of derivatives* **4**,**5**,**6** *and* **7**
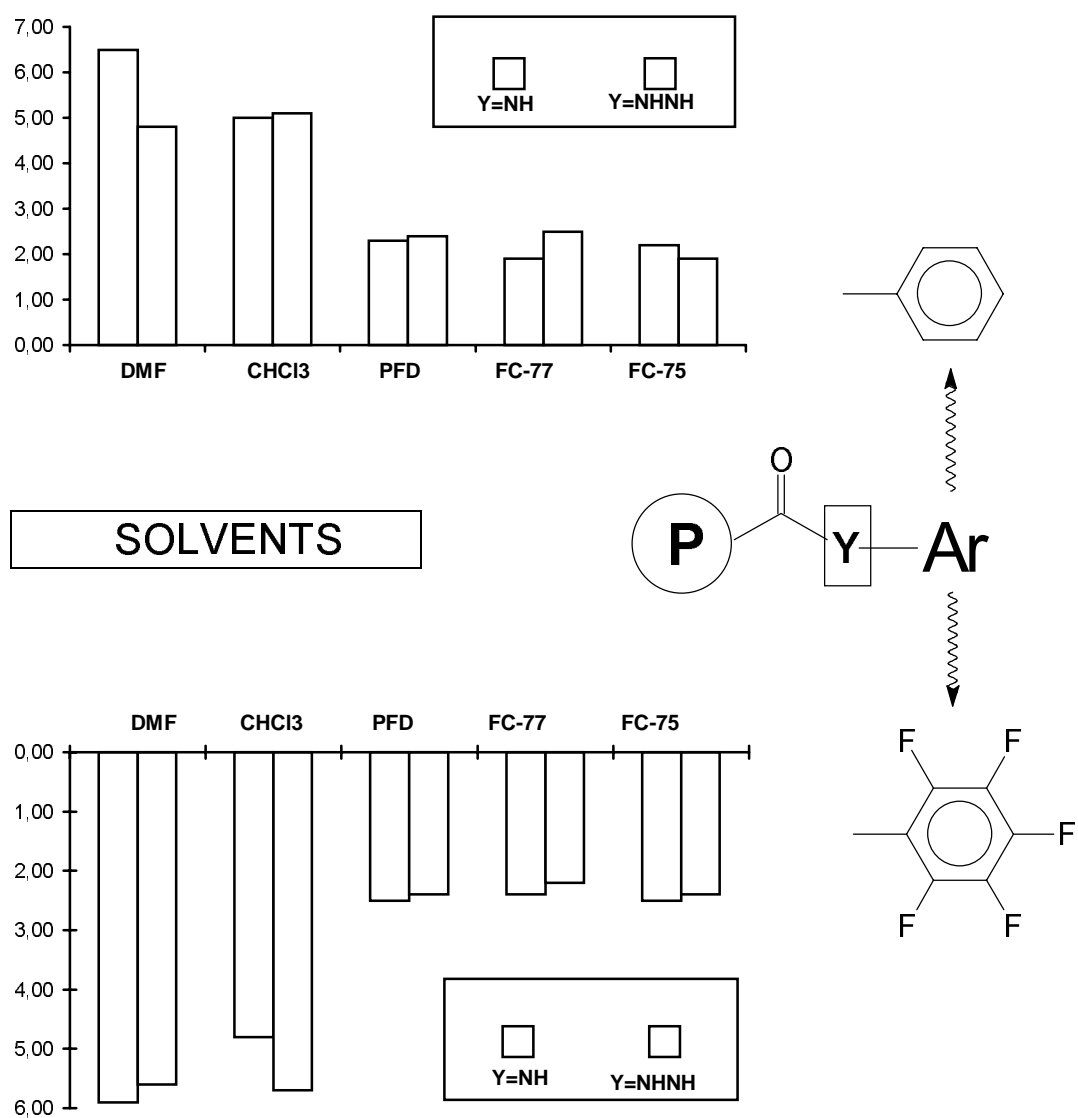
Experimental section

Materials

Commercially available p-nitrophenol (Fluka), acryloylchloride (Fluka), triethylamine (Fluka), azobisisobutyronitrile (Fluka), poly(vinylpyrrolidone) (Fluka), thionylchloride (Fluka), aniline (Aldrich), pentafluoroaniline (Fluorochem), phenylhydrazine (Aldrich), pentafluorophenylhydrazine (Fluorochem), perfluorodecaline (Fluorochem), Fluorinert FC-75 (3M, mainly perfluorocyclic ethers $C_8F_{16}O$), Fluorinert FC-77 (3M, mainly perfluorooctane) were used as received. Divinylbenzene (Merck, consisting also of 45% isomeric ethylvinylbenzenes) was washed with NaOH (5%) and water before use. The degree of functionalization of resins was determined by FTIR spectroscopy (Perkin-Elmer FT-IR 1720X) and combustion analysis (Perkin-Elmer 2400 CHN). Crosslinked copoly(styrene-p-nitrophenylacrylate) **1**, 4% DVB containing 2.61 mequiv of ester groups per gram of air-dry resin (3.2 mequiv of ester groups per gram of resin dried for 3 hours in vacuo at 110°C) was prepared by literature methods [49,51,52].

Preparation of crosslinked copoly(styrene-acrylic acid) (**2**)

5 g of air-dry copoly(styrene-p-nitrophenylacrylate) (**1**, 4% DVB) was suspended in 50 ml of tetrahydrofurane and 50 ml of a 1.5 M aqueous solution of NaOH was added. The reaction mixture was heated under reflux with stirring for 2 hours. The solid product was filtered off, washed with deionized water (10 x 50 ml), suspended in 50 ml of deionized water and acidified with diluted HCl until pH=4, again filtered off, washed with deionized water (3 x 50 ml), dried at room temperature for 20 hours and in vacuo at 60°C for 3 hours. The progress of the reaction was monitored by FTIR spectroscopy and combustion analysis and 2.24 g of dry polymer beads was obtained with the following composition: %C=76.20, %H=7.12, %N=0.0.

Preparation of crosslinked copoly(styrene-acryloyl chloride) (3)

5 g of dry copoly(styrene-acrylic acid) (**2**) was suspended in 60 ml of acetonitrile and 9.5 g of thionyl chloride was added. The reaction mixture was stirred at room temperature for 30 minutes. The solid product was filtered off, washed with acetonitrile (3 x 10 ml), dried at room temperature for 20 hours and 6.1 g of polymer beads was obtained. 1 g of air-dry product was further dried in vacuo at 60°C for 3 hours and 0.87 g of dry product was obtained with the following composition: %C=72.29, %H=6.27, %Cl=13.7

Reactions of crosslinked copoly(styrene-acryloyl chloride) (3) with amines and hydrazines

2 g of copoly(styrene-acryloyl chloride) (**3**) was suspended in 25 ml of acetonitrile, 1.96 g of triethylamine and the appropriate amount of amine (aniline, pentafluoroaniline) or hydrazine (phenylhydrazine, pentafluorophenylhydrazine) was added (molar ratio of acyl chloride function: amine= 1: 1.2). The reaction mixture was stirred at room temperature for 30 minutes and at 50°C for 5 hours.The solid product was filtered off, washed with acetonitrile (3 x 10 ml) dried at room temperature for 20 hours and the following amounts of products were isolated: anilide derivative (**4**): 2.57 g; pentafluoroanilide derivative (**5**): 3.15 g; phenylhydrazide derivative (**6**): 2.62 g; pentafluorophenyhydrazide derivative (**7**): 3.76 g;

1 g of air-dry product was further dried in vacuo at 100°C for 3 hours to obtain dry samples with the following compositions:

anilide derivative (**4**): 0.91 g, %C=81.16, %H=7.10, %N=5.06; 3.6 mequiv of anilido groups per gram (calculated 3.2 mequiv per gram),

pentafluoroanilide derivative (**5**): 0.95 g, %C=64.38, %H=4.63, %N=3.55; 2.5 mequiv of anilido groups per gram (calculated 2.5 mequiv per gram),

phenylhydrazide derivative (**6**): 0.93 g, %C=76.32, %H=7.44, %N=7.66; 2.8 mequiv of hydrazido groups per gram (calculated 3.0 mequiv per gram),

pentafluorophenyhydrazide derivative (**7**): 0.89 g, %C=60.97, %H=4.39, %N=7.06; 2.5 mequiv of hydrazido groups per gram (calculated 2.4 mequiv per gram).

Determination of the swelling capacities of polymer resins

1 ml of air-dry polymer resin was weighed, placed in a graduated cylinder, 10 ml of solvent was added and after 24 hours the volume of swollen beads was measured. The swelling capacities per gram are presented in the *Table*.

Acknowledgements

References

[1]   Labana S. S. (Ed.), *Chemistry and Properties of Crosslinked Polymers;* Academic Press, New York, 1977.
[2]   Seymour R. B. and Carraher Jr. C. E., *Structure-Property Relationships in Polymers;* Plenum Press, New York, 1984.
[3]   Ford W. T. (Ed.), *Polymeric Reagents and Catalysts;* American Chemical Society, Washington, D.C., 1986.
[4]   Laszlo P. (Ed.), *Preparative Chemistry Using Supported Reagents;* Academic Press, San Diego, 1987.
[5]   Sherrington D. C. and Hodge P. (Eds.), *Synthesis and Separations Using Functional Polymers;* John Wiley & Sons, Chichester, 1988.
[6]   Benhaur J. L. and Kinstle J. F. (Eds.), *Chemical Reactions on Polymers;* American Chemical Society, Washington, D.C., 1988.
[7]   Epton R. (Ed.), *Innovation and Perspectives in Solid Phase Synthesis. Peptides, Polypeptides and Oligonucleotides. Macro-organic Reagents and Catalysts;* SPCC (UK), Birmingham, 1990.
[8]   Tundo P., *Continuous Flow Methods in Organic Synthesis;* Ellis Horwood, Chichester, 1991.
[9]   Smith K. (Ed.), *Solid Supports and Catalysts in Organic Synthesis;* Ellis Horwood, Chichester, 1992.
[10] Eisenberg A. and King M., *Ion-Containing Polymers: Physical Properties and Structure;* Academic Press, New York, 1977.

[11] Flett D. S.(Ed.), *Ion Exchange Membranes;* Ellis Horwood, Chichester, 1983.
[12] Naden D and Streat M., *Ion Exchange Technology;* Ellis Horwood, Chichester, 1984.
[13] Lloyd D.R. (Ed.), *Materials Science of Synthetic Membranes;* American Chemical Society, Washington, D.C., 1985.
[14] Collins A.N., Sheldrake G.N., and Crosby J. (Eds.), *The Commercial Manufacture and Applications of Optically Active Compounds;* John Wiley & Sons, Chichester, 1992.
[15] Scranton A. B., Bowman C. N., and Peiffer R. W. (Eds.), *Photopolymerization. Fundamentals and Applications;* American Chemical Society, Washington DC, 1997.
[16] Dyer A., Hudson M. J., and Williams P. A. (Eds.), *Progress in Ion Exchange. Advances and Applications;* The Royal Society of Chemistry, Cambridge, 1997.
[17] Carraher Jr. C. E. and Gebelein C. G. (Eds.), *Biological Activities of Polymers;* American Chemical Society, Washington D.C., 1982.
[18] Wells J. I., *Pharmaceutical Preformulation: The Physicochemical Properties of Drug Substances;* Ellis Horwood, Chichester, 1988.
[19] Peppas N. A. and Langer R. S. (Eds.), *Advances in Polymer Science. 122. Biopolymers II;* Springer-Verlag, Berlin, 1995.
[20] Park K. (Ed), *Controlled Drug Delivery. Challenges and Strategies;* American Chemical Society Washington, DC, 1997.
[21] Davidson T. (Ed.), *Polymers in Electronics;* American Chemical Society, Washington, D.C., 1984.
[22] Guillet J., *Polymer Photophysics and Photochemistry: An Introduction to the Study of Photoprocesses in Macromolecules;* Cambridge University Press, Cambridge, 1985.
[23] Zachmann H.-G. (Ed.), *Advances in Polymer Science. 108. Structure in Polymers with Special Properties*; Springer-Verlag, Berlin, 1993.
[24] Narkis M. and Rosenzweig N. (Eds.), *Polymer Powder Technology;* John Wiley and Sons, Chichester, 1995.
[25] Hermkens P. H. H., Ottenheijm H. C. J., and Rees D. C., *Tetrahedron* **1996**, *52*, 4527-4554.
[26] Hermkens P. H. H., Ottenheijm H. C. J., and Rees D. C., *Tetrahedron* **1997**, *53*, 5643-5678.
[27] Armstrong R. W., Combs A. P., Tempest P. A., Brown S. D., and Keating T. A., *Acc. Chem. Res.* **1996**, *29*, 123-131.
[28] Thompson L. A. and Ellman J. A., *Chem. Rev.* **1996**, *96*, 555-600.
[29] Früchtel J. S. and Jung G., *Angew. Chem.* **1996**, *108*, 19-46.
[30] Lam K. S., Lebl M., and Krchňak V., *Chem. Rev.* **1997**, *97*, 411-448.
[31] Jung G., Ed., *Combinatorial Peptide and Nonpeptide Libraries;* VCH, Weinheim, 1996.
[32] Czarnik A. W. and DeWitt S. H. (Eds.), *A Practical Guide to Combinatorial Chemistry;* American Chemical Society, Washington DC, 1997.
[33] Arshady R. and Ledwith A., *Reactive Polymers* **1983**, *1*, 159-174.
[34] Zhu D.-W., *Synthesis* **1993**, 953-954.
[35] Chambers R. D. and Edwards A. R., *J. Chem. Soc. Perkin Trans. 1*, **1997**, 3623-3627.
[36] Studer A., Hadida S., Ferritto R., Kim S.-Y., Jeger P., Wipf P., and Curran D. P., *Science* **1997**, *275*, 823-826.
[37] DiMagno S. G., Dussault P. H., and Schultz J. A., *J. Am. Chem. Soc.* **1996**, *118*, 5312-5313.
[38] Gladysz J. A., *Science* **1994**, *266*, 55-56.
[39] Horvath I. T. and Rabai J., *Science* **1994**, *266*, 72-75.
[40] Cornils B., *Angew. Chem.* **1997**, *109*, 2147-2149.
[41] Klement I., Lütjens H., and Knochel P., *Angew. Chem.* **1997**, *109*, 1605-1607.
[42] Pozzi G., Cinato F., Montanari F., and Quici S., *J. Chem. Soc. Chem. Commun.* **1998**, 877-878.
[43] Pozzi G., Colombani I., Miglioli M., Montanari F., and Quici S., *Tetrahedron* **1997**, *53*, 6145-6162.
[44] Curran D. P. and Hadida S., *J. Am. Chem. Soc.* **1996**, *118*, 2531-2532.
[45] Juliette J. J. J., Horvath I. T., and Gladysz J. A., *Angew. Chem.* **1997**, *109*, 1682-1684.

[46] Bergbreiter D. E. and Franchina J. G., *J. Chem. Soc. Chem. Commun.* **1997**, 1531-1532.

[47] Arshady R., *Adv. Mater.* **1991**, *3*, 182-190.

[48] Arshady R., *Makromol. Chem.* **1984**, *185*, 2387-2400.

[49] Zupan M., Krajnc P., and Stavber S., *Polymer* **1996**, *37*, 5477-5481.

[50] Zupan M., Krajnc P., and Stavber S., *J. Pol. Sci.: Part A: Polymer Chemistry* **1998**, *36*, 1699-1706.

[51] Zupan M., Krajnc P., and Stavber S., *J. Pol. Sci.: Part A: Polymer Chemistry* **1996**, *34*, 2325-2331.

[52] Zupan M., Krajnc P., Trnovšek R., and Stavber S., *Acta Chim. Slov.* **1996**, *43*, 189-205.

Povzetek

Zamreženi kopoli(stiren-p-nitrofenilakrilat) (**1**) smo hidrolizirali do kopoli(stiren-akrilne kisline) (**2**) ter nadalje s tionil kloridom pretvorili v zamrežen kopoli(stiren-akriloil klorid) (**3**). Pri sobni temperaturi smo v acetonitrilu iz kopoli(stiren-akriloil klorida) (**3**) z aromatskimi amini (anilin, pentafluoroanilin) in aromatskimi hidrazini (fenilhidrazin, pentafluorofenilhidrazin) sintetizirali zamrežene amidne (**4**, **5**) in hidrazidne derivate (**6**, **7**). Stopnja nabrekanja polimernih nosilcev v topilih je odvisna od tipa funkcionalne skupine (amid, hidrazid), aromatskega dela (fenilni obroč, pentafluorofenillni obroč) in polarnosti topila (kloroform, dimetilformamid perfluorodekalin, perfluorooktan, perfluoro ciklični etri). Zamenjava fenilnega obroča s pentafluorofenilnim ne vodi do bistvenega povečanja nabrekanja v perfluoro topilih.

EFFECT OF POLYELECTROLYTE ON THE AGGREGATION OF CATIONIC SURFACTANTS IN AQUEOUS SOLUTIONS[1]

Ksenija Kogej and Jože Škerjanc

Faculty of Chemistry and Chemical Technology, University of Ljubljana, 1000 Ljubljana, Slovenia

Abstract: The effect of the specific nature of the polyelectrolyte on complexation with alkylpyridinium surfactants has been investigated. Two polyelectrolytes with the same linear charge density were studied, i.e. sodium poly(acrylate), NaPA, and sodium poly(styrenesulfonate), NaPSS. It has been found by fluorescence measurements that in the case of a more hydrophobic NaPSS the association of surfactant with the polyion is practically complete whereas for hydrophilic NaPA less than 80% of surfactant is associated with the polymer. Measurements of electrolytic conductivity, Λ, showed that the mobility of surfactant ions is greatly reduced in the presence of oppositely charged polyion. In NaPSS solutions, a pronounced minimum in Λ is seen in the range of cooperative binding. On the contrary, in NaPA solutions only a plateau region is observed. The difference in behavior has been explained by inclusion of the hydrophobic aromatic group on PSS^- into the surfactant minimicelle leading to formation of a very stable aggregate. This is accompanied by a release of a considerable amount of Na^+ and Cl^- ions into the solution. No such specific interaction is present between PA^- and surfactant aggregate. They are associated more loosely only through electrostatic interactions.

[1] Dedicated to the memory of Professor Anton Šebenik

INTRODUCTION

In the past decades considerable interest has developed in polymer-surfactant solutions because of the importance of these systems in a variety of applications. In the case of oppositely charged polyelectrolytes and surfactants, strong interactions are observed due to a contribution of electrostatic forces and cooperative hydrophobic effects between bound surfactant ions. This results in formation of micelle-like aggregates around the polyion chain, which are detected already much below the ordinary critical micelle concentration. The evidence for the existence of polyelectrolyte-surfactant complexes has come from indirect methods such as surface tension [1] and dye solubilization [2-5], and from direct measurements of binding by the use of surfactant ion-selective electrodes [6-9]. Sometimes, expressions 'minimicelle' [2] or polyelectrolyte induced micelle [4,5] are used in this context to stress the similarity with ordinary micelles. The surfactant concentration at which cooperative binding to polyelectrolyte starts depends on the nature of both, the surfactant and the polyelectrolyte. In particular, the surfactant head group and the length of its hydrocarbon tail as well as the polyion charge density play an important role.

In this contribution, we were interested in how the specific nature of the ionic groups on the polymer affects the formation of polyelectrolyte-surfactant complex. We investigated aggregation of dodecyl- (DPC) and cetyl- (CPC) pyridinium chlorides in the presence of two anionic polyelectrolytes, polystyrenesulfonate (PSS⁻) and polyacrylate (PA⁻).

(a)   (b)
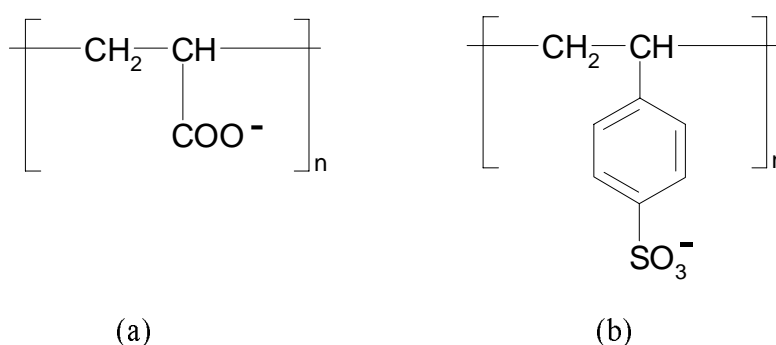
Figure 1: *Structure of the monomer unit of the polyelectrolyte: (a) polyacrylate; (b) polystyrenesulfonate.*

Polymer structures are shown in Figure 1. These two polyanions are characterized by the same linear charge-density parameter λ, defined as

$$\lambda = \frac{e_0^2}{4\pi\varepsilon_0\varepsilon kTb} \tag{1}$$

where e_0 is the protonic charge, ε_0 and ε are the permitivity of vacuum and the dielectric constant of solvent, k is the Boltzmann constant, and b is the average distance between two adjacent charges on the polymer chain. The structural parameter b is the same for all vinylic polymer chains (2.52 nm) and gives the value 2.83 for λ in aqueous solutions at 25 °C. Therefore, the difference between the two polyanions lies in the functional groups of the monomer unit. Due to the aromatic group attached to the chain, PSS⁻ is more hydrophobic than PA⁻. Some specific interactions between the surfactant and the polymer backbone can be expected in the polystyrenesulfonate case. We have chosen conductivity in combination with fluorescence measurements to probe the systems.

EXPERIMENTAL SECTION

Materials

Sodium poly(styrene sulfonate), NaPSS, with a molecular weight of about 70 000 g/mol and degree of sulfonation 1.0, supplied by Polysciences, Inc. (Warrington, PA) was prepared and purified by the procedure described in the literature [10]. Sodium poly(acrylate), NaPA, with a molecular weight around 10 000 g/mol, was prepared from polyacrylic acid, HPA (K & K Laboratories, Inc., Plainview, N. Y.) as reported previously [11]. N-dodecylpyridinium chloride, DPC, a gift from Merck-Schuchardt, and N-cetylpyridinium chloride, CPC (Kemika, Zagreb) were thoroughly purified by repeated recrystallization from acetone and vacuum dried at 50 °C. The fluorescence probe, 8-anilino-1-naphthalenesulfonic acid, ammonium salt (ANS), supplied by Fluka was used as received.

A constant concentration of NaPSS or NaPA, equal to 5×10^{-4} monomol/kg, was used in all experiments. Surfactant stock solutions, either in pure water or in aqueous polyelectrolyte solutions, were prepared by weight from dried substances. The specific conductivity of water used for the preparation of solutions was below 1.2×10^{-6} $\Omega^{-1}cm^{-1}$.

Fluorescence

ANS fluorescence spectra were recorded on a Perkin-Elmer Model LS-50 Luminescence Spectrometer with a water thermostated cell holder at 25°C. A 1 cm path quartz cuvette was used. A freshly prepared ANS stock solution was added to systems prior to measurements. The ANS fluorescence intensity at 483 nm was followed to obtain the total degree of coverage of the polyion with surfactant ions. The excitation wave length was 365 nm. Excitation and emission slit widths for recording the spectra were set to 5.0 nm, scan rate was 240 nm min^{-1}, and two scans were accumulated for each run.

Conductivity

The specific conductivity of solutions was measured at 25°C with a Metrohm 712 Conductometer using a Metrohm cell with a cell constant 0.095 cm^{-1}. The measurements were performed in aqueous solutions of pure surfactants and in polyelectrolyte-surfactant solutions at constant NaPSS or NaPA concentration. The concentration of surfactant was changed by a titration technique.

RESULTS AND DISCUSSION

Fluorescence

The fluorescence emission spectrum of ANS exhibits a marked dependence on the polarity of the solvating medium [12]. In nonpolar environment, its fluorescence maximum shifts to shorter wave-lengths (~483 nm) with concomitant increase in quantum yield. We have followed fluorescence intensity of ANS at 483 nm as a function
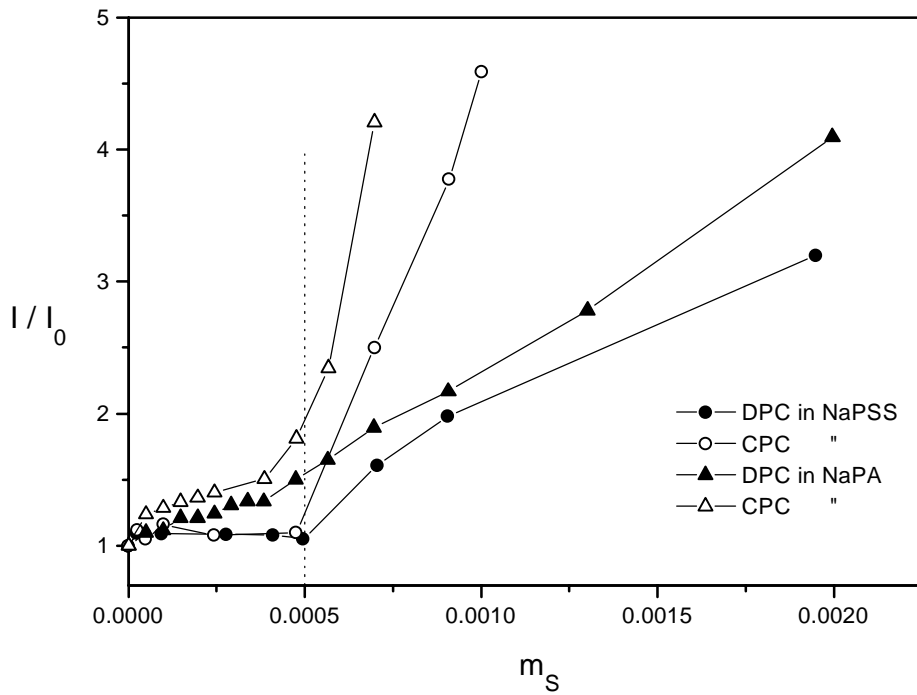
Figure 2: *The dependence of fluorescence intensity of ANS on DPC (CPC) concentration (m) in solutions of NaPSS and NaPA.*

Polyelectrolyte concentration: $m_P = 5 \times 10^{-4}$ m (dotted line).

of surfactant concentration. The results are shown in Figure 2 as plots of $I \, / \, I_0$ vs. surfactant concentration; I and I_0 are the fluorescence intensities of the probe in polyelectrolyte solutions with various surfactant concentrations and in pure polyelectrolyte solution, respectively. The $I \, / \, I_0$ ratio in NaPSS solutions is at first constant (around 1), indicating that the polarity of the surrounding medium is unchanged and equal to that of pure water. All the surfactant added binds to PSS chain. After the binding is finished, the $I \, / \, I_0$ increases sharply due to the presence of free surfactant in solution and consequently to the decreased polarity of the environment. From the concentration of surfactant at this threshold concentration, m_S, the total degree of coverage, β, of the polyelectrolyte chain with surfactant ions [2] was obtained from expression

$$\beta = \frac{m_S}{m_P} \qquad (2)$$

Here, m_p is the constant polyelectrolyte concentration. In this calculation, the concentration of free surfactant was not taken into account. For both surfactants in NaPSS solutions, this threshold surfactant concentration is approximately 5×10^{-4} mol/kg which gives β around 1. This is in agreement with the degree of binding determined by surfactant ion-selective electrode measurements [9] and implies that DPC and CPC are completely associated with polystyrenesulfonate anion.

The measurements in NaPA solutions show a somewhat different picture. Before commenting on this, we have to mention the following. Since ANS is negatively charged it can also interact strongly with cationic surfactants. It may form small aggregates with surfactant cations and even promote the release of DP^+ (CP^+) from polyelectrolyte-surfactant complex by simply displacing the association equilibrium [2]. The concentration of ANS used to probe NaPSS solutions was about 10% lower than the NaPSS concentration ($\sim 4.5 \times 10^{-4}$ mol/kg). The same concentration of ANS in NaPA solutions caused the equilibrium to shift in favor of the probe. The surfactant cations associated more readily with ANS than with polyacrylate anion and consequently no binding of DP^+ (CP^+) to PA^- could be detected. By decreasing the concentration of ANS to about one half of NaPA concentration ($\sim 2.5 \times 10^{-4}$ mol/kg) the usual plots were obtained (see Figure 2). This shows that the association of alkylpyridinium cations with PSS^- anion is much stronger than with PA^- anion.

We can see (cf. Figure 2) that the I / I_0 ratio in NaPA increases slightly also below the brake point. The binding to PA^- is completed at approximately 3.9×10^{-4} mol/kg for DPC and 4.0×10^{-4} mol/kg for CPC giving for β the values 0.78 and 0.8, respectively. This is slightly larger than β values reported in the literature [8]. The literature data for β obtained from surfactant ion-selective electrode measurements are 0.7 for tetradecylpyridinium bromide, TPB, and 0.75 for DPC, respectively. Our values are somewhat higher probably owing to the above mentioned simultaneous association of these surfactants with NaPA and ANS.

Comparison of β values in NaPSS and NaPA solutions with the same polyion concentration shows that the degree of binding of DPC and CPC is much lower in NaPA case in spite of the same linear charge density parameter λ for both polyanions. Also, the

aggregate formed between DP^+ (CP^+) and PSS^- seems to be more stable than the aggregate between DP^+ (CP^+) and PA^-.

Conductivity.

The molar conductivity, Λ, for pure surfactant solutions and for surfactant solutions in the presence of polyelectrolyte is presented in Figures 3 and 4. The Λ vs. $\sqrt{c}$ curves (c is the concentration of surfactant in mol/L, M) for pure surfactants show a usual dependence. The distinctive break in the curves observed at higher concentrations corresponds to micelle formation and from this the critical micelle concentration, cmc, was determined for both surfactants. The cmc values are 1.64×10^{-2} M and 8.6×10^{-4} M for DPC and CPC, respectively. They are in a reasonable agreement with the previously determined values [8,9].

The conductivity curves in the presence of polyelectrolyte will be discussed separately for two concentration regions: first, for surfactant concentrations above $\sim 5 \times 10^{-4}$ M (this concentration can be regarded as the 'equivalent' concentration because it is equal to the concentration of charged groups on the polymer), and second, for surfactant concentrations below the 'equivalent point' At surfactant concentrations above the 'equivalent point', the Λ curves in the presence of the polyion resemble behavior similar to pure surfactant solutions. They show a break at the so called apparent critical micelle concentration, cmc^*. This term is usually used for characterizing formation of free surfactant micelles in the presence of the polymeric component. The cmc^* is higher than the ordinary cmc due to the formation polyelectrolyte-surfactant complex at lower surfactant concentrations. The bound surfactant is not available for micellization, consequently, free micelles appear at somewhat higher total surfactant concentration. From cmc and cmc^* we can also estimate the total degree of binding of surfactant to polyelectrolyte from expression

$$\beta = \frac{cmc^* - cmc}{m_P} \qquad (3)$$
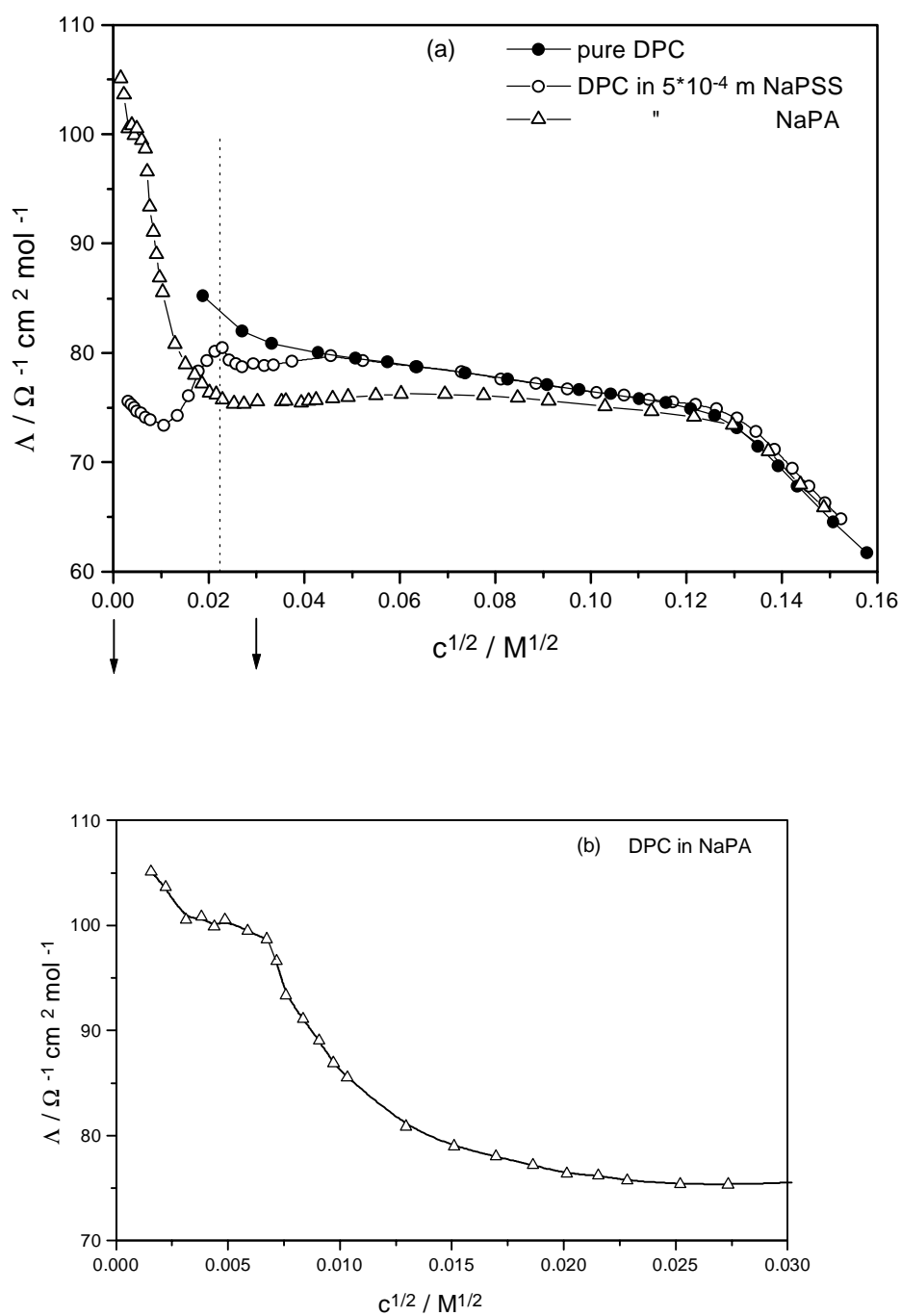
Figure 3. (a) *Molar conductivity, Λ, at 25°C in aqueous solutions of DPC in the absence and in the presence of NaPA or NaPSS.*

dotted line: polyelectrolyte concentration, $m_P = 5 \times 10^{-4}$ m.

(b) *the enlargement of the plot in NaPA solutions at surfactant concentrations below the 'equivalent point'.*
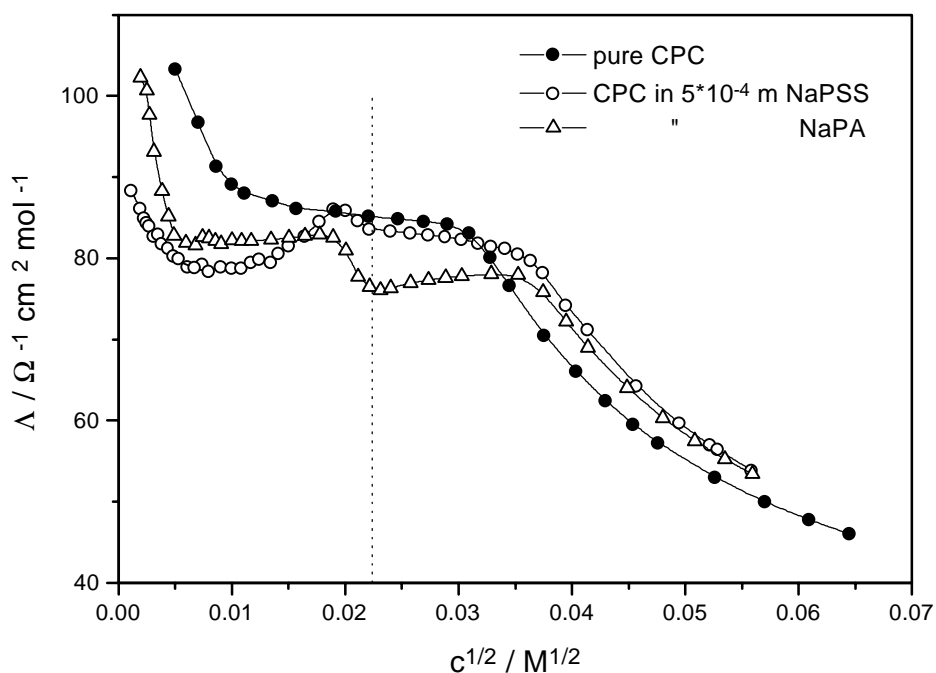
Figure 4. *Molar conductivity, Λ, at 25°C in aqueous solutions of CPC in the absence and in the presence of NaPA or NaPSS.*

dotted line: polyelectrolyte concentration, $m_P = 5 \times 10^{-4}$ m.

In NaPSS, cmc* values are 1.69×10^{-2} and 1.36×10^{-3} M and the corresponding β values are around 1 for DPC and CPC, respectively, again indicating quantitative 1:1 complexation between PSS^- and DP^+ (CP^+). In NaPA, we find cmc* 1.68×10^{-2} and 1.25×10^{-3} M, giving for β 0.80 and 0.78 for DPC and CPC, respectively. These values are in agreement with results obtained by fluorescence.

Below the 'equivalent point', conductivity curves in polyelectrolyte exhibit a very different behavior in comparison to pure surfactant solutions. In NaPSS, Λ first decreases with increasing concentration. In this range, the mobility of surfactant cations is strongly reduced due to the electrostatic field of the polyanion. After the minimum the conductivity starts to increase up to approximately the 'equivalent point'. The appearance of a minimum cannot be explained solely by electrostatic interactions

between surfactant minimicelle and polyelectrolyte chain, especially because the curves in NaPA solutions show no minima. In this case, Λ first also decreases sharply with increasing $\sqrt{c}$ but reaches a plateau region of rather constant value in the concentration range where minimum in NaPSS solutions has been observed (this concentration range is enlarged in Figure 3b for solutions of DPC in NaPA). The region of nearly constant Λ is afterwards followed by another steep decrease up to approximately the 'equivalent point'.

This remarkable difference in conductivity curves for alkylpyridinium cations in NaPSS and NaPA solutions leads to a conclusion that other effects besides the charge density of the polyion have to be taken into account. Since cooperative binding occurs in both systems [8,9] the observed difference must be due to the presence of the hydrophobic benzenesulfonate group in NaPSS which avoids contact with water. In fact, it has been shown [13] that a very stable and compact aggregate is formed in the case of NaPSS by inclusion of aromatic rings of PSS^- chain into the hydrophobic interior of the micelle (similar to ion pairing). In this way, the polyion chain wraps very tightly around surfactant minimicelles. This causes a release of small counterions originating from both, the polyion and the surfactant, into the solution and consequently, the conductivity starts to increase above a certain critical degree of complexation.

The minimum in DPC/NaPSS solutions is found at about 1×10^{-4} M (cf. Figure 3). For CPC/NaPSS it seems to be at somewhat lower concentrations, around 8×10^{-5} M (cf. Figure 4). However, because in this case the minimum is rather broad, it is difficult to position it precisely. In our former investigations of similar systems, i.e. solutions of NaPSS and alkyltrimethylammonium bromides [14], the minimum was ascribed to the point where the polyelectrolyte chain becomes saturated with surfactant minimicelles. Thereafter, it has been shown [14] that surfactant binds to the polymer in the monomer form only.

In the case of polyacrylate anion, the COO^- functional group has no tendency to avoid contact with water and to incorporate itself into the micellar aggregate. Therefore, the association between DPC (CPC) minimicelles and PA^- is purely electrostatic. We can conclude, that polyelectrolyte induced micelles of DPC (CPC) bind to PA^- as a

multivalent counterion without specific effects which would additionally stabilize the aggregate. The PA$^-$/DP$^+$ (PA$^-$/CP$^+$) complex is thus much more flexible and sensitive to the environment, the fact that was discussed previously in the light of strong effect of ANS on the association equilibrium. Also, lower values for parameter β in the case of NaPA reflect a weaker interaction between the polyanion and surfactant.

REFERENCES

[1]   B. Cabane, *J. Phys. Chem.* **1977**, *81*, 1639.
[2]   E. B. Abuin, J. C. Scaiano, *J. Am. Chem. Soc.* **1984**, *106*, 6274.
[3]   D. Chu, J. K. Thomas, *J. Am. Chem. Soc.* **1986**, *108*, 6270.
[4]   M. Almgren, P. Hansson, E. Mukhtar, J. van Stam, *Langmuir* **1992**, *8*, 2405.
[5]   P. Hansson, M. Almgren, *Langmuir* **1994**, *10*, 2115.
[6]   I. Satake, J. T. Yang, *Biopolymers* **1976**, *15*, 2263.
[7]   K. Hayakawa, P. J. Santerre, J. C. T. Kwak, *Macromolecules* **1983**, *16*, 1642.
[8]   A. Malovikova, K. Hayakawa, J. C. T. Kwak, *J. Phys. Chem.* **1984**, *88*, 1930.
[9]   J. Škerjanc, K. Kogej, G. Vesnaver, *J. Phys. Chem.* **1988**, *92*, 6382.
[10]   J. Škerjanc, M. Pavlin, *J. Phys. Chem.* **1977**, *81*, 1166.
[11]   J. Škerjanc, *Biophys. Chem.* **1974**, *1*, 376.
[12]   K. S. Birdi, H. N. Singh, S. U. Dalsager, *J. Phys. Chem.* **1979**, *83*, 2733.
[13]   Z. Gao, J. C. T. Kwak, R. E. Wasylishen, *J. Colloid Interface Sci.* **1988**, *126*, 1, 371.
[14]   K. Kogej, J. Škerjanc, *Langmuir*, submitted.

POVZETEK

Proučevali smo vpliv specifične narave polielektrolita na kompleksacijo z alkilpiridinijevimi surfaktanti. Izbrali smo dva polielektrolita z enako linearno gostoto naboja, natrijev poliakrilat, NaPA, in natrijev polistirensulfonat, NaPSS. Z merjenjem fluorescence smo ugotovili, da je v primeru bolj hidrofobnega NaPSS asociacija surfaktanta s poliionom skoraj popolna, medtem ko se na bolj hidrofilen polielektrolit NaPA veže manj kot 80% surfaktanta. Elektrolitska prevodnost raztopin Λ je pokazala, da se gibljivost ionov surfaktanta v prisotnosti nasprotno nabitega poliiona močno zmanjša. V raztopinah NaPSS smo v območju kooperativnega vezanja opazili izrazit minimum v krivulji $\Lambda(\sqrt{c})$. V raztopinah NaPA pa je, nasprotno, prevodnost v tem območju precej konstantna. Razliko v obnašanju smo razložili z dejstvom, da se hidrofobna aromatska skupina na PSS$^-$ vključi v notranjost surfaktantne minimicele, pri čemer nastane zelo stabilen agregat. Pri tem se v raztopino sprosti precejšnja množina Na$^+$ and Cl$^-$ ionov. Taka specifična interakcija med PA$^-$ in agregatom surfaktanta ni možna. Do asociacije slednjih dveh pride le zaradi elektrostatskih interakcij.

1-ACYL-3-HYDROXY-1*H*-PYRAZOLES AND RELATED DERIVATIVES AS USEFUL ACYLATING AGENTS[#]

Vladimir Kepe, Slovenko Polanc, and Marijan Kočevar

Faculty of Chemistry and Chemical Technology, University of Ljubljana, Aškerčeva 5,

1000 Ljubljana, Slovenia

ABSTRACT

A general application of 1-acyl-3-hydroxy-1*H*-pyrazoles **5** as useful acylating agents for alcohols or phenols, amines and hydrazines is described. The use of a hydrazide for a direct acylation of an alcohol in the presence of 4-ethoxymethylene-2-phenyl-5(4*H*)-oxazolone (**1**) is also discussed.

Acylation is one of the fundamental reactions in organic chemistry and can be carried out by wide variety of reagents [1]. Acyl groups play an important role in the chemistry of biomolecules [2], they are fragments of important natural products, such as peptides [2–3] or modified peptide bond isosteres [4], they serve as protecting groups [5], etc. Pyrazole derivatives are important synthons and reagents in organic synthesis and have found applications as pharmaceuticals, agrochemicals, dyestuffs, etc. [6]. They can be obtained by various methods from different starting materials [6–9]. In a previous communication pyrazoles were described as relatively inert acylating agents, although their alcoholysis was dramatically accelerated under the influence of a strong acid or base [10]. On the other hand, 1-acyl-3-hydroxy-1*H*-pyrazoles and related compounds

---

[#] Dedicated to the memory of Professor Anton Šebenik.

have not been so often investigated, although several acetyl derivatives have been pre-
pared and further studied [11−13]. Their potential as acylating *N*-acyl agents has not
been described, but it was found that 3-acetoxy group in 3-acetoxy-1-acetyl-5-methyl-
pyrazole has higher acetylating potential than its 1-acetyl group.

Recently, we have described a synthesis of 1-acyl-3-hydroxy-1*H*-pyrazoles **5** and
related derivatives from ethoxymethyleneoxazolone derivative **1** and hydrazides or
related derivatives **2** (Scheme 1) [6]. The method includes a migration of an acyl group
in the intermediary-formed pyrazolone derivative **4** to yield the rearranged 1-acyl-3-
hydroxy-1*H*-pyrazoles **5** in high yields. In contrast, in the reaction of the oxazolone
derivative **1** with two equivalents of an appropriate hydrazine derivative the
corresponding symmetrically *N,N′*-disubstituted hydrazines **6** were obtained together
with the oxazolone derivative **7**.
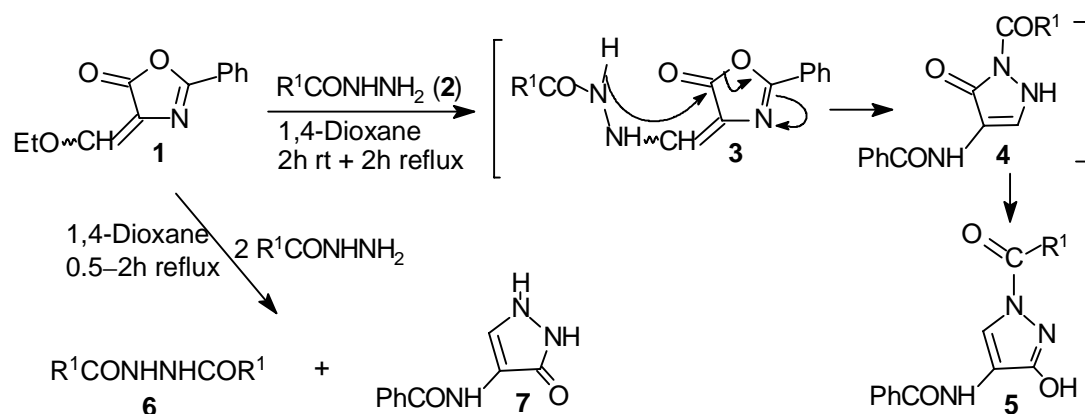
Scheme 1

Here, we report a possibility of using pyrazole derivatives **5a–e** as acylating
agents. In contrast to the previous investigation of pyrazoles for such purposes [10], we
wanted to explore the influence of an electron-rich hydroxy group on the acylating
potential of pyrazole derivatives. When a mixture of equimolar amounts of the oxazolone
derivative **1** and *p*-nitrophenylcarbohydrazide was heated for 30 h in a methanolic
solution, we isolated the corresponding methyl *p*-nitrobenzoate (**8**) in 74% yield.

$$1 \ + \ p\text{-}NO_2\text{-}C_6H_4\text{-}CONHNH_2 \xrightarrow[\Delta]{MeOH} p\text{-}NO_2\text{-}C_6H_4\text{-}CO_2Me$$

8
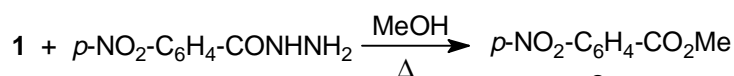
From the described reaction it is not clearly evident if pyrazole derivative is an acylating agent, since the acyl group might also be transferred onto methanol in the intermediary step. For this reason, the reaction of the pyrazole **5c** in methanol was carried out. It required a long heating period, but in the presence of an equimolar amount of sodium methoxide the reaction was over in 10 min at room temperature and we isolated methyl *p*-nitrobenzoate (**8**) in 72% yield (Scheme 2). Then we performed several reactions starting from equimolar amounts of the pyrazoles **5a–e** and various derivatives of type **9** (Y = O, NH) in boiling 1,4-dioxane and the corresponding products of type **10** were obtained in 55–87% yield (Table 1). By this method the acyl groups were transferred from pyrazoles **5a–e** to various amines, hydrazines, amino acid derivative and phenol yielding the corresponding amides, hydrazides or esters (**11–18**).
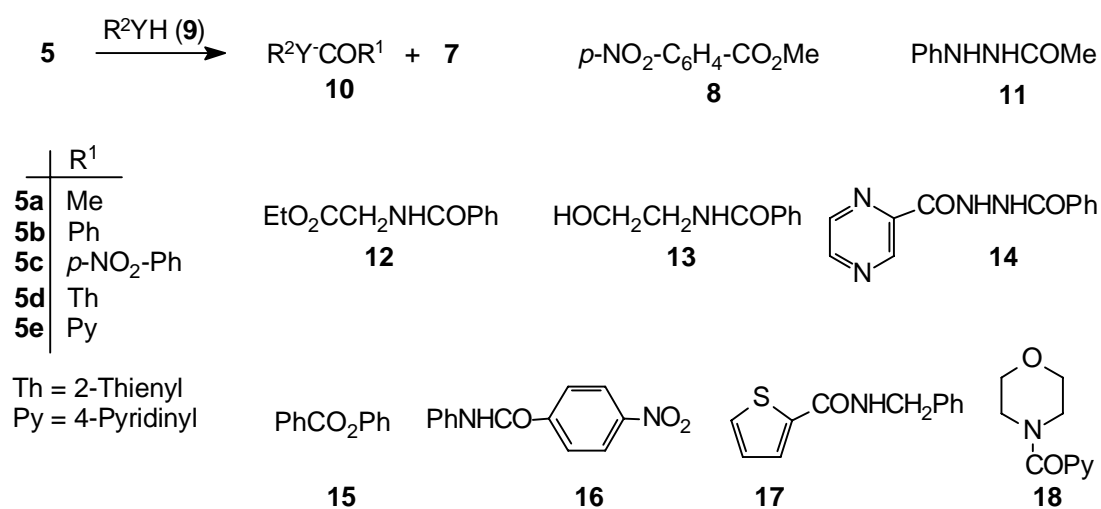
Scheme 2

For the synthesis of products **12** and **15** triethylamine was used as a catalyst. All other products were obtained after a short heating period of time in reasonable yields. With ethanolamine as a substrate, a selective *N*-acylation occurred to yield product **13**.

The separation of the products of type **10** from the pyrazolone derivative **7** was achieved by an alkaline water solution of the crude material from which the products separated or were extracted with a mixture of chloroform and 1,4-dioxane and finally purified by column chromatography.

Table 1. Reaction Conditions and Yields of Compounds 11-18

Entry	Pyrazole **5** (2 mmol)	Substrate **9** (2 mmol)	Conditions (dioxane, Δ)	Acylated Product	Yield (%)
1	**5a**	PhNHNH$_2$	2 h	**11**	67
2	**5b**	EtO$_2$CCH$_2$NH$_2$	2 h[a]	**12**	59
3	**5b**	HOCH$_2$CH$_2$NH$_2$	1 h	**13**	74[c]
4	**5b**	Pyrazinyl-CONHNH$_2$	2 h	**14**	84[d]
5	**5b**	PhOH	4 h[a]	**15**	55
6	**5c**	PhNH$_2$	2 h[b]	**16**	77
7	**5d**	PhCH$_2$NH$_2$	2 h	**17**	87
8	**5e**	Morpholine	1 h	**18**	72

[a]Et$_3$N was added as a catalyst. [b]Due to solubility problems DMF was used as a solvent. [c]Yield after isolation by column chromatography. [d]Isolation by work-up with 1 M NaOH, followed by filtration.

In conclusion, we have demonstrated the use 1-acyl-3-hydroxy-1*H*-pyrazoles as a convenient source of an acyl unit. The whole method starting from hydrazides represents a possible way of an activation of hydrazides, which are known as poor donors of acyl units due to their high resonance stability. The main advantages of this method are easily available and cheap chemicals, relatively mild reaction conditions and a simple work-up.

EXPERIMENTAL

Melting points were determined on a Kofler micro hot stage and are uncorrected. Thin-layer chromatography was carried out on Fluka silica gel TLC-cards. Column chromatography was carried out on Fluka silica gel 60 (220–440 mesh). 4-

Ethoxymethylene-2-phenyl-5(4*H*)-oxazolone (**1**) [14], 2-pyrazinecarbohydrazide [15] and 2-(benzoylamino)acetohydrazide [16] were prepared as described in the literature. 1,4-Dioxane was purified as described [17]. All other compounds and reagents were used as received from commercial suppliers (Fluka, Aldrich).

Preparation of Methyl 4-Nitrobenzoate (8).

Method A. A mixture of oxazolone **1** (0.436 g, 2 mmol) and 4-nitrobenzohydrazide (0.363 g, 2 mmol) was refluxed in methanol (10 mL) for 30 hours. The product was isolated by column chromatography on silica gel (ethyl acetate–petroleum benzine, 1:1). Yield 0.268 g (74%) of a white solid, which was identical with commercially available ester; mp 94–96 °C (lit [18] mp 94–95 °C).

Method B. Pyrazole **5c** (0.704 g, 2 mmol) was dissolved in a freshly prepared 1 M solution of NaOMe in methanol (2 mL). The reaction was completed in 10 min (TLC evidence), methanol was removed under reduced pressure and methyl 4-nitrobenzoate was isolated by column chromatography (ethyl acetate–petroleum benzine, 1:1). Yield 0.261 g (72%) of a white solid.

General Procedure for Reactions of Pyrazoles 5 with Nucleophilic Reagents 9.

A pyrazole **5** (2 mmol) was added to a solution of a nucleophile **9** (2 mmol) in dioxane (4 mL) and the reaction mixture was refluxed for 1–4 hours. The mixture was cooled, then chloroform (8 mL) and water (2 mL) were added. The pH value of the water layer was adjusted to 13 with 1 M NaOH in order to dissolve pyrazolone **7** in water. The layers were separated and the water layer was extracted with a mixture of chloroform (8 mL) and dioxane (4 mL). Organic layers were collected, washed with water (5 mL), dried over Na_2SO_4 and evaporated under reduced pressure. The products (with the exception of **14**) were purified by column chromatography and were obtained as TLC-pure compounds. Reaction conditions and yields of products **11**–**18** are given in Table 1.

The following products were obtained by the General Procedure:

N-(2,3-Dihydro-3-oxo-1*H*-pyrazol-4-yl)benzamide (7).

This compound can be isolated from the water layer by acidification to pH 5 with acetic acid and filtration of the resulting solid; mp 205–206 °C (lit [14] mp 204–205 °C).

N′-Phenylacetohydrazide (11).

This compound was prepared by refluxing pyrazole **5a** and phenylhydrazine for 2 h. Yield 0.201 g (67%) of a white solid; mp 125–127 °C (lit [19] mp 129 °C).

Ethyl 2-(benzoylamino)acetate (12).

This compound was prepared by refluxing pyrazole **5b** and glycine ethyl ester hydrochloride in the presence of triethylamine (0.6 mL, 4.3 mmol) for 2 h. Yield 0.245 g (59%) of a white solid; mp 59–60 °C (lit [20] mp 60.5 °C).

N-(2-Hydroxyethyl)benzamide (13).

This compound was prepared by refluxing pyrazole **5b** and 2-aminoethanol for 1 h. It was isolated by column chromatography on silica gel (chloroform–methanol, 5:1). Yield 0.244 g (74%) of a beige solid; mp 56–59 °C (lit [21] mp 58 °C).

N′-(2-Pyrazinylcarbonyl)benzohydrazide (14).

This compound was prepared by refluxing pyrazole **5b** and 2-pyrazinecarbohydrazide for 2 h. The reaction mixture was cooled, water (5 mL) was added and the pH value was adjusted to 10 with 1 M NaOH. The resulting solid was filtered off and washed with 1,4-dioxane. Yield 0.407 g (84%) of a white solid; mp 217–219 °C (lit [22] mp 217 °C).

Phenyl benzoate (15).

This compound was prepared by refluxing pyrazole **5b**, phenol and triethylamine (0.3 mL, 2.1 mmol) for 4 h. Yield 0.218 g (55%) of a white solid; mp 67−69 °C (lit [23] mp 70 °C).

N-**Phenyl-4-nitrobenzamide (16).**

This compound was prepared by refluxing pyrazole **5c** and aniline in DMF for 2 h. DMF was evaporated under reduced pressure, 1,4-dioxane (4 mL) was added and the product was isolated as described in the General Procedure. Yield 0.360 g (77%) of a yellowish solid; mp 219−220 °C (lit [24] mp 218 °C).

N-**Benzyl-2-thiophenecarboxamide (17).**

This compound was prepared by refluxing pyrazole **5d** and benzylamine in 1,4-dioxane for 2 h. Yield 0.378 g (87%) of white crystals; mp 117−120 °C (lit [25] mp 119.5−120.5 °C).

4-(4-Pyridinylcarbonyl)morpholine (18).

This compound was prepared by refluxing pyrazole **5e** and morpholine for 1 h. Yield 0.276 g (72%) of a white solid; mp 73−74 °C (lit [26] mp 75−76 °C).

ACKNOWLEDGMENT

REFERENCES

[1]   M. A. Ogliaruso, J. F. Wolfe, In *The Chemistry of Acid Derivatives: Supplement B*; Patai, S., Ed.; Interscience: Chichester, 1979; Part 1, pp 267–490.

[2]   R. J. Simmonds, *Chemistry of Biomolecules: An Introduction*; The Royal Society of Chemistry: Cambridge, 1992.

[3]   M. Bodanszky, *Peptide Chemistry;* Springer: Berlin, 1993.

[4]   J. Magrath, R. H. Abeles, *J. Med. Chem*. **1992**, *35*, 4279–4283.

[5]   T. W. Greene, P. G. M. Wuts, *Protective Groups in Organic Synthesis*; J. Wiley & Sons, Inc.: New York, 1991.

[6]   V. Kepe, F. Požgan, A. Golobič, S. Polanc, M. Kočevar, *J. Chem. Soc., Perkin Trans. 1*, **1998**, 2813–2816, and references cited therein.

[7]   P. Trebše, S. Polanc, M. Kočevar, T. Šolmajer, S. Golič Grdadolnik, *Tetrahedron*, **1997**, *53*, 1383–1390.

[8]   L. Vraničar, S. Polanc, M. Kočevar, *Tetrahedron*, in press.

[9]   V. Kepe, S. Polanc, M. Kočevar, *Heterocycles*, **1999**, in press.

[10]   C. Kashima, H. Harada, I. Kita, I. Fukuchi, A. Hosomo, *Synthesis* **1994**, 61–65.

[11]   M. Irie, T. Miyasaka, K. Arakawa, *J. Biochem. (Tokyo)* **1972**, *72*, 65–72.

[12]   K. Arakawa, T. Miyasaka, H. Ochi, *Chem. Pharm. Bull*. **1974**, *22*, 214–223.

[13]   H. Ochi, T. Miyasaka, K. Arakawa, *Bull. Chem. Soc. Jpn*. **1977**, *50*, 2991–2994.

[14]   J. W. Cornforth, *The Chemistry of Penicillin*; H. T. Clarke, J. R. Johnson, R. Robinson, Eds.; Princeton University Press: Princeton, 1949; pp 730–848.

[15]   G. Carrara, F. M. Chiancone, V. D'Amato, E. Ginoulhiac, C. Martinuzzi, U. M. Teotino, N. Visconti, *Gazz. Chim. Ital*. **1952**, *82*, 652–670; *Chem. Abstr*. **1954**, *48*, 6423d.

[16]   Th. Curtius *Chem. Ber*. **1890**, *23*, 3023–3033.

[17]   B. S. Furniss, A. J. Hannaford, P. W. G. Smith and A. R. Tatchell, *Vogel's Textbook of Practical Organic Chemistry*, Longman (co-published with Wiley), New York, 1989, 5th ed., p 407.

[18]   D. G. Markees, *J. Org. Chem*. **1958**, *23*, 1490-1492.

[19]   A. Kaufmann, *Chem. Ber*. **1909**, *42*, 3480–3483.

[20]   H. Franzen, *Chem. Ber*. **1909**, *42*, 2465–2468.

[21]   L. Knorr, P. Rössler, *Chem. Ber*. **1903**, *36*, 1278–1283.

[22]   K. Kakemi, T. Uno, T. Arita, H. Nakano, I. Shimada, Y. Ikegami, S. Kitazawa, *Yakugaku Zasshi* **1961**, *81*, 1609–1614; *Chem. Abstr*. **1962**, *56*, 10141h.

[23]   W. J. Wohlleben, *Chem. Ber*. **1909**, *42*, 4369–4375.

[24]   W. B. van Horssen, *Recl. Trav. Chim. Pays-Bas* **1936**, *55*, 245–262; *Chem. Abstr*. **1936**, *30*, 5198[9].

[25]   T. Kametani, S. Takano, O. Umezawa, H. Agui, K. Kanno, Y. Konno, F. Sato, H. Nemoto, K. Yamaki, H. Ueno, *Yakugaku Zasshi* **1966**, *86*, 823–828; *Chem. Abstr*. **1966**, *65*, 20093g.

[26]   R. M. Jacob, J. G. Robert, **Ger. 1,092,476** (1959); *Chem. Abstr*. **1962**, *56*, 8723e.

POVZETEK

Opisana je splošna metoda za uporaba 1-acil-3-hidroksi-1*H*-pirazolov **5** kot primernih acilirnih sredstev za alkohole ali fenole, amine in hidrazine. Opisan je tudi primer uporabe hidrazida ob prisotnosti 4-etoksimetilen-2-fenil-5(4*H*)-oksazolona (**1**) za neposredno aciliranje alkohola.

Solvent Effect in Photolysis of Chloro Substituted Benzyl Chlorides[†]

Berta Košmrlj and Boris Šket*

Faculty of Chemistry and Chemical Technology, University of Ljubljana, Aškerčeva 5, 1000 Ljubljana, Slovenia

Abstract:

The effect of solvent on photolyses of 3-chloro and 4-chloro substituted benzyl chlorides is described. Analysis of the products formed indicates that both radical and ionic intermediates are involved. In the first step, homolytic benzylic C-Cl bond cleavage occurs, resulting in a radical pair. Further reaction pathway, however, depends upon the solvent used. In cyclohexane and tetrahydrofuran, the products obtained are formed *via* an intermediate benzylic radical. Photolysis in acetonitrile, on the other hand, results in products, which can be interpreted through intermediate formation of both benzylic cation and benzylic radical. The presence of $LiAlH_4$ accelerates the reduction of the C-Cl bond in the aromatic ring, leading to toluene as the main product.

Introduction:

The photochemistry of heteroatomic benzylic bond has been the subject of investigation and mechanistic speculation for over 30 years. One of the intriguing discoveries is that partitioning between homolytic cleavage to give radicals and

---

[†] Dedicated to Prof. Dr. Anton Šebenik

heterolytic cleavage to give ions is closely balanced. The balance can be tipped by changing the solvent and leaving group.

In order to determine the mechanism of degradation different benzylic systems (PhCH$_2$X) were investigated: benzyl acetates (X=OAc) [1], sulphonium salts (X=(CH$_3$)$_2$S$^+$BF$_4^-$) [2], ammonium salts (X=(CH$_3$)$_3$N$^+$Cl$^-$) [3], phosphonium salts (X=Ph$_3$P$^+$Cl$^-$), and a group of homobenzylic systems. However, the most thoroughly studied examples have been benzyl halides (X = Cl, Br), which set the pattern that is followed by other benzylic systems.

The first photochemical studies were performed in the gas phase [4]. Direct photolysis of benzyl chloride led to benzyl radical and a chlorine atom. Zimmerman and Sandel [1] investigated the photolysis of 3- and 4-methoxybenzyl acetates and related derivatives in ethanol-water solution and observed that direct irradiation of 3-methoxybenzyl acetate as well as 3-methoxybenzyl chloride gave the appropriate alcohol, the ether and lesser amounts of free-radical products. The solvolytic products were taken as an evidence for the formation of an intermediate 3-methoxybenzylic cation. The nature of the state and the sequence of reactions leading to the cation were left unspecified.

The earliest studies of photochemical reactions of benzyl chloride in solution gave contradicting results. Ratcliff reported that benzyl chloride is solvolytically stable when irradiated in ethanol [3]. This was contradicted by Kuz'min and co-workers [5], who observed that direct irradiation of a range of chloromethyl and bromomethyl derivatives of aromatic hydrocarbons including benzyl chloride in alcohol-water solution led to the corresponding carbinols in high yields. Since the results were the same even when the reaction was carried out in solution saturated with oxygen, these authors concluded that photosolvolysis proceeds by direct heterolytic bond cleavage from the excited singlet state.

Cristol and Greenwald reported [6] that direct irradiation of benzyl chloride in methanol gave no benzyl methyl ether, which is the expected heterolytic cleavage product, but only products derived from benzyl radicals and chlorine atom. However, they reported that sensitization of benzyl chloride with the triplet sensitizers (acetone or acetophenone) in methanol resulted in exclusive formation of the anticipated solvolytic product. These results imply that the excited singlet state of benzyl chloride cleaves homolytically and that in the presence of the triplet sensitizer some other state, responsible for heterolytic cleavage is formed.

Hyömäki and Koskiakllio [7] studied direct irradiation of benzyl chloride in methanol-water mixtures. They observed formation of both the alcohol and ether products characteristic of heterolytic cleavage and the radical coupling products characteristic of homolytic cleavage of the carbon-chlorine bond. On the basis of the changes in the relative amounts of these products with the solvent composition, these authors suggested that the excited singlet state is homolytically cleaved and that chlorine atom formed either abstracts hydrogen atom from the solvent or oxidizes the benzylic radical to cation.

McKenna and co-workers [8] also irradiated benzyl chloride in methanol. Direct photolysis gave products characteristic of both ionic and free-radical pathways. The results were in good agreement with those reported by Hyömäki and Koskiakllio [7]. Due to the similar findings in the photolysis of ammonium salts, McKenna and co-workers proposed the following mechanism. In the first step, both the singlet and the triplet excited state of benzyl chloride are homolytically cleaved. The triplet radical pair can undergo an intersystem crossing into the singlet radical pair, which is either in the equilibrium with the ions formed by electron transfer or is a contributor to a resonance hybrid that includes both the ions and the singlet radical pair. From the studies of CIDNP effect it is known that the interconversion between singlet and triplet states of a radical pair where the partners are already adequately separated can occur at a rate comparable to that of the final separation of the partners. This effect is the result of electron-nucleus interactions while spin-orbit relaxation may also contribute when one of the partners is a halogen atom.

Cristol and Bindel [9,10] have carried out an intensive investigation of the photochemical transformations of benzyl chloride and some of its derivatives in *tert*-butyl alcohol. They reported that the products obtained in both the direct and acetone-sensitized irradiations are the same (derived by radical and ionic pathway), but they are formed in different proportions. Cristol and Bindel concluded that the state responsible for the formation of ionic intermediates is an unspecified short-lived upper triplet state.

The influence of metal hydrides:

It is known that the presence of metal hydrides ($NaBH_4$, $LiAlH_4$, etc.) has a great impact on the photoreduction of organic halogenides. Recent investigations on photoreduction of aryl halides [11-16] in the presence of $NaBH_4$ revealed three pathways that are supported by experimental observations:

a) In the excited molecule of an aryl halide a homolytic cleavage of C-X bond occurs in the first step, generating an aryl radical and a halogen atom. These radicals abstract in the second step hydrogen atom from BH_4^- giving $BH_3^{-\bullet}$ which initiates an $S_{RN}1$-like chain reaction to form the products (ArH, BH_3, HCl, NaCl) [11].

$$ArCl^* \longrightarrow Ar^\bullet + Cl^\bullet \xrightarrow{2\,BH_4^-} ArH + HCl + 2\,BH_3^{\bullet-}$$

$$BH_3^{\bullet-} + ArCl \xrightarrow[S_{RN}1]{} Ar^\bullet + Cl^- + BH_3$$
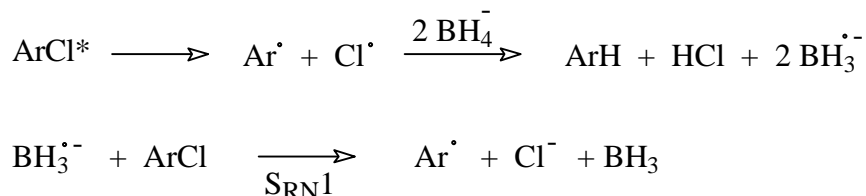
b) Excited aryl halide reacts with BH_4^- and direct transfer of hydride ion occurs. The resulting products are the same as in the previous pathway [12,14].

$$ArCl^* + BH_4^- \xrightarrow{\text{hydride ion transfer}} ArH + Cl^- + BH_3$$
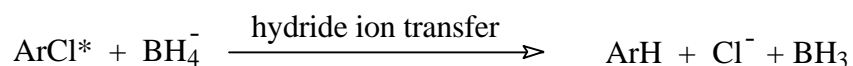
c) Single electron transfer occurs in the first step from BH_4^- resulting in a complex $[ArX^{-\bullet}BH_4^\bullet]$ which after intramolecular hydrogen atom transfer leads to previously mentioned products [15,16].

$$ArCl^* + BH_4^- \xrightarrow{\text{electron transfer}} \left[ArCl^{\bullet-}BH_4^\bullet\right] \xrightarrow{\text{hydrogen atom transfer}} ArH + Cl^- + BH_3$$
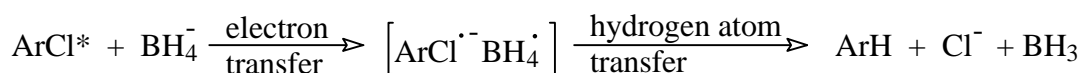
Similar reaction mechanisms were proposed for photoreduction of organic halides by $LiAlH_4$ [17-21].

Krishnamurthy and Brown [22] have shown that clear solution of $LiAlH_4$ in tetrahydrofuran reduces organic halides rapidly and quantitatively even at room temperatures. Such reactions are usually far faster than those where a suspension is used. The lower reactivity of suspension was assigned to insoluble impurities that might have coated the undissolved $LiAlH_4$ and hindered its migration into solution and subsequent reaction.

Results:

The solvent effect on the phototransformation of 3- and 4-chlorobenzyl chlorides was studied by direct irradiation in cyclohexane, tetrahydrofuran and acetonitrile solution.

Irradiation of 0.1 M solution of **1a** for 22 hours in cyclohexane (Scheme 1) at 253.7 nm resulted in 92 % conversion. The resulting mixtures contained, besides starting

substrate **1a,** 3-chlorotoluene (**2a**), toluene (**3**), 3-chlorophenylcyclohexylmethane (**4a**), cyclohexylphenylmethane (**5**), 1,2-bis(3-chlorophenyl)ethane (**6a**), 1-(3-chlorophenyl)-2-phenylethane (**7a**) and 1,2-diphenylethane (**8**). The product distribution is summarized in Table 1. Shortening of the reaction time from 22 to 4.5 hours led to both, decrease in conversion from 92 to 72 %, as well as to the change in product distribution (Table 1).

Irradiation of **1b** under the same reaction conditions as in the previous case (Scheme 1) resulted in 100 % conversion into a mixture of 4-chlorotoluene (**2b**), toluene (**3**), 4-chlorophenylcyclohexylmethane (**4b**), cyclohexylphenylmethane (**5**), 1,2-bis(4-chlorophenyl)ethane (**6b**), 1-(4-chlorophenyl)-2-phenylethane (**7b**) and 1,2-diphenylethane (**8**). The product distribution is summarized in Table 1. Again, shortening of the reaction time from 22 to 4.5 hours led to decreased conversion. The products formed were the same, however in changed relative ratio (Table 1).

Eight hours irradiation of 0.1 M solution of **1a** in tetrahydrofuran (Scheme 2) at 253.7 nm led to 100 % conversion. The products formed were toluene (**3**), 1,2-bis(3-chlorophenyl)ethane (**6a**), 1,2-diphenylethane (**8**), 3-chlorophenyl-(2-tetrahydrofuryl)-methane (**9a**) and phenyl-(2-tetrahydrofuryl)methane (**10**) and their relative ratio is shown in Table 2.

Irradiation of 0.1 M solution of 4-chlorobenzyl chloride (**1b**) in tetrahydrofuran (Scheme 2) under the same reaction conditions led to 100 % conversion into a mixture of 4-chlorotoluene (**2b**), toluene (**3**), 1,2-bis(4-chlorophenyl)ethane (**6b**), 1-(4-chloro-phenyl)-2-phenylethane (**7b**), 1,2-diphenylethane (**8**), 4-chlorophenyl-(2-tetrahydrofuryl)-methane (**9b**) and phenyl-(2-tetrahydrofuryl)methane (**10**). Distribution of products is summarized in Table 2.

Irradiation of 0.1 M solution of 3-chorobenzyl chloride (**1a**) for 2.5 hours in tetrahydrofuran in the presence of a threefold excess of LiAlH$_4$ resulted in 100 % conversion. The reaction mixture obtained, consisted of only 3-chlorotoluene (**2a**) and toluene (**3**) in the ratio of 1:8 (Table 2).

Irradiation of the tetrahydrofuran solution of 4-chlorobenzyl chloride (**1b**) under the same reaction conditions resulted in 100 % conversion to 4-chlorotoluene (**2b**) and toluene (**3**) in the ratio of 1:6 (Table 2).

Irradiation of 0.1 M solution of 3-chlorobenzyl chloride (**1a**) for 22.5 hours in acetonitrile (Scheme 3) resulted in 84 % conversion. The resulting reaction mixture contained, besides starting substrate, 1,2-bis(3-chlorophenyl)ethane (**6a**), 3-chloro-benzaldehyde (**11a**), 1-cyano-2-(3-chlorophenyl)ethane (**12a**), *N*-acetylamino-(3-

SCHEME 1: Photolysis of chloro substituted benzyl chlorides (**1**) in cyclohexane (**a**: 3-chloro; **b**: 4-chloro)
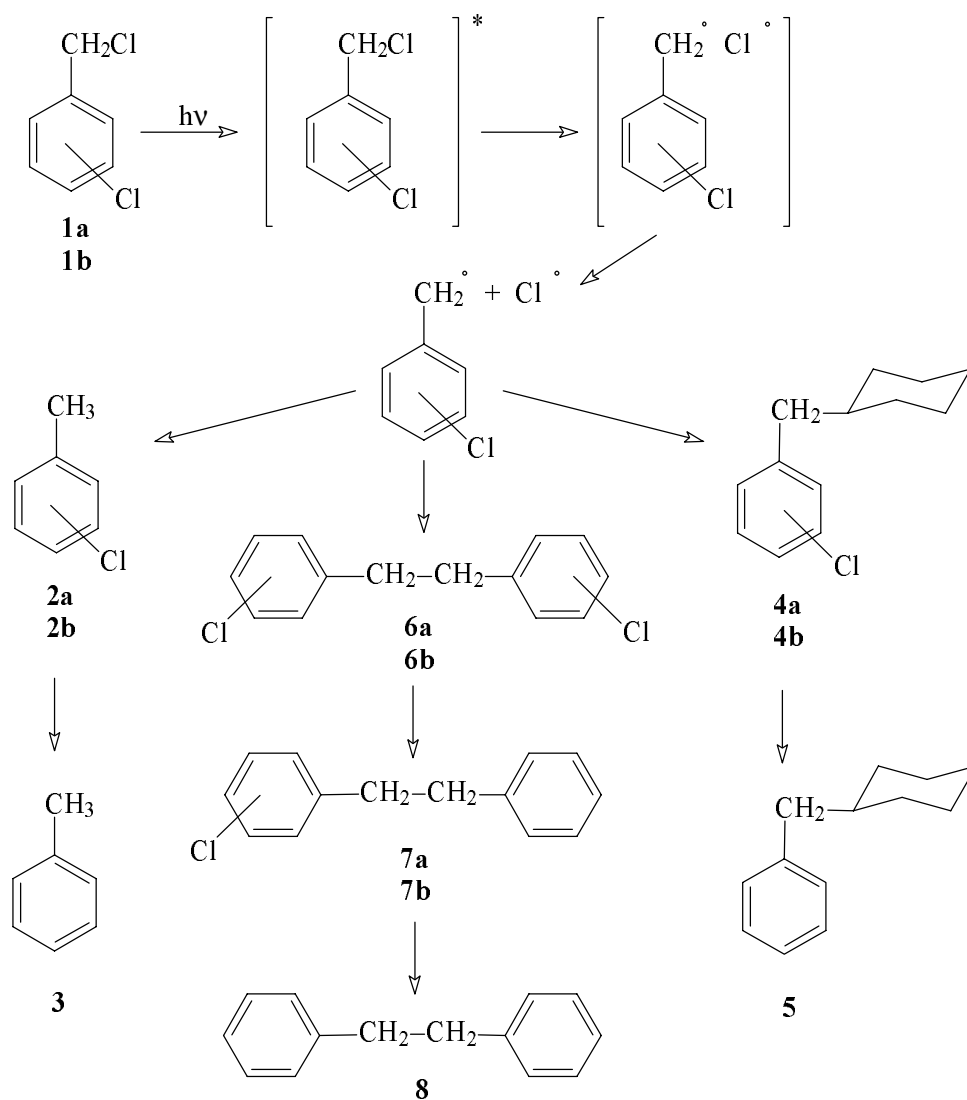
TABLE 1: Product distribution (relative yields (%))[a]

Starting compound[b]	1	2	3	4	5	6	7	8
3-chlorobenzyl chloride	8.0	1.7	0.3	33.4	30.5	9.1	9.5	7.5
3-chlorobenzyl chloride[c]	32.3	2.9	-	41.5	7.4	12.4	3.0	0.5
4-chlorobenzyl chloride	-	4.3	-	45.0	31.3	8.4	8.6	2.4
4-chlorobenzyl chloride[c]	18.2	1.1	-	40.0	16.3	13.8	7.3	3.3

a) Determined by GC/MS; b) Reaction conditions: substrate: 0.1 M; solvent: cyclohexane; irradiation time: 22 hours; $\lambda = 253.7$ nm. c) Irradiation time = 4.5 hours.

SCHEME 2: Photolysis of chloro substituted benzyl chlorides (**1**) in tetrahydrofuran (**a**: 3-chloro; **b**: 4-chloro)
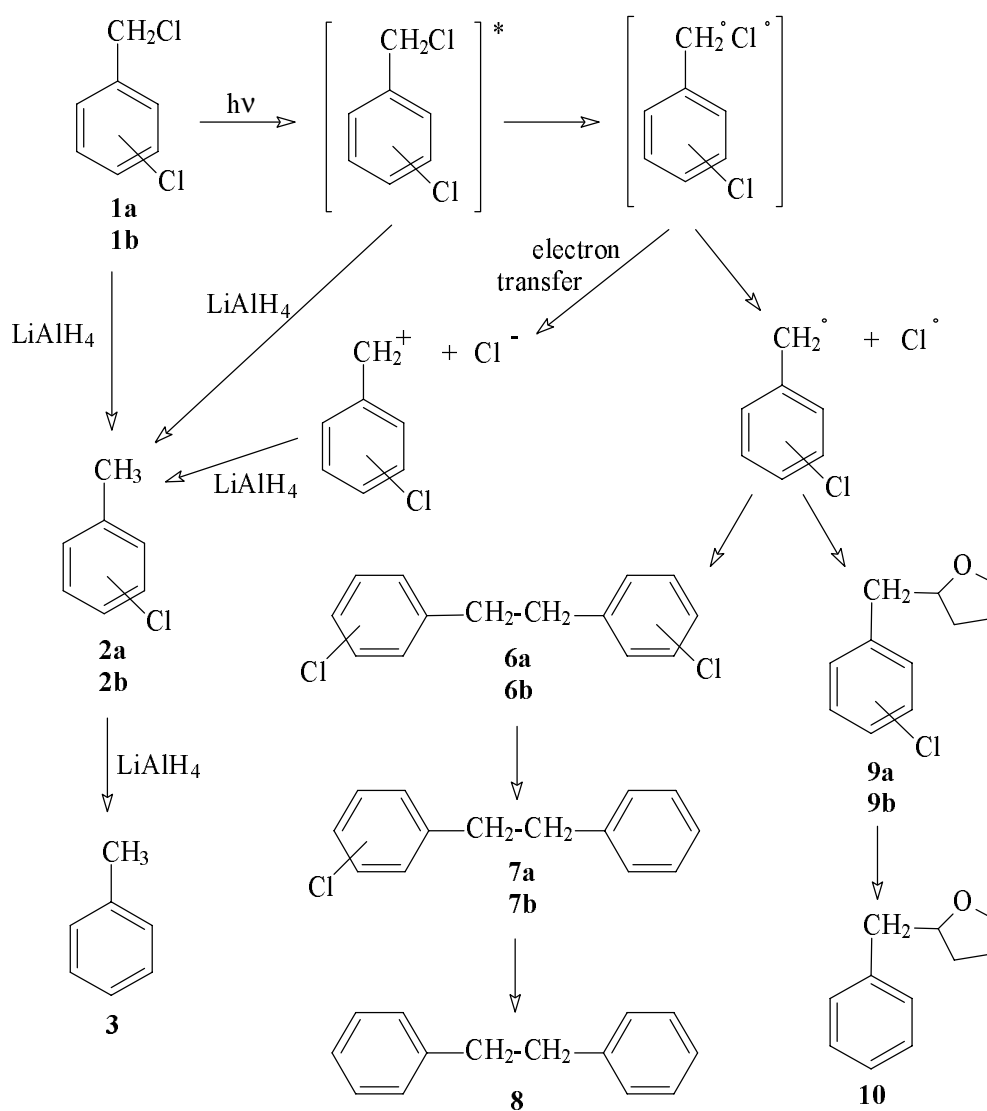
TABLE 2: Product distribution (relative yields (%))[a)]

Starting compound[b]	2	3	6	7	8	9	10
3-chlorobenzyl chloride	-	0.2	5.8	-	23.6	4.6	65.8
3-chlorobenzyl chloride[c)]	11.3	88.7	-	-	-	-	-
4-chlorobenzyl chloride	2.7	0.3	7.0	13.3	44.5	4.2	28.0
4-chlorobenzyl chloride[c)]	14.5	85.5	-	-	-	-	-

a) Determined by GC/MS; b) Reaction conditions: substrate: 0.1 M; solvent: tetrahydrofuran; irradiation time: 8 hours; λ = 253.7 nm. c) Addition of LiAlH$_4$: 0.3 M; irradiation time = 2.5 hours

SCHEME 3: Photolysis of chloro substituted benzyl chlorides (**1**) in acetonitrile

(**a**: 3-chloro; **b**: 4-chloro)
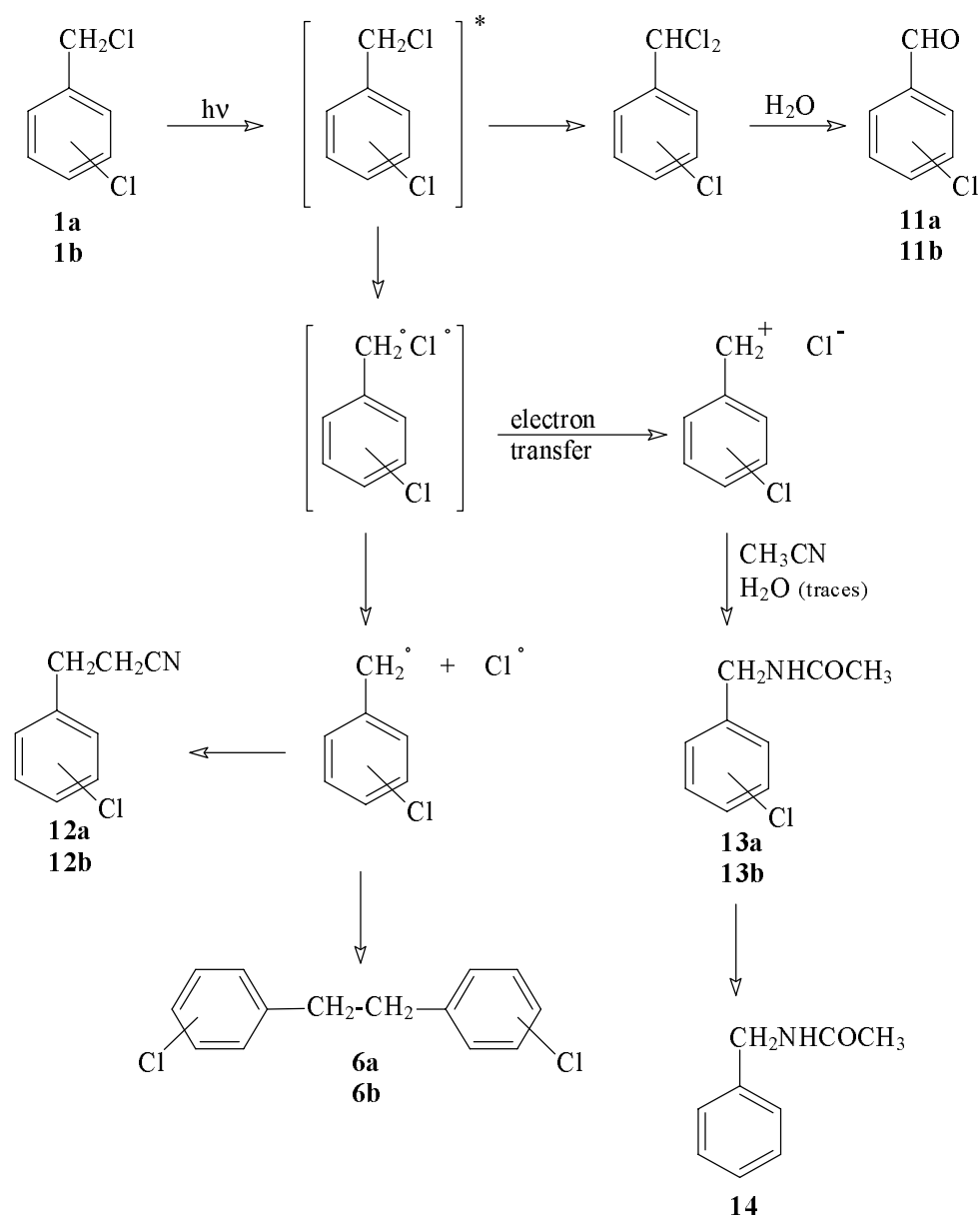
TABLE 3: Product distribution (relative yields (%))[a]

Starting compound[b]	1	6	11	12	13	14
3-chlorobenzyl chloride	15.6	5.5	4.5	2.4	68.9	3.1
4-chlorobenzyl chloride	24.2	5.0	3.6	-	67.2	-

a) Determined by GC/MS; b) Reaction conditions: substrate: 0.1 M; solvent: acetonitrile; irradiation time: 23.5 hours; λ = 253.7 nm.

chlorophenyl)methane (**13a**) and *N*-acetylaminophenylmethane (**14**) in the relative ratio, shown in Table 3. Irradiation of 0.1 M solution of 4-chlorobenzyl chloride (**1b**) in acetonitrile (Scheme 3) under the same reaction conditions led to 76 % conversion and the following products were detected: 1,2-bis(4-chlorophenyl)ethane (**6b**), 4-chlorobenzaldehyde (**11b**), *N*-acetylamino-(4-chlorophenyl)methane (**13b**) and *N*-acetylaminophenylmethane (**14**). Their distribution is summarized in Table 3.

Discussion:

The results obtained by photolyses of 3- and 4-chlorobenzyl chlorides (**1**) in cyclohexane (Scheme 1) suggest that the first step is the homolytic cleavage of the benzylic C-Cl bond and the formation of a biradical pair. Separation of radicals is facilitated by abstraction of hydrogen atom from cyclohexane by chlorine atom, which results in benzylic and cyclohexyl radicals. Generated radicals can react further in either of the following manners: a) combination of two benzyl radicals to form 1,2-diphenylethane derivatives (**6**, **7** and **8**), b) combination of benzyl radical and cyclohexyl radical to form cyclohexylphenylmethane derivatives (**4** and **5**) or c) benzyl radical abstraction of hydrogen atom from cyclohexane to form chlorotoluene (**2**) (Scheme 1, Table 1).

Photolyses of 3- and 4-chlorobenzyl chlorides (**1**) were further performed in tetrahydrofuran (Scheme 2), which is a good hydrogen donor and has also nucleophilic character. The results obtained revealed a similar reaction trend as observed in the case of cyclohexane as solvent. The main products obtained are 1,2-diphenylethane (**8**), formed by combination of two benzylic radicals, and phenyl-(2-tetrahydrofuryl)methane (**10**), generated by combination of 2-tetrahydrofuryl radical and benzyl radical (Scheme 2, Table 2). No products indicating intermediacy of benzylic cations were detected.

A substantial change in the reaction pathway was observed, when photolysis was performed in the presence of $LiAlH_4$. Chlorotoluene (**2**) and toluene (**3**) were the only products obtained (Table 2). Chlorotoluene (**2**) formation can be explained by either of the following processes:

- direct substitution of chloride ion by hydride ion

- reaction of the excited state of chlorobenzyl chloride with $LiAlH_4$

- benzylic cation formation from the radical pair followed by hydride ion transfer from $LiAlH_4$

The following reduction of C-Cl bond in the aromatic ring occurs *via* electron transfer from $LiAlH_4$ to the excited state of chlorotoluene (2) thus forming a complex, which after subsequent hydrogen atom transfer results in toluene (3) (Scheme 4).

SCHEME 4
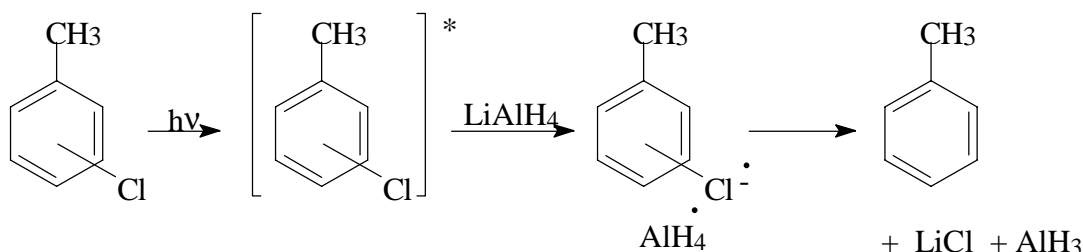
Photolyses of 3- and 4-chlorobenzyl chlorides (1) in acetonitrile (Scheme 3) have shown, that the choice of solvent plays a crucial role in the rate of radical separation as well as in the single electron transfer. Acetonitrile is a poor hydrogen donor, while a polarized -C≡N bond offers a potential reaction site for bonding of ionic intermediates.

Indeed, the content of radical products (1,2-diphenylethane derivatives 6, 7 and 8), formed in the photolysis of either 1a or 1b in acetonitrile, is very low (Table 3). This indicates that the ease of separation of the biradical pair into separated radicals and thus formation of benzylic radical depends on the reaction of chlorine atom with solvent through hydrogen atom abstraction. In the case of acetonitrile with poor hydrogen donor abilities, an electron transfer process, wherein benzylic cation is generated, becomes predominant. The cation thus formed reacts further with -C≡N bond, and after hydrolysis *N*-acetylaminobenzyl derivative (13) is obtained as the main product (Scheme 3).

Experimental part:

The photochemical reactions were performed in the Photochemical Reactors Ltd. MLU 18 with 6RPR 253,7 nm lamps.

The chromatographic analyses were made on Hewlett Packard HP6890 equipped with FID detector and HP-5 column (temperature program: 100(3)/20/270(10)) and on Varian 3700 equipped with TIC detector and OV-17(5%) column (temperature program: 84(2)/10/210(10)).

The GC/MS analyses were made on Hewlett Packard 6890 and VG-Analytical Autospec EQ spectrometer.

The starting compounds are commercially available and were used without further purification. Cyclohexane (LiAlH₄), tetrahydrofuran (LiAlH₄) and acetonitrile (CaH₂) were refluxed over mentioned drying agents and distilled in an inert atmosphere before use.

Typical experimental procedure: 2.0 mmol of substrate was dissolved in 20 ml of solvent and the reaction mixture was irradiated at 253.7 nm for 2.5 to 24 hours. Analysis of the reaction mixture was performed by GC and GC/MS and by comparison to the authentic samples: 4-chlorophenylcyclohexylmethane (**4b**) [23], cyclohexylphenyl-methane (**5**) [24], 1,2-bis(3-chlorophenyl)ethane (**6a**) [25], 1,2-bis(4-chlorophenyl)ethane (**6b**) [26], 1-(3-chlorophenyl)-2-phenylethane (**7a**) [27], 1-(4-chlorophenyl)-2-phenylethane (**7b**) [27], 4-chlorophenyl-(2-tetrahydrofuryl)methane (**9b**) [28], phenyl-(2-tetrahydrofuryl)methane (**10**) [29], *N*-acetylamino-(3-chlorophenyl)methane (**13a**) [30], *N*-acetylamino-(4-chlorophenyl)methane (**13b**) [30] and *N*-acetylaminophenylmethane (**14**) [31].

Irradiation in the presence of LiAlH₄: 1.0 mmol of substrate was dissolved in 9 ml of clear solution of LiAlH₄ in tetrahydrofuran (3.0 mmol, c = 0.3325 M) and irradiated for 2.5 hours. The solution was diluted with 10 ml of ether and poured into 10 ml of water to destroy the excess of LiAlH₄. Organic phase was dried over anhydrous Na₂SO₄ and concentrated under vacuum. Analysis of the reaction mixture was performed by GC and GC/MS and by comparison to the authentic samples.

References:

[1]   H. E. Zimmerman, V. R. Sandel, *J. Am. Chem. Soc.* **1963**, *85*, 915-922.

[2]   A. L. Maycock, G. A. Berchtold, *J. Org. Chem.* **1970**, *35*, 2532-2538.

[3]   M. A. Ratcliff, Jr., J. K. Kochi, *J. Org. Chem.* **1971**, *36*, 3112-3120.

[4]   F. Boyrakecken, J. E. Nicholas, *J. Chem. Soc. B.* **1970**, 691-694.

[5]   V. B. Ivanov, V. L. Ivanov, M. Kuz'min, *Zh. Org. Khim.* **1973**, *9*, 340-341.

[6]   S. J. Cristol,B. E. Greenwald, *Tetrahedron Lett.* **1976**, 2105-2108.

[7]   J. Hyömäki, J. Koskiakllio, *Acta Chem. Scand. Ser. A* **1977**, *A31*, 321-324.

[8]   D. C. Appleton, B. Brocklehurst, J. McKenna, J. M. McKenna, S. Thackeray, A. R. Walley, *J. Chem. Soc. Perkin Trans. 2* **1980**, 87-90.

[9]   S. J. Cristol, T. H. Bindel, *J. Org. Chem.* **1980**, *45*, 951-957.

[10]   S. J. Cristol, T. H. Bindel, *J. Am. Chem. Soc.* **1981**, 103, 7287-7293.

[11]   J. A. Barltrop, D. Bradbury, *J. Am. Chem. Soc.* **1973**, *95*, 5085-5086.

[12]   K. Tsujimoto, S. Tasaka, M. Ohashi, *J. Chem. Soc., Chem. Commun.* **1975**, 758-759.

[13]   G. A. Epling, E. Florio, *J. Chem. Soc., Chem. Commun.* **1986**, 185-186.

[14]   G. A. Epling, E. Florio, E. *Tetrahedron Lett.* **1986**, 675-678.

[15]   A. N. Abeywickrema, A. L. J. Beckwith, *Tetrahedron Lett.* **1986**, *27*, 109-112.

[16]   M. Kropp, G. B. Schuster, *Tetrahedron Lett.* **1987**, *28*, 5295-5298.

[17]   A. L. J. Beckwith, S. H. Goh, *J. Chem. Soc., Chem. Commun.* **1983**, 905-906.

[18]   A. L. J. Beckwith, S. H. Goh, *J. Chem. Soc., Chem. Commun.* **1983**, 907-907.

[19]   N. Shimizu, K. Watanabe, Y. Tsuno, *Bull. Chem. Soc. Jpn.* **1984**, *57*, 885-886.

[20]   E. C. Ashby, A. K. Deshpande, *J. Org. Chem.* **1994**, *59*, 3798-3805.

[21]   E. C. Ashby, C. O. Welder, *J. Org. Chem.* **1997**, *62*, 3542-3551.

[22]   S. Krishnamurthy, H. C. Brown, *J. Org. Chem.* **1982**, *47*, 276-280.

[23]   H. Tomioka, K. Tabayashi, Y. Ozaki, Y. Izawa, *Tetrahedron* **1985**, *41*, 1435-1440.

[24]   A. Klages, *Ber.* **1907**, *40*, 2360-2373.

[25]   K. Satyanarayana, N. Chidambaram, S. Chandrasekaran, *Synth. Commun.* **1989**, *19*, 2159-2166.

[26]   A. L. J. Beckwith, W. A. Waters, *J. Chem. Soc.* **1957**, 1665-1668.

[27]   F. Bergmann, J. Weizman, D. Schapiro, *J. Org. Chem.* **1944**, *9*, 408-414.

[28]   I. Al Adel, B. Adeoti Salami, J. Levisalles, H. Rudler, *Bull. Soc. Chim. Fr.* **1976**, 934-938.

[29]   T. Kariyone, *J. Pharm. Soc. Jpn.* **1925**, 515, 1-12.; *Chem. Abstr.* **1926**, *20*, 412.

[30]   G. Wiliams, *J. Chem. Soc.* **1930**, 37-46.

[31]   H. O. Nicholas, J. L. E. Erickson, *J. Am. Chem. Soc.* **1926**, *48*, 2174-2176.

Povzetek:

Proučevali smo vpliv topil na potek fotolize 3-kloro in 4-kloro substituiranih benzil kloridov. Kot topila smo izbrali cikloheksan, tetrahidrofuran in acetonitril. V vseh izbranih topilih v prvi stopnji poteče homolitska cepitev benzilne C-Cl vezi in nastane biradikalski par. Le-ta se v cikloheksanu ali tetrahidrofuranu pretvori v prosti benzilni radikal, nasprotno pa je v acetonitrilu primarni proces prenos elektrona v biradikalskem paru na halogenski atom in nastanek ionskega para. Redukcija C-Cl vezi v aromatskem obroču poteče šele v naslednji stopnji. Dodatek LiAlH$_4$ pospeši redukcijo, tako da nastaneta le 3-kloro- ali 4-klorotoluen in toluen.

THE SYNTHESES OF 1-(2-NAPHTHYL)PIPERAZINE DERIVATIVES. NOVEL SPIPERONE-CONTAINING PROBES[†]

Andrej Petrič*
Faculty of Chemistry and Chemical Technology, University of Ljubljana, SI-1000 Ljubljana, Slovenia

Jorge R. Barrio
Department of Molecular and Medical Pharmacology and the Laboratory of Structural Biology and Molecular Medicine, UCLA, School of Medicine, Los Angeles, California 90095, USA

Abstract

The synthesis of 1-(6-piperazino-2-naphthyl)-1-ethanone, a reactive fluorescent dye, is described. To this dye spiperone, a highly potent dopaminergic D_2 receptor ligand, was conjugated giving a new fluorescent probe. By the Knoevenagel reaction with malononitrile and subsequent deprotection, Vis range fluorescent probe was formed.

Introduction

The discovery of 2-(1,1-dicyanopropenyl-2)-6-dimethylaminonaphthalene [1] prompted us to explore the possibility of incorporating the favorable optical properties of this compound into biological probes for use with fluorescence microscopy. We initially envisaged structural modification of the compound by formal replacement of the dimethylamino group by an amine bearing a reactive functional group. Such a functional group would be utilized for attachment of a ligand, which would introduce specificity in the molecule towards enzymes or receptors maintaining, at the same time, fluorescent properties. We have already reported on a application of this approach with 4-piperidine-

---

[†] Dedicated to the memory of Prof. Dr. Anton Šebenik

methanol or 2-ethylaminoethanol as the dimethylamino group replacement, and using spiperone, a highly potent dopaminergic D_2 receptor ligand, as the specific ligand [2]. We have proven that in this way new pharmacological probes which possess very similar optical properties to those of the parent fluorophore can be prepared. Similar optical properties were also found in compounds in which the 4-ethylpiperazine moiety linked the spiperone and naphthalene moieties [3]. *In vitro* binding assays of such a compound against ³H-spiperone revealed high affinity for dopaminergic D_2 receptors. In this work we describe in detail synthetic procedures for the preparation of a series of piperazine-containing fluorescent compounds.

Results and discussion

The synthetic route to the title derivatives started with the preparation of 1-(6-piperazino-2-naphthyl)-1-ethanone (**3**). Thoroughly dried piperazine was treated with lithium metal in a mixture of anhydrous toluene and hexamethylphosphoric triamide (HMPT) to yield the lithium salt. The latter reacted with 1-(6-methoxy-2-naphthyl)-1-ethanone **1** to give compound **3** (**Scheme 1**).
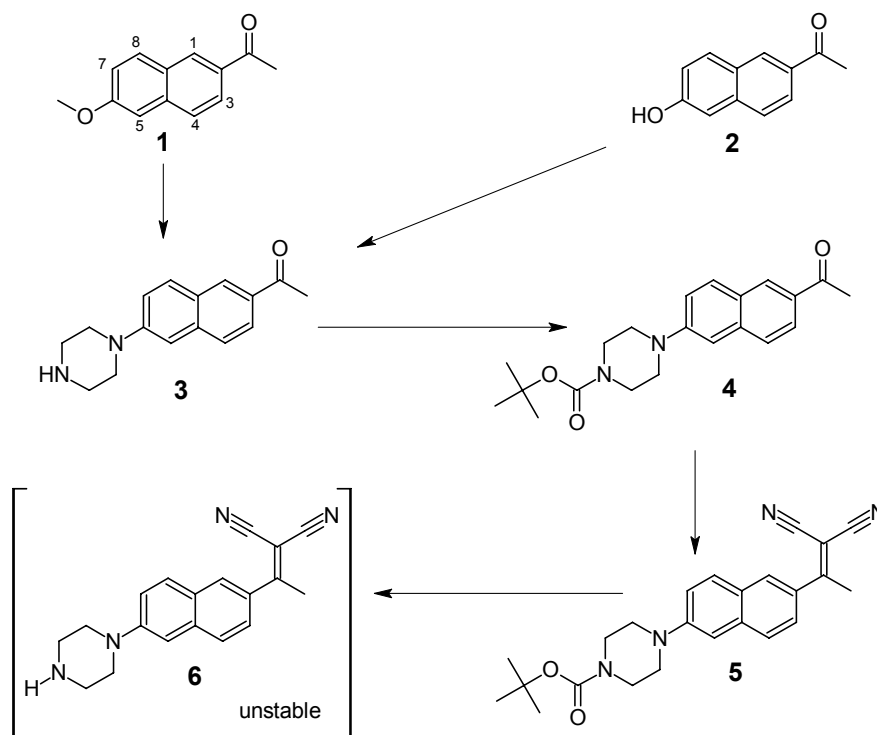
Scheme 1

Compound **3** was purified by column chromatography to remove 1-(6-dimethylamino-2-naphthyl)-1-ethanone, which was formed in a competing reaction of **1** with dimethylamine. It has been earlier described that HMPT decomposed under the reaction conditions releasing dimethylamine [4]. The Bucherer reaction [5] of 6-acetyl-2-naphthol with piperazine in the presence of sodium bisulfite gave a better yield of compound **3**, but due to the presence of the unreacted starting naphthol **2**, the chromatographic purification step could not be avoided.

An attempt to transform 1-(6-piperazino-2-naphthyl)-1-ethanone (**3**) into compound **6** resulted in a very low yield. We assumed that the free NH group in the piperazine ring catalyzed the decomposition of **6**. When we protected the free NH group in **3** with a *tert*-butyloxycarbonyl group, we obtained compound **4**. The transformation of **4** with malononitrile proceeded smoothly to give compound **5** in good yield. In the last step, the protective group was removed by treatment with trifluoroacetic acid (TFA) at room temperature. The product exhibited a ^{1}H NMR spectrum consistent with structure **6**, but was found to be unstable. This proved our initial assumption that the basic NH group can promote the decomposition of **6**, thus rendering this compound inappropriate starting material for further transformations.

The above observation led to the redesign of our synthetic approach as presented in **Scheme 2**. First, compound **3** was treated with an excess of 1,2-dibromoethane under phase transfer conditions to yield slightly unstable compound **7**, which was let to react with ketal protected spiperone in the next step and compound **8** was obtained. It served as a precursor for the preparation of a fluorescent probe **9**, with the excitation maximum in the UV range at approximately 340 nm. The transformation of **8** into **9** was reflected in expected changes in the ^{1}H NMR spectrum [6]. The lack of the two multiplets at approximately 3.75 and 4.00 ppm, corresponding to the ethylene protons of the ketal protecting group, and the downfield shift of the signals for protons 2 and 6 in the 4-fluorophenyl group supported the structure. Compound **8** also served as a precursor for the preparation of a fluorescent probe, with the excitation maximum in the visible range.

In the Knoevenagel reaction with malononitrile in pyridine, the acetyl group in **8** was transformed into the 1,1-dicyanopropenyl group, resulting in the yellow orange compound **10**. The target fluorescent probe for *in-vivo* probing of the dopaminergic D$_2$ receptors, which can be excited in the Vis range (approximately at 400 nm), was obtained upon mild, acid catalyzed, ketal protection removal from the spiperone moiety. It was found that compound **11** underwent slow decomposition at room temperature in a dichloromethane solution. The decomposition was prevented by the addition of 1 to 5% methanol and storage in a freezer.
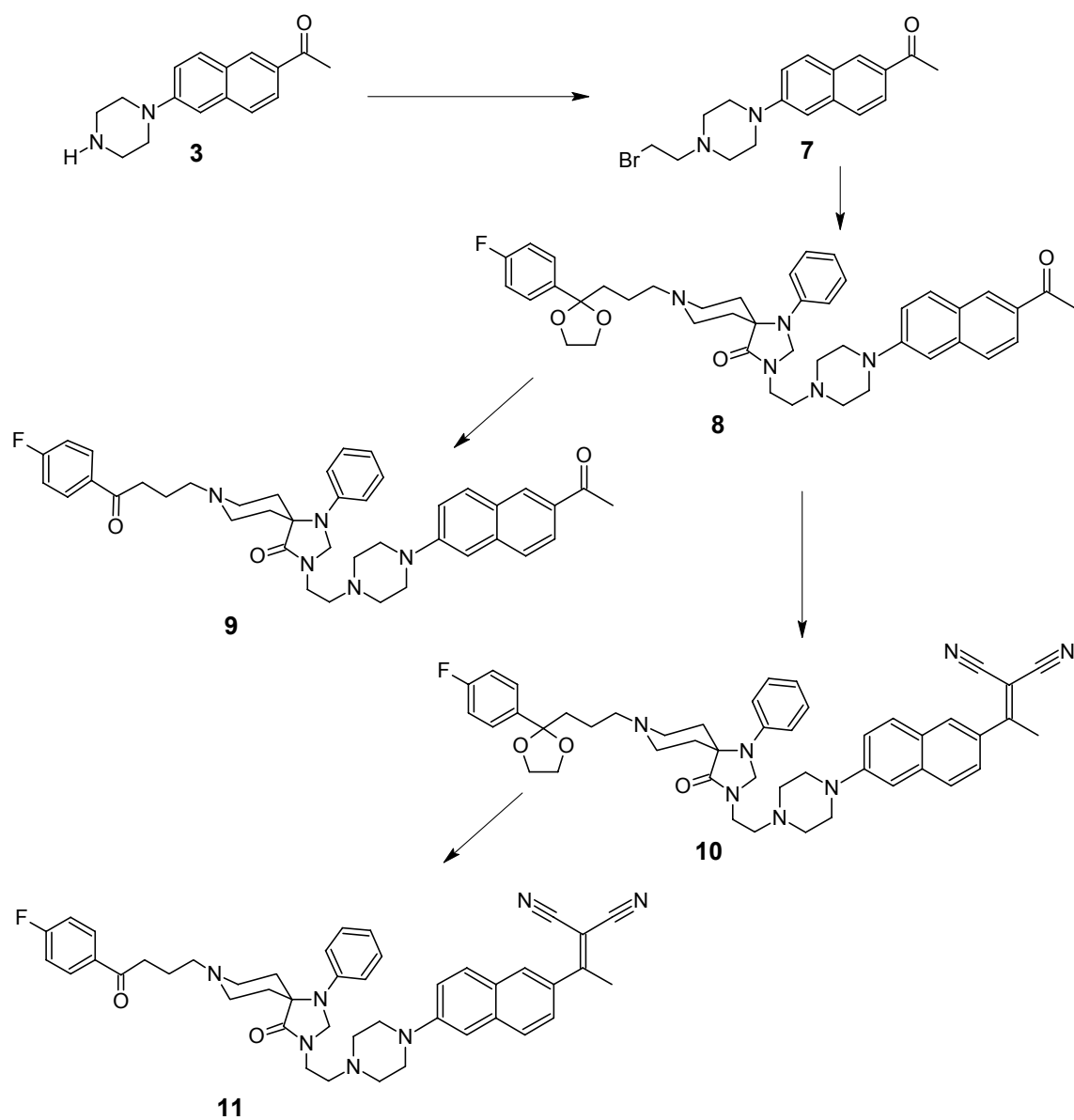
Scheme 2

Conclusions

A novel fluorescent reactive dye 1-(6-piperazino-2-naphthyl)-1-ethanone was prepared from 1-(6-methoxy-2-naphthyl)-1-ethanone or 6-acetyl-2-naphthol. It contains a free NH group available for the attachment of a ligand of choice. If such a ligand contains an electrophilic reactive center, novel fluorescent probes become available. If the intended ligand contains a nucleophilic center, which can be alkylated without significant deterioration of the binding properties, 1-6-[4-(2-bromoethyl)piperazino]-2-naphthyl-1-ethanone can be used instead. The optical properties of these compounds can be modified by the Knoevenagel reaction with malononitrile in which the acetyl group is transformed into a 1,1-dicyanopropenyl. This structural change induces the shift of the fluorescence excitation and emission maxima into the Vis range. Using spiperone, a highly potent ligand for the dopamine D_2 receptors, this approach was successfully tested.

Experimental

NMR spectra were obtained on Bruker AM 360 WB or DPX 300 Spectrometers. ^{1}H chemical shifts are reported in ppm downfield from TMS as internal standard. ^{19}F chemical shifts are reported relative to external fluorotrichloromethane. Deuteriochloroform was used as the solvent unless stated otherwise. Naphthalene ring atom numbering as specified for structure **1** in **Scheme 1** was used in reporting the spectral assignments, although the numbering according to the IUPAC Nomenclature rules differs [7]. Melting points were determined on a Electrothermal Melting Point Apparatus and are uncorrected. Elemental analyses were performed by Galbraith Laboratories, Inc., Knoxville, TN and Ms. Metka Kastelic at the Faculty of Chemistry and Chemical Technology, University of Ljubljana. Radial chromatography was performed on Chromatotron (Harrison Research, 840 Moana Court, Palo Alto, CA 94306). The rotors were prepared as recommended by Harrison Research using E. Merck Silica Gel (Cat. No. 7749-3). HPLC was performed on an Alltech Econosil C18

5 μm 4.6×250 mm column using water : acetonitrile : triethylamine = 40 : 60 : 2 as the solvent. UV detection at 254 nm was used. Solvents and reagents were purchased from Fisher, Aldrich or Fluka and were used as received unless noted otherwise.

1-(6-Piperazino-2-naphthyl)-1-ethanone (3). Method a: Anhydrous piperazine (7 g, 81.3 mmol; dried in a vacuum dessicator over KOH-drierite mixture for 3 days) was dissolved in a mixture of dry, freshly distilled toluene and hexamethyl phosphoric triamide (HMPT), 25 mL each. To the solution, 556 mg (80.1 mmol) of lithium rod, cut in small pieces under argon atmosphere, was added and the mixture was stirred under argon for 24 hours during which time all lithium has dissolved. Vacuum-dried **1** [8] (3.5g, 17.5 mmol) was added and stirring was continued for additional 65 hours. After quenching with 300 mL of water, extraction with dichloromethane (3×300 mL), drying with anhydrous magnesium sulfate, and evaporation, a mixture of white and yellow solids was obtained. Extraction with 300 mL of hot methanol gave raw material that was purified by column chromatography (70-230 mesh silica, 25×120 mm, 5% methanol in dichloromethane) to yield 1.54 g (35 %) of **3**. After recrystallization from ethyl acetate the sample melted at 170.5-172 °C. **Method b:** Compound **2** [2] (441 mg, 2.36 mmol) was heated at 140-150 °C with 6 g piperazine hydrate (30.9 mmol) and $NaHSO_3$ (244 mg, 2.35 mmol) for 24 hours when additional 2 g (19.2 mmol) of sodium bisulfite was added and heating was continued. After additional 24 hours more bisulfite (1 g) was added and heating was continued to the total reaction time of 72 hours. After cooling the mixture was extracted with methanol (2×50 mL). After evaporation of methanol the residue was suspended in water (50 mL) and extracted with ethyl acetate (5×80 mL). Combined extracts were dried (magnesium sulfate) and evaporated to give 430 mg of yellow solid. Radial chromatography (4 mm silica, methanol) gave 83 mg (19 %) of starting naphthol **2** and 276 mg (46 %; 56 %, based on unrecovered starting material) of product **3**. The product was in all respects identical to the compound obtained as described under **method a**. *Anal*. Calculated for $C_{16}H_{18}N_2O$: C, 75.56; H, 7.13; N, 11.01. Found: C, 75.82; H, 7.27; N, 10.92. ^{1}H NMR: δ 2.68 (s, 3H, CH_3), 3.09 and 3.35 (t, J= 4.95 Hz, 8H, piperazine), 7.10 (d, 1H, 5-H), 7.31 (dd, 1H, 7-H), 7.69 (d, 1H, 4-H),

7.83 (d, 1H, 8-H), 7.95 (d, 1H, 3-H), 8.34 (s, 1H, 1-H); $J_{5,7}$= 2 Hz, $J_{7,8}$= 8.4 Hz, $J_{1,3}$= 2 Hz, $J_{3,4}$= 8.4 Hz.

tert-Butyl 4-(6-acetyl-2-naphthyl)-1-piperazinecarboxylate (4). Compound **3** (254 mg, 1 mmol) was added to a stirred mixture of NaOH (1 g), tetra-*n*-butylammonium hydrogensulfate (100 mg), water (2 mL) and toluene (6 mL), followed by a solution of di-*tert*-butyl dicarbonate (230 mg, 1.05 mmol) of. The course of the reaction was followed by TLC (silica, 5% methanol in dichloromethane). Every 10 minutes additional amount of the dicarbonate was added until all starting material has reacted. A total of approximately 1.5 equivalents were used. A mixture of water and dichloromethane (60 mL each) was added and after thorough shaking the layers were separated. The aqueous layer was extracted with an additional 30 mL of dichloromethane. The combined organic extracts were dried with anhydrous magnesium sulfate. During this procedure the color of the solution turned from pink to light yellow. Evaporation *in vacuo* gave 295 mg (83 %) of **4**, which on recrystallization from dichloromethane - petroleum ether mixture melted at 153-154 °C *Anal.* Calculated for $C_{21}H_{26}N_2O_3$: C, 71.16; H, 7.39; N, 7.90. Found: C, 71.27; H, 7.60; N, 7.86. ^{1}H NMR: δ 1.50 (s, 9H, -C(CH$_3$)$_3$), 2.68 (s, 3H, CH$_3$), 3.33 and 3.64 (t, J= 4.9 Hz, 8H, piperazine), 7.10 (d, 1H, 5-H), 7.31 (dd, 1H, 7-H), 7.70 (d, 1H, 4-H), 7.85 (d, 1H, 8-H), 7.97 (d, 1H, 3-H), 8.35 (d, 1H, 1-H); $J_{5,7}$= 2 Hz, $J_{7,8}$= 9 Hz, $J_{3,4}$= 8.7 Hz.

tert-Butyl 4-[6-(2,2-dicyano-1-methylvinyl)-2-naphthyl]-1-piperazinecarboxylate (5). Compound **4** (177 mg, 0.5 mmol) was heated with 40 mg (0.6 mmol) of malononitrile in pyridine (4 mL) at 105-110 °C. After 5.5 hours additional 24 mg of malononitrile was added and heating was continued to a total of 13 hours. The mixture was cooled and evaporated *in vacuo*. Polar components of the mixture were removed by column chromatography (70-230 mesh silica, 20×120 mm, chloroform) and the product was finally purified by radial chromatography (silica, 2 mm, chloroform) to yield 155 mg (77%) of **5** that was recrystallized from dichloromethane - petroleum ether mixture,

M.p. 169-171 °C. *Anal.* Calculated for $C_{24}H_{26}N_4O_2$: C, 71.62; H, 6.51; N,13.92. Found: C, 71.62; H, 6.66; N, 13.87. ^{1}H NMR: δ 1.50 (s, 9H, -C(CH_3)_3), 2.72 (s, 3H, CH_3), 3.34 and 3.64 (t, J= 5.1 Hz, 8H, piperazine), 7.09 (d, 1H, 5-H), 7.33 (dd, 1H, 7-H), 7.58 (dd, 1H, 3-H), 7.74 (d, 1H, 4-H), 7.81 (d, 1H, 8-H), 8.02 (d, 1H, 1-H); $J_{5,7}$= 2 Hz, $J_{7,8}$= 9.1 Hz, $J_{1,3}$= 2 Hz, $J_{3,4}$= 9.1 Hz.

2-[1-(6-Piperazino-2-naphthyl)ethylidene]malononitrile (6). Compound **5** (10 mg) was treated with an excess of TFA (1 mL) at room temperature for 5 min followed by TFA was removal *in vacuo* at room temperature. TLC revealed the presence of a single compound. ^{1}H NMR: δ 2.72 (s, 3H, CH_3), 3.50 and 3.63 (broad, 8H, piperazine), 7.18 (broad s, 1H, 5-H), 7.29 (d, 1H, 7-H), 7.59 (d, 1H, 3-H), 7.79 (d, 1H, 4-H), 7.87 (d, 1H, 8-H), 8.04 (s, 1H, 1-H), 9.0 (broad, 1.5H, NH and acid); $J_{7,8}$= 8.8 Hz, $J_{3,4}$= 8.4 Hz. ^{19}F NMR: ? -76.2 (CF_3COO).

NMR of the residue revealed clean hydrolysis of the *tert*-butyloxycarbonyl group. The NMR sample was diluted by dichloromethane (10 mL), the solution washed with saturated NaHCO_3 solution (to remove traces of TFA), dried, and evaporated *in vacuo*. A light yellow oil was obtained which, on standing at room temperature, turned dark red. TLC analysis showed color change due to decomposition of **6** into several products, the most intense spot being low-Rf red-orange. Selected ^{1}H NMR signals after neutralization: δ 2.72 (s, 3H, CH_3), 3.09 and 3.35 (t, J= 5 Hz, 8H, piperazine), 7.08 (s, 1H, 5-H), 8.02 (s, 1H, 1-H).

1-{6-[4-(2-Bromoethyl)piperazino]-2-naphthyl}-1-ethanone (7). To a solution of NaOH (1g) and tetra-*n*-butylammonium hydrogensulfate (50 mg, 0.15 mmol) in water (2 mL) compound **3** was added (255 mg, 1 mmol) and the mixture was stirred for 45 min at room temperature. After the adition of 1,2-dibromoethane (2 mL), stirring was continued for 4 hours. TLC (silica, 5% methanol in dichloromethane) had revealed that the starting material was still present in the reaction mixture. Additional 1 mL of 1,2-dibromoethane was added and stirring was continued for a total of 20 hours. Water and

dichloromethane (50 mL each) were added to the mixture, the organic layer washed with water, dried and evaporated *in vacuo* at 35 °C. The solid was chromatographed by radial chromatography (4 mm silica, dichloromethane) to give 180 mg (50%) of pure (as determined by NMR) bromoethyl product **7.** This compound decomposes upon handling or when left at room temperature in the air, as determined by TLC on silicagel. It was necessary to use purified **7** immediately in the next step. ^{1}H NMR: δ 2.69 (s, 3H, CH$_3$), 2.74 and 3.40 (t, 8H, J= 4.8 Hz, piperazine), 2.89 and 3.50 (t, J= 7.2 Hz, 4H, CH$_2$CH$_2$), 7.10 (d, 1H, 5-H), 7.31 (dd, 1H, 7-H), 7.69 (d, 1H, 4-H), 7.83 (d, 1H, 8-H), 7.96 (d, 1H, 3-H), 8.35 (s, 1H, 1-H); J$_{5,7}$= 2 Hz, J$_{7,8}$= 8.8 Hz, J$_{3,4}$= 8.6 Hz.

1-(6-{4-[2-(8-{3-[2-(4-Fluorophenyl)-1,3-dioxolan-2-yl]propyl}-1-oxo-4-phenyl-2,4,8-triazaspiro[4.5]dec-2-yl)ethyl]piperazino}-2-naphthyl)-1-ethanone (8). To the solution of NaOH (1 g) and tetra-*n*-butylammonium hydrogensulfate (100 mg) in 2 mL of water, 8-{3-[2-(4-fluorophenyl)-1,3-dioxolan-2-yl]propyl}-1-phenyl-1,3,8-triaza-spiro[4.5]decan-4-one (spiperone ketal, 199 mg, 0.454 mmol)) [9,10] was added, followed by 1 mL of toluene. After stirring for 20 min, a solution of 180 mg (0.5 mmol) of **7** in toluene (9 mL) was added. The mixture was stirred at room temperature for 16 hours and, after addition of a mixture of ethyl acetate (100 mL) and water (50 mL), the organic layer was washed with 50 mL of brine. After drying with anhydrous magnesium sulfate and evaporation in vacuo, 387 mg of a yellow oil was obtained which was purified by chromatography (70-230 mesh silica, 21×120 mm, ethyl acetate) to give 258 mg (71%) of **8**. *HRMS* Calculated for C$_{43}$H$_{51}$N$_5$O$_4$F (M+H): 720.3925. Found: 720.3941. ^{1}H NMR: δ 1.49-3.65 (m, 29H, CH$_3$, spiperone, piperazine and ethylene between the latter two), 3.75 and 4.00 (m, 4H, OCH$_2$CH$_2$O), 4.75 (s, 2H, NCH$_2$N), 6.79-7.03 (m, 5H, Ar), 7.08 (d, 1H, 5-H(naphth.)), 7.23-7.32 (m, 3H, Ar and 7-H(naphth.)), 7.41 (m, 2H, Ar), 7.68 (d, 1H, 4-H(naphth.)), 7.82 (d, 1H, 8-H(naphth.)), 7.95 (d, 1H, 3-H(naphth.)), 8.34 (s, 1H, 1-H(naphth.)); J$_{3,4}$= 8.6 Hz, J$_{7,8}$= 8.9 Hz.

3-{2-[4-(6-Acetyl-2-naphthyl)piperazino]ethyl}-8-[4-(4-fluorophenyl)-4-oxobutyl]-1-

phenyl-1,3,8-triazaspiro[4.5]decan-4-one (9). Ketal **8** (10 mg, 0.014 mmol) was treated with 2 mL of methanol and 1 drop of concentrated hydrochloric acid. After stirring at room temperature for 3 hours the mixture was diluted with dichloromethane (50 mL) and washed with saturated sodium bicarbonate solution (20 mL). After drying with anhydrous magnesium sulfate and removal of the solvent, 8 mg of off-white foam was obtained. It was purified by chromatography on two 10×20 cm silica plates (0.2 mm layer thickness), using 5% methanol in dichloromethane as the solvent. Final purification was achieved by radial chromatography (1 mm silica, 5% methanol in dichloromethane). Appropriate fractions were collected and evaporated to give 5 mg (53 %) of pure **9**. ^{1}H NMR: δ 1.5-3.7 (m, 29 H, CH_3, spiperone, piperazine and ethylene between the latter two), 4.77 (s, 2H, NCH_2N), 6.82-7.03 (m, 3H, Ar), 7.09 (d, 1H, 5-H(naphth.)), 7.12 (t, J=8.5 Hz, 2H, Ar), 7.30 (m, 3H, Ar and 7-H(naphth.)), 7.68 (d, 1H, 4-H(naphth.)), 7.82 (d, 1H, 8-H(naphth.)), 7.95 (d, 1H, 7-H(naphth.)), 8.02 (m, 2H, Ar), 8.33 (s, 1H, 1-H(naphth.)); $J_{5,7}$= 2 Hz, $J_{7,8}$= 9 Hz, $J_{3,4}$= 8.5 Hz.

2-[1-(6-{4-[2-(8-{3-[2-(4-Fluorophenyl)-1,3-dioxolan-2-yl]propyl}-1-oxo-4-phenyl-2,4,8-triazaspiro[4.5]dec-2-yl)ethyl]piperazino}-2-naphthyl)ethylidene]malono-nitrile (10). Acetyl compound **8** (220 mg, 0.31 mmol) was heated and stirred at 70-85 ^{o}C under argon with malononitrile (101 mg, 1.5 mmol) in pyridine (6 mL) for 17 hours. After evaporation of the solvent *in vacuo* at 40 ^{o}C an orange-red oil (233 mg) was obtained and chromatographed (70-230 mesh neutral alumina, 16×360 mm, chloroform) to give 167 mg (67 %) of **10** as an orange oil. *HRMS* calcd. for $C_{46}H_{51}N_7O_3F$ (M+H): 768.4037. Found: 768.3994. ^{1}H NMR: δ 1.48-3.65 (m, 29H, CH_3, spiperone, piperazine and ethylene between the latter two), 3.75 and 4.01 (t, J= 7 Hz, 4H, OCH_2CH_2O), 4.75 (s, 2H, NCH_2N), 6.80-7.03 (m, 5H, Ar), 7.07 (d, 1H, 5-H(naphth.)), 7.32-7.38 (m, 3H, Ar and 7-H(naphth.)), 7.41 (m, 2H, Ar), 7.58 (dd, 1H, 3-H(naphth.)), 7.72 (d, 1H, 4-H(naphth.)), 7.80 (d, 1H, 8-H(naphth.)), 8.01 (s, 1H, 1-H(naphth.)); $J_{5,7}$= 2.7 Hz, $J_{7,8}$= 9. Hz, $J_{1,3}$= 2.5 Hz, $J_{3,4}$= 9 Hz.

2-(1-{6-[4-(2-{8-[4-(4-Fluorophenyl)-4-oxobutyl]-1-oxo-4-phenyl-2,4,8-triaza-spiro[4.5]dec-2-yl}ethyl)piperazino]-2-naphthyl}ethylidene)malononitrile (11).

Compound **10** (71 mg, 0.098 mmol) was stirred with 5 drops of concentrated hydrochloric acid in 10 mL of methanol for 4 hours. A mixture of 150 mL of dichloromethane and 50 mL of saturated sodium bicarbonate solution was added and the organic layer was washed with 50 mL of water. After drying with magnesium sulfate and evaporation of the solvent of an orange oil (45 mg, 67 %) was obtained. NMR analysis demonstrated removal of the ketal group. The product was purified by preparative TLC (2 mm silica, 5% methanol in dichloromethane). *HRMS* Calculated for $C_{44}H_{47}N_7O_2F$ (M+H): 724.3775. Found: 724.3791. ^{1}H NMR: δ 1.63-3.65 (m, 29H, CH_3, spiperone, piperazine and ethylene between the latter two), 4.75 (s, 2H, NCH_2N), 6.83-6.93 (m, 3H, Ar), 7.05 (d, 1H, 5-H(naphth.)), 7.12 (t, J=8.5 Hz, Ar), 7.26 (t, J=9.7 Hz, 2H, Ar), 7.31 (dd, 1H, 7-H(naphth.)), 7.56 (m, 1H, 3-H(naphth.)), 7.71 (d, 1H, 4-H(naphth.)), 7.78 (d, 1H, 8-H(naphth.)), 7.98-8.04 (m, 3H, Ar and 1-H(naphth.)); $J_{5,7}$= 2.5 Hz, $J_{3,4}$= 10 Hz, $J_{7,8}$= 10 Hz.

Acknowledgments

References and Notes

[1] A. Jacobson, A. Petric, A. Sinur, J. R. Barrio, *J. Am. Chem. Soc.* **1996**, *118*, 5572-5579.
[2] A. Petrič, T. Špes, J. R. Barrio, *Monatsh. Chem.* **1998**, *129*, 777-786.

[3] A. Petrič**,** A. F. Jacobson**,** J. R. Barrio, *Bioorg. Med. Chem. Lett.* **1998**, *8*, 1455-1460.

[4] T. Cuvigny, H. Normant, *C.R. Acad. Sci. Paris* **1971,** *272*, 1425-1430.

[5] N. L. Drake, *Organic Reactions* **1942,** Vol I, 105-128.

[6] G. Ambrožič, S. Čeh, A. Petrič, *Magn. Reson. Chem.* **1998**, *36*, 873-877.

[7] Chemical names were generated by ACD Labs' Name software package, courtesy of Dr. D. Kikelj, Faculty of Pharmacy, University of Ljubljana.

[8] L. Arsenijević, V. Arsenijević, A. Horeau, J. Jacques, *Org. Synth. Coll. Vol.* **1988**, *6*, 34-36.

[9] W. G. Scharpf, (1974) U.S. Pat. 3,839,342; *Chem. Abstr.* **1975,** *82,* 43416.

[10] D. O. Kiesewetter, W. C. Eckelman, R. M. Cohen, R. D. Finn, S. M. Larson, *Appl. Radiat. Isot.* **1986**, *37*, 1181.

Povzetek

Opisana je sinteza 1-(6-piperazino-2-naftil)-1-etanona, reaktivnega fluorescentnega barvila, ki ga je moč vzbujati z UV svetlobo. V nadaljevanju so opisane pretvorbe te spojine s spiperonom, močnim in selektivnim ligandom za dopaminske D_2 receptorje. S Knoevenagel-ovo reakcijo z malononitrilom in sledečo odstranitvijo zaščitne skupine, smo pripravili novo fluorescentno probo, ki jo je moč vzbujati z vidno svetlobo.

RECENT PROGRESS IN SOL-GEL DERIVED ELECTROCHROMIC DEVICES

B. Orel, A. Šurca , U. Opara Krašovec

National Institute of Chemistry, Hajdrihova 19, Ljubljana, Slovenia

Abstract

The future energy saving requirements placed on modern buildings will require that windows will have to meet higher standards, including: being able to reduce heat-loss while avoiding overheating of the building and gaining solar energy while assuring comfortable daylighting. These conflicting demands can be satisfied by using switchable or "smart" windows, the optical properties (transmittance and reflectance), of which can be varied between low and high transmitting states. This could be done either manually or automatically by the building's own energy management system. We report our progress towards making electrochromic devices for switchable "smart" window applications. The future development of the next generation of switchable windows is addressed.

INTRODUCTION

Heating, cooling and lighting account for the largest proportion of the total energy budget consumed in commercial and residential buildings. If the building of the future is to be "sustainable" in terms of energy consumption, then a step towards this will be the

use of active solar collector systems integrated into well designed energy management systems. Modern collector water-heating systems employ selective absorbers possessing a high efficiency for photothermal conversion. Selective absorbers, characterised by high solar absorptance (a_s) and low thermal emittance (e_T) - depressing total radiation losses, provide a net gain in solar conversion of more than 20 % compared to non-selective absorbers. This is because the working temperatures of selective absorbers are always higher. For example, in a domestic water-system the temperature difference at a working temperature of 40 °C is between 15 - 20 °C, when selective absorbers are used.

In Europe the annual requirement for glazed solar collectors with selective absorbers is estimated at 500000 m^2. The market is currently dominated by the electroplating industry: Black chrome and MTI in the USA, Batek in the Netherlands and GIBO in Germany. Ni-pigmented anodised aluminium absorbers are produced by Tecknoterm in Sweden, Metalux in Germany, Showa in Japan and Fenis in Turkey, while black nickel coated absorbers are produced by Maxorb in the United Kingdom. Electroplating is a highly developed technique but is increasingly under attack because of its high environmental impact.

More advanced technologies are being used including: reactive evaporation for making Ti-oxynitride coatings (TINOX, Germany) and reactive sputtering to make Cr-oxynitride coatings (Fraunhofer Institute for Solare Energiesysteme in Freiburg , Germany). These advanced vacuum techniques require sophisticated and expensive equipment resulting in high production costs. These are compensated for, or at least in part, by the high selectivity of the absorber coatings. Sol-gel Crystal Black coatings (Thermafin Manufacturing, L.C., USA) must also be mentioned, since by using sol-gel technology it is possible to make high quality coatings with high spectral selectivity more cheaply than by vacuum deposition.

Selective unglazed solar hot-air absorbers mounted on the facade represents a significant step forward towards reducing the total energy needs of a building. It is expected, that

solar facades could save approximately 2.5 % of the total energy budget, which is equivalent to approximately 1.2×10^{10} m^3 of CO_2 per year. Unglazed solar absorbers suitable for building facades are yet to reach the market. This is because there are at present no selective coatings durable to assure a long exploitation period - at least fifteen years. Solar facades must be aesthetically pleasing; the unglazed solar facade is the colour of the solar absorber, which is an unacceptable black. Since no satisfactory alternatives exist, the major challenge to material science research is to produce coloured selective absorbers with high solar absorptance ($a_s > 0.93$) and low thermal emittance ($e_T < 0.1$) [1].

It is also possible to reduce the heating demands of a building by improving thermal insulation, while a saving in the amount of energy needed for cooling a building can be achieved by increasing its mass and/or installing efficient ventilation systems. Both approaches - if not applied properly - might lead to a reduced thermal and visual comfort, adding to the phenomena known as "sick building syndrome". In hotter climates, the higher influx of the solar radiation through the windows can result in the overheating of the building interior. Alternatively, in colder climates the internal environment of highly thermally insulated buildings with small windows, may not provide adequate illumination. The amount of heat lost through a window depends on the material from which the window-frame is made, details of edge sealing and the ratio between the frame and the glazed areas. For modern buildings with extensive glazing heat-loss can be high. This heat-loss is expressed quantitatively in terms of the overall heat transfer coefficient (U-value in W/m^2K) [2]. Usually, the U-value of double glazed windows is between 2 - 3 W/m^2K, almost 10 times higher than the heat lost through the walls (Fig. 1). Modern windows with advanced glazing, with hard or soft low-emitting (low-e) coatings and filled with an inert gas, have a lower overall heat loss coefficient (1.5 - 2 W/m^2K), but their total solar energy transmittance (TSET) and visible light transmittance (T_{vis}) are rarely above 60 %. Windows employing monolithic aerogel, transparent insulation (e.g. capillary polycarbonate or honey comb materials) and vacuum glazing are alternatives to double and triple glazed windows with low e-coatings and an

inert gas (Kr, Xe) filling. These windows, with low U-values, can not respond "in-situ" to the variation in intensity of incoming solar radiation. By incorporating switchable
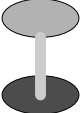
Fig. 1 Solar energy transmission TSET versus the centre-of-glass U-value (W/m^{2}K) for different windows (adapted from ref. [2]).

windows, the transmittance can be varied continuously between dark (low transmitting) and bleached (high transmitting) states, making it possible to avoid overheating during the day. This will reduce the amount of energy required for cooling in the summer, and

allow large area windows, with a high TSET to be incorporated into the building design without increasing the heating costs during the winter. In addition, switchable windows prevent the major visual discomfort caused by excessive glare.

Various switchable "smart" windows exist:

− Photochromic windows: transmittance change is a function of the irradiation dose.

− Thermochromic windows: transmittance change responds to the temperature variation of the glazing.

− Thermotropic windows: TSET decreases with increased scattering of the visible light at certain temperatures.

− Electrochromic windows: optical properties change under the action of a voltage or current pulse.

At present electrochromic (EC) windows are the best option, because they allow the transmittance to be varied either manually or automatically by the building's energy management system.

In this report we present our own progress towards making EC devices for "smart" window applications. This will include a brief description of sol-gel processing, the dip-coating technique and the most promising films and materials. The properties of the "all sol-gel" EC devices, regarding their colour change and overall spectral characteristics, will be discussed in greater depth. The future development of the next generation of switchable windows will also be addressed.

RESULTS

Within the frame-work of the Pilkington plc "Smartglass" project [3] our aims were to synthesise novel materials and films using sol-gel processing and dip-coating deposition and to manufacture an "all sol-gel" EC device (Fig. 2) with the following characteristics: a transmittance in the bleached (uncharged) state above 65 %, transmittance in the coloured state below 10 %, a switching speed less than 10 min and a cycling stability greater than 3000 cycles. In addition, the colour of the EC device in the charged state must offer alternative colours (dark neutral colours) other than blue, which is characteristic of charged WO_3 films.

glass
transparent conductive electrode
counter electrode
M^+ ionic conductor (M^+=Li^+ or H^+)
active electrode (WO_3)
transparent conductive electrode
glass

E (V)

(bleached state) $WO_3 + xe^- + xM^+ \longleftrightarrow M_x WO_3$ (coloured state)
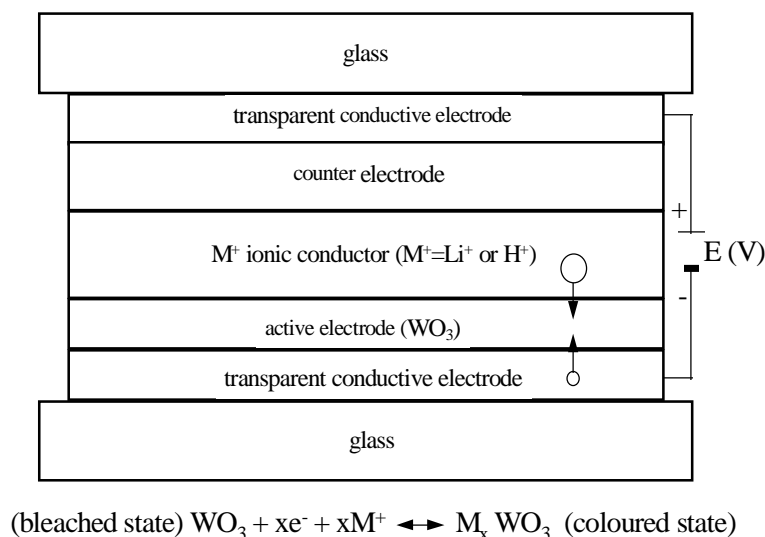
Fig. 2 Basic design of EC device. Transport of positive ions to obtain coloured state of the device is indicated.

An "all sol-gel" EC device is one in which all three internal layers, including the ionic conductor, are processed by the sol-gel route. Sol-gel processing exhibits many advantages over traditional techniques for the preparation of advanced and functional coatings with optical, chemical, electrooptical and mechanical properties [4]. By using the sol-gel method a high degree of homogeneity of the film is achieved, since the starting materials are mixed on a molecular level, i.e. in solution. The relatively low-cost of the precursors and the simplicity of the dip-coating process means that the potential

application of the sol-gel route is high. By using sol-gel processing a variety of dopants can be introduced to the initial sols in varying concentrations, yielding doped or mixed oxide films with much improved properties. In the frame of this project many different precursors and sol-gel routes were applied for manufacturing anodic/cathodic electrochromic and ion-storage films (Table 1).

Table 1 Thin films made by sol-gel route in our laboratory (for electrochromic and gasochromic device applications)

Cathodic electrochromics		**References**
• WO_3	peroxo sol-gel route	5,6
• Nb_2O_5	amorphous (300°C)	7
	pseudohexagonal TT-phase (520°C)	8
• $Li_{0.4}Nb_2O_{5.2}$, $Li_{0.2}Nb_2O_{5.1}$	pseudohexagonal TT-phase (520°C)	9
• PWA/TiO_2	amorphous xerogel	10,11
Anodic electrochromics		
• Ni - oxide		12,13
• Ni(Si) - oxide, Ni(La) - hydroxide		14,15
• Li_xNiO_2	layered	16
• Co_3O_4	spinel	17
• Co(Al,Si) - oxide	amorphous	18
• $LiCoO_2$	layered	16
• γFe_2O_3	maghemite	20
• Fe - oxide	amorphous	
Ion - storage films		
• CeO_2	crystalline (cerianite)	21
• CeO_2 - TiO_2	crystalline	22,23
• CeO_2 - SnO_2		24,25
• Mo: CeO_2, Si:CeO_2, Si:Mo:CeO_2		26
• $CeVO_4$	crystalline	27,28,29
• SnO_2	cassiterite	30,31
• Sb:SnO_2, Mo: Sb:SnO_2, Mo:SnO_2		32,33
• Ce:Sb:SnO_2		
• V/Ti - oxide, V/Ti/Zr - oxide,		34
• V/Ti/Ce - oxide		
• Nb/Fe - oxide	amorphous	35
• Fe/V - oxide	amorphous	
• Fe/Ti - oxide		36
• V_2O_5	amorphous	37,38
Gasochromic films		
• WO_3	amorphous	39,40,41,42

Counter-electrode films

We have concentrated a large part of our efforts into developing improved ion-storage counter-electrode films. The counter-electrode must have a high transmittance for visible light in the charged and discharged state and a ion-storage capacity exceeding 20 mC/cm^2. This ion-storage capacity is necessary if there is to be a sufficient number of ions to produce a deep coloration of the WO_3 active electrochromic film and for the device to remain stable. Our research shows that, between all the materials tested, $CeVO_4$ and V/Ti-oxide were the most efficient (Table 1).
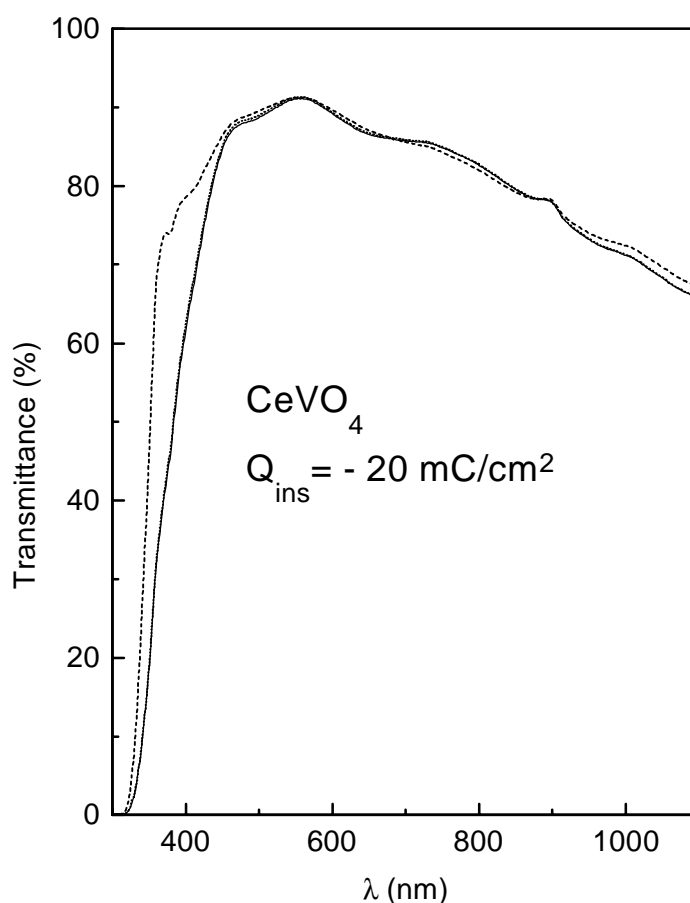
Fig. 3 In-situ UV-VIS spectroelectrochemical response of $CeVO_4$ films charged at -1.6 V and 1.6 V vs. Ag/AgCl: (———) as deposited, (-----) charged and (·······) discharged states [27].

Cerium vanadate [27] exhibits an ion-storage capacity greater than 20 mC/cm^2 and a high (90 %) transmittance in the visible region. The transmittance of the as-deposited and discharged states of the films are practical ly identical. The transmittance of charged and discharged states is marginal above 450 nm while bellow this wavelenght the films bleach with charging (Fig. 3). The spectral coloration efficiencies (η) are calculated according to the equation $\eta = \log (T_O/T_R)/\Delta Q$ [7], where T_O and T_R are the spectral transmittance of oxidised (T_O) and reduced (T_R) films between 350 - 1100 nm and ΔQ represent inserted or extracted charge. The η of CeVO$_4$ in the visible region is less than 2 cm^2/C and positive, whilst relatively strong negative coloration efficiencies (η) values are up to -40 cm^2/C are observed in the near UV ($\lambda < 450$ nm). The coloration efficiency of CeVO$_4$ films is the lowest among all known counter-electrode films. The excellent optical passiveness, together with high ion-storage capacity rank CeVO$_4$ films among the most promising counter-electrode materials for EC device applications.

Sol-gel derived V/Ti-oxide films with amorphous structure [34] exhibit even higher ion-storage capacity (30 mC/cm^2) as compared to CeVO$_4$ which - combined with high cyclic stability (few 1000 cycles), rank V/Ti- oxide films among the most promising counter electrodes. The quality of sol-gel films is comparable to the sputtered ones made in Pilkington plc. Sputtered V/Ti-oxide films are currently used in EC devices made by Pilkington plc and are coming to the market.

Films behave as optically passive counter electrodes (Fig. 4). The variation of films transmittance in bleached and coloured state is only 10 % which is still acceptable for the counter electrode with an optically passive response. The main drawback is relatively low transmittance of the cycled films in bleached state which is 10 % lower than that of the pristine films. In this respect V/Ti-oxide films are not as good as CeVO$_4$ films which beside higher transmittance in the bleach state also do not exhibit yellowish-green colour typical of the V/Ti-oxide films. This influences the colour of the EC windows (see below).
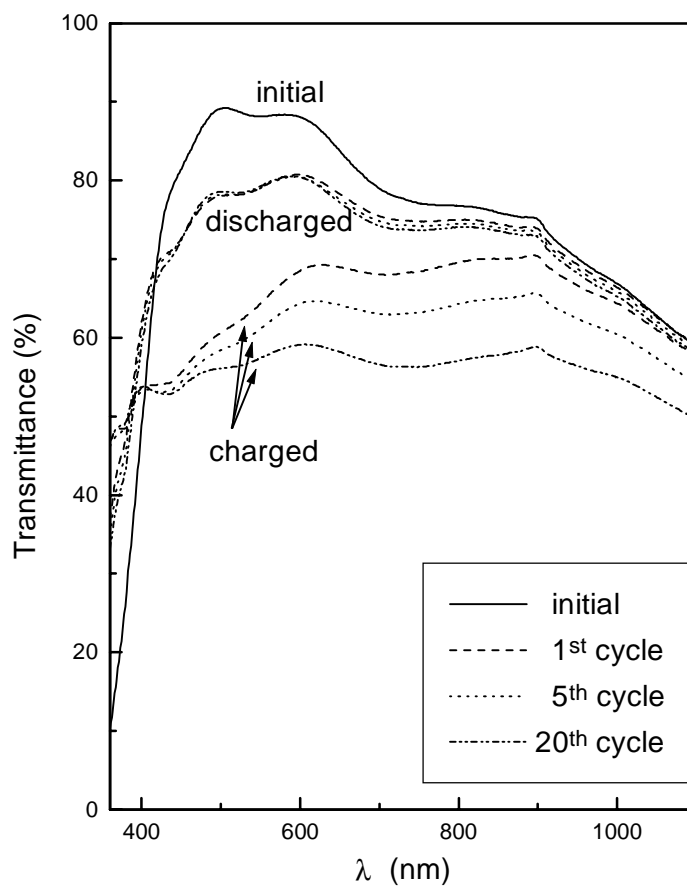
Fig. 4 In-situ UV-VIS spectroelectrochemical response of V/Ti-oxide films charged at -1.5 V and 1.5 V vs. Ag/AgCl [34].

Ionic conductors

The functioning of the EC device requires a Li^+ or H^+ ionic conductor serving as an electrolyte. At the same time the function of the ionic conductor is to laminate the active colouring and counter electrode layers together (laminated EC device).

Due to the low reaction temperatures, sol-gel synthesis offers many possibilities to introduce organic molecules into inorganic polymeric matrices. This can lead to the

synthesis of a large number of novel inorganic-organic hybrid materials with varying properties. Generally, hybrid materials depending on the nature of the chemical bonding between the organic and inorganic constituents can be divided into two classes [5]:

− Class I materials: only weak bonds exist between the organic and inorganic components (van der Waals, hydrogen, ionic bonds).

− Class II materials: covalent chemical bonds bind both parts together.

Organically modified electrolytes (ormolytes) present a good example of inorganic-organic hybrids. By varying several parameters in the sol-gel processing of the ormolyte we are able to obtain an ionic conductor with optimal properties, such as an ionic conductivity of 10^{-4} - 10^{-5} S/cm, dimensional stability and good flexibility. The present ormolyte is best described as a mixed class I - class II hybrid material where both weak physical bonds and covalent chemical bonds exist linking the silica network to the organic modifiers [5].

"All sol-gel" EC devices

The basic concept of an "all sol-gel" device is not new and consists of laminating two pieces of glass - each coated with an electrochromic (mostly cathodic) and counter electrode film, with a transparent polymeric H^+ or Li^+ ionic-conductor. In 1982 Randin [43] described the use of a poly(AMPS) H^+ ionic-conductor as a laminate for making WO_3-based EC devices. Later (1989), Granqvist *et. al.,* [44] successfully laminated sputtered WO_3 and V_2O_5 electrodes using a gel-type polymethyl-metacrylate (PMMA) Li^+ ionic-conductor.

An attempt to make a true "all sol-gel" EC device was reported by Judeinstein and Livage in 1988 [45], who succeeded to laminate a device consisting of a SnO_2 counter electrode and a sol-gel derived WO_3 with a TiO_2-gel ionic-conductor. Unfortunately, the SnO_2 counter electrode exhibited irreversible coloration. Özer *et. al.,* [46] used a sol-gel

made ITO counter-electrode and electro-chromically active TiO_2 but used a Li^+ doped polymeric electrolyte to laminate the device. The colouring/bleaching changes are good ($\Delta T \sim 80 - 40$ %) but the response time (50 s), is longer than that of a WO_3 EC devices made using the sol-gel route. It was Macêdo and Aegerter [47] who made the first "all sol-gel" EC device with a $WO_3 | TiO_2$ gel $| CeO_2/TiO_2$ configuration. The optical transmission changes of the device during the first cycle was 60 % < T < 20 % and the response time was in the order of a few seconds. This is comparable to EC devices obtained by other techniques, although, the delamination of the device was observed during extended cycling .
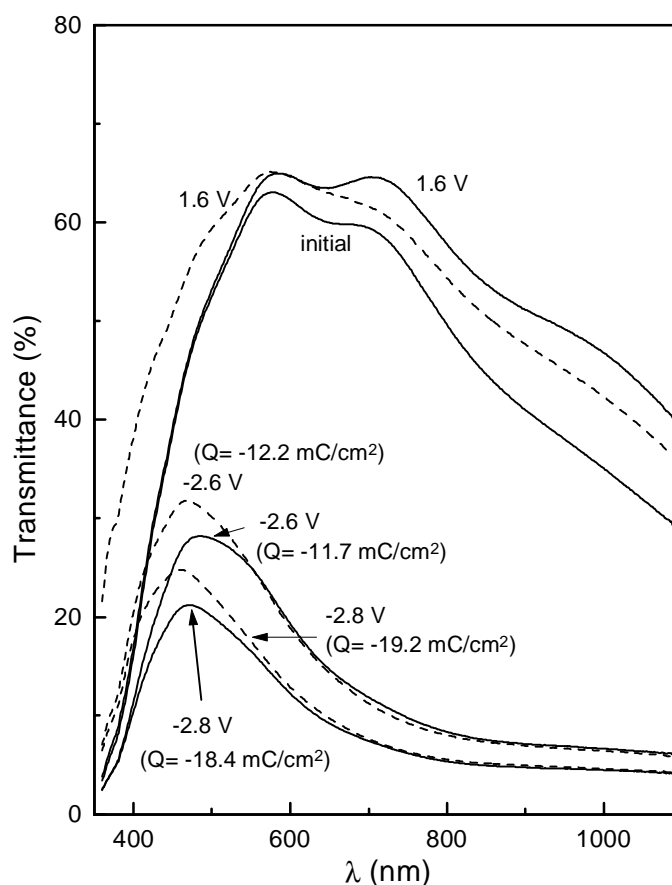
Fig. 5   Transmittance spectra of $WO_3 |$ ormolyte $|$ Nb/Fe - oxide EC device after (———) 10th and (··········) 2000th cycle [35].

Further discussion of the "all sol-gel" EC devices will be limited to their optical properties, since they demonstrate the advances made in developing the counter electrode films: CeVO$_4$ [27], SnO$_2$/Mo/Sb [33], V/Ti-oxide [34] and Nb/Fe-oxide [35], used in EC devices.

The **WO$_3$│ormolyte│Nb/Fe-oxide device** [35] (Fig. 5) when charged at 1.6 V exhibits a maximum transmittance of approximately of 60 %, but at -2.6 V the transmittance drops to 25 %. Lower transmittance values, below 20 %, can be easily obtained by applying higher negative potentials i.e. -2.8 V, but this results in a reduction in the cycling stability. The reason of lower cycling stability is the small ion-storage capacity (18 - 20 mC/cm^2) of the Nb/Fe-oxide counter electrode, which when reversing the potential is not able to store all the charge coming across the electrolyte from the WO$_3$ film. The deterioration of the electrolyte results from the accumulation of charge at the Nb/Fe-oxide/counter-electrode interface. Another problem is the low transmittance of device below 500 nm, caused by the low transmittance of the Nb/Fe-oxide counter electrode in charged state.

The **WO$_3$│ormolyte│SnO$_2$/Mo/Sb device** [5] (Fig. 6) is a better option than using a similar device containing a Nb/Fe-oxide counter electrode, since the SnO$_2$/Mo/Sb counter-electrode has a higher spectral transmittance in the visible region. This is particularly noticeable for the transmittance which the device exhibits in bleached state below 500 nm. Here the counter electrode transmits more radiation than Nb/Fe-oxide films. Conversely, the higher transmittance and better optical passiveness of the SnO$_2$/Sb/Mo counter electrode means that the EC device does not colour to such a low transmittance value. This is obvious in the near UV. Similar to the previous EC device, the transmittance in the coloured state can be enhanced by applying higher cathodic potentials to the WO$_3$ film. However, this also leads to an increase in the instability of the device. This demonstrates the importance of having a sufficiently high ion-storage capacity of the counter electrode.
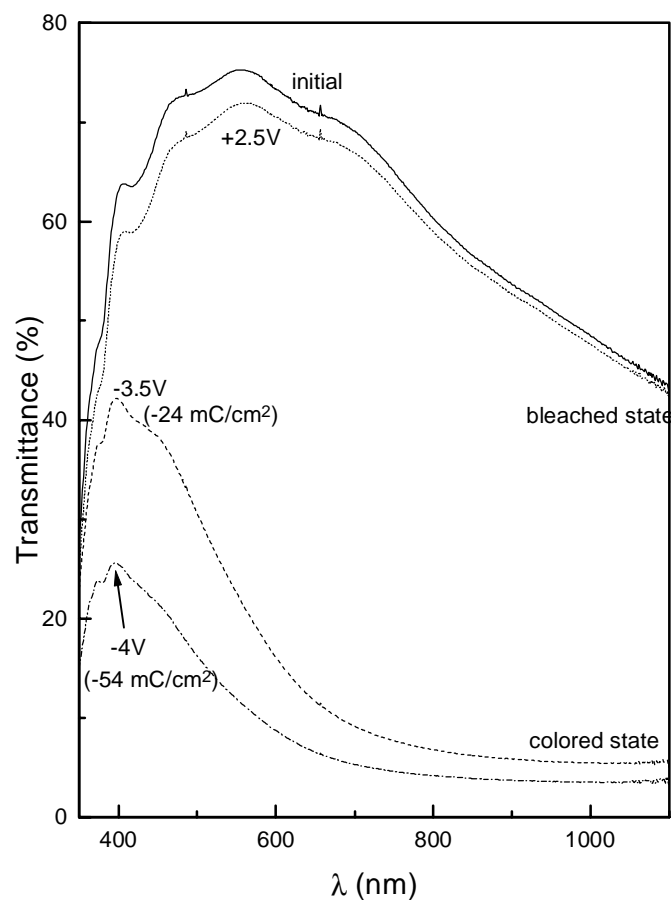
Fig. 6 Transmittance spectra of $WO_3 |$ ormolyte $| SnO_2$ /Sb/Mo EC device. Spectra of initial (——), coloured (– –), bleached (····) and irreversibly coloured (– ··) states are shown.

WO₃ | ormolyte | CeVO₄ (Fig. 7) [27,28] and **WO₃ | ormolyte | V/Ti-oxide** devices (Fig. 8) [34] represent the state-of-art regarding cycling stability and optical properties. The latter device, which is being manufactured by Pilkington plc, uses V/Ti-oxide films deposited using the sputtering technique. The switching characteristics of the complete "all sol-gel" EC device, assembled with sol-gel derived V/Ti-oxide [34] and CeVO₄ [27,28] counter-electrodes, are represented in Figs. 7 and 8. It is apparent that the transmittance of both types of devices in the bleach state is high, equivalent to the transmittance of the $WO_3 |$ ormolyte $| SnO_2$/Mo/Sb device. However, there is a distinctive, albeit relatively weak absorption of V/Ti-oxide films below 550 nm, which

has the detrimental effect of changing the colour of the film from yellow to a greenish-brown when charged. The optically passive response of the $CeVO_4$ counter-electrode film (Fig. 3) means that the final EC device (Fig. 7) remains transparent in the bleached state while the colour of the device in low transmitting states retains characteristic blue colouration of WO_3.
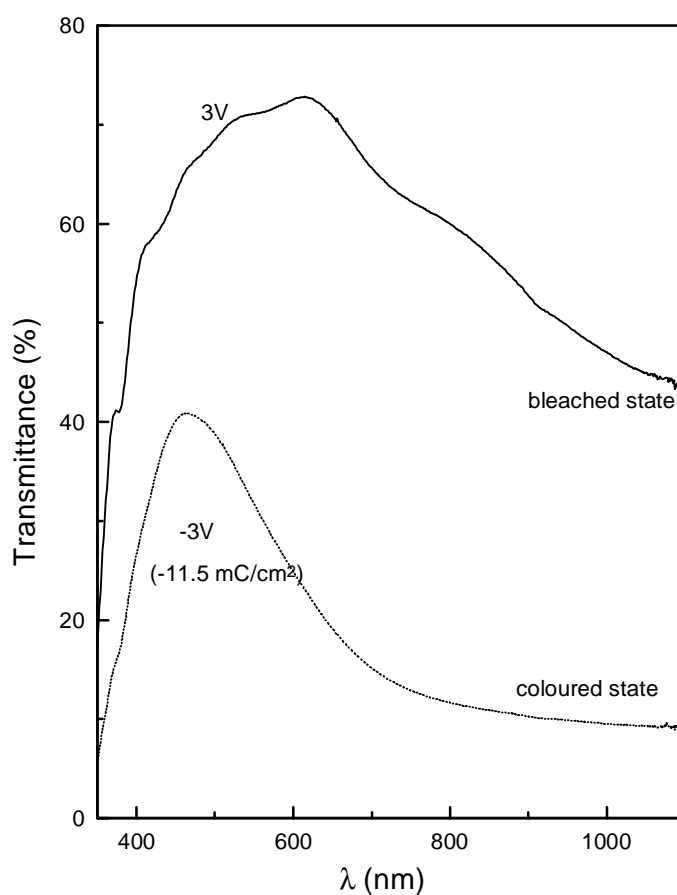
Fig. 7 Transmittance spectra of $WO_3 |$ ormolyte $| CeVO_4$ EC device in bleached and coloured states are shown. Charging was performed for 110 s at -3.0 V and discharging at 3.0 V vs. counter electrode.
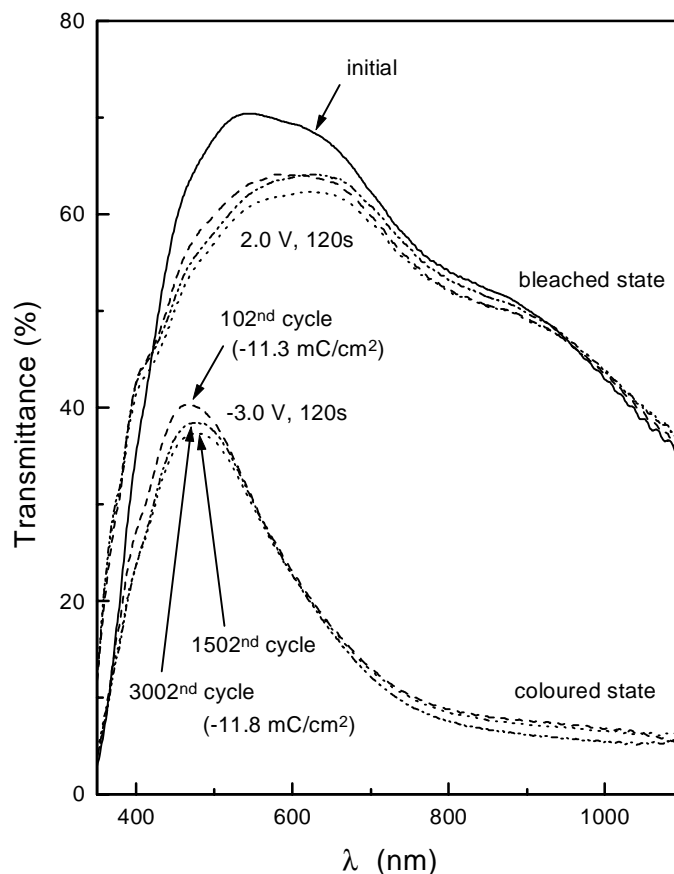
Fig. 8 Transmittance spectra of WO_3｜ormolyte｜V/Ti-oxide EC device. Charging was performed for 120 s at -3.0 V and discharging at 2.0 V vs. counter electrode.

CONCLUDING REMARKS

Electrochromic switchable windows are now commercially available but efforts to improve existing materials and to development of new electochromic devices with improved properties are in progress. WO_3 will continue to be the main active colouring film in the next generation of devices. Alternatives do exist and the Nb_2O_5 films prepared in our laboratory [7] exhibit a more neutral dark coloration, while hydrated Ni-oxide [15] and Co-oxide films [17] are viable options for EC devices using proton electrolytes.

Anodic LiCoO$_2$ or LiNiO$_2$ films can be used as counter electrodes in combination with lithium based electrolytes. These films colour simultaneously with the active WO$_3$ film and a transmittance below 10 % is obtainable.

New sol-gel ion-conductors for EC device application need to be developed because they can be applied using dip-coating deposition This will mean that less demanding technologies for assembling EC devices, for example vacuum pressing can be applied.

The EC device is not the only option for making switchable windows. Thermotropic windows have already being marketed in car sun-roof applications, but because they cause blurring of the light in the low transmitting state they remain limited to specific building applications. Switchable windows can also be made utilising a process known as gasochromism [40,48]. This involves controlling the optical modulation of a catalytically active tungsten oxide film coated on the inside of a double glazed window. The film is then coloured by exposure to diluted hydrogen and bleached using "cleaned" air. The advantage of a gasochromic switchable window is in its simplicity, requiring only a single layer of WO$_3$.

New building regulations demand ever higher standards of efficient energy usage and management, in which switchable windows will play an increasingly important role. The search for novel materials for use in new and better switchable devices remains a fertile ground for research for the foreseeable future.

REFERENCES

[1]   EC-Joule project *Solar Facades* PL 971140.
[2]   V. Wittwer, A. Gombert, W. Graf, M. Köhl; *Proceedings SPIE,* **1995**, *2531*, 2.
[3]   EC Joule project *High Performance Variable solar Control Glazing* PL 950588.
[4]   C. J. Brinker, G. W. Scherer, *Sol-Gel Science*; Academic Press Inc., Boston 1990.
[5]   B. Orel, U. Opara Kra{ovec, U. Lavren~i~ [tangar, P. Judeinstein,

J. Sol-Gel Science and Technology **1998**, *11*, 87.

[6] B. Orel, U. Opara Kra{ovec, M. Ma~ek, F. [vegl, U. Lavren~i~ [tangar, *Sol. Energy Mater. & Sol. Cells* (accepted).

[7] M. Ma~ek, B. Orel, U. Opara Kra{ovec, *J. Electrochem. Soc.* **1997**, *144*, 3002.

[8] M. Ma~ek, B. Orel, *Sol. Energy Mater. & Sol. Cells* (accepted).

[9] B. Orel, M. Ma~ek, J. Grdadolnik, A. Meden, *J. Solid State Electrochem.* **1998**, *4*, 221.

[10] U. Lavren~i~ [tangar, B. Orel, M. G. Hutchins, K. Kalcher, *J. Non-Cryst. Solids* **1994**, *175*, 251.

[11] U. Lavren~i~ [tangar, B. Orel, A. Régis, Ph. Colomban, *J. Sol-Gel Science and Technology* **1997**, *8*, 965.

[12] A. [urca, B. Orel, B. Pihlar, P. Bukovec, *J. Electroanal. Chem.* **1996**, *408*, 83.

[13] A. [urca, B. Orel, B. Pihlar, *J. Sol-Gel Science and Technology* **1997**, *8*, 743.

[14] A. [urca, B. Orel, B. Cerc-Koro{ec, P. Bukovec, B. Pihlar, *J. Electroanal. Chem.* **1997**, *433*, 57.

[15] A. [urca, B. Orel and B. Pihlar, *J. Solid State Electrochem.* **1998**, *2*, 38.

[16] F. [vegl, B. Orel, *J. Sol-Gel Science and Technology* (accepted).

[17] F. [vegl, B. Orel, M. G. Hutchins, K. Kalcher, *J. Electrochem. Soc.* **1996**, *143*, 1520.

[18] F. [vegl, B. Orel, P. Bukovec, K. Kalcher, M. G. Hutchins, *J. Electroanal. Chem.* **1996**, *418*, 53.

[19] F. [vegl, B. Orel, M. G. Hutchins, *J. Sol-Gel Science and Technology* **1997**, *8*, 765.

[20] B. Orel, M. Ma~ek, F. [vegl, K. Kalcher, *Thin Solid Films* **1994**, *246*, 131.

[21] U. Lavren~i~ [tangar, B. Orel, I. Grabec, B. Ogorevc, K. Kalcher, *Sol. Energy Mater. & Sol. Cells* **1993**, *31*, 171.

[22] U. Lavren~i~ [tangar, B. Orel, I. Grabec, B. Ogorevc, *Acta Chim. Slov.* **1994**, *41*, 39.

[23] Z. Crnjak Orel, B. Orel, *Phys. Stat. Sol. B* **1994**, *186*, K33.

[24] Z. Crnjak Orel, B. Orel, *J. Mater. Sci.* **1995**, *30*, 2284.

[25] Z. Crnjak Orel, B. Orel, *Sol. Energy Mater. & Sol. Cells* **1996**, *40*, 205.

[26] U. Lavren~i~ [tangar, U. Opara, B. Orel, *J. Sol-Gel Science and Technology* **1997**, *8*, 751.

[27] U. Opara Kra{ovec, B. Orel, R. Reisfeld, *Electrochem. Solid State Lett.* **1998**, *2*, 1.

[28] U. Opara Kra{ovec, B. Orel, A. [urca, N. Bukovec, R. Reisfeld, *Solid State Ionics* (accepted).

[29] G. Picardi, F. Varsano, F. Decker, U. Opara Kra{ovec, A. [urca, B. Orel, *Electrochim. Acta* (submitted).

[30] B. Orel, U. Lavren~i~ [tangar, Z. Crnjak Orel, P. Bukovec, M. Kosec, *J. Non-Cryst. Solids* **1994**, *67*, 272.

[31] B. Orel, U. Lavren~i~ [tangar, K. Kalcher, *J. Electrochem. Soc.* **1994**, *141*, L127.

[32] B. Orel, U. Lavren~i~ [tangar, U. Opara, M. Gaber{~ek, K. Kalcher,

J. Mater. Chem. **1995**, *5*, 617.

[33] U. Opara Kra{ovec, B. Orel, S. Ho~evar, I. Mu{evi~, *J. Electrochem. Soc.* **1997**, *144*, 3398.

[34] A. [urca, B. Orel, B. Pihlar, *Electrochim. Acta* (accepted).

[35] B. Orel, M. Ma~ek, U. Lavren~i~ [tangar, *J. Electrochem. Soc.* **1998**, *145*, 1607.

[36] M. Ma~ek, B. Orel, *J. Sol-Gel Science and Technology* **1997**, *8*, 771.

[37] A. [urca, B. Orel, G. Dra`i~, B. Pihlar, *J. Electrochem. Soc.* (accepted).

[38] A. [urca, B. Orel, *Electrochim. Acta* (submitted).

[39] M. Zayat, R. Reisfeld, H. Minti, B. Orel, F. [vegl, *J. Sol-Gel Science and Technology* **1998**, 11, 161.

[40] B. Orel, N. Gro{elj, U. Opara Kra{ovec, M. Gaber{~ek, P. Bukovec, R. Reisfeld, *Sensors and Actuators B, Chemical* **1998**, *50*, 234.

[41] B. Orel, U. Opara Kra{ovec, N. Gro{elj, M. Kosec, G. Dra`i~, R. Reisfeld, *J. Sol-Gel Science and Technology* (accepted).

[42] N. Gro{elj, M. Gaber{~ek, U. Opara Kra{ovec, B. Orel, G. Dra`i~, *Solid State Ionics* (submitted).

[43] J. P. Randin, *J. Electrochem. Soc.* **1982**, *129*, 1215.

[44] A. M. Anderson, C. G. Granqvist, J. R. Stevens, *Appl. Opt.* **1989**, *28*, 3295.

[45] P. Judeinstein, J. Livage, A. Zarudiansky, P. Rose, *Solid State Ionics*, **1988**, *28-30*, 1722.

[46] N. Özer, F. Tepehan, N. Bozkurt, *Thin Solid Films* **1992**, *219*, 193.

[47] M.A. Macêdo, M. Aegerter, *J. Sol-Gel Science and Technology* **1994**, *2*, 667.

[48] A. Georg, W. Graf, D. Schweiger, V. Wittwer, P. Nitz, H. R. Wilson, *Solar Energy* **1998**, *62*, 215.

ACKNOWLEDGMENT

Povzetek

Zahteve po energijskem varčevanju postavljajo vse višje standarde zasteklitve. V modernih stavbah moramo zmanjšati toplotne izgube oz. preprečiti pregrevanje preko oken, hkrati pa moramo zagotoviti primerno osvetlitev prostorov. Inteligentna okna predstavljajo nove rešitve, ki zadoščajo zgornjim zahtevam in so sposobna prilagajati svoje optične lastnosti (transmisijo in refleksijo) trenutnemu sončnemu sevanju. Do sedaj so bili odkriti štirje načini, ki omogočajo optično modulacijo: fotokromizem, termokromizem, termotropizem in elektrokromizem. V članku opisujemo napredek, ki smo ga naredili v načem laboratoriju na področju elektrokromnih oken, pripravljenih po sol-gel postopkih in s tehniko potapljanja. Zaključujemo s predlogi, ki naj bi v bodočnosti izboljšali učinkovitost inteligentnih oken.

SOLUTION POLYMERIZATION OF METHYL METHACRYLATE IN THE PRESENCE OF THE QUATERNARY AMMONIUM CHLORIDE

Ines Vodopivec Podgornik and Anton Perdih

Faculty of Chemistry and Chemical Technology, University of Ljubljana, 1000 Ljubljana, Slovenia

Abstract

In the solution polymerization of an inhibitor containing methyl methacrylate in toluene initiated by dibenzoyl peroxide, the addition of a quaternary ammonium chloride reduces the lag time and decreases the polymerization rate. The complex mixture formed from the inhibitor in this reaction system seems responsible for these effects.

INTRODUCTION

The use of quaternary ammonium compounds in the preparation of polymers from vinyl monomers is not as common as in other fields of polymer science. Baxendale et al. [1] noted the enhancement of the polymerization rate on addition of $RNMe_3$ Br in the aqueous solution polymerization. Lebedev et al. [2] recognised quaternary ammonium compounds as active agents in emulsion polymerization. Rasmussen and Smith [3,4]

utilised the ability of quaternary ammonium compounds to phase transfer the persulfate anion to initiate the polymerization. Freedman [5] reviewed the progress in this area. Ghosh and Maity [6-8] studied the influence of some quaternary ammonium bromides and chlorides in the solution polymerization of methyl methacrylate. They found that the initiation was inhibited by hydroquinone indicating a radical mechanism, as well as that some basic aprotic solvents enhance the polymerization rate whereas some protic ones diminish it. They also proposed two mechanisms of action of quaternary ammonium compounds. Jagodic and Perdih [9] demonstrated that different anions in quaternary ammonium compounds have different influences on the reaction constant and the lag time of bulk polymerization of methyl methacrylate. In the same system, Perdih [10] tested a larger number of counteranions and found that in several cases the interchange of anions between quaternary ammonium compounds and dibenzoyl peroxide prevailed by far as the first step of reaction. In view of these results the influence of a quaternary ammonium chloride in the solution polymerization of methyl methacrylate seemed to be worth reexamining.

EXPERIMENTAL

Chemicals

Methyl methacrylate (**MMA**) stabilized with 10 mg/kg Topanol A (2-*tert.*-butyl-4,6-dimethylphenol) (**Inh**) was obtained from Akripol, Trebnje. Dibenzoyl peroxide (**DBPO**) and alkyl benzyl dimethylammonium chloride (**QCl**) were obtained from Merck, Darmstadt, whereas toluene and methanol from Kemika, Zagreb.

Polymerization

Polymerizations were performed in a 1 L glass reactor equipped with a mixing system and thermostated to 79.5 ± 0.5°C. The monomer solution contained MMA and toluene, 100 g each. After attaining constant temperature, QCl was dissolved in the mixture. After its dissolution, 0.7 g of DBPO was added. In predetermined intervals, 2 mL of

solution was removed, mixed with 100 mL of methanol and after staying overnight at room temperature the precipitate was filtered off, washed with methanol, dried and weighed. Each experiment was performed at least three times.

Analyses

The lag time was estimated by extrapolation of the linear part in the conversion plot to zero conversion, and the polymerization rate from its slope.

Mean molecular weights (M_w) were determined by size exclusion chromatography on a Waters/Varian chromatograph equipped with μ-Styragel 10^3, 10^4 columns, with tetrahydrofuran as solvent and relative to polystyrene standards.

Thin layer chromatography was performed on silica sheets (Merck No. 5554) with benzene as the mobile phase and UV detection.

RESULTS AND DISCUSSION

In previous work [9,10] the bulk polymerization of MMA was followed by dilatometry. In order not to take into account the low MW compounds observed earlier [10], the methanol insoluble polymer was determined by gravimetry.

From the conversion vs. time curves were deduced the data presented in Table 1. These data demonstrate that the inhibition period (lag time) as well as the rate of polymerization decrease with increasing the amount of QCl in the reaction mixture. The polymerization rate constant and Mw of the formed polymer tend to level off at a molar ratio of inhibitor : QCl of over **1 : 5**. The lag time decreases with increasing addition of QCl and levels off at a molar ratio of inhibitor : QCl of about **1 : 10**. This is somewhat similar to the situation in bulk MMA [10] where the lag time levelled off at an approx. eightfold excess of QCl. According to [10], QCl reacts with DBPO to form chlorine and/or peroxybenzoyl chloride, whereas MMA, anisole, or phenol get chlorinated if

present. The QCl exponent observed in the present work is -0.16. For bromide salt, it was positive at low QBr concentrations and negative at higher ones [6].

Table 1. Lag time (t_l), polymerization rate constant (k), and mean molecular weight (M_w) of the formed polymethylmethacrylate at various QCl concentrations. [MMA] = 4.52 mol L^{-1}, [DBPO] = 0.013 mol L^{-1}, [Inh] = 2.5*10^{-5} mol L^{-1}

QCl*10^4 (mol L^{-1})	Inh : QCl	t_l (min)	k*10^4 (L$^{1/2}$ mol$^{-1/2}$ s^{-1})	M_w (kg mol^{-1})
0	1 : 0.00	58	5.32	50
0.25	1 : 0.98	53	4.76	
1.24	1 : 4.88	46	3.57	110
2.48	1 : 9.76	35	3.25	
4.52	1 : 17.8	34	3.02	120

In the present work DBPO is in a 26 to 500 fold molar excess over QCl. The decrease in the concentration of DBPO caused by its reaction with QCl is thus less than 4% of its initial value. This small decrease in DBPO concentration can not account for almost halving the lag time and the polymerization rate. Thus the decrease and levelling off of the lag time and the polymerization rate can not be ascribed to the decrease of initial DBPO content but to another effect. The chlorination of the inhibitor seems at first sight the most probable candidate since phenol has been chlorinated during previous tests [10]. The decrease of the inhibition period together with the rate of polymerization indicate that on reaction of the inhibitor with DBPO and QCl, its inhibiting activity decreases to a final value and at the same time it is converted into a retarder. In bulk MMA, on increasing addition of QCl, at the usual inhibitor concentration, a decreasing inhibition was observed and no retardation [10]; increasing retardation was observed if the inhibitor concentration was increased up to ten times above the usual. Both the decreasing inhibition and increasing retardation have been observed in the toluene - MMA solution at the usual concentration of the inhibitor.

To test the hypothesis that the chlorinated inhibitor is responsible for the observed effects, the inhibitor, DBPO, and QCl in a molar ratio of 1: 2 : 5 were reacted in toluene at room temperature as well as at 80°C. After removing the polar matters including benzoic acid and the Q-benzoate, thin layer chromatography of the products revealed a mixture of at least 12 UV-absorbing compounds. This is in sharp contrast to the composition of the inhibitor containing one major and one trace compound as well as to the results of reaction of phenol [10] where only 2-chlorophenol and a dichlorophenol were detected. On the other hand, the number of formed compounds is nearly twice that presented by Chirinos-Padrón and Allen [11] for oxidation products of simple phenolic antioxidants with peroxides. The formed mixture had the same influence on the polymerization of noninhibited MMA in solution as if the solution contained the inhibitor and QCl. Simple chlorinated phenols tested for comparison expressed a much weaker inhibiting and retarding action than the mentioned reaction mixture. From the existing evidence can be concluded that the reaction of a phenolic inhibitor with DBPO is faster in the presence of QCl giving rise to a more complex product mixture responsible for the reduction of lag time and retardation of polymerization.

REFERENCES

[1] J.H. Baxendale, M. G. Evans, J. K Kilham, *Trans, Faraday Soc.* **1946**, *42*, 668-675.
[2] Yu. V. Lebedev, S. N. Trubitsyna, M. A. Askarov, M. F. Margaritova, *Vysokomol. Soed., Ser. B.* **1973**, *15*, 612-618.
[3] J.K. Rasmussen, H.K. Smith, *Makromol. Chem.* **1981**, *182*, 701-703.
[4] J.K. Rasmussen, H.K. Smith, *Polym. Sci. Technol.* **1984**, *24*, 105-119.
[5] H.H. Friedman, *Pure Appl. Chem.* **1986**, *58*, 857-868.
[6] P. Ghosh, S. N. Maity, *Eur. Polymer J.* **1978**, *14*, 855-859.
[7] P. Ghosh, S. N. Maity, *Eur. Polymer J.* **1979**, *15*, 787-795.
[8] P. Ghosh, S. N. Maity, *Eur. Polymer J.* **1980**, *16*, 1115-1119.
[9] F. Jagodic, A. Perdih, *IUPAC Macro'83, Section I, Polymer Chemistry, Abstracts,* Bucharest, **1983**, pp. 341-344.

[10]   A. Perdih, *Polymer Bull.* **1989**, *21*, 151-158.
[11]   A. J. Chirinos-Padrón, N. S. Allen, in: S. Halim Hamid, M. B. Amin, A. G. Maadhah, eds. *Handbook of Polymer Degradation*; M. Dekker, New York, **1992**, p. 268.

POVZETEK

Pri raztopinski polimerizaciji inhibitor vsebujočega metilmetakrilata v toluenu, sproženi z dibenzoil peroksidom, dodatek kvarternega amonijevega klorida skrajša začetni čas in zmanjša hitrost polimerizacije. Za ta pojav je vzrok zmes spojin, ki nastanejo iz inhibitorja v tem reakcijskem sistemu.

Volume Changes of Ionization of Ethylenemalonic acid

Janez Cerar and Jože Škerjanc

Faculty of Chemistry and Chemical Technology, University of Ljubljana,1000 Ljubljana, Slovenia

Abstract

Densities of aqueous solutions of 1,1-cyclopropanedicarboxylic acid (ethylenemalonic acid) have been determined at 25 $^{\circ}$C for various degrees of neutralization of the acid. From the densimetric titration curve the apparent molar volume of undissociated acid, as well as the volume changes for ionization of the first and the second carboxylic group, ΔV_1 and ΔV_2, respectively, have been calculated. The resulting values at infinite dilutions, $\Delta V_1^{\infty} = -7.0$ ml/mol COOH$_{(1)}$ and $\Delta V_2^{\infty} = -28.9$ ml/mol COOH$_{(2)}$ are comparable to those found for other weak diprotic acids.

INTRODUCTION

During our recent physicochemical studies with aqueous solutions of fullerenehexamalonic acid it became evident that parallel studies with solutions of ethylenemalonic acid (EMA; 1,1-cyclopropanedicarboxylic acid) could be helpful in interpreting the experimental results. Therefore, some measurements with water solutions of this diprotic organic acid have been undertaken. In this contribution we present densimetric studies. On the basis of these experiments the apparent molar volume of unionized EMA, $>\langle_{COOH}^{COOH}$, have been calculated, as well as the volume change for ionization of the first and of the second carboxylic groups.

EXPERIMENTAL SECTION

Materials. Ethylenemalonic acid (EMA, 1,1-cyclopropanedicarboxylic acid, $\geq 98\%$) was supplied by Fluka. In all experiments three times quartz distilled water was used.

The concentration of the stock solution of EMA was determined by potentiometric and conductometric titrations with NaOH.

Potentiometric titration curves were recorded at 25°C by Metrohm automatic titrator 736 GP Titrino using glass and calomel electrodes.

Densities of the solutions were measured with a Paar digital density meter DMA 60 with external measuring cell DMA 602. An ultrathermostat attached to the instrument controlled the temperature at 25.00 ± 0.002°C. The accuracy of density measurements was within $\pm 4.5 \cdot 10^{-6}$ g cm^{-3}.

RESULTS AND DISCUSION

The densimetric titration curve of aqueous solutions of ethylenemalonic acid is presented in Figure 1. As expected, the slope of the curve changes at the degree of neutralization $\alpha_n = 0.5$. From these values the apparent molar volume, ϕ_V, has been calculated from

$$\phi_V = \frac{1}{\rho_o}\left(\overline{M} - \frac{\rho - \rho_o}{c}\right) \tag{1}$$

where ρ and ρ_o are densities of a solution and water, respectively, and $\overline{M}$ is the molar mass of partially neutralized EMA. From eq 1 calculated values of ϕ_V are plotted as function of the degree of neutralization, α_n, in Figure 2. The value $\alpha_n = 1$ corresponds to complete neutralization of both carboxylic groups. Since the measurement were performed with solutions in which the solute concentration was small, the distinction between the degree of ionization, α, and neutralization, α_n

$$\alpha = \alpha_n + \left(\left[H^+\right] - \left[OH^-\right]\right)/c \tag{2}$$
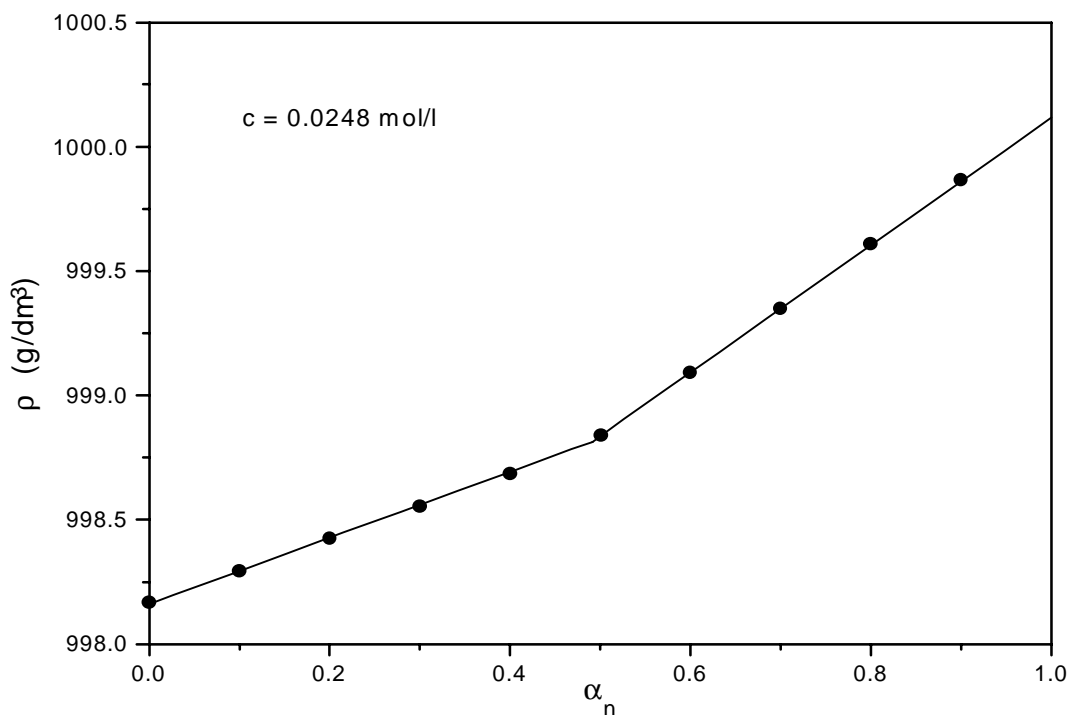
Figure 1. Densimetric titration of aqueous solutions of ethylenemalonic acid at 25 ^{o}C and at concentration $c = 0.0248$ mol/L.

needed to be taken into account. In eq 2, which follows from the electroneutrality condition, the concentration of H$^+$ ions, [H$^+$], was calculated from the measured pH by taking into account the activity coefficient of H$^+$ ion calculated from the Debye-Hückel limiting law. In most cases the concentration of OH$^-$ ions, [OH$^-$], can be neglected. Obviously, the degree of ionization of the first carboxylic group, α_1, is $\alpha_1 = 2\alpha$ for $0 \leq \alpha_n \leq 0.5$, and of the second group, α_2, is $\alpha_2 = 2\alpha - 1$ for $0.5 \leq \alpha_n \leq 1$. Figure 2 shows that the apparent molar volume first decreases with the increasing degree of neutralization until $\alpha_n = 0.5$, and after that a sharper decrease of the curve is observed. The added NaOH first reacts with the strong COOH$_{(1)}$ groups producing a break in the curve at the first equivalent point, followed by much steeper decrease of the curve when the weaker COOH$_{(2)}$ group starts to ionize.

From the experimental values for the acid and its monosodium and disodium salts we can
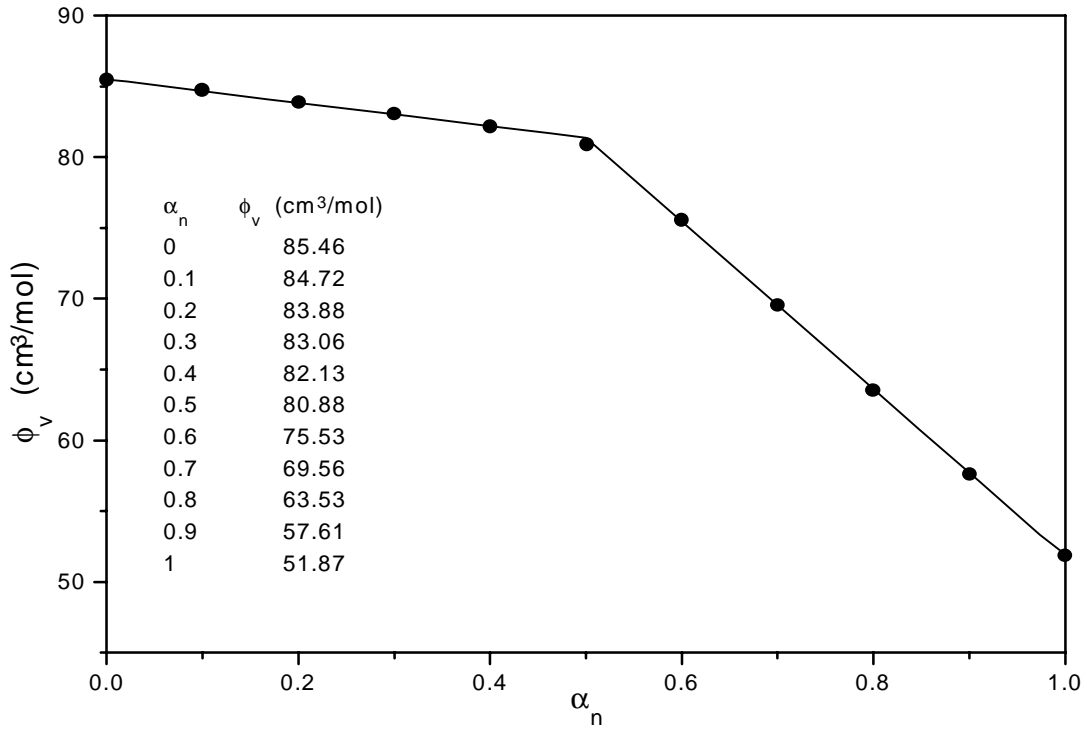
Figure 2. Apparent molar volume of partly neutralized EMA in water at 25 $^{\circ}$C as a function of the degree of neutralization. Concentration $c = 0.0248$ mol/L.

estimate the apparent molal volume, ϕ_u, of undissociated acid, as well as the volume changes for ionization of the first and the second carboxylic groups, ΔV_1 and ΔV_2, respectively. The conductivity measurements have disclosed [1] that the ionization reaction

$$>\!\!\langle {COOH \atop COOH} \rightarrow >\!\!\langle {COO^- \atop COOH} + H^+ \tag{3}$$

proceeds far at experimental concentrations. Therefore, the molecules and ions must contribute to the measured apparent molar volume, ϕ_V. It is well known that the additivity principle [2]

$$c\phi_V = \sum c_i \phi_i \tag{4}$$

may be expected to be fulfilled very closely at high dilutions, and to be a reasonable approximation at moderate concentrations. By applying eq 4 to the process 3 we obtain

$$c\phi_V = c(1 - \alpha_1)\phi_u + c\alpha_1\phi_{d1} + c\alpha_1\phi_{H+} \tag{5}$$

where ϕ_{d1} stands for the apparent molar volume of the $>\langle^{COO^-}_{COOH}$ constituent. Upon rearranging eq 5 we get

$$\phi_u = \frac{\phi_V}{1 - \alpha_1} - \frac{\alpha_1}{1 - \alpha_1}(\phi_{H^+} + \phi_{d1}) \tag{6}$$

The value of ϕ_{d1} was obtained from the extrapolated value of ϕ_V at $\alpha_1 = 1$ ($\alpha_n = 0.5$), which is ϕ_V of the $>\langle^{COONa}_{COOH}$ species, taking into account the value of the apparent molar volume [3] of Na^+ ion at the experimental concentration. The degree of ionization, α_1, of the first carboxylic group at $\alpha_n = 0.5$ has been calculated from eq 2. From eq 6 calculated value of ϕ_u is $\phi_u = 89.7$ ml /mol EMA.

We can calculate also the volume change of ionization for the process 3, ΔV_1, from

$$\Delta V_1 = \phi_{H^+} + \phi_{d1} - \phi_u \tag{7}$$

The resulting value is -6.7 ml/mol EMA, which is the ionization volume for the first carboxylic group. Similarly, we can obtain the ionization volume, ΔV_2, for the second ionization step

$$>\langle^{COO^-}_{COOH} \rightarrow >\langle^{COO^-}_{COO^-} + H^+ \tag{8}$$

$$\Delta V_2 = \phi_{H^+} + \phi_{d2} - \phi_{d1} \tag{9}$$

The apparent molar volume of the $>\langle^{COO^-}_{COO^-}$ species, $\phi_{d2} = 54.7$ ml/mol EMA, has been obtained from the experimental value of ϕ_V at $\alpha_n = 1$ ($\alpha_2 = 1$), taking into account $\phi_{V(Na+)}$

at the experimental concentration, which has been calculated from its conventional value at infinite dilution, $\phi_{Na^+}^\infty$, and the limiting expression of Debye and Hückel [4]

$$\phi_i = \phi_i^\infty + 0.660\, z_i^2 \left(\sum v_i z_i^2 \right)^{1/2} \sqrt{c} \tag{10}$$

The resulting value is $\Delta V_2 = -27.9$ ml/mol $COOH_{(2)}$. We see that both ionization volumes are negative, a situation that is normal because of the electrostriction of water produced by the ions resulting in a ionization process.

For solutions in which EMA is partly neutralized with NaOH combination of eqs 3-7 gives

$$\phi_V = \phi_u + \alpha_1 \Delta V_1 + 2\alpha_n (\phi_{Na^+} - \phi_{H^+}) \tag{11}$$

for the range $0 \le \alpha_n \le 0.5$. From this expression we can obtain the intermediate volumes of ionization between the individual experimental points

$$\Delta V_1 = \frac{\Delta \phi_V}{\Delta \alpha_1} - 2(\phi_{Na^+} - \phi_{H^+})\frac{\Delta \alpha_n}{\Delta \alpha_1} \tag{12}$$

Similarly, for the range $0.5 \le \alpha_n \le 1$ we get

$$\phi_V = (\phi_{Na^+} + \phi_{d1}) + \alpha_2 \Delta V_2 + 2\alpha_n (\phi_{Na^+} - \phi_{H^+}) \tag{13}$$

and

$$\Delta V_2 = \frac{\Delta \phi_V}{\Delta \alpha_2} - 2(\phi_{Na^+} - \phi_{H^+})\frac{\Delta \alpha_n}{\Delta \alpha_2} \tag{14}$$

It has to be mentioned that for the range $0.5 \le \alpha_n \le 1$ the quotient $2\Delta\alpha_n/\Delta\alpha_2 \approx 1$. From eqs 12 and 14 calculated values of the intermediate volumes of ionization are presented in Figure 3. The sharp decrease of the curve at $\alpha_n = 0.5$ can be ascribed to the releasing of the proton from both carboxylate groups to which it is bound by the intramolecular
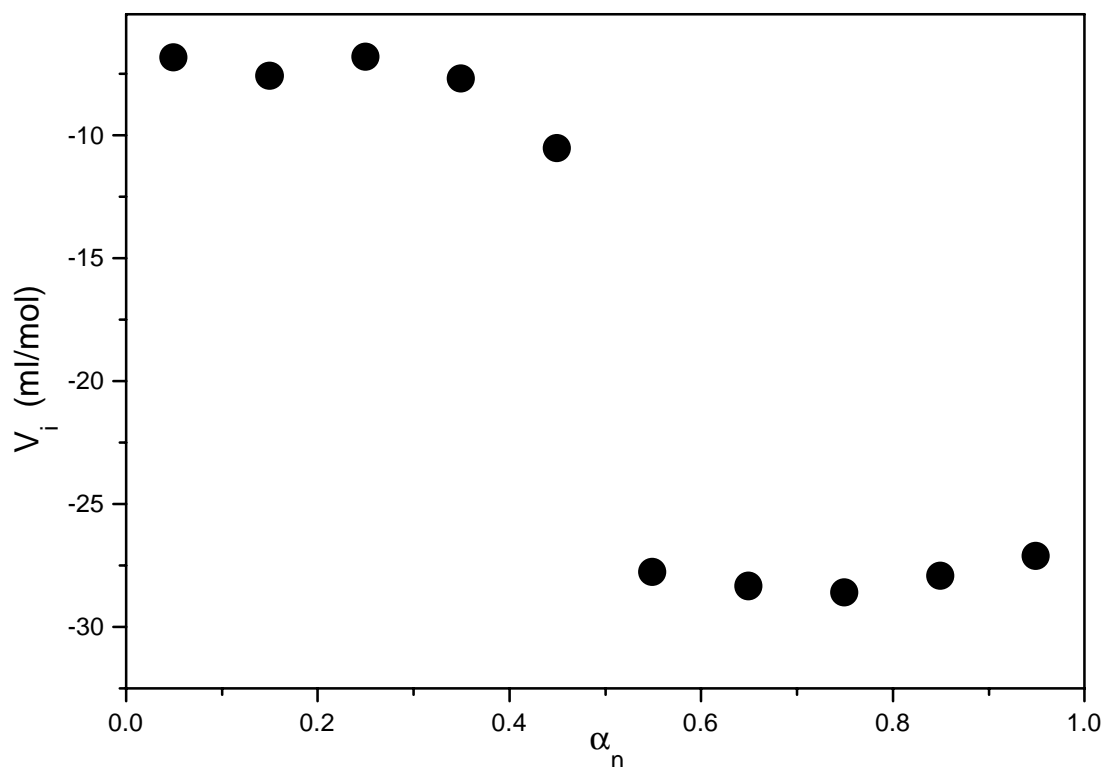
Figure3. Volume change on ionization of partly neutralized EMA at 25 $^{\circ}$C as a function of the degree of neutralization. Concentration c = 0.0248 mol/L.

hydrogen bounds above α_n = 0.5. It is interesting that a similar ΔV_i curve has been observed with the high molecular weight copolymer of maleic acid with ethylene obtained by direct dilatometry [5].

Usually the ionization volumes at infinite dilution are reported. The apparent molar volumes of the H^+, Na^+, and the ethylenemalonate anions, $>\langle^{COOH}_{COO^-}$ and $>\langle^{COO^-}_{COO^-}$, have been expressed from eq 10, and for the apparent molar volume of undissociated acid ϕ_u it was assumed that $\phi_u = \phi_u^{\infty}$. The resulting values of the ionization volumes are $\Delta V_1^{\infty} = -7.0$ ml/mol COOH$_{(1)}$ and $\Delta V_2^{\infty} = -28.9$ ml/mol COOH$_{(2)}$. These values are comparable to those found for other weak acids.

REFERENCES

[1] W. L.German, G. H. Jeffery, A. I. Vogel, *J. Chem. Soc.* **1935**, 1624-1630.
[2] H. S. Harned, B. B. Owen, *The Physical Chemistry of Electrolytic Solutions*; Reinhold, New York, pp 396-406.
[3] F. J. Millero, *Chem. Rev.* **1971**, *71*, 147-176.
[4] S. Glasstone, *Thermodynamics for Chemists;* Van Nostrand, New York, 1953, pp 436.
[5] J. Škerjanc, *J. Phys. Chem.* **1978**, *82*, 2313-2316.

POVZETEK

Vodnim raztopinam 1,1-ciklopropandikarboksilne kisline (etilenmalonske kisline) smo za različne stopnje nevtralizacije kisline pri 25 $^{\circ}$C izmerili gostote. Iz tako dobljene denzimetrične titracijske krivulje smo izračunali navidezni molski volumen neionizirane kisline in volumske spremembe za ionizacijo prve in druge karboksilne skupine ΔV_1 in ΔV_2. Dobljeni vrednosti pri neskončnem razredčenju, $\Delta V_1^{\infty} = -7.0$ ml/mol COOH$_{(1)}$ in $\Delta V_2^{\infty} = -28.9$ ml/mol COOH$_{(2)}$, sta primerljivi z rezultati, ki so jih dobili z drugimi šibkimi dvobaznimi kislinami.

SHORT-RANGE INTERACTION IN A POLYELECTROLYTE SOLUTION CONTAINING A MIXTURE OF MONO- AND DIVALENT COUNTERIONS

D. Dolar and M. Bešter Rogač

Faculty of Chemistry and Chemical Technology, University of Ljubljana,

1000-Ljubljana, Aškerčeva 5, Slovenia

ABSTRACT

The osmotic coefficient and the excess free energy have been calculated for a polyelectrolyte solution with mixtures of mono and divalent counterions. The results have been obtained by applying the cylindrical cell model in the Poisson-Boltzmann approximation. The short-range interaction between polyion and counterions, described by a square-well potential, has also been taken into account. The results of osmotic coefficient are presented as functions of the equivalent fraction of monovalent counterions for different values of ionic radii, depth of the potential well, and concentration.

INTRODUCTION

The cylindrical cell model which considers the electrostatic interactions among ions has usually been applied for the interpretation of thermodynamic properties of polyelectrolyte solutions with a fair success. Several times it appears, however, that the

discrepancy between experimental results and theoretical calculations is rather large [1,2,3] and consequently, it has stimulated some attempts [4,5,6] in order to improve the calculations by introducing the non-Coulombic, short-range interaction into the model.

In the present study we are interested in a polyelectrolyte solution containing a mixture of mono and divalent counterions. The first theoretical approach to this problem has been published long ago [7] followed by an experimental verification [8,9,10]. The same system has also been treated by applying the line charge model [11]. In both cases the electrostatic interaction has only been taken into account. In this contribution the influence of short-range interactions between polyion and counterions, represented by a square-well potential, on the osmotic coefficient and excess free energy will be presented.

THE MODEL AND THE POTENTIAL

The polyelectrolyte solution is represented as an ensemble of cylindrical **cells with radius R and length h (h $\gg$ R). In the axis of each cell is fixed a cylindrical polyion of radius a and length h $=\nu b$, where b is the lenght of the monomer unit. The charge of the polyion is $-\nu\, e_0$,** supposed to be spread uniformly over its surface. In the free volume of the cell is a mixture of mono and z-valent counterions with the total charge equal in number but opposite in sign to the charge of the polyion. By denoting the radius of monovalent counterions with r_1 and z-valent with r_2, it follows for the distances of closest approach $a_1 = a + r_1$ and $a_2 = a + r_2$. The short-range interactions of the non-Coulombic type are represented by a square-well potential V_{nc} for monovalent counterion:

$$V_{nc} = \infty, \qquad 0 \leq r < a_1$$
$$V_{nc} = -E_1, \qquad a_1 \leq r \leq b_1 \qquad\qquad (1)$$
$$V_{nc} = 0, \qquad\; b_1 < r \leq R$$

and for z-valent counterions:

$$V_{nc} = \infty, \qquad 0 \leq r < a_2$$
$$V_{nc} = -E_2, \qquad a_2 \leq r \leq b_2 \qquad\qquad (2)$$
$$V_{nc} = 0, \qquad b_2 < r \leq R$$

where r is the cylindrical coordinate and E_1 and E_2 are positive quantities. By supposing the additivity of Coulombic and non-Coulombic potential and by denoting

$$\eta_1 = e^{E_1/kT} \quad \text{and} \quad \eta_2 = e^{E_2/kT} \qquad\qquad (3)$$

the Poisson-Boltzmann equation for this system reads

$$\frac{1}{r}\frac{d}{dr}\left(r\frac{d\psi}{dr}\right) = -\frac{e_o}{\varepsilon_o\varepsilon}\left[n_1^o \exp\left(-\frac{e_o\psi}{kT}\right)\eta_1 + z\,n_z^o \exp\left(-\frac{z\,e_o\psi}{kT}\right)\eta_2\right] \qquad (4)$$

with the boundary conditions

$$\left(\frac{d\psi}{dr}\right)_a = \frac{ve_o}{2\pi\varepsilon_o\varepsilon\,a\,h}, \quad \left(\frac{d\psi}{dr}\right)_R = 0 \;. \qquad\qquad (5)$$

The values of the parameters η_1 and η_2 are given in equations (1) and (2). In equations above ø is the electrostatic potential, k the Boltzmann constant, T the absolute temperature, e_o the elementary charge, ε_o the vacuum and $\varepsilon\,\varepsilon_o$ the solvent permittivity, n_1^o and n_z^o the number density of mono and z-valent counterions at $\psi = 0$.

To simplify the notation the dimensionless quantities are introduced

$$\left.\begin{array}{l} y = -\dfrac{e_o\psi}{kT}, \quad t = \ln\dfrac{r}{a}, \quad \gamma = \ln\dfrac{R}{a} \\[2mm] t_1 = \ln\dfrac{a_1}{a}, \quad t_{11} = \ln\dfrac{b_1}{a}, \quad t_2 = \ln\dfrac{a_2}{a}, \quad t_{22} = \ln\dfrac{b_2}{a} \\[2mm] \lambda = \dfrac{ve_o^2}{4\pi\varepsilon_o\varepsilon kTh} \end{array}\right\} \qquad (6)$$

The parameter λ is proportional to the linear charge density of the polyion which is the basic property of each polyelectrolyte. Furthermore, we introduce the equivalent fractions N_1^o and N_z^o in the place where $\psi = 0$ and their average values $\overline{N}_1$ and $\overline{N}_z$

$$\left. N_1^o = \frac{n_1^o}{n_1^o + z\,n_z^o}, \quad N_z^o = \frac{z\,n_z^o}{n_1^o + z\,n_z^o}, \quad \overline{N}_1 = \frac{\overline{n}_1}{\overline{n}_1 + z\,\overline{n}_z}, \quad \overline{N}_z = \frac{z\,\overline{n}_z}{\overline{n}_1 + z\,\overline{n}_z} \atop \text{and the ratio} \quad \xi = \frac{\overline{n}_1 + z\,\overline{n}_z}{n_1^o + z\,n_z^o} \,. \right\} \quad (7)$$

The Poisson-Boltzmann equation and the boundary conditions now read

$$\frac{d^2 y}{dt^2} = \frac{4\lambda}{(e^{2\gamma}-1)\xi} e^{2t} \left[\eta_1 N_1^o e^y + \eta_2 N_z^o e^{zy} \right]$$

$$\left(\frac{dy}{dt} \right)_0 = -2\lambda, \quad \left(\frac{dy}{dt} \right)_\gamma = 0 \qquad (8)$$

The average values $\overline{N}_1$ and $\overline{N}_z$ may be obtained from

$$\overline{N}_1 = \frac{2\,N_1^o}{\xi(e^{2\gamma}-1)} \int_0^\gamma \eta_1 e^{y+2t} dt, \quad \overline{N}_z = \frac{2\,N_z^o}{\xi(e^{2\gamma}-1)} \int_0^\gamma \eta_2 e^{zy+2t} dt \qquad (9)$$

Within the integration interval, $0 \le t \le \gamma$, each of the parameters η_1 and η_2 assumes three different values as indicated in equations (1) and (2). Let us repeat this condition in the new notation

$$\eta_1 = \begin{cases} 0, & 0 \le t < t_1 \\ \eta_1, & t_1 \le t \le t_{11} \\ 1, & t_{11} < t \le \gamma \end{cases} \qquad \eta_2 = \begin{cases} 0, & 0 \le t < t_2 \\ \eta_1, & t_2 \le t \le t_{22} \\ 1, & t_{22} < t \le \gamma \end{cases} \qquad (10)$$

Because equation (8) cannot be solved analytically we applied the Runge-Kutta method of the third order for numerical computation. The values of N_1^o and N_Z^o were chosen arbitrarily and the parameter ξ was found by an appropriate iteration procedure.

THE FREE ENERGY AND THE OSMOTIC COEFFICIENT

The excess free energy A_{ex} of a polyelectrolyte has three contributions

$$A_{ex} = U_{nc} + U_c - TS_{cf} \tag{11}$$

where U_{nc} is the non-Coulombic contribution, U_c the Coulombic contribution and S_{cf} is the configurational entropy [12]. U_{nc} was calculated from

$$U_{nc} = -E_1 \int_{a_1}^{b_1} n_1^o e^y \eta_1 dV - E_2 \int_{a_2}^{b_2} n_Z^o e^{zy} \eta_2 dV \tag{12}$$

The final expression is

$$U_{nc} = -2\nu kTV_m \left\{ \eta_1 \ln \eta_1 n_1^o \int_{t_1}^{t_{11}} e^{y+2t} dt + \eta_2 \ln \eta_2 n_Z^o \int_{t_2}^{t_{22}} e^{zy+2t} dt \right\} \tag{13}$$

where $V_m = \pi a^2 b$ is the volume of the monomer unit. The Columbic contribution U_c was calculated in two different ways, according to equations (14) and (15), giving different but equivalent expressions

$$U_c = \frac{1}{2} \int_V \rho \psi \, dV + \frac{1}{2} \int_S \sigma \psi(a) \, dS \tag{14}$$

$$U_c = \frac{\varepsilon_o \varepsilon}{2} \int_V (grad\,\psi)^2 \, dV \tag{15}$$

where ρ is the local volume charge density and σ is the charge density on the surface of the polyion. The configurational entropy S_{cf} due to nonuniform distribution of counterions within the cell was calculated from

$$S_{cf} - = -k \sum_{i=1}^{z} \int \left(n_i \ln n_i - \bar{n}_i \ln \bar{n}_i \right) dV \tag{16}$$

where n_i is the local concentration of mono and z-valent counterions and $\bar{n}_i$ its average value.

From equation (14) it follows

$$U_c = \frac{1}{2} \nu\,k\,T\,y(0) - \nu\,k\,T\,V_m \left\{ \int_0^\gamma \eta_1 n_1^o e^{y+2t} y \, dt + \int_0^\gamma \eta_2 n_z^o e^{zy+2t} y \, dt \right\} \tag{17}$$

and from equation (15)

$$U_c = \frac{\nu\,k\,T}{4\lambda} \int_0^\gamma \left(\frac{dy}{dt} \right)^2 dt \;. \tag{18}$$

In both integrals of equation (17) the condition (10) has to be taken into account. The expression for S_{cf} is too long and for that reason it is not reproduced here.

The calculation of A_{ex} is a very long procedure and it will not be presented here. Therefore, we give only the final expression of the excess free energy per monomer unit by introducing equation (14) into equation (11)

$$\left(\frac{A_{ex}}{\nu\,k\,T} \right)_1 = \frac{1}{2} y(0) + \bar{N}_1 \ln \frac{N_1^0}{\xi \bar{N}_1} + \frac{\bar{N}_z}{z} \ln \frac{N_z^0}{\xi \bar{N}_z} +$$

$$V_m \eta_1 n_1^o \int_0^\gamma e^{y+2t} y \, dt + V_m \eta_2 n_z^o \int_0^\gamma e^{zy+2t} z y \, dt \tag{19}$$

and equation (15) into equation (11)

$$\left(\frac{A_{ex}}{\nu\,k\,T}\right)_2 = \frac{1}{4\lambda}\int_0^\gamma\left(\frac{dy}{dt}\right)^2 dt + \overline{N}_1 \ln\frac{N_1^0}{\xi\overline{N}_1} + \frac{\overline{N}_z}{z}\ln\frac{N_z^0}{\xi\overline{N}_z} +$$

$$2V_m\eta_1 n_1^o\int_0^\gamma e^{y+2t}y\,dt + 2V_m\eta_2 n_z^o\int_0^\gamma e^{zy+2t}z\,y\,dt \quad .$$

(20)

In equations (19) and (20) the fraction $(e^{2\gamma} - e^{2t_1})/(e^{2\gamma} - e^{2t_2})$ was approximated by 1 which simplifies the writing and does not make an appreciable error. By multiplying equation (19) by 2 and substracting equation (20) from it, we obtain the simple expression

$$\frac{A_{ex}}{\nu\,k\,T} = y(0) - \frac{1}{4\lambda}\int_0^\gamma\left(\frac{dy}{dt}\right)^2 dt + \overline{N}_1\ln\frac{N_1^0}{\xi\overline{N}_1} + \frac{\overline{N}_z}{z}\ln\frac{N_z^0}{\xi\overline{N}_z} \quad ,$$

(21)

very suitable for numerical evaluation.

The osmotic coefficient can be obtained from the partial derivative of A_{ex} with respect to volume [13]. The most convenient expression [12], adapted for this case is

$$\Phi = \frac{n_1^o + n_z^o}{\overline{n}_1 + \overline{n}_z}$$

(22)

which reads in our notation
$$\Phi = \frac{z\,N_1^o + N_z^o}{\xi\left(z\,\overline{N}_1 + \overline{N}_z\right)} \quad .$$

(23)

RESULTS AND DISCUSSION

All equations in the previous section were developed for the general case of mono and z-valent counterions. The numerical calculations have been made, however, for mixtures of mono and divalent counterions which are more frequently encountered in biological and industrial systems. For all calculations the following values of the

parameters characterizing the polyion were applied: a = 0.8 nm, b = 0.252 nm, and λ = 2.84. For counterions the following values of ionic radii were taken: r_1 = 0.33 nm (e. g. Cs^+) which gives a_1 = 1.13 nm, and r_2 = 0.46 nm (e. g. Be^{2+}) [14] which gives a_2 = 1.26 nm. In Figure 3 we have for comparison a_1 = 0.8 nm; 1.0 nm; 1.13 nm and a_2 = 0.8 nm; 1.1 nm; 1.26 nm. The relation between the concentration parameter γ and concentration c_m in moles of monomer units per liter is

$$\gamma = \ln\frac{R}{a} = -\frac{1}{2}\ln\left(10^3 N_A V_m\right) - \frac{1}{2}\ln c_m, \tag{24}$$

where N_A is the Avogadro number. Thus, we have γ = 1.5 (c_m = 0.163 mol/l), γ = 2 (c_m = 0.06 mol/l), γ = 3 (c_m = 0.00812 mol/l), and γ = 4 (c_m = 0.0011 mol/l). For almost all calculations the value γ = 2 was applied. The range of the short-range interaction, b_1 = 1.4 nm and b_2 = 1.6 nm, was the same in all cases.
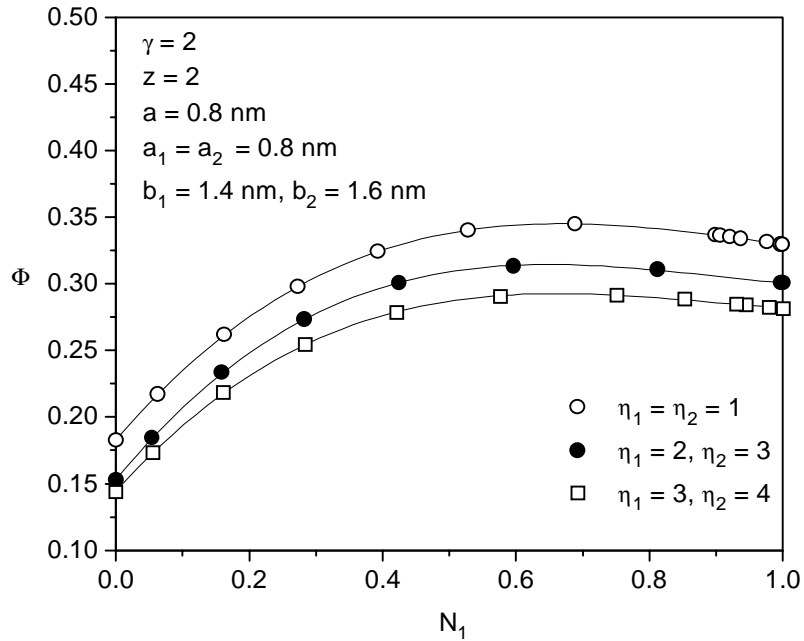
FIGURE 1. The influence of the short-range interaction on the osmotic coefficient. Counterions are point charges.
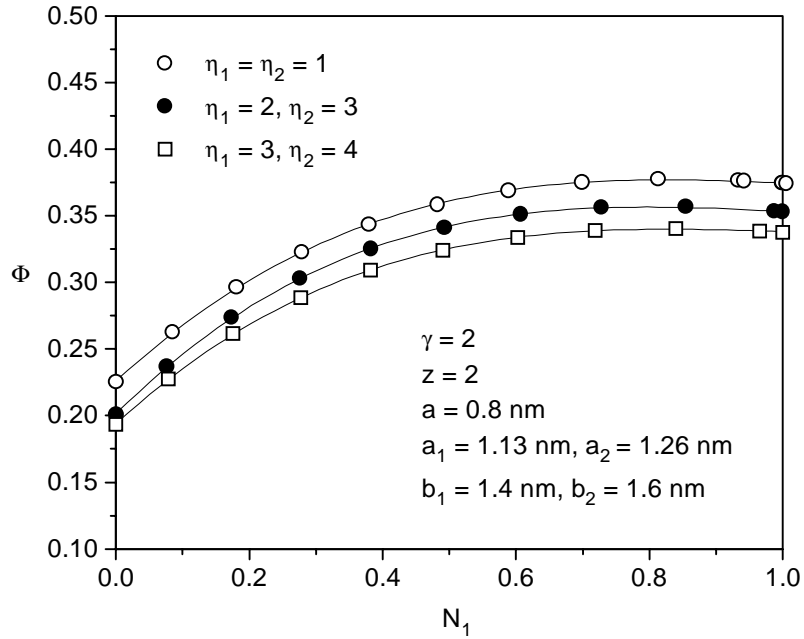
FIGURE 2. The influence of the short-range interaction on the osmotic coefficient. Radii of counterions are $r_1 = 0.33$ nm and $r_2 = 0.46$ nm.

The greater part of the figures presented in this article is devoted to the osmotic coefficient because, it can be obtained directly from the experiment, and gives an approximate information about the distribution of counterions inside the cell. The concentration of counterions at the border of the cell is decisive for the value of the osmotic coefficient, as shown in equation (22). A low value of Φ signifies that counterions are gathering around the polyion and, as a result, a decrease of concentration is produced at the border of the cell. A comparison of Figures 1 and 2 reveals that a lower depth of the potential well (higher values of η_1 and η_2) gives rise to a stronger attraction of counterions to the polyion, irrespective of the ionic size and the value of $\overline{N}_1$. Furthermore, larger counterions are less attracted by the polyion causing a higher value of Φ, as seen in Figure 3. The dependence of the osmotic coefficient on concentration is presented in Figure 4 and 5 for two different cases. For lower concentrations (higher values of the parameter γ) the well expressed maxima appear what has been confirmed by the experiments [8].
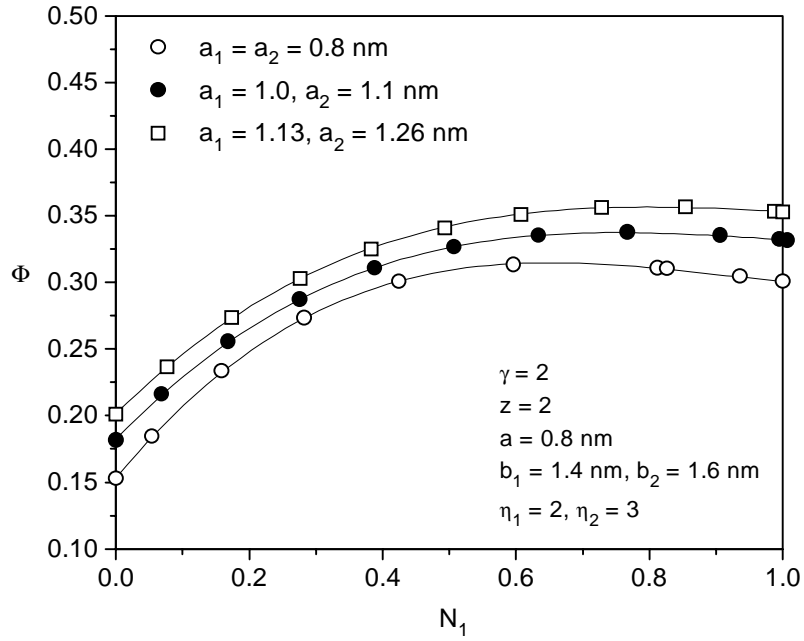
FIGURE 3. The influence of radii of counterions on the osmotic coefficient.
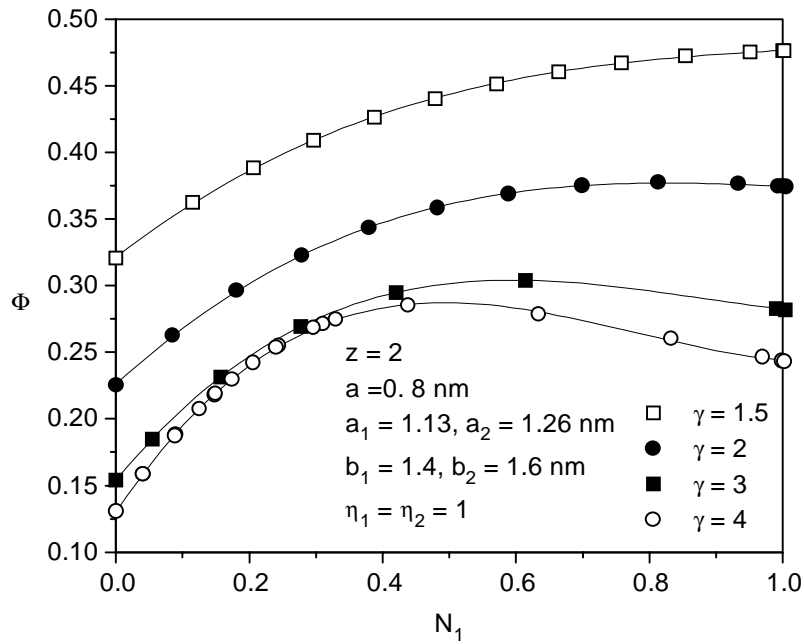
FIGURE 4. Dependence of the osmotic coefficient on concentration in the absence of the short-range interaction.
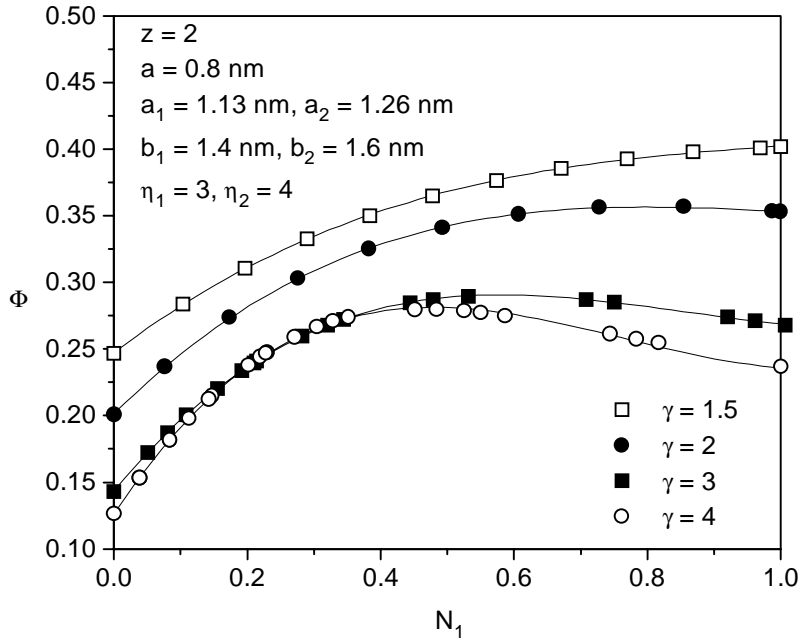
FIGURE 5. Dependence of the osmotic coefficient on concentration in the presence of the short-range interaction.

In Figures 6 and 7 the excess free energy is plotted against $\overline{N}_1$ for different values of γ and of the parameters η_1 and η_2. In this case, a simple interpretation which would be analogous to that applied with osmotic coefficient is not possible.
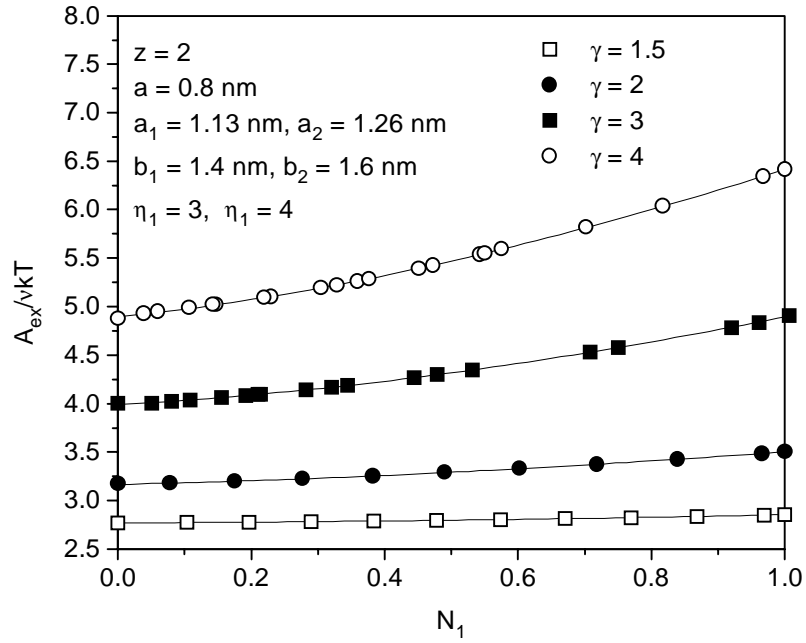
FIGURE 6. Dependence of $A_{ex}/\mathrm{í}kT$ on concentration.
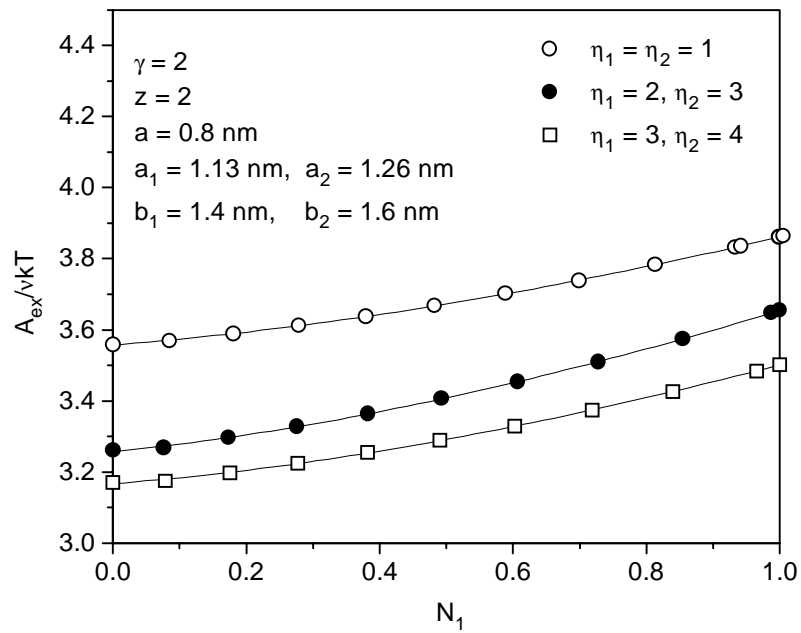
FIGURE 7. The influence of short-range interaction on $A_{ex}/\mathrm{í}kT$.

REFERENCES

[1] P. W. Hales, G. Pass, *Eur. Polym. J.* **1981,** *17,* 657-659.

[2] G. Vesnaver, M. Rudež, C. Pohar, J. Škerjanc, *J. Phys. Chem.* **1984**, *88*, 2411-2414.

[3] G. Vesnaver, Z. Kranjc, C. Pohar, J. Škerjanc, *J. Phys. Chem.* **1987**, *91*, 3845-3848.

[4] D. Dolar, IX. Yugoslav Symposium on Electrochemistry, Dubrovnik, Book of Abstracts, Serbian Chem. Soc., Belgrade, **1985**, pp 47- 50.

[5]   V. Vlachy, *Eur. Polym. J.* **1988**, *24*, 737-740.

[6]   D. Dolar, M. Bešter, *J. Phys. Chem.* **1995**, *99*, 4763-4767.

[7]   D. Dolar, A. Peterlin, *J. Chem. Phys.* **1969**, *10*, 3011-3015.

[8]   D. Dolar, D. Kozak, IUPAC International Symposium on Macromolecules, Leiden, Book of Abstracts, Inter Scientias Inc., The Hague, **1970**, Vol. 1, pp 363-366. The results of this article are reproduced in Ref. 9 and 10.

[9]   A. Katchalsky, *Pure Appl. Chem.* **1971**, *26*, 327-373.

[10] D. Dolar, in *Polyelectrolytes*, ed. E. Selegny, M. Mandel, U. P. Strauss, D. Reidel, Dordrecht, The Netherlands, **1972**, pp 97-113**.**

[11] G. S. Manning, *ibid.* pp 9-37.

[12] R. A. Marcus, *J. Chem. Phys.* **1955**, *23*, 1057-1068.

[13] S. Lifson, A. Katchalsky, *J. Polym. Sci.* **1954**, *13*, 43-55.

[14]   B. E. Conway, *Ionic Hydration in Chemistry and Biophysics*, Elsevier Scientific Publishing Company, **1981**, pp 73.

POVZETEK

Za raztopino polielektrolita z mešanico eno- in dvovalentnih protioiinov smo na osnovi celičnega modela s cilindrično simetrijo in z uporabo Poisson-Boltzmannove enačbe izračunali osmozni koeficient in presežno prosto energijo. Pri računu smo upoštevali tudi kratkosežne interakcije med poliionom in protiioni, opisane s pravokotnim potencialom. Vrednosti osmoznega koeficienta smo podali kot funkcijo ekvivalentnega ulomka enovalentnih protiionov za različne vrednosti ionskih radijev, globine potencialne jame in koncentracije.

INFLUENCE OF ALKYLUREAS ON THE FLUORESCENCE PROPERTIES OF MODEL DIPEPTIDES AND RIBONUCLEASE A

Nataša Poklar, Aleksandra Mecilošek and Gorazd Vesnaver

Department of Chemistry, University of Ljubljana, Aškerčeva 5, 1000 Ljubljana,

Slovenia

Abstract: The influence of guanidinium hydrochloride (GuHCl), urea and some alkylureas on the stability of bovine ribonuclease A (RNase A) in aqueous solutions at 25 $^{\circ}$C was investigated by measuring the protein intrinsic fluorescence emission as a function of the added denaturant concentration. It was shown that GuHCl is significantly stronger denaturing agent than urea and that in solutions of alkylureas a full RNase A denaturation cannot be achieved even at the highest possible denaturant concentrations. Such behavior was ascribed to lower denaturing efficiency and/or lower solubility of alkylureas. These findings were fully supported by the results of RNase A fluorescence polarization measurements performed in the same denaturant solutions. The fluorescence emission spectra of RNase A were also compared with the corresponding spectra of the model dipeptide containing one tyrosine residue. It was shown that the changes in the RNase A intrinsic fluorescence emission observed at high denaturant concentrations are due primarily to the unfolding of the protein.

INTRODUCTION

It is well known that almost all proteins contain natural fluorophores tyrosine (Tyr), tryptophan (Trp) and phenylalanine (Phe) and that upon excitation at 280 nm where only Tyr and Trp absorb the fluorescence emission is due primarily to Trp [1-3]. The emission spectra of Trp residues are highly sensitive to the polarity of their immediate surrounding and to the presence of all kinds of quenchers. As a result, the

position and the magnitude of Trp emission maximum depends on those factors which affect the exposure of Trp residues to the water phase. In other words, measuring of the Trp fluorescence excited at 280 nm is suitable for following the unfolding equilibria of those proteins that contain Trp alone or Trp together with Tyr. The emission of the other natural fluorophore, Tyr, occurs at around 303 nm and is almost insensitive to solvent polarity. In spite of its high absorption at 280 nm the Tyr emission from most proteins is small and frequently hard to detect. The main reason for that is quenching of Tyr emission by various groups and ions in the Tyr immediate vicinity and by energy transfer from Tyr to Trp residues. The observed weak Tyr emission from proteins thus depends on their three dimensional structure. Consequently, the unfolding of proteins that contain only Tyr residues can be followed by measuring their intrinsic fluorescence emission intensity at 303 nm [1-3].

Bovine ribonuclease A (RNase A) is a protein which has been frequently used, due to its structural simplicity and commercial availability, for studying the influence of various physicochemical agents on the conformational stability and the unfolding - refolding equilibria of proteins. RNase A is a small monomeric enzyme with molecular weight of 13.7 kDa that consists of 124 amino acids. It contains four disulfide bonds and six Tyr residues, three of them being buried within the protein molecule when it is in its native state [4-5]. According to the far-UV CD spectra it shows structural characteristics of $\alpha+\beta$ type proteins [6]. The three-dimensional X-ray structure of RNase A shows that it is a kidney-shaped molecule containing a N-terminal α-helix and two other short helices packed against a central twisted antiparallel β-sheet [7]. In this work we investigated the influence of denaturants GuHCl, urea and some alkylureas on the RNase A stability in aqueous solutions at 25°C by measuring its intrinsic fluorescence as a function of added denaturant concentration. We also performed the same type of measurements on aqueous solutions of model dipeptides containing Tyr or Trp residues. From the comparison of the RNase A and the corresponding model dipeptide emission spectra we tried to estimate the contributions to the observed changes in the protein emission intensity that result from the RNase A unfolding induced by the addition of denaturants.

EXPERIMENTAL PROCEDURES

Materials

Two dipeptides containing tryptophan, Glycyl-L-Tryptophan (Gly-L-Trp) and L-Leucyl-L-Tryptophan (L-Leu-L-Trp) and two dipeptides containing tyrosine, Glycyl-L-Tyrosine (Gly-L-Tyr) and L-Leucyl-L-Tyrosine (L-Leu-L-Tyr) (Fig. 1) and ribonuclease A type XII-A from bovine pancreas (RNase A) were purchased from Sigma Chemical (St. Louis, MO) and used without further purification.
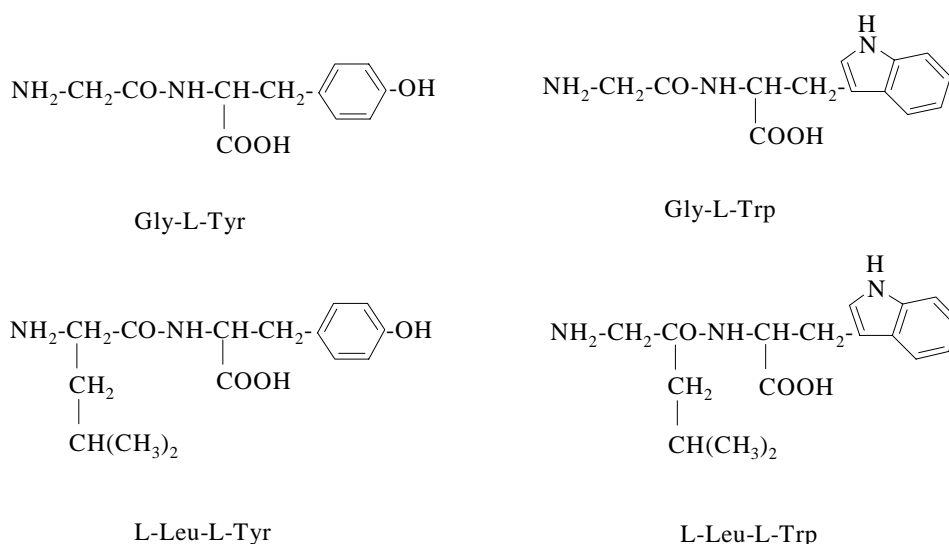
Figure 1: *Model dipeptides containing tyrosine or tryptophan residue.*

Ultrapure urea was a product of Kemika (Zagreb, Croatia). Guanidine hydrochloride, methylurea, N,N'-dimethylurea, ethylurea, and buthylurea were supplied by Fluka (Buch, Switzerland). Before use, all ureas and GuHCl were recrystalized from hot ethanol and dried for 48 hours under a vacuum at 40 $^{\circ}$C in the presence of phosphorus pentoxide. Glycine buffers (0.1 M glycine, 0.1 M NaCl / 0.1 M HCl) with appropriate pH (1.1, 3.0, 3.5) and solution of RNase A in triple distilled water (pH = 7.0-7.4) were used.

Aqueous dipeptide stock solutions were prepared by weighing dried dipeptides on a precision analytical balance (Sartorius Research RC 210S, Goettingen, Germany) and dissolving them in a known amount of water. Solutions of dipeptides in aqueous solutions of the desirable denaturant concentration were then prepared by weighing into a given quantity of stock solution appropriate amounts of solid ureas and triple distilled water. The final concentration of dipeptides in all urea and alkylurea solutions was $1.5 \cdot 10^{-5}$ M.

Protein aqueous stock solutions were prepared daily by weighing a proper amount of the dry protein into the triple distilled water. Protein concentration in aqueous solution at 20 ^{o}C was determined spectrophotometrically by using $E_{1cm}^{1\%} =$ 7.38 at 278 nm [8]. From the stock solution of RNase A, solutions of the desirable denaturant concentration were prepared in the same way as the dipeptide solutions. The concentration of RNase A in all solutions used for fluorescence measurements was $1.0 \cdot 10^{-5}$ M.

Intrinsic Fluorescence measurements

Intrinsic fluorescence emission spectra of dipeptides and RNase A in the presence of different concentrations of denaturants were measured on a Perkin-Elmer Model LS-50 Luminescence Spectrometer equipped with a water thermostated cell holder using a 1 cm pathlength quartz cuvette. Slit widths with a nominal band pass of 5 nm were used for both excitation and emission beams. Intrinsic fluorescence emission spectra were recorded in the range from 280 to 460 nm after exciting at 275, 280 or 295 nm. All fluorescence measurements were taken at 20 ^{o}C with the scan rate of 250 nm / min. The fluorescence emission spectrum of pure solvent (background intensity) was always subtracted from the corresponding emission spectrum of the model dipeptide or RNase A. The intrinsic fluorescence spectra were corrected for PM-tube response using fluorescence spectrum of Quinine sulfate (c = $2.5 \cdot 10^{-7}$ M) in 0.1 M solution of perchloric acid as a standard.

Polarization measurements

Fluorescence polarization measurements of protein were made on the same spectrophotometer equipped with an automated polarizing accessory. The excitation and emission slit widths were 5 nm. All measurements were carried out by exciting at 275 nm, while corresponding emission wavelength was 303 nm. The grating correction factor G and degree of polarization P were obtained as [9]

$$G = \frac{F_{HV}}{F_{HH}}; \qquad P = \frac{F_{VV} - GF_{VH}}{F_{VV} + GF_{VH}} \qquad (1)$$

where F_{VV}, F_{VH}, F_{HV}, and F_{HH} are the fluorescence intensity components in which the subscripts refer to the horizontal (H) and vertical (V) position of the excitation and emission polarizers, respectively.

Thermodynamic Analysis of Equilibria

Assuming that the protein unfolding is a reversible "all or none" transition, the standard Gibbs free energy of denaturation, ΔG_D^o, can be expressed as

$$\Delta G_D^o = -RT \cdot \ln K_D \qquad (2)$$

where the apparent equilibrium constant for the denaturation process, K_D, is given by the equation

$$K_D = \frac{f_D}{f_N} = \frac{y_N - y}{y - y_D} \qquad (3)$$

in which y is the measured property (in this study the protein intrinsic emission intensity) and N and D refer to the native and denatured state, respectively. Numerous studies of protein denaturation by denaturing agents such as GuHCl, urea or alkylureas have shown that over the denaturant concentration range in which the denaturation process can be followed, ΔG^o_D varies at a constant temperature linearly with the denaturant concentration as [10-11]

$$\Delta G_D^o = \Delta G_{D,H_2O}^o - m \cdot c_D \qquad (4)$$

In this empirical relation $\Delta G^o_{D,H_2O}$ is the standard Gibbs free energy of denaturation in the absence of denaturant, obtained with a linear extrapolation of ΔG^o_D to zero denaturant concentration and factor m is the rate of change of ΔG_D^o with denaturant

concentration, c_D. The validity of the described linear extrapolation has been discussed by a number of authors from both the theoretical [12-14] and experimental point of view [15-16].

<div align="center">RESULTS AND DISCUSSION</div>

Fluorescence emission of model dipeptides containing Tyr or Trp residues.

Measurements of the fluorescence emission spectra of the model dipeptides Gly-L-Tyr, L-Leu-L-Tyr, Gly-L-Trp and L-Leu-L-Trp dissolved in the triple distilled water showed no dependence on the excitation wavelength, λ_{exc} (Table 1). They did show, however, that the fluorescence intensities of Tyr and Trp combined with Leu are higher than those obtained from Tyr and Trp combined with Gly. It seems, that leucine residue which is bulkier than the glycine one creates less polar environment around Tyr and Trp causing their fluorescence to increase. Since both Tyr and Trp are known to increase their fluorescence emission significantly already in slightly less polar solvents [1-2] such explanation seems reasonable.

Table 1: *The wavelength at the emission maximum, λ_{max}, and the corresponding fluorescence intensity, $F_{\lambda_{max}}$, of the model dipeptides in aqueous solutions at 25°C (c = 1.5·10^{-5} M) as a function of the excitation wavelength, λ_{exc}.*

	λ_{exc} nm	λ_{max} nm	*$F_{\lambda_{max}}$ arbitrary units
Gly-L-Tyr	275	303.0 ± 1	485
	280	302.0 ± 1	485
	295	305.0 ± 1	6
L-Leu-L-Tyr	275	302.5 ± 1	597
	280	302.0 ± 1	549
	295	-	-
Gly-L-Trp	275	359.5 ± 1	562
	280	358.5 ± 1	570
	295	358.5 ± 1	218
L-Leu-L-Trp	275	359.5 ± 1	892
	280	359.0 ± 1	886
	295	358.5 ± 1	368

*The relative error involved in measurement the fluorescence emission intensity is estimated to not exceed 3 %.

The concentration dependence of the emission intensity at λ_{em} = 358 nm, F_{358}, of 1.5×10^{-5} M Gly-L-Trp in urea and alkylurea solutions relative to the corresponding fluorescence intensity in water, F^{o}_{358}, is shown in Fig. 2A.
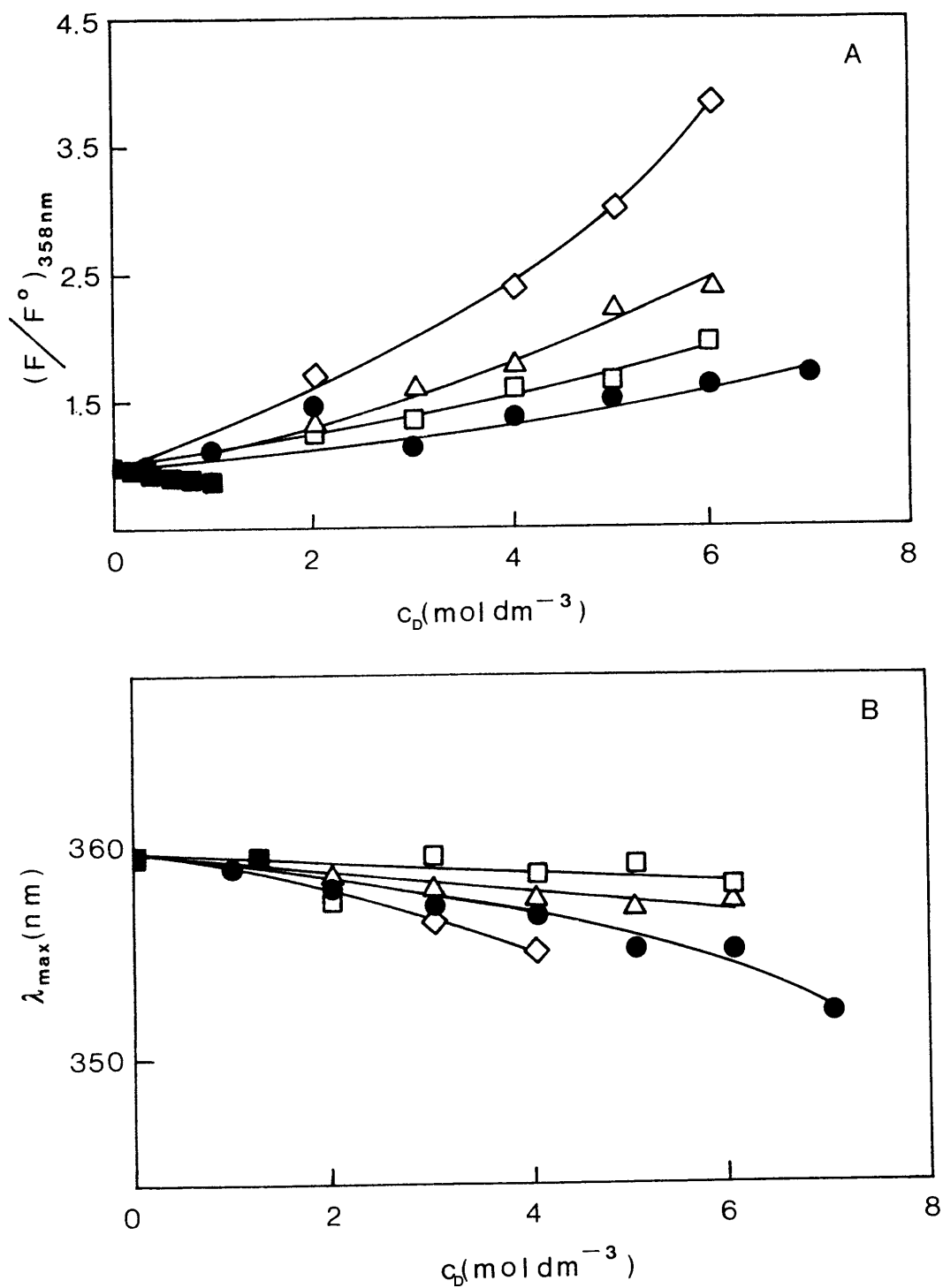
Figure 2: The relative fluorescence emission intensity measured at 358 nm (F/F^o)$_{358}$ (Panel A) and the emission maximum wavelength shift λ_{max} (Panel B) of Gly-L-Trp in aqueous solutions(c = 1.5·10^{-5} M) at 25 °C in the presence of urea (   ), methylurea (∆), N,N'-dimethylurea (◊), ethylurea (●) and butylurea (■) as a function of denaturant concentration, c$_D$. λ_{exc} was 295 nm. F^o refers to the fluorescence intensity of Gly-L-Trp in triple distilled water.

It can be seen that the observed relative fluorescence intensity, $(F/F^o)_{358}$, increases with increasing urea and alkylurea concentration in the following order: butylurea < ethylurea < urea < methylurea. < N,N'-dimethylurea. Similar dependence upon the solvent composition is observed also with the wavelength of the Gly-L-Trp emission maximum, λ_{max}. With increasing denaturant concentration and increasing size of the alkylgroup substituted on the urea molecule λ_{max} shifts toward lower values (Fig. 2B).

For Gly-L-Tyr the relative fluorescence intensities measured at $\lambda_{em} = 303$ nm, $(F/F^o)_{303}$, are not so high as for Gly-L-Trp and increase with denaturant concentration only in urea and N,N'-dimethylurea solutions (Fig. 3A). Furthermore, λ_{max} does not shift with increasing concentration or hydrophobicity of alkylureas and stays at 303 nm (Fig. 3B).

Comparison of our results with the literature data on the fluorescence spectra of Tyr and Trp derivatives shows good consistency. The fluorescence emission spectrum of Trp is known to be highly sensitive to solvent polarity and to quenching by variety of reasons [2]. Numerous works have shown that the emission maximum of Trp-derivatives which occur in water at 350-360 nm shifts in less polar solvents to significantly lower values (in hexane ~ 300 nm) [2, 17-18]. In contrast, the reported emission of Tyr and its derivatives occurs in water at around 303 nm and shows no, or very little sensitivity to solvent polarity [2, 18]. Similar behavior of both fluorophores was observed also in this work.

The observed shifts of Trp emission spectra were attributed to the changes of local solvent polarity caused by the addition of urea and its derivatives. With the increasing urea and alkylurea concentration and also with the increasing size of the alkyl groups on the urea molecules the Gly-L-Trp, Gly-L-Tyr, L-Leu-L-Trp or L-Leu-L-Tyr surrounding environment becomes less polar. As a result, the observed emission spectra of Trp-residues which reflect the polarity of their immediate surroundings are shifted toward blue. In contrast, the corresponding spectra of Tyr-residues remain unchanged due to the poor sensitivity of this fluorophore to changes in solvent polarity. The fluorescence intensity studies performed on solutions of Trp, Tyr and some of their derivatives have shown that the fluorescence emission intensity of these

fluorophores in general increases (with Tyr to smaller extent) as the solvent becomes less polar. It has been suggested that the excited singlet states of Trp and Tyr interact with neighboring water molecules to form excited state-water complexes and that such complexation competes with the radiative decay of the fluorophore excited state [2, 18]. Thus, the observed enhancement of the Trp and Tyr fluorescence intensity that accompanies the addition of urea and alkylureas to aqueous solutions of Trp and Tyr dipeptides may be due to a decreased water concentration in the immediate vicinity of the fluorophores. The consequent reduction of the amount of the excited state-water complexes or formation of weaker complexes than those derived from water will lead to a less pronounced nonradiative deactivation of the excited states and thus to an increase in the fluorescence quantum yield.

As already mentioned, a process that competes with the enhancement of the fluorescence emission intensity is fluorescence quenching. This complex process is due to the fluorophore - neighboring molecules interactions such as hydrogen bonding, acid-base chemistry or charge transfer, to name a few. The Tyr fluorescence is known to be quenched by the presence of nearby uncharged amino groups [2]. Apparently, a transfer of protons from the Tyr aromatic hydroxyl groups to these proton acceptors takes place during the lifetime of the excited state leading to a quenching of the tyrosine fluorescence. Therefore, the addition of urea and alkylureas to Tyr aqueous solutions will result in quenching of the emission fluorescence of Tyr-fluorophores. This quenching will compete with the previously described enhancement of fluorescence intensity due to the less aqueous solvent in the immediate vicinity of Tyr fluorophores and the resulting relative fluorescence $(F/F^o)_{303}$ will be lower than the corresponding value observed for Trp. In some solvents the $(F/F^o)_{303}$ value may even drop below 1. Inspection of Figs. 2 and 3 clearly shows that the suggested qualitative explanation for the dependence of fluorescence intensity of Trp and Tyr residues in model dipeptides upon the addition of urea and alkylureas is in good agreement with experimental data.

A variety of reasons have been suggested for the well known absence of tyrosine fluorescence in proteins and one of them is the energy transfer from Tyr to Trp. The efficiency of this transition depends strongly upon the distance between the
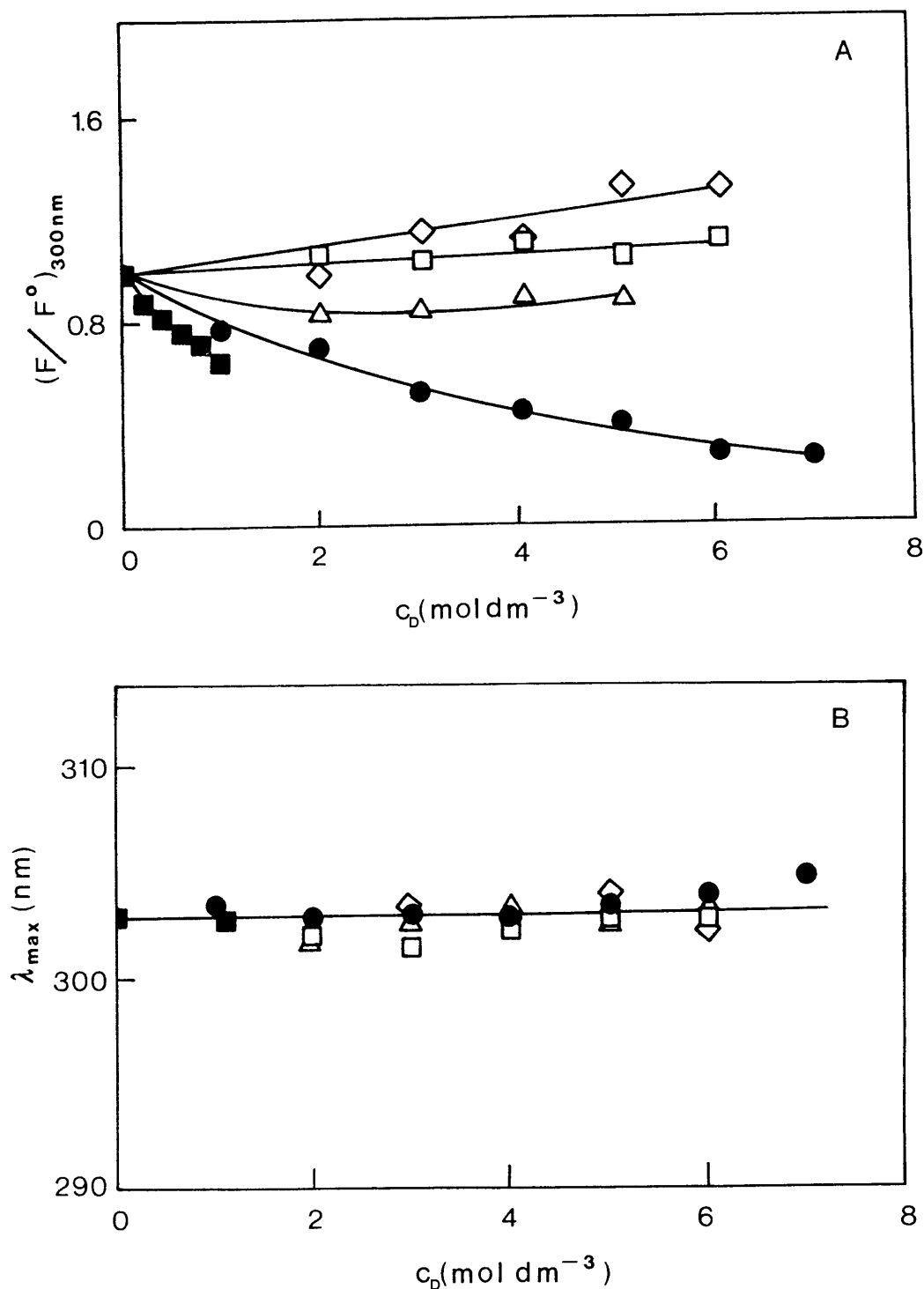
Figure 3: The relative fluorescence emission intensity measured at 303 nm $(F/F^o)_{358}$ (Panel A) and the emission maximum wavelength shift λ_{max} (Panel B) of Gly-L-Tyr in aqueous solutions($c = 1.5 \cdot 10^{-5}$ M) at 25 °C in the presence of urea (   ), methylurea (Δ), N,N'-dimethylurea ($\lozenge$), ethylurea ($\bullet$) and butylurea ($\blacksquare$) as a function of denaturant concentration, c_D. λ_{exc} was 275 nm. F^o refers to the fluorescence intensity of Gly-L-Tyr in triple distilled water.

Tyr-donors and Trp-acceptors and therefore, as numerous studies have shown, it depends on the three dimensional structure of the protein [1-2]. Consequently, the addition of denaturants, such as urea or alkylureas, to protein solutions is accompanied by changes in the energy transfer efficiencies which are reflected in changes of the measured fluorescence emission intensities. The question is, whether these changes are due only to changes of protein conformation or also to specific interactions of denaturant molecules with Tyr and Trp residues. In an attempt to clarify this question we performed a series of fluorescence measurements in solutions of the model dipeptides, Gly-L-Tyr and Gly-L-Trp, at constant total dipeptide concentration of 10^{-5} M and at Tyr:Trp ratios of 1:1, 1:2 and 11:5 to which different amounts of urea and alkylureas were added. At 1:1 and 1:2 ratios we did not observe any difference between the measured spectra and those calculated using the principle of additivity of pure Gly-L-Tyr and Gly-L-Trp spectra at the corresponding concentrations. At ratio of 11:5, however, the difference between the measured and calculated spectra is noticeable (Fig. 4).
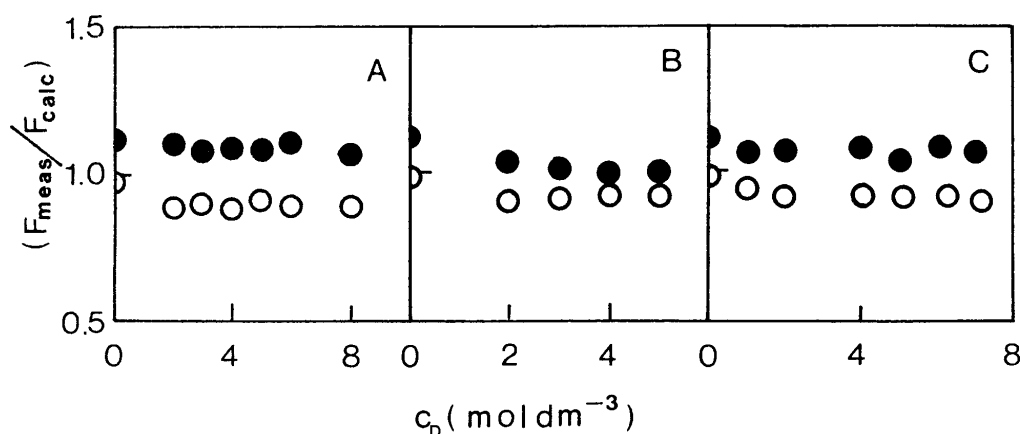
Figure 4: *The energy transfer from Tyr (O) to Trp (●) at 25 °C in aqueous solutions of the total dipeptide concentration of 1.5·10^{-5} M and Gly-L-Tyr to Gly-L-Trp ratio of 11 to 5 in the presence of urea (Panel A), N,N'-dimethylurea (Panel B) and ethylurea (Panel C). λ_{exc} was 275 nm. The fluorescence emission intensity, F_{meas} for Tyr in the mixture solution was measured at 303 nm and for Trp at 358 nm, respectively. These intensities were compared to the corresponding values, F_{calc}, calculated for the Gly-L-Trp : Gly-L-Tyr ratio of 11:5 from the pure spectra of Gly-L-Trp and Gly-L-Tyr.*

The comparison of the measured and calculated fluorescence intensities shows that the measured Tyr emission at 303 nm is for about 10% lower and the measured Trp emission at 358 nm for about 10% higher than the corresponding emission intensities calculated using the principle of additivity. Inspection of Fig. 4 further shows that at the given experimental conditions the observed Try-to-Trp energy transfer of about 10% does not depend on the urea or alkylurea concentration and is thus not sensitive to any specific interactions between Tyr or Trp residues and urea or alkylurea molecules. This result is irrelevant for RNase A since it does not contain any Tyr residues, however, it should be taken into account in denaturation studies followed by fluorescence of those proteins that contain both Tyr and Trp.

Fluorescence emission and fluorescence polarization of RNase A.

Upon excitation at 275 nm, the fluorescence emission of RNase A in urea solutions increases with increasing urea concentration while the position of emission maximum (λ_{max} = 303 nm) remains unchanged (Fig. 5).
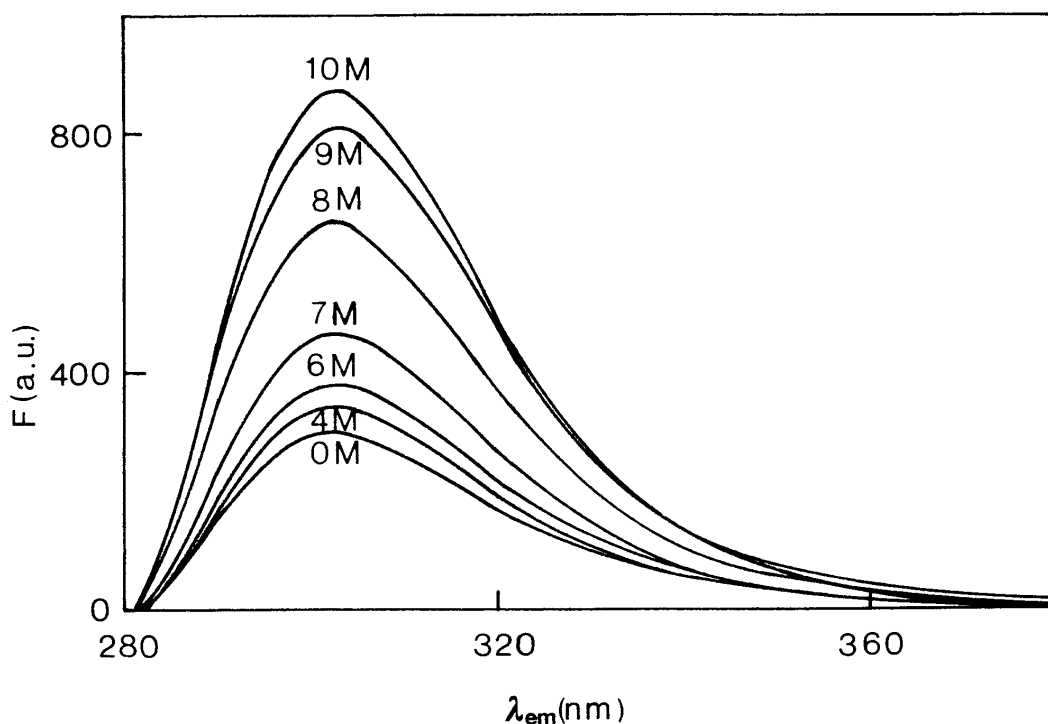
Figure 5: *The fluorescence emission spectra of RNase A (c = 1.0·10^5 M) in the aqueous solutions of urea at urea concentrations between 0 to 10 M; λ_{exc} = 275 nm, F the fluorescence intensity in arbitrary units.*

Clearly, the unfolding of RNase A that occurs at high urea concentrations results in increased average exposure of the protein Tyr residues to the water phase. Because of that, quenching of Tyr by the nearby peptide bonds and charged and uncharged carboxyl and amino groups is reduced and as a result an increase in the fluorescence emission is observed. Similar dependence of RNase A fluorescence emission on denaturant concentration was observed also in solutions of GuHCl and some alkylureas. As can be seen from Fig. 6 where the relative fluorescence emission, $(F/F^o)_{303}$, is presented as a function of denaturant concentration, the unfolding of RNase A seems to be completed only in urea and GuHCl solutions. In solutions of methyl- and N,N'-dimethylurea which are obviously less efficient denaturants than GuHCl or urea only the beginning of RNase A unfolding can be observed at the highest possible denaturant concentrations.
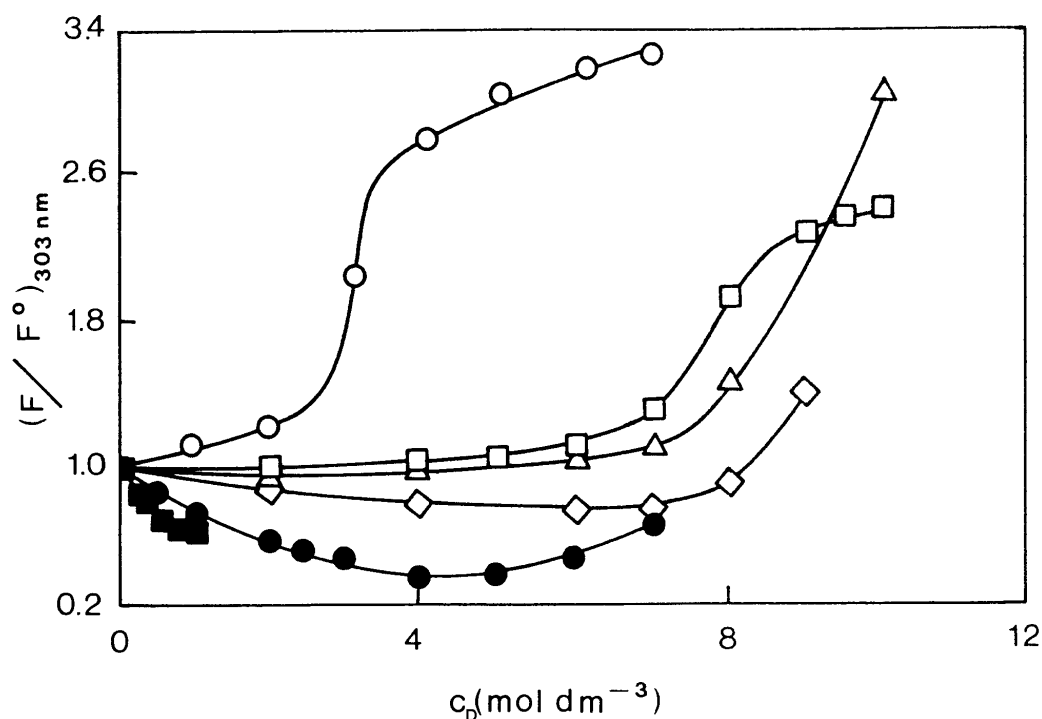
Figure 6: The relative fluorescence emission intensity of RNase A (c = 1.0·10^{-5} M) at 303 nm and 25 °C, $(F/F^o)_{303}$, in the presence of GuHCl (O), urea ( ), methylurea (Δ), N,N'-dimethylurea (◊), ethylurea (●) and butylurea (■) as a function of denaturant concentration. λ_{exc} was 275 nm. F^o refers to the fluorescence intensity of RNase A in triple distilled water.

Furthermore, in buthylurea solutions in which very high denaturant concentration cannot be reached due to the solubility problem nothing but decreasing of $(F/F^o)_{303}$ with increasing denaturant concentration is observed (Fig. 6). This decreasing is also observed at low denaturant concentration in N,N'-dimethylurea and ethylurea solutions and is more pronounced with alkylureas possessing larger hydrophobic groups. It seems, that it is caused by some additional quenching of Tyr fluorescence by denaturant molecules. Evidently, the measured fluorescence emission dependence on the denaturant concentration results from the competition of two opposing effects; the increasing of the fluorescence emission due to increasing exposure of Tyr residues to the aqueous phase and the decreasing of the fluorescence emission due to the increased quenching by the denaturant molecules. The existence of this second contribution is confirmed by the results presented in Figs. 3A and 6 which show that at low denaturant concentrations the fluorescence of the RNase A Tyr residues and the corresponding fluorescence of Tyr residues in the model dipeptide Gly-L-Tyr are similarly affected by urea and alkylureas.

The effect of GuHCl, urea and methylurea on the fluorescence polarization of RNase A is presented in Fig. 7. Obviously, the measured fluorescence is sensitive to RNase A conformational changes, although this sensitivity is less pronounced than with fluorescence emission intensity. In fact, only the RNase A conformational changes induced by addition of GuHCl, urea and methylurea can be followed by measuring the accompanying changes in the protein fluorescence polarization. As shown in Fig. 7 the polarization of RNase A fluorescence in solutions of GuHCl, urea and methylurea decreases with increasing denaturant concentration indicating an increase in the flexibility of Tyr side chains and an increase in the randomization of the RNase A tertiary structure.

Comparison of the results presented in Figs. 6 and 7 further shows that the denaturant concentration region in which according to fluorescence emission measurements the protein undergoes conformational transition overlaps for GuHCl, urea and methylurea with the denaturant concentration region in which changes in fluorescence polarization are observed.
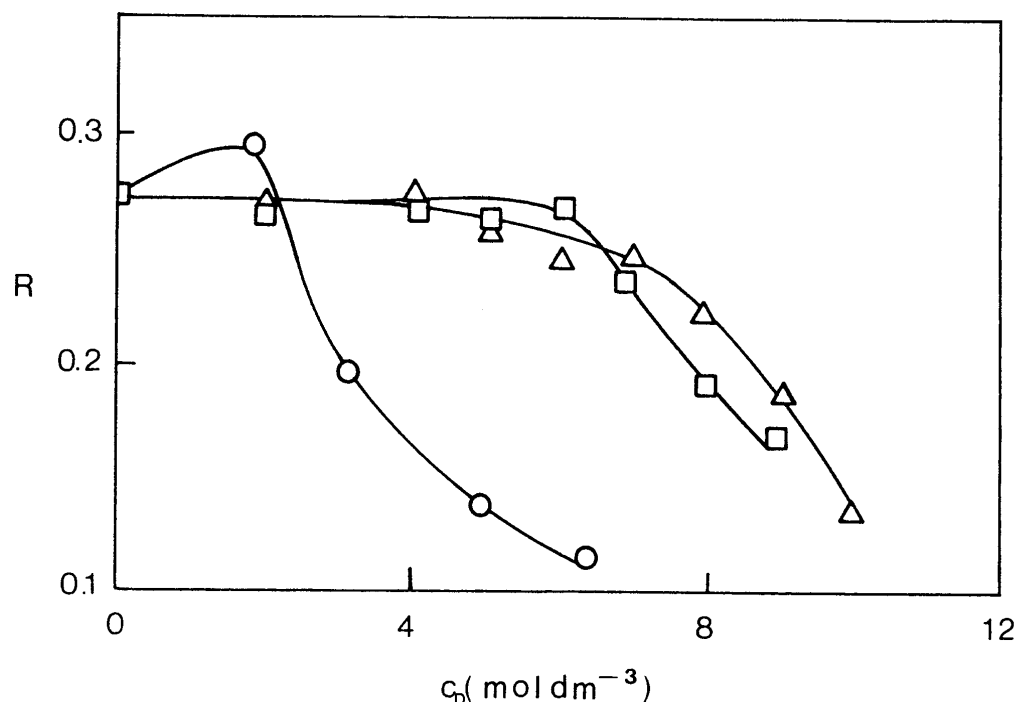
Figure 7: *The fluorescence polarization of RNase A in aqueous solutions (c = 1.0·10^-5 M) at 303 nm and 25 °C in the presence of GuHCl (O), urea ( ) and methylurea (△) as a function of denaturant concentration, c_D. λ_{exc} = 275 nm, λ_{em} = 303 nm.*

Thermodynamic analysis of RNase A fluorescence emission data.

Assuming that the unfolding of RNase A is a two state process the corresponding equilibrium constants and ΔG^o_D values can be calculated from eqs. 2 and 3. Using these values we were able to show that over the GuHCl or urea concentration range in which the RNase A denaturation could be followed the calculated ΔG^o_D varies linearly with the denaturant concentration as predicted by eq. 4. The characteristic values of $\Delta G^o_{D,H2O}$, the denaturant concentration $c_{1/2}$ at which half of RNase A molecules are unfolded and at which $\Delta G^o_D = 0$ and factor m are presented in Table 2. The $c_{1/2}$ value in GuHCl ($c_{1/2}$ = 3.0 M) is lower than in urea ($c_{1/2}$ = 7.6 M) indicating that GuHCl is a more efficient denaturant than urea. With other denaturants the fully denatured state of RNase A could not be reached because of their less pronounced denaturation abilities and/or to low solubilities. Inspection of Table 2 shows that values of the standard Gibbs free energy of denaturation in water at 25 °C, $\Delta G^o_{D,H2O}$, obtained in GuHCl and urea solutions by linear extrapolation of ΔG^o_D values

to zero denaturant concentration are 27.5 and 28.0 kJ/mol, respectively. Although such extrapolations from regions of high concentrations are rather unsafe, the agreement of $\Delta G^o_{D,H2O}$ values determined from solutions of both denaturants is excellent. Furthermore, these $\Delta G^o_{D,H2O}$ values are very close to the corresponding $\Delta G^o_{D,H2O}$ values obtained in GuHCl (26.5 kJ/mol) and urea (34 kJ/mol) solutions from DSC measurements [19]. Another quantity that may be used for the characterization of the denaturation efficiency of a given denaturant is the factor *m* appearing in eq. 4. Its physical significance is not completely clear although according to several studies [12-16] it may reflect the difference between the accessibility of the surface areas of the denatured and native state for a given denaturant. In other words, its value may be considered as a measure of the compactness of the protein denatured state. According to such characterization GuHCl with its high *m* value of 9.2 can be considered as much stronger denaturing agent of RNase A than urea whose *m* value is only 3.7. It is to be noted that similar results were obtained also from DSC studies of RNase A denaturation from which *m*-values of 8.0 for GuHCl and 4.1 for urea were derived [19].

Table 2: *Thermodynamic characteristic of solvent denaturation of RNase A at 25°C in aqueous GuHCl and urea solution obtained from fluorescence intensity measurements at 303 nm by applying the eqs. 2 - 4; λ_{exc} was 275 nm.*

	$\Delta G^o_{D,H2O}$ (kJ/mol)	m (kJ·L/mol^2)	$c_{1/2}$ (mol/L)
GuHCl	27.4 ± 1.5	9.2 ± 0.6	3.0 ± 0.4
	(26.5 ± 5)	(8.0 ± 1.6)	(3.3 ± 0.6)
Urea	28.0 ± 0.2	3.7 ± 0.2	7.5 ± 0.5
	(34.2 ± 7)	(4.1 ± 0.8)	(8.3 ± 1.6)

The data in parenthesizes are from DSC measurements [19].

ACKNOWLEDGMENTS

fluorescence emission and polarization measurements of RNase A in the presence of guanidinium hydrochloride.

REFERENCES

[1]   J.R. Lakowicz, *Principles of Fluorescence Spectroscopy:* Plenum Press, New York, 1986.

[2]   J.R. Lakowicz, *Modern Physical Methods in Biochemistry:* Elsevier, New York 1988, pp. 1-25.

[3]   I.D. Campbell and R.A. Dwek, *Biological Spectroscopy:* The Benjamine Publishing Comp.Inc., 1984, pp. 90-125.

[4]   H.A. Scheraga, *Fed. Proc.* **1967**, *26*, 1380-1387.

[5]   J. Santoro, C. Gonzales, M. Bruix, J.L. Neira, J.L. Nieta, J. Herranz, M. Rico, *J. Mol. Biol.* **1993**, *229*, 722-734.

[6]   P. Manavalan, Jr. C. Johnson, *Nature* **1983**, *305*, 831-832.

[7]   A. Wlodawer, L.A. Svensson, L. Sjolin, G.L. Gilliland, *Biochemistry* **1988**, *27*, 2705-2717.

[8]   R.A. Scott, H.A. Scheraga, *J. Am. Chem. Soc.* **1963**, *85*, 3866-3873.

[9]   K.M. Rajkowski, N. Cittanowa, *J. Theor. Biol.* **1981**, 93, 691-696.

[10]   C. Tanford, K.C. Aune, *Biochemistry* **1970**, *9*, 206-211.

[11]   R.F. Greene, C.N. Pace, *J. Biol. Chem.* **1974**, *249*, 5388-5393.

[12]   J.A. Schellman, *Biopolymers* **1978**, *17*, 1305-1322.

[13]   J.A. Schellman, *Biopolymers* **1987**, *26*, 459-559.

[14]   D.O. Alonso, K.A. Dill, *Biochemistry* **1991**, *30*, 5974-5985.

[15]   J.A. Knapp, C.N. Pace, *Biochemistry* **1974**, *13*, 1289-1294.

[16]   J.K. Myers, C.N. Pace, J.M. Scholtz, *Protein Sci* **1995**, *4*, 2138-2148.

[17]   J.C. Garcia-Borron, J. Escribano, M. Jimenez, J.L. Iborra, *Anal Biochem.* **1982**, *125*, 277-285.

[18]   P.M. Froehlich, M. Yeats, *Anal. Chim. Acta* **1976**, *87*, 185-191.

[19]   N. Poklar, N. Petrovčič, M. Oblak, G. Vesnaver, *in preparation.*

POVZETEK

Vpliv guanidinijevega hidroklorida (GuHCl), sečnine in nekaterih alkil sečnin na stabilnost ribonukleaze A (RNase A) v vodnih raztopinah pri 25 °C smo raziskovali z merjenjem lastne emisijske fluorescence proteina v odvisnosti od koncentracije dodanega denaturanta. Pokazali smo, da je GuHCl znatno močnejši denaturant od sečnine in da v raztopinah alkil sečnin ne moremo doseči popolne denaturacije RNase A celo pri najvišjih možnih koncentracijah denaturanta. Vzrok za takšno obnašanje smo pripisali nižjim denaturacijskim sposobnostim in / ali nižjim topnostim alkil sečnin. Rezultati merjenja emisijske fluorescence se za RNase A v raztopinah omenjenih denaturantov dobro ujemajo z rezultati merjenj odgovarjajoče fluorescenčne polarizacije, ki smo jih izvedli pri enakih pogojih merjenja. Fluorescenčne emisijske spektre RNase A smo primerjali tudi z ustreznimi izmerjenimi spektri modelnega dipeptida, ki vsebuje eno tirozinsko skupino. Pokazali smo, da so spremembe lastne emisijske fluorescence RNase A, ki jih opazimo pri visokih koncentracijah denaturantov v prvi vrsti posledica razvitja proteina.

THERMODYNAMICS OF MICELLIZATION OF N-ALKYLPYRIDINIUM CHLORIDES: A POTENTIOMETRIC STUDY

Barbara Simončič, Jože Špan

University of Ljubljana, Faculty of Natural Sciences and Engineering,
Department of Textiles, Ljubljana, Slovenija

Abstract

The critical micelle concentration (CMC) and the thermodynamic functions ΔG^o_{mic}, ΔH^o_{mic} and ΔS^o_{mic} for the micellization process of the two pyridinium cationic surfactants N-dodecylpyridinium chloride (DPC) and N-cetylpyridinium chloride (CPC) in aqueous solution were studied by a potentiometric method using surfactant cation-sensitive membrane electrodes. The e.m.f. of the galvanic cell was measured as a function of surfactant concentration at temperatures of 15, 25, 35 and 45°C at different concentrations of added NaCl (0.00, 0.01, 0.05, 0.1 and 0.5 mol kg^{-1}). The properties of the DPC/CPC mixture were also investigated. The results indicate that the CMC decreases as the hydrophobic character of the surfactant increases and that the addition of NaCl favours the micellization of both studied surfactants. Increase of temperature from 25°C to 45°C did not cause a noticeable change in the CMC of DPC, but resulted in a slight increase in the CMC of CPC. Inspection of the data for thermodynamic functions of micellization shows that the micellization of the studied surfactants is governed mainly by hydrophobic interactions between the surfactant cations, and that CPC forms micelles more readily than DPC under the same conditions.

Introduction

Surfactants are widely used in different practical applications such as washing, cleaning, wetting, dispersing, emulsifying and foaming. The use of surfactants as levelling and retarding agents in textile dyeing is also of great importance. Cationic surfactants are commonly used in these processes. There are two characteristic features of surfactants, surface activity and the ability to form micelles in solution, which affect

the performance of surfactants. According to the literature data [1-5], much research has been focused on the development of new methods for studying the behaviour of surfactant solutions and the influence of different factors on surfactant properties.

In this paper, a potentiometric method was used to study the thermodynamic aspects of the micellization of the two cationic surfactants N-cetylpyridinium chloride and N-dodecylpyridinium chloride in aqueous solutions in single component and mixed surfactant systems. This method, based on the use of surfactant cation-sensitive membrane electrodes, allows direct determination of the concentration at which surfactant cations tend to form micelles in solution.

Experimental

Surfactants N-dodecylpyridinium chloride (DPC), N-cetylpyridinium chloride (CPC) and sodium dodecylsulfate (SDS) were commercial products from Aldrich-Chemical Co. and were purified by four recrystallizations from acetone. All solutions were prepared in double distilled water by weight and expressed in molal concentrations.

Ion selective electrodes were prepared according to the well-known method [6] that was described previously [7]. These electrodes include the surfactant cation - surfactant anion complex incorporated within a poly(vinyl chloride) gel membrane.

Potentiometric measurements were carried out in the following electrode cell:
Ag Ι AgCl Ι reference solution; $1 \cdot 10^{-4}$ mol kg^{-1} S$^+$Cl$^-$ + 0.1 mol kg^{-1} NaCl Ι polymer membrane + S$^+$DS$^-$ Ι test solution of S$^+$Cl$^-$, ΙΙ KCl (satd.) Ι Hg$_2$Cl$_2$ Ι Hg,
where S$^+$ represents the DPC or CPC surfactant cation and DS$^-$ the SDS surfactant anion. The electrode was tested against a reference calomel electrode (Model HEK 0301, Iskra, Slovenia) via an ammonium nitrate salt bridge and the potential difference was measured with an MA 5740 mV-meter (Iskra, Slovenia).

The dependence of e.m.f. of the cell versus the surfactant concentration, m_S, in the test solution was measured in the concentration range $4 \cdot 10^{-6}$ to $4 \cdot 10^{-2}$ mol kg^{-1} for DPC and $2 \cdot 10^{-6}$ to $3 \cdot 10^{-3}$ mol kg^{-1} for CPC in aqueous solution at 15, 25, 35 and 45°C ($\pm 0.1^o$C), and also in the presence of different fixed amounts of added NaCl (0.01,

0.05, 0.10 and 0.50 mol kg^{-1}). Potentiometric measurements were also performed in mixtures of the studied surfactants DPC and CPC at 25°C, in two different ways. The first experiment included e.m.f. measurements at different concentrations of CPC in the test solution containing fixed amounts of DPC (1·10^{-4} and 1·10^{-3} mol kg^{-1}). For this experiment the CPC cation-sensitive membrane electrode was used. In the second experiment a mixture of CPC and DPC (1:1) was added to the test solution in discrete steps, and the resulting potential difference was measured using the CPC- as well as the DPC-selective membrane electrode.

Results

In order to estimate the CMC of the studied surfactants a series of plots of measured e.m.f. (E) versus the logarithm of the concentration (log m_S) of DPC and CPC in aqueous solutions at different temperatures and concentrations of added NaCl salt were made. Fig. 1 and 2 show some representative plots. Plots of E versus log m_S for DPC and CPC in mixtures of the studied surfactants at 25°C are shown in Fig. 3.
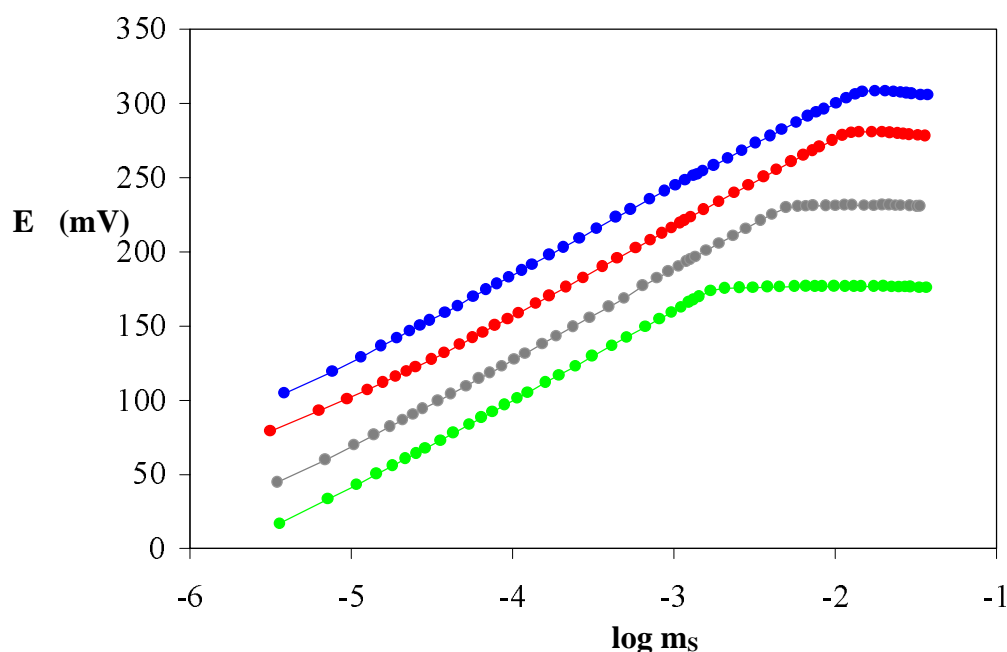
Fig. 1. Plots of e.m.f. (E) of the cell vs the log of DPC concentration (log m_S) in the presence of different concentrations of NaCl at 35°C.
-●-●-: 0 m NaCl, -●-●-: 0.01 m NaCl, -●-●-: 0.10 m NaCl, -●-●-: 0.50 m NaCl.
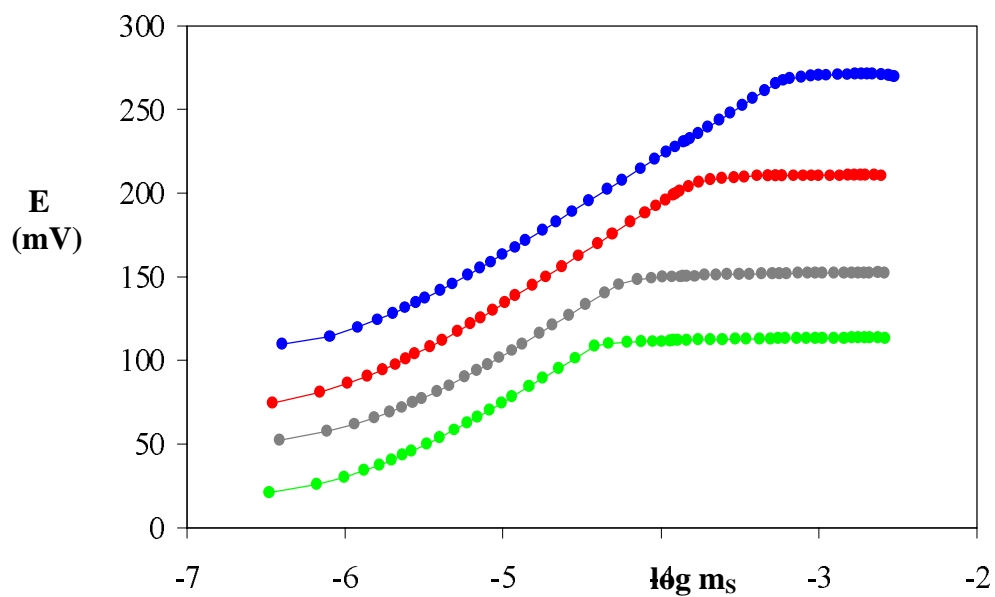
Fig. 2. Plots of e.m.f. (E) of the cell vs the log of CPC surfactant concentration (log m_S) in the presence of different concentrations of NaCl at 35^oC.
-●-●-: 0 m NaCl, -●-●-: 0.01 m NaCl, -●-●-: 0.05 m NaCl, -●-●-: 0.10 m NaCl.
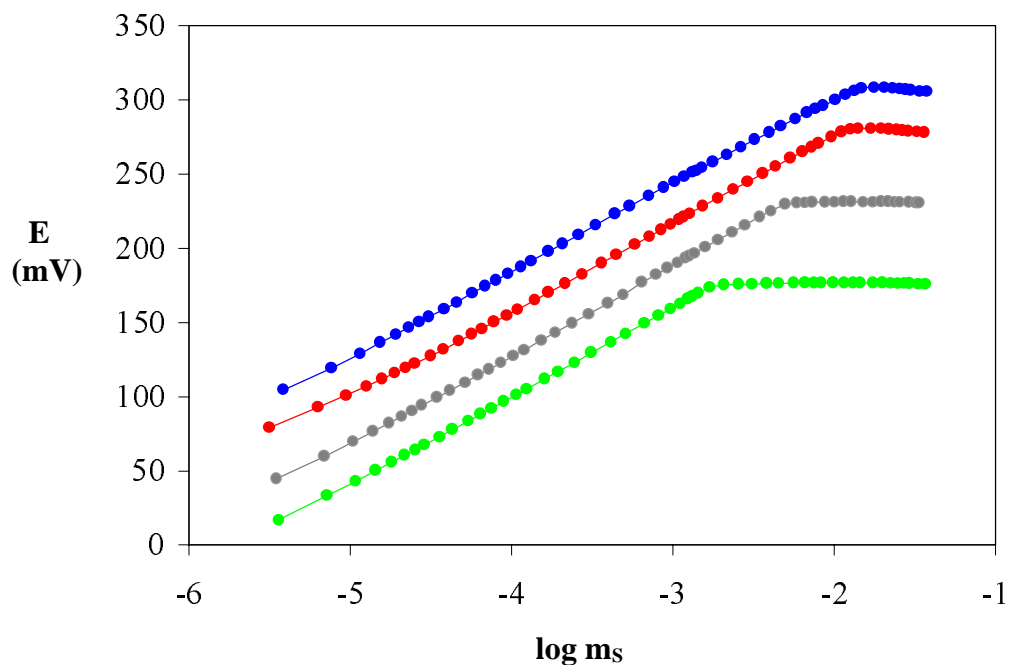
Fig. 3. Plots of e.m.f. (E) of the cell vs the log of surfactant concentration (log m_S) for DPC or CPC in mixtures of the studied surfactants at 25^oC.

-●-●-: E vs log m_S of CPC in $1.0 \cdot 10^{-4}$ m DPC, -●-●-: E vs log m_S of CPC in $1.0 \cdot 10^{-3}$ m DPC, -●-●-: E vs log m_S of CPC in the mixture of CPC and DPC (1:1), -●-●-: E vs log m_S of DPC in the mixture of CPC and DPC (1:1).

As evident from the figures, the e.m.f. response is linear over the concentration range $1 \cdot 10^{-6}$ mol kg^{-1} to the CMC with excellent agreement with the Nernstian response [8], and that a break of the potentiometric curve was observed above the CMC. The concentration at the point of intersection of the two linear portions of the E - log m_S plots was taken as the CMC and is presented in Table 1.

TABLE 1
Thermodynamic functions of micellization of DPC and CPC in aqueous solutions

Surfactant	T (^{o}C)	NaCl (mol/kg)	CMC (mol/kg)	K_g	ΔG^{o}_{mic} (kJ/mol)	ΔH^{o}_{mic} (kJ/mol)	ΔS^{o}_{mic} (J/molK)
DPC	15	0.00	$1.56 \cdot 10^{-2}$	0.83	-18.8	-4.4	50.0
		0.01	$1.30 \cdot 10^{-2}$				
		0.10	$5.24 \cdot 10^{-3}$				
		0.50	$1.82 \cdot 10^{-3}$				
	25	0.00	$1.49 \cdot 10^{-2}$	0.80	-19.4	-4.4	50.3
		0.01	$1.18 \cdot 10^{-2}$				
		0.10	$4.99 \cdot 10^{-3}$				
		0.50	$1.79 \cdot 10^{-3}$				
	35	0.00	$1.34 \cdot 10^{-2}$	0.75	-19.9	-4.4	50.3
		0.01	$1.22 \cdot 10^{-2}$				
		0.10	$5.06 \cdot 10^{-3}$				
		0.50	$1.88 \cdot 10^{-3}$				
	45	0.00	$1.34 \cdot 10^{-2}$	0.73	-20.3	-4.4	50.6
		0.01	$1.18 \cdot 10^{-2}$				
		0.10	$5.26 \cdot 10^{-3}$				
		0.50	$1.96 \cdot 10^{-3}$				
CPC	15	0.00	$5.98 \cdot 10^{-4}$	≈0.69	-32.1	6.5	134.0
		0.01	$1.30 \cdot 10^{-4}$				
		0.10	$3.56 \cdot 10^{-5}$				
	25	0.00	$5.31 \cdot 10^{-4}$	0.75	-32.8	6.5	131.8
		0.01	$1.53 \cdot 10^{-4}$				
		0.05	$5.91 \cdot 10^{-5}$				
		0.10	$3.64 \cdot 10^{-5}$				
	35	0.00	$4.38 \cdot 10^{-4}$	0.75	-34.8	6.5	134.0
		0.01	$1.85 \cdot 10^{-4}$				
		0.05	$6.71 \cdot 10^{-5}$				
		0.10	$4.43 \cdot 10^{-5}$				
	45	0.01	$2.18 \cdot 10^{-4}$	/	/	/	/

148

		0.10	$4.89 \cdot 10^{-5}$				
DPC–CPC mixture	25	0.00	$4.27 \cdot 10^{-4}$ * $3.81 \cdot 10^{-4}$ **	/	/	/	/

* CPC cation-sensitive membrane electrode was used

** DPC cation-sensitive membrane electrode was used

The CMC values determined for DPC are in good agreement with the literature data, where in pure water a CMC value of $1.24 \cdot 10^{-2}$ mol dm^{-3} at 30°C was obtained by isothermal microcalorimetry [9], a value of $1.62 \cdot 10^{-2}$ mol dm^{-3} at 25°C from surface tension measurements and a value of $1.78 \cdot 10^{-2}$ mol dm^{-3} at 25°C from conductance measurements [10]. On the other hand, the CMC value of $5.31 \cdot 10^{-4}$ mol kg^{-1} determined for CPC at 25°C in pure water is lower than the literature value of $9.0 \cdot 10^{-4}$ mol dm^{-3}, which was obtained by Hartley [11]. It is interesting that our CMC value of $8.7 \cdot 10^{-3}$ mol kg^{-1} determined for SDS at 25°C, using the same ion selective electrode, is in good agreement with the value of $8.0 \cdot 10^{-3}$ mol dm^{-3} obtained by Kale et. al. from potentiometric measurements [12]. The CMC values as a function of the temperature and the concentration of added NaCl for DPC and DPC are shown in Fig. 4.

Fig. 4. Experimental ... oncentrations of a... stems.
-●-●-: DPC in pu... 0.10 m NaCl,
-●-●-: DPC in ... in 0.10 m

Thermodynam... mass-action approach. Theref... CPC may be described as [13]:

$$nS^+ + (n-p)C^- \rightleftharpoons \quad (1)$$

$$(n-p) \equiv Kg$$
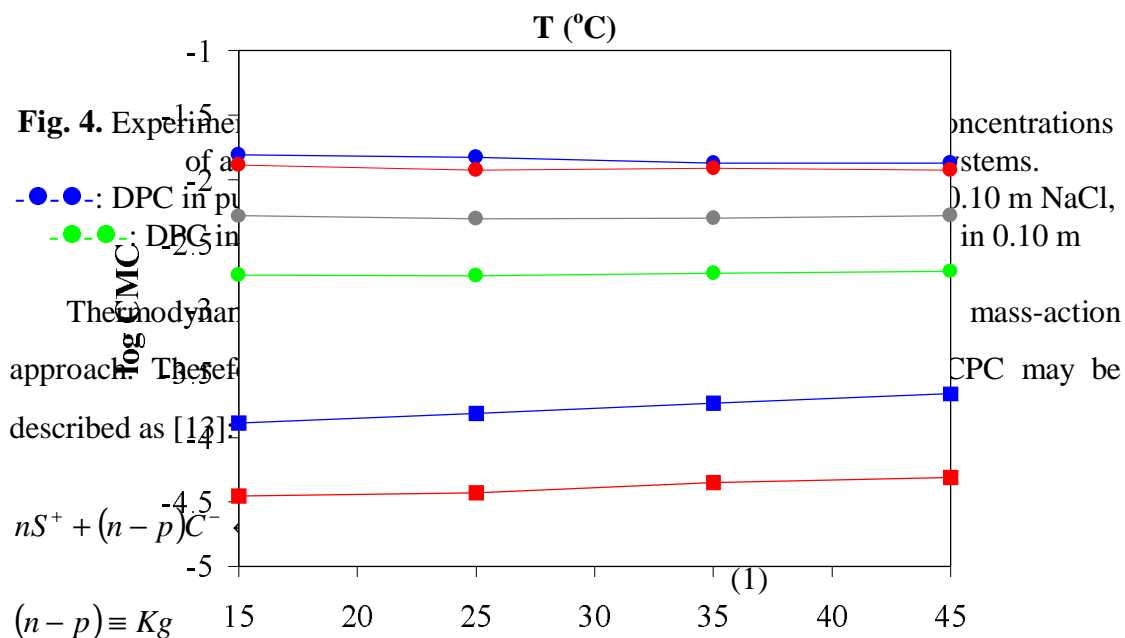
where S^+ represents the surfactant cations, C^- the chloride counterions, and M^{p+} the aggregate of n surfactant monomers with an effective charge of p. K_g is the effective coefficient of electrical energy of micellization.[11].

The standard free energy, ΔG^o_{mic}, of micellization per mole of monomeric surfactant can be calculated as follows [11]:

where m_S and m_C are the molal concentrations of the surfactant cation and the chloride counterion in the solution at the CMC respectively, and γ_+ and γ_- are the activity coefficients of the surfactant and chloride ions. The activity coefficients can be calculated from the Debye-Hückel equation [11]:

$$(3)$$

where α is the mean distance of approach of the ions and is taken 0.6Å for the surfactant ion and 0.3Å for the Cl⁻ counterion. The total ionic strength, I, of the solution is equal to:

$$I = \frac{1}{2}\sum_i m_i z_i^2$$

$$(4)$$

Assuming that ΔG^o_{mic} does not change significantly with change in the concentration of m_C, then K_g can be evaluated from the negative slope of the linear plot of [log CMC + log γ_+] versus [log m_C + log γ_-] [11].

For determining the standard enthalpy change, ΔH^o_{mic}, and the standard entropy change, ΔS^o_{mic}, for the micellization process, the well-known equations [14]:

$$(5)$$

$$\Delta S^o_{mic} = \frac{\Delta H^o_{mic} - \Delta G^o_{mic}}{T} \qquad (6)$$

were used. From eqn (5) it can be seen that if $\Delta G^o_{mic}/T$ is plotted against $1/T$, the slope of the curve at any temperature is equal to ΔH^o_{mic} at this temperature. The results show that the relationship between $\Delta G^o_{mic}/T$ and $1/T$ is practically linear within experimental error, indicating ΔH^o_{mic} is constant over the measured temperature range. It should be emphasized, that because of the small CMC changes over the measured temperature range, the inaccuracies in the log(CMC) vs T slopes are rather large, therefore the ΔH^o_{mic} value calculated from eqn (5) should be considered as only approximate. The thermodynamic quantities for micellization of DPC and CPC are collected in Table 1.

Discussion

The results show that the surfactant's structure, the addition of electrolyte and the temperature influence the micellar properties of the studied surfactants. As expected, the CMC depends on the hydrophobic character of the surfactants. It decreases with increasing length of the hydrocarbon chain of the surfactant. When the number of carbon atoms in the hydrophobic group rises from 12 to 16 the CMC decreases by a factor of 28 at 25^oC in pure water. This factor changes only slightly with change in temperature. It is also seen that the small amount of added NaCl decreases the CMC of the studied surfactants (Fig. 4). This is due to the decrease in the electrical repulsion between the positively charged head groups in the micelle in the electrolyte solution. The effect of added NaCl on the CMC is much more pronounced for CPC than for DPC. Experimental data also indicate that an increase in the temperature appears to cause a minimal change in the CMC for DPC over the measured temperature range, and that the CMC of CPC increases slightly with increasing temperature (Fig. 5), independent of the added salt concentration. This behaviour is consistent with the fact that disruption of the structured water surrounding the hydrophobic group induced by the temperature increase, is more effective for CPC with its longer alkyl chain than for

DPC. These results are in good agreement with the results obtained for alkylpyridinium bromides [15].

The CMC of the mixture of DPC and CPC is lower than that of CPC and of DPC in single-component systems. In this case, mixed micelles of the studied surfactants occur in the mixture and the system is said to exhibit synergism in mixed micelle formation [11,16].

The results also show that the ΔH^{o}_{mic} value calculated for DPC is negative indicating that the micellization process of the studied surfactant is exothermic. The value of –4.4 kJ/mol for DPC is in good agreement with literature data obtained for alkylpyridinium bromide by potentiometric and calorimetric measurements [15]. On the other hand it should be mentioned that the ΔH^{o}_{mic} value of +6.5 kJ/mol observed for CPC is not in agreement with the explanation that exothermicity increases with increasing alkyl chain length [13,15]. It is seen that this value is positive in sign indicating the endothermic process. This result could be a consequence of a large error in calculating the temperature derivative of CMC at very low CMC values.

According to the large, positive values of ΔS^{o}_{mic} for both studied surfactants, the system becomes more random after micellization. The positive values of ΔS^{o}_{mic} clearly indicate that the micellization of the studied surfactants in aqueous solution is governed mainly by hydrophobic interactions between the surfactant cations resulting in the breakdown of the structured water surrounding the hydrophobic groups. Because more water is released during micellization of surfactacts with longer alkyl chains the ΔS^{o}_{mic} value of 131.8 J/molK determined for CPC at 25°C is larger than the value of 50.3 J/molK obtained for DPC under the same experimental conditions.

Inspection of the values of ΔG^{o}_{mic} for DPC and CPC shows, that ΔG^{o}_{mic} decreases with increasing temperature meaning that an increase in temperature tends to drive the equilibrium toward the hydrophobic bonding, and that CPC forms micelles more readily than DPC under the same conditions.

References

[1]   M. J. Rosen, A. W. Cohen, M. Dahanayake and X. Hua, *J. Phys. Chem.*, **1982**, 86, 541-545.

[2]   K. Shinoda, M. Kobayashi and N. Yamaguchi, *J. Phys. Chem.*, **1987**, 91, 5292-5294.

[3]   J. M. Rio, G. Prieto, F. Sarmiento and V. Mosquera, *Langmuir*, **1995**, 11, 1511-1514.

[4]   J. E. Desnoyers, G. Caron, S. Beaulieu and G. Perron, *Langmuir*, **1995**, 11, 1905-1911.

[5]   J. Eastoe, P. Rogueda, D. Shariatmadaria and R. Heenan, *Colloids and Surfaces*, **1996**, 117, 215-225.

[6]   S. G. Cutler, P. J. Meares and D. G. Hall, *Electroanal. Chem.*, **1977**, 85, 145-148.

[7]   B. Siomončič and J. Špan, *Dyes and Pigments*, **1998**, 1, 1-14.

[8]   W. E. Morf, *The Principles of Ion-Selective Electrodes and of Membrane Transport.* Akademiai Kiado, Budapest, Hungary, 1981.

[9]   T. Mehrian, A. Keizer, A. J. Korteweg and J. Lyklema, *Colloids and Surfaces A: Physicochemical and Engineering Aspects*, **1993**, 71, 255-267.

[10]   M. J. Rosen, M. Dahanayake and A. W. Cohen, *Colloids and Surfaces*, **1982**, 5, 159-172.

[11]   M. J. Rosen, *Surfactants and Interfacial Phenomena*, John Wiley and Sons, Inc., New York, USA, 1989.

[12]   K. M. Kale, E. L. Cussler and D. F. Evans, *J. Phys. Chem.*, **1980**, 84, 593-598.

[13]   R. J. Hunter, in *Foundations of Colloid Science*, Clarendon Press, Oxford, 1987, vol. 1, p. 593.

[14]   W. J. Moore, *Physical Chemistry*, 5th edn., Longman, London, GB, 1972.

[15]   M. Bežan, M. Malavašič, G. Vernaver, *J. Chem. Soc. Faraday Trans.*, **1993**, 89(14), 2445-2449.

[16]   K. Ogino and M. Abe, Mixed Surfactant Systems, Surfactant Science Series, Vol. 46, Marcel Dekker, Inc., New York, USA, 1993.

Povzetek

Kritično koncentracijo micelov (CMC) in termodinamske funkcije micelizacije ΔG^o_{mic}, ΔH^o_{mic} in ΔS^o_{mic} dveh kationskih piridinijevih tenzidov N-dodecilpiridinijevega klorida (DPC) in N-cetilpiridinijevega klorida (CPC) v vodni raztopini smo določili s potenciometrično metodo, ki temelji na uporabi ionoselektivne membranske elektrode, občutljive za katione tenzida. Meritve napetosti galvanskega člena v odvisnosti od koncentracije tenzida smo opravili pri temperaturah 15, 25, 35 in 45°C pri različnih dodatkih soli NaCl (0.00, 0.01, 0.05, 0,10 in 0.50 mol kg^{-1}). Ob tem smo proučevali tudi lastnosti mešanice tenzidov DPC in CPC. Iz rezultatov meritev je razvidno, da se z večanjem hidrofobnega karakterja tenzida CMC zmanjšuje. Dodatek NaCl v raztopino proučevanih tenzidov pogojuje micelizacijo DPC kot tudi CPC. Zvišanje temperature od 25°C do 45°C bistveno ne vpliva na spremembo CMC tenzida DPC, medtem ko povzroči rahlo naraščanje CMC tenzida CPC. Na podlagi vrednosti termodinamskih funkcij lahko zaključimo, da so pri procesu micelizacije proučevanih tenzidov v vodni raztopini pomembne hidrofobne interakcije.

EXCESS MOLAR VOLUMES OF BINARY LIQUID MIXTURES OF CYCLOHEXANE - CARBON TETRACHLORIDE AND TOLUENE - BENZENE AT VARIOUS TEMPERATURES

A. Petek, V. Doleček

Faculty of Chemistry and Chemical Engineering, University of Maribor, Smetanova 17,

2000 Maribor, Slovenia

Abstract: Excess molar volumes of binary mixtures of cyclohexane - carbon tetrachloride at 288.15, 293.15, 298.15 K and of toluene - benzene at 293.15, 298.15, 308.15 K have been determined using a vibrating tube densimeter.
Flory's theory of liquid mixture has been applied to calculate the excess enthalpy of cyclohexane - carbon tetrachloride at 298,15 K; the calculated value for the equimolar mixture is in fairly good agreement with experimental results.

INTRODUCTION

Excess molar volumes of binary mixtures of cyclohexane - carbon tetrachloride and toluene - benzene are presented in this paper. The toluene - benzene system which forms nearly ideal solutions has been used as reference system.

The aim of our work was to calculate the excess enthalpy from measured excess volumes, using the statistical Flory's theory of liquid mixtures [1]. Flory has developed an approach which relates the excess properties of a mixture to measurable macroscopic properties of pure liquid components by a partition function. This theory has been very useful in predicting the thermodynamic properties of binary mixtures of nonpolar

molecules such as hydrocarbons (normal, branched, cyclic and aromatic) and halocarbons [2,3]. In this work we use this approach to the mixture of cyclohexane - carbon tetrachloride with a moderate polarity.

EXPERIMENTAL

Cyclohexane (Kemika, Zagreb), carbon tetrachloride (Carlo Erba), toluene (Kemika) and benzene (Riedel - de Haen), with p.a. stated purity, were used without further purification. The investigation of sources of errors in V^E by Lepory et al. [4] showed namely, that purity of substances was not a crucial factor in V^E measurements.

Densities were measured, using a vibrating tube densimeter A.Paar DMA 60/602, at 288.15, 293.15, 298.15 and 308.15 K. Temperature control of the cell was $\pm 5 \cdot 10^{-3}$ ^{0}C. Before each series of measurements, the instrument was calibrated with doubly distilled water and dry air at atmospheric pressure. The density d, of any liquid relative to the density of pure water d_w, is given by

$$d = d_w + k \, (T^2 - T^2_w)$$ (1)

where k is the characteristic of a particular oscillator. T^2 and T^2_w are vibration periods of the tube, filled with liquid and with water, respectively. The determined densities [5,6] are accurate to at least $\pm 10^{-5}$ g cm^{-3}. For pure cyclohexane, benzene, toluene and carbon tetrachloride they agreed well with literature values [7-10,12-14]. The mixtures were prepared by weight. The values of V^E determined from density measurements are accurate within ± 0.0005 cm^3 mol^{-1}.

RESULTS AND DISCUSION

Excess molar volumes V^E of binary mixtures of cyclohexane (1)- carbon tetrachloride (2) and toluene (1) - benzene (2) were calculated from the corresponding density measurements using the equation

$$V^E \, (cm^3 \, mol^{-1}) = x_1 \, M_1 \, (d_m^{-1} - d_1^{-1}) + x_1 \, M_1 \, (d_m^{-1} - d_2^{-1})$$ (2)

where x_i is the molar fraction of component i, and d_m and d_i are the densities of the mixture and pure component i, respectively. M_i are the molar masses of the pure components. The obtained results are listed in Table 1 and Table 2.

Table 1: Densities and excess molar volumes V^E of binary mixtures of toluene(1) - benzene(2) at 293.15, 298.15 and 308.15 K

293.15 K			298.15 K			308.15 K		
X_2	d (g cm^{-3})	V^E (cm^3 mol^{-1})	X_2	d (g cm^{-3})	V^E (cm^3 mol^{-1})	X_2	d (g cm^{-3})	V^E (cm^3 mol^{-1})
0.00000	0.86685	0.0000	0.00000	0.86223	0.0000	0.00000	0.85299	0.0000
0.10676	0.86771	0.0280	0.09093	0.86291	0.0238	0.07520	0.85346	0.0209
0.16292	0.86818	0.0421	0.16471	0.86349	0.0415	0.24456	0.85459	0.0645
0.23090	0.86876	0.0593	0.23253	0.86403	0.0585	0.26568	0.85461	0.0851
0.29499	0.86937	0.0696	0.24830	0.86416	0.0621	0.28276	0.85486	0.0736
0.34447	0.86987	0.0752	0.29065	0.86456	0.0662	0.31242	0.85507	0.0809
0.38214	0.87027	0.0779	0.33250	0.86494	0.0728	0.37459	0.85559	0.0875
0.40612	0.87050	0.0828	0.37787	0.86536	0.0797	0.40639	0.85587	0.0898
0.45288	0.87099	0.0882	0.41849	0.86578	0.0814	0.47647	0.85652	0.0922
0.48365	0.87135	0.0880	0.48448	0.86647	0.0849	0.59077	0.85766	0.0910
0.51775	0.87175	0.0882	0.52499	0.86691	0.0861	0.59490	0.85770	0.0912
0.54412	0.87202	0.0931	0.57627	0.86751	0.0837	0.68986	0.85876	0.0817
0.58951	0.87264	0.0851	0.59444	0.86772	0.0835	0.73848	0.85933	0.0755
0.65377	0.87346	0.0820	0.63416	0.86821	0.0801	0.75586	0.85955	0.0717
0.75732	0.87492	0.0667	0.69181	0.86894	0.0746	0.80325	0.86016	0.0612
0.81199	0.87572	0.0580	0.73162	0.86947	0.0689	0.85483	0.86082	0.0515
0.86405	0.87641	0.0588	0.79248	0.87032	0.0577	0.90854	0.86159	0.0341
0.90216	0.87717	0.0339	0.85753	0.87128	0.0425	0.95616	0.86229	0.0182
0.94521	0.87777	0.0338	0.89630	0.87187	0.0328	1.00000	0.86298	0.0000
1.00000	0.87888	0.0000	0.95441	0.87282	0.0132			
			1.00000	0.87356	0.0000			

Table 2: Densities and excess molar volumes V^E of binary mixtures of cyclohexane(1) - carbon tetrachloride(2) at 288.15, 293.15 and 298.15 K

288.15 K			293.15 K			298.15 K		
X_2	d (g cm^{-3})	V^E (cm^3 mol^{-1})	X_2	d (g cm^{-3})	V^E (cm^3 mol^{-1})	X_2	d (g cm^{-3})	V^E (cm^3 mol^{-1})
1.00000	1.60374	0.000	1.00000	1.59311	0.000	1.00000	1.58427	0.000
0.95162	1.55895	0.035	0.95243	1.55008	-0.008	0.95118	1.53959	0.039
0.89768	1.50984	0.063	0.89964	1.50223	0.026	0.89982	1.49347	0.062
0.85224	1.46883	0.096	0.85152	1.45925	0.051	0.84930	1.44861	0.088
0.80115	1.42346	0.121	0.79943	1.41332	0.077	0.79976	1.40527	0.106
0.69971	1.33524	0.154	0.69900	1.32651	0.116	0.70118	1.32036	0.156
0.59972	1.25030	0.191	0.59972	1.24271	0.156	0.59743	1.23358	0.174
0.49878	1.16713	0.179	0.49878	1.16003	0.150	0.49892	1.15360	0.146
0.39881	1.08633	0.192	0.40045	1.08070	0.198	0.40045	1.07416	0.235
0.30000	1.00839	0.190	0.30077	1.00295	0.160	0.29962	0.99606	0.187
0.20020	0.93158	0.166	0.15004	0.88850	0.099	0.20087	0.92094	0.168
0.14949	0.89325	0.145	0.09949	0.85101	0.067	0.15021	0.88361	0.086
0.10266	0.85857	0.081	0.05004	0.81477	0.028	0.10291	0.84864	0.064
0.04667	0.81738	0.023	0.00000	0.77838	0.000	0.04739	0.80818	0.019
0.00000	0.78320	0.000				0.00000	0.77386	0.000

Each set of experimental results as fitted to the Redlich - Kister equation [11]

$$V^E \ (cm^3 \ mol^{-1}) = x_1 \ x_2 \ \sum_{i=0}^{n} \ A_i \ (1 - 2 \ x_2)^i \qquad (3)$$

Values of coefficients A_i are listed in Table 3, together with the standard deviation of the fit, σV^E, defined as

$$\sigma V^E = \left[\sum (V_{exp}^E - V_{calc}^E)^2 \ / \ (N - n) \right]^{1/2} \quad , \qquad (4)$$

where N is the number of data points and n is the number of coefficients.

Table 3: Coefficients A_i and standard deviation σV^E of equation (3)

	$T \ (K)$	A_0	A_1	A_2	A_3	$\sigma V^E \ (cm^3 \ mol^{-1})$
cyclohexane-carbon	288.15	0.7967	0.2549	0.1356	-0.1290	0.013
tetrachloride	293.15	0.6903	0.2970	-0.2709	-0.1113	0.012
	298.15	0.8129	0.5045	-0.1836	-0.8788	0.022
toluene-benzene	293.15	0.3535	-0.0356	-0.0218	-0.0320	0.0052
	298.15	0.3465	-0.0291	-0.0491	0.0090	0.0012
	308.15	0.3770	-0.0092	-0.0211	-0.0867	0.0167

The V^E of both mixtures are positive throughout. However, they are significantly smaller for toluene-benzene mixture, which is nearly ideal solution, than for the cyclohexane-carbon tetrachloride system. Positive values can be explained by the predominance of expansion in volume, caused by the loss of dipolar association and difference in size and shape of component molecules, over contraction in volumes, due to the dipole-dipole and dipole-induced dipole interactions.

Ocon, Tojo, Espada [12] have determined V^E of cyclohexane-carbon tetrachloride at 293.15 K. Our results for this mixture at 293.15 K are compared with literature ones in Fig.1; it can be seen, that our values are higher in a part of the curve ($X_2 = 0.4$-0.5). The reason may be in additional purification of chemicals [12].
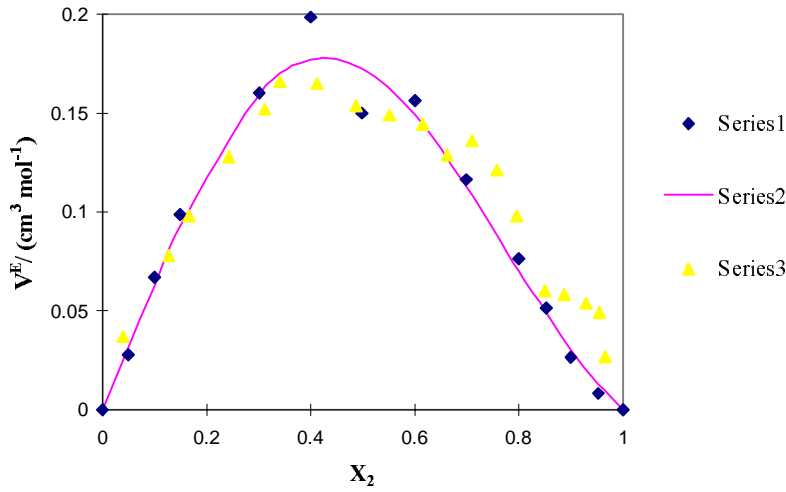
Fig.1: Experimental V^E for cyclohexane-carbon tetrachloride at 293.15 K (series 1); Ocon, Tojo, Espada (series 3); calculated values based upon equ. 3 (series 2)

Analysis in terms of the Flory theory

The interaction parameter χ_{12} in Flory's theory can be calculated from experimental excess volume data and should be used further to obtain H^E. Details were given by Flory (1965) and Abe, Flory (1965). Symbols in the following equations have their usual meaning and are explained at the end of the text:

$$V^E = \frac{(\tilde{v}^0)^{7/3}}{(4/3) - (\tilde{v}^0)^{1/3}} (\tilde{T} - \tilde{T}^0) (X_1 V_1^* + X_2 V_2^*), \tag{5}$$

$$H^E = X_1 P_1^* V_1^* (1/\tilde{v}_1 - 1/\tilde{v}) + X_2 P_2^* V_2 (1/\tilde{v}_2 - 1/\tilde{v}) + X_1 V_1^* \Theta_2 \chi_{12}/\tilde{v}, \tag{6}$$

where $\tilde{v}^0 = \Phi_1 \tilde{v}_1 + \Phi_2 \tilde{v}_2$, $\tag{7}$

$$\tilde{T} = \frac{\Phi_1 P_1^* T_1 + \Phi_2 P_2^* \tilde{T}}{\Phi_1 P_1^* + \Phi_2 P_2^* - \Phi_1 \Theta_2 \chi_{12}}, \tag{8}$$

$$\tilde{v}_i^{1/3} - 1 = \frac{\alpha_i T}{3(1 + \alpha_i T)}, \tag{9}$$

$$\Phi_1 = 1 - \Phi_2 = \frac{X_1 V_1^*}{X_1 V_1^* + X_2 V_2^*} \tag{10}$$

The key quantity of the theory, the interchange energy parameter χ_{12}, was fitted to equimolar experimental values of V^E for cyclohexane-carbon tetrachloride at 298.15 K. The resulting χ_{12} was used to calculate H^E, along with the pure component parameters

(α_i from Wood, Gray [14] and γ_i from Holder, Whalley [15]) as given in Table 4. Comparison between calculated and experimental (Adcock and McGlashan [16]) excess enthalpy, and TS^E is given in Table 5.

Table 4: The parameters of pure liquid component used in Flory′s theory

component	c-C_6H_{12}	CCl_4
$V_i \, (cm^3 / mol)$	108.75	97.08
$\alpha_i \cdot 10^3 \, (K^{-1})$	1.217	1.229
$\gamma_i \, (J / cm^3 \, K)$	1.067	1.143
$\tilde{v}_i$	1.2904	1.2927
$\tilde{T}_i$	0.06314	0.06345
$P_i^* \, (J / cm^3)$	532	569
$V_i^* \, (cm^3 / mol)$	84.28	75.10
$T_i^* \, (K)$	4720	4697
Φ_i	0.5288	0.4712
Θ_i	0.5192	0.4808

Table 5: Calculated (Flory′s theory) and experimental H^E (X=0.5) and TS^E (X=0.5) values for the cyclohexane-carbon tetrachloride system, at 298.15 K

χ_{12}	H^E (J/mol)		$T S^E$ (J/mol)	
	calc.	exp.	calc.	exp.
7.9	167	149	78.3	46.5

From Table 5 it can be seen, that the theory predicts H^E reasonably well, even though the calculated value exceeds the experimental by 12%. The agreement in excess entropy is worse; but it is well known, that Flory′s theory can not provide a better conformity for a moderate polarity of molecules.

LIST OF SYMBOLS

H^E excess molar enthalpy

P_i^* characteristic pressure of pure component

T_i^* characteristic temperature of pure component

$\tilde{T}_i$ reduced temperature of component I

V^E excess molar volume

V_i molar volume of pure component

V_i^* characteristic volume of pure component

$\tilde{v}_i$ reduced volume of pure component

X_2 mole fraction of component 2

Θ_2 site fraction of component 2

Φ_2 segment fraction of component 2

γ thermal pressure coefficient

α thermal volume coefficient

χ_{12} interaction parameter

REFERENCES

1. P.J.Flory, *J. Am. Chem. Soc.* **1965**, *87*, 1833-1838

2. A.Abe, P.J.Flory, *J. Am. Chem. Soc.* **1965**, *87*, 1838-1846

3. R.Battino, *Chem. Reviews*, **1971**, *71*, 5-31

4. L.Lepori, M.Mengheri, V.Mollica, *J. Phys. Chem.* **1983**, *87*, 3520-3525

5. V.Hrženjak, *Diplomsko delo* **1995**, FKKT Maribor, 1-33

6. K.Frece, *Diplomsko delo* **1991**, FKKT Maribor, 1-45

7. M.Akl Awwad, A.Kifah Jabra, *Fluid Phase Equil.* **1989**, *47*, 95-102

8. P.Berti, L.Lepori, E.Matteoli, *Fluid Phase Equil.* **1989**, *44*, 285-294

9. D.V.S.Jain, N.S.Dhar, *Fluid Phase Equil.* **1990**, *58*, 173-180

10. W.Riddick, W.B.Bunger, *Organic Solvents* **1970**, John Wiley, NY

11. O.Redlich, A.Kister, *Ind. Eng. Chem.* **1948**, *40*, 345-348

12. J.Ocon, G.Tojo, L.Espada, *An. Chim.* **1969**, *65*, 633-639

13. O.Kiyohara, G.C.Benson, *J. Chem. Thermodyn.* **1977**, *9*, 807-809

14. S.E.Wood, J.A.Gray, *J. Am. Chem. Soc.* **1952**, *74*, 3729-3733

15. G.A.Holder, E.Whalley, *Trans. Faraday Soc.* **1962**, *58*, 2095

16. D.S.Adcock, M.L.McGlashan, *Proc. Roy. Soc.* **1954**, London, *A226*, 266-282

Povzetek: Z gostotomerom smo izmerili gostote raztopin cikloheksana z ogljikovim tetrakloridom pri 288,15, 293,15 in 298,15 K ter raztopin toluena z benzenom pri 293,15, 298,15 in 308,15 K in iz njih izračunali presežne molske volumne.
S pomočjo Flory-jeve teorije za raztopine smo za sistem cikloheksan-ogljikov tetraklorid pri 298,15 K izračunali presežno molsko entalpijo; izračunana vrednost za ekvimolarno mešanico se relativno dobro ujema z experimentalno določeno.

Stability and folding studies of two homologous proteins, human stefins A and B.

Eva Žerovnik[1], Roman Jerala[2] , Louise Kroon-Žitko[1] and Vito Turk[1]

[1] Department of Biochemistry and Molecular Biology, Jožef Stefan Institute,

Jamova 39, 1000 Ljubljana, Slovenia

[2] Laboratory for Molecular Modeling and NMR Spectroscopy, National Institute of Chemistry,

Hajdrihova 19, 1000 Ljubljana, Slovenia

Dedicated to the memory of Professor Savo Lapanje

Abstract: In a shorter Introduction we describe the usual experimental means of how to study protein stability and folding. Our work on stability of human stefins A and B, determined by chemical, heat and pH denaturation, is described next. We explain the folding mechanism of human stefin B (as determined thus far) and compare it to homologous human stefin A, in particular, the dependence of folding rates on the concentration of GuHCl. pH denaturation of human stefin B (E.Žerovnik et al., Eur. J. Biochem. 1997, 245, 364-372) and its folding to the native state are described in more detail.

Introduction

Denaturation [1,2] studies allow the measurement of some basic thermodynamic properties of proteins, which also can be calculated from coordinates of the 3D structures [3]. The mechanism of folding is more difficult to determine as there may be many routes and many intermediate states leading to the native state. The major drive to the native state stems from thermodynamics even though, there are cases where kinetic barriers route proteins into trapped intermediates or meta-stable native states [4]. It is now apparent that 3-state folding with a sequentially placed intermediate on the route from unfolded to the native state is no more an exception [5-7]. The "old" and "new"

views of protein folding [8,9] differ mainly in the way they describe this complex reaction. The old view stresses common conformations - states, whereas the new view points to each separate conformation [9].

Experimentalists collect data on thermodynamics and kinetics of protein folding. One usually starts by determining the stability from heat, pH and chemical denaturation. If multiple spectroscopic probes give coincident transitions this means that there are no populated intermediates. 2-state transition is also revealed by identity of Van't Hoff and calorimetric enthalpies which are obtained by differential scanning calorimetry (DSC).

To determine the kinetics of folding and unfolding, lots of data have to be collected under different experimental conditions. The changes should be studied by different spectroscopic probes which monitor different structural aspects of the process. Rate constants should be determined as a function of denaturant concentration, temperature, pH and selected mutations. Even though the kinetic data can be fit to plausible models these still need to be confirmed. One useful experiment to distinguish between intermediate and native states is measuring unfolding after various times of refolding [10].

New biophysical techniques [11] permit results of high quality and time resolution. For example, advances have been made in multidimensional NMR, where the difficult task of investigating the denatured and partially folded states is achievable [12, 13]. To see which h-bonded structures of protein become protected during folding, quenching of hydrogen to deuterium exchange is followed by NMR or MS measurements. The changes in compactness during folding are getting measured using small angle X-ray scattering [14].

Human stefins A and B were chosen for studies of protein stability and folding due to their relative simplicity : small M_r and no disulphide bonds. Both posess a number of prolines which are in the trans conformation. Sequence similarity of stefins A and B amounts to 56 % and they fold in a very similar 3D conformations (less than 1 Å

deviation of the backbone C-atoms). Despite these similarities they exhibit marked differencies in stability and mechanism of folding. We have determined stability and kinetics of folding using several spectroscopic probes, and have measured the kinetics by fluorescence as a function of temperature, pH and GuHCl concentration. In order to determine the rate-limiting step, the folding was started from various denatured states.

Denaturation and folding studies of human stefins A and B

The two proteins were first isolated from human sources [15-17]. Later, many homologues were identified in the animal kingdom [18-20] and in plants [21]. In Table 1, some representative aminoacid sequences are aligned. Human stefins A and B are members of the cystatin superfamily of cysteine proteinase inhibitors [21,22]. They have been cloned and expressed in E.coli [23,24] and the yield of expression subsequently improved [25]. The 3 D structures of each are determined by X-ray crystallography (human stefin B in complex with papain [26] and by solution NMR (human stefin A [27, 28]).

Initial study was done on folding of human stefin A [29]. GuHCl denaturation [29] , monitored by near UV CD, far UV CD and tyrosine fluorescence, with a midpoint at 2.8 ± 0.1 M GuHCl (25°C, pH 8), showed a reversible, two state unfolding transition. The kinetics of slow folding was measured (10°C, pH 8) by the same three probes. In 2.0 M GuHCl, the kinetics were rather slow (k = 0.002 s^{-1} by all three probes). The amplitudes of the observable phases were 90±10 % by tyrosine fluorescence and near UV CD, but only 20% by the far UV CD. This can be interpreted as kinetically 2-state folding from an initial intermediate possessing 80% of the signal in the far UV CD. "Double jump" experiments were performed and have shown that the slow changes in tyrosine fluorescence reach their complete amplitude only after longer times of unfolding. Except for proline isomerization this might be due to slow unfolding of the core.

In subsequent years, we have focused on recombinant human stefin B. Its denaturation by heat, acid and GuHCl, monitored by fluorescence, near UV and far UV CD [30], were found noncoincident which was explained by the presence of a molten globule - type [31-34] of intermediate [30, 35]. In contrast to stefin A which is thermally extremely stable, the behavior of stefin B is quite different. Differential scanning calorimetry (DSC) was used to obtain thermodynamic data from the thermal unfolding of both proteins [36] as well as some cystatins [37]. The reasons for the big difference in thermal stability between stefins A and B were sought using structural thermodynamics [38]. Reversible DSC scans of stefin A could be analysed in terms of a 2-state transition whereas stefin B unfolded in an irreversible transition (at pH 8 and 6.5, 0.13 M salt). The asimetry of the DSC peaks was characteristic of unfolding of a dimer. At pH 5, the transition of stefin B became reversible and permitted thermodynamic analysis [36].

Table 1

Sequence alignment of some representative stefins; the N-terminal extension is omitted from pig leukocyte CPI (5 residues) [20]. The bold letters stress identity to human stefin B, underlined are residues which are the same to human stefin A. Recombinant human stefin B differs in the third residue (Ser3) from the wild type Cys3.

```
res No                    10         20         30         40         50
human r. stef.B  MMSGAPSATQ PATAETQHIA DQVRSQLEEK YNKKFPVFKA VSFKSQVVAG
bovine stefin B[44] MMCGGTSATQ PATAETQAIA DKVKSQLEEK ENKKFPVFKA LEFKSQLVAG
human stefin A   MIPDDLSEAK PATPEIQEIV DKVKPQLEEK TNETYGKLEA VQYKTQVVAG
bovine stefin A[19] MIPGGLTEAK PATIEIQEIA NMVKPQLEEK TNETYEEFTA IEYKSQVVAG
pig leuko. CPI[20] MLAGGLTEPR PATPEIQEIA NKVKPQLEEK TNKTYEKFEA IIYRSQVVAG
```

```
res No                    60         70         80         90
human r.stef.B   TNYFIKVHVG DEDFVHLRVF QSLPHENKPL TLSNYQTNKA KHDELTYF
bovine stefin B[44] KNYFIKVQVD EDDFVHIRVF ESLPHENKPV ALTSYQTNKG RHDELTYF
human stefin A   TNYYIKVRAG DNKYMHLKVF KSLPGQNEDL VLTGYQVDKN KDDELTGF
bovine stefin A[19] INYYIKIQTG DNRYIHIKVF KSLPQQSHSL ILTGYQVDKT KDDELAGF
pig leuko. CPI[20] TNYYIKVHVG GNNYVHIRVF QSLPHQEDPL KLIGYQVDKT KDDELTGF
```

pH denaturation of human stefin B was studied in more detail by spectroscopic and DSC techniques [39]. The pH titration was performed at "low" salt (buffers described in [39], 0.033 M NaCl) or at "high" salt (the same buffers [39], 0.42 M NaCl). Near and far UV CD spectra were recorded as a function of pH. Some representative far UV CD spectra are shown in Fig1. The pH denaturation was recorded at 200, 208, 222 and 277 nm, and

showed two transitions, at pH 4.1 and 5.7. At pH 5.7 only minor changes at 200, 208 and 222 nm are observable (due to minor changes in secondary structure) which is supported by recent NMR experiments on N^{15} labeled stefin B. At pH 4.1, rather large and cooperative changes occur at all wavelengths. The final, acid intermediate (denatured) state I_1 (below pH 3.3) has some properties of a "less structured" molten globule [33], in particular, in binding ANS. Adding salt to I_1 produces a transition to a "more structured" molten globule I_2. All CD and fluorescence data were acquired at $18^{\circ}C$ as the population of intermediate states changes with temperature. Instead of
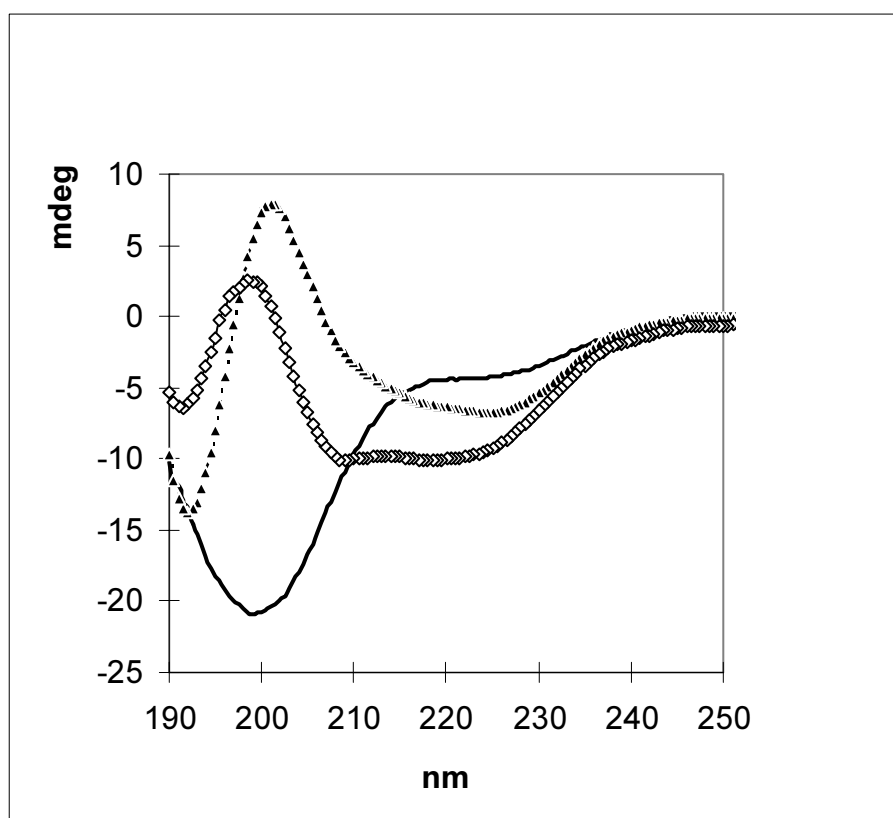
Figure 1. Far UV CD spectra of human stefin B in various denatured and intermediate states: N (0.01 M phosphate buffer pH 6.5), I_2 (0.01 glycine 0.25 M sulphate, pH 3.3), I_1 (0.01 M glycine , pH 3.3); from top to the bottom at 200 nm.

studying pH denaturation at several temperatures, we have heated samples at various pH values. DSC data [39] have shown that thermal denaturation deviates from 2-state with decreasing pH which was explained by a rather low enthalpy of unfolding of the acid intermediate state I_1. As this state is populated to 100 % only below pH 3.3 where

enthalpy could not be measured due to the low melting temperature, no firm conclusion on the enthalpy of unfolding of state I_1 could be made. In contrast, the second, more structured acid intermediate I_2 demonstrates a measurable enthalpy of unfolding.

[1]D NMR spectra [39] of the acid induced intermediates of human stefin B have been measured and have confirmed that I_2 posesses some tertiary structure (high field methyl resonances) in contrast to I_1. It is hoped that by using N^{15} and C^{13} labelled samples and acquiring 2D and 3D NMR spectra much more detail would be obtained also of the other two acid intermediate states I_1 and I_2. (R.J., experiments underway). The compactness of the acid intermediate states and their oligomeric nature was probed by SEC [40].
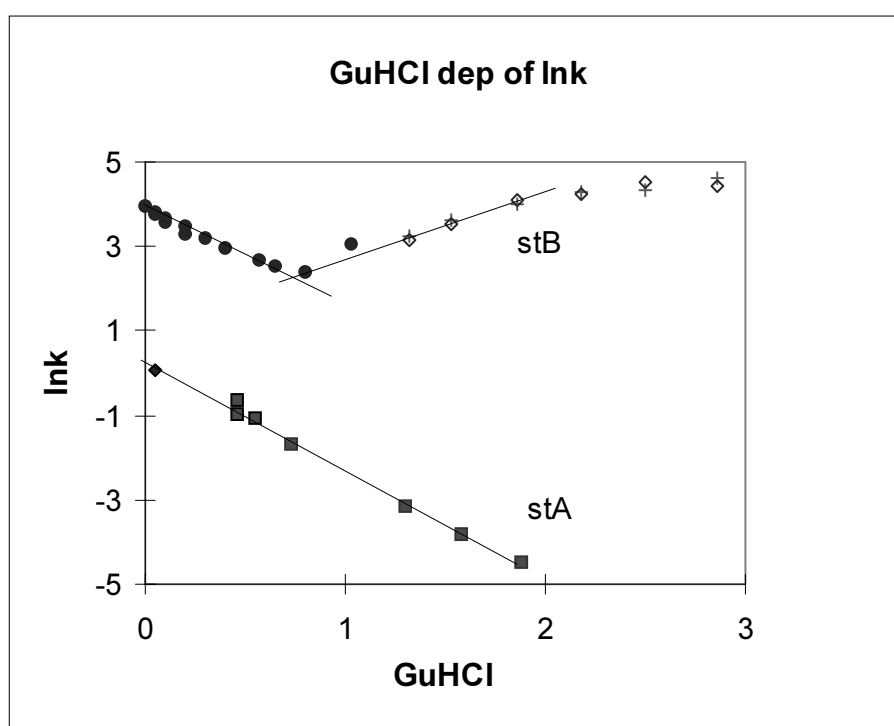
Figure 2. Logarithm of the rate constants against GuHCl molarity. Folding of human stefin B was started from the acid intermediate state at pH 2.7. This was found the same as when started from the GuHCl denatured state at 3.45 M GuHCl. (not shown). Unfolding was started from the native state at pH 6. Folding of human stefin A was started from the GuHCl denatured state (4.4 M GuHCl). The initial values at zero GuHCl have been obtained by folding the acid denatured state to zero GuHCl at otherwise the same conditions (pH 6, 20°C).

The folding mechanism of stefin B has been studied [41,42] and compared to that of stefin A. We also have studied the influence of pH and TFE on the folding reaction[41]. Using several spectroscopic probes (CD in the near, CD in the far, tyrosine and ANS fluorescence - Table 2), it was found that the kinetics of folding of human stefin B differ from those of stefin A. Not only is the major phase of folding 40-times faster (at zero GuHCl, - Fig.2), this protein demonstrates an additional slow phase. The slow phase of 25 % amplitude (Table 2) could be ascribed to proline isomerization but pH dependence of the amplitude and double jump experiments do not prove it univocally. An intermediate seems a more likely hypothesis. In the very initial stages of folding, a "burst" phase of the signal at 230 nm was observed [41]. Its amplitude was 60% ± 5% of the total change.

In a second paper [42], folding was started from different initial states : GuHCl unfolded, TFE denatured, acid denatured and acid intermediate state. The folding rates were found to be the same, so that the rate limiting step must also be the same. In Fig.3, folding from acid denatured state A_D is shown as monitored by ANS fluorescence. ANS binding on folding of stefin B and many other proteins is very informative. The initial increase can be explained as compactization [32,34] which is supported by X-ray scattering [43]. The decrease of ANS fluorescence occurs along with appearance of the native-like states (Fig.3 B,C).

To conclude : Many more experiments still have to be done to be able to understand the folding of these two homologous proteins. We hope to study their mutants and to follow dimerization reactions which seem connected to stefin B folding. In cooperation with other laboratories it will be possible to determine the rate of compactization (time-resolved X-ray scattering [43] and details of structure formation (real time NMR [45]).

Table 2

       Comparison of the folding kinetics of human stefins A and B as measured by the near and far UV CD, tyrosine and ANS fluorescence. Data are taken from [41]. The folding of stefin B was started by 6-times dilution from 3.45 M GuHCl and of stefin A from 4.4 M GuHCl, both, to pH 6. The measurements were done at 20 $^\circ$C. Rate constants are in s^{-1} and amplitudes as % of the observed change. "Burst phase" amplitudes in the far UV CD are 60% and 45 % of the total change, respectively, for stefins B and A. No amplitude is given for ANS fluorescence, only the sign.

human stefin B folding

probe	k_1'	k_1/A_m	k_2'	k_2/Am
Tyr fl.		14.2/77%		0.05/23%
ANS fl.	86(+)	12.8(-)	0.34(+)	0.022(-)
CD far		10.5/76%		0.045/24%
CD near		10.8/75%		0.039/25%

human stefin A folding

probe	k / Am
Tyr fl.	0.18 / 100%
ANS fl.	no change
CD far	0.18 / 100%
CD near	0.16 / 100%

Acknowledgments

Figure 3. Kinetics of folding of human stefin B recorded by ANS fluorescence. The folding was started from state A_D at pH 1.8 ± 0.2 (dialysis against water / HCl pH 1.8) and proceeded into 0.02 M phosphate buffer. After 6-fold dilution the final pH was 6.0 ± 0.1.
A) the initial ANS fluorescence increase - folding to an intermediate ($k'' = 533$, $k' = 92$ s^{-1})
B, C) folding to the native state is tri-phasic ($k_1 = 11$ s^{-1}, $k_2 = 0.053$ s^{-1} and $k_3 = 0.004$ s^{-1})

Povzetek : Najprej je podan kratek uvod v eksperimentalni del študija stabilnosti in folding a proteinov. Nato opisujemo naše delo s človeškima stefinoma A in B. Kinetiko folding a stefina B smo merili z več probami in jo primerjali s kinetiko folding a stefina A. Merili smo tudi odvisnost hitrosti od koncentracije GuHCl, pH-ja in temperature. pH denaturacija človeškega stefina B (E.Žerovnik et al., Eur.J.Biochem. 1997, 245, 364 - 372) in folding do nativnega stanja iz kislo denaturiranega, sta opisana nekoliko bolj natančno.

References

[1] C.Tanford, Adv.Prot.Chem. 1968, 23, 121 -   .
[2] S.Lapanje,Physicochemical Aspects of Protein Denaturation , Wiley-Interscience, N.York, **1973**
[3] K.P. Murphy, E.Freire, Adv.Prot.Chem. **1992**, 43, 313 - 361.
[4] T.E. Creighton , Nature **1992**, 356, 194 - 195.
[5] S. Khorasanizadeh, I.D. Peters, H. Roder, Nat.Struct.Biol.**1996**, 3, 193 - 204.
[6] D.K. Heidary, L.A. Gross, M. Roy, P.A. Jennings, Nature Struct.Biol. **1997**, 4, 1-10.
[7] R.L. Baldwin , Fold.&Design **1996**, 1, R1 -R8.
[8] K.A. Dill , H.S. Chan, Nat.Struct.Biol. **1997**, 4, 10 -19.
[9] H.S.Chan, K.A.Dill, Proteins **1997**, 8, 2-33.
[10] F.X. Schmid, In : Protein Folding 1992, T.E. Creighton, ed., Freeman & Co., pp. 197 - 238.
[11] K.W. Plaxco, C.M. Dobson , Curr.Opin.Struct.Biol. **1996**, 6, 630-636.
[12] D. Eliezer, J. Yao, J. Dyson, P.E. Wright, Nat.Struct.Biol. **1998**, 5, 148 - 155.
[13] P. Fan , C. Bracken, J. Baum, Biochemistry **1993**, 32, 1573 - 1582.
[14] J. Trewhella, Curr.Opin.Struct.Biol. **1997**, 7,702 - 708.
[15] J.Brzin, M.Kopitar, V.Turk, W. Machleidt,
      Hoppe Seyler's Z. Physiol.Chem.**1983**, 364, 1475 - 1480.
[16] W.Machleidt, U. Borchart , H. Fritz, J.Brzin, A.Ritonja, V.Turk,
      Hoppe Seyler's Z.Physiol.Chem. **1983**, 364, 1481 - 1486.
[17] A.Ritonja, W.Machleidt, A.J.Barrett, Biochim.Biophys.Res.Commun.**1985**, 131, 1187 - 1192.
[18] B.Turk, I.Križaj, B.Kralj, I.Dolenc, T.Popović, J.G. Bieth, V.Turk,
      J.Biol.Chem. **1993**, 268, 7323 - 7329.
[19] B.Turk, A.Ritonja, I.Bjork, V.Stoka, I.Dolenc, V.Turk, FEBS Lett. **1995**, 101 - 105.
[20] B.Lenarčič, A.Ritonja, I.Dolenc, V.Stoka, S.Berbić, J. Pungerčar, B.Štrukelj,
      V.Turk, FEBS Lett. **1993**, 336, 289 - 292.
[21] W.M. Brown, K.M. Dziegielewska, Protein Sci **1997**, 6, 5 - 12.
[22] V.Turk, W.Bode, FEBS Lett. **1991**, 285, 213 - 219.
[23] R.Jerala, M.Trstenjak, B.Lenarčič, V.Turk, FEBS Lett. **1988**, 239, 41 - 44.
[24] M. Strauss, J.Stollwerk, B.Lenarčič, V.Turk, K.D.Jany, H.G. Gassen ,
      Hoppe Seyler 1988, **369**, 1019 - 1030.
[25] R.Jerala, L.Kroon-Žitko, V.Turk, Protein Expr.Purif. **1994**, 5, 65 - 69.
[26] M.T.Stubbs, B.Laber , W. Bode, R. Huber, R. Jerala, B. Lenarčič, V.Turk,
      EMBO J.**1990**, 9, 1939 - 1947.
[27] J.R.Martin, C.J.Craven, R.Jerala, L.Kroon-Žitko, E.Žerovnik, V.Turk, J.P. Waltho,
      J.Mol.Biol.**1995**, 246, 331 - 343.
[28] J.R.Martin, R.Jerala, L.Kroon-Žitko, E.Žerovnik, V.Turk, J.P. Waltho,
      Eur.J.Biochem. **1994**, 225, 1181 - 1194.
[29] E. Žerovnik, B. Lenarčič, R.Jerala, V.Turk , Biochim.Biophys.Acta **1991**, 1078, 313 - 320.
[30] E.Žerovnik, R.Jerala, L.Kroon-Žitko, R.H.Pain, V.Turk, J.Biol.Chem. **1992**, 267, 9041 - 9046.
[31] K.Kuwajima, Proteins : Struct.Fun.& Gen. **1989**, 6, 87 - 103.
[32] O.B. Ptitsyn, R.H. Pain, G.V. Semisotnov, E. Žerovnik, O.I.Razgulyaev,
      FEBS Lett. **1990**, 262, 20 - 24.
[33] O.B. Ptitsyn (**1992**). In *Protein folding*,
      Creighton T.E., Ed., Freeman & Co., New York, pp.243 - 300.

[34]   H. Christensen, R.H. Pain, In *Mechanisms of Protein Folding*, R.H Pain., ed.,
         Oxford Univ.Press ,1994, pp. 55-76.
[35]   E.Žerovnik, R.Jerala, L.Kroon-Žitko, V.Turk, R.H.Pain,
         Biol.Chem. Hoppe-Seyler **1992**, 373, 453 - 458.
[36]   E.Žerovnik, K.Lohner, R.Jerala, P.Laggner, V.Turk, Eur.J.Biochem. **1992**, 210, 217 - 221.
[37]   E.Žerovnik, N.Cimerman, J.Kos, V.Turk, K.Lohner, Biol.Chem. **1997**, 378, 1199 - 1203.
[38]   R.Jerala, E.Žerovnik, K.Lohner, V.Turk, Prot.Engineering **1994**, 7, 977 - 984.
[39]   E.Žerovnik, R.Jerala, L.Kroon-Žitko, V.Turk, K.Lohner, Eur.J.Biochem**1997**, 245, 364 - 372.
[40]   E.Žerovnik, R.Jerala, N.Poklar, L.Kroon-Žitko, V.Turk,
         Biochim.Biophys.Acta **1994**, 1209, 140 - 143.
[41]   E.Žerovnik, R.Virden, R.Jerala, V.Turk, J.P.Waltho, Proteins: Struct.Fun.&Gen **1998**, in press
[42]   E.Žerovnik,R.Jerala, R.Virden, L. Kroon-Žitko, V. Turk, J.P.Waltho,
         Proteins: Struct.Fun.&Gen. **1998**, in press
[43]   L. Chen, G. Wildegger, T. Kiefhaber, K.O. Hodgson, S.Doniach,
         J.Mol.Biol. **1998**, 276, 225 - 237.
[44]   I.Križaj, B.Turk, V.Turk, FEBS Lett.**1992**, 298, 237-239.
[45]   J.Balbach, V.Forge, W.S. Lau, N.A. van Nuland, K.Brew, C.M.Dobson,
         Science **1996**, 274, 1161 - 1163..

INFLUENCE OF POLYMERIZATION PARAMETERS ON THE MOLECULAR WEIGHT OF POLYANILINE

Maja Vilčnik, Majda Žigon*, Marko Zupan, Anton Šebenik
Faculty of Chemistry and Chemical Technology, University of Ljubljana, Slovenia
*National Institute of Chemistry, Ljubljana, Slovenia

ABSTRACT

The yield of polymerization and the molecular weight of polyaniline (PAN) were determined in dependence on the ratio of aniline and amoniumperoxodisulphate, temperature, reaction time and pH. It was found that polymerization yield and molecular weight decrease with the increasing ratio oxidant to aniline, pH and temperature. The pH of the reaction mixture rapidly decreases due to the release of proton from 0.80 to 0.35 and during the polymerization slowly increases back to the starting value. The polydispersity is in the wide range and is almost constant with the changing reaction parameters. After the reduction of emeraldine base to leucoemeraldine base, the molecular weight decreases due to the difference in the hydrodinamic volume of quinoid segments in comparision with that of benzenoide, as well as to intermolecular hydrogen bonds between amine and imine groups of benzenoid and quinoide segments of emeraldine base, and the decomposition of the -C-N- bonds after the reduction.

INTRODUCTION

Polyaniline (PAN) has attracted considerable attention since MacDiarmid *et al*. [1] reinvestigated this material as a conducting polymer due to its simple synthesis, good environmental stability, and adequate level of electrical conductivity. Polyaniline is unique among conducting polymers in that its electrical properties can be reversibly controlled

both by charge-transfer doping and by protonation. The wide range of associated electrochemical and optical properties, coupled with good stability, make polyaniline potentially attractive for application as an electronic material. Recent work has shown that polyaniline prepared at room temperature is of fairly low molecular weight [2] and contains defect sites [3]. It is hoped that better-quality polyaniline, with fewer defect sites and higher molecular weight may lead to improvements in its mechanical and electrical properties.

Polyaniline can be synthesized by both electrochemical and chemical oxidative polymerization [5]. Considerable effort has been made to develop relationships between synthesis conditions and properties of polyaniline obtained by electrochemical polymerization [6]. By contrast, relatively little attention has been paid to the chemical polymerization of aniline due to its very complex and undefined structure [7,8,9].

The aim of our work was controlled polymerization of aniline at different reaction conditions using amoniumperoxodisulfate as an oxidant. The course of this reaction was followed by determination of the yield of copolymerization, molecular weight and of its polydispersity in dependence on the reaction parameters. The influence of the reaction parameters on electrical conductivity and energy gap was determined.

EXPERIMENTAL

Materials: Aniline (AN) was a product of Aldrich. Amoniumperoxodisulfate and hydrochloric acid were products of Merck. Phenylhydrazine (Fluka) and 3-chloroperoxybenzoic acid (Aldrich) were used for preparing the leucoemeraldine and the pernigraniline bases. All these and other chemicals in this work were used without further purification. 1-methyl-2-pyrrolidinone (NMP), triethylamine (TEA) and lithium chloride (LiCl) mixture was used as the solvent.

Polymerization: Polymerization of AN (0.0548 mol) was carried out in a reaction vessel at the temperature range from -5 to 10°C. We followed the yield of polymerization in dependence on the ratio of the aniline to amoniumperoxodisulfate and on the concentration of HCl. The oxidant was added after 2 hours and then the reaction continued for 2 additional hours. The dark green polyaniline hydrochlorides were separated, and then washed with 1M HCl and methanol to obtain a colourless solution without any oligomers. The polymers were dried in vacuum to dark green products. The exact reaction conditions are described in Tables 1, 2 and 3. The dark green powders were neutralised with water solution of NH$_3$ and then were dried. The products which consisted of all three PAN bases, were dissolved in NMP, and then reduced with phenylhydrazine to

leucoemeraldine base [10], or were oxidised with 3-chloroperoxybenzoic acid to pernigraniline base [11].

Molecular weight determination: Before measuring of the molecular weight, the solubility of the PAN was determined. The best solvent for PAN was a mixture of the NMP, TEA and LiCl in the weight ratio of 100:0.5:0.5. The molecular weights were measured by GPC with Ultra-Styragel 10μ columns using mixture of NMP, and LiCl as the eluent in the weight ratio 100:0.5. The flow rate was 0.5 ml/min. Polystyrene and polyvinylpyridine standards were used for calibration. As a detector, the diode array UV detector at 330 nm was used.

Measurements: The structure, sequence monomer distribution, chain end groups, purity and the presence of impurities were followed by NMR spectroscopy of the polymers. The one and two dimensional homo and hetero correlation ^{1}H, and ^{13}C spectra were measured by Varian VXR 300 MHz and INOVA 600 MHz NMR spectrometers. The samples were dissolved in a mixture of NMP, TEA and DMSO-d$_6$. All signals were quoted on TMS as internal standard. For the determination of individual signals in the NMR spectra and for quantitative measurements of benzenoid and quinoid segments in the polymer, a number of model compounds, their relaxation times, proton coupling and decoupling spectra were taken. For the assignation of ^{13}C NMR spectra, the attached proton test (APT) and model substances were used. FTIR spectra were measured by Perkin Elmer spectrometer using the KBr pallets technique. For resistance measurements, individual films from NMP solution, according to a procedure described elsewhere, were prepared [12]. The impendance spectroscopy with the pellet samples between two carbon wires attached at both sides was used.

RESULTS AND DISCUSSION

Polyanilines are interesting compounds from the point of view of fundamental aspects of the mechanism of charge transport in conducting polymers. The conductivity along the polyaniline backbone can be affected by the degree of oxidation of the polymer (the relative amount of amine and imine groups), the protonation acid and the percentage of protonation [9]. The conductivity is also affected by the degree of water and solvent content, which presumably can affect the charge transport between chains, and also by the morphology and texture of the polymer, the molecular weight and degree of crystallization.

Mechanism of polymerization: The structure of individual polyaniline bases and distribution of the oxidised and reduced units in the chains were determined by ^{13}C and

APT NMR and FTIR spectroscopy (Figure. 1). The spectra of all polyaniline bases are very complex because of many individual distributions of the quinoid and benzenoid rings

Figures available in printed version only

Figure 2: Dependence of the pH on reaction time at 0^OC, ratio oxidant/aniline 1.00:1.

in polyaniline chains, different end groups, minor substituents and products of various possible side reactions such as branching, cyclization, crosslinking, conformation effects and reduction in ring symmetry. The simplest is the spectrum of the leucoemeraldine base with two main signals of benzenoid rings which represent 1-4 substitution and a number of small signals of end groups. The general assignation of individual signals is marked on the spectra.

Although there is still some uncertainty regarding the exact mechanism of aniline polymerization, it is likely that radical cation species are produced as a result of oxidative attack on the aniline monomer. These then condense with the loss of protons to give the protonated semi-oxidised emeraldine form of polyaniline as the reaction product [4]. The following scheme of polymerization can be predicted (Scheme 1).

Cationic chain polymerization is usually carried out at low polymerization temperatures, which favour propagation over competition with side reactions. Solvents with a high

dielectric constant favour both initiation and propagation leading to high molecular weight products [8]. One of the characteristics of step-growth polymerization is that the molecular weight of the polyaniline rises steadily throughout the reaction, and therefore long reaction time is essential to obtain high molecular weight products.

Solubility of PAN: The formed nonprotonated emeraldine base is soluble in NMP but the macromolecules produce aggregates. This was seen from the light scattering measurements of the particle size of polyaniline solutions in NMP. The -NH- protons on the polymer backbone are partly blocked with inter and intra molecular hydrogen bonding. The aggregates are formed due to interactions such as physical entanglements or hydrogen bonding with the size up to 15µm [13]. Triethylamine increases the solubility of polyaniline and, in combination of LiCl, it breaks the aggregates to the dissolved macromolecules and the fictive high molecular weight decreases to the real value. The presence of TEA acts as a dedoping agent, being a proton-acceptor with his lone electron pair on nitrogen.

Determination of molecular weight: Determination of the molecular weight by GPC is questionable due to the presence of aggregates in NMP, formed by hydrogen bonds between the amine and imine segments and also due to possible interaction between the solute and the stationary phase. The NMP and TEA changes the characteristics of the columns. In the case of emeraldine base, the -NH- and =N- groups produce a stronger interaction between individual macromolecules as in the case of leucoemeraldine base, where only interactions between -NH- groups are possible. For this reason, individual electrolites can reduce the interactions. We tried different contents of LiCl and TEA. LiCl hinders lone electron pairs of nitrogen and prevents hydrogen bonds. The presence of triethylamine increases the solubility of polyaniline, but the column is not stable due to additional interactions. This is evident from GPC chromatograms, which have multimodal molecular weight distribution with a high portion of fictive high molecular weight fractions. The multimodal molecular weight distribution disappeared by the addition of LiCl, which also prevents the interaction of solute to the mobile and stationary phase [3]. The optimal content was determined from the dependence of the retention time on the content of LiCl, when the molecular weight reached the minimal value. The chromatograms with unimodal distribution were obtained using NMP with LiCl as solvent in the weight ratio 100:0.5. The size of aggregates is about 50 times higher than the observed molecular weight. This proves that the inter and intramolecular electrostatic interactions between polymer chains are disrupted by the addition of LiCl [3,14].

Influence of the temperature: Molecular weight of polyaniline rapidly decreases with increasing reaction temperature due to the condensation of radical cation species which

lose protons to give the protonated emeraldine form (Table 3). Cationic chain polymerization is usually carried out at low polymerization temperatures in the solvents with a high dielectric constant, which favours both initiation and propagation leading to high molecular weight [4,8]. The low temperature increases the dipole moment and this favours the production of high molecular weight polyaniline compared to materials prepared at room temperature. The ^{13}C NMR spectra shows that the polyaniline synthesized at lower temperatures consists of almost para-substituted phenylene rings linked by amine groups with a few small signals which indicate defect sites on the benzene ring [14-17]. The fact that the yield and molecular weight increase linearly with decreasing reaction temperature, confirms the cationic step-growth mechanism of the polymerization.

The influence of the oxidant: Molecular weight decreases linearly with the increasing content of the amoniumperoxodisulphate due to the partial oxidation of individual segments, which are not further reactive for cataionic step-growth polymerization (Table 1). The same holds for the increase of the content of hydrochloric acid (Table 2). Higher concentration of hydrochloric acid decreases the propagation of cationic spices. In accordance with the reaction mechanisms the acidity of the reaction mixture increases during polymerization due to the release of a proton [18]. The pH of the reaction mixture rapidly decreases from 0.80 to 0.35 and during polymerization slowly increases back to the starting value (Figure 2). Due to the decreasing pH, the reaction equlibria favour the termination of macrocations, which leads to a lower molecular weight of polyaniline.

Influence of the reduction: In all cases the molecular weight of emeraldine base decreases after the reduction to leucoemeraldine base. There are however several reasons. The hydrodynamic volume of rigid quinoid segments is bigger than that of benzenoid. Secondly, the intermolecular hydrogen bonds between amine and imine groups of benzenoid and quinoid segments of emeraldine base decompose after the reduction of quinoid structures. The third reason is the decomposition of some -C-N- bonds after the reduction.

Electrical conductivity: Polyaniline acts as an electrically conductive material only in the protonation form of emeraldine salt. Its electrical conductivity is about $6.7 \cdot 10^{-2}$ S/cm, due to the doping of emeraldine base by hydrochloric acid. The conductivity rapidly decreases with the reduction of emeraldine base to leucoemeraldine base to the value of $8.5 \cdot 10^{-10}$ S/cm. After the oxidation of emeraldine base to pernigraniline base, electrical conductivity decrease to $4.1 \cdot 10^{-9}$ S/cm. In the case of emeraldine salt, quinoid rings with hybridised π orbitals which are resonance stabilised, enable charge transport between chains, although the three other rings of polyaniline are in nonconductive benzenoid form. In the case of fully reduced leucoemeraldine base, all rings are in benzenoid form, each isolated one from

other by -NH- groups and each macromolecule is in nondoping form. There is no charge transport nor along single macromolecules neither between macromolecules. Electrical conductivity decreases for 10^8 for emeraldine base and 10^7 times for leucoemeradine base. The electrical conductivity and mechanical properties of polyaniline increase with the decreasing reaction temperature and are optimal almost at stechiometrical ratio between the oxidant, hydrochloric acid and aniline. The formed films are compact with good mechanical properties. The conductivity of polyaniline does not depend on the temperature of surroundings which indicates a small energy gap.

CONCLUSION

The highest molecular weight and yield of polymerization of polyaniline were obtained at a low temperature and at an equivalent ratio between aniline oxidant and hydrochloric acid. The formed films are compact with good mechanical properties.

ACKNOWLEDGEMENT

REFERENCES

[1]. A.G. MacDiarmid, J.C. Chiang, M. Halpern, W.S. Huang, S.L. Mu, N.L. Somasiri, W. Wu and S.I. Yaniger, *Mol. Cryst. Liq. Cryst.*, **1985**, 121, 173

[2]. P.N. Adams, D.C. Apperley and A.P. Monkman, *Polymer*, **1993**, 34, 328

[3]. A.M. Kenwright, W.J. Feast, P.N. Adams, A.J. Milton, A.P. Monkman and B.J. Say, *Polymer*, **1992**, 33, 4292

[4]. P.N. Adams, P.J. Laughlin, A.P. Monkman and A.M. Kenwright, *Polymer*, **1996**, 37, 3411

[5]. J.C. Chiang and A.G. MacDiarmid, *Synth. Met.*, **1986**, 13, 193

[6]. W.S. Huang, B.D. Humphrey and A.G. MacDiarmid, *J. Chem. Soc. Faraday Trans.*, **1986**, 82, 2385

[7]. C.H. Ong, S.H. Goh and H.S.O. Chan, *Polym. Bull.,* **1997**, 39, 627

[8]. P.N. Adams, P.J. Laughlin, A.P. Monkman, *Synth. Met.*, **1996**, 76, 157

[9]. G. Boara and M. Sparpaglione, *Synth. Met.*, **1995**, 72, 135

[10]. Y. Wei, K. F. Hsueh, G. W. Jang, *Macromolecules*, **1994**, 27, 519

[11]. Y. Sun, A. G. MacDiarmid, A. J. Epstein, *J. Chem. Soc., Chem. Commun.*, **1990**, 529

[12]. M. Angelopoulos, G. E. Asturias, S. P. Ermer, A. Ray, E. M. Scherr, A. G. MacDiarmid, *Mol. Cryst. Liq. Cryst.*, **1988**, 160, 151

[13]. M. Angelopoulos, Y.H. Liao, B. Furman, T. Graham, *Mat. Res. Soc. Symp. Proc.,* **1996**, 413, 637

[14]. S. Ni, J. Tang, F. Wang, L. Shen, *Polymer*, **1992**, 33, 3607

[15]. T. Hagiwara, M. Yamaura, K. Iwata, *Synth. Met.*, **1998**, 26, 195

[16]. A.C. Kolbert, S. Cardarelli, K.F. Thier, N.S. Sariciftci, Y. Cao A.J. Heeger, *Physic. Rev.*, **1995**, 51, 1541

[17]. A.M. Kenwright, W.J. Feast, P. Adams, A.J. Milton, A.P. Monkman, B.J. Say, *Synth. Met.*, **1993**, 55-57, 666

[18]. J. Stejskal, P. Kratochvil, A.D. Jenkins, *Polymer*, **1996**, 37, 367

POVZETEK

Določili smo vpliv razmerja med anilinom in amonperoksidisulfatom, temperature, časa reakcije in pH na izkoristek polimerizacije in molsko maso polianilina (PAN). Izkoristek polimerizacije in molska masa padata z rastočim razmerjem med oksidantom in anilinom, pH in temperaturo. Na začetku pH reakcijske zmesi intenzivno pade od 0,80 do 0,35 zaradi odcepa protonov in med reakcijo počasi raste na začetno vrednost. Polidisperznost je v širokem območju in je neodvisna od reakcijskih parametrov. Po redukciji emeraldine v leukoemeraldino bazo molska masa pade zaradi razlike hidrodinamskih volumnov benzenoidnih in kinoidnih segmentov, kot tudi zaradi intermolekularnih vodikovih vezi med aminskimi in iminskimi skupinami benzenoidnih in kinoidnih segmentov emeraldine baze ter zaradi razpada -C-N- vezi pri redukciji.

Volumetric Properties of Alkali Metal p-Toluenesulphonates in Water as a Function of Temperature

C. Pohar and S. Skale

Faculty of Chemistry and Chemical Technology, University of Ljubljana, 1000 Ljubljana, Slovenia

Abstract

Density data are presented for alkaline salts of p-toluenesulphonic acid at temperatures from 5 to 40 ^{O}C up to concentrations of ~2 mol/kg. The apparent molar volumes, $V_{2\phi}$, were calculated for these solutions from the density measurements. The apparent molar volumes were fitted to the equation of Redlich and Meyer to determine two important parameters: i) the apparent molar volume at infinite dilution, $V_{2\phi}^o$, and ii) the deviation constant b_V. At 25 ^{O}C the additivity rule of the individual ionic contributions was confirmed. Further, $V_{2\phi}^o$ increases with increasing temperature for all the salts, while the parameters b_V monotonically decrease from positive to negative values (in the order Li<Na<K<Rb<Cs) as the temperature is increased. The effect of temperature on the apparent molar volumes of the p-toluenesulphonates in water at infinite dilution is similar to that of other simple electrolytes.

Key words: Alkaline p-Toluenesulphonates; Apparent Molar Volume; Density; Apparent Molar Expansibility.

Dedicated to the memory of Prof. Savo Lapanje

Introduction

Thermodynamic properties of electrolyte solutions expressed as apparent or partial molar quantities are useful in characterizing solute-solvent and solute-solute interactions. One approach toward a deeper understanding of interactions in polyelectrolyte solutions is to study the monomer system. It is reasonable to expect the electrochemical properties of the sulphonic group in polystyrenesulfonate solutions to be similar to those in low molecular analogues, i.e. various substituted benzenesulphonic acids and their salts [1]. Study of the monomer system is, moreover, facilitated by the fact that accurate theories are available for the analysis of experimental data on solutions of simple electrolyte.

The excess thermodynamic properties of electrolyte solutions, i.e. osmotic coefficients, heats of dilution, or volume changes on dilution, are determined by the ion-ion and ion-solvent interactions. Additional information about interactions in solution may be obtained by studying the system at various temperatures since different interaction potentials have different temperature dependencies [2]. Recently, the heats of dilution (ΔH_D, c$\rightarrow$0.002 mole-dm^{-3}) at various temperatures have been measured [3] for aqueous solutions of the alkaline salts of p-toluenesulphonic acid. In the another publication [4], a preliminary theoretical analysis of the osmotic coefficients, heats of dilution and volume changes on dilution based on Friedman's theory [5] was presented. Unfortunately, except for the osmotic coefficients and heats of dilution, a complete investigation of the concentration dependence of other properties of the alkali p-toluenesulphonates is lacking. In the literature we found the partial molar volume data of p-toluenesulphonic acid and its sodium salt for the temperature of 25 ^{O}C [6], but no measurements for other temperatures were presented so far. Since the concentration dependence of the apparent or partial molar volume over a sufficiently wide range of temperature is needed to verify the theoretical models of electrolyte solution, we measured the densities of Li, Na, K, Rb and Cs salts of p-toluenesulphonic acid in water at 5, 15, 25, and 40 ^{O}C. From the concentration dependence of the apparent molal volumes and with the use of the Redlich-Meyer equation [7], the apparent molal volumes at infinite dilution and the parameter b_V were determined. The differences in values of these quantities between various salts were interpreted with respect to

structural interactions[8-10]. Note that extensive reviews of the volumetric properties of electrolyte solutions have been published by Millero [11,12].

Experimental

Toluene-4-sulphonic acid monohydrate (or p-toluenesulphonic acid monohydrate, abbreviated to HTS.H_2O, Merck 99%) was used as a starting material for preparation of alkaline (Li, Na, K, Rb, Cs) p-toluenesulphonates (TS). All salts were prepared by neutralization of an acid solution by the corresponding metal hydroxide or carbonate until a pH of about 5 was obtained. The concentration of the acid stock solution was determined by potentiometric titration, while the concentrations of stock salt solutions were measured spectrophotometrically. In all the experiments water doubly distilled in quartz was used.

The densities of solution d were measured at a given temperature using a Paar digital precision density meter, Model DMA 620, with a reproducibility of 10^{-5} g-cm^{-3}. About 10 measurements at each concentration were carried out for each solution. Calibrations at each temperature were made with pure water [13], and with dry air at least twice a day. The temperature of the cell compartment was controlled to ±0.01 ^{O}C using a Heto circulating thermostat. The temperature was measured in a water bath with a platinum resistance thermometer (Degusa Pt1000) and a thermistor inserted into the cell of the density meter. The water bath and the density meter were located so that a stream of water at constant temperature travelled between them.

The apparent molar volumes $V_{2\Phi}$ were calculated from the densities d using [12]

$$V_{2\Phi} = \frac{M_2}{d} + \frac{1000(d^0 - d)}{mdd^0}$$

(1)

where d^0 is the density of pure water, m the molality and M the molar mass of the solute.

The experimental error in $V_{2\Phi}$, which stems from uncertainties in the density measurements, exceeds that from the uncertainties in concentration. The error was

estimated to be $< \pm 1$ cm^3-mol^{-1} at the lowest measured concentration and decreases with increasing concentration.

Results

Experimentally obtained densities are given in Table I for each of the salts and the acid, as a function of molality and temperature. Table I also lists the apparent molar volumes calculated by Equation (1).

TABLE I.   Densities and Apparent Molar Volumes of Aqueous Alkaline p-Toluenesulphonate Solutions as a Function of Concentration at Various Temperatures.

HTS 5 ^{O}C

m [a]	d [b]	$V_{2\Phi}$ [c]
0.0104	1.00055	115.56
0.0505	1.00280	115.66
0.1053	1.00582	115.86
0.5559	1.02913	116.34
1.0573	1.05208	116.82
1.1815	1.05752	116.77
1.3301	1.06360	116.92
1.4162	1.06717	116.89
1.6218	1.07514	117.05

HTS 15 ^{O}C

m	d	$V_{2\Phi}$
0.0094	0.99961	118.42
0.0466	1.00159	118.61
0.0764	1.00316	118.64
0.2959	1.01434	118.96
0.6487	1.03109	119.14
0.8232	1.03892	119.15
1.0903	1.05034	119.16
1.4221	1.06360	119.22
1.8729	1.08042	119.16
2.1339	1.08952	119.13

[a] Units: mol-kg^{-1}
[b] g-cm^{-3}
[c] cm^3-mol^{-1}.

HTS 25 ^{O}C

m	d	$V_{2\Phi}$
0.0095	0.99754	120.69
0.0471	0.99946	120.90
0.0775	1.00099	121.07
0.2984	1.01177	121.28
0.6561	1.02801	121.47
0.8321	1.03548	121.56
1.1057	1.04664	121.55
1.4359	1.05937	121.46
1.9029	1.07577	121.50
2.1728	1.08473	121.44

HTS 40 ^{O}C

m	d	$V_{2\Phi}$
0.0479	0.99462	122.38
0.0776	0.99608	122.50
0.3024	1.00680	122.76
0.6540	1.02235	123.01
0.8312	1.02980	122.97
1.1198	1.04118	123.06
1.4590	1.05380	123.04
1.9248	1.06967	123.07
2.2040	1.07871	122.97

LiTS 5 ^{O}C

m	d	$V_{2\Phi}$
0.0109	1.00065	114.94
0.0505	1.00313	115.08
0.1021	1.00631	115.23
0.4326	1.02575	115.54
0.9349	1.05262	115.72
1.2196	1.06659	115.79
1.3115	1.07085	115.87
1.5196	1.08043	115.86
1.6724	1.08713	115.91
1.9019	1.09687	115.94

LiTS 15 ^{O}C

m	d	$V_{2\Phi}$
0.0105	0.99973	117.92
0.0515	1.00218	118.04
0.1069	1.00544	118.13
0.5756	1.03129	118.45
0.9694	1.05104	118.46
1.2667	1.06510	118.29
1.4204	1.07192	118.31
1.5718	1.07846	118.31
1.7285	1.08518	118.22
1.8988	1.09236	118.07

LiTS 25 ^{O}C

m	d	$V_{2\Phi}$
0.0105	0.99766	120.13
0.0520	1.00004	120.36
0.1067	1.00315	120.42
0.5777	1.02817	120.69
0.9725	1.04729	120.61
1.2742	1.06087	120.56
1.4570	1.06879	120.46
1.5987	1.07463	120.47
1.7865	1.08219	120.43
1.9264	1.08777	120.34

LiTS 40 ^{O}C

m	d	$V_{2\Phi}$
0.0106	0.99282	121.38
0.0517	0.99515	121.60
0.1073	0.99825	121.69
0.5774	1.02277	122.03
0.9804	1.04182	122.04
1.2777	1.05494	121.96
1.4318	1.06146	121.90
1.5950	1.06806	121.91
1.7701	1.07507	121.81
1.9185	1.08080	121.76

NaTS 5 ^{O}C

m	d	$V_{2\Phi}$
0.0107	1.00081	114.78
0.0509	1.00397	115.05
0.1004	1.00781	115.17
0.4287	1.03190	115.98
0.9321	1.06507	116.74
1.0858	1.07434	116.98
1.2408	1.08343	117.13
1.5461	1.10020	117.56
2.0830	1.12727	118.04

NaTS 15 ^{O}C

m	d	$V_{2\Phi}$
0.0186	1.00052	117.72
0.2563	1.01797	118.35
0.5133	1.03561	118.76
0.7930	1.05359	119.03
1.0755	1.07055	119.27
1.3229	1.08448	119.49
1.4769	1.09276	119.61
1.6947	1.10408	119.72
1.8991	1.11412	119.88
2.0779	1.12258	119.99

NaTS 25 ^{O}C

NaTS 40 ^{O}C

m	d	$V_{2\Phi}$	m	d	$V_{2\Phi}$
0.0186	0.99843	119.93	0.0184	0.99357	120.78
0.2559	1.01535	120.57	0.2519	1.01010	121.40
0.5114	1.03243	120.86	0.5025	1.02677	121.64
0.7846	1.04949	121.15	0.7816	1.04413	121.86
1.0731	1.06634	121.37	1.0474	1.05966	122.00
1.3143	1.07963	121.49	1.2918	1.07319	122.07
1.4768	1.08819	121.56	1.4386	1.08099	122.10
1.6828	1.09855	121.69	1.6535	1.09191	122.19
1.8873	1.10851	121.74	1.8519	1.10167	122.19
2.0727	1.11714	121.80	2.0246	1.10983	122.21

KTS 5 ^{O}C

KTS 15 ^{O}C

m	d	$V_{2\Phi}$	m	d	$V_{2\Phi}$
0.0096	1.00080	123.81	0.0133	1.00020	127.59
0.0514	1.00436	124.10	0.0639	1.00433	127.79
0.1008	1.00854	124.18	0.1337	1.00992	128.01
0.4309	1.03479	125.13	0.6580	1.04850	128.90
0.8165	1.06248	125.85	0.8195	1.05931	129.09
0.9504	1.07153	125.98	1.0002	1.07092	129.25
1.0973	1.08107	126.15	1.1277	1.07882	129.33
1.2625	1.09121	126.48	1.2541	1.08641	129.43
1.4109	1.10022	126.55	1.4055	1.09512	129.59
1.5724	1.10956	126.71	1.6109	1.10656	129.70

KTS 25 ^{O}C

KTS ^{O}C

m	d	$V_{2\Phi}$	m	d	$V_{2\Phi}$
0.0134	0.99811	130.57	0.0132	0.99327	131.43
0.0645	1.00214	130.83	0.1319	1.00245	131.80
0.1342	1.00752	131.00	0.6596	1.03964	132.58
0.6682	1.04536	131.79	0.8025	1.04896	132.54
0.8250	1.05547	131.94	0.9908	1.06058	132.72
1.0109	1.06698	132.06	1.1161	1.06799	132.84
1.1432	1.07484	132.14	1.4031	1.08422	133.00
1.2709	1.08215	132.26	1.6158	1.09578	132.96
1.4134	1.09013	132.31			
1.6321	1.10183	132.41			

RbTS 5 ^{O}C

RbTS 15 ^{O}C

m	d	$V_{2\Phi}$	m	d	$V_{2\Phi}$
0.0097	1.00120	129.67	0.0090	1.00021	133.79
0.0500	1.00626	129.86	0.0505	1.00526	134.05
0.0976	1.01216	130.11	0.4023	1.04562	134.79
0.2107	1.02586	130.40	0.7966	1.08633	135.38
0.3192	1.03854	130.76	1.0107	1.10672	135.61
0.4261	1.05073	130.89	1.0935	1.11433	135.67
0.5645	1.06587	131.26	1.2118	1.12500	135.71
0.6937	1.07957	131.44	1.3905	1.14036	135.91
0.8371	1.09415	131.74	1.5548	1.15397	136.02

RbTS 25 ^{O}C

RbTS 40 ^{O}C

m	d	$V_{2\Phi}$	m	d	$V_{2\Phi}$
0.0091	0.99814	136.09	0.0089	0.99329	136.59
0.0500	1.00303	136.30	0.0499	0.99816	136.88
0.1370	1.01320	136.55	0.1374	1.00835	137.19
0.3981	1.04220	137.12	0.3959	1.03701	137.55
0.7859	1.08163	137.49	0.7809	1.07606	137.95
1.0100	1.10259	137.71	0.9964	1.09632	138.06
1.0788	1.10878	137.80	1.0692	1.10296	138.06
1.2127	1.12056	137.88	1.1935	1.11387	138.20
1.3959	1.13617	137.92	1.3824	1.13000	138.24
			1.5304	1.14200	138.37

CsTS 5 ^{O}C

CsTS 15 ^{O}C

m	d	$V_{2\Phi}$	m	d	$V_{2\Phi}$
0.0099	1.00160	137.62	0.0104	1.00078	141.37
0.0385	1.00633	137.84	0.0495	1.00709	141.54
0.0665	1.01091	137.99	0.1116	1.01694	141.77
0.3009	1.04777	138.60	0.7055	1.10246	142.83
0.4405	1.06854	138.89	0.8002	1.11487	142.88
0.5578	1.08530	139.23	0.9184	1.12981	143.06
0.6888	1.10344	139.44	1.0216	1.14251	143.19
0.8348	1.12290	139.66	1.1136	1.15360	143.23
1.2457	1.17346	140.44	1.2552	1.17014	143.32

CsTS 25 °C			CsTS 40 °C		
m	*d*	$V_{2\Phi}$	*m*	*d*	$V_{2\Phi}$
0.0494	1.00492	143.65	0.0103	0.99387	143.59
0.1099	1.01437	143.88	0.0490	1.00001	143.78
0.3445	1.04945	144.39	0.1099	1.00953	144.03
0.6945	1.09759	144.76	0.3434	1.04443	144.43
0.7977	1.11085	144.95	0.6904	1.09217	144.84
0.9103	1.12498	145.02	0.7931	1.10549	144.87
1.0184	1.13814	145.09	0.9039	1.11939	144.99
1.0955	1.14726	145.19	1.0118	1.13255	145.08
1.2307	1.16283	145.33	1.0874	1.14161	145.08
			1.2214	1.15713	145.21

The apparent molal volumes at infinite dilution $V_{2\Phi}^{o}$ were calculated using Equation (2) proposed by Redlich and Meyer [7]:

$$V_{2\Phi} - S_V c^{1/2} = V_{2\Phi}^{o} + b_V c \tag{2}$$

where S_V (in dm$^{3/2}$-cm^3-mol$^{-3/2}$) is the Debye-Hückel limiting slope, which for 1:1 type electrolytes is the following function of temperature t (in °C) [12]

$$S_V = 1.4447 + 1.6799x10^{-2}t - 8.4055x10^{-6}t^2 + 5.5153x10^{-7}t^3 \tag{3}$$

and b_V (in cm^3-dm^3-mol^{-2}) is the empirical deviation constant. The experimental results for LiTS and KTS are also shown graphically in Figures 1 and 2. The apparent molar volumes of alkaline p-toluenesulphonates at infinite dilution and the deviation constants b_V at various temperatures are collected in Table II. The possible experimental errors are given in parentheses.
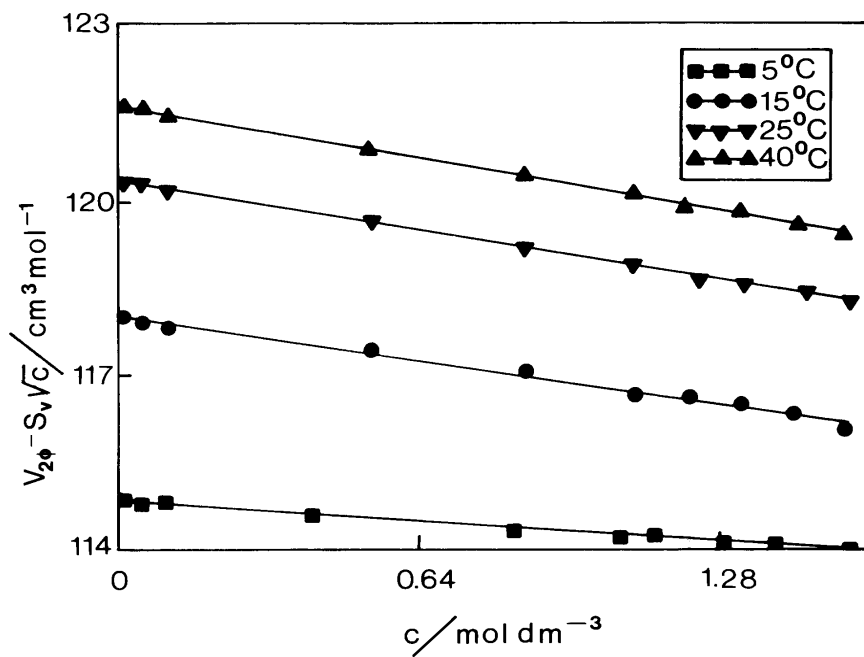
Figure 1. Plot of $V_{2\Phi} - S_V\sqrt{c}$ vs. molarity for LiTS in water at various temperatures; S_V from Equation (3).
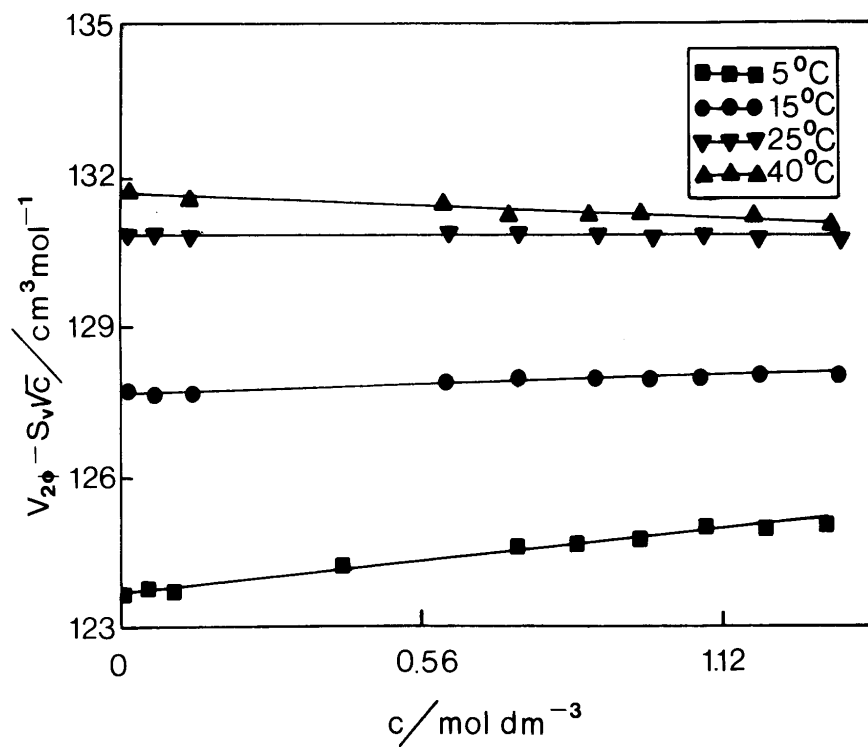
Figure 2. Plot of $V_{2\Phi}$ - S_V $\sqrt{\bar{c}}$ vs. molarity for KTS in water at various temperatures; S_V from Equation (3).

TABLE II. Apparent Molar Volumes of Alkaline p-Toluenesulphonates at Infinite Dilution and the Deviation Constant b_V at Various Temperatures.

HTS   LiTS

t^d	$V_{2\Phi}^0$	b_V	$V_{2\Phi}^0$	b_V
5	115.36 (0.30)	-0.08 (0.30)	114.77 (0.24)	-0.48 (0.24)
15	118.27 (0.23)	-0.77 (0.23)	117.75 (0.25)	-1.08 (0.25)
25	120.57 (0.23)	-0.90 (0.23)	119.97 (0.24)	-1.24 (0.24)
40	121.95 (0.11)	-1.02 (0.11)	121.17 (0.25)	-1.31 (0.25)

^{d} ^{0}C

NaTS   KTS

t	$V_{2\Phi}^0$	b_V	$V_{2\Phi}^0$	b_V
5	114.63 (0.26)	0.87 (0.260)	123.68 (0.34)	1.04 (0.34)
15	117.47 (0.21)	0.19 (0.21)	127.38 (0.3)	0.29 (0.30)
25	119.67 (0.21)	-0.15 (0.21)	130.36 (0.30)	-0.05 (0.30)
40	120.49 (0.22)	-0.60 (0.22)	131.14 (0.44)	-0.44 (0.44)

RbTS   CsTS

t	$V_{2\Phi}^0$	b_V	$V_{2\Phi}^0$	b_V
5	129.49 (0.96)	1.20 (0.96)	137.46 (0.64)	1.26 (0.64)
15	133.64 (0.55)	0.37 (0.55)	141.17 (0.62)	0.42 (0.62)
25	135.90 (0.47)	0.05 (0.47)	143.24 (0.60)	0.14 (0.60)
40	136.41 (0.42)	-0.38 (0.42)	143.35 (0.59)	-0.32 (0.59)

Discussion

The apparent molar volumes presented in this work cannot be compared directly with literature values since, to our knowledge, no such data were published. It is possible, however, to make some comparison of the temperature dependence of $V_{2\Phi}^0$ with those solutes for which data are available. To test the consistency of the experimental results, the additivity of the apparent molar volumes at infinite dilution at 25 ^{O}C was examined. The differences between the parameters $V_{2\Phi}^0$, Δ are given in Table III. One can notice that the differences Δ for alkaline p-toluenesulphonates are very close to those for alkaline chlorides. The discrepancies lie within the experimental error of the determination of $V_{2\Phi}^0$. This result is not unexpected since at the infinite dilution limit the ion-ion interactions vanish and the $V_{2\Phi}^0$ values represent only ion-water interactions.

In the case of complete dissociation the Δ values depend only on the difference by which different ions affect the structure of water.

Table III. Differences, Δ, of the $V_{2\Phi}^0$ Values for Alkaline Chlorides and Alkaline p-Toluenesulphonates at 25 ^{O}C.

Ion	Cl$^-$ [10]	Δ	TS$^-$
Li$^+$	16.91	103.06	119.97
Δ	-0.29		-0.30
Na$^+$	16.62	103.05	119.67
Δ	10.19		10.69
K$^+$	26.81	103.55	130.36
Δ	5.13		5.54
Rb$^+$	31.94	103.96	135.90
Δ	7.23		7.34
Cs$^+$	39.17	104.07	143.24

To examine the effect of temperature on $V_{2\Phi}^0$ for alkaline p-toluenesulphonates, the results for $V_{2\Phi}^0$ were expressed as a polynomial function of temperature and the polynomial was then differentiated with respect to temperature. This way a function was obtained which allowed calculation of the apparent molar expansibility of the solute at the infinite dilution limit [12] :

$$E_{2\Phi}^0 = \left(\partial V_{2\Phi}^0 \Big/ \partial T \right)_P \tag{4}$$

Figure 3 shows $E_{2\Phi}^0$ for Li and K p-toluenesulphonate solutions as a function of temperature. $E_{2\Phi}^0$ values for LiCl and KCl [12] are included in Figure 3 for comparison. The conclusion is that the values of $E_{2\Phi}^0$ for alkaline p-toluenesulfonate solutions decrease with increasing temperature, as in the case of other simple electrolytes.
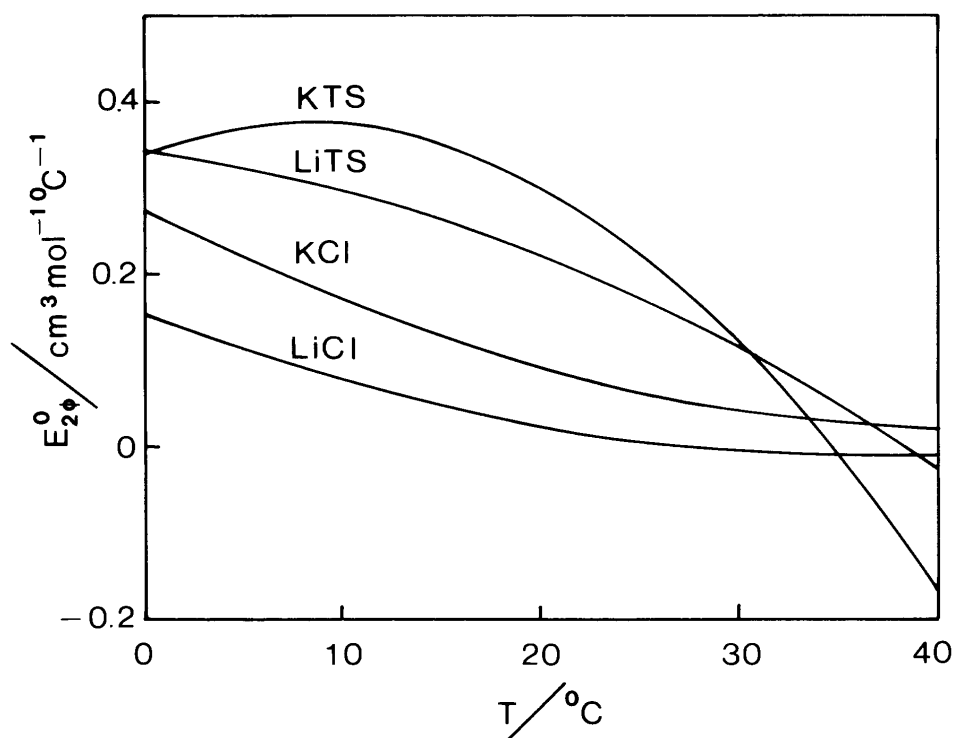
Figure 3. Partial molar expansibility of aqueous LiTS, KTS, LiCl and KCl at infinite dilution as a function of temperature.

There are, however, differences in the magnitude of $E_{2\Phi}^{0}$ and in the shape of the curve. It seems reasonable to attribute this effect to the influence of the large aromatic anion on the structure of water. (See also Figure 4). Hepler [14] has pointed out that from the thermodynamic relation

$$\left(\frac{\partial \overline{C}_{P}^{0}}{\partial P}\right)_{T} = -T\left(\frac{\partial^{2}\overline{V}^{0}}{\partial T^{2}}\right)_{P} = -T\frac{\partial \overline{E}^{0}}{\partial T} \tag{5},$$

where $\overline{C}_{P}^{0}$ is the partial molar heat capacity at infinite dilution, one can discern the type

of effect. A positive value of $\left(\dfrac{\partial \overline{C}_{P}^{0}}{\partial P}\right)_{T}$, or a negative value of $\dfrac{\partial \overline{E}^{0}}{\partial T}$, is evidence of the

structure breaking effect of the solute. It seems then reasonable to regard the ion of the aromatic electrolyte (cf. Figure 4) as having a dual character: it has a "structure making" effect on water on the aromatic side and a "structure breaking" effect on the side of the sulphonic group. The former effect expands, and the latter diminishes the apparent size

of an ion. Both types of effect are temperature dependent. At higher temperatures electrostriction becomes more important leading to a reduction of size [12].
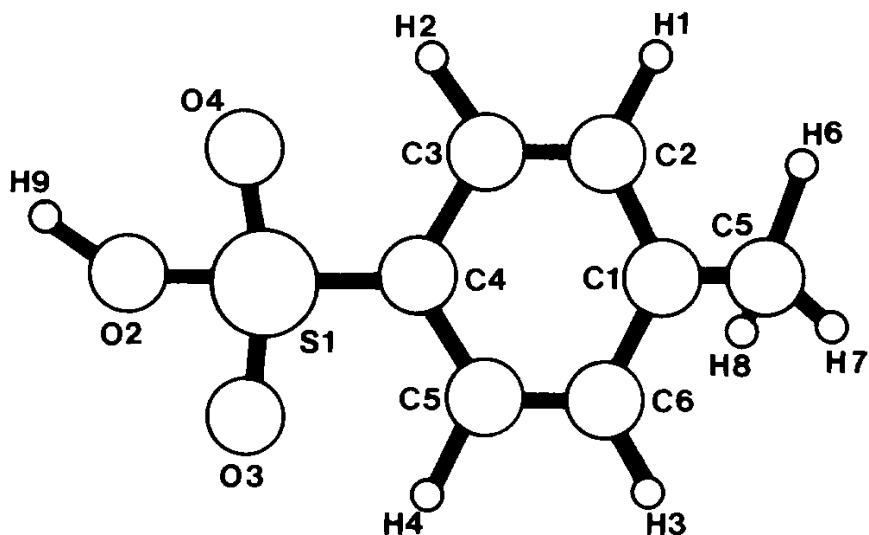
Figure 4. The structure of p-toluenesulphonic acid.

The values obtained for b_V in Equation (2) are tabulated in Table II. Since there is no theory that covers this empirical term it is not known what significance to attach to it, although it probably has to do primarily with solute-solute interactions. One can see, however, that b_V is positive at lower temperatures and becomes less positive or more negative, as the temperature rises. This behaviour is consistent with that found by Helgeson and Kirkham [15] for several inorganic salts, and recently also by Strong et al. [16] for some methyl substituted benzoic acids and their sodium salts.

Finally, it should be mentioned that direct comparison of the apparent molal volumes of polyelectrolytes with those of model electrolytes is not possible. Škerjanc [17] has demonstrated experimentally and theoretically a sharp fall of $V_{2\Phi}$ with decreasing polyelectrolyte concentration. These results lead to the conclusion that $V_{2\Phi}$ data obtained by linear extrapolation of $V_{2\Phi}$ to zero concentration [18,19] should be accepted with a great deal of caution. Furthermore, the apparent molar volumes of polyelectrolytes are not additive, the reason being the so-called site binding of counterions [20].

References

[1] G. E. Boyd, F. Vaslow, A. Schwarz and J. W. Chase, *J. Phys. Chem.,* **1967,** 71, 879.

[2] G. Vesnaver, M. Rudež, C. Pohar and J. Škerjanc, *J. Phys. Chem.,* **1984,** 88, 2411.

[3] K. Otrin Debevc, C. Pohar and V. Vlachy, *J. Solution Chem.,* **1996,** 25,787.

[4] C. Pohar, K. Otrin Debevc and V. Vlachy, *Acta Chim. Slovenica*, **1997**, 44, 79.

[5] P. S. Ramanathan and H. L. Friedman, *J. Chem. Phys*, **1971,** 54, 1086.

[6] D. O. Bonner and R. W. Gable, *J. Chem. Eng. Data*, **1970,** 15, 499.

[7] O. Redlich, D. M. Meyer, *Chemical Reviews*, **1964,** 64, 221.

[8] H. S. Frank and M. W. Evans, *J. Chem. Phys.,* **1945,** 11, 507.

[9] W. Y. Wen and S. Saito, *J. Phys. Chem.*, **1964,** 68, 2639.

[10] J. E. Desnoyers, M. Arel, G. Peron and C. Jolicoeur, J. Phys. Chem., **1969,** 73, 346.

[11] F. J. Millero, *Chemical Reviews*, **1971,** 71, 147.

[12] F. J. Millero in *Water and Aqueous solutions*, R. H. Horne ed., Wiley, New York, **1972,** Chap.13.

[13] G. S. Kell, *J. Chem. Eng. Data,* **1967,** 12, 66.

[14] L. G. Hepler, *J. Phys. Chem.*, **1965,** 69, 965.

[15] H. C. Helgeson and D. H. Kirkham, *Am. J. Sci.*, **1976,** 276, 97.

[16] L. E. Strong, M.Bowe., J. White, and K. Abi-Selah, *J. Solution Chem.*, **1994,** 23, 541.

[17] J. Škerjanc, *J. Phys. Chem.*, **1973, 77,** 2225.

[18] N. Ise and T. Okubo, *J.Amer. Chem. Soc.*, **1968,** 90, 4527.; *Macromolecules*, **1969,** 2, 401.

[19] B. E. Conway, J. E. Desnoyers, and A. C. Smith, *Phyl. Trans. Roy. Soc. London*, **1964,** 256, 389.

[20] C. Tondre and R. Zana, *J. Phys. Chem.*, **1972,** 76, 3451.

Povzetek

Izmerili smo gostote raztopin alkalijskih soli p-toluensulfonske kisline pri temperaturah 5, 15, 25 in 40 ^{o}C in v koncentracijskem območju od 0.01 do 2 mol-kg^{-1}. Iz dobljenih podatkov smo izračunali navidezne molske volumne $V_{2\Phi}$. Z uporabo Redlich-Meyerjeve enačbe smo določili navidezne molske volumne pri neskončnem razredčenju $V_{2\Phi}^{o}$ in deviacijske parametre b_V. Ugotovili smo, da velja pravilo o aditivnosti navideznih ionskih volumnov pri temperaturi 25 ^{O}C. Vrednosti $V_{2\Phi}^{o}$ naraščajo, vrednosti parametrov b_V, pa padajo z naraščajočo temperaturo. Temperaturna odvisnost volumskih lastnosti raztopin alkalijskih p-toluensulfonatov je podobna temperaturni odvisnosti alkalijskih kloridov.

ANALYSIS OF OSMOTIC PRESSURE DATA FOR AQUEOUS PROTEIN SOLUTIONS VIA A ONE - COMPONENT MODEL [1]

Yu. V. Kalyuzhnyi[a,b], J. Reščič[b] and V. Vlachy [b]

[a] Institude for Physics of Condensed Matter, Lviv, Ukraine
[b] Faculty of Chemistry and Chemical Technology, University of Ljubljana, Aškerčeva 5, 1000 Ljubljana, Slovenia.

Abstract
A modification of the one-component model of protein solutions is presented that accounts for the self-association of protein molecules in solution. In addition to the usual screened Coulomb interaction the protein molecules can form dimers, but no higher clusters are allowed. Essentially, we treat the solution as a mixture of hard spheres and hard dumb-bells characterized by some effective diameter. A simple variational approach is proposed to relate the effective diameter to the parameters of the solution under investigation, i.e. the real diameter of the protein, its charge and concentration. The new method is used to analyse the reported data for the osmotic pressure of three different proteins with various degrees of self-association. The method, which requires little numerical work, seems to be able to explain the osmotic pressure behaviour of protein solutions in terms of a single parameter, i.e. the fraction of dimers in solution.

Introduction

Professor Savo Lapanje in the Preface to his monograph on protein denaturation [1] wrote: "the physicochemical aspects of protein denaturation represent the basis

---

[1]Dedicated to the memory of Professor Savo Lapanje

for understanding all other aspects of this important phenomenon". In other words, knowledge of the protein-protein and protein-solvent interactions is a prerequisite for understanding of their properties in solution. It appears, however, to be very difficult to build a consistent microscopic picture of these complex systems. The structure and thermodynamics of protein solutions will result from a subtle balance between the protein-protein interaction, protein-electrolyte and protein-solvent interaction, including the influence of the electrolyte-solvent and solvent-solvent interaction. It is clear that a general theory for these ternary systems, based on Hamiltonian models, cannot be expected soon. Yet, there is need to study the sources of nonideality in protein solutions and to interpret the experimental results in the light of molecular theories. One such attempt is presented in this paper.

Among experimental techniques used to identify the principal interactions in macro-molecular solutions, measurements of the osmotic pressure play very important role (see, for example [2], [3], [4], [5]). The first measurements of the osmotic pressure in aqueous protein solution were conducted as early as 1899 [6] and since that time os-mometry has become an important tool for characterization of proteins in solution. Very recently, some of us have applied this experimental technique to study the association of human serum albumin (HSA) in aqueous solutions in mixtures with phosphate buffer [5]. These measurements indicate strong deviations from ideality, the osmotic pressure being influenced by factors like pH, the concentration of added electrolyte and protein concentration. The osmotic pressure measurements [5] were complemented by an X-ray study of the same system and the protein association was identified as the principal source of the nonideality. So far, only the experimental results were presented and no theoretical predictions were compared with our experimental data for HSA [5].

Traditionally, osmotic pressure data are interpreted in terms of the second virial coefficient, B_2. This automatically limits the theoretical analysis to solutions which are very dilute with respect to the protein component. A more satisfying approach is to include higher virial coefficients through a suitable integral equation theory. In some cases [7], good agreement between the experiment and theory can be obtained. Unfortunately, integral equation theories, based on the concentration expansion (the first term of this expansion is proportional to B_2) are not well suited for systems with a strong attractive interaction [8]. For the strongly nonideal systems studied here, where the osmotic coefficient does not approach unity even in a dilute regime, the classical integral equation theories become inapplicable. For example, the hypernet-ted chain approximation, an otherwise successful theory for charged solutions, does

not yield convergent results under conditions where strong attractive forces yield to partial association of ions. In the last decade, however, statistical-mechanical theories were developed which permit us to study model solutions, where the particles form dimers or even higher clusters [9].

Very recently, Kalyuzhny and Vlachy [10] have proposed a theoretical model in which the protein molecules, in addition to the usual Coulomb forces, interact via a short-range directional attractive force. Our approach is based on the theory developed by Wertheim [9] for treating associated systems. Parameters of the short-range interaction are chosen to result in formation of dimers. This model provides a basis to quantify the effects of macroion association on factors such as protein and electrolyte concentration, charge and size of the protein and others. The major disadvantage of the proposed theory is that it requires a solution of the integral equations for the multicomponent system and it is therefore less applicable for daily analysis of experimental results.

In the present paper we propose a much simpler approach to analyse osmotic pressure data in protein solutions: the method is an extension of the one-component model and should apply equally well to both associated and nonassociated systems. In the proposed theory the solution is treated as a mixture of dimers (pairs of protein molecules) and monomers. The particles forming the mixture are assumed to have some "effective" size which differs from their "real" (molecular) size. This way we can use a known formula to obtain the osmotic pressure for a hard sphere - hard dumb-bell mixture [11]. The effective size of the particles reflects the interactions between the protein molecules in solution; it is obtained using the variational principle [12], taking into account the "real" size of the protein, its charge, the concentration of added electrolyte and other parameters which characterize the solution under investigation.

Theoretical Part

Ternary solutions containing protein, a simple electrolyte and water are too complicated for a complete description on the molecular level. Fortunately, many experimental properties of globular proteins can be explained using a simple one-component model wherein a pseudo- solvent (simple electrolyte and water) modifies the interactions between the protein molecules. In this article we present an extension of this approach to account for the possible self-association of the protein molecules in solution.

The aqueous solution of a globular protein is represented as a two-component mix-

ture of charged hard spheres (monomers) and charged hard sphere diatomics (dumb-bells), mimicking the dimers. The effect of added electrolyte is modelled by the screened Coulomb potential acting between each pair of monomer units. Thus, the total pair potential $U(r)$ between the diatomic sites, the diatomic site and the charged hard sphere and between the charged hard spheres is of the following form:

$$U(r) = U_h(r) + U_Y(r) \qquad (1)$$

where $U_h(r)$ is the hard-sphere potential, and

$$U_Y(r) = \frac{A}{r} \exp(-\kappa r), \qquad (2)$$

where

$$A = \frac{z_p^2 L_B \exp(\kappa\sigma)}{(1 + \kappa\sigma/2)} \qquad (3)$$

In Eqs. (2,3) κ is the Debye-Hückel screening parameter defined as

$$\kappa^2 = 4\pi L_B N_A c_s \qquad (4)$$

where $e_0 z_p$ is the macroion charge, σ is the hard-sphere (molecular) diameter, c_s is the molar electrolyte concentration and N_A is the Avogadro number. Further, L_B is the Bjerrum length given by

$$L_B = \frac{e_0^2}{4\pi\epsilon_0\epsilon_r k_B T}, \qquad (5)$$

where $\epsilon_0\epsilon_r$ is the permittivity of the solution, k_B Boltzmann's constant and T the absolute temperature.

To calculate the thermodynamic properties of the model system described above we utilize a simple thermodynamic perturbation theory and the Boublik equation of state for a mixture of hard convex bodies [11]. First, the original system interacting via the potential given by Eq. (1) is replaced by a reference system represented by the two-component mixture of hard spheres and hard dumb-bells (representing dimers) of some "effective" diameter. The effective hard-sphere diameter σ_{ef} for the dumb-bell sites and hard spheres, reflecting the screened Coulomb interaction, is then determined using the condition proposed by Lado [12]:

$$4\pi \int_0^\infty r^2 dr [e^{-\beta U(r)} - e^{-\beta U_h(\sigma_{ef}, r)}] \frac{\partial y_h(\sigma_{ef}, r)}{\partial \sigma_{ef}} = 0 \qquad (6)$$

In this calculation the dumb-bell elongation L is $L = \sigma$. An alternative is to choose the value of L in such a way that the dumb-bell excluded volume is the same as of

original hard spheres. The choice of L, however, does not affects σ_{ef} significantly. In order to evaluate integral in Eq. (6) we need to know y_h; the so-called cavity distribution function for the hard-sphere system [13]. The hard-sphere cavity distribution function $y_h(\sigma_{ef}, r)$ was calculated using the Henderson-Grundke prescription [14]. It is important to stress that condition given by Eq. (6) enforces thermodynamic consistency; the energy and the virial route to osmotic pressure yield exactly the same result [12].

In the last step, Boublik's equation for the osmotic coefficient [11] is applied in the form:

$$\Phi = \frac{\beta P}{N k_B T} = \frac{1}{1-v} + \frac{2r_c s}{\rho(1+x)(1-v)^2} + \frac{2qs^2(1-v/3)}{3\rho(1+x)(1-v)^3}, \tag{7}$$

where

$$r_c = \frac{1}{4}\rho(1+x)\sigma_{ef}\left[\frac{1}{2}(1-x)(1+\frac{1}{2}\sigma)+x\right], \tag{8}$$

$$s = \frac{1}{2}\rho(1+x)\pi\sigma_{ef}^2\left[\frac{1}{2}(1-x)(1+\sigma)+x\right], \tag{9}$$

$$v = \frac{\pi}{12}\rho(1+x)\sigma_{ef}^3\left[\frac{1}{2}(1-x)(1+\frac{3}{2}\sigma-\frac{1}{2}\sigma^3)+x\right], \tag{10}$$

$$q = \frac{1}{8}(1+x)\rho\sigma_{ef}^2\left[(1+\frac{1}{2}\sigma)^2+x\right]. \tag{11}$$

In Eqs. (7-11) x is the fraction of the hard spheres, ρ is the total number density of the monomeric units (stoichiometric number concentration of protein) in the system, defined by

$$\rho = \rho_0 + 2 * \rho_d \tag{12}$$

In the last equation (12) ρ_0 is the number density of hard spheres and ρ_d the number density of dumb-bells. One important advantage of the perturbation theory described above is that it requires very little numerical work in comparison with the theories based on the integral equation approach [10]. Equation (6) was solved numerically using Newton - Raphson method.

Analysis of experimental data

The theory outlined in the previous section yields results for the osmotic coefficient (or osmotic pressure) which can be compared with the experimental values. The computational procedure is the following. First, we calculate the interaction potential given by Eq. (1) using the "real" (molecular) parameters of the system of
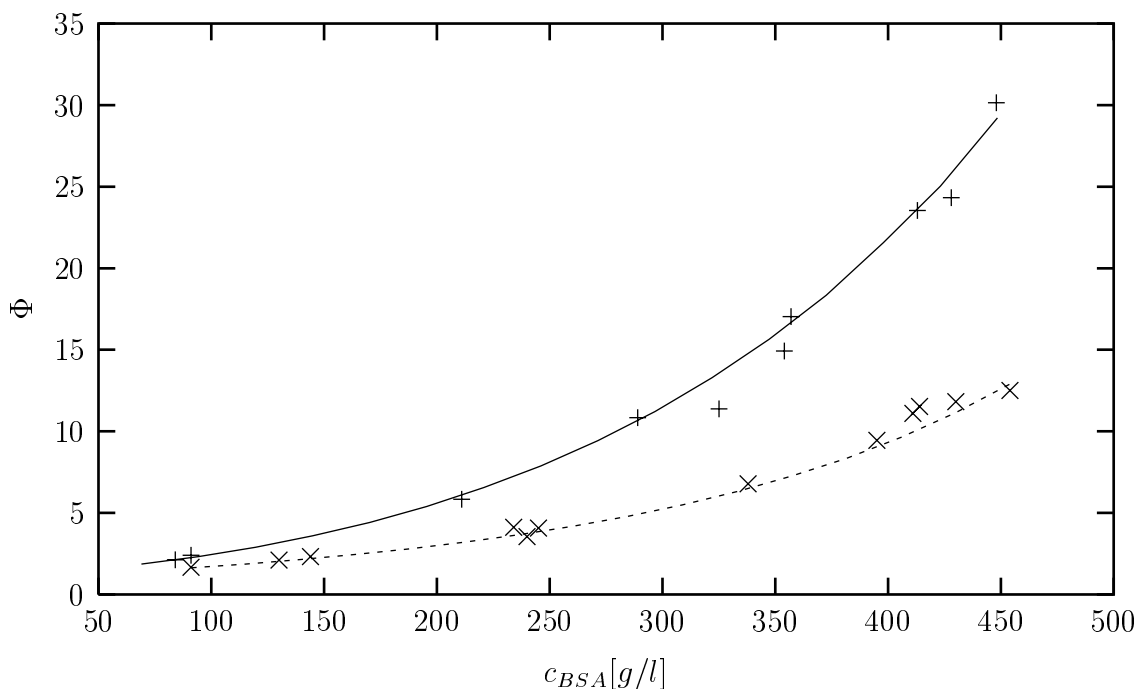
Figure 1: Osmotic coefficient $\Phi = \Pi/\Pi_{id}$ as a function of BSA concentration [3]. Theoretical predictions at pH 7.3 are represented by the solid line and at pH 5.4 by the dashed line; experimental data at pH 7.3 (+++) and at pH 5.4 (xxx). Protein charges are -20 and -9 at pH 7.3 and 5.4, respectively.

interest. This information is used as input to Eq. (6) which determines the effective dimensions of the hard sphere - hard dumb-bells mixture. Once the effective diameter for the model mixture is known the osmotic coefficient can be determined from Eq. (7). The calculated osmotic coefficient (or pressure) can be fitted to experimental results to obtain the fraction of dimers in the solution. The results for three different proteins in solution are presented below.

First we apply our analysis to the osmotic pressure measurements of bovine serum albumin (BSA) in 0.15 M sodium chloride. These results are shown in Fig. 1, where the osmotic coefficient is given as a function of the protein concentration. The lines in figures are 'eye best fit'. The experimental data are from ref. [3]. The protein molecular weight used in the calculation of osmotic coefficient is 69,000 g/mol. Under these conditions (for other parameters see the caption to the figure) no self-association of protein molecules is detected - the fraction of dimers giving good agreement with experiment is zero. Note, however, that these results apply to a very high concentration of BSA molecules. In Fig. 2 we present the results for the human serum albumin (HSA) solutions recently studied by some of us [5]. Again the osmotic coefficient is analysed as a function of the protein concentration
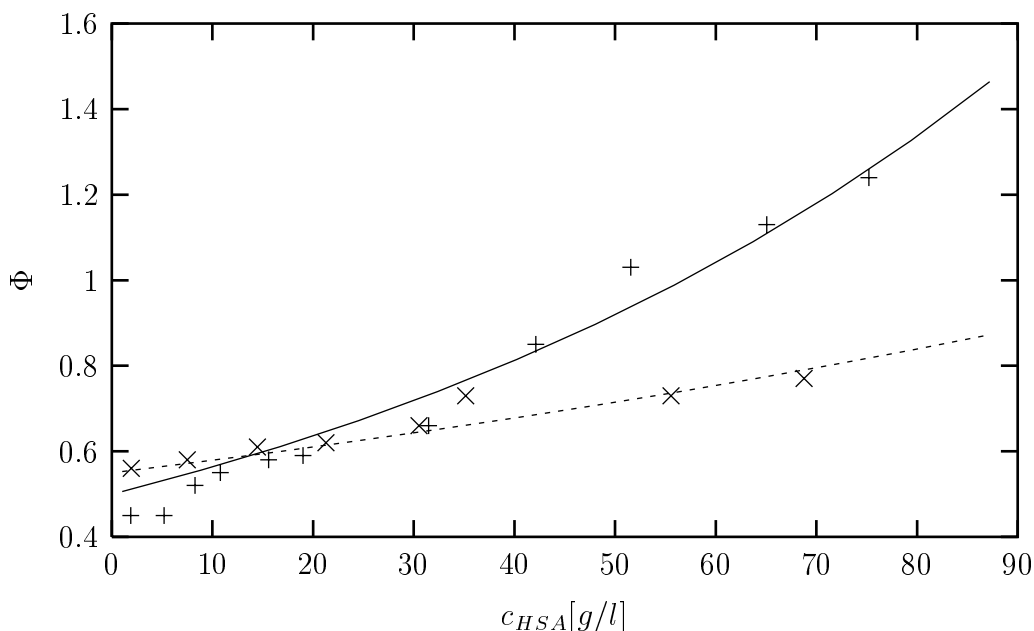
Figure 2: Osmotic coefficient as a function of the HSA concentration [5]. Theoretical predictions at pH 8.0 are represented by the solid line and at pH 5.4 by the dashed line; experimental data at pH 8.0 (+++) and at pH 5.4 (xxx). The number of negative charges on the HSA molecule are 22 and 0 at pH 8.0 and 5.4, respectively.

and for two different pH values. The concentration of added phosphate buffer was 0.1 M. The protein molecular weight used in this calculation was 66,700 g/mol and the charges on the protein [17] are given in caption to this figure. In this case the strong nonideality in solution can be explained by the formation of dimers. A reasonably good agreement between calculation and experiment is obtained when the fraction of dimers is equal to 1 (full dimerization) and 0.9, for pH values equal to 8.0 and 5.4, respectively. Appreciable association in dilute solutions of HSA has been confirmed by an X-ray scattering study [5].

The third figure (Fig. 3) presents the osmotic pressure results for moderately concentrated BSA solutions at two different pH values (for experimental details see [15], [16]). The number of (negative) charges on the protein molecule is 21 and 17 at pH 7.3 and 6.9, respectively. The ionic strength of the added simple electrolyte is 0.1 M. The fraction of dimers used as input in these calculations was 0.3. Equally good agreement between theory and experiment was also obtained for pH = 8.0, but these results are not shown here. Diammeter of both HSA and BSA molecules used in calculations is 6.0 nm.

In the final example studied in this paper we present the results for α -chymotrypsin solutions. In Fig. 4 the osmotic pressure is plotted as a function of protein concen-
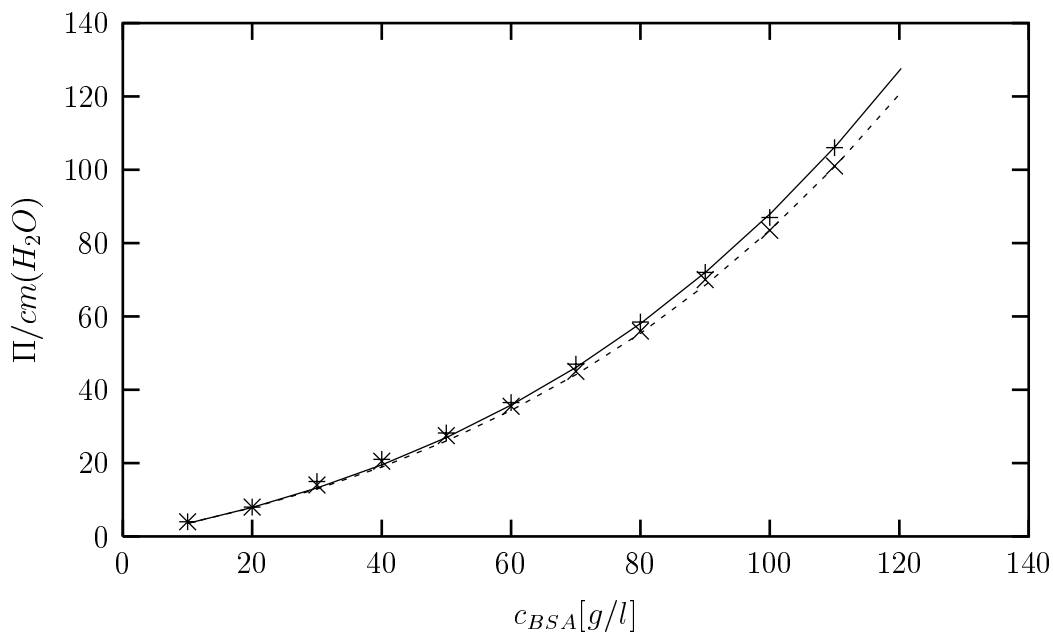
Figure 3: Osmotic pressure Π as a function of BSA concentration [15], [16]. Theoretical predictions at pH 7.3 are represented by the solid line and at pH 6.9 by the dashed line; experimental data at pH 7.3 (+++) and at pH 6.9 (xxx).
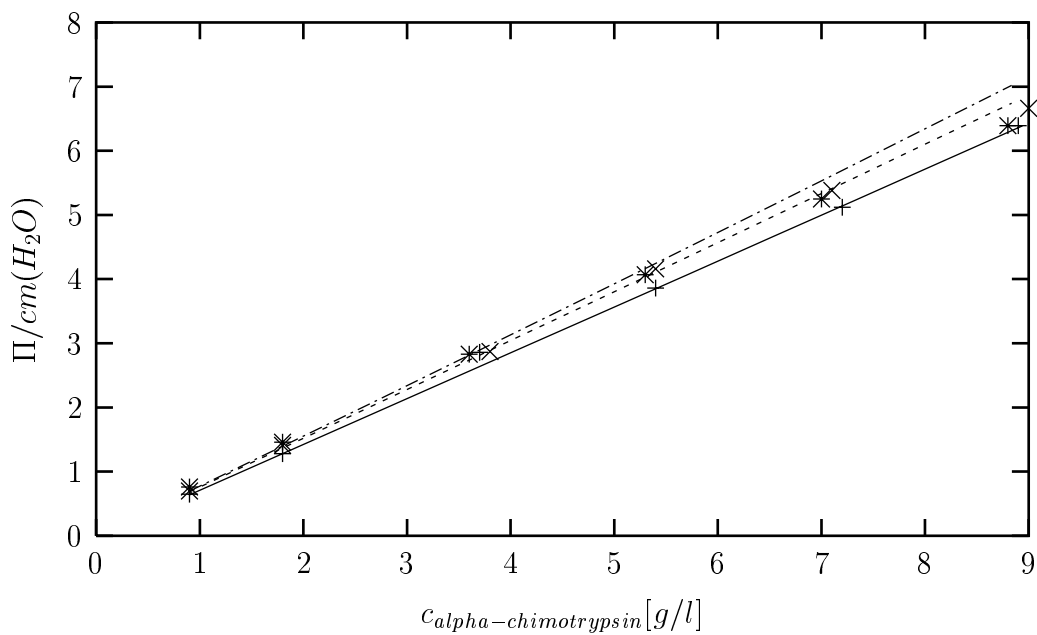
Figure 4: Osmotic pressure Π as a function of α-chymotrypsin concentration [4]. Theoretical predictions at pH 8.25 are represented by the solid line, at pH 6 by the dashed line and at pH 4 by the dashed-dotted line. Experimental data at pH 8.25 are denoted by (+++), at pH 6 by (xxx) and at pH 4 by (***).

tration for three different values of pH. Experimental values are taken from ref. [4]; the ionic strength of the added simple electrolyte is 0.3 M in this example and the number of charges on the protein for the three pH values is 0 (pH=8.25), 3 (pH=6.0) and 10 (pH=4.0). The protein diammeter is 2.17 nm. The fraction of dimers used to calculate the lines in Fig. 4 are 0.48 (pH=8.25), 0.38 (pH=6), and 0.35 (pH=4).

Discussion

The nonideality of protein solutions may originate from several sources; the association between protein molecules is one of them. It is known that this association plays an important role in the control of enzyme activity. To know the degree of protein self-association and the factors which control this phenomenon is therefore important. Among experimental methods, membrane osmometry is a traditional method of measuring the nonideality of protein solutions.

In an attempt to explain the osmotic pressure data of aqueous solutions of globular proteins, we propose a simple perturbation theory. The idea was to develop a theoretical model that predicts how factors such as protein size and charge (pH), salt concentration and protein aggregation affect the osmotic pressure. The perturbation theory presented in this paper has two advantages: i) it does not require massive numerical work as do integral equation theories, and, ii) it applies equally well to associated and non-associated systems of molecules. The analysis of experimental data for three different proteins in a broad range of protein concentration, (varying pH and concentration of added simple electrolyte) is presented in the previous section. The results indicate that we can fit the experimentally obtained osmotic pressure by adjusting the fraction of dimers in solution. In this way, the fraction of dimers in solution can be determined. With this respect, the theory proposed above is positioned somewhere between the molecular theories based on Hamiltonian models [10] and fully empirical methods [16] of data analysis. At this level of the theory only formation of dimers is considered. At higher degrees of dimerization (e.g. the system presented in Fig. 2), the contribution of higher clusters may become appreciable, what essentially limits applications of the theory only to situations where the degree of pairing is low. It is not impossible, however, to extend the calculation to treat trimers and higher clusters or, for example, to account for the interpenetration of the protein molecules. We hope to present some of these developments in the near future.

References

[1] S. Lapanje, *Physicochemical Aspects of Protein Denaturation:* Wiley, New York, 1978.

[2] M. P. Tombs and A. R. Peacocke, *The Osmotic Pressure of Biological Macromolecules*, Clarendon, Oxford, 1974.

[3] V. L. Vilker, C. L. Colton, and K. A. Smith, *J. Colloid. Interface Sci.*, **1981**, *79*, 548.

[4] C. A. Haynes, K. Tamura, H. R. Korfer, H. W. Blanch, and J. M. Prausnitz, *J. Phys. Chem.*, **1992**, *96*, 905.

[5] J. Reščič, V. Vlachy, A. Jamnik, and O. Glatter, *Biophys. Chem.*, submitted.

[6] E. H. Starling, *J. Physiol.*, **1899**, *24*, 317.

[7] V. Vlachy and J.M. Prausnitz, *J. Phys. Chem.*, **1992**, *96*, 6465.

[8] Yu. V. Kalyuzhnyi, M. F. Holovko, and A. D. J. Haymet, *J. Chem. Phys.*, **1991**, *95*, 9151.

[9] M. S. Wertheim, *J. Stat. Phys.*, **1984**, *35*, 19 - 35; **1986**, *42*, 459 - 477.

[10] Yu. V. Kalyuzhnyi and V. Vlachy, *J. Chem. Phys.*, **1998**, *108*.

[11] T. Boublik, *J. Chem. Phys.*, **1975**, *63*, 4084.

[12] F. Lado, *Mol. Phys.*, **1984**, *52*, 871.

[13] J. P. Hansen and I. R. MacDonald , *Theory of Simple Liquids*, Academic Press, London, **1986**.

[14] D. Henderson and E. W. Grundke, *J. Chem. Phys.*, **1975**, *63*, 601.

[15] A. P. Minton, *Biophys. Chem.*, **1995**, *57*, 65.

[16] K. M. Kanal, G. D. Fullerton, I. L. Cameron, *Biophys J.*, **1994**, *66*, 153.

[17] N. Fogh-Andersen, P. J. Bjerrum, O. Siggaard-Andersen, *Clin. Chem*, **1993**, *39/1*, 48.

Povzetek

Članek obravnava razširitev enokomponentnega modela raztopine globularnih proteinov v vodi. Novi model omogoča študij asociiranih sistemov, kjer molekule ali ioni tvorijo pare. Poleg običajnega, zaradi prisotnosti elektrolita zasenčenega coulombskega potenciala delujejo med proteinskimi molekulami tudi kratkosežne sile, ki vodijo do nastanka parov. Gruče, ki vsebujejo tri ali večmolekul, smo v tem delu prezrli. Raztopino smo obravnavali kot mešanico, ki jo sestavljajo toge kroglice (monomer) in pa v par povezane toge kroglice (dimer). Za takšen primer je bila izpeljana enačba stanja, ki je dana v analitični obliki. Velikost togih kroglic, ki smo jo uporabili v računu, ne ustreza molekularnim dimenzijam proteina, ampak že odraža tudi njihovo interakcijo s topilom in dodanim elektrolitom. Razširjeni model omogoča analizo termodinamičnih količin pri neasociiranih kot tudi pri asociiranih raztopinah in zahteva razmeroma malo numeričnega dela. Uporabnost predlaganega modela smo prikazali z analizo izmerjenih osmoznih tlakov v raztopinah treh različnih proteinov in sicer v širokem območju koncentracij in pH vrednosti. Kot rezultat podajamo delež asociiranih molekul v teh raztopinah.

A SILVER/SILVER SULPHIDE SELECTIVE ELECTRODE PREPARED BY MEANS OF CHEMICAL TREATMENT OF SILVER WIRE

D.Dobčnik, I.Gros and M.Kolar

Faculty of Chemistry and Chemical Engineering, University of Maribor, Slovenia

Summary. The preparation and usability of a sulphide ion selective electrode, prepared by means of chemical pretreatment of silver wire with an ammonium perdisulphate solution, and the sulphidization in an alkaline sulphide solution are described. The electrode is suitable for direct potentiometric measuring of sulphide in alkaline solutions of concentrations down to 1×10^{-6} mol/L. The 45 min required for each chemical treatment are enough for the preparation of the described electrode.

INTRODUCTION

Ag/Ag_2S electrodes are prepared by means of anodic polarization of a silver rod in a solution of sodium sulphide [1], by dipping the platinum spiral, coated with porous silver, into a solution of hydrogen sulphide [2], by sulphidizing the silver wire with sulphur vapor in nitrogenous atmosphere [3] as well as by sulphidizing with cooper-alloyed silver wire in a saturated alkaline solution of sodium sulphide [4]. The authors state that even after six days of chemical treatment no black sulphide layer was observed on the surface of a pure silver wire (99.99%) which suggests that the silver sulphide layer is probably produced through an anodic reaction of a localized corrosion process [4].

The preparation conditions and the performance of a small size Ag/Ag_2S selective electrode are described. The analytical behaviour of this electrode, produced by chemical treatment of a silver wire, is described in terms of potential-concentration curves, electrode selectivity and titration procedures.

A series of electrodes have been prepared and investigated. Their response and selectivity to Ag^+ and S^{2-} were measured and compared with those of a commercial Orion silver/sulphide electrode. Several titrations were performed to evaluate the performances of the electrode. The investigated electrode was found as a good substitute for the commercial silver/sulphide electrode in a wide variety of practical analytical systems. A simple preparation by means of chemical pre-treatment of a silver wire with an ammonium perdisuphate solution and sulphidization in alkaline sulphide solution were performed. The electrode has proven to be suitable for direct potentiometric measuring of sulphide in alkali solutions of concentrations down to 1×10^{-6} mol/l. The 45-min required for chemical treatments are enough for the preparation of the described electrodes.

EXPERIMENTAL

Reagents

All the chemicals used were of the analytical grade and all the solutions were prepared in doubly distilled water.

A SAOB [5] solution was prepared by dissolving 2 moles of NaOH, 0.2 moles of ascorbic acid and 0.2 moles of Na_2EDTA in water and diluting them to a final volume of 1000 mL.

Standard silver solutions were prepared from a stock solution (0.1 mol Ag^+/L) by sequential dilution with 0.1 mol/L KNO_3.

A stock solution of Na_2S was prepared by dissolving the reagent grade Na_2Sx9H_2O in 25%(v/v) SAOB [5]. It was standardized iodometrically by titration with a $Na_2S_2O_3$ solution. Standard solutions were prepared from a stock solution by sequential dilution with 25%(v/v) SAOB.

Preparation of electrodes

The pure silver wire (99.99% Ag) between 0.8 and 1.0 mm in diameter was connected with a cooper wire and adhered into a glass tube with epoxy resin. The free Ag-wire should be 10 to 15 mm long. The wire is furtheron treated in HNO_3 (1+1) for approximately 10 s and thoroughly washed with doubly distilled water; then was immersed into a 0.1 mol/L solution of $(NH_4)_2S_2O_8$ for 15 min. After being washed with the doubly distilled water, the electrode was sulphidized in a 0.1 mol/L alkaline solution of Na_2S for 30 min. Finally the electrode was thoroughly washed with doubly distilled water.

Apparatus

All potentiometric measurments on sulphide electrodes were performed with a digital mV/pH meter ISKRA MA 5730. The ISKRA saturated calomel electrode (SCE) with 0.1 mol/L KNO_3 salt bridge was used as a standard reference elektrode.

Comparative measurments were made with ORION 94-16 sulphide electrode.

All measurments were carried out at 298 ± 0.1 K.

RESULTS AND DISCUSSION

Surface analysis

The depth-profile diagram obtained by the Auger electron spectrometer (PHI SAM model 545 A) shows a quantitative elemental composition of atomic layers on the surface of the silver wire. As can be seen from Fig.1, the stoichometric composition of Ag_2S is found only in the first atomic layers on the surface of the silver wire. The broadening of the concentration profile is typical of the rough surface of the chemically etched metal surface [6, 7].

Available in printed version only

Figure 1. The AES composition-depth profile of a sulphidized silver wire obtained by sputtering with 1 keV Ar^+ ions at a 47^0 incidence angle and a raster size of 10 mm x 10 mm.

Potentiometric behaviour

Response of the silver/silver sulphide wire electrode to Ag^+ and S^{2-} ions

The equilibrium potentials observed during the serial dilution of 0.1 mol/L silver nitrate in the measuring cell were plotted against $logC_{Ag^+}$. A linear response with a slope of 58.8 mV per concentration decade (59.1 mV/decade for a theoretical Nernstian response) was obtained in the concentration range from 10^{-1} to less than 10^{-5} mol/L, followed by a non linear region at lower concentrations (Fig. 2). The same procedure was used for the sulphide ion response plot in an alkaline SAOB solution containing ascorbic acid. A linear response for E vs. $logC_{S^{2-}}$ over the range from 0.1 to nearly 10^{-6} mol/L with the slope of 28.1 mV per concentration decade (29.55 mV/decade theoretical) was recorded as shown in Figure 3. A deviation from linear behaviour was observed in the concentration range from 10^{-6} to 10^{-7} mol/L.
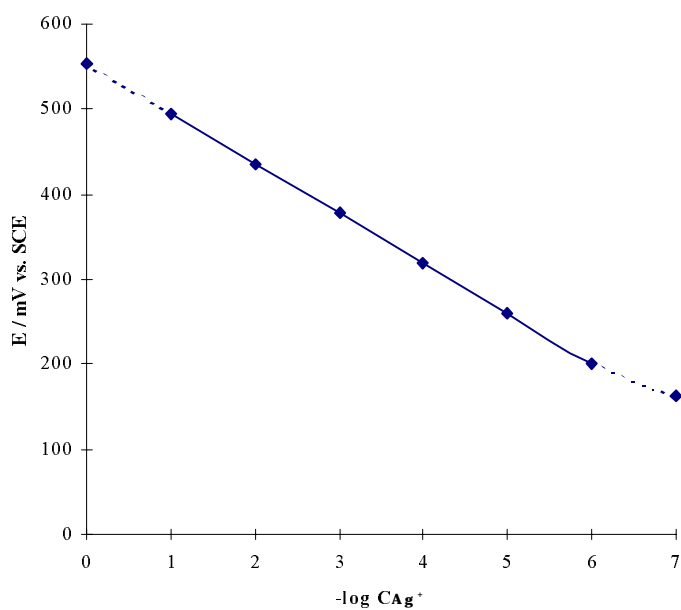
Figure 2. Response of the silver / silver sulphide electrode to the
silver ion concentrations in 0.1 mol/L KNO₃
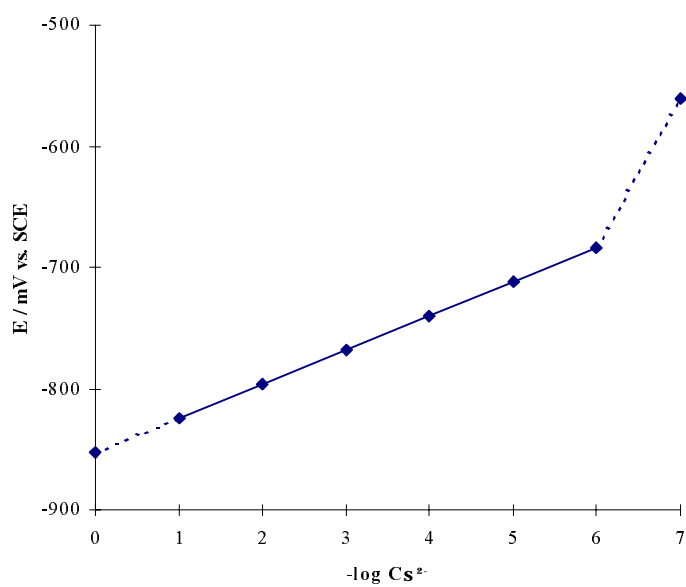
Figure 3. Response of the silver / silver sulphide electrode to the
sulphide ion concentrations in 25% (v/v) SAOB

The extrapolated intercepts at $\log C_{Ag^+}$ and $\log C_{S^{2-}} = 0$ in Figures 2 and 3 give us the values $K_{Ag^+} = 553.7$ mV and $K_{S^{2-}} = -852.8$ mV vs. SCE. Using this data and considering the potential of SCE (242.0 mV) two expressions that correlate the potential and the concentration of measuring ion can be written:

$$E_{S^{2-}} = -610.8 - 28.1 \log C_{S^{2-}}$$

$$E_{Ag^+} = +795.7 + 58.8 \log C_{Ag^+}$$

The effects of several anions, namely Cl^-, Br^-, SCN^-, I^-, NO_3^-, $S_2O_3^{2-}$, SO_4^{2-} and $C_2O_4^{2-}$ on the sulphide potential response of the electrode were tested by using the mixed solution technique [8] with a constant level of sulphide concentration 1×10^{-5} mol/L and increasing concentrations of anions in the range between 10^{-1} and 10^{-6} mol/L.

The anions have no influence in this concentration region on the measurement of sulphide. The results show that the investigated electrode can be used for selective analytical measurements in a wide variety of practical systems.

Potentiometric titrations

The wire electrode was also tested as an end-point indicator electrode in potentiometric titrations involving Ag^+ or S^{2-} ions. For comparison, the titrations were followed simultaneously with home made Ag/Ag_2S electrodes and commercial silver/sulphide electrodes. The shape of the potentiometric titrations of Ag^+ ions and the actual potential values close to and beyond the end points were in excellent agreement.

Also, the comparison of the potentiometric titration of sulphide with Pb^{2+} in alkaline solution indicates that the titration curve and end point observed coincide to a satisfactory degree (Fig. 4, 5, 6, 7) throughout some differences in potential between both electrodes.
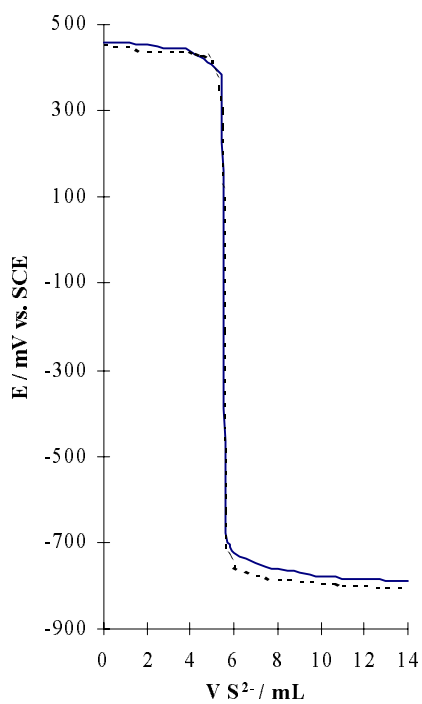
Figure 4. Ag^{+} titration with 0.1 mol/L S^{2-}
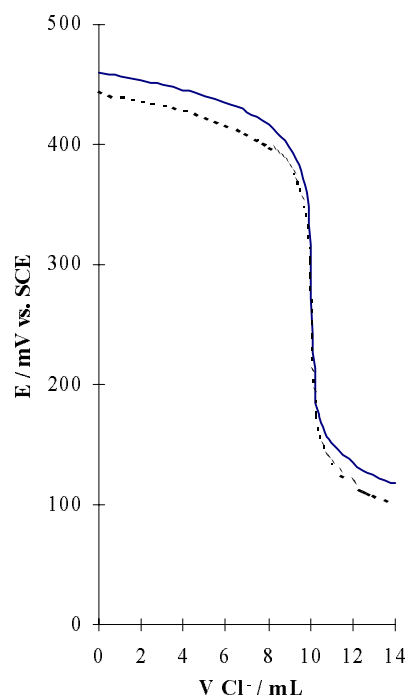
Figure 5. Ag^{+} titration with 0.1 mol/L Cl^{-}
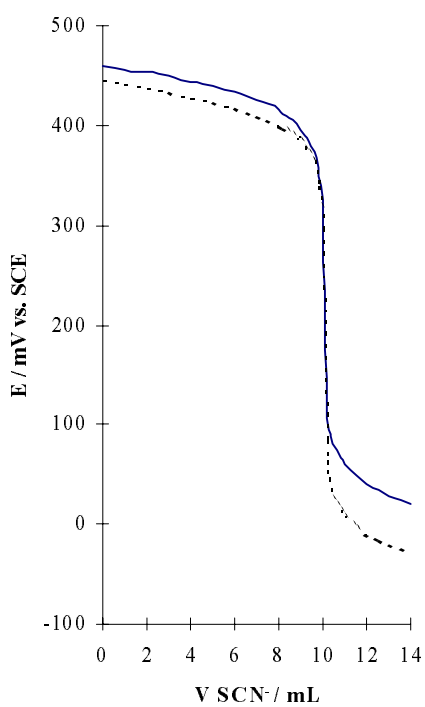
Figure 6. Ag^{+} titration with 0.1 mol/L SCN^{-}
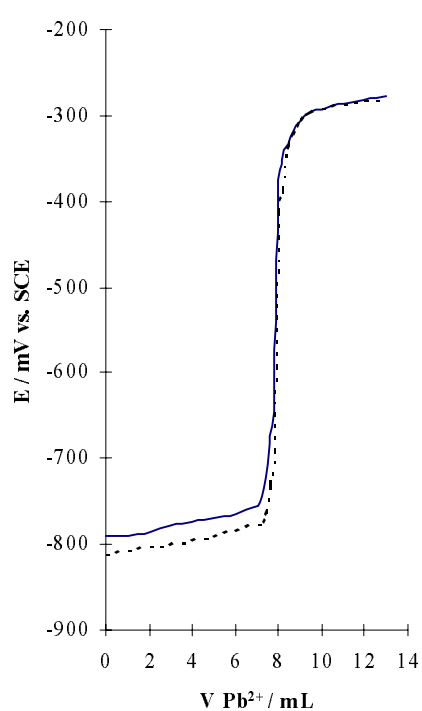
Figure 7. Sulphide titration in alkaline solution with 0.1 mol/L Pb^{2+}

REFERENCES

[1] L.T. Abfalt, D. Jagner, *Anal Chim Acta* **1971**, 56, 477.

[2] D. J. G. Ives, G.J. Janz, *Reference electrodes;* Academic Press, New York 1961, p. 382

[3] R.E. Van de Laast, *Analyst* **1977**, 102, 509.

[4] Nj. Radić, K. J. Mulligan, Jr. H. B. Marc, *Anal Chem* **1984**, 56, 297.

[5] Instruction Manual; *Sulphide ion electrode, silver ion electrode model 94-16;* ORION Research Inc.,

   Cambridge, Mass, 1977.

[6] A. Zalar, S. Hofmann, *Nucl Instr Meth Phys Res* **1987**, B 18, 655.

[7] A. Zalar, S. Hofmann, *Vaccum* **1987**, 37, 169.

[8] E. Pungor, K. Toth, *Anal Chim Acta* **1969**, 47, 291.

Povzetek: Opisujemo pripravo sulfidne ionoselektivne elektrode s kemijsko obdelavo srebrne žice v amonijevem peroksodisulfatu in v alkalni sulfidni raztopini. Elektroda omogoča direktne potenciometrične meritve koncentracij sulfidnih ionov v alkalnih raztopinah navzdol do 10^{-6} mol/L. Priprava elektrode je enostavna in hitra.

STABLE ISOTOPES DETERMINATIONS IN SOME FRUIT JUICES TO DETECT ADDED SUGAR

Marjan Guček[1], Jože Marsel[1*], Nives Ogrinc[2], Sonja Lojen[2]

[1]Department of Analytical Chemistry, Faculty of Chemistry and Chemical Technology,
University of Ljubljana, 1000 Ljubljana, Slovenia

[2]Department of Environmental Sciences, J. Stefan Institute, 1000 Ljubljana, Slovenia

Abstract

A method was developed to detect the adulteration of fruit juices. By means of stable isotope determinations, it is possible to detect exogenous sugar addition to natural juices. Since sugars photosynthesized by the Calvin cycle (orange, apple, beet) have $\delta^{13}C$ values much lower than their Hatch-Slack counterparts (cane sugar). Thus, it is possible to detect cane sugar addition. The δD in nitrated sugars enables the determination of beet sugar addition to natural juices. Commercially available Slovenian fruit juices were investigated. The results showed that none of the juices investigated was illegally adulterated.

INTRODUCTION

Stable isotopes have been extensively used for more than 15 years for the authentication and quality control of foodstuffs [1]. The most commonly employed stable isotopes in food analyses are ^{13}C, ^{2}H, ^{18}O, ^{14}N and ^{34}S, but the most important, regarding

---

* Author for correspondence

the analytical information, are ^{13}C, ^{2}H and ^{18}O, whereas ^{14}N and ^{34}S are used only occasionally. The abundance of a stable isotope in a compound is easily measured by means of Isotope Ratio Mass Spectrometry (IRMS).

Natural products exhibit small variations in their isotopic composition that are particularly amenable for provenance studies. The fluctuations are a result of isotopic fractionation that occurs during the synthesis of a given constitutional compound of a foodstuff. The causes for discrepancies in the isotopic composition are mostly different photosynthetic cycles used by plants. Moreover, milieu conditions, geographical position, rainfall and other factors also contribute to isotopic fractionation but to a lesser extent [2]. Synthetic products and compounds show different isotopic abundances, thus, enabling the differentiation among compounds of natural and those of artificial origin.

Natural variations in the stable isotope abundances in plant components provide a useful means to detect the adulteration of food. Carbon ^{13}C is especially useful in this regard. To incorporate CO_2 during photosynthesis, plants follow three biological cycles, resulting in carbohydrates with different isotopic compositions. The most plants use the C3 or Calvin cycle, whereas the fewer plant species, C4 or Hatch-Slack and CAM mode [3]. Most fruits and vegetables follow Calvin cycle, with the most well-known exceptions being corn and sugar cane which obey Hatch-Slack cycle. Due to the kinetic isotope effect, C4 plants and their metabolites are slightly enriched in ^{13}C compared to their C3 counterparts. By measuring the $^{13}C/^{12}C$ ratio, it is possible to distinguish between natural products produced by C3 plants and those synthesized by C4 plants.

Juices - both fruit and vegetable - are very popular commercial products, and there have been many attempts to adulterate them with low-cost beet, cane sugar or corn syrups. Adulterations of juices can be achieved in various ways. Exogenous sugar can be added to natural juice or to juice made of concentrate, and then diluted with water. It is also possible to dilute concentrate and sell such juice as genuine. It was expected that in Slovenia the first case of adulteration might be present.

Fortunately, with the advances in measuring stable isotope abundances, adulteration of juices has become increasingly risky, since the addition of exogenous sugar is easily traced [4 - 8]. It is possible to distinguish, e.g. between orange juice sugar (Calvin

pathway) and cane sugar (Hatch-Slack pathway) by measuring the ^{13}C content of the sugars. Though, the compounds may have the same chemical composition, they differ in isotopic content due to different photosynthetic pathways.

The problems arise when the exogenous sugar added was photosynthesized using the same cycle as the fruit plant (e.g. beet sugar added to orange or apple juice). Such a case of adulteration is expected in Slovenia since beet is the main sugar source. Though, there are slight variations in ^{13}C content among C3 plants, these differences are not sufficient for the verification of adulteration from the point of view of analytical reliability. That is why other stable isotopes and approaches are utilized to establish a reliable method for all possible cases of juice adulteration. The deuterium content is a useful tracer which can differentiate between plants and their metabolites belonging to the same photosynthetic pathway.

The hydroxyl hydrogen atoms of sugars are easily exchanged with water and so the overall deuterium content of sugars no longer corresponds to that in the original fruit. Thus, it is necessary to first remove the readily exchangeable hydroxyl hydrogen atoms before performing deuterium isotopic analysis. The best solution is the nitration of isolated and lyophilized sugars. One can measure the deuterium content in juice water (plus the content of ^{18}O) to detect the dilution of a juice concentrate [9 - 11]. By measuring the deuterium content of sugars isolated from a juice, it is possible to detect the addition of exogenous sugar [12 - 14]. All these approaches use Isotope Ratio Mass Spectrometry (IRMS) to determine the stable isotope content. The deuterium content can also be established using Site-specific Natural Isotope Fractionation NMR (SNIF/NMR) [2, 15, 16]. In this case, sugars must be converted to ethanol upon which the deuterium content at a specific site is measured.

Besides fruit juices, stable isotopes can be used to detect the adulteration of honeys [17, 18] brandies and addition of artificial aromas to different foodstuffs [19, 20].

In the present study, a method was introduced to detect the suspected adulteration of commercially available juices in Slovenia. The research focused on ^{13}C and the deuterium content of sugars. The juices under investigation were products from domestic companies but for comparison imported products were also tested. Although only orange

and apple juices were investigated, the method can be easily modified to detect adulteration of other fruit and vegetable juices and also wine [12, 21].

EXPERIMENTAL

Isolation of sugars

   The method for isolating sugars from juices was taken from Koziet *et al.* [7]. The samples comprised of freshly squeezed oranges and lemons, 7 commercially available orange juices, an apple juice and a juice made of mixed fruits.

   The insoluble constituents of cca. 50 ml of a juice were eliminated by centrifugation (30 min at 4000 rpmin). The supernatant was decanted. To precipitate soluble organic and amino acids, 2 g of calcium oxide p.a. (Merck, Germany) were added to the solution while stirring well and heating on a water bath at 90 $^{\circ}$C for three minutes. In the case of natural lemon juice 4 g of CaO were added since lemon juice contains more organic acids than orange and apple juice. The sample was then centrifuged (10 min at 4000 rpmin) and the supernatant, which contained mainly sugars, was acidified to cca. pH = 5 using sulfuric acid (1 M). The solution was refrigerated at 4 $^{\circ}$C overnight to allow the calcium sulfate to precipitate. The final solution contained mainly sugars (fructose, glucose and sucrose), with dissolved calcium sulfate and some colorants as minor constituents. Such a solution is directly amenable to the combustion unit preceding the instrumentation unit for ^{13}C isotopic analysis, whereas, the preparation of samples for deuterium isotopic analysis acquires additional preparation.

Solutions of sugars were lyophilized (66 hours) and a mixture of sugars was obtained.

Nitration of sugars

   Two nitration methods were attempted, both leading to successful results [12]. The first method uses a mixture of fuming nitric acid, acetic anhydride and acetic acid as a nitration reagent, while the second reagent is a mixture of fuming nitric acid and

concentrated sulfuric acid. Since the second method closely resembles the former, only one procedure is given.

25 ml of fuming nitric acid (Fluka) was cooled to 0 ^{o}C (on ice) and a mixture containing 15 ml of acetic anhydride and 15 ml of acetic acid (both Fluka) was slowly added. The temperature was kept below 5 ^{o}C, since at higher temperatures an extremely vigorous reaction can occur. To the nitration mixture approximately 3 g of sugars were added and allowed to react overnight. The mixture was poured into icy water where the nitrated sugars precipitated. The precipitate was thoroughly washed with water to remove all traces of acid. The nitrated sugars were dried under vacuum for 3 days to completely remove the water. The nitrated sugars formed a sticky yellowish residue and could be directly used for the deuterium isotopic determination.

Isotopic measurements of ^{13}C

The isotopic ratio of a sample is expressed as a relative value against the PDB (Pee Dee Belemnite from South Carolina, USA) standard. However, since the PDB no longer exists, a secondary standard NBS 22 (mineral oil, IAEA, Vienna) was used to calibrate the working standard (urea, 232 mg/ml).

All the measurements are expressed in relative terms against PDB. The assigned value of ^{13}C/^{12}C ratio for PDB is:

$$R = {}^{13}C/{}^{12}C = 0,0112372$$

For the other samples delta notation (δ^{13}C) is used in isotopic measurements with the expression:

$$\delta^{13}C = (R_{sample} - R_{standard})/R_{standard} \cdot 1000 \qquad [‰]$$

The instrumentation comprises of a combustion unit coupled to a mass spectrometer modified to achieve a high resolution [22, 23, 24]. In our case, isotope-ratio mass spectrometer ANCA-NT (Europa Scientific, Great Britain) was used. ANCA is a specific

line for use with raw samples in environmental and nutritional research enabling to measure $^{13}C/^{12}C$ ratio of solid, liquid and gaseous samples.

The combustion unit is maintained at 1000 $^{\circ}C$ and the reduction column at 600 $^{\circ}C$. Carbon dioxide is formed in the combustion column and analyzed in the mass spectrometer which discriminates between $^{12}CO_2^+$ and $^{13}CO_2^+$. By dividing the areas under peaks for these two ions, the ratio $^{13}C/^{12}C$ is obtained which is used to calculate the $\delta^{13}C$ value of a sample.

Isotopic measurements of ^2H

The determination of the deuterium content is a rather laborious and time-consuming procedure since the samples have to be combusted in a separate unit (off-line). The water formed has to be converted to hydrogen before the δD value can be measured.

However, the reduction of water to hydrogen is a rather sensitive procedure in terms of analytical reproducibility. It can be achieved in three ways: using zinc metal [25], chromium metal [26] or equilibrating water with hydrogen gas of known isotopic composition [27, 28]. In our study, the method based on zinc was utilized.

A home-made combustion unit was used (Figure 1), assembled according to Dunbar *et al*. [12] with some modifications. Approximately 30 mg of vacuum-dried nitrated sugars is combusted in a flow of air, previously passing through silicagel and active charcoal. During combustion at cca. 600 $^{\circ}C$ water and other gases (nitrous oxides, carbon dioxides) are formed which flow through a reduction column packed with copper oxide CuO and maintained at 900 $^{\circ}C$. Water is trapped in an ethanol-liquid nitrogen trap, while the other gases are pumped away. Afterwards, the water is transferred into a special vacuum-tight reaction vessel, containing zinc, and lyophilized.
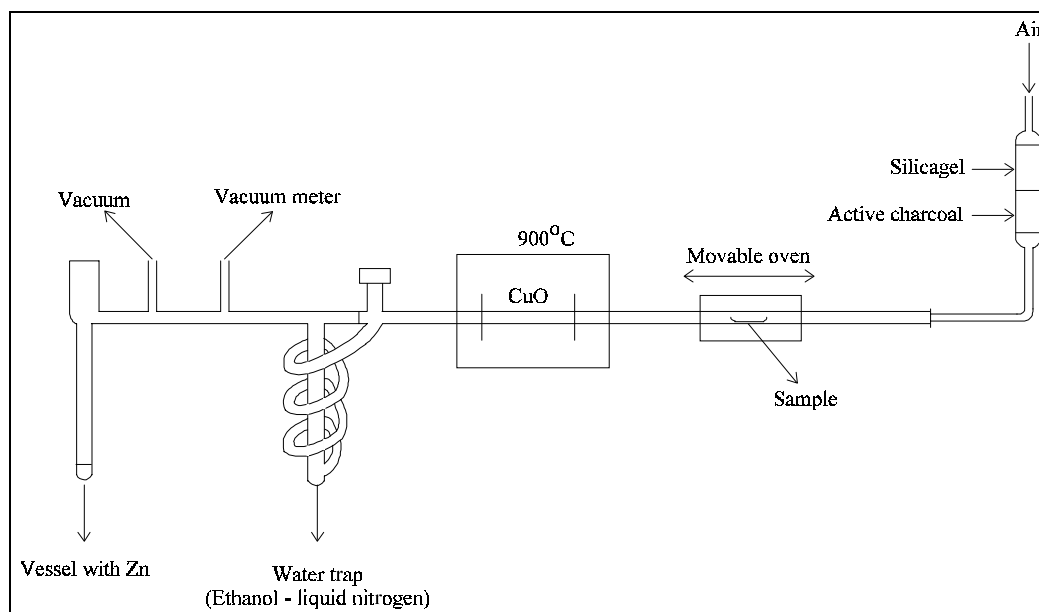
Figure 1: Schematic representation of the combustion unit

The reaction vessels, which are vacuum-tight closed, are then placed in an aluminum-block furnace at 490 ^{o}C and left to react for 4 hours. Thus, hydrogen is formed which is then measured with the mass spectrometer (MAT 250, Varian) against a suitable standard. As a primary standard in deuterium isotope determinations SMOW (Standard Mean Ocean Water) is used, nevertheless, in our study secondary standards were used: Water1 with δD = -90‰, Water2 with δD = -55‰ and polyethylene with δD = -110‰.

RESULTS AND DISCUSSION

At the beginning of the study, the isotopic measurements were performed on pure sugars and natural juices. Natural juices of orange and lemon were obtained by squeezing fresh fruits, thus, there were no doubts about the authenticity of the juices. The samples of sugars included beet sugar from Slovenia (Tovarna sladkorja Ormož) and two samples of cane sugar: one from Brazil and the other one from Australia.

Genuine juices were prepared according to the procedure described above, whereas, sugars were directly analyzed for $\delta^{13}C$ and nitrated for δD determination.

Table 1 shows the results for $\delta^{13}C$ determinations.

Table 1: $\delta^{13}C$ values for natural juices and some commercially available sugars

Sample	$\delta^{13}C$ (average)	No. of replicates	Standard deviation
Beet sugar (SLO)	-25.4	3	0.1
Cane sugar (BRA)	-11.3	3	0.2
Cane sugar (AUS)	-10.8	3	0.2
Orange juice	-22.93	5	0.07
Lemon juice	-24.1	5	0.2

The data in Table 1 clearly demonstrate that sugar cane is a C4 plant whereas oranges, lemons and beet are plants using C3 photosynthetic pathway. The standard deviation of the $\delta^{13}C$ determination is better than 0.2, or in relative terms, better than 1%. The difference between $\delta^{13}C$ for beet sugar and the same value for orange juice is more than one unit, however, this is not sufficient to detect beet sugar adulteration since climate and geographic position greatly affect the $\delta^{13}C$. The interval of the $\delta^{13}C$ values for orange juices is between -22.1 and -25.6‰ [29], thus, covering the interval of the $\delta^{13}C$ values for beet sugar. That is why the deuterium content of a sample must be taken into account to detect an illegal addition of beet sugar to a pure juice. The data of the deuterium content determinations are collected in Table 2.

Table 2: δD values of sugars and a natural orange juice

Sample	δD*
Nitrated beet sugar	-118
Nitrated cane sugar (BRA)	-78
Nitrated cane sugar (AUS)	-38
Natural orange juice	-48

*an average of two replicate measurements

Due to the laborious and time-consuming procedure of the deuterium content determination, only two replicate measurements were performed. The deuterium content

determinations suffer from memory effects during combustion and due to incomplete combustion. Both hindrances can be partly eliminated by prolonged heating of the sample container before and during combustion. The data in Table 2 clearly demonstrate that δD values for beet sugar differ from orange juice, thus, giving a reliable basis for detecting the addition of exogenous beet sugar. The range of the δD values for nitrated beet sugar is -130.4 to -108.2 permil in Germany [12], from -178 to -108 permil in USA [9] and for North America from -160 to -109 permil according to [8]. The δD values for Slovenian beet sugar resemble to the German values which is logical considering a similar geographical position and the climate milieu. On the other hand, the δD values for oranges are less negative: from -50 to 0 permil [8] and from -43 to -13 permil [9]. An adulterated orange juice (to which beet sugar was added) should have a δD value between -100 and -60 permil. Moreover, the δD value itself can serve as a tracer for the estimation of the percentage of sugar added.

The next step involved an attempt to adulterate natural orange juice with beet and cane sugar. To aliquots of 10 ml of orange juice (representing approximately 1 g of sugars) 0, 0.05, 0.1, 0.5 and 1 g of beet or cane sugar was added, thus, obtaining adulterated juices with 0, 5, 9, 33 and 50% adulteration, respectively. Afterwards, the ^{13}C content was established. The results are plotted on Figure 2.
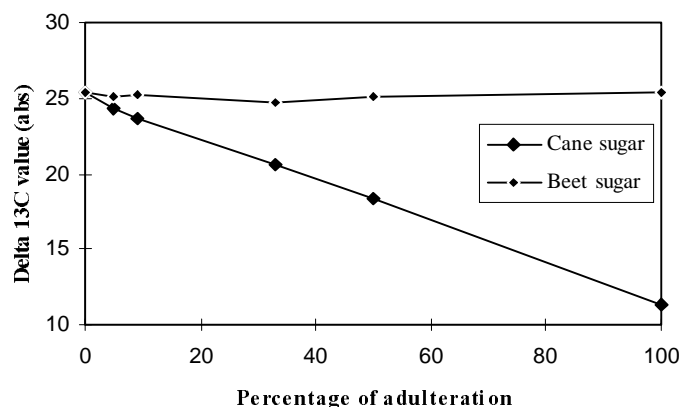
Figure 2: δ^{13}C values of orange juices adulterated with cane or beet sugar

The graphs show a decreasing $\delta^{13}C$ value (in absolute terms) with an increased percentage of adulteration with cane sugar, however, there is no trend observed in the case of beet sugar addition since the beet sugar and orange sugar are produced by C3 plants and their $\delta^{13}C$ values show similar patterns. The 'cane sugar plot' has an inherent analytical value because it enables an estimate of the percentage of cane sugar added to juices of the fruits photosynthesized by the Calvin pathway.

A list of the tested commercially available juices and the measured $\delta^{13}C$ and δD values are given in Tables 3 and 4, respectively.

Table 3: The list of juices analyzed

Number	Type of juice	Producer and mark	Specification
1	natural orange juice	lab-squeezed	100%, no sugar added
2	orange juice	FRUCTAL (SLO)	100%, no sugar added
3	orange nectar	FRUCTAL (SLO)	50%, sugar added
4	orange juice	DANA, Dan (SLO)	100%*
5	orange juice	VITAL Mestinje (SLO)	100%, no sugar added
6	orange juice	FRUCTAL, Sunny day	100%, no sugar added
7	orange juice	Happy day (Austria)	100%, no sugar added
8	orange juice	Santal (Spain)	100%, no sugar added
9	apple juice	FRUCTAL (SLO)	100%, no sugar added
10	mixed fruits	Kasfruit (Spain)	100%, no sugar added

*no declaration that no sugar is added, though, they declare it is an 100% orange juice

Table 4: Results of isotopic measurements of various juices

Number	Producer and mark	$\delta^{13}C$ [permil]*	δD[permil]**
1	lab-squeezed	-22.9	-48
2	FRUCTAL (orange, 100%)	-24.8	-53
3	FRUCTAL (orange nectar)	-17.8	-28
4	DANA, Dan	-24.9	-23
5	VITAL Mestinje, Frupi	-25.1	-25
6	FRUCTAL, Sunny day	-24.9	-37
7	Happy day (Austria)	-24.6	-27
8	Santal (Spain)	-24.7	-15
9	FRUCTAL (apple, 100%)	-25.9	-57
10	Kasfruit (Spain)	-23.3	-32

*an average of three replicate measurements
**an average of two replicate measurements

The results of isotopic measurements in the Table 4 lead to interesting conclusions. On the basis of ^{13}C determinations one can conclude that one of the juices contains cane

sugar. Nevertheless, the producer declares that sugar was added to the juice. It is interesting to note, however, that cane sugar was added, though, the predominant sugar source in Slovenia is beet sugar. The deuterium content determinations agree with the values for natural juices. Thus, no exogenous beet sugar seems to have been added to the juices analyzed.

The isotopic ratio determinations of sugars in juices prove to be a reliable method for detection of adulteration through exogenous sugar addition. The main disadvantage of the method are the time consuming steps in deuterium determination: isolation, nitration of sugars and their combustion in a special unit. Thus, a more promising approach seems to be a novel method by which deuterium content is measured by means of SNIF/NMR [15, 16].

Acknowledgments

REFERENCES

[1] H. W. Krueger, R. H. Reesmann, *Mass Spectrom. Rev*. **1982**, 1, 205-236
[2] H.-L. Schmidt, *Fresenius Z. Anal. Chem.* **1986**, 324, 760-766
[3] D. Voet, J. G. Voet, *Biochemistry*; John Wiley&Sons, 1995, pp 640-659
[4] A. Rossmann, J. Koziet, G. J. Martin, M. J. Dennis, *Anal. Chim. Acta* **1997**, 340, 21-29
[5] R. W. Durst, R. E. Wrolstad, D. A. Krueger, *J. AOAC Int*. **1995**, 78, 1195-1204
[6] N. H. Low, *J. AOAC Int*. **1996**, 79, 724-737
[7] J. Koziet, A. Rossmann, G. J. Martin, P. R. Ashurst, *Anal. Chim. Acta* **1993**, 271, 31-38
[8] J. Bricout, J. Koziet, *J. Agric. Food Chem*. **1987**, 35, 758-760
[9] L. W. Doner, H. O. Ajie, L. S. L. Sternberg, J. M. Milburn, M. J. DeNiro, K. B. Hicks, *J. Agric. Food Chem*. **1987**, 35, 610-612
[10] L. W. Doner, A. R. Brause, D. R. Petrus, *J. AOAC Int*. **1992**, 75, 1107-1111
[11] J. Koziet, A. Rossmann, G. J. Martin, P. Johnson, *Anal. Chim. Acta* **1995**, 302, 29-37
[12] J. Dunbar, H.-L. Schmidt, R. Woller, *Vitis* **1983**, 22, 375-386
[13] O. Breas, C. Guillou, F. Reniero, E. Sada, G. Tanet, *Rapid Commun. Mass Spectrom.* **1996**, 10, 246-249
[14] J. Dunbar, H.-L. Schmidt, *Fresenius Z. Anal. Chem*. **1984**, 317, 853-857

[15] G. G. Martin, V. Hanote, M. Lees, Y.-L. Martin, *J. AOAC Int*. **1996**, 79, 62-72

[16] G. J. Martin, J. Koziet, A. Rossmann, J. Dennis, *Anal. Chim. Acta* **1996**, 321, 137-146

[17] J. S. Bonvehi, F. V. Coll, *Food Science Technol. Int*. **1995**, 1, 25-28

[18] A. Rossmann, C. Luellmann, H.-L. Schmidt, *Z. Lebensm. Unters. Forsch*. **1992**, 195, 307-311

[19] M. Gensler, A. Rossmann, H.-L. Schmidt, *J. Agric. Food Chem*. **1995**, 43, 2662-2666

[20] G. Lamprecht, F. Pichlmayer, E. R. Schmid, *J. Agric. Food Chem*. **1994**, 42, 1722-1727

[21] O. Breas, F. Reniero, G. Serrini, *Rapid Commun. Mass Spectrom*. **1994**, 8, 967-970

[22] A. Newman, *Anal. Chem*. **1996**, 68, 373A-377A

[23] W. A. Brand, *J. Mass Spectrom*. **1996**, 31, 225-235

[24] W. Meier-Augenstein, *LC-GC Int*. **1997**, January

[25] C. Kendall, T. B. Coplen, *Anal. Chem*. **1985**, 57, 1437-1440

[26] M. Gehre, R. Hoefling, P. Kowski, G. Strauch, *Anal. Chem*. **1996**, 68, 4414-4417

[27] T. B. Coplen, J. D. Wildman, J. Chen, *Anal. Chem*. **1991**, 63, 910-912

[28] H. J. Tobias, K. J. Goodman, C. E. Blacken, J. T. Brenna, *Anal. Chem*. **1995**, 67, 2486-2492

[29] L. Doner, D. Bills, *J. AOAC Int*. **1982**, 95, 608-614

Povzetek

Uvedli smo metodo, s katero je možno zaslediti potvarjanje sadnih sokov. S pomočjo merjenja izotopskih razmerij je mogoče določiti dodatek sladkorja naravnim sokovom. Sladkorji, ki nastanejo preko Calvinovega cikla (pomaranča, jabolka, sladkorna pesa), imajo $\delta^{13}C$ vrednosti mnogo nižje kot ustrezni sladkorji, ki nastanejo preko Hatch-Slackovega cikla (sladkorni trs). Na ta način je mogoče zaslediti dodatek sladkorja iz sladkornega trsa. Na drugi strani pa δD vrednosti nitriranih sladkorjev omogočajo določitev dodatka sladkorja iz sladkorne pese. Metodo smo uporabili na nekaterih komercialno dostopnih slovenskih sadnih sokovih. Ugotovili smo, da noben izmed preiskanih sokov ni vseboval ilegalno dodanega sladkorja.

MERCURY AND METHALLOTHIONEIN-LIKE PROTEINS IN THE PARTICULATE CELL FRACTION OF HUMAN CEREBELLAR NUCLEUS DENTATUS

I. Falnoga, M. Tušek-Žnidarič, R. Milačič

Jožef Stefan Institute, Jamova 39, 1111 Ljubljana, Slovenia

ABSTRACT

The particulate fraction (pellet) of human cerebellar nucleus dentatus from a retired mercury mine worker with a high mercury and selenium content (2.35 ìg/g, 1.02 ìg/g) was subjected to mild extraction of Hg binding proteins with a buffer containing 10% mercaptoethanol (ME). The amount of mercury solubilised in this procedure was very low, about 3% of the pellet Hg content. Nevertheless, in the ME extract the presence of metallothionein-like proteins (MT-LP) were found by Sephadex G-75 gel chromatography and subsequent metal analysis. They were detected as Cu, Zn, Pb, Hg MT-LP, where the binding of Cu was much the highest and Hg was present only in traces. These data indicate that in accordance with literature discussions MT in nucleus dentatus could be involved in Cu metabolism and in short term heavy metal detoxification (Pb, Hg).

INTRODUCTION

In a wider investigation of mercury (Hg) accumulation and retention in autopsy samples from Idrija mercury mine employees it was found that in certain samples of retired workers, namely thyroid, hypophysis, cerebellar tissue - nucleus dentatus and kidney cortex, almost all the retained mercury and selenium were located in the cell particulate fraction (pellet) [1,2]. Similar results have been reported for kidney tissue of a deceased dentist by Björkman et al [3].

In the cell particulate fractions mercury was accompanied by selenium in a molar ratio near to one. In the literature it is supposed that both elements can be present as insoluble Hg selenide and/or sulphide polymers [4], or as insoluble metal-protein complexes (maybe Hg-Se as a part of metallothionein or its degradation products) [5], mostly localised in lysosomes.

Metallothioneins (MTs) are a group of inducible low-molecular-weight, cystein-rich, metal binding cytosol proteins which can represent a part of the cell´s defence mechanism against metal toxicity, oxidative stress and inflammation [6,7]. Among many other functions they can serve as efficient buffers for toxic concentrations of essential and nonessential metal ions entering the system. Although metallothionein (MT) is a cytoplasmic protein, it can also accumulate in lysosomes and in some cases it has been observed in the cell nucleus [6,7,8,9]. Interesting data were found particularly with copper MT [7,8,9]. As liver copper concentrations increase, the metal often accumulates in aggregated (polymeric, granular) forms of copper MT which occur in the particulate fraction (including lysosomes) of copper- loaded liver tissue. These aggregated forms of copper can be solubilised under alkaline or reducing conditions [10].

Concerning these observations and the thesis of Suzuki et al [11] that "MT may be involved in the storage, transport, excretion, homeostasis and detoxification of heavy metals in the central nervous system", especially in nucleus dentatus and some other brain areas, we were interested in the mercury retained in the nucleus dentatus from a retired mercury worker, principally in the presence of mercury metallothionein (MT).

The aim of the present study was to extract Hg-proteins from the particulate cell fraction the way done in studies with Cu [12], and to partially characterise the metallothionein-like proteins with Hg, Cu and Zn affinity.

MATERIALS AND METHODS

Autopsy sample

The autopsy sample was obtained from the brain cerebellum (nucleus dentatus) of a retired Idrija mercury mine employee. The time between death and autopsy was not

longer than 48 hours. The subject was aged 64 years, exposed to elemental mercury vapour for 18.5 years and then retired for 16.3 years. The cause of death was heart attack. The sample was immediately frozen, and kept below - 18°C until use.

Preparation of Particulate Fraction, Mercury Extraction and Sephadex G-75 Chromatography

The nucleus dentatus obtained was used for separation of pellet (particulate fraction) and supernatant. The pellet was subjected to mild Hg protein extraction with a buffer containing 10% mercaptoethanol (ME), and the MT- like proteins isolated by gel chromatography.

Tissue homogenate was prepared in nitrogen-saturated 10 mM Tris HCl buffer (pH 7.6, 4°C) containing 1mM dithiothreitol (DTT), strained through a 250-nm nylon net and ultracentrifuged for 1h at 100 000g in an Centrikon T-2070 (Kontron instruments) ultracentrifuge (rotor TFT 70.38). The supernatant was removed. The pellet (nuclei, mitochondria, lysosomes, microsomes) was suspended in 10 mM Tris HCl buffer (pH 7.6) containing 10% mercaptoethanol (ME), frozen and thawed three times to aid disruption of membranes and left overnight at 4°C. The mixture was then ultracentrifuged in the same way as cell homogenate to obtain an ME extract and sediment of the particulate fraction (modified procedure of Riordan and Richards) [12]. Aliquots of cell fractions were used for metal analysis.

The ME extract of the particulate fraction (2.5 mL) was applied to a calibrated 1.6 x 60 cm Sephadex G-75 column, and eluted in a nitrogen atmosphere at 4°C with buffer (10 mM Tris HCl, pH 7.6). The UV absorption at 280 and 254 nm and the concentrations of metals (Hg, Cu, Zn, Pb) were determined in the column eluents.

The column was standardized with marker proteins of known molecular weight (MW) (Pharmacia, Serva): blue dextran (2 000 000), bovine serum albumin (MW 67 000), ovalbumin (MW 44 000), chymotrypsinogen A (MW 25 000) myoglobin (MW 17 800), and cytochrome c (MW 12 400). Blue dextran was used to determine the void volume of the column. The standard marker proteins were eluted with 10 mM Tris HCl (pH 7.6), and the elution was monitored at 280 nm.

Metal Determination

Several methods were used for quantitative determination of total Hg, Zn, Cu, Cd and Pb in the biological samples analysed in this study: radiochemical neutron-activation analysis (RNAA), flame atomic absorption spectroscopy (flame AAS) and electrothermal atomic absorption spectroscopy (ET AAS). The analytical methods used for determination of particular elements in different samples are summarized in Table 1.

Table 1.   Samples, Elements and Methods

Sample	Element	Method
Nucleus dentatus	Hg, Se Cu, Zn	RNAA [13] RNAA [14]
100 000 g supernatant	Hg, Se Cu, Zn	RNAA [13] RNAA [14]
Pellet	Hg, Se	RNA [13]
Pellet extract	Hg, Se	RNAA [13]
Fractions from the Gel- filtration column	Hg Zn Cu Pb	RNAA [13] flame AAS RNAA [14] ET AAS

RESULTS

The nucleus dentatus sample contained 2.40ìg of Hg and 1.00ìg of Se/g wet weight. The amount of tissue Hg in the 100 000g supernatant (*cytosol)* was less than 1%. The concentration of supernatant Se was under the limit of detection. Almost all Hg and Se, with an atomic ratio near 1 (0.913), were retained in pellet. In view of these results the pellet was selected for mild Hg extraction. Buffer with 10% ME was used to attempt solubilization and extraction of polymerised MT (S-S bond splitting). The extraction of Hg found was very low, about 3% of the pellet Hg content. Tissue separation and extraction data are shown in Table 2.

Using gel chromatography the presence of MT-like proteins was detected in the ME pellet extract as Cu,Zn,Pb,Hg MT-like protein, where the presence of Cu was the

most marked. Fig.1 (A,B and C) depicts the elution profiles of the ME extract of pellet on a calibrated Sephadex G-75 column where the cytochrome c molecular weight range is characteristic of MT. UV absorbances were determined at 280 and 254 nm. The lack of absorbance at 280 (the absence of aromatic amino acids) and a peak at 254 nm (the presence of metallo-mercaptide bonds) in the range of cytochrome c are additional characteristics of MT. The absence of a peak at 254 nm is the consequence of the low concentration of protein. Fig.1 (A,B,C) shows the elution profiles of mercury, lead, and the essential elements Zn and Cu. The distribution of the measured elements is mutually unlike, but in the molecular range of cytochrome c the peaks of all elements are present, although their concentrations found in this range are different in the order: Cu >Zn > Pb >Hg.

The major Hg and Zn peaks correspond to very low MW substances (< 3000), Fig.1 (A, B). The strong UV absorbance of ME (at 254 nm) can probably account for the absorbance peak detected in the same region [15]. In the study of Roesiajadi and Drum [15] related to ME buffer and mercury-binding proteins in Mytilus gills, they showed that ME can shift mercury from mercury binding proteins to low molecular weight substances. The same conclusion could also be valid in our case. It is possible that ME removed part of the bound Hg and Zn from MT-like proteins and shifted both elements to substances with very low MW (Mr < 3000, i.e. the last peaks on the chromatogram, Fig. 1 A,C). The same phenomenon is not obvious for Cu. MTs bind Cu atoms cooperatively and tenaciously [16].

Table 2: Element concentrations in tissue and cell fractions from nucleus dentatus of retired mercury miner.[1]

NUCLEUS DENTATUS	Hg ìg/g	Hg %	Se ìg/g	Cu ìg/	Zn ìg/
Tissue (2g)	2.36	100	1.02	6.33	4.45
100 000 g supernatant (11g)	0.003	~0.7	<0.01	0.44	0.46
Pellet (1.95g, 1.72g*)	2.35	100	1.09	-	-
100 000 g pellet ME extract (5.5g)	0.034	~3	0.034	-	-

1 - separation data are described in materials and methods, - - no data,
* - mass of the pellet used for extraction

Fig. 1
pellet
The M:
10 mn
and Zn
of cyto
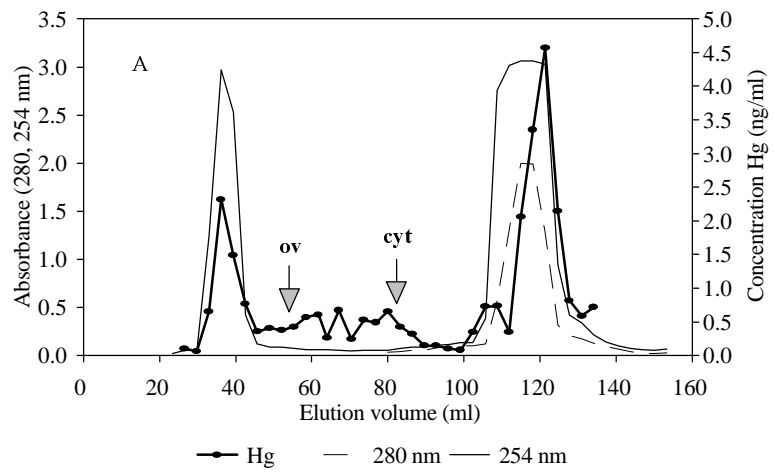
| extract of the

and eluted with
for Hg (A), Cu
. The positions
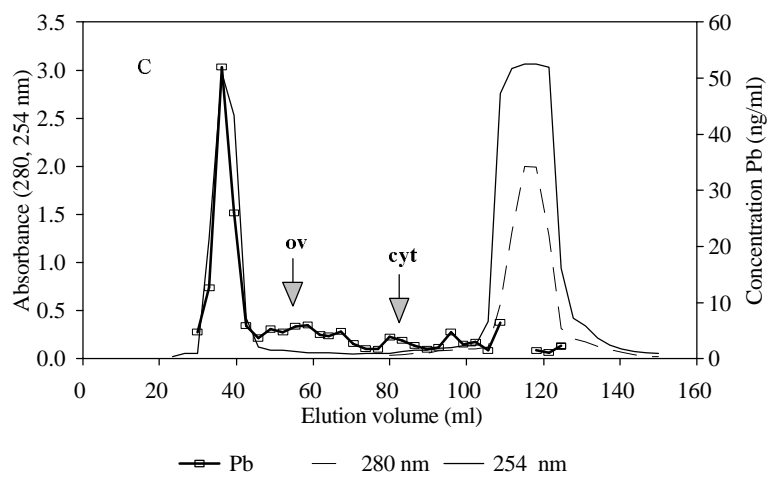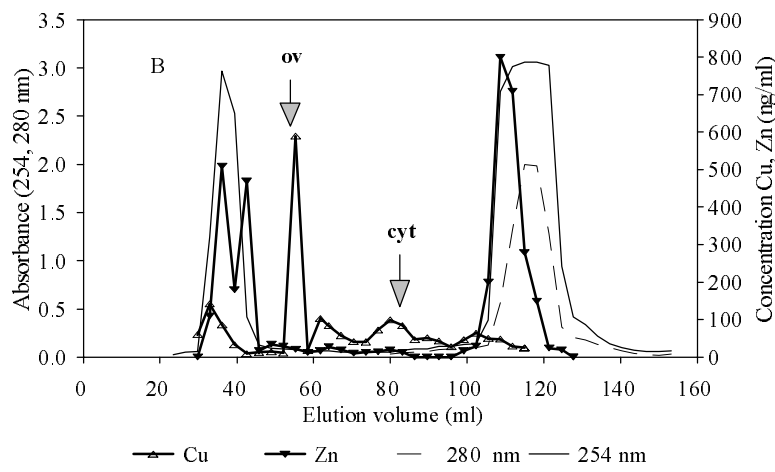
DISCUSSION

Our investigation revealed that buffer (10 mM Tris HCl) containing 10% mercaptoethanol (ME) dissolved only a small proportion of retained Hg and Se from nucleus dentatus pellet, about 3% and 7%. We found a similar result for a thyroid pellet sample from a retired mercury mine worker where the buffer contained 1% SDS (sodium dodecyl sulphate) (our unpublished data). These low extraction results are in concordance with another extraction study of the **kidney of a deceased dentist where a buffer (10 mm Tris HCl) containing a mixture of two reagents, 5 ìmol/ml ME and 1% SDS was used [3]. But considering the Hg extraction efficiencies of different buffers used for dolphin liver samples [17] it would b**e sensible to repeat the procedure with 20 mm ammonium acetate containing 4% SDS. In any case it is evident that in tissues from subjects with former exposure to Hg the deposits of Hg and Se are almost insoluble by mild extraction procedures. Regarding these data the suggestion that both elements can be present as insoluble Hg selenide polymers [4] seems more convincing than storage in aggregated metallothioneins [5].

In the ME pellet extract MT-like proteins were identified as Cu,Zn,Pb,Hg MT-LP. The binding of copper was outstanding and Hg was present only in traces, as seen from Fig. 1 (A,B,C). In view of literature data about liver granular Cu MT [8,9,10]and a study of granular forms of MTs accumulated in astrocytoma cells in the presence of interleukin-1 and heavy metals [18], we suppose that the nucleus dentatus cell pellet contained MT aggregates, which were dissolved by mercaptoethanol (S-S bond cleavage). As ME can act both as a reductant and a chelating agent, it is possible that the height of the Hg and Zn MT peaks might be diminished (discussed in Results).

Despite some procedural uncertainties connected with the effects of mercaptoethanol on Hg and Zn, it is significant that this is the first observation of nucleus dentatus MT-like proteins by gel-filtration chromatography and subsequent metal analysis of the MT fractions. Until now they were noticed and localized only by immunohistochemical techniques in nucleus dentatus of *macaca fascicularis* [18], and in nucleus dentatus of human brain [20, 11, 21] in the nuclei, cytoplasm and vascular feet

of astrocytes. In brain three MT isoforms (MT-I, MT-II, MT-III) exist, but in astrocytes MT-I and MT-II appear to be abundant and MT-III conspicuously absent [22]. In recent discussions about MT-I and MT-II isoforms within astrocytes, both forms have been associated with compartmentalization of zinc, and other metals (Cu) between neurons and astrocytes, regulation of metal intracellular concentrations and with tolerance to heavy metal and free radical neurotoxicity [22, 23, 24]. The data from our investigation indicate that MT in nucleus dentatus could be involved in Cu, Zn metabolism and in short term heavy metal detoxification (Pb, Hg) (Fig.1). Their involvement in the long term storage of Hg seems very questionable.

Undoubtedly it should be pointed out that it is becoming more difficult to operate with only a partial characterisation of Cu MTs, as recently (1997) a new family of Cu proteins has been discovered. Within the cell, Cu appears to be distributed among Cu-requiring proteins (enzymes) through the use of so-called Cu chaperons [16]. Until now in humans chaperons have been identified as cytosolic soluble copper binding low molecular weight proteins with cysteine residues (HAH 1 with 68 amino acids, COX 17 with 63 amino acids) [16, 25]. It could be said that MTs are important for Cu sequestration in a nonexchangeable form and chaperons are involved in intracellular Cu distribution [16]. As the connection of chaperons with Cu storage or aggregation in cellular organelles is not known, we suppose that their discovery does not affect the interpretation of results made in our investigation.

ACKNOWLEDGMENTS

REFERENCES

[1] I. Falnoga, I. Kregar, P. Stegnar, and M. Tušek-Znidarič, in: P.W.F. Fischer, M.R. L´Abbé, K.A. Cockell, and R.S. Gibbson, *Trace Elements in Man and Animals - 9. Proccedings of The Ninth International Symposium on Zrace Elements in Man and Animals;* NRC Ressearch Press, Ottawa,

Canada,1997, pp 489-490.

[2] I. Falnoga, *Absorption, distribution and elimination of mercury in experimental animals exposed to mercury vapour*, *Ph.D. Thesis*, University of Ljubljana, 1995 (in Slovene).

[3] L. Björkman, B. Palm, M. Nylander, and M. Nordberg, *Biol. Trace Element Res.*, **1994**, 40, 255-265.

[4] G. Dancher, and B. Møller-Madsen, *J. Histochem. Cytochem.,* **1985**, 33, 219-228 .

[5] T. Aoi, T. Higuchi, R. Kidokoro, R. Fukumura, A.Yagi, S. Ohguchi, A. Sasi, H. Hayashi, N. Sakamoto, and T. Hanaichi, *Human Toxicol.,* **1985**, 4, 637-642.

[6] J. H. R Kägi, and A. Schäffer, *Biochemistry,* **1988**, 27, 8509-8515.

[7] M. G. Cherian, and H. M. Chan, in K.T. Suzuki, N. Imura, and M. Kimura, *Metallothionein III*; Birkhäuser Verag, Basel-Boston-Berlin, 1993, pp 87-109.

[8] I. Bremner, in J.F. Riordan, and B. L. Vallee, *Methods in Enzimology*; Academic Press, Inc., pp. 1991, vol. 205, pp 584-599.

[9] I. Bremner, in K.T. Suzuki, N. Imura, and M. Kimura, *Metallothionein III*; Birkhäuser Verag, Basel-Boston-Berlin, 1993,pp 112-114.

[10] I. Bremner, in M. Anke, D. Meissner, and C. F. Mills, *Trace Elements in Man and Animals - TEMA 8,* 1993, pp 507-515.

[11] K. Suzuki, K. Nakajima, N. Otaki, M. Kimura,U. Kawaharada, K. Uehara, F. Hara, Y. Nakazato, and M. Takatama, *Path. Int.*, **1994**, 44, 20-26.

[12] J.R. Riordan, and V. Richards, *J. Biol. Chem.,* **1980**, 255, 5380-5383.

[13] A.R. Byrne, and L. Kosta, *Talanta,* **1974**, 21, 1083-1092.

[14] M. Dermelj, A. Vakselj, V. Ravnik, and B. Smodis, *Radiochem. Radioanal. Lett.*, **1979**, 41, 149-160.

[15] G. Roesijadi, and A.S. Drum, *Comp. Biochem. Physiol.,* **1982**, 71B, 455- 459.

[16] K.A. Koch, Ma O. Pena, and D.J. Thiele, *Chemistry & Biology*, **1997**, 4, 549-560.

[17] Y. Shibata, M. Morita, and K. Fuwa, *Adv. Biophys.,* **1992***,* 28, 31-80.

[18] Y. Kikuchi, M. Irie, T. Kasahara, J. Sawada, and T. Terao, *FEBS Lett.,* **1993***,* 317, 22-26.

[19] K. Suzuki, K. Nakajima, U. Kawaharada, F. Hara, K. Uehara, N. Otaki, M. Kimura, and Y.Tamura, *Acta Histochem. Cytochem.*, **1992**, 25, 609-616.

[20] H.G.T. Blaauwgeers, P.A.E. Sillevis Smitt, J.M.B.V. De Jong, and D. Troost, *Glia,* **1993**, 8, 62-70.

[21] K. Nakajima, and K. Suzuki, *Neurochem. Int.*, **1995**, 27, 73-87.

[22] M. Aschner, *FASEB J.*, 1996, 10, 1129-1136.

[23] M. Aschner, *NeuroToxicology,* **1996**, 17, 93-106.

[24] J.W. Neal, S.K Singhrao, B. Jasani, and G.R. Newman, *Neuropathol. Appl. Neurobiol.*, **1996,** 22, 243-247.

[25] I.H. Hung, R.L.B. Casareno, G. Labesse, F.S. Mathews, and J.D. Gitlin, *J. Biol. Chem.,* **1998**, 273, 1749-1754.

POVZETEK

Iz avtoptičnega vzorca nukleusa dentatusa malih možgan upokojenega rudarja smo pripravili partikularno celično frakcijo. Vsebovala je visoko vsebnost živega srebra in selena (**2.35 ìg/g, 1.02 ìg/g**). Z milo ekstrakcijo (pufer z 10% merkaptoetanolom/ME) smo poskusili raztopiti beljakovine z vezanim živim srebrom. Količina tako raztopljenega Hg je bila zelo nizka, okoli 3% vsebnosti Hg v partikularni frakciji. V ekstraktu smo s pomočjo gelske filtracije na Sephadex G-75 koloni in določitve kovin v eluatu identificirali metalotioninom podobne beljakovine (MT-PB). Zaznali smo jih kot Cu,Zn,Pb,Hg MT-LP, kjer je bila vezava bakra najbolj izstopajoča, živo srebro pa je bilo prisotno le v sledovih. Glede na to in na literaturne podatke predvidevamo, da so MT v nukleusu dentatusu lahko vpleteni v metabolizem Cu ter kratkoročno detoksifikacijo težkih kovin (Hg, Pb).

ON CHARACTERIZATION OF MOLECULAR ATTRIBUTES[†]

Milan Randic

Department of Mathematics, Drake University, Des Moines, Iowa, 50311 and National

Institute of Chemistry, Ljubljana, Slovenia

Abstract: We report here on recent developments in the characterization of molecular branching, molecular cyclicity, molecular shape, and chirality using graph theoretical invariants.

INTRODUCTION

Quantitative characterizations of molecular structural features has been overlooked and neglected for too long time. It is not uncommon to come across qualitative statements about molecular branching, molecular cyclicity, or molecular shape. Thus, for example, occasionally we find stated in chemical textbooks that the boiling points of alkanes decrease with the degree of molecular branching, even though the branching in alkanes has not been rigorously defined. In fact, such a statement has motivated Wiener [1] to develop his graph theoretical approach to structure-property correlation analysis.

It is generally accepted that most molecular properties critically depend on molecular size and molecular shape. Yet while molecular size can be characterized

---

[†] Presented as a lecture at the X. ECSM, June 10-12, 1998, Maribor, Slovenia

relatively well by number of molecular descriptors, e. g., the number of atoms in a molecule (particularly non-hydrogen atoms), or molecular weight, the characterization of molecular shape remains elusive. Similar situation is with the characterization of molecular cyclicity, chirality, the degree of folding, degree of planarity, molecular complexity, aromaticity, and several other molecular attributes. The same extends to a degree to the characterization of molecular similarity and molecular diversity, the properties that relate to a class of molecules rather than to an individual chemical structure. In this report we will review recent developments in characterization of several of the mentioned molecular attributes.

DESIDERATA

First, let us emphasize the distinction between the characterization of a molecule and the representation of molecular structure. The characterization refers to description of molecular structures by one or more descriptors (parameters, graph theoretical or topological indices, structural indices). The representation refers to giving a molecule unique label, name, code, which permits its full reconstruction. In the language of computer science we may say that molecular representation corresponds to an input information on a molecule (or molecular graph) while molecular characterization corresponds to mathematical property of a structure, which typically comes as an output of computer manipulation with a structure.

There are hundreds of molecular descriptors. For example, the program CODESSA evaluates some 400 graph theoretical descriptors and quantum chemical parameters for molecules to be considered in a structure-property-activity study [2]. Such a large number of descriptors raises the question how to select descriptors, besides the question how to interpret the resulting regressions, the problems that have hardly received due attention. We will briefly address this topic in this report.

The slow advance in quantitative characterization of molecular attributes is primarily due to lack of precise definition of such attributes. What is molecular shape? How should molecular branching be defined? Can we measure the degree of chirality? Even the questions that at the first sight appear not difficult, like what is molecular size,

how is to be defined and how is one to measure molecular size need some scrutiny. Many molecules have the same number of atoms (or heavy atoms) and could be viewed as having the same size. But an index of limited resolution (such as the number of carbon atoms in alkanes, or number of carbon atoms and hetero-atoms in organic molecules) has also limited applicability when one is interested in minor variation in molecular properties, e. g., the variation in properties of isomers. Molecules having the same number o atoms in general will have different molecular volumes and different molecular weight. Is molecular volume or molecular weight to be used as the preferred descriptor of molecular size?

As we will see there may be more than one way of measuring quantitatively the same molecular attribute. When statistical methods are used for study of the structure-property relationship two deciding factors ought to be considering: (1) The quality of the statistical analysis (measured by the correlation coefficient r, the coefficient of determination r^2, the standard error s, the Fisher ration F or other statistical parameters); and (2) The possibility of structural interpretation of the results. Even a cursory screening of chemical literature shows that the above two important factors are too often ignored, if not fully, at least partially. This makes comparative QSAR, which should point to best statistical models and the best molecular descriptors for specific situations, difficult if not impossible. The emphasis in the development of molecular descriptors ought to be on the quality of the descriptors, which is measured by how well they cover the molecular structure-property space rather than how well they discriminate among structures. The structure discrimination is an important property of a descriptor and indirectly points to the capability of a descriptor to capture diverse structural features of a molecule. However, if those feature are at the same time not critical for determining the relative manifestation of property of interest descriptor which has high discriminatory power will be of little interest even if it has relatively simple structural interpretation (which most of highly discriminatory indices don't have).

In the following sections we will outline the recent development for characterization of a selection of molecular attributes. All the results outlined are relatively new, some of the results reported here have even not yet been published. For additional introductory material and in particular for extensions of the graph theoretical

approaches to the charcterization of 3D structures, which because of space we will not consider here, we would like to direct readers to ref. [4-6], which review most of recent developments in that area.

CHARACTERIZATION OF MOLECULAR BRANCHING

Already in 1973 Lovasz and Pelikan suggested the leading or the first eigenvalue of the adjacency matrix as a molecular branching index [3]. The connectivity index χ [7], was initially called the branching index, and was thought to be a useful descriptor of molecular branching. Indeed, χ parallels quite well the boiling points in smaller alkanes, which parallel qualitatively the degree of branching. However, the connectivity index χ can be also computed for linear structures and cyclic structures without branches, so the name "connectivity index" instead of "branching index" which was suggested by Kier [8], is a better name for this index. Both branching indices have some limitations as they do not discriminate between several structures that show apparently different branching pattern. Thus, for example the leading eigenvalue for 3-methylheptane and 2,5-dimethylhexane is the same ($\lambda_1 = 2.00000$), while the connectivity index is same for 3-methylheptane and 4-methylheptane ($\chi = 0.80806$). Recently Kirby discussed the limitations of both these indices and offered some remedies that in particular improve the performance the connectivity index for larger alkanes [9].

Is there another branching index that does not show the limitations shown by the leading eigenvalue of the adjacency matrix and the connectivity index? Recently such a novel index was proposed [10]. It is based on the path matrix, a newly introduced matrix for graphs in which the matrix elements are expressed as the path subgraphs of a graph considered [11]. To obtain matrix in a numerical form one selects a mathematical property of interest for the subgraphs that appear as matrix elements. When one selects the leading eigenvalues (λ_1) of the subgraphs and then takes the leading eigenvalue of so constructed matrix one obtain the novel branching index (designated a $\lambda\lambda_1$). For example, the new branching index for 3-methylheptane, 4-methylheptane and 2,5-dimethylhexane are 10.2359, 10.2211 and 10.1712 respectively. The $\lambda\lambda_1$ index for

reported for all alkanes having n=10 or fewer carbon atoms [12]. It has also been reported for selected larger trees that have several coincidental topological indices [13]. So far no two trees having the same ll_1 index have been found. In Table 1 below we illustrate the path matrix and in Table 2 the path eigenvalue matrix for 2-methylpentane.
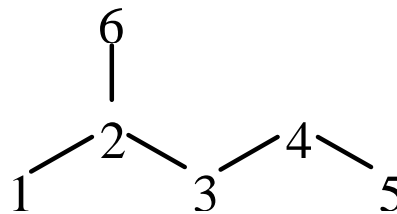
Table 1

0	p_1	p_2	p_3	p_4	p_2
p_1	0	p_1	p_2	p_3	p_1
p_2	p_1	0	p_1	p_2	p_2
p_3	p_2	p_1	0	p_1	p_3
p_4	p_3	p_2	p_1	0	p_4
p_2	p_1	p_2	p_3	p_4	0

Table 2

0	1.00000	1.41421	1.61803	1.73205	1.41421
1.00000	0	1.00000	1.41421	1.61803	1.00000
1.41421	1.00000	0	1.00000	1.41421	1.41421
1.61803	1.41421	1.00000	0	1.00000	1.61803
1.73205	1.61803	1.41421	1.00000	0	1.73205
1.41421	1.00000	1.41421	1.61803	1.73205	0

The elements of Table 2 are the leading eigenvalue of the adjacency matrices of paths p_1-p_4. The leading eigenvalue of so constructed path matrix is the new branching index.

CHARACTERIZATION OF MOLECULAR CYCLICITY

Within the Chemical Graph Theory [14, 15] characterization of molecular cyclicity received some attention. Bonchev, Mekenyan and Trinajstic [16] were the first to propose cyclicity index for molecules. They developed a set of rules that were paralleled the relative magnitude of the Wiener index [17] for cyclic molecules. Although later their approach was improved [18] it still maintains its original *ad hoc* character in that occasionally human intervention was called for in order to resolve unforeseen ambiguities. Can one design molecular cyclicity index that will be less dependent on human intervention?

Recently a novel cyclicity index was proposed which show promise. It has a high discrimination power and hopefully will resolve the questions of relative cyclicity among molecules with limited if any human intervention [19]. The index is based on the so called D/DD quotient matrix constructed from the elements of the graph distance matrix D [20], and the graph Detour matrix DD [21]. The element d_{ij} of the distance matrix is given by the distance between vertices i and j measured by the number of bonds between them, while the element dd_{ij} of the detour matrix is defined as the length of the longest path between vertices i and j. The i, j element of the quotient matrix D/DD is given by the ratio d_{ij}/dd_{ij}. The new index of molecular cyclicity is obtained as the average row sum of the so constructed matrix (suitably normalized). In Table 3 below we illustrate the D/DD matrix for the small bicyclic structure shown at the right of the table.

Table 3

0	1/4	2/4	2/4	1/4
1/4	0	1/4	2/3	1/3
2/4	1/4	0	1/4	2/3
2/4	2/3	1/4	0	1/4
1/4	1/3	2/3	1/4	0
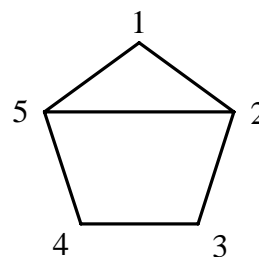
A comparison of two molecules having the same number of atoms but different cyclic structure shows that molecule with more cycles will have smaller row sums because it will allow for many atom pairs longer detour paths. Importantly, the approach permits construction of indices that apply locally, to individual rings and cycles.

CHARACTERIZATION OF MOLECULAR SHAPE

The shape, just as chirality, is not only the characteristic of three dimensional objects, although clearly the shape and chirality are very apparent properties of 3-dimensional objects and molecules. Objects embedded in 2 dimensional space also may have distinct shape. Even objects of a lesser dimension may show different shapes, as illustrated by shapes of fractals, the dimension of which typically varies between one and two (if embedded in a plane). Graphs despite being widely referred to as two dimensional objects are, strictly speaking, one dimensional mathematical objects [20]. One can however speak of the shape of a graph despite that graphs allow different pictorial representation and lack rigid structure. Simple indices of shapes of graphs are "girth," "thickness," "eccentricity," (see ref. [20] for details), which to some degree discriminate among graphs of widely different forms. Kier [22] was first to propose shape indices for molecular graphs, the so called kappa shape indices. The kappa shape indices have been widely used in QSAR [23].

A close look at the definition of Kier's κ indices reveals their somewhat arbitrary character. The indices are based on comparison between selected descriptors for the extreme shapes for graphs having n vertices. For trees the extreme graphs are on one hand the linear graph (or a path graph) having n vertices and on the other hand the so called "star" graph in which all vertices are connected to a central vertex. The extreme graphs, the path graph and the star graph have visibly different count of paths. Kier has used the count of paths in these extreme cases as the reference points in his definition of the respective shape indices. One could say that κ shape indices represent a measure of a departure of molecular shape from that of the extreme cases, which have set the scale for such measurement. Hence, we may speak of κ as a relative shape indices.

Can we design an absolute shape index for molecular graphs, an index which will not require other structures as the reference points as has been the case with Kier's kappa indices? Recently such new shape indices have been proposed [24]. An absolute index has an apparent advantage that it does not require a choice of the reference structures. Instead of using paths for characterization of the structures, including the extreme reference structures, on the "shape" scale we combine the count of paths of different length and the count of walks of different length for characterization of molecular shape. We will illustrate the approach on graph of 2-methylpentane. We will assume the standard numbering of carbon atoms. For each atom first we find the count of paths (p_i) and count of walks (w_i). The count of walks could continue indefinitely, since the lengths of walks is unbounded, but we stopped to match the walks to the paths because we will make the quotients (p_i/w_i):

	Paths				Walks				Path/Walks			
Atom	p_1	p_2	p_3	p_4	w_1	w_2	w_3	w_4	q_1	q_2	q_3	q_4
1	1	2	1	1	1	3	4	11	1	2/3	1/4	1/11
2	3	1	1		3	4	11		1	1/4	1/11	
3	2	3			2	5			1	3/5		
4	2	1	2		2	3	7		1	1/3	1/7	
5	1	1	1	2	1	2	3	7	1	1/2	1/3	2/7
6	1	2	1	1	1	3	4	11	1	2/3	1/4	1/11

Molecular shape indices are obtained by taking 1/6 of the sum of all (p_i/w_i) atomic contributions giving in the case of 2-methylpentane: $q_1=1.00000$, $q_2=0.50278$, $q_3=0.17785$, $q_4=0.07792$.

The few applications of the new shape indices on selected properties of alkanes have shown that these indices lead to significantly better regressions than the Kier's kappa shape indices In Table 4 below we show the statistical parameters for several thermodynamic properties of heptane isomers when using two shape indices p_2/w_2 and p_3/w_3 (the index p_1/w_1 is always 1 and is therefore of no interest).

Table 4

Property	Coefficient of regression r	Standard error s	Fisher Ratio F
Boiling points	0.9340	2.33 ^{o}C	51.3
Pitzer steric factor	0.9729	0.438	133.0
Entropy	0.9451	1.57	62.8
Heat of formation	0.9819	0.078	201.4
Critical Heat	0.9609	0.373	89.5
Critical Pressure	0.9840	0.229	228.9
Heat of formation (vapor)	0.9705	0.520	121.7

No other simple molecular descriptors when restricted to the nine isomers of heptane give so good results.   It remains however to be seen how will these indices be generalized and extended to molecular having heteroatoms.

CHARACTERIZATION OF MOLECULAR CHIRALITY

Lord Kelvin has pointed out already at the beginning of this century that chirality exists in spaces of different dimension, besides the generally recognized cases of chirality for objects in 3D [25].   We will restrict our attention here to chirality of molecules embedded in 2D and will illustrate novel and the first molecular descriptors of the chirality on smaller benzenoids.   It is generally accepted that a chiral molecule and its antipodal counterpart if looked in an isolation will have all their mathematical or physical properties identical.   Since molecular descriptors are nothing but mathematical properties of a structure it appears impossible to come with a design of a molecular descriptor, topological index, or quantum chemical parameter, which will distinguish a molecule and its enantiomer.   In fact, all the reported topological indices, and there are several hundreds of such, are the same for a structure and its enantiomer.   Chiral structures are

discriminated when considered in a chiral environment, such as occurs when a chiral molecule approaches a receptor (which as a rule is also chiral).

So how can one design a descriptor which will give different values for a chiral molecule and its mirror image? The task appears impossible, yet very recently the first graph theoretical invariant (i. e., mathematical property) was designed that differentiate mirror image from its parent structure [26]. We will outline this construction on benzo[a]anthracene (shown below), which when embedded in a plane represents a chiral structure.
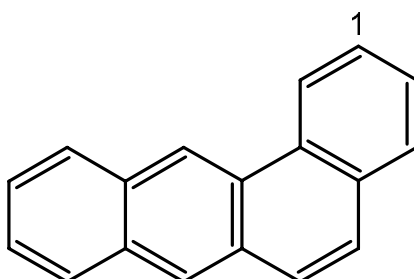
Observe that if we decide to "walk" around the molecular periphery from selected atom (like atom #1) the two opposing direction of walk produce different walking pattern. We may speak of asymmetry of atomic environment along the perimeter and can measure this asymmetry by some graph theoretical descriptor. Let us first make a list of atomic valences as we go around the molecular periphery. For example, starting from atom 1 and including it, we have:

clockwise	2, 2, 2, 3, 2, 2, 3, 2, 3, 2, 2, 2, 2, 3, 2, 3, 3, 2
anticlockwise	2, 2, 3, 3, 2, 3, 2, 2, 2, 2, 3, 2, 3, 2, 2, 3, 2, 2.

In the next step we will make the corresponding sequences for the partial sums by adding successively elements of the series:

clockwise	2, 4, 6, 9, 11, 13, 16, 18, 21, 23, 25, 27, 29, 32, 34, 37, 40, 42
anticlockwise	2, 4, 7, 10, 12, 15, 17, 19, 21, 23, 26, 28, 31, 33, 35, 38, 40, 42.

The above sequences, both belonging to carbon atom # 1, contain some information on the asymmetry of the periphery of the molecule when, starting from atom # 1, we go around the molecular periphery in opposite directions. In the next step we want to extract from the two sequences a single descriptor. One can define such descriptor by considering the difference between the anticlockwise (mathematical positive sense) and clockwise orientation (mathematically negative sense). For the above illustration we obtain as the difference $D_1 = 14$, the subscript 1 relates to the atom selected. When this is completed for all atoms one obtains the results shown below:
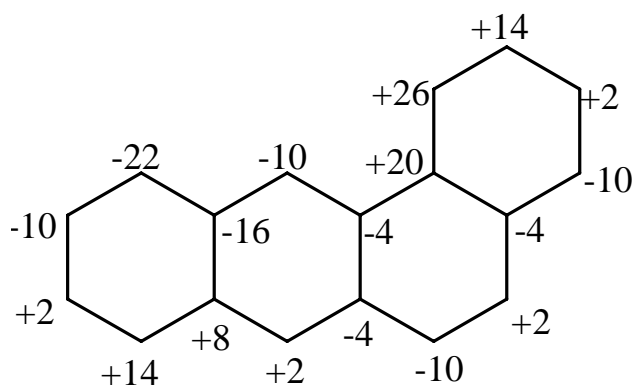
Clearly some atoms have more asymmetric environment while others show a lesser differentiation between two opposing directions of walking around the molecular periphery. The same calculation can be performed for the mirror image structure. The difference will only be in the sign of the individual contributions, while the corresponding atoms will maintain the same magnitudes. The calculations for a molecule and its enantiomer differ only in the exchange of the clockwise sequence for anticlockwise and vice versa.

We will use the derived D_i values for construction of a chirality index. Consider first simply the sum of $\Sigma\ D_i$ values. It is zero, and this is true for its mirror image. However, if we calculate the sums of the odd powers of the D_i numbers we will in general obtain non zero result. In the case of benzanthracene using a simple normalization based on the number of atoms in a structure we obtain:

$$\Sigma(D_i)^3/18^3 \qquad \Sigma(D_i)^5/18^5 \qquad \Sigma(D_i)^7/18^7 \qquad \Sigma(D_i)^9/18^9 \qquad \Sigma(D_i)^{11}/18^{11}$$

| benzanthracene | +2.17284 | +5.07240 | +10.97954 | +23.70935 | +51.05061 |
| mirror image | -2.17284 | -5.07240 | -10.97954 | -23.70935 | -51.05061 |

Alternative normalization could be considered but at this stage of the development of chirality indices the emphasis has been on the constructing the "impossible" rather than adjusting the derived index for a specific application. As we see the molecule and its enantiomer have positive and negative chirality indices respectively. The above is the first graph theoretical invariant (or call it the first topological index) that discriminates among enantiomers. If molecule is achiral all the components $(D_i)^m/n^m$ (m being odd and n is the number of atoms in the structure) occur in pairs, positive and negative, resulting in all sums $\Sigma(D_i)^m/n$ to be zero.

There is an important conceptual consequence of the possibility to construct chirality indices as those illustrated above. Hitherto chirality has been viewed as a *relative* property. That means that in order to assign a relative chirality label, such as left or right (e. g. *d* and *l* sugar) a molecule M and its mirror image M* have to be compared to some standard. For most molecules one come across this is possible, but as Ruch has pointed out for some objects this is not necessarily possible [26]. Thus, for example, one can speak of the left and the right shoe, or the left and the right glove, because these object can be matched to the left and the right hands which are assumed to be the standard of reference. However, as indicated by Ruch, one can come across chiral potatoes and not be able to tell which is left and which is right. Moreover, as has been pointed out by Randic and Razinger [28], the classification of chiral molecules analogous to the left and the right isomers may depend on the standard chosen. So for one standard one may obtain for a molecule M and its enantiomer M* to be classified to correspond to standards A and A*, but for some other standards the assignment of the label (* or no *) may reverse. This clearly points to the relative nature of classification of molecules and their enantiomers.

In our case the situation is different. We do not need standards to determine the chiral character of a molecule M and its enantiomer. If the chirality indices are positive we have M^+ if they are negative we have M^-, independent of any such assignment for any other pair of molecules.

CONCLUDING REMARKS

In this report we have limited our attention to molecules represented by molecular graphs rather then molecules represented as 3D structure. Some of the recent development outlined here can be readily extended to 3D structures, other, including the chirality indices, may require more efforts and some imagination. Be as it may, the purpose of this communication has been to raise consciousness among the practitioners towards the need for meaningful, that is, structurally interpretable and conceptually simple descriptors. Despite there being hundreds of descriptors apparently there is still room for the improvement. Selection of descriptors to be used in structure-property-activity studies should not be delegated solely to the computers although the statistical criteria will continue to be useful for preliminary screening of descriptors taken from a large pool. Often in an automated selection of descriptors a descriptor will be discarded because it is highly correlated with another descriptor already selected. But what is important is not whether two descriptors parallel one another, i.e., duplicate much of the same structural information but whether they in those parts that are important for structure-property correlations. If they differ in the domain which is important for the property considered both descriptors should be retained, if they differ in the parts that are not relevant for the correlation of considered property then one of them can be discarded. Hence, the residual of the correlation between two descriptors should be examined and kept or discarded depending on how well it can improved the correlation based on already selected descriptors. Alternatively, one should replace the set of descriptors used by descriptors that can be extracted from them through the orthgonalization procedure that has been introduced in regression analysis [29-33], perhaps somewhat belatedly, but should not because of the late start be overlooked in the future.

REFERENCES

1. Wiener, remarks at the after dinner talk at the first International Conference on Mathematical Chemistry, Athens, Ga

2. A. R. Katritzky, V. Lobanov and M. Karelson, *Codessa (Comprehensive Descriptors for Structural and Statistical Analysis)*, University of Gainesville, Fl., 1944.

3. L. Lovasz and J. Pelikan, On the eigenvalue of trees, *Period. Math. Hung*. **1973**, *3,* 175-182.

4. M. Randic and M. Razinger, On Characterization of 3D Molecular Structure, in: *From Chemical Topology to Three-Dimensional Geometry* (A. T. Balaban, Ed.), Plenum Press, New York, 1997.

5. M. Randic, On characterization of chemical structure, *J. Chem. Inf. Comput. Sci*. **1997**, *37,* 672-687.

6. M. Randic, Topological Indices, in: *Encyclopaedia of Computational Chemistry* (P. von Rague Schleyer, Editor-in-Chief), Wiley & sons, London (in press).

7. M. Randic, On characterization of molecular branching, *J. Am. Chem. Soc*. **1975**, *97,* 6609-6615.

8. L. B. Kier, L. H. Hall, W. J. Murray and M. Randic, Molecular connectivity I. Relationship to non-specific local anaesthesia, *J. Pharm. Sci*. **1975**, *64,* 1971-1974.

9. E. C. Kirby, Sensitivity of topological indices to methyl group branching in octanes and azulenes, or what does a topological index index? *J. Chem. Inf. Comput. Sci*. **1994**, *34,* 1030-1035.

10. M. Randic, On molecular branching, *Acta Chim. Slov*. **1997**, *44,* 57-77.

11. M. Randic, D. Plavsic and M. Razinger, Double invariants, *MATCH* **1997**, *35,* 243-259.

12. M. Randic, On structural ordering and branching of acyclic hydrocarbons, *J. Math. Chem.* (submitted)

13. M. Randic, X. Guo, and S. Bobst, Use of path matrices for characterization of molecular structure, *Proc. Workshop on Mathematical Chemistry*, Rutgers Univesity, May 1998.

14. *Chemical Applications of Graph Theory*, (A. T. Balaban, Ed.), Academic Press, London, 1976.

15. N. Trinajstic, *Chemical Graph Theory,* CRC Press, Boca Raton, Fl.

16. D. Bonchev, O. Mekenyan and N. Trinajstic, Topological characterization of cyclic structures, *Int. J. Quant. Chem.* **1980**, *17,* 845-893.

17. H. Wiener, Structural determination of paraffin boiling points, *J. Am. Chem. Soc*. **1947**, *69,* 17-20.

18. D. Bonchev, A. T. Balaban, X. Lui, and D. Klein, Molecular cyclicity and centrality of polycyclic graphs. I. Cyclicity based on resistance distances or reciprocal distances, *Int. J. Quant. Chem.* **1994**, *50,* 1-20.

19. M. Randic, On characterization of cyclic structures, *J. Chem. Inf. Comput. Sci*. **1997**, *37,* 1063-1071.

20. F. Harary, *Graph Theory*, Addison-Wesley, Reading, Ma, 1969.

21. D. Amic and N. Trinajstic, On the detour matrix, *Croat. Chem. Acta* **1995**, *68,* 873-882.

22. L. B. Kier, Shape indexes of orders one and three from molecular graphs, *Quant. Struct.-Act. Relat.* **1986**, *5,* 1-7.

23. L. B. Kier, Indexes of molecular shape from chemical graphs, *Med. Res. Rev.* **1987**, *7,* 417-440.

24. M. Randic, New shape indices for molecular graphs, in preparation for publication.

25. Lord Kelvin, *Baltimore Lectures on Molecular Dynamics and the Wave Theory of Light*, pp. 439, 619, C. J. Clay and Sons Publisher, London (1904).

26. M. Randic, unpublished

27. E. Ruch, *Angew. Chem. Intl. Edn. Engl.* **1977**, *16,* 65.

28. M. Randic and M. Razinger, Molecular shapes and chirality, *J. Chem. Inf. Comput. Sci.* **1996**, *36,* 429-441.

29. M. Randic, Orthogonal molecular descriptors, *New J. Chem.* **1991**, *15,* 517-525.

30. M. Randic, Resolution of ambiguities in structure-property studies by use of orthogonal descriptors, *J. Chem. Inf. Comput. Sci.* **1991**, *31,* 311-320.

31. M. Randic, Fitting of nonlinear regressions by orthogonalized power series, *J. Comput. Chem.* **1993**, *14,* 363-370.

32. M. Randic, Curve-fitting paradox, *Int. J. Quant. Chem: Quant. Biol. Symp.* **1994**, *21,* 215-225.

33. M. Randic, Orthosimilarity, *J. Chem. Inf. Comput. Sci.* **1996**, *36,* 1092-1097.

Povzetek. V članku poročamo o uporabi in najnovejšem razvoju invariant teorije grafov za karakterizacijo razvejanosti molekul, cikličnosti, zunanje oblike ter njihove kiralnosti.

FUNCTIONS OF 17ß-HYDROXYSTEROID DEHYDROGENASE TYPE 4

Gabriele Möller[1], Frauke Leenders[2], Monika Markus[3], Bettina Husen[4],

Yvan de Launoit[5], Jerzy Adamski[1]

[1]GSF Research Center for Environment and Health, Institute for Mammalian Genetics, 85764

Neuherberg, [2]University Clinic Charité, Institute for Pharmacology and Toxicology, Berlin, [3]Medical

School Hannover, Hannover, [4]Institute for Anatomy, University of Greifswald, Greifswald, Germany,

[5]CNRS, Institut Pasteur, Lille, France,

Address the correspondence to J. Adamski, email: adamski@gsf.de

Abstract
Five types of 17β-hydroxysteroid dehydrogenases catalyzing the conversion of estrogens and androgens at position C17 have been identified so far. The porcine peroxisomal 17β-hydroxysteroid dehydrogenase type 4 (17ß-HSD 4) catalyzes the oxidation of estradiol with high preference over the reduction of estrone. The 17ß-HSD 4 reveals only 25% amino acid similarity with 17ß-HSD 1, 2, 3 and 5 enzymes. The highest levels of 17ß-HSD 4 mRNA transcription and specific activity are found in liver and kidney followed by ovary and testes. In porcine gonads the immunofluorescence assigned the 17ß-HSD 4 to granulosa cells, Leydig and Sertoli cells. A 2.9 kb mRNA codes for an 80 kDa (737 amino acids) protein featuring domains which are not present in the other 17βHSDs. Although five Asn-Xaa-Ser/Thr (Xaa - unspecified amino acid) sites are found in the 80 kDa protein the enzyme is not glycosylated.The 80 kDa protein is N-terminally cleaved to a 32 kDa enzymatically active fragment. Both the 80 kDa and the N-terminal 32 kDa (amino acids 1-323) protein are the first enzymes that are able to perform the dehydrogenase reaction not only with steroids at the C17 position but also with 3-hydroxyacyl-CoA. The central part of the 80 kDa protein (amino acids 324-596) catalyzes the 2-enoyl-acyl-CoA hydratase reaction with high efficiency. The C-terminal part of the 80 kDa protein (amino acids 597-737) facilitates the transfer of 7-dehydrocholesterol and phosphatidylcholine between membranes *in vitro*. The unique multidomain structure of the 80 kDa protein permits the catalysis of several reactions so far thought to be performed by complexes of different enzymes.

Abbreviations

aa - amino acid, bp - base pairs, EDH - 32 kDa N-terminal fragment of porcine 17ß-estradiol dehydrogenase, E_2 - 17ß-estradiol, E_1 - estrone, HSD - 17ß-hydroxysteroid dehydrogenase, hHSD 4 -human 17ß-hydroxysteroid dehydrogenase type 4, pHSD 4 - porcine 80 kDa primary transcript of 17ß-hydroxysteroid dehydrogenase 4, GST - glutathione-S-transferase, VHF - very hydrophobic fraction

Several dehydrogenases convert steroids at the position C17

Biological potency of estrogens and androgens is regulated by conversions at position C17 by 17ß-hydroxysteroid dehydrogenases (HSD). Several enzymes with close substrate specificities are participating in that process. The identification and characterization of individual human HSDs was limited by scanty amounts of tissue available for purification. However, analyses performed with homogenates or with subcellular fractions allowed the kinetical differentiation of several enzymes such as the soluble 17ß-hydroxysteroid oxidoreductase of placenta or the structure-associated 17ß-estradiol dehydrogenase of uterus epithelium [1-3]. Before molecular biology techniques became widespread the readily available human placenta allowed the purification of the first human 17ß-hydroxysteroid dehydrogenase (HSD 1) which became a model for studies of steroid converting enzymes. After cloning and elucidation of the gene structure [4,5] it represents the best characterized human 34 kDa steroid dehydrogenase interconverting 17ß-estradiol and estrone with similar velocities. Detailed kinetical studies [6] have shown that placenta expresses additional HSDs and one of them, namely HSD 2, was cloned recently [7] (Table 1). This enzyme is a 43 kDa microsomal dehydrogenase revealing a two-fold higher rate of oxidation than reduction for both estrogens and androgens. A further enzyme, the HSD 3 is most abundant in testes and represents a transmembrane microsomal 35 kDa protein with a strong preference for the reduction of androgens [8]. The recently cloned mouse and human 17ß-HSDs type 5 have not yet been fully characterized [9,10]. The complexity of the 17ß-hydroxysteroid dehydrogenases was reviewed recently [11-14].

The oxidative 17ß-HSD activity found in human uterus endometrium could not be unequivo-cally ascribed to the known enzymes [3]. Attempts to isolate the endometrial 17ß-HSD from the particulate fraction of homogenates [15] resulted in 40-fold enrichment. However, because of difficulties in collecting and paucity of starting material the enriched fractions were not applied to amino acid sequencing and antibody production. Entenmann et al. discovered in porcine endometrium oxidative activity for 17ß-estradiol [16]. This microsomal activity revealed comparable kinetical parameters (NAD^+-dependency, K_m less than 1 µM). The parameters suggested a role in the inactivation of hormones.

Table 1. Human 17ß-hydroxysteroid dehydrogenases

enzyme	tissue	subcellular localization	mass kDa	best substrate	K_m µM	catalysis *in vivo*	ref.
17ß-HSD 1	placenta ovary	soluble	34	estrone estradiol	8.6 5.9	reduction	[4]
17ß-HSD 2	placenta liver	microsomal	43	testosterone estradiol	0.4 0.2	oxidation	[7]
17ß-HSD 3	testis	microsomal	35	androstenedione estrone	0.5 0.5	reduction	[8]
17ß-HSD 4	liver kidney	peroxisomal	80	estradiol androstenediol	0.2 0.4	oxidation	[17]
17ß-HSD 5	liver testis	microsomal	34	androstenedione	-	reduction	[10]

Purification of the porcine 17ß-estradiol dehydrogenase 4

Porcine uterus could be easily collected at a preparative scale. The separation of epithelial layer from the myometrium was achieved by curretage [18]. The most critical step of the purification turned out to be the solubilization of 17ß-estradiol dehydrogenase activity from the particulate fraction (38,000 x g) pellets of homogenates as activity was either deteriorated or not extracted [19]. The best results were obtained with the nonionic detergent Brij 35 with which 6% of enzyme activity was solubilized. Extracts were applied to DEAE-Sepharose, depleted of free detergent on Amberlite XAD-2 and further purified by affinity chromatography on Blue Sepharose [20]. In epithelial cells the proportion of oxidation to reduction at optimal assay conditions is 30:1 and remains unchanged until the affinity chromatography step. However, the activity of the 17ß-estradiol dehydrogenase was eluted with 0.7 M KCl while the estrone reductase activity (free of dehydrogenase) required 1.8 M KCl for the elution. Therefore, oxidation and reduction of steroids in porcine uterus epithelium is performed by two distinct enzymes. This has already been suggested by Bogovich and Payne for the testosterone/androstenedione transformations in rat testes [21]. Because of the separation of a genuine reductase the rate of oxidation to reduction increased to 360:1 for 17ß-HSD rich fraction. Further purification on Butyl Sepharose resulted in two products rich in 17ß-estradiol dehydrogenase activity: a major moderate hydrophobic fraction (EDH) and a minor very hydrophobic fraction (VHF). They were processed in parallel by gel filtration and ion-exchange chromatography on Mono S (Fig. 1). The EDH fraction was purified to homogeneity (4081-fold enrichment) and

revealed a single band at 32 kDa in the denaturing SDS-PAGE. The VHF was a mixture of proteins of 32, 45 and 80 kDa (2402-fold enrichment).
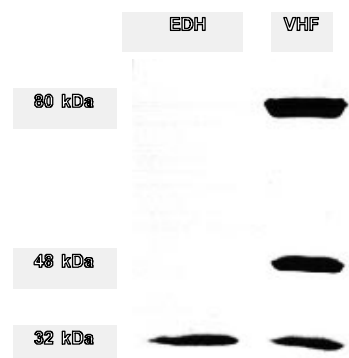
Fig. 1. Purified porcine 17ß-HSD 4

VHF is a mixture of a 80 kDa protein, its cleavage products of 32 and 48 kDa and actin [20].

Characterization of EDH and VHF

Both purification products, the EDH and the VHF, show the same K_m for steroids and cofactors as those measured with two-substrate kinetics in the particulate fraction of homogenates of porcine uterus epithelium (Table 2). They reveal an ordered mechanism of reaction with the cofactor binding first [20,22]. EDH and VHF share as well the substrate specificity, which is highest for 17ß-estradiol and, unexpectedly, comparably high for Δ5-androstene-3ß,17ß-diol (K_m = 0.2 µM). Other androgens or progestagens are not converted.

Table 2. Kinetic parameters of porcine 17ß-estradiol dehydrogenase 4

parameter	$E_2 \rightarrow E_1$	$E_2 \leftarrow E_1$
optimal pH	7.8	6.6
K_m for steroid	0.22 µM	1.10 mM
best cofactor	NAD^+	NADPH
K_m for cofactor	44 mM	21 mM

The molecular mass was estimated in denaturing SDS-PAGE and under native conditions by gel filtration and density gradient centrifugation [20]. The 32 kDa protein has a capability of forming dimers with an apparent molecular weight of 75 kDa. The interactions in the VHF are more complex. A homodimer of two 80 kDa proteins may

correspond to a low molecular mass form (170 kDa) and a heterocomplex including 32, 45 and 80 kDa proteins to a high molecular mass form (240 kDa) observed in density gradients. Identification of VHF components was a prerequisite for understanding the intrinsic interactions. It was achieved by investigations with antibodies and by amino acid sequencing. Goat and rabbit polyclonal antibodies raised against 32 kDa EDH reacted with the 32 and 80 kDa protein of VHF. The mouse monoclonal antibody (mab) W1 recognized only the 32 kDa protein and the mab F1 both the 32 and 80 kDa proteins [20,23]. Neither antibody reacted with the 45 kDa protein. The identity of the latter band with ß-actin was shown by amino acid sequencing and by western blots. The 80 kDa band of VHF revealed the presence of peptides known from the sequence of actin, the 32 kDa protein and some unassigned sequences [24]. The nature of the 80 kDa protein remained unclarified until its molecular cloning. The 32 kDa protein was identical in both purification products EDH and VHF and represented a new 17ß-estradiol dehydrogenase addressed as 17ß-HSD 4.

Processing of the porcine 80 kDa protein

The single open reading frame of the cDNA codes for an 80 kDa protein which undergoes a complex processing. It is N-terminally cleaved, probably after the sequence Ala320-Ala-Pro-Ser324, to a 32 kDa fragment representing EDH [25]. The comparison of specific activities of the purified EDH and VHF suggest that the primary translation product is enzymatically active. The EDH may reversibly interact with actin and some of the enzyme molecules are covalently crosslinked with actin through side groups of γ-glutamyl and ε-lysyl amino acids forming a 78 kDa complex [24]. The 78 kDa actin-EDH complex and the 80 kDa primary translation product are not resolved by SDS-PAGE. The comigration explains the detection of actin in the 80 kDa band of western blots [26]. The interactions forming homodimers of EDH and heterocomplexes of EDH, 80 kDa protein and actin must be of a nature withstanding at least in part the conditions of solubilization from the particulate fraction and further purification steps. Such partial dissipation leads to isolation of two fractions representing EDH (homogenous 32 kDa protein) and the VHF (EDH, actin, EDH-γ-glutamyl-ε-lysyl-actin and primary translation product).

Molecular cloning of the porcine and human 17ß-estradiol dehydrogenases type 4

With degenerated PCR-primers, designed according to partial amino acid (aa) sequence of the 32 kDa EDH, a fragment of 405 base pairs (bp) was amplified from porcine endometrium cDNA. It had a single open reading frame coding for an amino acid sequence

which was identical to the 32 kDa EDH as confirmed by Edman degradation. Using this fragment as a probe a 2.9 kb cDNA was isolated from a porcine λZAP kidney cDNA library. The sequence was later confirmed in porcine uterus [26]. The cDNA coded in a single open reading frame for a protein of 80 kDa (named pHSD 4) consisting of 737 aa and was not similar to any known steroid dehydrogenases [27,28]. About 70% of its amino acid sequence was already known from peptides of the 32 and 80 kDa proteins. Screening of human cDNA λgt11 libraries of liver and placenta was performed with a fragment corresponding to nucleotides 271 to 683 of the porcine enzyme. A 3 kb cDNA was identified which coded for a 80 kDa protein of 736 aa (addressed as hHSD 4) representing the human counterpart of the porcine enzyme [17]. Ortholog proteins were recently cloned in mouse [29] and rat [30].

Tissue distribution of porcine and human 17ß-HSD 4

In the studied porcine tissues the oxidation of 17ß-estradiol is predominating over the reduction. Highest pHSD4 concentrations are found in liver and kidney followed by uterus, lung, ovary and testes (Table 3).

Table 3. Distribution of 17ß-estradiol dehydrogenase activity in porcine tissues

tissue	$E_2 \rightarrow E_1$ $\mu U/mg$	$E_2 \leftarrow E_1$ $\mu U/mg$	immunocytochemistry
liver	687.5	5.6	hepatocytes
kidney	336.4	0.7	epithelium of proximal tubuli
ovary	293.9	1.5	granulosa cells
lung	185.4	0.8	bronchial epithelium
testes	69.2	1.8	Leydig cells
uterus	30.1	1.2	luminal and glandular epithelium
skeletal muscle	10.9	ND	myocytes
prostate	0.8	0.1	ND
blood erythrocytes	ND	ND	ND

Activities were measured in the particulate fractions of homogenates in tissue from boars or gilts in the luteal phase of the ovarian cycle [20]. Immunohistology was performed with rehydrated paraffin sections using monoclonal antibody F1-peroxidase conjugates as described [31], ND - not detected.

A slightly different expression pattern was seen in human tissues. The highest mRNA level of human 17ß-HSD 4 was observed in liver, followed by heart, prostate and testis. Moderate expression occurred in lung, skeletal muscle, kidney, pancreas, thymus,

ovary, intestine and term placenta. Weak signals were observed in brain, spleen, colon and lymphocytes. In all cases only a single band at 3 kb was discernible [17]. The wide distribution of 17ß-HSD 4 may in part explain oxidative activities measured in human tissues [32]. The expression of 17ß-HSD 4 is in contrast with that of 17ß-HSD 1 and 2 predominantly seen in placenta. Several human cancer cell lines also express 17ß-HSD 4. Estrogen receptor positive mammary cell line T47D express more hHSD 4 mRNA transcript than BT-20, MDA-MB-453 and MDA-MB-231 which are estrogen receptor negative. The megakaryotic cell line DAMI reveals a very high levels of hHSD 4 mRNA while less is present in hepatocellular carcinoma HEP-G2 and early embryonic Tera-1 cell lines [17].

Subcellular distribution of pHSD 4

Immunocytochemical and immunofluorescence studies in porcine uterus restricted the pHSD 4 to luminal and glandular epithelium [31] similar to analyses of human endometrium [33,34]. However, the staining was not diffuse in the cytoplasm but showed punctated appearance. The intensity of the mab F1-peroxidase staining followed the changes of porcine EDH activity. It raised 4-fold after day 5 of the ovarian cycle and rapidly decreased after day 17 similar to the levels of progesterone. At day 4 faint spots of fluorescence appeared in the cytoplasm of gladular epithelium. The spots accumulated at the cell basis between days 11 through 17 (luteal phase) and disappeared within one day. The pattern of immunofluorescence staining suggested that pHSD 4 is localized in vesicles. The latter have been isolated from porcine uterus epithelium homogenates by sequential density gradients of isopycnic 30% Percoll and linear 0.3 - 2 M sucrose in vertical rotors [23,35,36]. The vesicles harboring the 17ß-HSD activity equilibrated at the density of 1.18 g/ml, were 120 - 200 nm in diameter, revealed a moderate electron dense matrix bounded by a single membrane and were morphologically and enzymatically distinct from mitochondria, lysosomes, fragments of plasma membrane, endoplasmic reticulum and the Golgi apparatus. In immunogold electron microscopy the labelling with mab F1 (recognizing the 32 kDa EDH and the 80 kDa protein) and W1 (reacting with EDH only) confirmed that all forms of the enzyme are present in the same vesicles, both in tissue and in the isolated fraction [36].

Several clues pointed to the identity of EDH containing vesicles as peroxisomes: (1) the morphology and density is similar to that of peroxisomes, (2) the 80 kDa primary transcript features the peroxisomal targeting signal Ala-Lys-Ile and a putative recognition sequence (Ala-Ala-Pro) for a protease processing peroxisomal proteins [37] and (3) the 80

kDa protein is similar to enzymes participating in peroxisomal ß-oxidation of fatty acids. Indeed, typical peroxisomal markers such as catalase and acyl-CoA oxidase colocalized with pHSD 4 in immunogold labelling studies in uterus, kidney and liver [38,39]. Therefore, peroxisomes participate in the inactivation of steroids.

Features of the amino acid sequence of a new type of 17ß-estradiol dehydrogenases

The amino acid sequences of porcine and human 80 kDa HSD 4 are very similar (84%). They reveal a three-domain structure (Fig. 2) unknown for other dehydrogenases [40].

Fig 2. Similarities of amino acid sequences
(complete in printed version)
FOX2 - multifunctional enzyme of *Saccharomyces cerevisiae*, SCAD - short chain alcohol dehydrogenase, SCP2 -sterol carrier protein 2, SCPx - sterol carrier protein X, % identity is given along the arrows

FOX2

17-HSD 4

SCPX

About 300 aa of the N-terminal sequence have low overall similarity of 27% to the short chain alcohol dehydrogenase (SCAD) family. Similarity to the human HSD 1, 2 and 3, which consist of a single domain of the short chain dehydrogenase type, is less than 25%. Exceptionally high homology (50%) is observed to the first domain of the multifunctional fatty acid hydratase-dehydrogenase-epimerase of *Candida tropicalis* [41] and the FOX2 enzyme of *Saccharomyces cerevisiae* [42].

The copurification of EDH and actin suggested the possibility of specific interactions. The EDH sequence (aa 73 -119) contains a motif similar to that of aldolase [25,43] and to those of SH3-domains which are reported to participate in reversible actin binding [44]. The proteolytic cleavage of 80 kDa protein releases the complete SCAD domain.

Amino acid sequences of human, porcine and mouse 80 kDa proteins reveal several potential glycosylation sites (Asn-Xaa-Ser/Thr, Xaa - unspecified amino acid): e.g 6 in the porcine and 3 in the human HSD 4 [17,26,29]. Except for Asn401 (porcine) or Asn400 (human) they are localized in the N-terminal parts. Since the 17ß-HSD 4 is a peroxisomal enzyme and glycosylated proteins have not yet been described in these organelles we explored potential modifications. In the porcine protein 5 glycosylation sites are present in the SCAD domain and one is located in the domain similar to fatty acid hydratases. Amino acid sequencing has shown that 4 of the 5 N-terminal sites are not posttranslationally modified [26]. Further information has been provided by lectin staining. The 32 kDa 17ß-HSD 4 was either purified from kidney (native enzyme) or as a recombinant GST fusion protein from *E.coli* (glycosylation excluded). No labelling was seen with biotinylated lectins isolated from *Triticum vulgaris*, *Phaseolus vulgaris* and *Abrus preactoriusor*. However, lectins of *Tetragonolobus purpureas* (strong labelling), *Glycine max* and *Helix pomatia* (both weak signal) have shown affinity for both proteins and therefore must represent unspecific binding. Results suggest that the 17ß-HSD 4 is not glycosylated.

The central aa 343-607 domain of pHSD 4 and the aa 343-606 domain of hHSD 4 are 40% identical (Fig. 2) with the C-terminal domains of fatty acid hydratase/dehydroge-nase of *Saccharomyces cerevisiae* [42] and *Candida tropicalis* [41]. Although the relationship of ß-oxidation enzymes to the members of the short chain alcohol dehydrogenase family has been reported [45] the high resemblance of the 80 kDa proteins to multifunctional enzymes is unique and suggests a common ancestor.

The C-terminal segments of 17ß-HSD 4 are 39% similar to the sterol carrier protein 2 (SCP2) [46], including the peroxisome-targeting signal [47] Ala-Lys-Ile (pHSD 4) and Ala-Lys-Leu (hHSD 4). At present it is not known if any cleavage between the central and SCP2 domains is taking place. The peroxisomal 13 kDa SCP2 protein was reported to participate in the transfer of lipids and cholesterol which is important for the shuttling of sterols during steroid synthesis [37,46,48]. The organisation of the central and C-terminal domain in the porcine and human HSD 4 is similar to the structural pattern of the 60 kDa SCPx protein. The latter reveals an N-terminal homology to 3-ketoacyl CoA thiolase (ß-oxidation enzyme), a C-terminal similarity to SCP2 and is not proteolytically cleaved between the two domains [49]. However, it was recently demonstrated that SCP2 and SCPx are expressed from a single gene via alternative transcription initiation from two distinct promoters [50].

Simultaneous occurrence of domains responsible for steroid metabolism, ß-oxidation and sterol transport in a single protein has not yet been observed. The 17ß-HSD 4 proteins are the first of such type.

Multifunctionality of 17β-HSD 4

In order to check for the presence of activities predicted by amino acid similarities of the 80 kDa protein (Fig. 2) its three domains were expressed separately as GST fusion proteins. Essentially pure fusion proteins were obtained after a single passage through glutathione-agarose. Cleavage of the fusion proteins on the glutathione-agarose column with thrombin released single peptides (Fig. 3). The authenticity of the recombinant proteins was checked by DNA sequencing and by N-terminal amino acid sequencing of the first 10 residues.
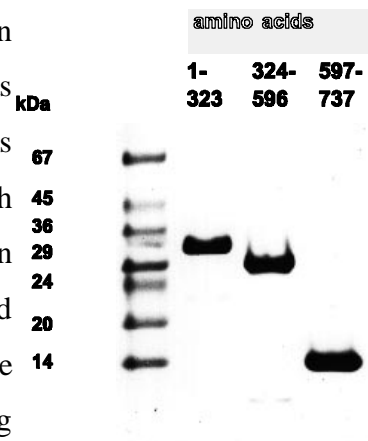
Fig. 3. SDS-PAGE and Coomassie blue staining of expressed domains of 17ß HSD 4

The domains were expressed as GST fusion proteins in *E.coli* , bound to glutathione agarose, cleaved with thrombin and eluted [40]

The N-terminal domain (aa 1-323) catalyzed both the 17ß-hydroxysteroid- and the 3-hydroxyacyl-CoA dehydrogenase reactions (Table 3). Kinetic parameters (K_m, V_{max}) of the expressed full length 80 kDa protein were close to those observed for the single expressed domains or for the native purified enzyme (EDH or VHF) [40].

Table 3. Kinetic parameters of domains of porcine 17ß-HSD 4

Sample	17ß-hydroxysteroid dehydrogenase		fatty acid-CoA hydratase		fatty acid-CoA dehydrogenase	
	K_m μM	V_{max} nmol x l^{-1} x min^{-1} x mg. prot.$^{-1}$	K_m μM	V_{max} μmol x l^{-1} x min^{-1} x mg. prot.$^{-1}$	K_m μM	V_{max} μmol x l^{-1} x min^{-1} x mg. prot.$^{-1}$
Purified 32 kDa	0.2	0.15	ND	ND	ND	ND
Recombinant 32 kDa	0.3	0.14	ND	ND	ND	ND
VHF	0.3	0.19	34.0	4.44	34.8	3.31
Recombinant 80 kDa	0.4	0.11	37.1	3.92	35.3	2.91
Recombinant central domain	ND	ND	34.7	1.36	21.9	1.25

Kinetic parameters of 17ß-HSD 4 were assayed with estradiol, fatty acid-CoA hydratase with crotonyl-CoA and fatty acid-CoA dehydrogenase with acetoacetyl-CoA [40]. Recombinant 32 kDa and 80 kDa proteins were assayed in homogenates of transfected cells and were corrected for background conversion [51]. The recombinant central domain was characterized after purification on gluthatione-agarose and thrombin cleveage, ND - activity not detected.

This was the first observation of an enzyme performing the dehydrogenase activity not only with steroids but also with 3-hydroxyacyl-CoA-derivates of fatty acids. Furthermore the central domain (aa 324 - 596) was responsible for the 2-enoyl-acyl-CoA hydratase activity (Fig. 5)

Fig. 5. Hydratase and dehydrogenase activities of 17ß-HSD 4.

The reactions are catalyzed by the N-terminal and central domains, respectively.

Estimated K_m-values for the hydratase and fatty acid dehydrogenase are similar to those of other enzymes of ß-oxidation of fatty acids [52,53]. Both K_m for steroids and fatty acids are in the physiological range.

As suggested by the similarity to SCP2 we investigated the recombinant C-terminal domain and the purified native enzyme for the ability to transfer 7-dehydrocholesterol and phosphatidylcholine. The specific transfer activities of the VHF and 80 kDa protein are close to those of SCPx [54]. More direct evidence for the involvement of the SCP2-related domain in the sterol and lipid transfer was obtained with the porcine recombinant peptide. Both the GST-SCP2 fusion product and the SCP2 domain were acitve in transfer. The purified porcine SCP2 peptide increases the transfer of 7-dehydrocholesterol and phosphatidylcholine 147- and 158-fold over the control levels (transfer by BSA), respectively (Fig. 6).
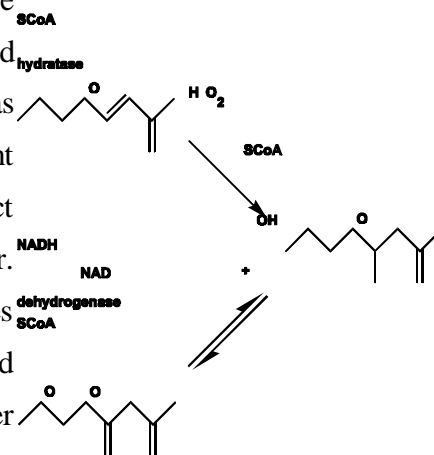
Fig. 6. Transport of cholesterol by 17ß-HSD 4
(availèable in printed version)
hSCP2 - human SCP2, hSCPX - human SCPX, GST-hSCP2 - fusion protein of
glutation-S-transferase and hSCP2, pSCP2 - C-terminal domain of 17ß-HSD 4, control:
BSA - bovine serum albumin [54].

Physiological significance

The high degree of resemblance in the amino acid sequence of porcine and human HSD 4 makes similarities in their enzymic properties likely. Table 1 compares the HSD 1 - 5 and depicts differences in catalytic parameters, posttranslational processing and subcellular localization. The catalytical property of porcine 32 kDa EDH revealing the virtually uni-directional oxidative activity, clearly define it as a steroid inactivating enzyme [55], since it produces estrone which shows little affinity to estradiol receptor. The ovarian cycle-triggered positioning of peroxisomes in glandular epithelium suggests the participation of the cytoskeleton in the regulation of hormone levels. Interactions of EDH with actin are also indicatory for that. The conversion of 17ß-estradiol to estrone might be complemented by hydroxylations in positions 6α or 7α [56] and producing steroids devoid of estradiol receptor affinity and permitting fast release from cells after formation. The V_{max} and K_m values for EDH are similar to those for estrone hydroxylases [57] and allows the metabolic conversion 17ß-estradiol → estrone → 6α / 7α-hydroxy-estrone without rate-limiting steps.

Our discovery of the 17ß-HSD 4 in peroxisomes stimulated the discussions about the possible role of peroxisomes in steroid metabolism [38]. The enzyme has yet unseen ability to be stimulated by both (1) progestins [58], which is a common feature of other 17ß-HSDs [59,60], and (2) peroxisomal activators such as WY14,643 [30,61] or clofibrate (M. Markus, J. Adamski unpublished results). The stimulation produces a tissue-specific response: progestins induce 17ß-HSD 4 about 10-fold in uterus epithelium but not in liver whereas a clofibrate treatment has no effects on uterus but results in 3-fold induction in the liver. It is unknown whether the differences are caused by local concentrations of receptors, modulation of receptor action by spatially restricted factors or alternated promoter usage similar to that observed for the estrogen receptor in osteoblasts and breast tissue [62]. The 17ß-HSD 4 inactivates D5-androstene-3ß, 17ß-diol to dehydroepiandrosterone (DHEA), a

known peroxisomal proliferator [63]. Although both DHEA and clofibrate induce peroxisomes they have opposite effects on the concentrations of triglycerides and cholesterol in blood. DHEA increases tthe levels of lipids while clofibrate acts as a hyperlipidemic drug. Decreased expression of enzymes which inactivate estradiol including Cyp2C11, and the reported increased expression of aromatase (converting testosterone to estradiol) may explain why male rats exposed to diverse peroxisomal proliferators have higher serum estradiol levels. These higher estradiol levels in male rats have been thought to be mechanistically linked to Leydig cell hyperplasia and adenomas. Increased conversion of estradiol to the less active estrone by 17ß-HSD 4 induction may explain how exposure to the di-(2-ethylhexyl)-phthalate leads to decreases in serum estradiol levels and suppression of ovulation in female rats [61,64].

The possible competition between fatty acids and steroids for the active center of enzyme would be a new aspect of enzymatic regulation. Also the functionality of the multi-domain structure (17ß-HSD 4 + hydratase + SCP2) is unknown. Nevertheless, the high level of conservation of amino acid sequence (85% identity) between human, mouse, rat and porcine 17ß-HSD 4 suggests an essential function of this type of protein.

References

[1]   Engel, L.L. and Groman, E.V., *Recent Progress in Hormone Research* **1974**, 30, 139-169.
[2]   Tseng, L. and Gurpide, E., *Endocrinology* **1974**, 94, 419-425.
[3]   Tseng, L. and Mazella, J., *J. Steroid Biochem.* **1981**, 14, 437-442.
[4]   Peltoketo, H., Isomaa, V., Mäentausta, O. and Vihko, R., *FEBS Letters* **1988**, 239, 73-77.
[5]   Luu-The, V., Lachance, Y., Labrie, C., Leblanc, G., Thomas, J.L., Strickler, R.C. and Labrie, F., *Mol. Endocrinol.* **1989**, 3, 1310-1312.
[6]   Blomquist, C.H., Lindemann, N.J. and Hakanson, E.Y., *Arch. Biochem. Bioph.* **1985**, 239, 206-215.
[7]   Wu, L., Einstein, M., Geissler, W.M., Chan, H.K., Elliston, K.O. and Andersson, S., *J. Biol. Chem.* **1993**, 268, 12964-12969.
[8]   Geissler, W.M., Davis, D. L.,Wu, L., Bradshaw, K. D., Patel, S., Mendonca, B. B., Elliston, K. O., Wilson, J. D., Russell, D. W., Andersson, S *Nat. Genet* .**1994**, 7, 34-39.
[9]   Deyashiki, Y., Ohshima, K., Nakanishi, M., Sato, K., Matsuura, K. and Hara, A., *J. Biol. Chem.* **1995**, 270, 10461-10467.
[10]   Zhang, Y., Dufort, I., Soucy, P., Labrie, F. and Luu-The, V., *Proc. 77th Ann. Meeting*

Endocrine Soc. **1995**, Abstract # 622

[11]   Reed, M.J., *J. Endocrinol.* **1991**, 129, 163-165.

[12]   Andersson, S., *J.Endocrinol.* **1995**, 146, 197-200.

[13]   Poutanen, M., Isomaa, V., Peltoketo, H. and Vihko, R., *Ann. Med.* **1995**, 27, 675 - 682.

[14]   Penning, T.M., *Endocr Rev* **1997**, 18, 281-305.

[15]   Pollow, K., Lübbert, H. and Pollow, B., *J. Steroid Biochem.* **1976**, 7, 315-320.

[16]   Entenmann, A.H., Sierralta, W.D. and Jungblut, P.W., *Hoppe-Seyler´s Z. Physiol. Chem.* **1980**, 361, 959-968.

[17]   Adamski, J., Normand, T., Leenders, F., Monte, D., Begue, A., Stehelin, D., Jungblut, P.W. and de Launoit, Y., *Biochem. J.* **1995**, 311, 437 - 443.

[18]   Sierralta, W., Truitt, A.J. and Jungblut, P.W., *Hoppe-Seyler´s Z. Physiol. Chem.* **1978**, 359, 517-528.

[19]   Adamski, J., Husen, B., Marks, F. and Jungblut, P.W., *J. Steroid Biochem. Mol. Biol.* **1992**, 43, 1089-1093.

[20]   Adamski, J., Husen, B., Marks, F. and Jungblut, P.W., *Biochem. J.* **1992**, 288, 375-381.

[21]   Bogovich, K. and Payne, A.H., *J. Biol. Chem.* **1980**, 255, 5552-5559.

[22]   Marks, F., *Ph.D. Thesis* **1992**, University of Hannover

[23]   Adamski, J., *Eur. J. Cell Biol.* **1991**, 54, 166-170.

[24]   Adamski, J., Husen, B., Thole, H.H., Groeschel-Stewart, U. and Jungblut, P.W., *Biochem. J.* **1993**, 296, 797-802.

[25]   Leenders, F., Husen, B., Thole, H.H. and Adamski, J., *Mol. Cell. Endocrinol.* **994**, 104, 127-131.

[26]   Leenders, F., Adamski, J., Husen, B., Thole, H.H. and Jungblut, P.W., *Eur. J. Biochem.* **1994**, 222, 221-227.

[27]   Persson, B., Krook, M. and Jörnvall, H., *Eur.J. Biochem.* **1991**, 200, 537-543.

[28]   Krozowski, Z., *J. Steroid Biochem. Mol. Biol.* **1994**, 51, 125-130.

[29]   Normand, T., Husen, B., Leenders, F., Pelczar, H., Baert, J. L., Begue, A., Flourens, A. C., Adamski, J., de Launoit, Y. *J. Steroid Biochem. Mol. Biol.* **1995**, 55, 541-548.

[30]   Corton, J.C., Bocos, C., Moreno, E.S., Merritt, A., Marsman, D.S., Sausen, P.J., Cattley, R.C. and Gustafsson, J.Å., *Mol. Pharmacology* **1996**, 50, 1157-1166.

[31]   Husen, B., Adamski, J., Szendro, P.I. and Jungblut, P.W., *Cell & Tissue Research* **1994**, 278, 227-233.

[32]   Martel, C., Rheaume, E., Takahashi, M., Trudel, C., Couet, J., Luu, T.V., Simard, J. and Labrie, F., *J. Steroid Biochem. Mol. Biol.* **1992**, 41, 597-603.

[33]   Scublinsky, A., Marin C and Gurpide, E., *J. Steroid Biochemi.* **1976**, 7, 745-747.

[34]   Mäentausta, O., Sormunen, R., Isomaa, V., Lehto, V.-P., Jouppila, P. and Vihko, R., *Laboratory Investigation* **1991**, 65, 582-587.

[35]   Adamski, J., Sierralta, W.D. and Jungblut, P.W., *Eur. J. Cell Biol.* **1987**, 45, 238-245.

[36]   Adamski, J., Husen, B., Marks, F. and Jungblut, P.W., *Biochem. J.* **1993**, 290, 777-782.

[37]   Mori, T., Tsukamoto, T., Mori, H., Tashiro, Y. and Fujiki, Y., *Proc. Natil. Acad. Sci. USA* **1991**, 88, 4338-4342.

[38]   Markus, M., Husen, B., Leenders, F., Jungblut, P.W., Hall, P.F. and Adamski, J., *Eur. J. Cell Biol.* **1995**, 68, 263-267.

[39]   Markus, M., Husen, B. and Adamski, J., *J. Ster. Biochem. Mol Biol.* **1995**, 55, 617 - 621.

[40]   Leenders, F., Tesdorpf, J.G., Markus, M., Engel, T., Seedorf, U. and Adamski, J., *J. Biol. Chem.* **1996**, 271, 5438-5442.

[41]   Nuttley, W.M., Aitchison, J.D. and Rachubinski, R.A., *Gene* **1988**, 69, 171-180.

[42]   Hiltunen, J.K., Wenzel, B., Beyer, A., Erdmann, R., Fossa, A. and Kunau, W.H., *J. Biol. Chem* **1992**, 267, 6646-6653.

[43]   O´Reilly, G. and Clarke, F., *FEBS Letters* **1993**, 321, 69-72.

[44]   Bar-Sagi, D., Rotin, D., Batzer, A., Mandiyan, V. and Schlessinger, J., *Cell* **1993**, 74, 83-91.

[45]   Baker, M.E., *FASEB Journal* **1990**, 4, 222-226.

[46]   Seedorf, U. and Assmann, G., *J. Biol. Chem.* **1991**, 266, 630-636.

[47] De Hoop, M.J. and Ab, G., *Biochem. J.* **1992**, 286, 657-669.

[48] Keller, G.A., Scallen, T.J., Clarke, D., Maher, P.A., Krisans, S.K. and Singer, S.J., *J. Cell Biol.* **1989**, 108, 1353 - 1361.

[49] Pfeifer, S.M., Sakuragi, N., Ryan, A., Johnson, A.L., Deeley, R.G., Billheimer, J.T., Baker, M.E. and Strauss, J.F., *Arch. Biochem. Bioph.* **1993**, 304, 287-293.

[50] Ohba, T., Holt, J.A., Bilheimer, J.T. and Strauss III, J.F., *Biochemistry* **1995**, 34, 10660 - 10668.

[51] Carstensen, J.F., Tesdorpf, J.G., Kaufmann, M., Markus, M.M., Husen, B., Leenders, F., Jakob, F., de Launoit, Y., Adamski, J. *J. Endocrinol.* **1996**, 150, 3 - 12.

[52] Steinman, H.M. and Hill, R.L., *Methods in Enzymology* **1975**, 35, 136-139.

[53] Palosaari, P.M. and Hiltunen, J.K., *J. Biol. Biochem.* **1990**, 265, 2446-2449.

[54] Seedorf, U., Engel, T., Assmann, G., Leenders, F. and Adamski, J., *J. Steroid Biochem. Mol. Biol.* **1995**, 55, 549-53.

[55] Gurpide, E. and Marks, C., *J. Clin. Endocrinol. Metab.* **1981**, 52, 252-255.

[56] Maschler, I., Ball, P., Bayerköhler, G., Gaues, J. and Knuppen, R., *Steroids* **1983**, 41, 597-607.

[57] Adamski, J., Hohls, E. and Jungblut, P.W., *Exp. Clin. Endocrinol.* **1994**, 102, 388 - 393.

[58] Kaufmann, M., Carstensen, J., Husen, B. and Adamski, J., *J. Steroid Biochem. Mol. Biol.* **1995**, 55, 535 - 539.

[59] Poutanen, M., Isomaa, V., Kainulainen, K. and Vihko, R., *Int.J. Cancer* **1990**, 46, 897-901.

[60] Tseng, L. and Gurpide, E., *Endocrinology* **1975**, 97, 825-833.

[61] Corton, J.C., Bocos, C., Moreno, E.S., Merritt, A., Cattley, R.C. and Gustafsson, J.A., *Biochimie* **1997**, 79, 151-62.

[62] Grandien, K., Backdahl, M., Ljunggren, O., Gustafsson, J.A. and Berkenstam, A., *Endocrinology* **1995**, 136, 2223 - 2229.

[63] Prough, R.A., Webb, S.J., Wu, H.Q., Lapenson, D.P. and Waxman, D.J., *Cancer Res.* **1994**, 54, 2878 - 2886.

[64] Srivastava, S. and Srivastava, S.P., *Toxicology Letters* **1991**, 57, 235-239.

UTILIZATION OF THE CHIROPTICAL SPECTROSCOPIES FOR THE STRUCTURE ELUCIDATION OF FLAVONOIDS AND RELATED BENZOPYRAN DERIVATIVES[†]

Albert Lévai

Department of Organic Chemistry, Lajos Kossuth University, P.O.Box 20,

H-4010 Debrecen, Hungary

Abstract

Chiroptical stpectroscopies, mainly the optical rotatory dispersion (ORD) and the circular dichroism (CD) played an important role for the structure elucidation of various naturally occurring organic compounds, with the flavonoids among them, during the last four decades. The aim of the present review article is to provide characteristic examples on the utilization of these techniques in the flavonoid chemistry.

Introduction

Flavonoids are well known natural products of the plant kingdom [1-3]. Several groups of the naturally occurring flavonoids, e.g. flavans, flavanones, isoflavans, isoflavanones, etc. are chiral molecules and are isolated in enantiopure form as optically active substances. Numerous flavonoid glycosides are optically active plant products as well. For this reason, the chiroptical techniques are very convenient and efficient tools

[†]Dedicated to the late Prof. Dr. Günther Snatzke on the occasion of his 70th birth anniversary

for their structure elucidation mainly for the determination of the absolute configuration of their stereogenic centres.

Of the chiroptical techniques, the optical rotatory dispersion (ORD) was utilized first by using the commercially available spectropolarimeter manufactured and marketed by the Rudolph company since 1953. According to Djerassi [4], this instrument "undoubtedly represented the prince who awoke the sleeping beauty of the rotatory dispersion". This prince offered a new opportunity for the flavonoid chemistry by the determination of the absolute configuration of the optically active flavonoids (vide infra). However, because of an easier and more convenient correlation of the structure or stereochemistry and the circular dichrosim (CD) spectra if compared to the ORD properties of a particular molecule, the circular dichroism (CD) spectroscopy came to the front since the middle of the sixties [5]. Owing to the fact that a successful measurement of a CD spectrum requires less than one milligram substance, this technique is especially convenient and helpful method for the structure elucidation of naturally occurring optically active organic compounds. Reference substances with established absolute configuration or the so-called empirical rules like the octant rule [6] and sector rules [7] help to correlate the stereochemistry and the chiroptical properties of optically active flavonoids.

In our present review article, we plan to summarize the most important results of the utilization of the chiroptical spectroscopies in the flavonoid chemistry. One of the aims of this account is to direct the attention of chemists engaged in optically active flavonoids to the utility of the chiroptical techniques.

Flavanones

Since flavanones (2-phenylchromanones) are the first representatives of the known naturally occurring optically active flavonoids, it seems to be expedient to start the discussion of the application of the so-called chiroptical techniques in the flavonoid chemistry with the flavanones. Optically active flavanones, *viz.* (-)-matteucinol and (-)-demethoxymatteucinol were isolated by Fujise and Kubota [8] already in 1934. Data

relating to the determination of the absolute configuration of the stereogenic centre of optically active flavanones were, however, published only in 1960. The absolute configuration of (-)-hesperetin (**1**), (-)-liquiritigenin (**2**) and (+)-sakuranetin (**3**) (Fig. 1)

1: $R^1 = OH$, $R^2 = OMe$
2: $R^1 = H$, $R^2 = OH$
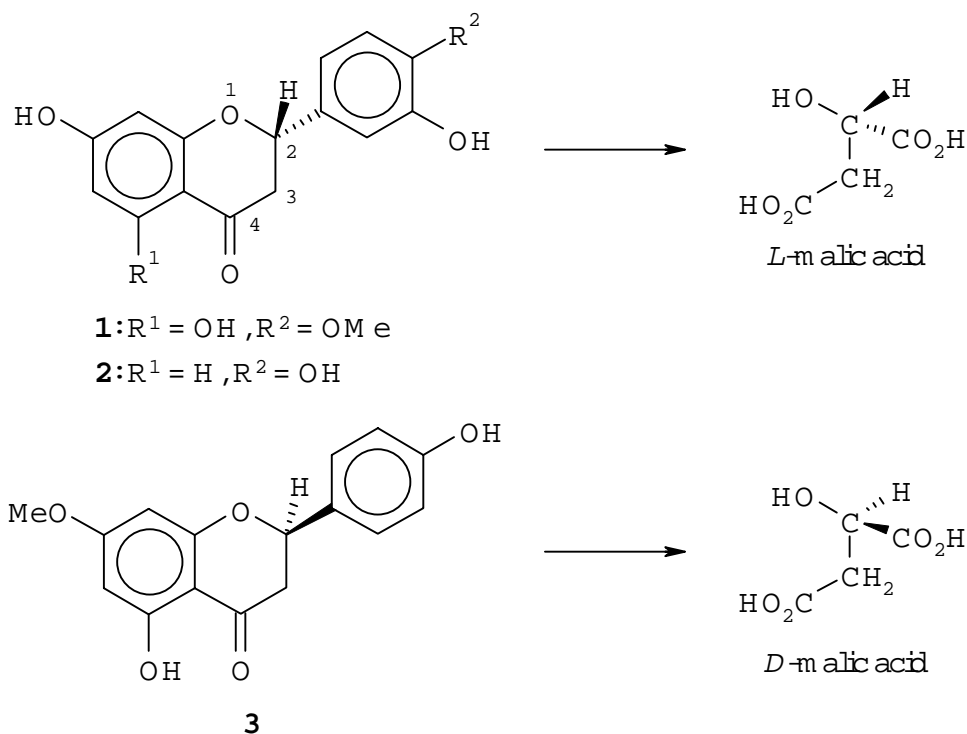
Figure 1

was established by chemical degradation by Arakawa and Nakazaki [9]. These compounds were subjected to ozonization and subsequent oxidation in order to obtain malic acid of known absolute configuration (Fig. 1, L-malic acid from the (-)-flavanones **1** and **2** and D-malic acid from the (+)-flavanone **3**) which gave unequivocally the absolute configuration of the investigated flavanones. Moreover, these results can be used as reference data for the determination of the absolute configuration of other flavanones with the help of chiroptical spectroscopies, e.g. optical rotatory dispersion (ORD) or circular dichroism (CD).

First utilization of a chiroptical spectroscopic method, *viz.* optical rotatory dispersion (ORD) in the flavonoid chemistry was published by Gaffield and Waiss [10]. They reported that (-)-flavanones **1** and **2** with *2S* absolute configuration [8] showed a

positive Cotton effect between 320-330 nm due to the n→π* transition. However, the dextrorotatory (+)-sakuranetin (**3**) of *2R* absolute configuration displayed a negative Cotton effect in the same wavelength region assigned to an n→π* transition as well. Circular dichroism (CD) spectra of flavanones including compounds **1-3** were measured fist by Arakawa and Masui [11]. Later, the CD spectra of a series of naturally occurring flavanones were studied by Gaffield [12] and the CD spectra of the unsubstituted flavanone enantiomers by Snatzke et al. [13], respectively. Very recently, Kojima et al. [14] applied the CD spectroscopy for the determination of the absolute configuration of optically active flavanones isolated from *Iris tenuifolia*. All these CD measurements reveal that the sign of the n→π*-band CD maximum of flavanones are independent on the substitution pattern of the aromatic rings. For this reason, the sign of the n→π*-band CD maximum can be utilized for the determination of the absolute configuration of the stereogenic centre of flavanones. Thus, the negative n→π*-band CD maximum proves the absolute configuration to be *2R*, while a positive sign of this CD maximum reveals a *2S* absolute configuration (Fig. 2). Of course, additional Cotton effects appear at shorter wavelengths, but it is not necessary to correlate their signs with the absolute

2R-flavanones
negative n→π*-band CD

2S-flavanones
positive n→π*-band CD
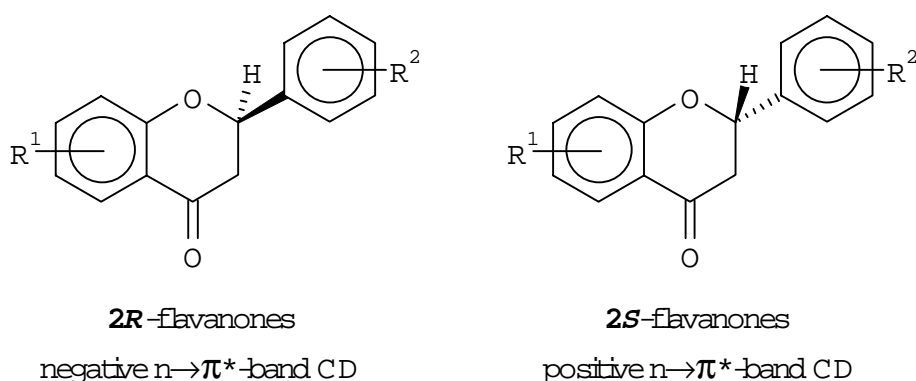
Figure 2

configuration of the molecule. Consideration of the sign of the n→π*-band CD is enough for this purpose. It is worth mentioning that Gaffield [10] attempted to apply the Snatzke's modified octant rule [15] for the prediction of the sign of the n→π*-band CD maximum as well.

Although it is not the aim of this review article to discuss the utility of the chiroptical techniques for related heterocyclic compounds with heteroatom other than oxygen, we mention that the CD spectroscopy was successfully applied for the determination of the absolute configuration of optically active 1-thioflavanones and the so-called "azaflavanones" by Antus et al. [16].

3-Hydroxyflavanones (dihydroflavonols) are well known and important natural products isolated from numerous plants [1-3]. Owing to their two stereogenic centres,

2R,3S
positive n→π*-band CD

2R,3R
positive n→π*-band CD

2S,3R
negative n→π*-band CD

2S,3S
negative n→π*-band CD
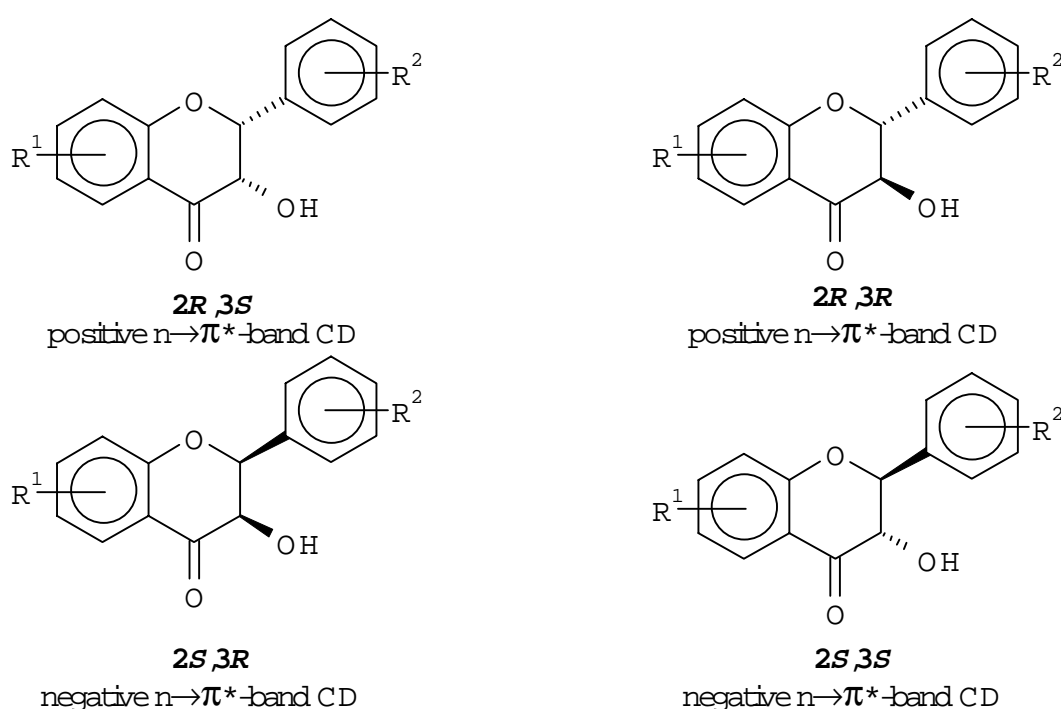
Figure 3

they can exist in four optically active stereoisomers (Fig. 3). CD spectroscopy was successfully used for the determination of their absolute configuration [10,12,14,17,18]. A positive n→π*-band CD maximum in the 330-340 nm wavelength region proves the *2R* configuration for both the *cis* and *trans* isomers. However, a negative CD maximum belonging to a similar wavelength value reveals a *2S* absolute configuration for the other two stereoisomers. Configuration at the C-3 atom can then be deduced from these data (Fig. 3). As in the case of flavanones (vide supra), although several CD maxima are generally measured, it is enough to use the sign of the n→π*-band CD maximum around

330-340 nm to determine the absolute configuration of both stereogenic centres of the 3-hydroxyflavanones.

Isoflavanones

Recently, opticaly active isoflavanones (3-phenylchromanones) have also been isolated from various plant sources [19,20]. First utilization of a chiroptical spectroscopy for synthetic isoflavanones was described by Farkas et al. [21] in 1969. They measured the ORD spectra of some isoflavanone glycosides and determined the absolute configuration of the aglycone of the (-)-5-acetoxy-7-methoxy-4'-(tetra-O-acetyl-β-D-glucosyloxy)isoflavanone by this method. CD spectroscopy was used to determine the absolute configuration of the recently isolated isoflavanones [19,20]. A positive n$\rightarrow\pi^*$-band CD maximum in the 325-352 nm wavelength region reveals a *3R* absolute configuration on the basis of the modified octant rule [15] (Fig. 4).

3R -isoflavanones
positive n$\rightarrow\pi^*$-band CD

1a*S*,7a*R*
positive n$\rightarrow\pi^*$-band CD

1a*R*,7a*S*
negative n$\rightarrow\pi^*$-band CD
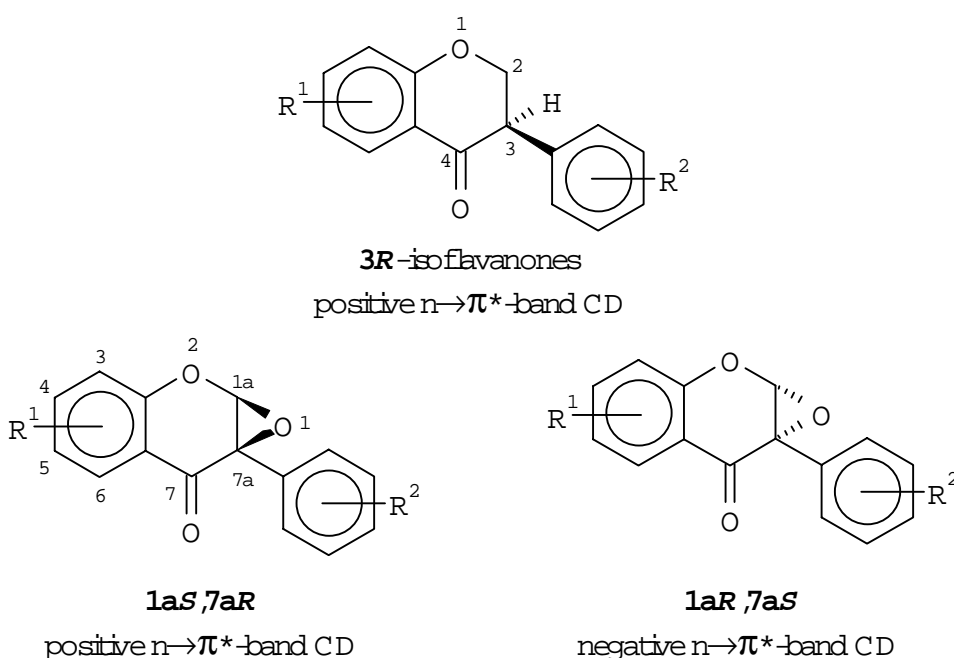
Figure 4

A newest development in the application of the CD spectroscopy for the determination of the absolute configuration of isoflavanone derivatives is our own study

on optically active isoflavone epoxides [22] (Fig. 4). It has been found that a negative n→π* CD maximum of the (-)-compounds uniquivocally proves the *1aR,7aS*, while a positive sign of the same CD band of their (+)-enantiomers reveals the *1aS,7aR* absolute configuration by using the Snatzke's "inverse octant rule" [15]. These results are in full harmony with those determined by X-ray diffraction analysis [23]. Thus, it can be concluded that in the case of the optically active isoflavanones or 3,4-epoxyisoflavanones the knowledge of the sign of their n→π*-band CD maximum is enough to determine the absolute configuration of their stereogenic centres by using the modified octant rule or the inverse octant rule both introcuded by Snatzke [15].

Flavans

In the present review two groups of flavan derivatives, *viz.* 3-hydroxyflavans and 4-substituted flavans are discussed, the available CD data of which make possible some general considerations.

3-Hydroxyflavans

The stereochemical problems of the 3-hydroxyflavans (catechins and epicatechins) have been summarized in a detailed review article [24]. The absolute configuration of the stereogenic centres of these flavan derivatives were generally determined either by using the Prelog's atrolactic acid method [25] or by azonolysis [26] prior to the availability of the CD spectroscopy. From the early seventies the CD spectroscopy has been successfully used for this purpose as well [27-31].

The absorption bands of these chromophores are found in two regions: around 280 nm ($^1B_{2u}$ transition) and at about 240 nm ($^1B_{1u}$ transition). In their CD spectra Cotton effects are expected in these two regions. The CD spectra of a series of 3-hydroxyflavans at 25 and -185 °C have been measured by Korver and Wilkins [27]. According to their study, the sign of the Cotton effect due to the $^1B_{2u}$ transition is determined by the chirality of the hetero ring, which in turn is connected with the absolute configuration of the stereogenic centre at position 2 (Fig. 5). Thus, the *2R* absolute configuration gives rise to a negative CD band, while a *2S* absolute

configuration to a positive one [27]. The contribution of the C-3 stereogenic centre to this CD band is small. On the basis of low temperature measurements they managed to evaluate the contribution of the phenyl group at the C-2 atom as well. Therefore, it can be concluded that the CD spectroscopy can be advantageously utilized for the determination of the absolute configuration of the 3-hydroxyflavan derivatives.

2R,3S-3-hydroxyflavan

2S,3R-3-hydroxyflavan

2R,3R-3-hydroxyflavan

2S,3S-3-hydroxyflavan
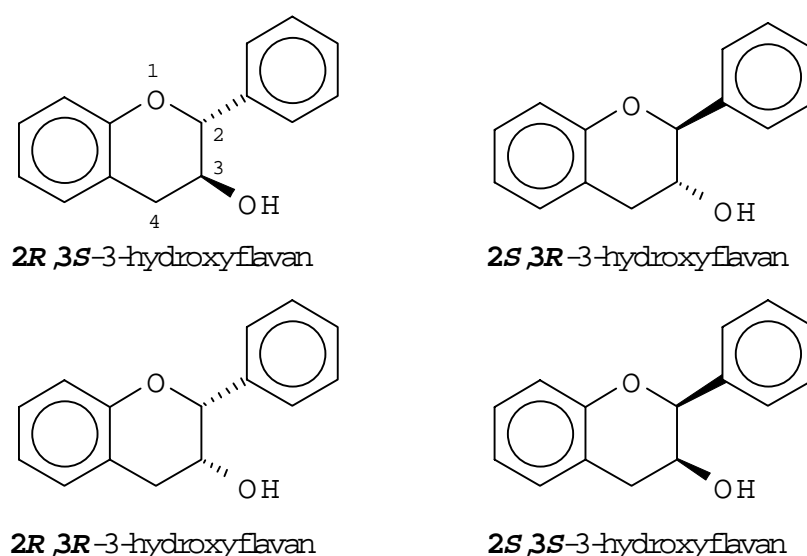
Figure 5

4-Substituted flavans

A series of 4-substituted *cis-* and *trans*-flavan derivatives have been prepared by Bognár et al. [32-36] by the optical resolution and subsequent chemical transformations of 4-amino- and 4-hydroxyflavans. The CD spectra of these compounds have been studied by Snatzke et al. [13]. The absolute configuration of the two stereogenic centres of these compounds result from their conversion into flavanone enantiomers of known absolute configuration [33]. Moreover, the CD spectroscopy could also be utilized for the determination of the conformation of these 4-substituted flavans. The evaluation of the second- and third-sphere contributions revealed a *sofa* conformation for both their *cis-* and *trans*-isomers [13] (Fig. 6). Sofa conformation has also been suggested by Korver and Wilkins [27] in the case of 3-hydroxyflavans. A sector rule for the

estimation of the influence of the 4-substituent has also been proposed by Snatzke et al. [13].

R:OH, NH₃⁺ Cl, NHAc, NHBz
cis-compounds

R:OH, OAc
trans-compounds
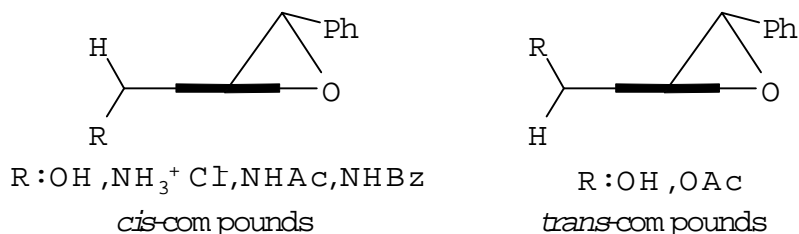
Figure 6

Isoflavans

ORD and CD measurements have been used for the determination of the absolute configuration of naturally occurring isoflavan derivatives [37-41]. Asolute configuration of the (*3S*)-5,7,3',4'-tetramethoxyisoflavan (**4**) (Fig. 7) was established by its chemical correlation with *S*-(-)-methylsuccinic acid [42]. This compound served as a reference for the determination of the absolute configuration of other optically active isoflavans by means of chiroptical methods. The ORD spectra of the *3S*-isoflavans showed a negative Cotton effect in the 260-300 nm region [37]. In the CD spectra of the *3S*-compounds around 280 nm also a negative maximum, while at about 230-240 nm a positive one were measured. The sign was opposite in both regions for the *3R*-enantiomers. On all these bases, it can be concluded that the chiroptical techniques can be beneficially used for the determination of the absolute configuration of optically active isoflavans as well (Fig. 7).

3R-isoflavan   *3S*-isoflavan   **4**
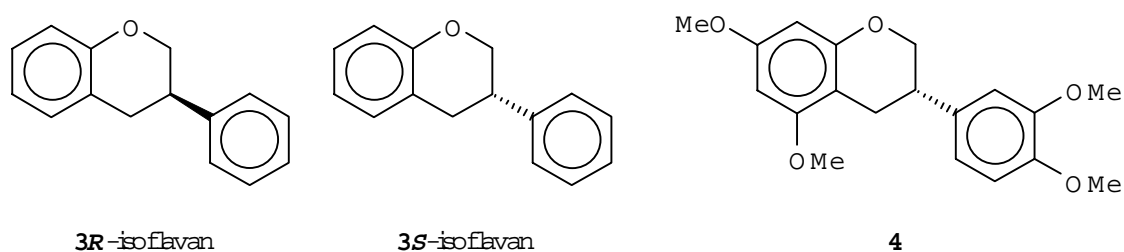
Figure 7

Flavone and isoflavone glycosides

Natural flavones and isoflavones are frequently present in their plant sources attached to mono- or oligosaccharides [1-3]. Both the C-glycosides and O-glycosides of these two types of flavonoids have been isolated from a wide variety of plants [1-3]. Owing to their sugar component, all these natural products are optically active compounds making possible the utilization of the chiroptical techniques for their structure elucidation. Herein we provide some characteristic examples for such application of the ORD and CD spectroscopies.

C-Glycosylflavones

The CD spectra of 6- and 8-glycosylflavones (Fig. 8) have been investigated by Gaffield et al. [43,44]. Their studies prove that the sign of the Cotton effect at 250-275 nm depends upon the position of the C-glycosyl residue on the flavone if the sugar belongs to the D-series and the glycosidic linkage is β. In this region all the 6-C-glycosylflavones displayed a positive, and the 8-C-glycosylflavones a negative Cotton effect. On this basis the CD spectroscopy appears to be a sensitive method for the differentiation of the 6- and 8-C-glycosylflavones.

6-C-glycosylflavones   8-C-glycosylflavones
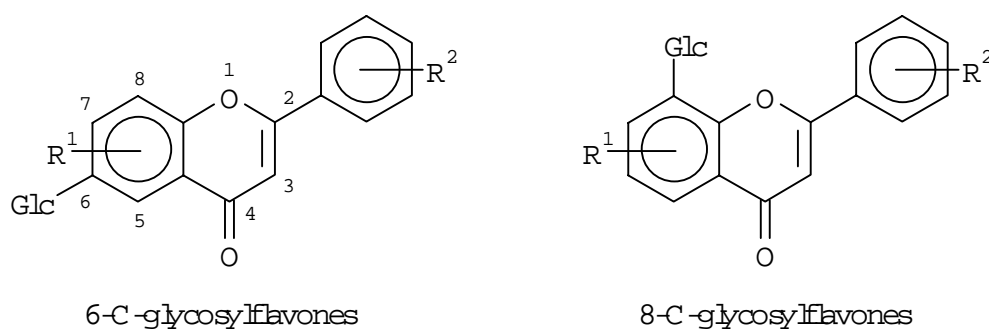
Figure 8

In view of these findings attempts have been made to use the CD for the differentiation of O-glycosylflavones and O-glycosylisoflavones as well. Prior to the discusssion of the chiroptical properties of the O-glycosylflavones and the O-glycosylisoflavones, CD properties of the simple phenyl glycosides should be mentioned.

According to detailed investigations, both $^1B_{2u}$ and $^1B_{1u}$ CD maxima are negative for phenyl β-D-glycosides and positive for the α-anomers [45,46]. This relationship, however, is not necessarily true for glycosides with a more complicated chromophore, e.g. flavone or isoflavone molecules.

O-Glycosylflavones

CD spectra of few O-glycosylflavones are available in the literature [47,48], but the published data do not make possible the establishment of such a relationship between the chiroptical properties and the site of the glycosidic linkage as in the case of C-glycosylflavones [43,44]. To improve these informations, we decided to investigate a systematic series of flavone glycosides, *viz.* the quercetin glucosides, where the aglycone (3,5,7,3',4'-pentahydroxyflavone), the sugar component (D-glucose) and the glycosidic linkage (β) are the same [49] (Fig. 9). Compounds under study (**5-12**) were synthesized by Farkas et al. [50-52].
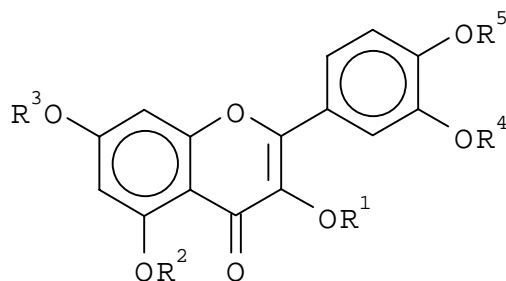
5–12

5: $R^1 = Glu, R^2 = R^3 = R^4 = R^5 = H$ **9**: $R^1 = R^4 = Glu, R^2 = R^3 = R^5 = H$

6: $R^1 = R^3 = R^4 = R^5 = H, R^2 = Glu$ **10**: $R^1 = R^5 = Glu, R^2 = R^3 = R^4 = H$

7: $R^1 = R^2 = R^4 = R^5 = H, R^3 = Glu$ **11**: $R^1 = R^3 = Glu, R^2 = R^4 = R^5 = H$

8: $R^1 = R^2 = R^3 = R^4 = H, R^5 = Glu$ **12**: $R^1 = R^2 = R^4 = H, R^3 = R^5 = Glu$

Glu: β-D-glucosyl

Figure 9

278

A negative CD maximum was observed for all compounds between 340 and 375 nm which seems to belong to the n→π* transition. The magnitude of this maximum somewhat alters with the position of the glycosidic linkage. Around 250 nm a characteristic intense positive band was measured for the 3-O-glucoside and a negative one for the 5- and 4'-O-glucosides, respectively. 7-Glucosylquercetin, in which the free rotation of the sugar component is not hindered, exhibited only one negative maximum at 375 nm. The CD spectra of the quercetin diglucosides displayed a superposition of the CD spectra of the corresponding two monoglucosides.

O-Glycosylisoflavones

The sugar component of naturally occurring O-glycosylisoflavones known so far are attached to the aglycone through the hydroxyl group either at C-7 or C-4' of isoflavone by a β-linkage [1-3] (Fig. 10). The position of the glycosidic linkage has been elucidated by means of chemical degradation or by NMR spectroscopy.

negative n→π*-band CD   positive n→π*-band CD
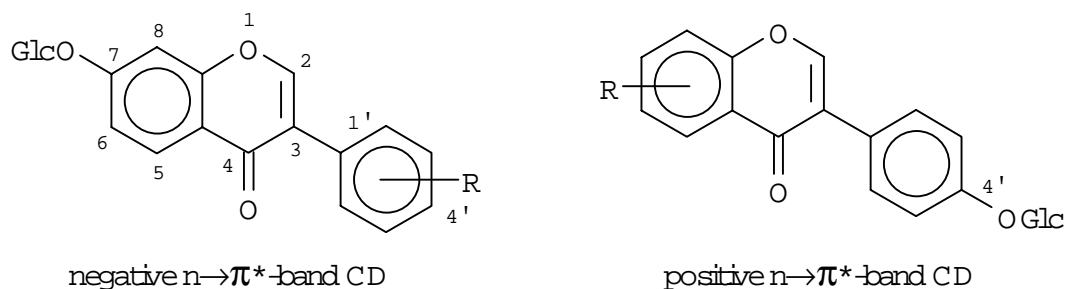
Figure 10

The CD spectra [48,53] of a series of synthetic 7-β-glycosyloxyisoflavones [54-56] and natural 4'-β-glycosyloxyisoflavones have been measured. These measurements revealed that the sign of the CD maximum due to the n→π* transition (330-350 nm) is dependent on the site of the glycosidic linkage: it is negative for 7-β-glycosyloxyisoflavones and positive for 4'-β-glycosyloxyisoflavones (Fig. 10). These findings refer only to such isoflavone O-glycosides where a D-sugar is attached to the aglycone by a β-linkage. Therefore, the CD spectroscopy can serve as a simple and

convenient method for the elucidation of the site of the glycosidic linkage of newly isolated natural isoflavone glycosides.

Biflavones

First representatives of the optically active biflavones, the (-)-5,5‴-dihydroxy-4',4‴,7,7‴-tetramethoxy-8,8‴-biflavone (Fig. 11 (-)-**13**) was isolated from *Araucaria cunninghamii* and *A. cooki* in 1968 [57]. Later, several other optically active biflavones, *viz.* cupressuflavones [57-59], amentoflavones [60,61] and agathisflavones [62] have also been isolated from various plant sources. Their chirality is due to the atropisomerism of the biflavone moiety. Recently, synthesis of optically pure biflavones has also been achieved [63-65]. However, the first data for the determination of their absolute configuration were published only in 1995 by Lin et al. [63]. X-ray diffraction analysis of the (+)-bis-5,5‴-camphonate of (+)-**13** (Fig. 11) revealed an *aR* absolute configuration by correlation with the known configuration of the camphorsulfonate group. This compound served as a reference for the determination of the absolute configuration of other optically active biflavones by CD spectroscopy [63-65]. By means of a combined utilization of the X-ray diffraction analysis and the CD spectroscopy Lin et al. [63] assigned an *aR* configuration to the (+)-biflavones and and *aS* one to their (-)-enantiomers, whereas Harada et al. [59,65] an *aR* configuration to compound (-)-**13** (Fig. 11) on the basis of the same CD data. This contradiction has not hitherto been solved by the reinvestigation of the absolute configuration of the optically active biflavones.

R = H : (+)-**13**　　　　　　　　R = H : (−)-**13**

R = M e: (+)-**14**　　　　　　　R = M e: (−)-**14**
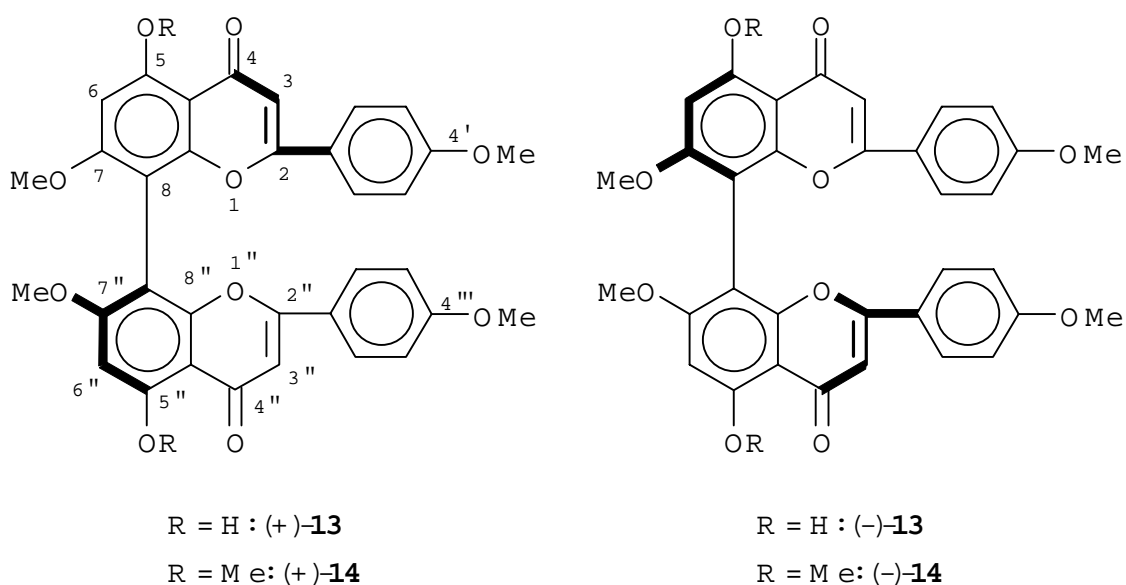
Figure 11

Other benzopyran derivatives

4-Hydroxychromans

Optically active 4-hydroxychromans have been prepared by kinetic resolution of (±)-chroman-4-ols by microbial lipases using vinyl acetate as acyl donor [66,67]. Under these reaction conditions (+)-chroman-4-ols were converted into their acetates and the (-)-chroman-4-ols remained unchaged materials in high enantiomeric excess (Fig. 12). The absolute configuration of these optically active chroman derivatives has been determined by CD spectroscopy [68] either by using the so-called helicity rule [13,16] or by measuring the exciton-coupled CD spectra of the 4-benzoyloxychromans [68]. These measurements revealed a *4R* configuration to the (+)-4-acetoxychromans and *4S* one to the (-)-4-hydroxychromans (Fig. 12).
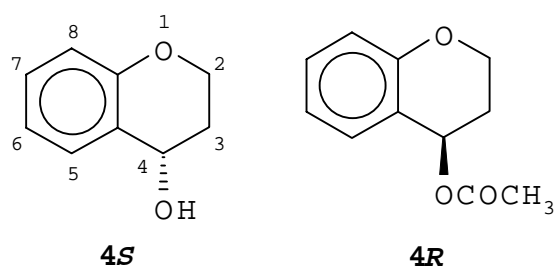
Figure 12

2,2-Dimethyl-3,4-epoxychromans

Optically active 2,2-dimethyl-3,4-epoxychromans have been synthesized by several research groups [69-77] by the catalytic enantioselective epoxidation of 2,2-dimethyl-2*H*-chromenes by using Mn(III)salen catalysts. However, no direct determination of their absolute configuration has been published prior to our paper [77] in 1996. Jacobsen et al. [78] described the measurement of the CD spectra of some optically active 2,2-disubstituted 3,4-epoxychromans, but without mentioning the correlation of the CD data with the configuration of their epoxides. In our own study [77], absolute configuration of one optically active 2,2-dimethyl-3,4-epoxychroman was determined by X-ray diffraction analysis which then could be used as reference substance for the CD study of the related epoxides. Thus, the (+)-compounds proved to be the *3R,4R*-enantiomers and the (-)-ones are the *3S,4S*-enantiomers determined by CD measurements (Fig. 13). These CD data [77] may serve as reference for the configurational assignment of related 3,4-epoxychromans by CD spectroscopy or even on the basis of the sign of their specific rotation.
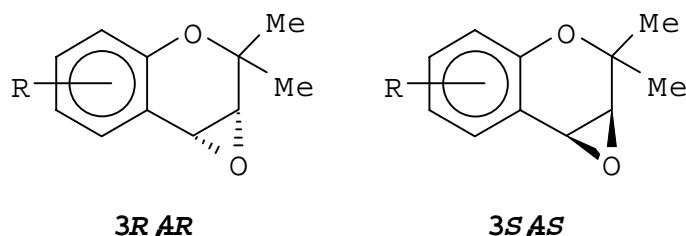
Figure 13

3,4-Dihydroxy-2,2-dimethylchromans

All four optically active stereoisomers of the 3,4-dihydroxy-2,2-dimethyl-7-methoxychroman (Fig. 14) were synthesized by Jennings [79]. Absolute configuration of these compounds were determined by the CD measurement of their bis-p-N,N-dimethylaminobenzoate by means of the exciton chirality method [80].
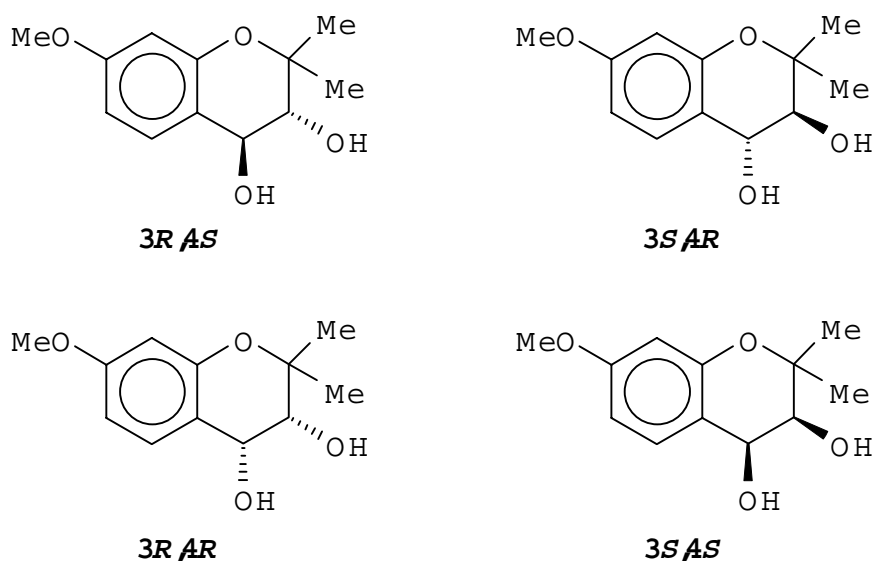
Figure 14

In summary, the present review is aimed to show the utility of the chiroptical spectroscopic methods through the eyes of a synthetic chemist who looks for tools to determine the stereochemistry of optically active flavonoids. Theoretic backgrounds of chiroptical techniques discussed here are, therefore, omitted.

Acknowledgement

References

1. T. A. Geissman, *The Chemistry of Flavonoid Compounds*, Pergamon Press, Oxford, 1962.
2. J. B. Harborne, T.J. Mabry, J. Mabry, *The Flavonoids*, Chapman and Hall, London, 1975.
3. J.B. Harborne, *The Flavonoids: Advances in Research science 1980*, Chapman and Hall, London, 1988.
4. C. Dejerassi, *Optical Rotatory Dispersion*, McGraw-Hill Book Company, Inc., New York, 1960.
5. G. Snatzke, *Optical Rotatory Dispersion and Circular Dichroism in Organic Chemistry*, Heyden and Son Ltd, London, 1967.
6. W. Moffit, R.B. Woodward, A. Moscowitz, W. Klyne, C. Djerassi, *J. Am. Chem. Soc.* **1961**, *83*, 4013-4018.
7. F. Ciardelli, P. Salvadori, *Fundamental Aspects and Recent Developments in Optical Rotatory Dispersion and Circular Dichroism*, Heyden and Son Ltd, London, 1973.
8. S. Fujise, T. Kubota, *Ber Dtsch. Chem. Ges.* **1934**, *67*, 1905-1908.
9. H. Arakawa, M. Nazaoki, *Liebigs Ann. Chem.* **1960**, *636*,111-117.
10. W. Gaffield, A. C Waiss, Jr., *J. Chem. Soc., Chem. Commun.* **1968**, 29-31.
11. H. Arakawa, Y. Masui, *Bull. Chem. Soc. Jpn.* **1969**, *42*, 1452-1453.
12. W. Gaffield, *Tetrahedron* **1970** *26*, 4093-4108.
13. G. Snatzke, F. Snatzke, A.L. Tőkés, M. Rákosi, R. Bognár, *Tetrahedron* 1973, *29*, 909-912.
14. K. Kojima, P. Gombosurengyin, P. Ondognyi, D. Begzsurengyin, O. Zevgeegyin, K. Hatano, Y. Ogihara, *Phytochemistry* **1997**, *44*, 711-714.
15. G. Snatzke, *Tetrahedron* **1965**, *21*, 413-448.
16. S. Antus, E. Baitz-Gács, J. Kajtár, G. Snatzke, A. L. Tőkés, *Liebigs Ann. Chem.* **1994**, 497-502.
17. W. Gaffield, *Chem. Pharm. Bull.* **1996**, *44*, 1102-1103.
18. H. van Rensburg, P.S. van Heerden, B.C.B. Bezuidenhoudt, D. Ferreira, *Tetrahedron* **1997**, *53*, 14141-14152.
19. G.B. Russell, *Aust. J. Chem.* **1997**, *50*, 333-336.
20. C. Galeffi, P. Rasoanaivo, E. Federici, G. Palazzino, M. Nicoletti, B. Rasondratovo, *Phytochemistry* **1997**, *45*, 189-192.
21. L. Farkas, M. Nógrádi, S. Antus, Á. Gottsegen, *Tetrahedron* **1969**, *25*, 1013-1019.
22. A. Lévai, W. Adam, R.T. Fell, R. Gessner, T. Patonay, A. Simon, G. Tóth, *Tetrahedron*, in press.
23. W. Adam, R.T. Fell, A. Lévai, T. Patonay, K. Peters, A. Simon, G. Tóth, *Tetrahedron:Asymmetry* **1998**, *9*, 1121-1124.
24. K. Weinges, W. Bähr, W. Ebert, K. Göritz, H.D. Marx, *Fortschr. Chem. Org. Naturst.* **1969**, *27*, 158-260.
25. A.J. Birch, J.W. Clark-Lewis, A.V. Robertson, *J. Chem. Soc.* **1957**, 3586-3594.
26. E. Hardegger, H. Gempeler, H. Züst, *Helv. Chim. Acta* **1957**, *40*, 1819-1822.
27. O. Korver, C.K. Wilkins, *Tetrahedron* **1971**, *27*, 5459-5465.
28. R.S. Thompson, D. Jacques, E. Haslam, R.J.N. Tanner, *J. Chem. Soc., Perkin Trans. 1* **1972**, 1387-1399.
29. D.W. Engel, M. Hattingh, H.K.L. Hundt, D.G. Roux, *J. Chem. Soc., Chem. Commun.* **1978**, 695-696.
30. M.W. Barrett, W. Klyne, P.M. Scopes, A.C. Fletcher, L.J. Porter, E. Haslam, *J. Chem. Soc., Perkin Trans. 1* **1979**, 2375-2377.
31. H. van Rensburg, P.S. van Heerden, D. Ferreira, *J. Chem. Soc., Perkin Trans. 1* **1997**, 3415-3421.
32. R. Bognár, A. L. Tőkés, M. Rákosi, *Magy. Kém. Foly.* **1970**, *76*, 271-274.
33. M. Rákosi, A.L. Tőkés, R. Bognár, *Tetrahedron Lett.* **1970**, 2305-2308.
34. R. Bognár, J.W. Clark-Lewis, A.L. Tőkés, M. Rákosi, *Aust. J. Chem.* **1970**, *23*, 2015-2025.
35. R. Bognár, A.L. Tőkés, M. Rákosi, *Acta Chim. Acad. Sci. Hung.* **1973**,*79*, 357-363.
36. M. Rákosi, A.L. Tőkés, R. Bognár, *Acta Chim. Acad. Sci. Hung.* **1975**,*87*, 161-164.
37. K. Kurosawa, W.D. Ollis, B.T. Redman, I.O. Sutherland, O.R. Gottlieb, H.M. Alves, *J.Chem. Soc., Chem. Commun.* **1968**, 1265-1266.
38. L. Verbit, J.W. Clark-Lewis, *Tetrahedron* **1968**, *24*, 5519-5527.
39. D.M.X. Donnelly, P.J. Keenan, J.P. Prendergast, *Phytochemistry* **1973**, *12*, 1157-1161.
40. M.D. Woodward, *Phytochemistry* **1980**, *19*, 921-927.

41. S. Yahara, R. Saijo, T. Nohara, R. Kouishi, J. Yamahara, T. Kawasaki, K. Miyahara, *Chem. Pharm. Bull.* **1985**, *33*, 5130-5133.

42. J.W. Clark-Lewis, *Rev. Pure Appl. Chem.* **1962**, *12*, 96-116.

43. W. Gaffield, R.H. Horowitz, *J. Chem. Soc., Chem. Commun.* **1972**, 648-649.

44. W. Gaffield, R.M. Horowitz, B. Gentili, J. Chopin, M.L. Bouillant, *Tetrahedron* **1978**, *34*, 3089-3096.

45. T. Sticzay, C. Peciar, S. Bauer, A.L. Tőkés, A. Lévai, R. Bognár, *Chem. zvesti* **1974**, *28*, 90-94.

46. A. Lévai, A. Lipták, I. Pintér, G. Snatzke, *Acta Chim. Acad. Sci. Hung.* **1975,** *84,* 99-107.

47. W. Voelter, O. Oster, G. Jung, E. Breitmeier, *Chimia* **1971**, *25*, 26-27.

48. T. Sticzay, S. Bistricky, C. Peciar, A. Lévai, R. Bognár, *Chem. zvesti* **1975**, *29*, 538-543.

49. A. Lévai, *Flavonoids and Bioflavonoids Current Research Trends* (Eds. L. Farkas, M. Gábor, F. Kállay), Akadémiai Kiadó, Budapest, 1977, pp. 295-306.

50. L. Farkas, M. Nógrádi, B. Vermes, A. Wolfner, H. Wagner, L. Hörhammer, H. Kramer, *Chem. Ber.* **1969**, *102*, 2583-2587.

51. L. Farkas, B. Vermes, M. Nógrádi, *Chem. Ber.* **1972**, *105*, 3505-3510.

52. L. Farkas, B. Vermes, M. Nógrádi, *Chem. Ber.* **1974**, *107*, 1518-1525.

53. A. Lévai, R. Bognár, C. Peciar, S. Bistricky, T. Sticzay, *Acta Chim. Acad. Sci. Hung.* **1973**, *79*, 365-367.

54. R. Bognár, A. Lévai, *Acta Chim. Acad. Sci. Hung.* **1973**, *77*, 435-442.

55. A. Lévai, R. Bognár, *Acta Chim. Acad. Sci. Hung.* **1973**, *79,* 191-195.

56. A. Lévai, R. Bognár, *Acta Chim. Acad. Sci. Hung.* **1974**, *81*, 93-96.

57. M. Ilyas, J.N. Ushami, S.P. Bhatnager, W. Rahman, A. Pelter, *Tetrahedron Lett.* **1968**, 5515-5517.

58. M. Ilyas, O. Seligmann, H. Wagner, *Z. Natursforsch.* **1977**, *32c*, 206-209.

59. N. Harada, H. Ohno, H. Uda, M. Parveen, N.U. Kahn, B. Achari, P.K. Dutta, *J. Am. Chem. Soc.* **1992**, *114*, 7687-7692.

60. A. Pelter, R. Warren, K.K. Chexal, B.K. Handa, W. Rahman, *Tetrahedron Lett.* **1971**, *27*, 1625-1634.

61. R. Madhav, *Tetrahedron Lett.* **1969**, 2017-2019.

62. N.U. Kahn, M. Ilyas, W. Rahman, T. Mashima, M. Okigawa, N. Kawano, *Tetrahedron* **1972**, *28*, 5689-5694.

63. F. J. Zhang, G.Q. Lin, Q.C. Huang, *J. Org. Chem.* **1995**, *60*, 6427-6430.

64. G.Q. Lin, M. Zhong, *Tetrahedron Lett.* **1997**, *38*, 1087-1090.

65. A.Y. Li, T. Nehira, M. Hagiwara, N. Harada, *J. Org. Chem.* **1997**, *62*, 7222-7227.

66. M. Majerič, M. Gelo-Pujic, V. Sunjič, A. Lévai, P. Sebők, T. Tímár, *Tetrahedron:Asymmetry* **1995**, *6*, 937-944.

67. S. Ramadas, G.L.D. Krupadanam, *Tetrahedron:Asymmetry* **1997**, *8*, 3059-3066.

68. Zs. Majer, M. Hollósi, A. Lévai, M. Majerič, V. Sunjič, *Spectroscopy Lett.* **1995**, *28*, 1181-1190.

69. N.H. Lee, A.R. Muci, E.N. Jacobsen, *Tetrahedron Lett.* **1991**, *32*, 5055-5058.

70. A. Hatayama, N. Hosoya, R, Irie, Y. Ito, T. Katsuki, *Synlett* **1992**, 407-409.

71. N. Hosoya, R. Irie, T. Katsuki, *Synlett* **1993**, 261-263.

72. H. Sasaki, R. Irie, T. Katsuki, *Synlett* **1993**, 300-302.

73. R. Irie, N. Hosoya, T. Katsuki, *Synlett* **1994**, 255-256.

74. N. Hosoya, A. Hatayama, R. Irie, H. Sasaki, T. Katsuki, *Tetrahedron* **1994**, *50*, 4311-4322.

75. P. Pietikäinen, *Tetrahedron Lett.* **1995**, *36*, 319-322.

76. W. Adam, J. Jekő, A. Lévai, Cs. Nemes, T. Patonay, P. Sebők, *Tetrahedron Lett.* **1995**, *36*, 3669-3672.

77. W. Adam, J. Jekő, A. Lévai, Zs. Majer, Cs. Nemes, T. Patonay, L. Párkányi, P. Sebők, *Tetrahedron:Asymmetry* **1996**, *7*, 2437-2446.

78. S.L. Vander Velde, E.N. Jacobsen, *J. Org. Chem.* **1995**, *60*, 5380-5381.

79. R.C. Jennings, *Tetrahedron Lett.* **1982**, *23*, 2693-2696.

80. N. Harada, K. Nakanishi, *Accounts Chem. Res.* **1972**, *5*, 257-263.

Povzetek. Kirooptične spektroskopske metode, še posebej optična rotacijska disperzija (ORD) in cirkularni dihroizem (CD), so odigrale pomembno vlogo pri določanju strukture različnih naravnih organskih spojin. Namen članka je prikazati uporabo teh metod na na primeru flavonoidov.

HETARYLDIENES: PROMISING BUILDING BLOCKS TO NEW POLYHETARYL DERIVATIVES

György Hajós and András Kotschy[&]

Chemical Center, Institute of Chemistry, Hungarian Academy of Sciences

H-1525 Budapest POBox 17

[&] *Present address: Eötvös Loránd University, General and Inorganic*

Department of Chemistry

H-1518 Budapest 112 POBox 32

CONTENT

Introduction

I. SYNTHESIS

A. Syntheses involving compilation of the diene chain
    A.1.Wittig-type syntheses
        A.1.1. Starting from hetaryl aldehydes
        A.1.2. Starting from hetaryl acroleins
        A.1.3. Starting from hetarylphosphoranes
        A. 1.4. Starting from hetarylmethylene phosphonic esters
    A.2. Synthesis of the diene chain by the use of other condensation reactions
        A.2.1. From methyl substituted hetarenes
        A.2.2. By miscellaneous condensation reactions
    A.3. Synthesis of the diene chain by other methods
        A.3.1. From a nitrile with Grignard reagent
        A.3.2. Syntheses utilising dehydration
        A.3.3. Synthesis of the diene chain dehydrobromation

Introduction

Numerous literature data from the recent years reveal that properly substituted dienes bearing a hetaryl substituent can be used as interesting and useful building blocks for several syntheses. This recognition prompted the authors to provide a survey on synthetic methods leading to these compounds and also to summarise the most important application possibilities for their transformations. According to the dual goal of this paper, the first part deals with the synthetic variations classified according to the reaction types and, at the end of the descriptive part of this chapter, a collective table summarises the experimental data and references of the most important synthetic routes to hetaryldienes. The second part, subsequently, describes the most relevant transformations of hetaryldienes.

I. SYNTHESIS

A. Syntheses involving compilation of the diene chain

A.1.Wittig-type syntheses

Two main approaches: the classical Wittig reaction (reaction of an aldehyde with a phosphorane) and the Wittig-Horner-Emmons reaction (reaction of an aldehyde with a phosphonic ester) have been widely used for the formation of one of the double bonds of hetaryldienes. Both of these can be classified depending on which functional group (*i.e.* the aldehyde function or the phosphorous reagent) has been provided by the hetarene compound.

A.1.1. Starting from hetaryl aldehydes

One of the most general routes to hetaryldienes is the Wittig reaction of hetarylaldehydes with allyltriphenylphosphonium bromide under basic conditions. Since the appropriate

aldehydes are often fairly stable and - in some cases - commercially available compounds, this procedure is highly suitable for the synthesis of various hetaryldienes.

Scheme 1
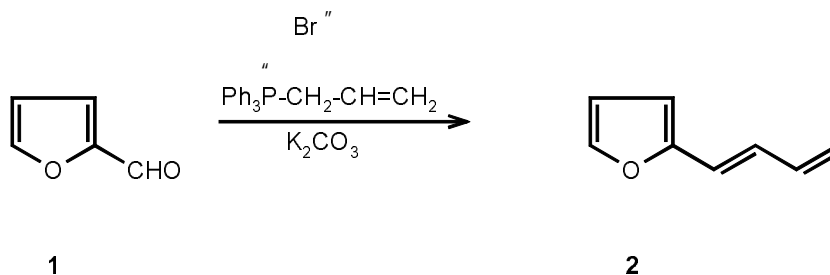
Scheme 2
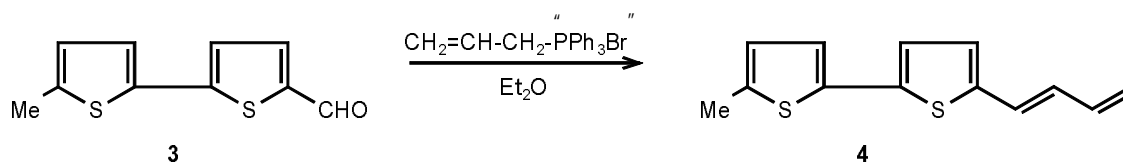
Thus, 2-furanaldehyde (**1**) leads to 1-(2-furyl)butadiene (**2**) in high yield [1] and, similarly, the bisthienyl aldehyde **3** affords the corresponding diene **4** [2] which is in fact a naturally occurring compound isolated from *Bidens radiata* [3].

A special application of this synthesis to piperidyl substituted dienes has also been reported [4]: the thienyl and pyridyl aldehydes **5** when treated with the amino substituted triphenylphosphorane derivative **6** afforded the 1-hetaryl-3-aminodienes **7** in good yield.

Scheme 3

Het = thienyl or pyridyl
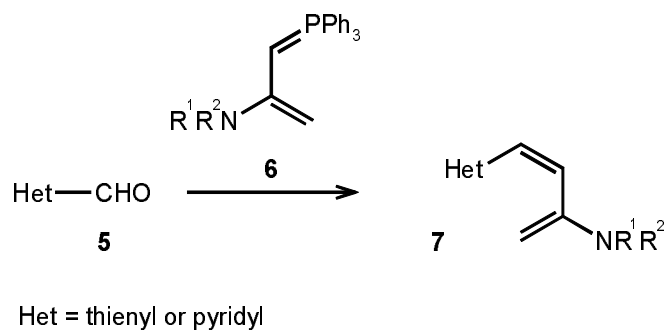
A.1.2. Starting from hetaryl acroleins

In contrast to the above procedures where one of the double bonds of the diene chain was delivered as a substituent of the Wittig reagent, numerous applications starting from hetaryl acrylaldehydes have been elaborated. Thus, in this synthetic strategy one double bond is provided by the hetarene-ring-containing component and the second one is formed by the Wittig reaction with the phosphorane-containing single carbon atom unit.

Scheme 4

8　　　　　　　　　　　　**9**
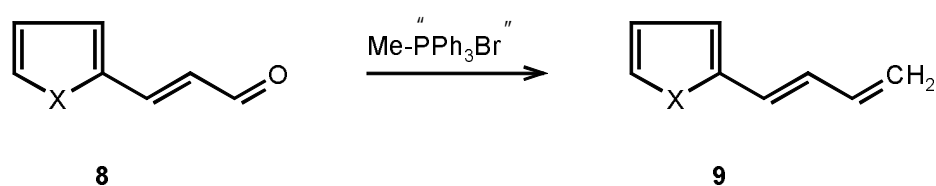
Thus, ß-(2-furyl)- and (2-thienyl)acroleine (**8**, X = O, S) when reacted with methyltriphenylphosphonium bromide under basic conditions afforded 1-(2-furyl)- and 1-(2-thienyl)butadiene (**9**) in moderate yield [5]. Synthesis of the pyrrolyl substituted diene **13** has also been accomplished in a similar manner: the starting aldehyde **10** was converted first with formylpropylidene phosphorane (**11**) - also by a Wittig reaction - to the methacrylaldehyde analogue **12** which with a second molecule of the reagent was converted to the diene product **13** [6].

Scheme 5

10　　　　　　　　　　　　**12**

13
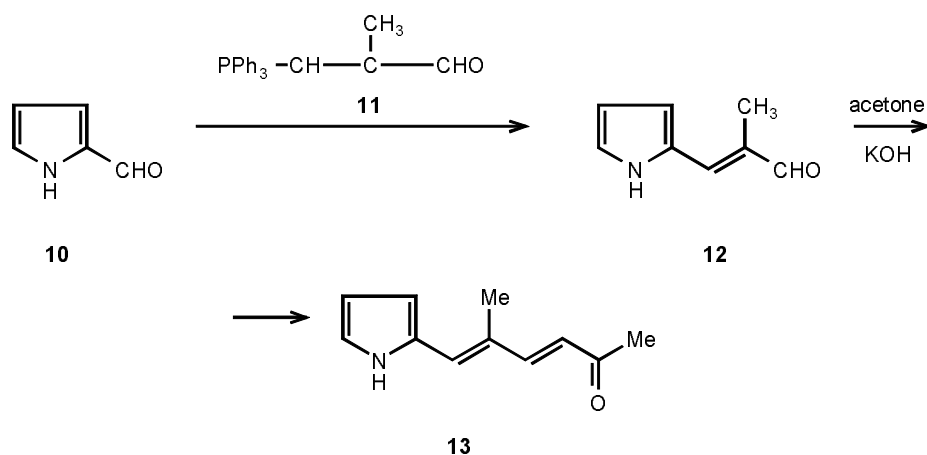
The intermediate methacrylaldehyde derivative **12** can also be treated with different reagents. Thus, reaction with the diethylphosphonate **14** gave the dienyl aldehyde **15**, whereas use of reagent **16** led to the formation of the cyano-substituted diene **17**. [7]

Scheme 6
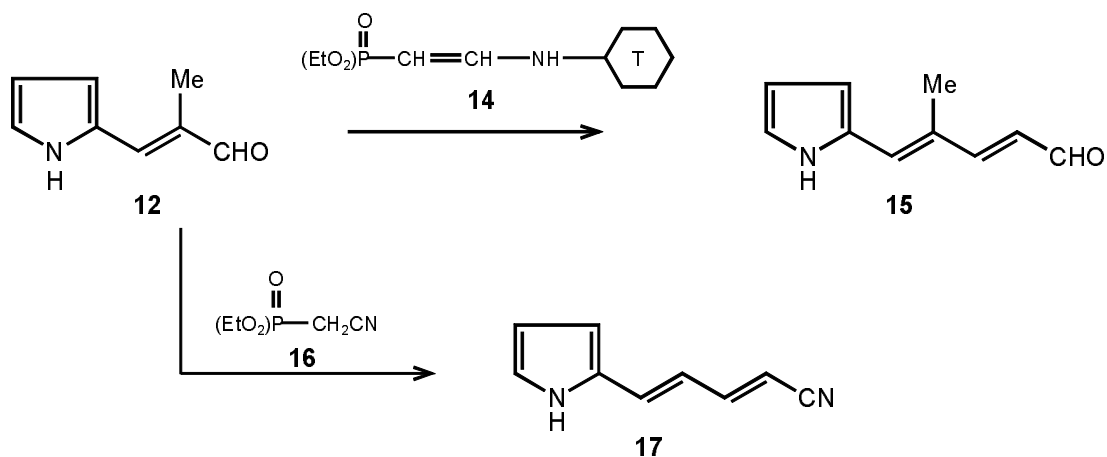
Scheme 7
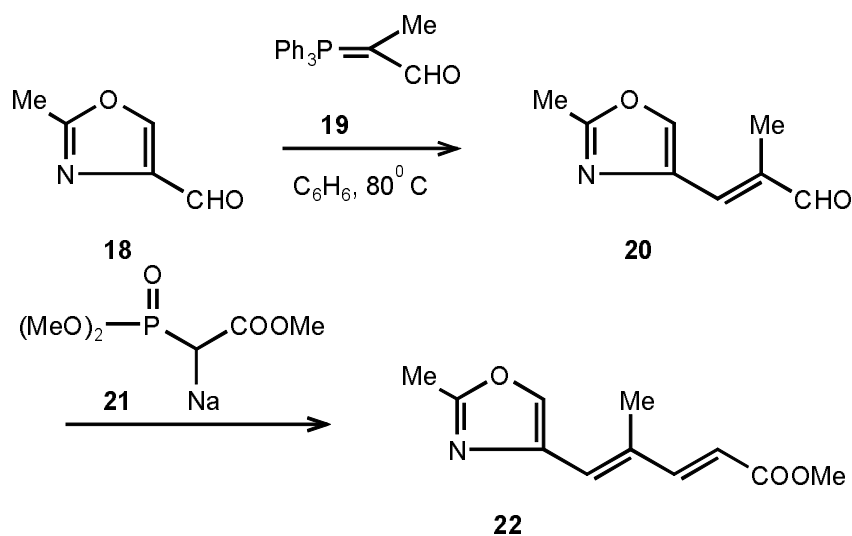
A similar synthetic strategy as above has been applied for the synthesis of the oxazolyldiene carboxylic ester **22**: reaction of the starting aldehyde **18** and phosphorane **19** gave first the hetarylmethacrylaldehyde derivative **20** which upon treatment with the phosphonic ester (**21**) afforded **22** in high yield [8].

A.1.3. Starting from hetarylphosphoranes

Scheme 8
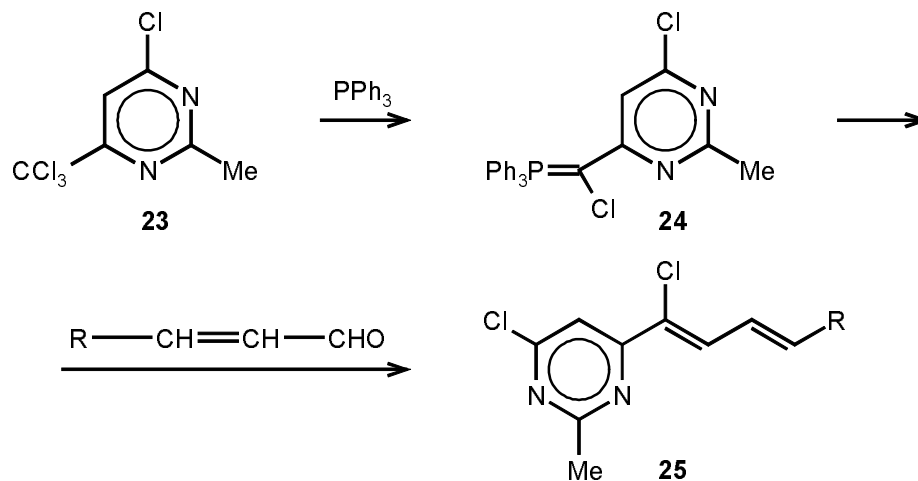
Several synthetic approaches to hetaryldienes have been described where the Wittig reaction was carried out by starting from a hetarylphosphorane. Such derivatives can generally be obtained from trichloromethyl substituted hetarenes. Thus, 4-chloro-2-methyl-6-trichloromethylpyrimidine (23) was transformed by triphenylphosphine to the phosphorane 24 first which upon reaction with an unsaturated aldehyde gave the end product 25 [9].

Scheme 9
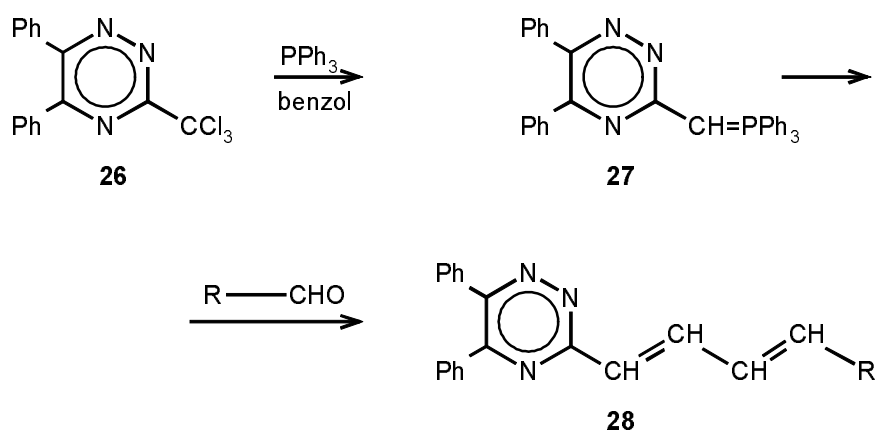
A similar method has been applied for the synthesis of two as-triazinyldiene derivatives (28, R = Me and Ph): 5,6-diphenyl-3-trichloromethyl-[1,2,4]triazine (26) was

transformed - by using two molar equivalents of triphenylphosphine - to the phosphorane **27** which reacted with the appropriate aldehyde to give the final product **28** [10]. The method also proved to be suitable for the synthesis of five membered hetarene derivatives: the chloromethyl substituted tetrazole **29** easily gave the phosphorane **30** which was reacted with cinnamic aldehyde (**31**) under mild conditions to yield the phenyl substituted tetrazolyldiene **32**.

Scheme 10
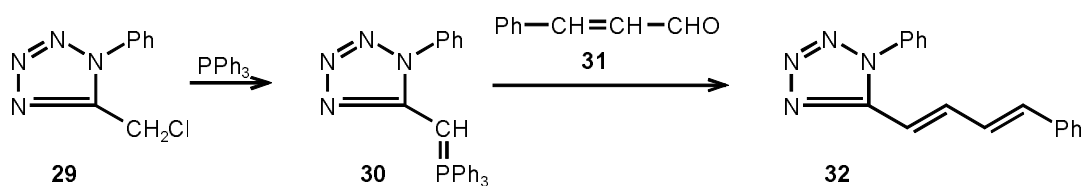
A. 1.4. Starting from hetarylmethylene phosphonic esters

As mentioned in the introductory part, the Wittig-Horner-Emmons synthesis of hetaryldienes can also be accomplished by the reaction of a hetarylphosphonic ester and an aldehyde. The following three examples convincingly show that this methodology can be usefully applied to the synthesis of various hetarene derivatives

Scheme 11
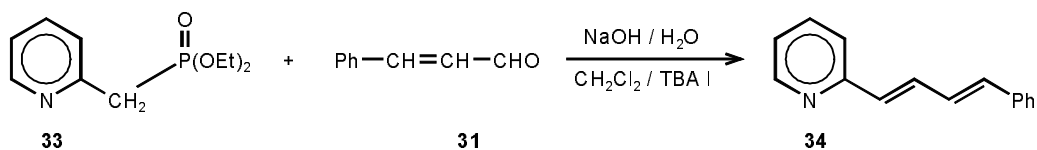
Reaction of cinnamic aldehyde (**31**) with diethyl 2-pyridylmethylphosphonic ester (**33**) under phase transfer conditions gave 1-(2-pyridyl)-4-phenylbutadiene (**34**) [11, 12]. The isoxazolylmethylphosphonic ester (**35**) when reacted with the aldehyde **36** afforded the corresponding isoxazolylbutadiene (**37**) [13], whereas the benzthiazolylphosphonic ester **39** - easily obtainable from the bromomethyl compound **38** - was reacted with *p*-dimethylaminocinnamic aldehyde **40** and yielded the deep yellow benzthiazolylbutadiene **41** [14].

Scheme 12
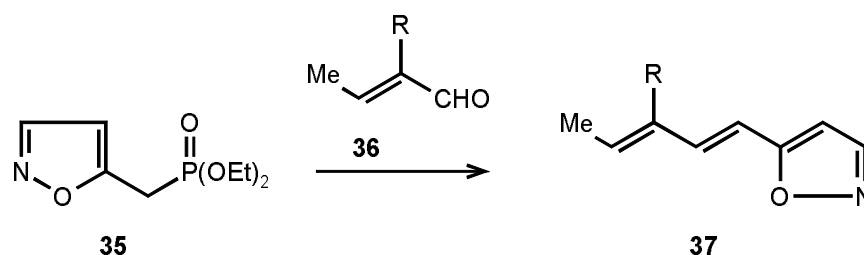
Scheme 13
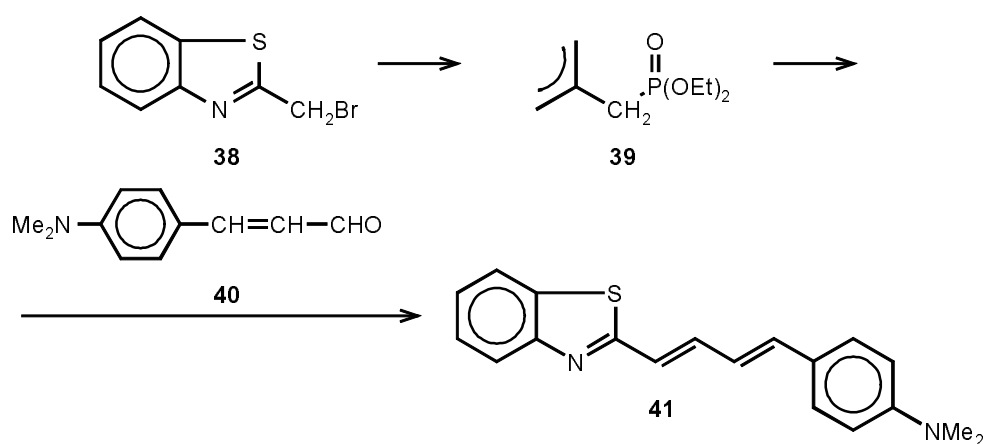
A.2. Synthesis of the diene chain by the use of other condensation reactions

A.2.1. From methyl substituted hetarenes

α-Methylhetarenes generally undergo condensation reactions with aldehydes under acidic or basic conditions to give olefins. This reactivity can be usefully exploited for the synthesis of hetaryldienes with unsaturated aldehydes as reaction partners. According to this procedure various methylpyridines like 2-picoline (**42**) [15], 4-picoline (**43**), 2,6-dimethylpyridine (**44**) and [2,4,6]collidine (**45**) [16] can be converted to the corresponding substituted 1-pyridyl-4-phenylbutadienes **46**, **47**, **48**, and **49**, respectively. The yields of these conversions are, unfortunately, rather poor in most cases.

Scheme 14

$$Ph-CH=CH-CHO$$
31
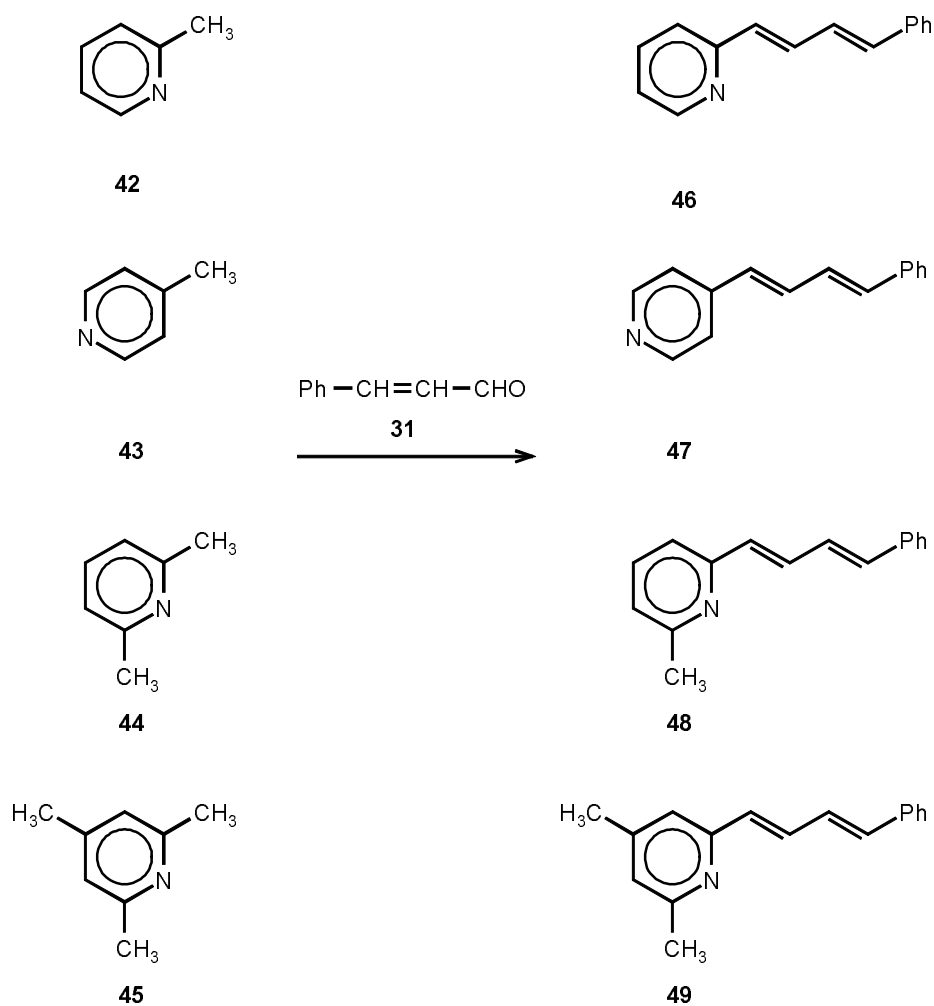
Scheme 15
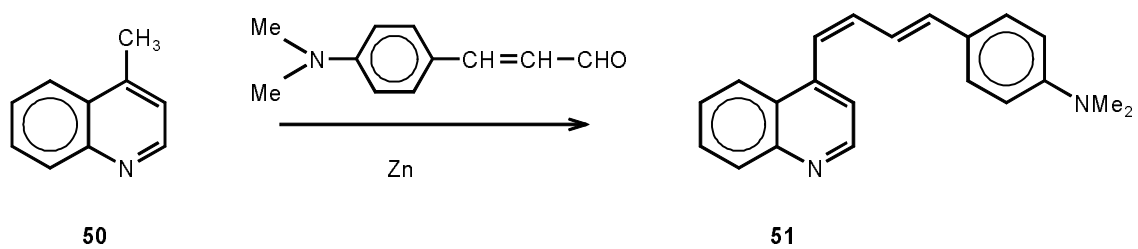
This approach can be applied to benzologues, other six membered heterocycles, and five membered heteroaromatics, too. Thus, 4-methylquinoline **50** leads to the substituted phenyldiene **51** [17], 3-methylbenzoxazinone **52** affords, similarly, the diene **53** [18],

whereas 2-methylthiazole (**54**) can be converted to 1-(2-thiazolyl)-4-phenylbutadiene (**55**) although only in poor yield [19].

Scheme 16

52 → **53**

Scheme 17

54 → **55**
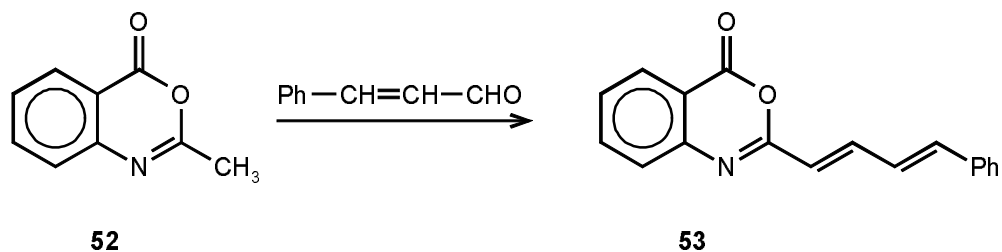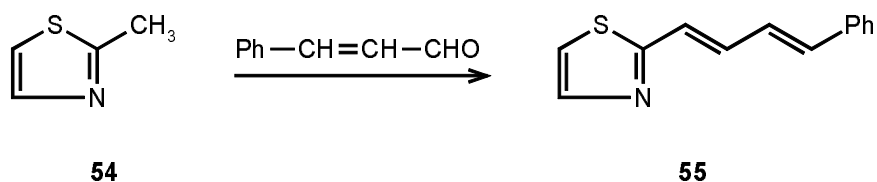
Condensation reaction of the hetarylmethyl group is particularly easy with quaternary compounds. Accordingly, the N-methylated salt **56** reacts smoothly with cinnamaldehyde to give the diene **57** [20], the six membered pyridinium and pyrylium salts **58** (X = N or O, respectively) can be readily converted to the corresponding dienes (**59**) in high yield [21].

Scheme 18

56 → **57**

Scheme 19

X = O, N-Me

R^1 or $R^2 = NMe_2\text{-CH=CH-CH=CH-}$
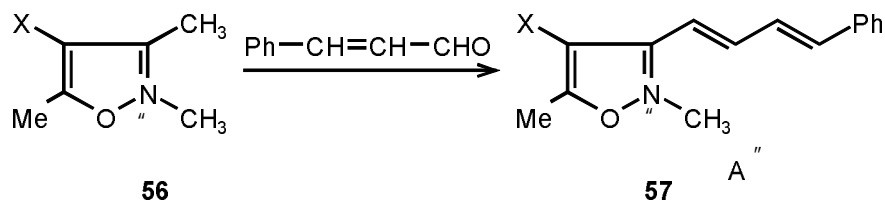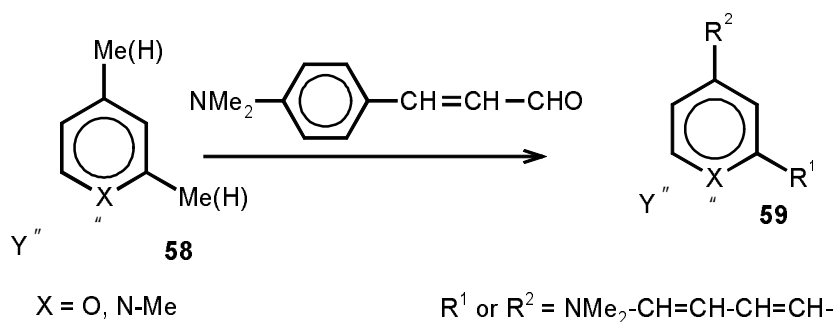
Instead of aldehydes, masked aldehydes like substituted vinamidinium salts can also be successfully used as reagents in the same transformations. This is nicely demonstrated by the following two examples: both α-picoline (**42**) and 2-methyloxazolidine (**61**) react with tetramethyl-vinamidinium chloride - which can be regarded as a masked γ-aminoacroleine - to give 1-(2-pyridyl)-4-dimethylaminobutadiene (**60**) and 1-(2-oxazolidinyl)-4-dimethylaminobutadiene (**62**), respectively.

Scheme 20
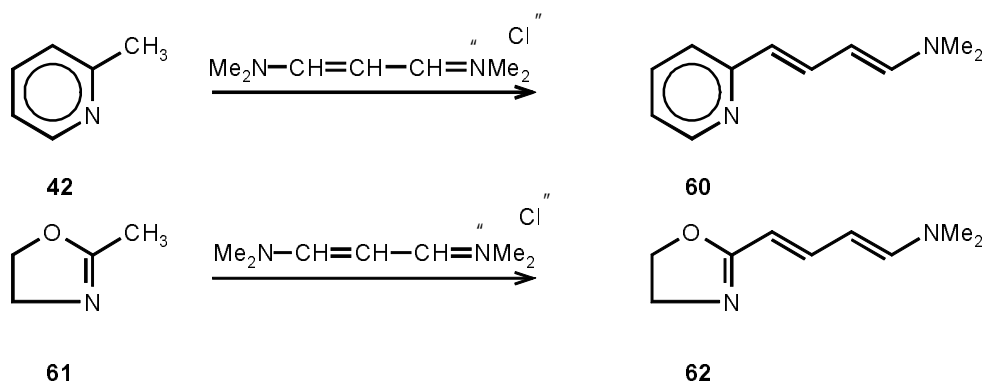
A.2.2. By miscellaneous condensation reactions

Hetarenes bearing an active methylene group in the side chain are also suitable starting materials for condensation reactions with unsaturated aldehydes to hetaryldienes. Thus, 2-cyanomethylbenzothiazole (**63**) when reacted with cinnamaldehyde affords 1-benzothiazolyl-1-cyano-4-phenylbutadiene (**64**) in high yield [22]. The same transformation - similar to the previous chapter - can also be carried out by vinamidinium

salts as masked aldehydes. Thus, 2-cyanomethyl substituted azoles (**65**) can easily be transformed to the corresponding 1-azolyldieneamines (**66**) [23].

Scheme 21

Scheme 22

X = O, S, N-Me
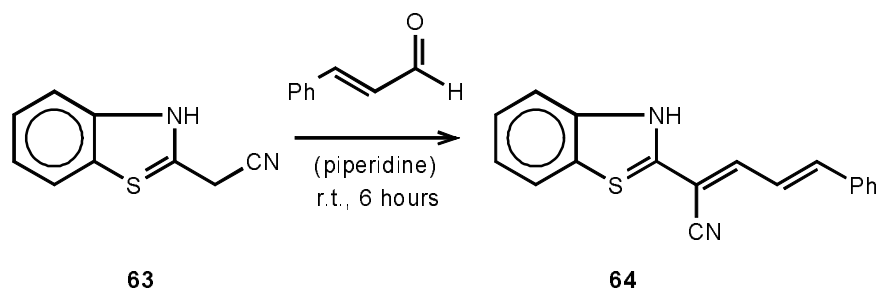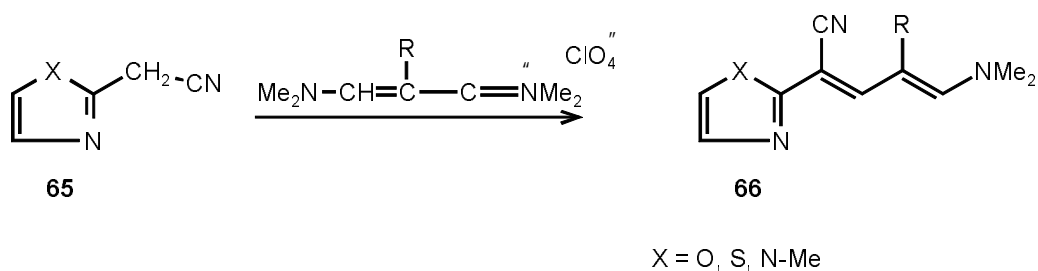
α,β-Unsaturated aldehydes attached to a hetarene can participate in condensation reaction with the active methylene group of methyl azidoacetate (**68**) to give 4-azido substituted 1-hetaryldiene 4-carboxylic esters. Thus, the aldehyde **67** (Het = various five membered heteroaromatics) afforded the diene compound **69** [24, 25].

Scheme 23
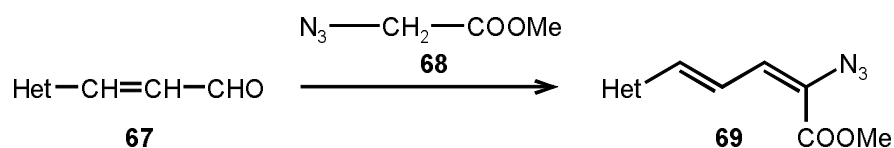
Scheme 24
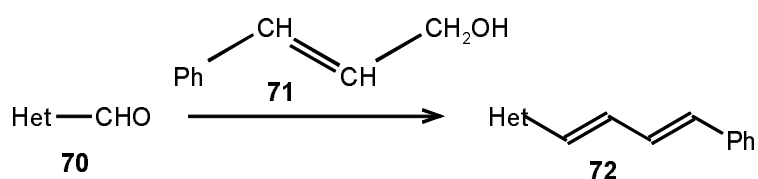
Finally, cinnamic alcohol (**71**) can react with a hetarene aldehyde (**70**) to give 1-hetaryl-4-phenylbutadienes **72**. This conversion has successfully been applied for 2-furyl-, 2-thienyl- and 3-pyridyl derivatives [24].

A.3. Synthesis of the diene chain by other methods

A.3.1. From a nitrile with Grignard reagent

A special group of hetaryldienes: those bearing also an amino moiety in position 1 is available by the reaction of hetarylnitriles **73** and allylmagnesium chloride (**74**). The primarily formed complex when worked up with aqueous ammonia affords the 1,1-disubstituted diene products (**75**) [26].

Scheme 25
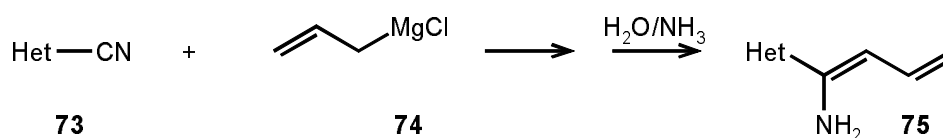
A.3.2. Syntheses utilising dehydration

In numerous cases the diene chain of hetaryldienes has been formed by dehydration reaction of a substituted allylalcohol derivative. The removal of water proceeds in some cases under very mild conditions. Thus, the thienyl derivative **76** can easily be transformed by potassium hydrogensulfate to the thienyldiene **77** [27], which product, however, proved to be rather unstable.

Scheme 26
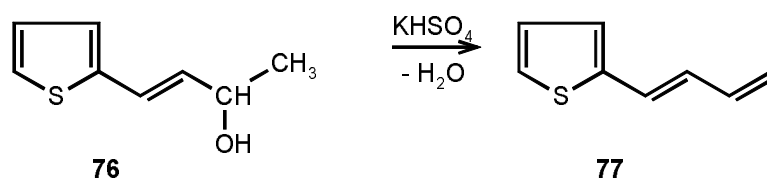
Treatment of **78** (Het = thienyl or furyl) with dimethylformamide dimethylacetal (**79**) leads to similar results, the difference from the transformation **76** → **77** is that a decarboxylation step takes also place and the 1,3-disubstituted diene **80** (Het = 2-furyl and 2-thienyl) is formed [28].

Scheme 27
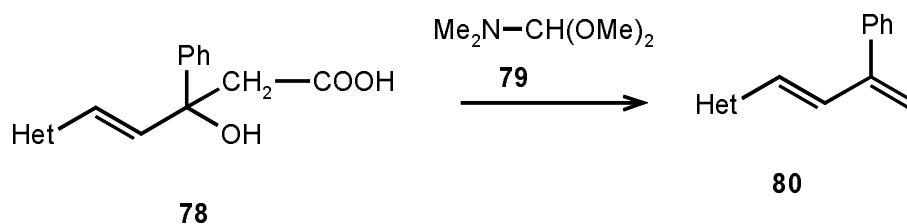
In contrast to the above two starting hetarylethenyl derivatives (**76** and **78**), hetarenes bearing a substituent through a saturated carbon atom can also serve as a precursor to dienes as shown by the following three examples.

Scheme 28
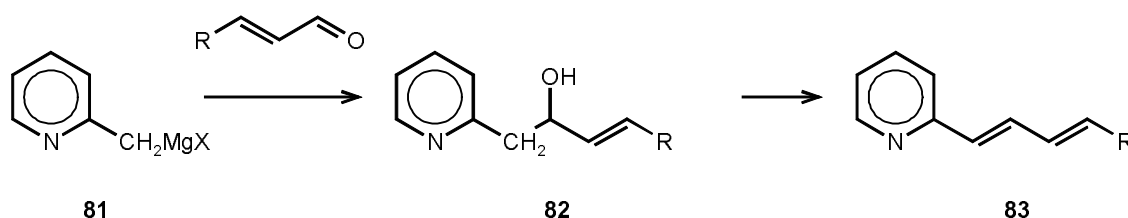
The secondary allylalcohol **82** which can be synthesised from the pyridyl Grignard reagent **81** and an acroleine derivative undergoes facile elimination to give the corresponding 1,4-disubstituted diene **83** [29]. A similar starting compound (**85**) can be prepared from pyridyl aldehyde **84** and allylmagnesium bromide which upon treatment with thionyl chloride affords pyridyldienes (**86**) unsubstituted at position 4 [30]. An analogous methodology was also successfully applied to the synthesis of a thiazolyldiene (**90**): the lithiated derivative of 2-methyl-5-phenylthiazole (**87**) when reacted with the substituted formylketene dithioacetal (**88**) gave first the secondary alcohol addition product **89** which underwent water elimination on treatment with boron trifluoride etherate to give the thiazolyldiene **90** [31].

Scheme 29
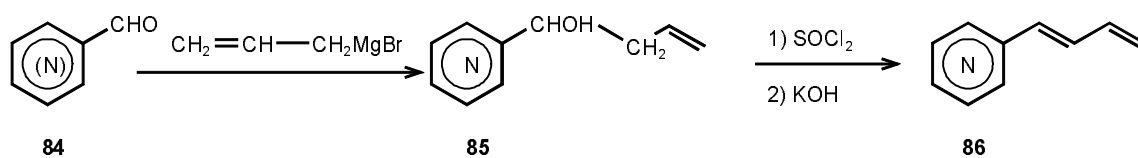
Scheme 30
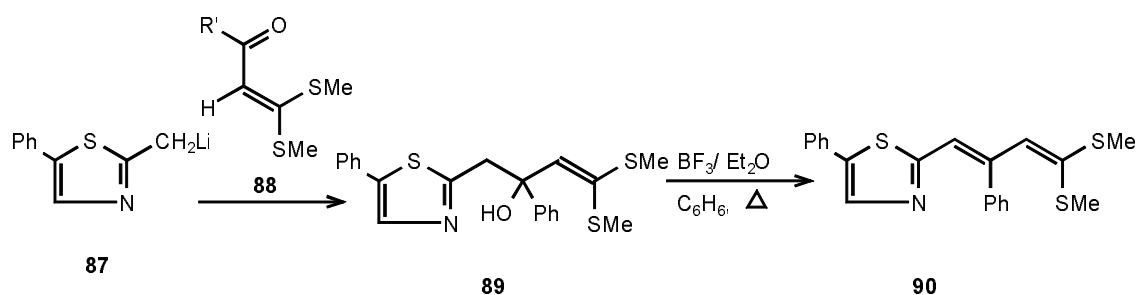
A.3.3. Synthesis of the diene chain by dehydrobromation

One example is known where the diene side chain of a hetaryldiene has been formed by successive bromination and dehydrobromation steps starting from a butylhetarene: 5-butylpyridine 2-carboxylic acid (**91**, "fusarinic acid") proved to be a suitable starting compound for this purpose and afforded the 3-pyridyldiene derivative (**92**) in 4 reaction steps [32].

Scheme 31

91

E = COOH

92
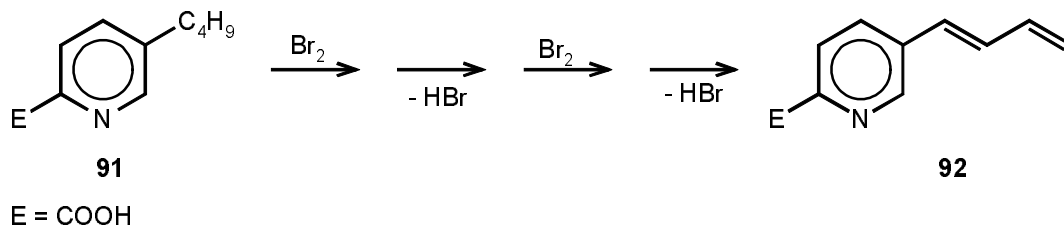
A.3.4. Formation of the diene chain by oxo-enol tautomerism

ß-Hetaryl-α,β-unsaturated ketones can also serve as starting compounds to dienes if the keto function can participate in an oxo-enol tautomerism and undergoes further transformation to a derivative of the enol tautomeric form. This method has been applied in the case of the furyl-ethenylketone **93** which upon trimethylsilylation afforded the trimethylsilyloxy substituted furyldiene **94** [33].

Scheme 32

93

94
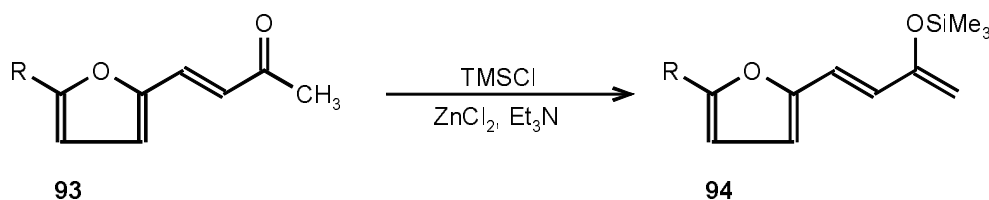
A.3.5. Peterson olefin formation

The "Peterson" olefin formation has also been successfully applied to the synthesis of a series of hetaryldienes. In this procedure the 9-BBN derivative **95** is reacted first with a hetaryl aldehyde to give - *via* formation of the transition state **96** and subsequent rearrangement - the intermediate (**97**). This compound undergoes *syn* elimination in the presence of a base (sodium hydroxide or sodium ethoxide) to give the final hetaryldiene **98**. Because of the *syn* nature of the last elimination step, the product has necessarily a 1-*cis* geometry [34].

Scheme 33

95   **96**

97   **98**
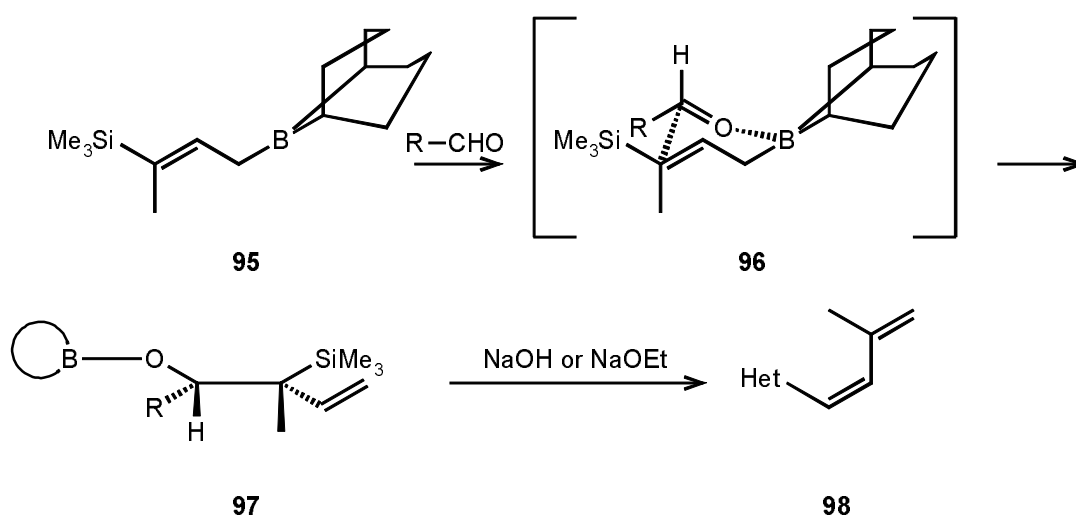
B. Synthesis of hetaryldienes from other functionalised polyenes

In the following two chapters (B.1. and B.2.) such reactions affording hetaryldienes will be described that start from already existing dienes, and the hetarene side chain is either introduced by a coupling reaction or formed by a ring closure.

B.1. Cross-coupling reaction of substituted dienes

Transition metal catalysed cross-coupling reaction is a straightforward method for attaching a polyene to a hetaryl group. Thus, compound **99** was coupled first with a bromohetarene to give the acetylene-containing product **100** which upon reduction with zinc yields the dienethioether **101**. Both steps take place in good to excellent yields and can be applied to a variety of heteroaromatic (*i.e.* R = 2-furyl, 2- and 3-thienyl, 2- and 3-pyridyl) halides [35].

Scheme 34

99   **100**   **101**
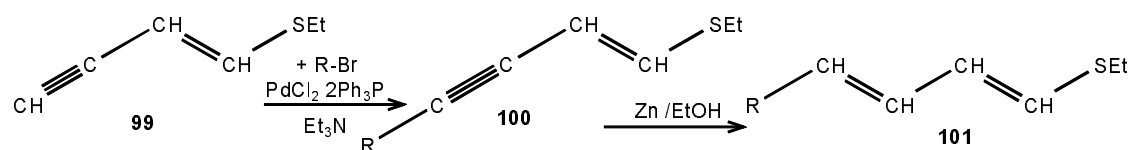
A more complicated synthetic strategy taking use of the cross-coupling methodology has been applied to a double coupling of 1-bromo-4-phenylthiodiene (**102**). In this case, two successive couplings have been carried out: the first one taking place at the bromine atom at 0 °C, followed by the coupling at the other terminal of the chain, *i.e.* on the PhS group which can be completed at room temperature to give the final diene **103**.

Scheme 35

R' = 2-thienyl
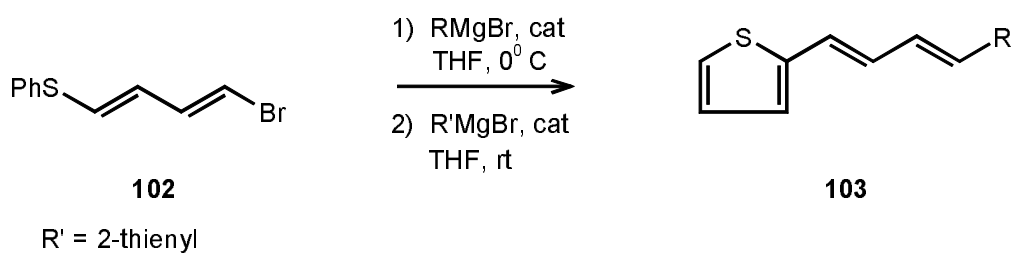
B.2. Ring closure reaction to hetarenes starting from substituted dienes

B.2.1. Formation of 5-membered rings

The iminium salt **104** containing a reactive chlorine atom in the γ position was found to be suitable starting compound for a ring closure to thiophene derivatives. If the R substituent of **104** is a phenyldienyl chain this procedure affords substituted 1-(2-thienyl)-4-phenyldienes (**105**) [36].

Scheme 36

R = Ph-(CH=CH)₂-
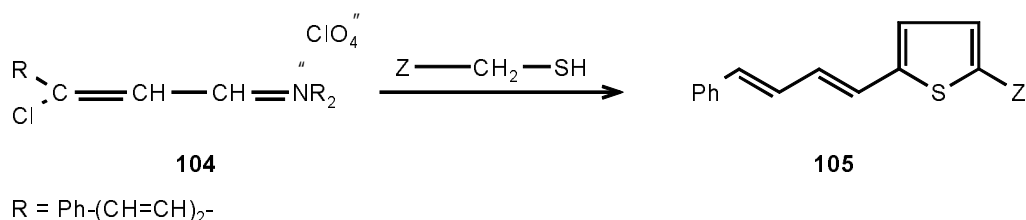
Scheme 37
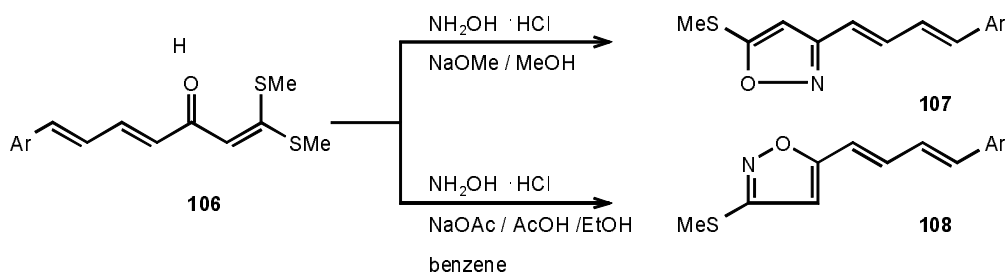
Ring closure of the side chain of diene **106** with hydroxylamine was carried out under two different reaction conditions: in the presence of sodium methoxide the isoxazolyldiene **107** was obtained, whereas in a mixture of sodium acetate-acetic acid-ethanol-benzene the reaction proved to be regiospecific in the other way around and afforded the isomeric **108** product [37].

Scheme 38
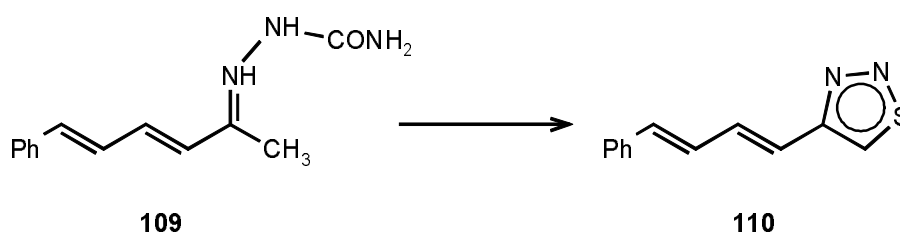
Ring closure to the 1,2,3-thiadiazole compound bearing a diene side chain (**110**) starting from the semicarbazone **109** has also been reported [38].

A fairly complicated route starting from the variously substituted polyene **111** to a series of 2-furyldienes has been described: in the first step a ring closure to form the furan ring takes place to afford the intermediate **112**, which by a base-promoted deprotonation (and by the shift of the remaining electrons as shown by the arrows) induces a [1,8] elimination to yield the furyldiene **113**. [63].

Scheme 39
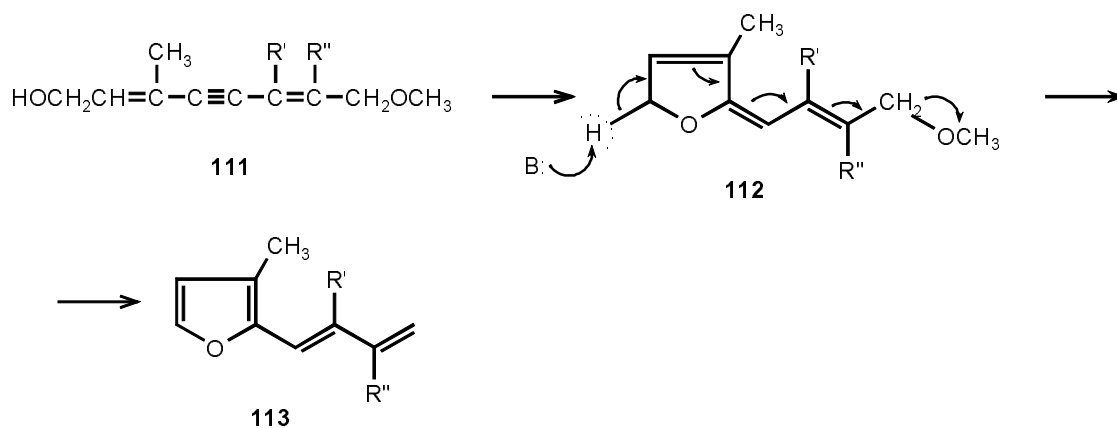
The oxazinyl substituted diene (**53**) discussed already in an earlier chapter (A.2.1.) of this paper underwent a ring opening and subsequent ring closure reaction to yield a tetrazolyldiene: in the first step an azidoazomethine (**114**) was formed which underwent a 1,5-dipolar cyclisation to the final product **115** [18].

Scheme 40
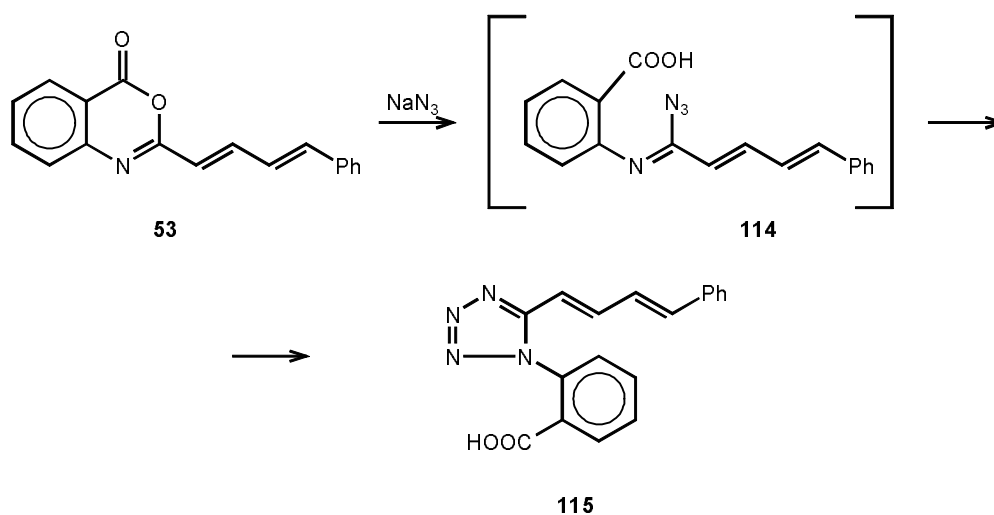
B.2.2. Formation of 6-membered rings

Two examples can be found in the literature where a six membered hetarene is formed by ring closure as a substituent of a diene chain. The first such case was published in the early fifties: the dienyl-methylglyoxal derivative **117** which was obtained from diacetyl (**116**) and cinnamic aldehyde was subjected to a condensation reaction with o-phenylenediamine to give the quinoxalyldiene compound **118** [39].

Scheme 41
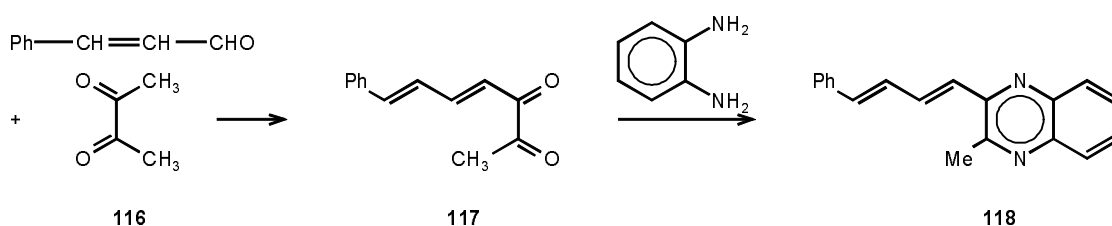
A more general route has been elaborated for pyrimidinyldienes: the aryldiene bearing an α,β-unsaturated ketone side chain (**119**) was treated with guanidine (**120**) under basic conditions to give 1-(2-amino-4-alkoxipyrimidin-6-yl)-4-aryl diene (**121**) dienes in acceptable yield [40].

Scheme 42
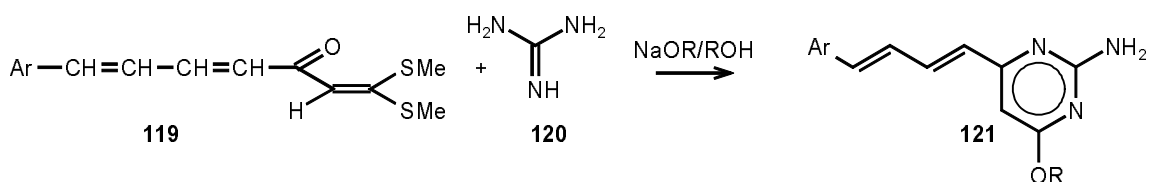
C. Formation of hetaryldienes by ring opening reactions

C.1. Ring opening of neutral systems

The tetracyanocyclobutane derivative **123** which was obtained as a [2+2] cycloadduct of the ethenylpyrazole compound **122** and tetracyanoethylene (TCE) was found to open up in methanol to the tricyanodienylpyrazole **124** in excellent yield. The reaction also involves the elimination of one molecule of hydrogen cyanide [41].

Scheme 43
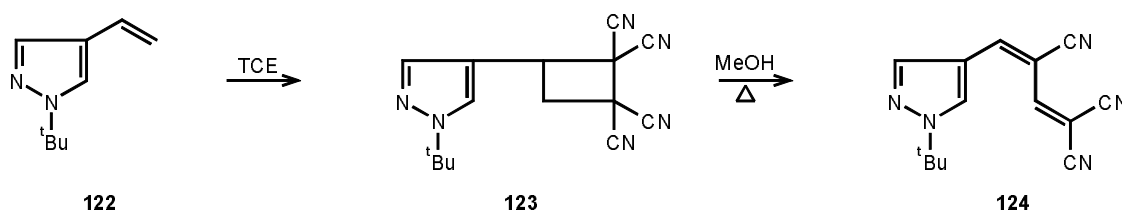
Scheme 44
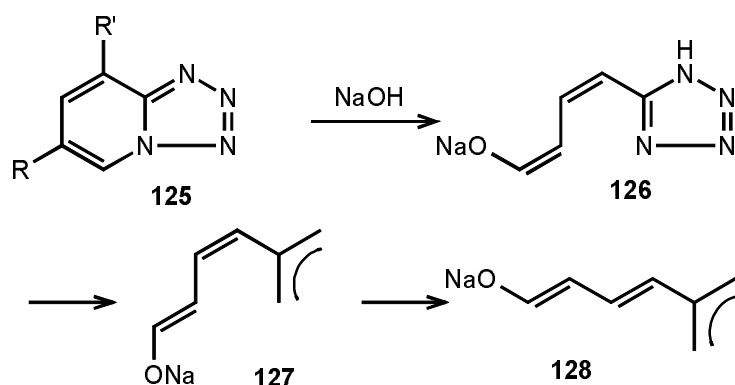
Variously substituted tetrazolopyridines (**125**) were found to undergo ring opening to tetrazolyldienes under basic conditions to yield sodium dienolates. Detailed NMR study of this reaction revealed that the ring opening results both in a 1-*cis*-3-*cis*-(**126**) and a 1-*cis*-3-*trans*-diene (**127**), and both can be converted to the more stable 1-*trans*-3-*trans* isomer (**128**). [42]. A similar transformation was found with a [1,2,3]triazolopyridine derivative (**129**): this compound when treated with lithium aluminiumhydride afforded a triazinyldiene (**130**) [43].

Scheme 45

129   **130**
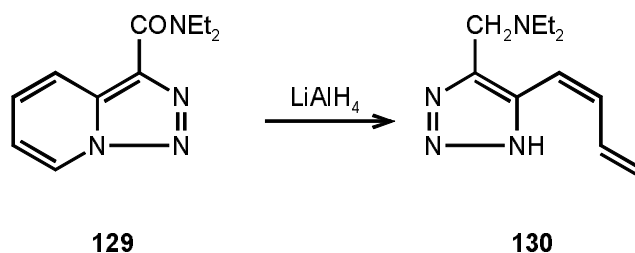
An interesting ring opening of benzofurazan **131** to an isoxazolyldiene (**132**) under irradiation has been reported [44]: three different geometric isomers have been found and isolated from the reaction mixture.

Scheme 46

131   **132**
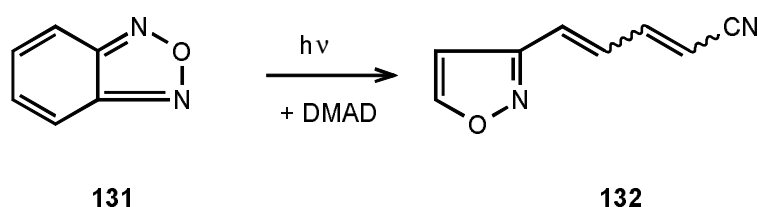
C.2. Ring opening of positively charged systems with a bridge head nitrogen atom

Numerous examples reveal that fused azinium salts containing a bridge-head nitrogen atom are excellent precursors for hetaryldienes. In these reactions a nucleophilic reagent is needed which can attack the azinium moiety to form an addition product first which - via a retroelectrocyclisation - affords the diene bearing the hetero ring fused originally to the particular azine. The below cases convincingly show the general applicability of this procedure.

The ring opening of quinolizinium salts (**133**) to pyridyldieneamines was studied in details The reaction proceeds in acceptable yield with various secondary amines (derivatives **134** are formed) [45] and is almost quantitative in the case of reactions with ammonia to the free aminodienes **135**, [46]. The reaction has been nicely extended for benzologues yielding quinolyl and isoquinolyldienes [47].

Scheme 47
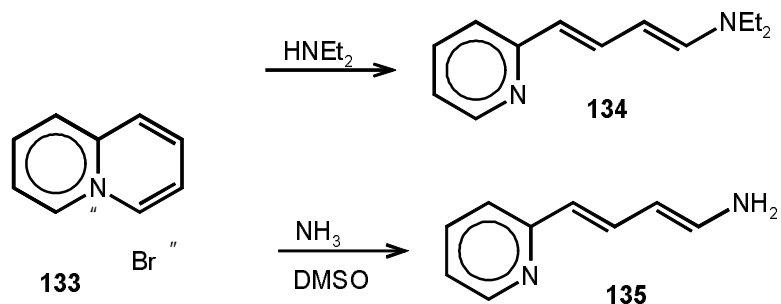
Grignard-reagents as nucleophiles have also been applied to the ring opening reactions of quinolizinium salts (**136**) to pyridyldienes. In these transformations the alkyl or aryl group of the reagent acts as a nucleophile to be attached to the terminal position of the diene chain: e.g. 1-hetaryl-4-phenylbutadienes (**137**) have been synthesised by this route [48]. The method was applied to the tricyclic benzologues (**138**) as well affording pyridyl- (**139**), quinolyl- (**140**) and isoquinolyldienes (**141**) [49].

Scheme 48
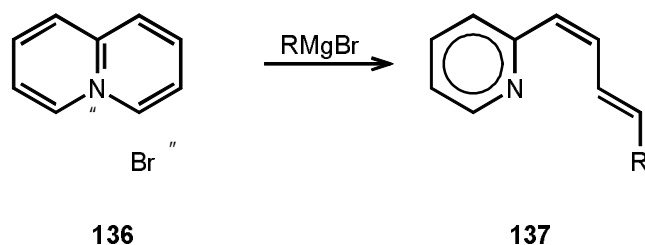
Scheme 49
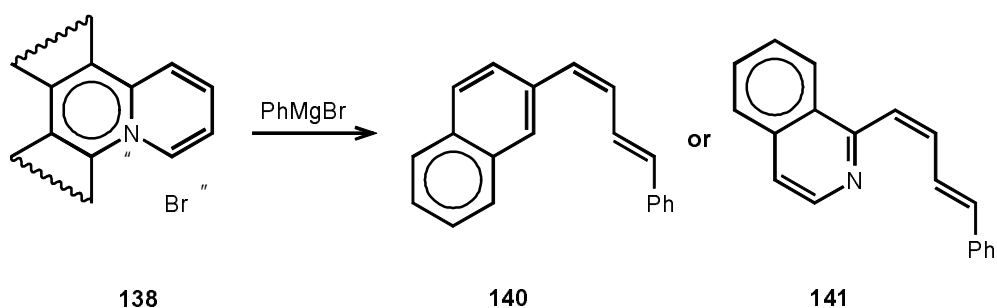
Similar to the above cases of azinoazinium (*i.e.* 6+6 fused) salts, azoloazinium systems (5+6 fused rings with bridgehead nitrogen atom) behave in an analogous manner when reacted with nucleophilic reagents.

The most extensive studies in this respect have been carried out with tetrazolopyridinium salts (**142**). [50, 51, 52]. As a nucleophile, sodium borohydride, tetraalkylammonium cyanide, sodium alkoxide and various secondary amines have been used. The hydride reagent gave the 1-*cis*-3-*trans* tetrazolyldiene (**143**), whereas a fully *cis* diene (**144**) was obtained as the main product with cyanide anion. In the case of the alkoxide reagent, generally a mixture of the 1-*cis*-3-*trans* (**145**) and 1-*cis*-1-*cis* dienes (**146**) have been obtained. Reaction of the tetrazolium salt **142** with secondary amines resulted in formation of a fully *trans* dieneamine (**147**). If the reaction, however, has been carried out with the sodium salt of the secondary amine, 1-*cis*-3-*trans* dieneamine were formed first which, in most cases in the presence of protic solvents or a trace of acid were transformed to the more stable *trans-trans* isomers.

Scheme 50
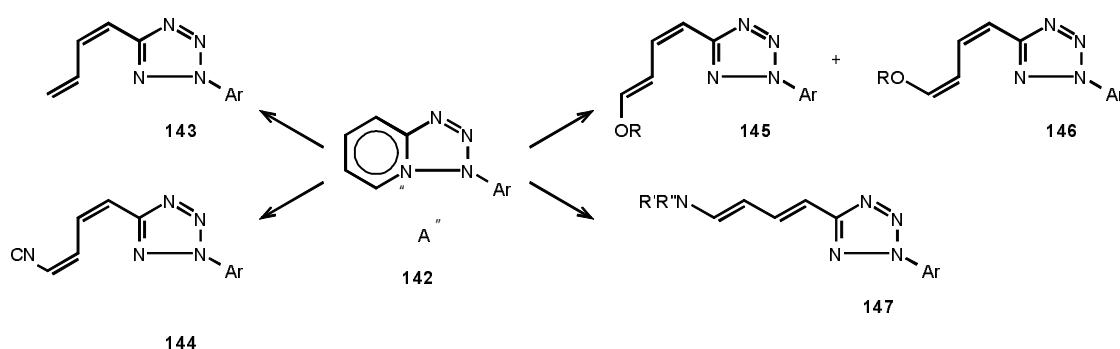
An interesting behaviour of the thiazolo[3,2-a]pyridinium salts (**148**) has been published [53]. This compound reacted with secondary amines (*e.g.* with morpholine) at room temperature to give the addition product **149** which was isolated in crystalline form.

When the reaction was carried out, however, in refluxing acetonitrile, the *trans-trans* thiazolyldieneamine **151** was formed, obviously via the intermediate **150**.

Scheme 51
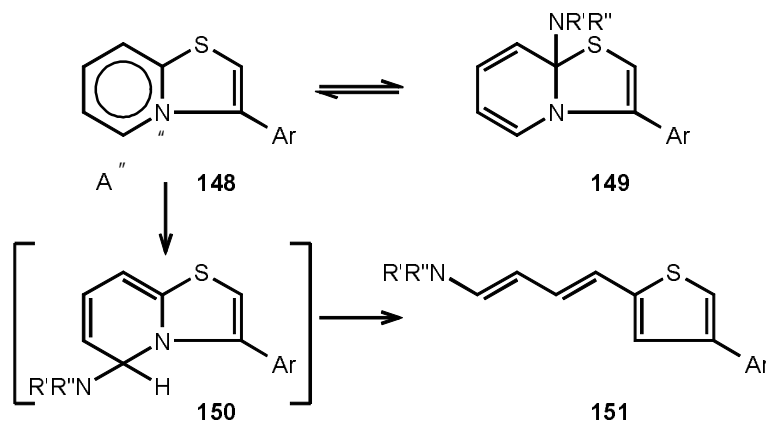
C.3. Ring opening of partially reduced fused systems with bridge-head nitrogen atom

In contrast to the above cases, partially reduced fused heteroaromatics can also undergo ring opening to yield hetaryldienes. Thus, the tetrahydroquinolizinium salt **152** when treated with sodium acetate at higher temperatures affords pyridyldiene **153** [54].

Scheme 52

Scheme 53

154   **155**   **156**
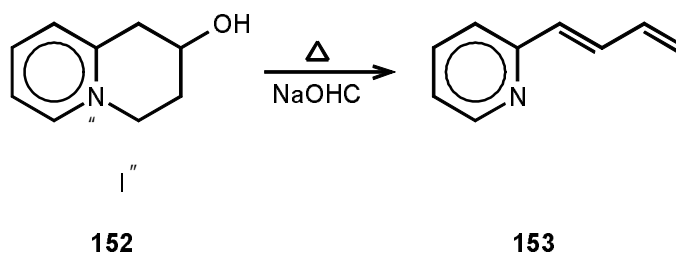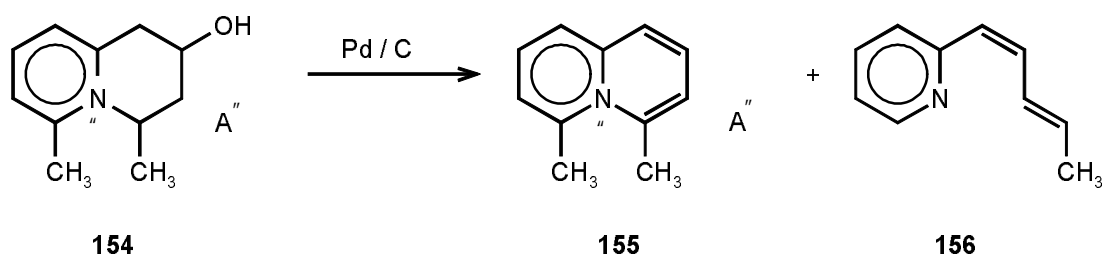
The same type of ring opening was also observed in the case of the dimethyl substituted tetrahydroquinolizinium salt **154** when treated with Pd/C catalyst. Two products: the partially oxidised salt **155** as well as the ring opened diene **156** were obtained [55]

D. Synthesis of hetaryldienes by rearrangements.

The isoxazolidine derivative **157** was found to undergo an exothermic reaction when heated to 145 °C to give the **158** isoxazole derivative in very good yield which upon chromatography on alumina underwent a rearrangement to 1-[4-allyl-3-methyloxazolyl-5]diene (**159**) almost in quantitative yield [56].

Scheme 54

157   **158**

159

Scheme 55

160   **161**
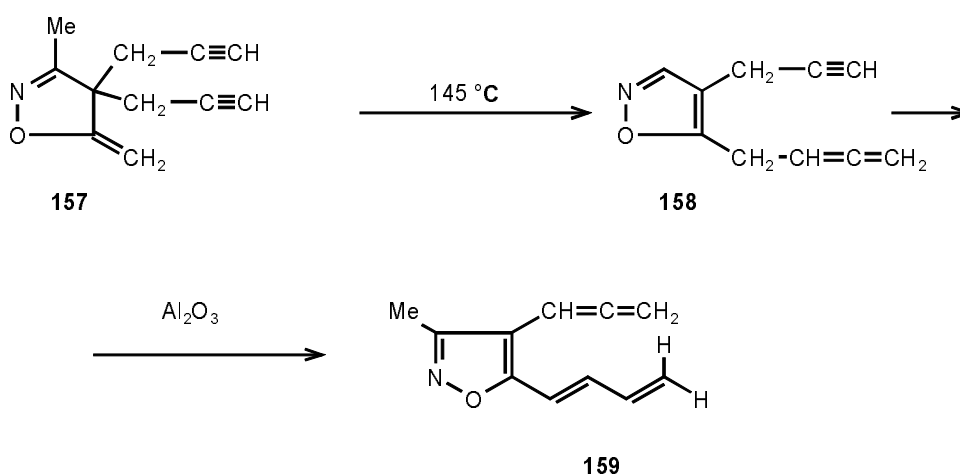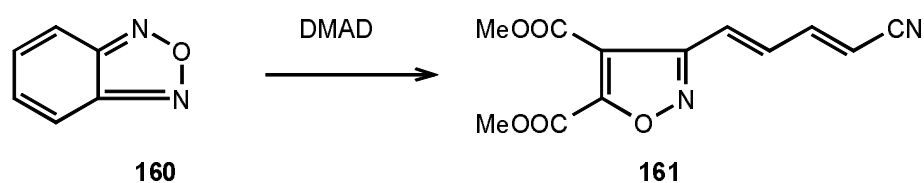
Another and more general rearrangement to hetaryldienes was found with benzoxadiazole **160**: this compound when reacted with dimethyl acetylenedicarboxalate affords - via a fairly unusual addition - the cyano substituted isoxazolyldiene **161** [44, 57]. Similarly, benzoselenodiazoles react with benzyne in an analogous manner and lead to the benzisoselenazolyldiene **163**. As indicated by the R substituents the fused benzene ring of the products derived from the reagent, whereas the fused benzene ring of the starting compound **162** undergoes ring opening to afford the diene chain [58, 59].

Scheme 56

162   **163**
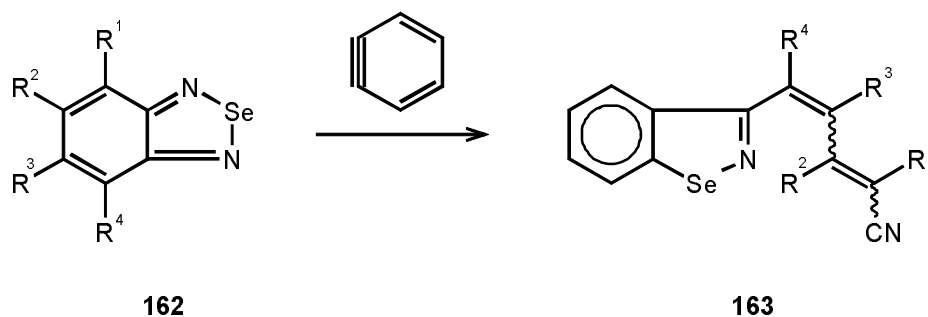
Table 1 cont.

Het	$R_{1\text{-}3}$	R_4	mp	yield (%)	method	ref

E. Collective Table

Table 1   Experimental data and references of hetaryldienes
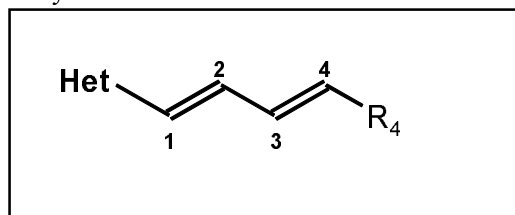
Het	$R_{1\text{-}3}$	R_4	mp (bp$^{\text{Hgmm}}$)	yield (%)	method	ref

5-MEMBERED RINGS WITH ONE HETEROATOM

Het	$R_{1\text{-}3}$	R_4	mp (bp$^{\text{Hgmm}}$)	yield (%)	method	ref
(2-methylfuran)	-	H	-	87	A1	[1]
	-	H	bp 54^{11}	51	B	[5]
	-	Ph	103-4	84	A2	[12]
	-	Ph	103-4	44	F	[60]
	-	-	4-CN-4-COOMe	44	76	F
	[24]					
	R_1= CN	NMe_2	-	-	F	[23]
$R_1 = NH_2$	H	yellow oil	70	G	[26]	
3-Ph	H	oil	62	G	[28]	
3-R	H	-	64	G	[61]	
	3-OSiMe₃	H	bp $73\text{-}4^2$	86	G	
	[33]					

Het	$R_{1\text{-}3}$	R_4	mp (bp$^{\text{Hgmm}}$)	yield (%)	method	ref
(2,5-dimethylfuran, Me–O) 3-OSiMe₃	H	bp 85^4	80	G	[33]	

.

Table 1 cont.
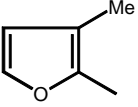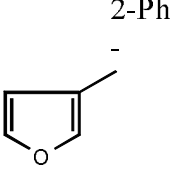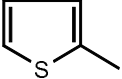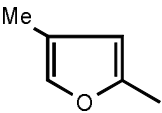
Het	R$_{1-3}$	R$_4$	mp	yield (%)		
(furan, 3-Me, 2-Me)	--					
2-Ph	H	-	-	G	[62]	
-	H	bp 76[10]	64	H	[63]	
(3-methylfuran) R^2= Me	H	bp 87[11]	79			
R^3= Me	H	bp 92[17]	74			
-	4-CN-4-COOMe	68	52	F	[24]	
(2-methylthiophene, S)	--					
	-	SEt	70[1]			
[35]	-	SEt	bp. 121-6$^{0.4}$	80		
	-	H	bp 84[12]	40		
-		H	oil	57		
-	4-pentenyl	-	51	H	[65]	
-	4-CN-4-COOMe	62	72	F	[24]	
-	Ph	147-9	48	F	[60]	
-		2-(Me_3Si)-ethenyl	-	50		
(furan, 4-Me, 2-Me)		3-Ph	H	oil		
[28]						

Table 1 cont.
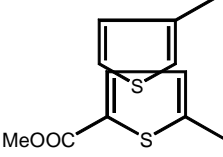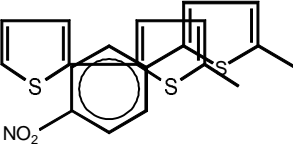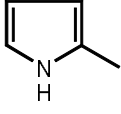
Het	R_1-3	R_4	mp	yield (%)	
	R_1= CN	NMe_2			
	-	4-CN-4-COOMe	52	78	
	-	SEt	bp 65[1]	65	
	R_3=piperidyl	H	oil	80	
	-	H	unmeasurable	61	
-	Ph	130-1	70	H	[36]
-	Ph	193	80	H	[36]

Table 1 cont.

Het	R_{1-3}	R_4	mp	yield (%)
	-	4-CN-4-COOMe	-	-
	-	Ph	192-5	34
	-	COOMe	136	60
	-	CN	70-73	24
	R_2 = Me	H	oil	67
	R_2 = Me	COMe	112	92
	R_2 = Me	CHO	solid	poor
	R_2=Me	COOMe	114	74
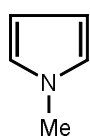
| | R_1= CN | NMe$_2$ | - | - |

5-MEMBERED RINGS WITH TWO OR MORE HETEROATOMS
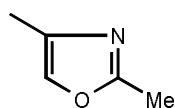
| | R_2 = Me | COOMe | 88-89 | 89 |

Table 1 cont.
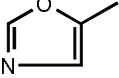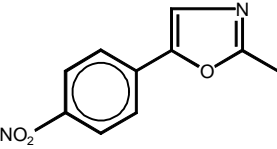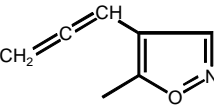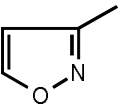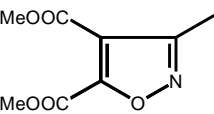
Het	R$_{1-3}$	R$_4$	mp	yield (%)
	R$_1$= Me -	NMe$_2$ NMe$_2$	bp 87-100$^{0.0}$ 97-100	44 44
	-	Me	157-63	25
	-	H	77-9	94
	2-OAc, 3-Br	H	oil	poor
	-	CN	-	-

Table 1 cont.
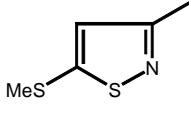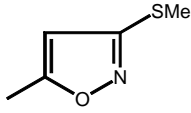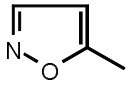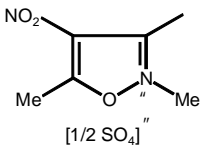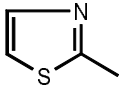
Het	R$_{1-3}$	R$_4$	mp	yield (%)	
(5-MeS-3-Me-isothiazole)	-	Ph	102-3	41	
	-	p-MeO-phenyl	112-3	44	H
	-	3,4-diMeO-phenyl	118-9	41	
(3-SMe-5-Me-isoxazole)	-	p-anisyl	102-3	58	
	-	3,4-diMeO-phenyl	108-9	63	
(5-Me-isoxazole)	-	Me	oil	75	
	R$_3$=Me	Me	oil	70	
(4-NO$_2$-3-Me-5-Me-isoxazolium, 2-Me, [1/2 SO$_4$])	-	Ph	175-6	67	
(2-Me-thiazole)	-	Ph	89-90	poor	
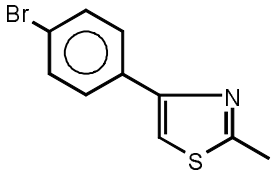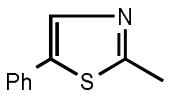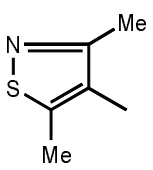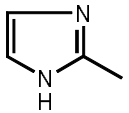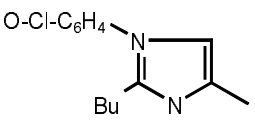
Table 1 cont.

Het	R$_{1-3}$	R$_4$	mp	yield (%)
	- - - -	morpholyl piperidyl pyrrolidyl N-Me-piperazyl	158-9 126-8 113-5 129-31	55 52 56 54
	2-Ph	4,4-bis-SMe	brown liquid	38
	-	-	oil*	87
	R$_2$ = Me	H	oil	63
	-	COOEt	low melting solid	38

Table 1 cont.
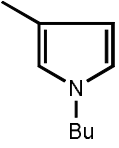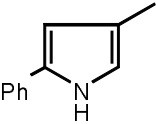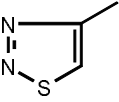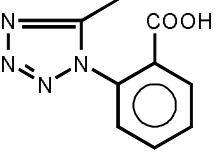
Het	R_{1-3}	R_4	mp	yield (%)
	R^2=CN	diCN	160	95
	-	H	50	89
	-	Ph	124-6	18
	-	Ph	178	62
	-	H	65	74
	R^1=Me	-	96	88
	R^2=Me	-	125	80
	R^3=Me	-	41	34
	-	Me	65*	74
	-	Ome	164 (1-Z)	38
	-	Ome	97 (1-E)	12

Table 1 cont.
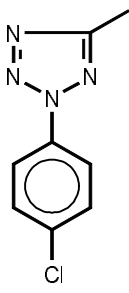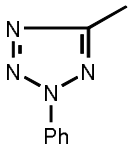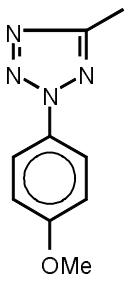
Het	R$_{1-3}$	R$_4$	mp	yield (%)
	-	Oet	67 (1-Z)	34
	-	Oet	54 (1-E)	12
	-	Opr^i	84 (1-Z)	5
	-	Opr^i	77 (1-E)	75
	-	Obu^t	106 (1-E)	79
	-	CN	160 (1-Z)	67
	-	CN	142 (1-E)	15
	-	imidazolyl	151 (1-E)	92
	-	benzimidazolyl	198 (1-E)	82
	-	indolyl	164 (1-E)	85
	-	7-Cl-phenothiazinyl	164 (1-E)	38
	-	morpholyl	94 (1-E, 3-Z)	69
	-	morpholyl	161 (1-E, 3-E)	61
	-	aziridy l	79-81*	82
	-	morfolyl	136(1-E,3-E)	56
	-	morfolyl	128	53

Table 1 cont.

Het	R₁₋₃	R₄	mp	yield (%)

Het	R_{1-3}	R_4	mp	yield (%)

(1-phenyl-5-methyltetrazole structure) — Ph — 161-2 — 74
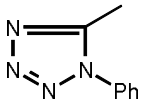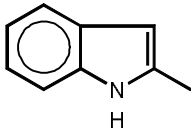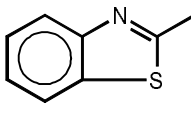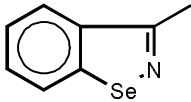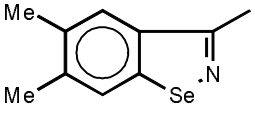
BENZOLOGUES OF 5 MEMBERED HETEROCYCLES

(2-methylindole structure) — R_2 = Me / R_3 = Me — H / H — solid / 132-3 — 88 / 38

(2-methylbenzothiazole structure) — R_1= CN / – — Ph / p-Me$_2$N-Ph — 153 / 197-9 — 90 / 91

(benzisoselenazole structure) — – — CN — 140-1 — 88

(dimethyl benzisoselenazole structure) — – — CN — 102-4 — 58

Het	R_{1-3}	R_4	mp	yield (%)
(1-phenyl-5-methyltetrazole)	–	Ph	161-2	74

BENZOLOGUES OF 5 MEMBERED HETEROCYCLES

Het	R_{1-3}	R_4	mp	yield (%)
(2-methyl-1H-indole)	R_2 = Me	H	solid	88
	R_3 = Me	H	132-3	38
(2-methylbenzothiazole)	R_1= CN	Ph	153	90
	–	p-Me$_2$N-Ph	197-9	91
(benzisoselenazole)	–	CN	140-1	88
Me, Me-substituted (benzisoselenazole)	–	CN	102-4	58
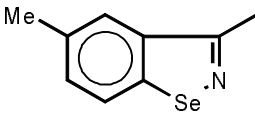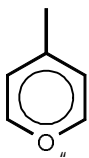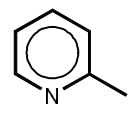
Table 1 cont.

Het	R_{1-3}	R_4	mp	yield (%)

| | - | CN | 144-54 | 12 |

6 MEMBERED RINGS WITH ONE HETEROATOM

| | - | p- NMe_2 -phenyl | 145 | 93 |

	-	Ph	121-3	44
	-	Ph	121	44
	-	Ph	121-3	68
	-	Ph	121-2	-
	-	Ph	123-4	-
	-	H	152 (picrate)	-
	-	H	bp 70^1	-
	-	H	oil	84
	-	H	bp $66^{1.5}$	91
	-	Me	bp $48^{0.08}$	56
	-	Me	153-5	30
	-	NMe_2	oil	50

Table 1 cont.
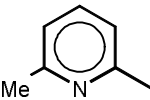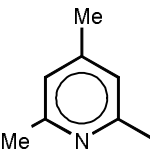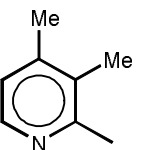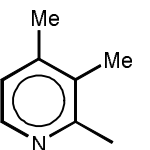
Het	R$_{1-3}$	R$_4$	mp	yield (%)
	-	NMe$_2$	bp 130-5$^{0.3}$	-
	-	NH$_2$	-	quantitative
	-	Net$_2$	-	65
	-	SEt	bp 80[1]	54
	-	piperidyl	58-60	68
	-	morpholyl	112	56
	R$_1$ = NH$_2$	H	oil	78
	R$_2$ = Me	H	oil	92
	R$_2$ = iPr-NH$_2$	iPrNH	171-2	45
(Me, N, Me pyridine)	-	Me	bp 90-91[1]	30
	-	Ph	108	-
	-	Ph	103-4	-
(Me, Me, N, Me pyridine)	-	piperidyl	96	93
	-	Ph	103-4	-
(Me, Me, N, Me pyridine)	-	morpholyl	119	55

Table 1 cont.
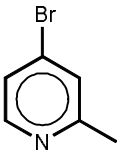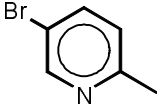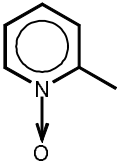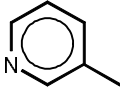
Het	R_{1-3}	R_4	mp	yield (%)
(4-bromo-2-methylpyridine)	-	NEt_2	-	10
(5-bromo-2-methylpyridine)	-	Net_2	-	5
(2-methylpyridine N-oxide)	-	Ph	170-1	76
(3-methylpyridine)	-	SEt	bp 90^1	63
	-	Ph	104-5	77
	-	NMe_2	145-7	94
	-	Ph	100-2	59
	-	H	bp $60^{0.2}$	72
	R_3=piperidyl	H	oil	81
	R_2 = Me	H	oil	83

Table 1 cont.
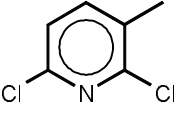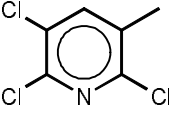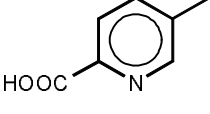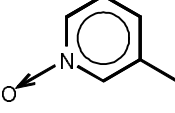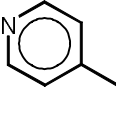
Het	R$_{1-3}$	R$_4$	mp	yield (%)
	-	Ph	120-2	63
	-	Ph	133-5	51
	-	H	105-6	-
	-	Ph	196-8	65
	-	Ph	158-60	52
	-	Ph	137-8	-
	-	Ph	159	-
	-	H	bp 71$^{1.5}$	63
	R$_2$ = Me	H	oil	91

Table 1 cont.
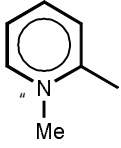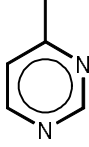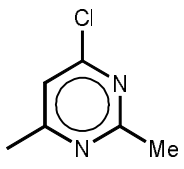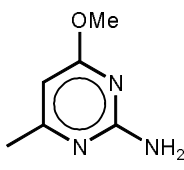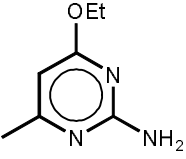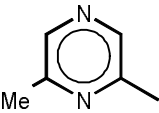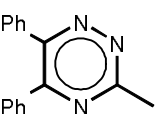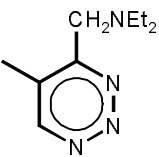
Het	R$_{1-3}$	R$_4$	mp	yield (%)
![pyridine structure]	-	p- NMe$_2$ -phenyl	224-6	75
![pyrimidine structure]	-	Ph	101	8

6-MEMBERED RINGS WITH TWO OR MORE HETEROATOMS

Het	R$_{1-3}$	R$_4$	mp	yield (%)
![chloro pyrimidine structure]	-	Me	72-3	42
	-	Ph	121-3	50
![OMe pyrimidine structure]	-	Ph	166	62
	-	p-tolyl	201	60
	-	p-anisyl	193	62
	-	3,4-disubst.Ph	186	55
	-	p-anisyl	171	57
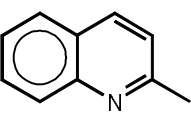
Table 1 cont.

Het	R_{1-3}	R_4	mp	yield (%)

| | - | Ph | 149-50 | 54 |
| | - | p-tolyl | 171 | 57 |

| | - | Ph | - | - |

| | - | Me | 142-4 | 78 |
| | - | Ph | 146-7 | 62 |

| | - | H | bp $100^{0.01}$ | 60 |

BENZOLOGUES OF 6 MEMBERED HETEROCYCLES

	-	piperidyl	175-6	quantitative
	-	Ph	57-58	144
	-	Ph	117	13

Table 1 cont.

Het	R_{1-3}	R_4	mp	yield (%)
	-	NMe$_2$	165-6	7
	- -	Ph piperidyl	122-3 113-4	48 76
	-	Ph	170	60
	-	Ph	138	-

*mixture of E and Z isomers

Method A1: from a hetarylaldehyde and allylphosphorane, see section A.1.1.; Method A2: from a hetarylaldehyde and allylphosphonic acid, see section A.1.1.; Metho
phosphorous reagents, see section A.1.2.; Method C: from hetarylphosphoranes, see section A.1.3.; Method D: from hetarylmethylenephosphonic esters, see section A.
condensation reaction, see section A.2.1.; Method F: by miscellenious condensation reactions other than E, see section A.2.2.; Method G: by various methods describe
fubctionalised polyenes, see sections B.1. and B.2..; Method J: by ring opening reactions, see sections C.1., C.2., and C.3.; Method K: obtained by rearrangements, see

II. REACTIONS

This part of the paper covers the transformations of hetaryldienes - except reactions that do not involve the change of the diene moiety - classified according to their nature. To better understand the reactivity of hetaryldienes one has to study the electronic and steric features of these molecules.

F. Structure and reactivity

Generally a 1,3-diene moiety has a planar arrangement upheld by the conjugation of its π-electrons. The connection of a hetaryl ring to any position of the diene chain would in principle mean spreading out the conjugation on the molecule and coplanarity of the aromatic ring(s) with the diene chain, which suggests that in reactions where the attacking entity approaches the molecule from the top or the bottom (which is the usual pattern) the steric influence directing the incoming reagent originate primarily from other, non-planar substituents. On the other hand the aryl moiety and other conjugating substituents (which by virtue of conjugation have to lie in the plain of the diene chain) do fundamentally determine the electron- and orbital-distribution of the diene chain and thus its reactivity patterns.

Semiempirical calculations using the AM1 Hamiltonian and the MOPAC 6.0 package show (Table 2) that on introduction of a conjugating substituent the energy of the highest occupied molecular orbital (HOMO) increases considerably (cf. entries 1,2,3,5) and the π-contribution (HOMO $2p_z$ coefficient) of the diene carbon atoms to the HOMO orbital in positions β and δ to the substituent is significantly enhanced relative to positions α and γ. The results also reveal that the change of the geometry of a double bond (cf. entries 3,4 and 5,6) or introduction of a non-conjugating substituent (cf. entries 5,7) have only a minor effect on the HOMO orbital energy and population. Similar considerations lead to the conclusion (also supported by molecular modelling) that the

carbon atoms of higher HOMO coefficient in the diene chain do also accommodate a higher electron density and thus have a larger partial negative charge than the other positions.

Scheme 57
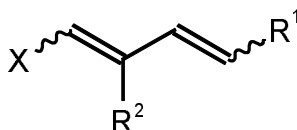
Table 2

Calculated HOMO orbital energies (E_{HOMO}, eV) and $2p_z$ coefficients (q_{2pz}, absolute value) of some dienes (AM1, MOPAC 6.0)

Entry	X	R^2	R^1	E_{HOMO}	C^{α}-q_{2pz}	C^{β}-q_{2pz}	C^{γ}-q_{2pz}	C^{δ}-q_{2pz}
1	H	H	H	-9,33	0,56	0,43	0,43	0,56
2	E-Ph	H	H	-8,63	0,41	0,44	0,24	0,39
3	E-NMe$_2$	H	H	-8,08	0,37	0,53	0,24	0,43
4	Z-NMe$_2$	H	H	-8,10	0,35	0,54	0,21	0,34
5	E-NMe$_2$	H	E-2-Me-tetrazol-5-yl	-8,02	0,33	0,49	0,26	0,45
6	E-NMe$_2$	H	Z-2-Me-tetrazol-5-yl	-8,01	0,34	0,52	0,22	0,43
7	E-NMe$_2$	Me	E-2-Me-tetrazol-5-yl	-7,90	0,34	0,51	0,21	0,39

Based on the calculations the following reactivity patterns can be predicted for hetaryldienes: besides the reactions characteristic of olefins (*e.g.* saturation, 2+2 photo-cycloaddition, rearrangements) hetaryldienes might be expected to undergo regioselective cycloaddition reactions as electron-rich 2π or 4π components, with the reagent atom of higher LUMO contribution being connected to the diene carbon of higher HOMO contribution, and are susceptible to electrophilic attack at positions β and δ relative to the strongest donating substituent. Due to the fairly even orbital and charge

distribution along the diene chain in transformations where only one of the two double bonds takes part the selection will usually be based on steric susceptibility rather than electronic differences.

G. Reactions with electrophiles

This chapter collects the reactions of hetaryldienes with electrophiles. As mentioned previously these attacks are expected to take place at positions β and δ. In most cases electrophilic attack on the hetaryl ring might also occur as a competing reaction.

G.1. Protonation

As olefins are usually sensitive to acids, easily undergoing isomerisation, rearrangement or polymerisation, quantitative protonation reactions have little practical use with hetaryldienes. The use of acid catalysis was found beneficial in certain cases which will be discussed at the appropriate transformations.

Scheme 58
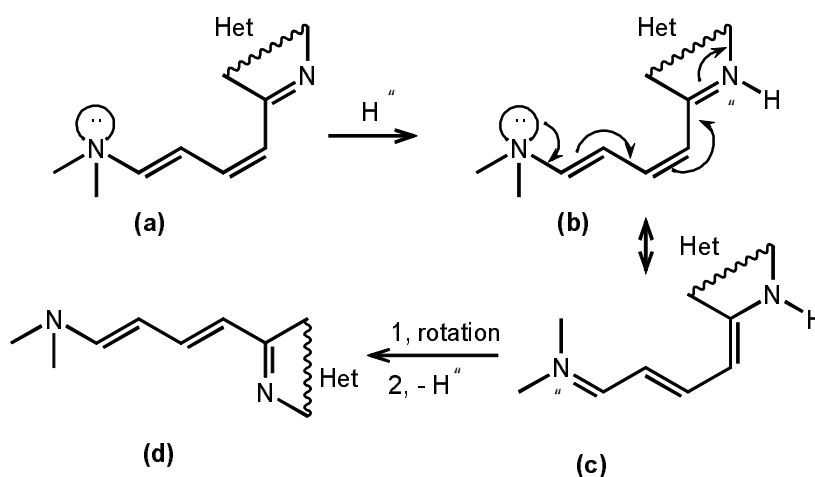
In some cases the hetaryldiene structure can make the proton catalysed isomerisation very facile. In *1Z,3E*-1-hetaryl-4-amino dienes (scheme 58, **a**) the diene chain bears a lone pair donor atom at one terminus (e.g. nitrogen) and a hetaryl moiety at the other

terminus in a way that it can formally be conjugated to a pyridine type nitrogen. Protonation of the heterocycle gives an iminium ion (**b**) which - if the amine nitrogen is ready to contribute its lone pair - can also be described by a mesomeric form (**c**) where the formally double 1,2-bond becomes single thus allowing rotation around the bond and deprotonation results in the thermodynamically more stabile *1E,3E* form (**d**). The process was applied to the synthesis of *E,E* hetaryldienamines [83].

G.2. Reaction with other electrophiles

Although electrophiles other than proton can also lead to non-desired side-reactions so their use as a reagent with hetaryldienes is fairly limited, interesting comparison can be made between the few published reactions of hetaryldienamines and their carbocyclic analogues.

The tetrazolyldienamine **164** was found to react with aryldiazonium salts at the β position and after aqueous work up the α-hydrazono-aldehyde **165** was isolated in moderate yield (52%) [84]. The analogous dienamine derived from Δ^4-androstene-3,17-dione (**166**) was readily attacked by aryldiazonium salts in the δ position and was converted after treatment with phosphorous oxychloride and hydrolysis to steroidoindoles (**167**) [85].

Although treatment of **164** with diethyl azodicarboxylate (DEAD) led to the addition of the δ-CH bond onto the azo-part and formation of **168** in good yield (60%) - formally an electrophilic attack followed by hydrogen shift - the reaction is believed to follow a cycloaddition-elimination pathway through the dihydro-pyridazine intermediate **169** [84]. A decalin-derived cyclic dienamine with fixed *cisoid* geometry (unable to furnish the cycloaddition intermediate) was attacked at the β-position by DEAD [86] and **170** was formed in moderate yield (42%). The reaction is thought to proceed via the addition of the electron-rich β carbon onto the azo-bond followed by hydrogen shift.

Scheme 59

Ar: 4-Cl-phenyl

X: F, Cl

Scheme 60

164 →

E = CO$_2$Et
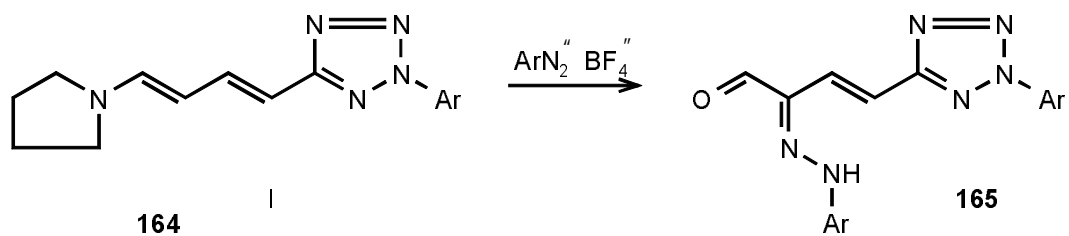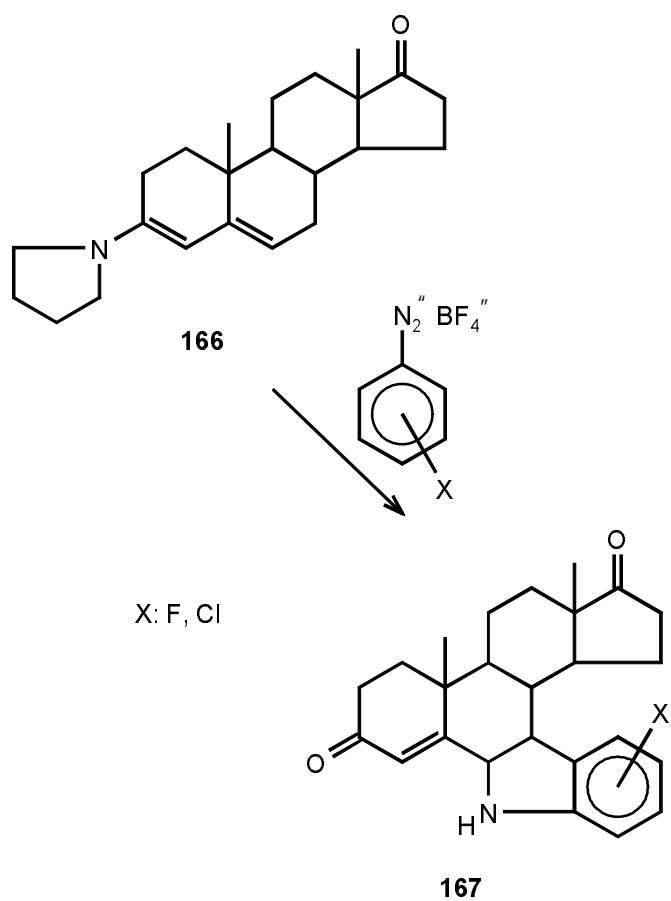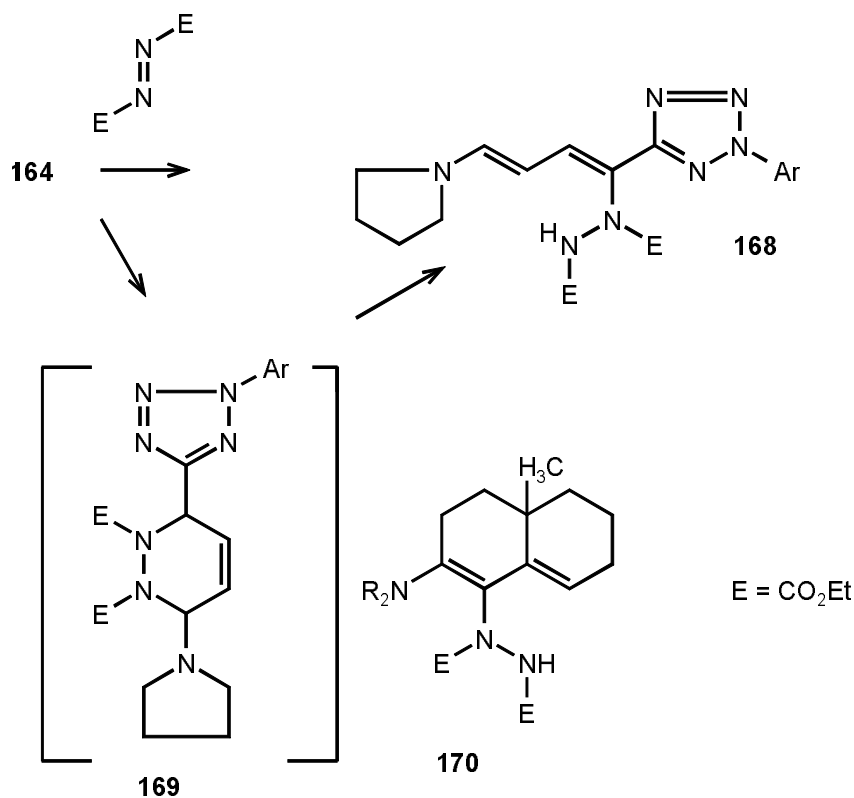
H. Cycloaddition reactions

As the frontier orbital analysis of hetaryldienes in chapter F reveals high lying HOMO orbitals one would assume that they are ideally Set to participate 4+2 and 4+6 cycloadditions as 4π components. As the same HOMO orbital applies if we consider the dienes as ene systems, reactions taking place on electron rich olefins (such as 2+3 dipolar cycloaddition, "inverse electron demand" Diels-Alder reaction or 2+8 cycloaddition) will also find practical use amongst hetaryldienes.

H.1. Dienes as 4π components

H.1.1. Diels-Alder (4+2) cycloadditions

The first report on the Diels-Alder reaction of a hetaryldiene goes back to 1950, when 2'-thienlylbutadienes (**171a**) were found to react with maleic anhydride (X=O) to give the bicyclic product (**172a**) [87]. A similar reaction was published [86] using hetaryldienamines (**171b**) and N-phenyl-maleinimide (X=NPh). Here the primary adduct (**172b**) underwent spontaneous elimination to yield the cyclohexadienofurane (**173b**) in good yield (72%). A similar Diels-Alder reaction - elimination sequence was also used to rationalise the formation of the 3-hetaryl-phthalic acid dimethyl esters (**174**) from the hetaryldienamine (**171b**) and dimethyl acetilenedicarboxylate (DMAD) reported in the same paper.

Scheme 61
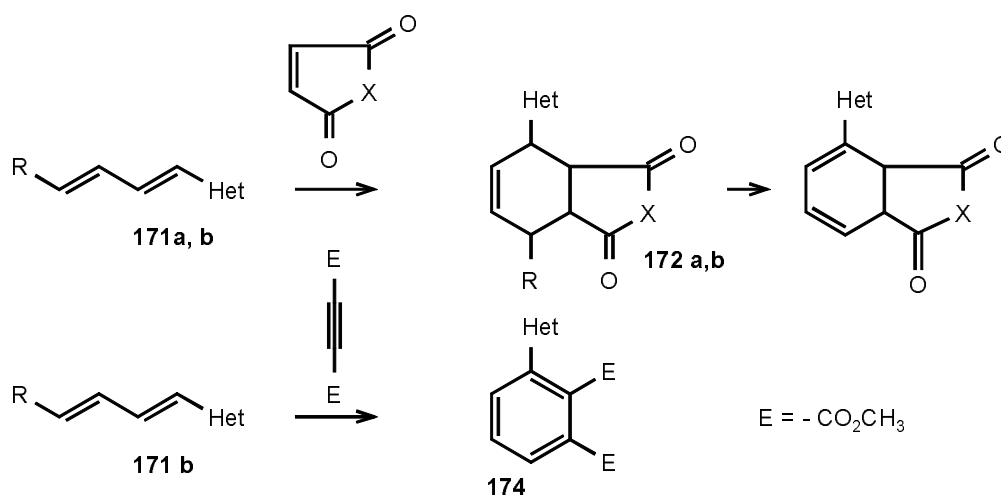
a: Het = 2'-thienyl, R = H, X = O

b: Het = 2(4-chlorophenyl)-tetrazolyl-5, R = morpholino, X = NPh

Although the use of α,β-unsaturated oxo-compounds as dienophiles with electron-rich olefins goes back to 1942 [88] their reaction with hetaryldienes was only reported recently. Cinnamaldehyde and methylvinylketone - activated by a catalytic amount of strong Broensted acid reacted with a series of hetaryldienamines (**175**) to give cyclohexenes. The intermediates eliminated the amine moiety spontaneously and

cyclohexadienes were formed which were isolated (**176**) or oxidised to benzene derivatives (**177**). The wide range of yields (17-80%) was attributed to the different acid sensitivity of the starting dienes and products [89].

Scheme 62
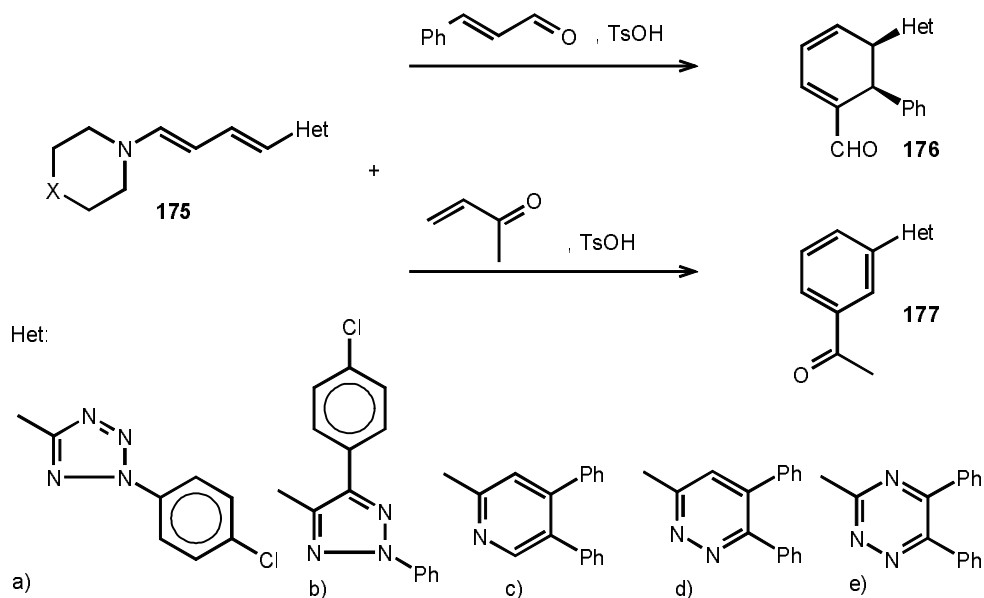
The highly reactive 1,2,3,3-tetrachlorocyclopropene system was used in the synthesis of cyclopropenobenzene (**180**) starting from a 2'-thienyl-diene (**178**). The first step of the procedure is the Diels-Alder reaction of **178** yielding the fused cyclohexene (**179**) in 33% yield, which was converted to the end product **180** in 28% yield by potassium *tert*-butoxide [90].

Nitrosobenzene was found to react as a hetero-dienophile when treated with pyridyl-dienes (**181a-c**) to yield dihydrooxazine derivatives (**182a-c**). The intermediates containing 2'-pyridyl or 4'-pyridyl substituents (**182a,c**) were transformed into the pyrrol derivatives **183a,c** on treatment with base, while their 3'-pyridyl analogues remained intact under the applied conditions [91].

An unusual diene, the cationic N-(2-butadienyl)-pyridinium salt (**184**) was reacted with electron deficient or strained olefins (**185**) in acetonitrile at 140 °C in a sealed vessel to give the cyclohexene cationic derivatives (**186**) in good yield (79-92%) [92].

Scheme 63

Th : 2'-thienyl

Py : 1-, 2-, 3- pyridyl; R=H,CH₃
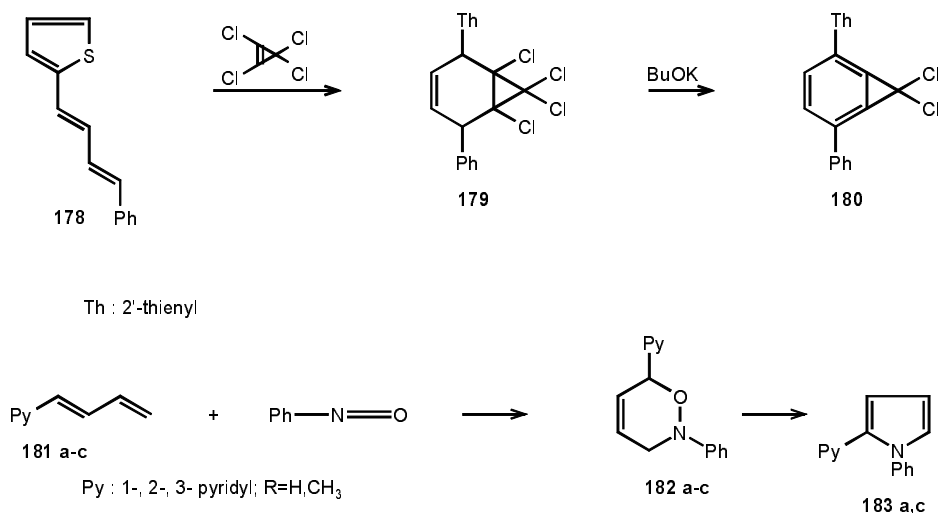
Scheme 64
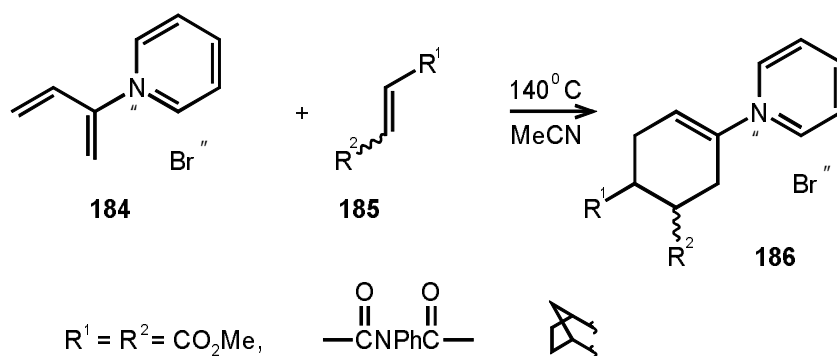
The "irregular" Diels-Alder behaviour of the cyclic polyene **187** - it reacts with DMAD on its furan moiety if n=1 to yield **188** in 90%, but doesn't react with DMAD if n=2 [93] - was attributed to the anti-aromatic character of **188** (n=2) and **187** (n=1) and the aromatic stabilisation in **188** (n=1) and **187** (n=2).

Scheme 65

187

188

E = CO₂CH₃ n=1,2

$E = CO_2CH_3$ n=1,2

Scheme 66

189

1) LDA

2)

190

191 air

192
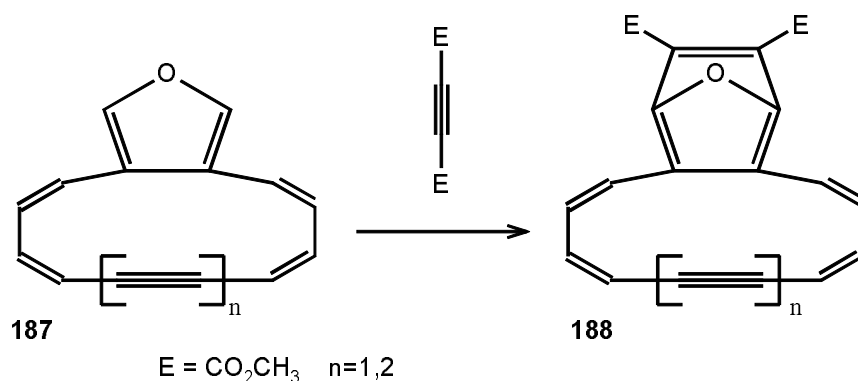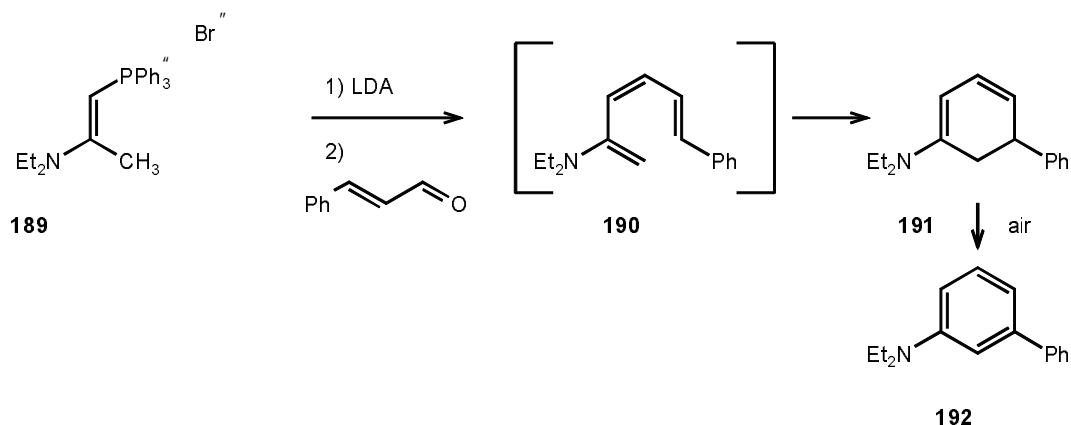
The intramolecular Diels-Alder reaction is frequently used in the synthesis of polycyclic systems. The ring construction step might utilise a stable starting material and forcing reaction conditions or the facile transformation of an *in situ* formed intermediate. This latter case is represented in the formation of the biphenyl-derivative **192**. The enamino-phosphonium salt (**189**) was converted to the hexatriene intermediate (**190**) which cyclised to the cyclohexadiene (**191**). Oxidation of **191** afforded the aromatic product **192** [4].

The cyclisation of pyridyldienes (**193-195**) to quinolines and isoquinolines under mild conditions is prohibited by the *E* geometry of the 1,2-double bond. Under forcing conditions, however a side chain isomerisation may occur and the formed isomers (**196** and its analogues) undergo intramolecular Diels-Alder reaction to give dihydroquinolines

and dihydroisoquinolines (**198-201**). The regioselectivity of the process was shown to be dependent on the substitution pattern of the diene chain [94].

Scheme 67

199:200

P=H   1:2

P=XH$_3$ 3:1
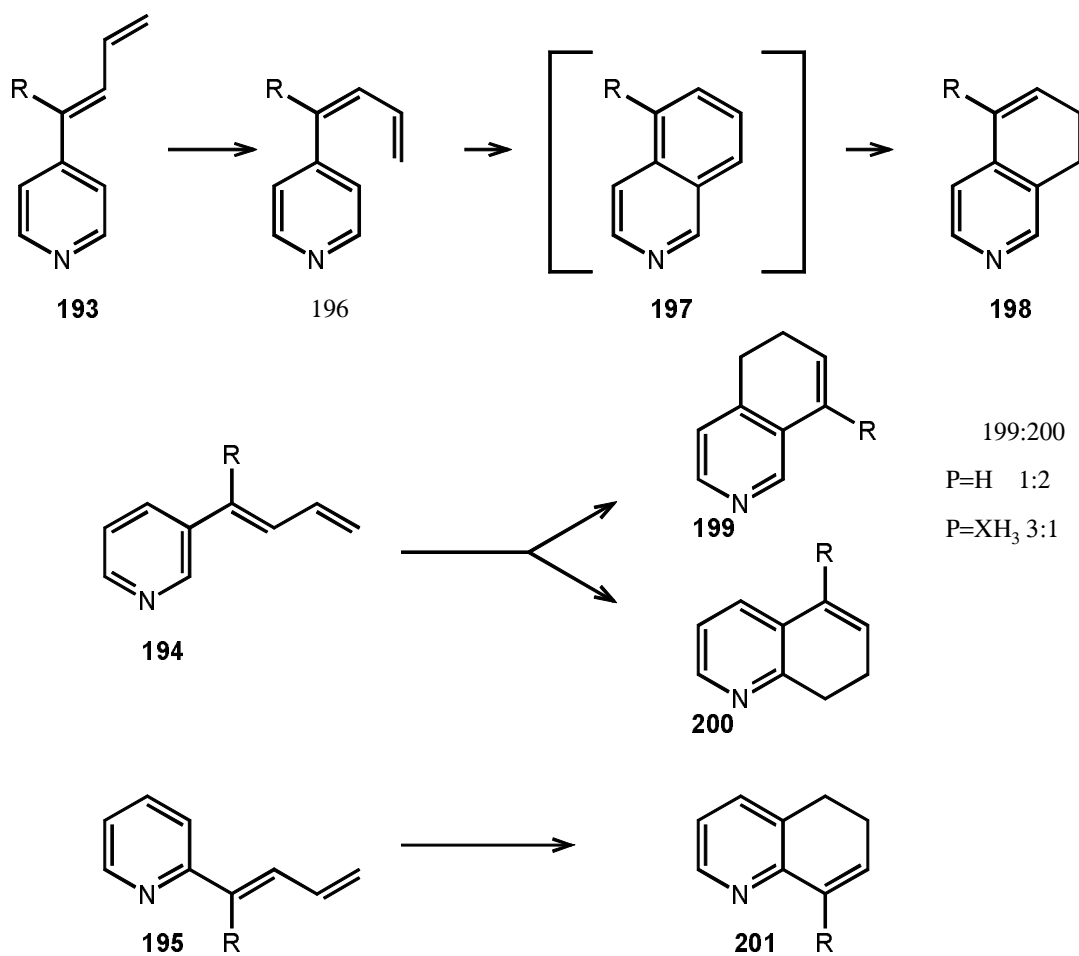
Scheme 68
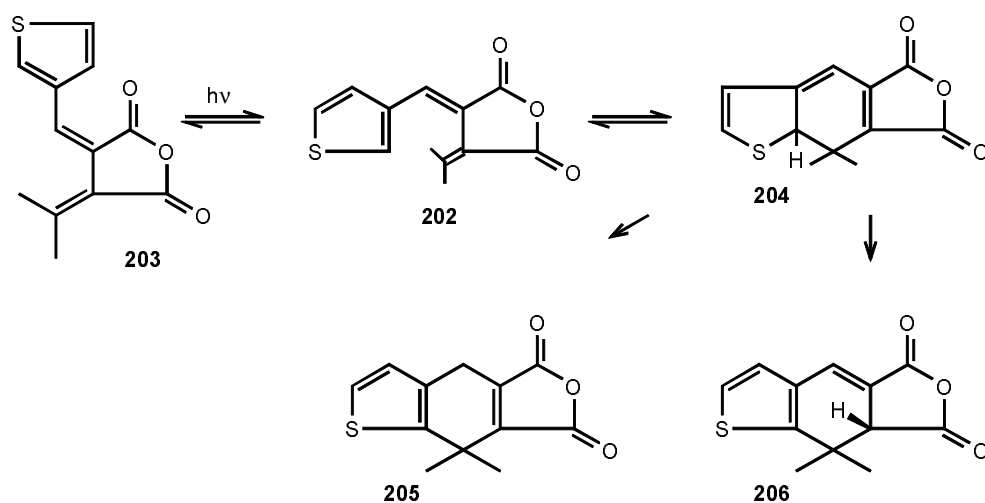
The *E*-thienyldiene (**202**) was converted selectively into a series of intramolecular reaction products (**203-206**). On prolonged irradiation at 366 nm a *ca.* 7:3 equilibrium mixture of the *E-Z* fulgides (**202**) and (**203**) was formed. When **202** was heated to 140 °C it cyclised to **204** which on irradiation with white light regenerated **202**. Carrying out the same reaction in the presence of a catalytic amount of trifluoroacetic acid **202** was converted quantitatively into **205**, the reaction proceeding probably through **204**. Heating of **202** in 1,2-dichlorobenzene in a sealed tube at 180 °C led to the quantitative formation of **206** in an hour. Attempts to achieve the acid catalysed transformation of **206** into **205** were unsuccessful.

The acid catalysed Diels-Alder dimerisation of the dehydroprenylindole (**208**) is thought to be the key step in the biosynthesis of yuehchukene (**209**). The process starts by the oxidation of prenylindole (**207**) to dehydroprenylindole (**208**) which in the presence of acid gives its protonated form **208p**. Diels-Alder reaction of **208** with **208p** followed by cyclisation leads to the natural product 209 [74].

Scheme 69

207 → H" → **208p**, **208** →

209
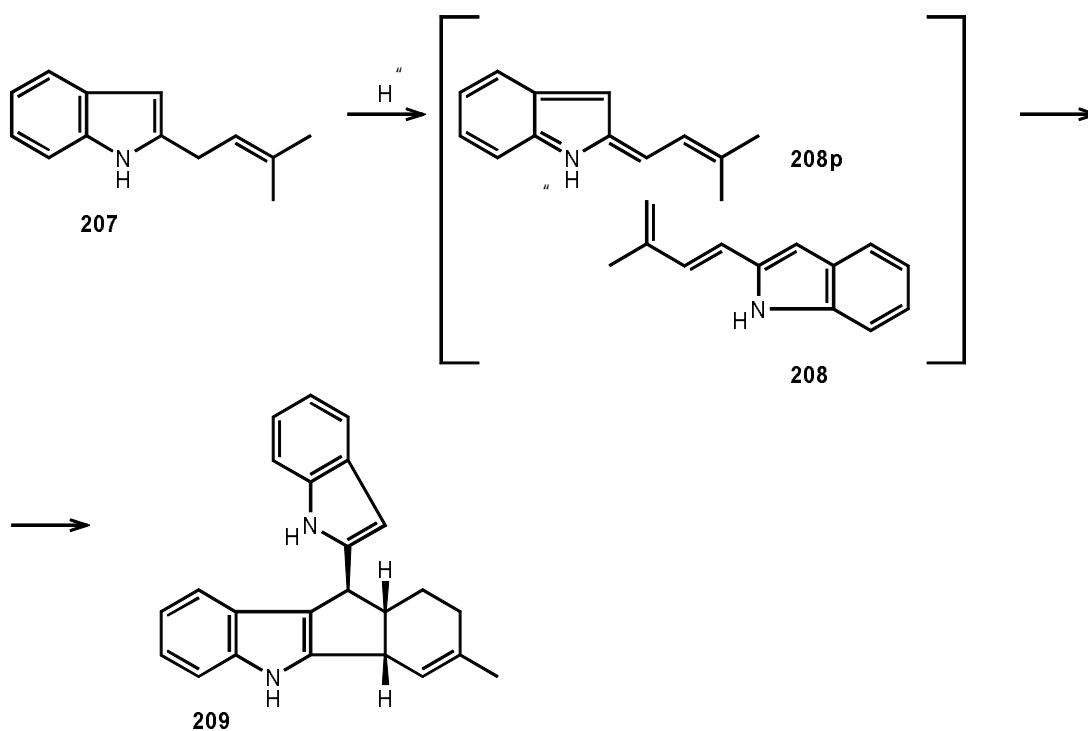
A strong Broensted acid was used to achieve the ring closure of the pyridyl-dienylether **210** to the quinolizinium derivative **211** in quantitative yield [58]. It is interesting to note that this ring closure procedure represents the reversal of the commonly employed ring opening technique of bridgehead nitrogen containing condensed salts with nucleophiles.

Scheme 70

210 → HClO$_4$ / quant. → **211**

E = " CO$_2$Me

Scheme 71

X = O, S, NMe   R = H, OMe, Bz
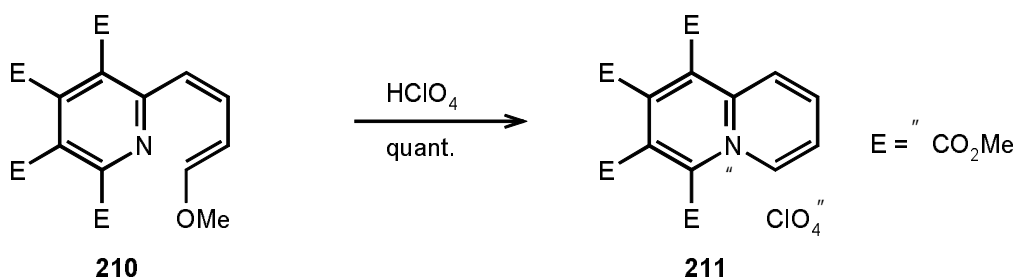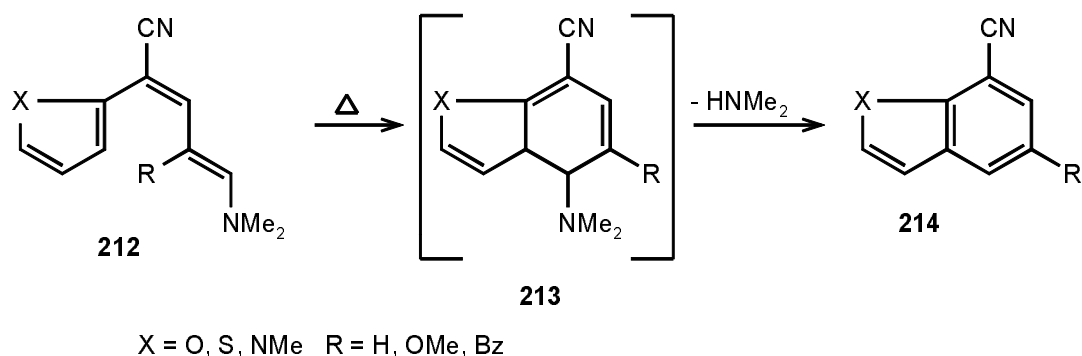
The previous examples demonstrated clearly that intramolecular cycloadditions proceeding with the destruction of an aromatic system require forced conditions. The same applies to the intramolecular Diels-Alder reaction of hetaryldienes (212) which yielded benzo[b]furans, -thiophenes and indoles (214) through the 213 intermediates [23].

H.1.2. 4+6 cycloadditions

Another class of "Woodward-Hoffmann allowed" thermal cycloadditions is of the less frequently exploited 4+6 cycloadditions. Acyloxyfulvenes (216) reacted with hetaryldienamines (215) as 6π systems and after the elimination of the amine moiety azulenes (217) were formed in moderate yield (46-65%) [86].

Scheme 72
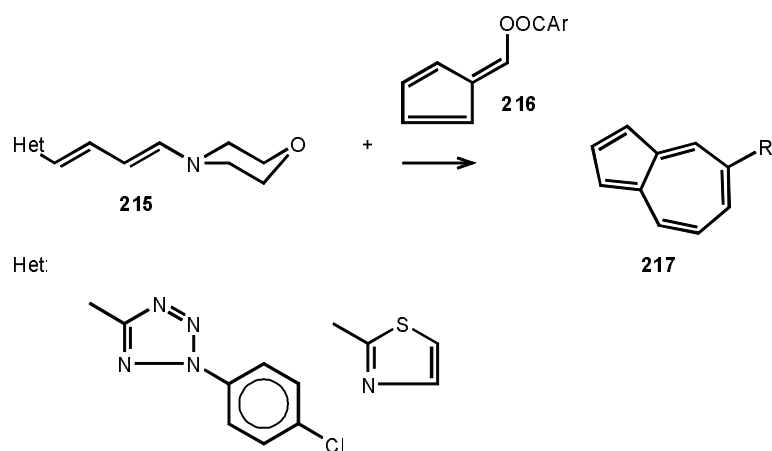
H.2. Dienes as 2π components

H.2.1. 2+2 cycloadditions

Although the photochemical 2+2 cycloaddition of olefins is frequently used in organic synthesis its extension to hetaryldienes is limited. The only report on this subject discusses the solid phase photochemical transformation of the 2'-thienyldiene (**218**) into its dimer (**219**) on irradiation [96].

Scheme 73

Ar = 2,6-dichlorophenyl
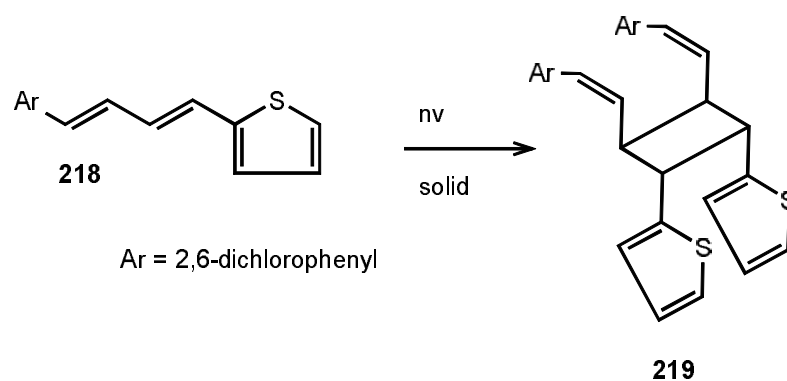
H.2.2. 2+3 cycloadditions

Hetaryldienes having an electron-rich diene system react readily with 1,3-dipoles; the site of attack mostly determined by the steric hindrance of the double bonds and regioselectivity governed by electronic factors. The pyridyl-eneyne (**220**) reacted with its terminal acetylene bond when treated with the nitrileoxides (**221**) and gave pyridylvinylisoxazoles (**222**) in moderate yield [97]. The analogous reaction of the pyridylbutadiene (**223**) gave the isoxazoline derivative (**225**) in good yield. No other isomers were detected in the reaction mixtures.

Scheme 74

R: Ph, CO$_2$Et
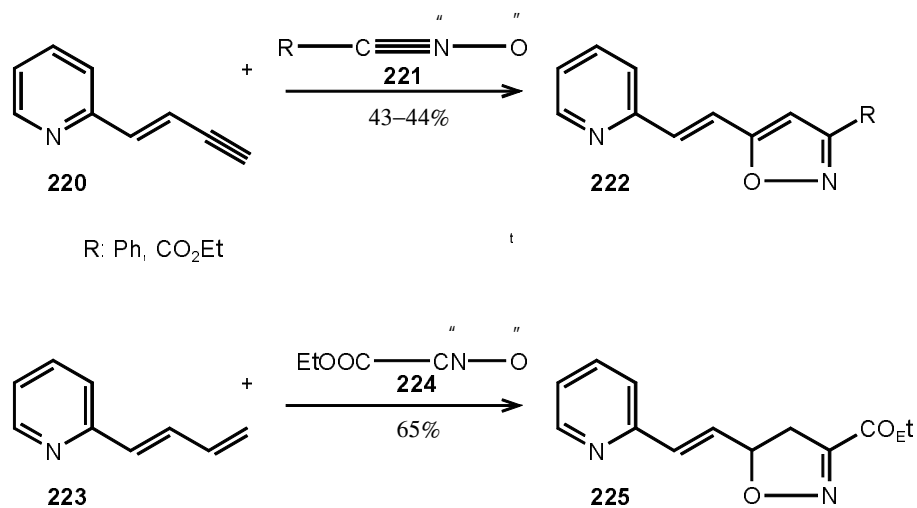
The tetrazolyldienamine (**226a**) gave tetrazolylvinyltriazole (**227a**) on treatment with arylazides [84] *via* a dipolar cycloaddition followed by morpholine elimination. The analogous product (**227b**) formed in the transformation of morpholinobutadiene (**226b**) suggests that the amine moiety takes part in the stabilisation of the transition state (cf. chapter H.2.4.).

Scheme 75

226 a,b   **227 a,b**

a: R = H, 2-(4-chlorophenyl)-tetrazolyl   b: R=H
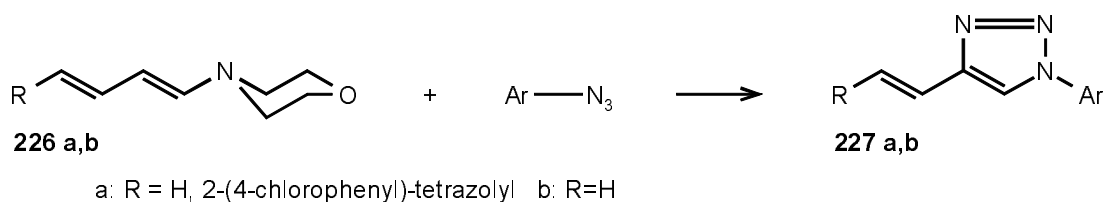
H.2.3. "Inverse electron-demand" Diels-Alder (2+4) cycloadditions

Hetaryldienes having an additional p-donating substituent, especially dienamines have high lying HOMO orbital which makes them suitable dienophiles in the "inverse electron-demand" Diels-Alder reaction. A series of *E,E*-hetaryldienamines (**228**) were reacted with 3,6-dimethyl 1,2,4,5-tetrazine dicarboxylate (**229**) and *E*-azolylvinylpyridazines

(230) were isolated in moderate to good yield [83, 98]. In each case the tetrazine reacted with the enamine part retaining the geometry of the 1,2 double bond. A series of the analogous *Z,E*-azolyldienamines (231) gave the corresponding *Z*-azolylvinylpyridazines (232) [98].

Tetrazolyl-methoxy-butadiene (233) which consists as a mixture of the *Z,Z* and *Z,E* isomers was expected to give a product with a *Z*-side chain geometry but reaction of 233 with 229 in boiling toluene resulted in the formation of the *E*-azolylvinylpyridazine (234). As neither the starting material nor the product isomerised under the applied conditions the surprising behaviour was attributed to the reaction intermediate (235) [98] which was isolated and shown to posses an azolyl-dienamine substructure capable of isomerisation (cf. chapter G.1.)

Scheme 76
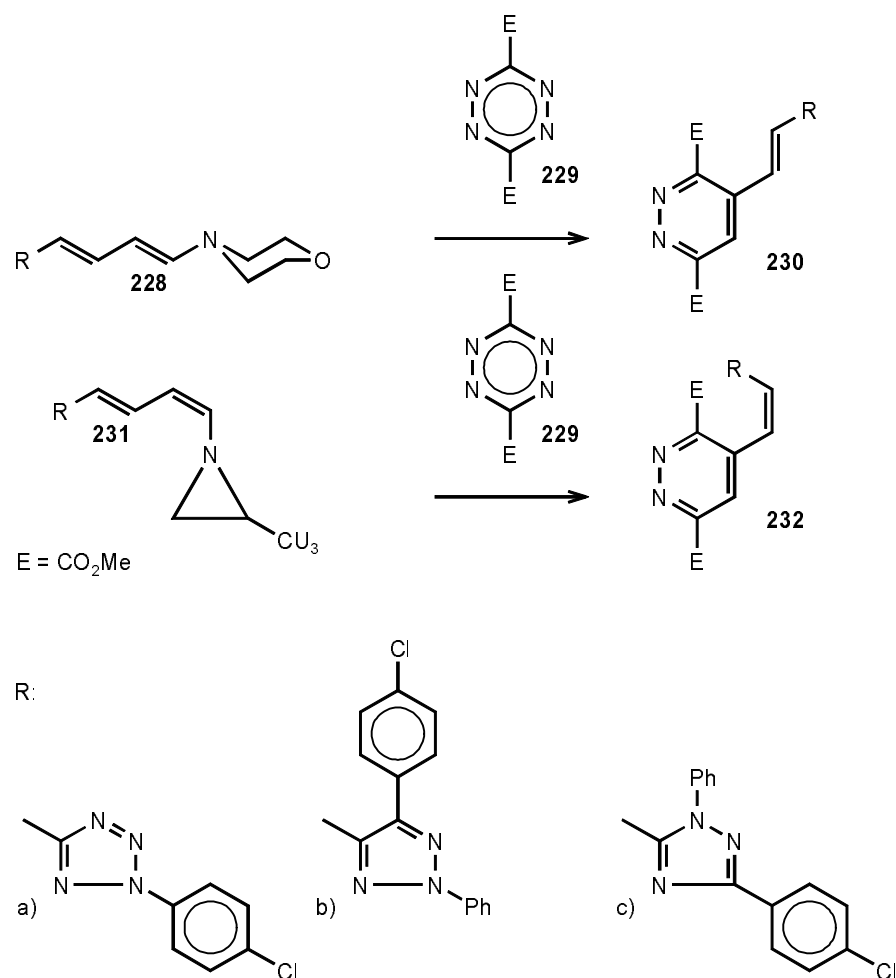
Attempts directed at the capturing of the primarily formed dihydropyridazine intermediate by introduction of a methyl group into the appropriate position of the hetaryldiene diene and thus disabling amine elimination failed as the reaction took a different course. The dienamine (**236**) took up two equivalents of the tetrazine (**237**) and a 1:1 mixture of hetarylpyridazine (**238**) and amino-dihydropyridazine (**239**) was formed in each case. Experimental evidence suggests that the reaction proceeds via a double "inverse electron demand" Diels-Alder addition-disproportionation pathway [99].
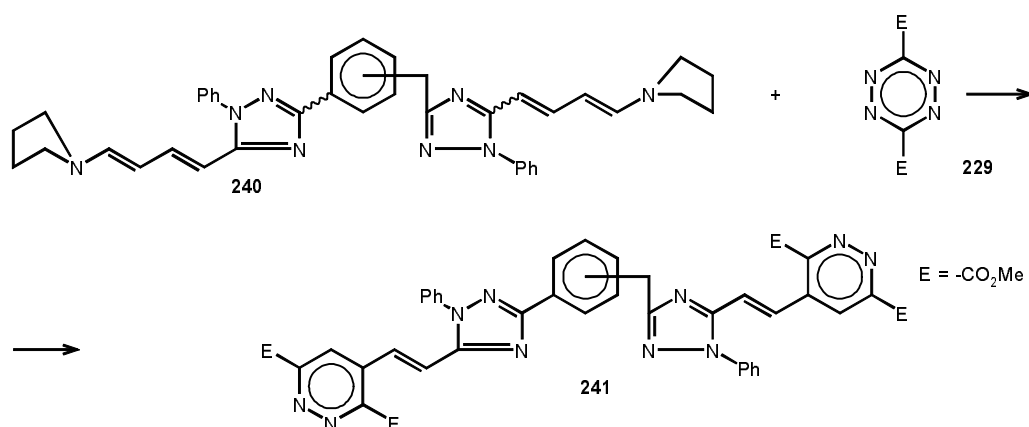
Scheme 77
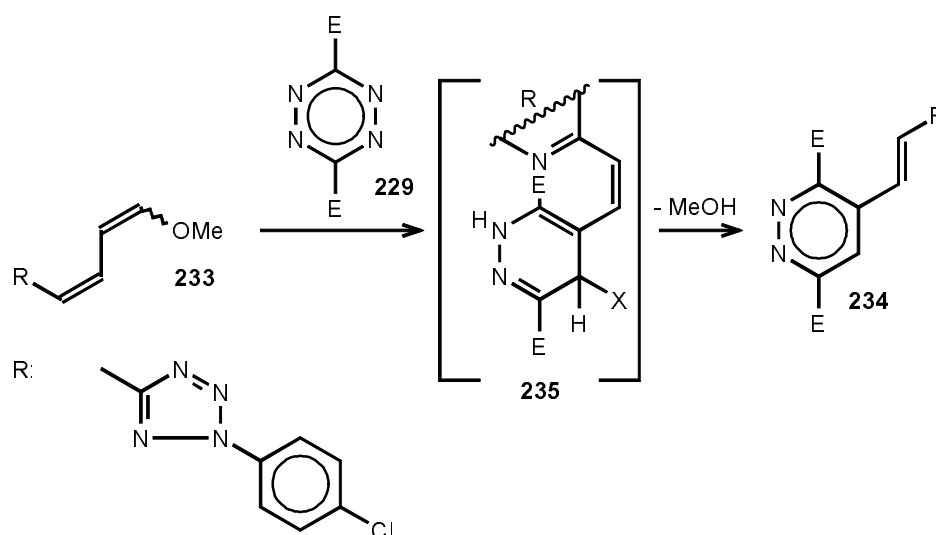
Scheme 78
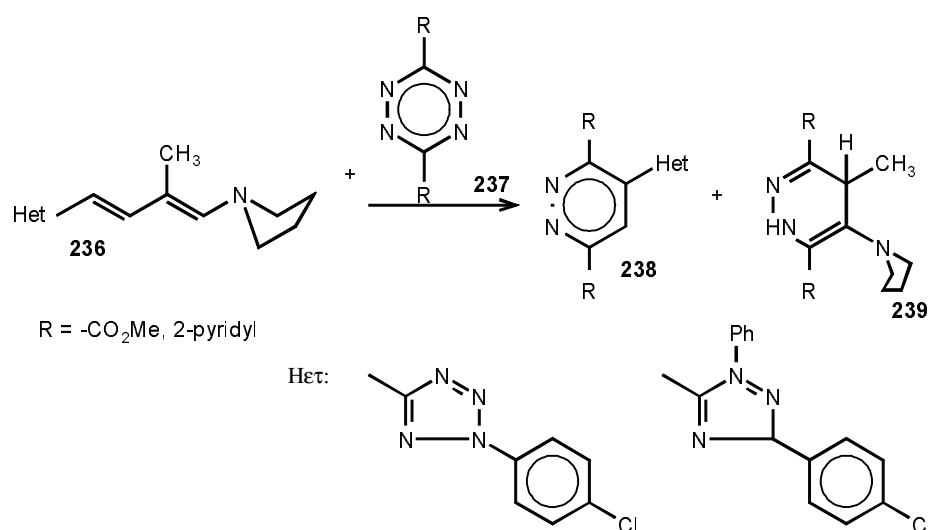
The application of the "inverse electron demand" Diels-Alder reaction in polymer synthesis is a topic of current interest. The synthesis of hetaryldienamines was extended to their bis-analogues (**240**) which in a model experiment also reacted smoothly with the tetrazine **229** and the bis-adduct **241** was formed in good yield [100].

Scheme 79

H.2.4. 2+8 cycloadditions

The 2+8 cycloaddition of electron-rich olefins with electron deficient conjugated tetraenes is an analogue of the inverse Diels-Alder reaction. A representative of this class is the reaction of the tetrazolyldienamine **243a** with benzofuroxane which yielded the tetrazolylvinylquinoxaline dioxide **245** in poor yield (23%) [84]. The analogous transformation of morpholino-butadiene (**243b**) resulted in the formation of the enamino-quinoxaline-bis-oxide **244** in 75% yield [101]. Unlike in the case of arylazides (chapter H.2.2.) the site of attack in these reactions seems to be determined by steric factors.

Scheme 80

a: R = H, 2-(4-chlorophenyl)-tetrazolyl-5; b: R=H
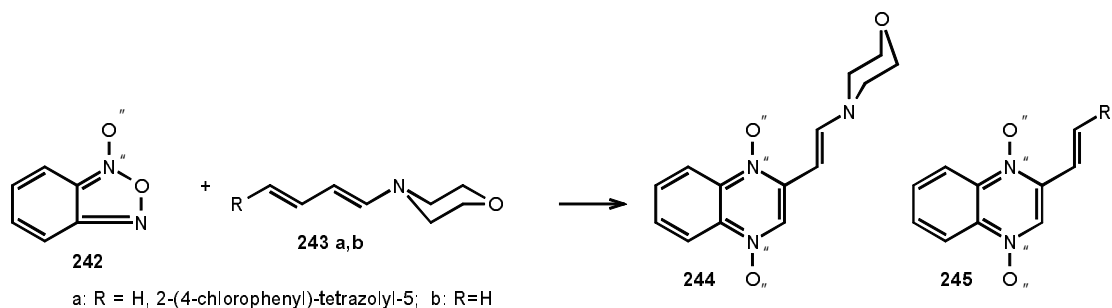
I. Rearrangements

The rearrangement of hetaryldienes requires the incorporation of sensitive or reactive functionalities which can be activated in the course of the process. Azido-hetaryldienes (**246**) for example eliminate nitrogen on heating to give nitrenes which ring close spontaneously to pyrrol derivatives (**247**) [24, 25].
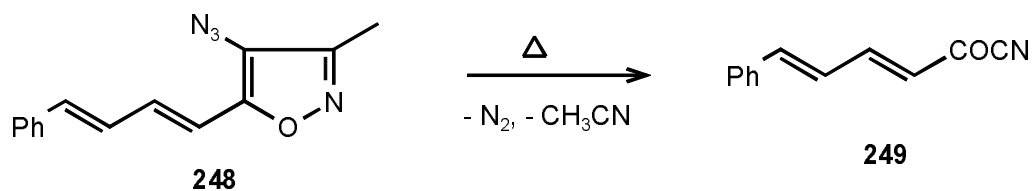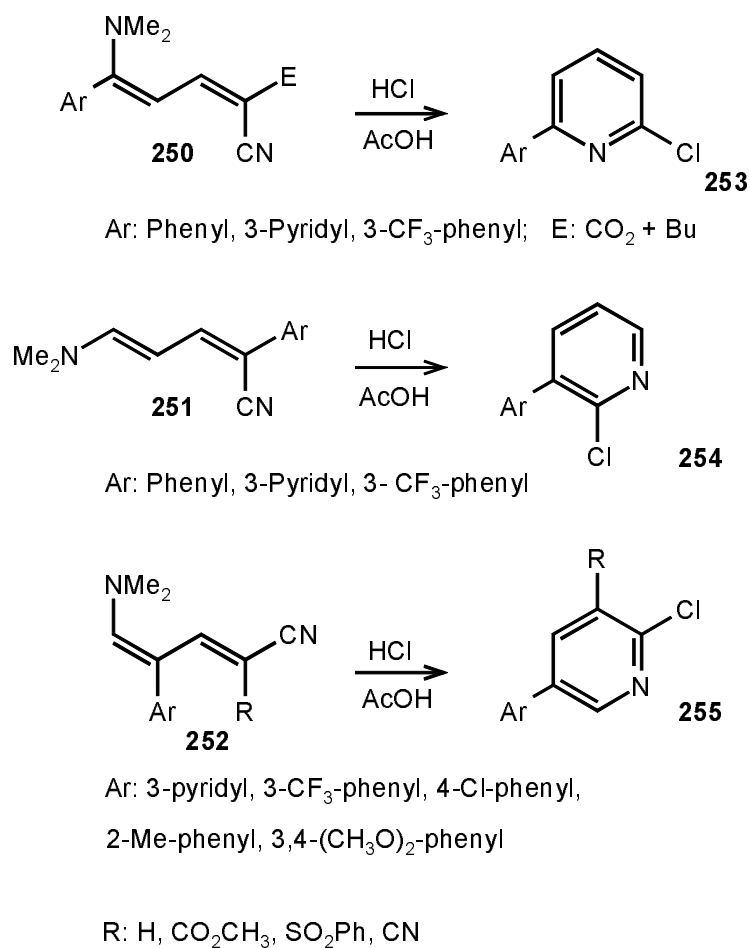
Scheme 81
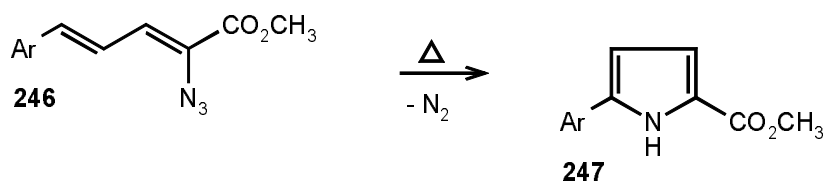
Ar: Phenyl, 2'-Thienyl, 3'-Thienyl, 2'-Furyl, 3'-Furyl, 2'-Pyrrolyl

Interestingly, the placement of the azide onto the heterocycle instead of the diene chain led to a different reaction. Although the nitrene formed from **248** could have ring closed onto the diene, the isoxazolyldiene **248** lost nitrogen and acetonitrile on heating to give the acylnitrile **249**.

Scheme 82

Scheme 83

Ar: Phenyl, 3-Pyridyl, 3-CF$_3$-phenyl;   E: CO$_2$ + Bu

Ar: Phenyl, 3-Pyridyl, 3- CF$_3$-phenyl

Ar: 3-pyridyl, 3-CF$_3$-phenyl, 4-Cl-phenyl,

2-Me-phenyl, 3,4-(CH$_3$O)$_2$-phenyl

R: H, CO$_2$CH$_3$, SO$_2$Ph, CN

The 1-cyano-4-dimethylaminobutadiene part provides the means for the transformation in the hydrogen chloride mediated rearrangement of the hetaryldienes **250-252** to the hetarylpyridine derivatives **253-255**. Yields are strongly substituent and substitution

pattern dependent and vary in the range of 30-95% [79]. Using methanolic ammonia to promote ring closure instead of hydrogen chloride-acetic acid the chlorine is replaced by an amine function in the products.

Appropriately substituted benzo[b]thiophenes (256) were shown to undergo stereoselective thermal rearrangement to benzothieno[3,2-b]pyrrolizine derivatives (257) [102] the stereochemical outcome of the process strongly dependent on the polarity of the applied solvent. Toluene as a reaction medium favoured the formation of the (β-E)-isomer (86% isolated yield), while the use of acetic acid led to the (α-E)-isomer in 73% yield.
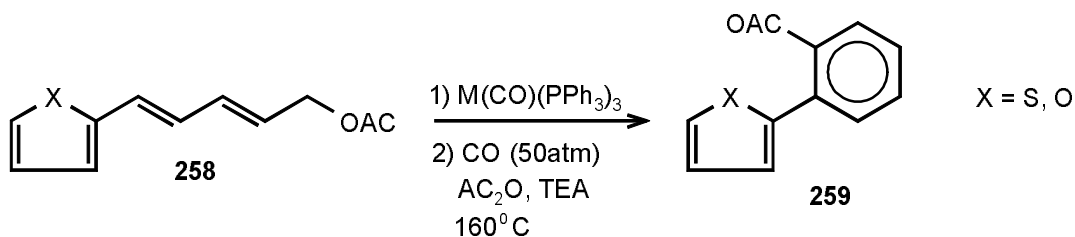
Scheme 84


E: -CN, -CO₂Me
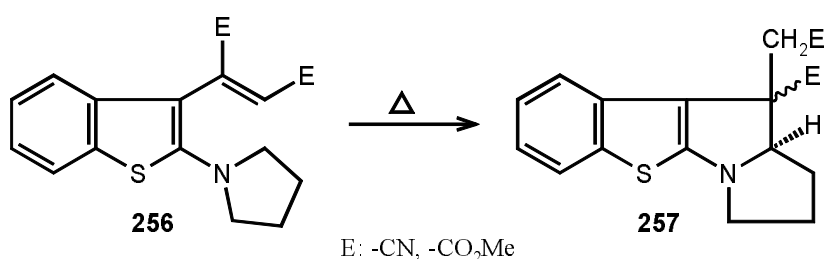
J. Miscellaneous transformations

The palladium catalysed transformation of allylic acetates was extended to furyl- and thienyl-vinylogs. Allylic carbonylation of 258 followed by rearrangement and acetylation under the applied conditions led to the *o*-hetaryl-phenol derivatives (259) in moderate yield [95].

Scheme 85

The iron carbonyl complex of the bis-benzodisilazinyl-diene (**260**) reacted with 2,4-dibromo-pentan-3-one (**261**) and a cyclopentanone moiety was formed in the reaction onto one of its double bonds (**262**). The low yield of the transformation (20%) makes this reaction more a sign to show new fields to explore than a practical application [104].

Scheme 86
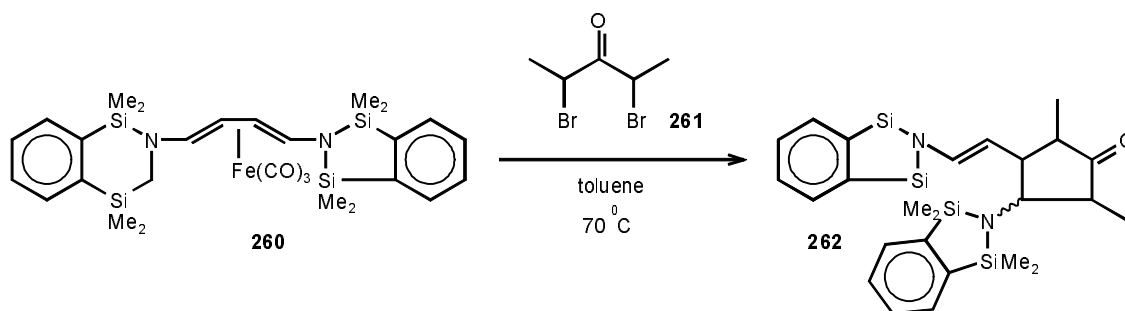
III. LITERATURE

[1] T. B. Attra, Y. L. Bigot, R. El Gharbi, M. Delmas and A. Gaset, *Synth. Commun.* **1992**, *22*, 1421-1425.

[2] M. D'Auria, A. DeMico, F. D'Onofrio and G. Piancatelli, *J. Org. Chem.* **1987**, *52*, 5243-5247.

[3] S. L. Jensen, N. A. Sörensen, *Acta Chem. Scand.* **1961**, *15*, 1885.

[4] J. Barluenga, I. Merino and F. Palacios, *Tetrahedron Lett.* **1990**, *31*, 6713-6716.

[5] J. W. Van Reijendam, G. J. Heeres and M. J. Janssen, *Tetrahedron* **1970**, *26*, 1291-1299.

[6] Y. Badar, W. J. S. Lockley, T. P. Toube, B. C. L. Weedon and L. R. G. Valadon, *J. Chem. Soc.* **1973**, 1416-1424.

[7] Y. Badar, A. K. Chopra, H. W. Dias, M. B. Hursthouse, A. R. Khokhar, M. Ito, T. P. Toube and B. C. L. Weedon, *J. Chem. Soc.* **1977**, 1372-1376.

[8] D. L. Boger and T. T. Curran, *J. Org. Chem.* **1992**, *57*, 2235-2244.

[9] T. Kato, N. Katagiri, T. Takahashi and Y. Katagiri, *J. Heterocycl. Chem.* **1979**, *16*, 1575-1578.

[10] S. Konno, M. Sagi, E. Takaharu, S. Fujimura, K. Hayashi and H. Yamanaka, *Chem. Pharm. Bull.* **1988**, *36*, 1721-1726.

[11] C. Piechucki, *Synthesis* **1974**, 869-870.

[12] C. Piechucki, *Synthesis* **1976**, 187-188.

[13] P. DeShong, J. A. Cipollina and N. K. Lowmaster, *J. Org. Chem.* **1988**, *53*, 1356-1364.

[14] E. B. Knott, *J. Chem. Soc.* **1965**, 3793-3795.

[15] E. Späth, *Chem. Ber.* **1941**, *74*, 873-879.

[16] H. Proske, *Chem. Ber.* **1909**, *42*, 1450-1457.

[17] C. T. Bahner and J. N. Fain, *J. Org. Chem.* **1957**, 1109.

[18] W. I. Awad, *J. Prakt. Chem.* **1973**, *315*, 1152-1160.

[19] H. Erlenmeyer, O. Weber, P. Schmidt, G. Küng, C. Zinsstag and B. Prijs, *Helv. Chim. Acta* **1948**, *31*, 1142-1156.

[20] A. Alberola, A. M. G. Nogal and F. J. Pulido, *Heterocycles* **1983**, *20*, 1035-1042.

[21] M. Matsui, S. Kawamura, K. Shibata and H. Muramatsu, *Bull. Chem. Soc. Jpn.* **1992**, *65*, 71-74.

[22] G. A. M. Nawwar, H. F. Zohdi, R. H. Swellen and S. A. Osman, *Heterocycles* **1992**, *34*, 457-464.

[23] C. Jutz, R. M. Wagner and H.-G. Löbering, *Angew. Chem.* **1974**, *21*, 781-782.

[24] J-P. Boukou-Poba, M. Farnier and R. Guilard, *Tetrahedron Lett.* **1979**, *19*, 1717-1720.

[25] W. Hinz, R. A. Jones, S. U. Patel and M-H. Karatza, *Tetrahedron* **1986**, *42*, 3753-3758.

[26] G. Erker, M. Riedel, S. Koch, T. Jödicke and E-U. Würthwein, *J. Org. Chem.* **1995**, *60*, 5284-5290.

[27] E. A. Braude, J. S. Fawcett and D. D. E. Newman, *J. Chem. Soc.* **1952**, 4155-4157.

[28] J. Mulzer, G. Brüntrup, U. Kühl and G. Hartz, *Chem. Ber.* **1982**, *115*, 3453-3686.

[29] E. Profft and H-W. Linke, *Chem. Ber.* **1960**, *93*, 2591-2602.

[30] J. Firl, *Chem. Ber.* **1968**, *101*, 218-225.

[31] A. Thomas, H. Ila and H. Junjappa, *Tetrahedron* **1990**, *46*, 4295-4302.

[32] K. Steiner , U. Graf and E. Hardegger, *Helv. Chim. Acta* **1963**, *46*, 690-693.

[33] G. A. Tolstikov, E. E. Shultz, G. M. Sapharova, L. V. Spirichin and A. A. Panashenko, *Zh. Org. Khim.* **1990**, *26*(6), 1283-1296.

[34] D. Sattsangi and K. K. Wang, *Tetrahedron Lett.* **1992**, *33*(35), 5025-5028.

[35] M. Fossatelli, A. C. T. H. M. van der Kerk, S. F. Vasilevsky and L. Brandsma, *Tetrahedron Lett.* **1992**, *33*, 4229-4232.

[36] J. Liebscher and H. Hartmann, *J. Prakt. Chem.* **1976**, *318*, 731-744.

[37] M. L. Purkayastha, B. Patro, H. Ila and H. Junjappa, *J. Heterocycl. Chem.* **1991**, *28*, 1341-1349.

[38] A. Shafiee, M. Vosooghi and I. Lalezari, *J.Heterocycl. Chem.* **1980**, *17*, 545-547.

[39] F. Bohlmann, *Chem. Ber.* **1951**, *84*, 860-865.

[40] L. W. Singh, A. K. Gupta, H. Ila and H. Junjappa, *Synthesis* **1984**, 516-518.

[41] J. Sepúlveda-Arques, M. Medio-Simón and L. Piqueres-Vidal, *Monatsh. Chem.* **1989**, *120*, 1113-1118.

[42] B. Stanovnik and M. Tišler, *Chimia* **1971**, *25*, 272-273.

[43] G. Jones, D. J. Mouat and D. J. Tonkinson, *J. Chem. Soc.* **1985**, 2719-2723.

[44] I. Yavari, S. Esfandiari, A. J. Mostashari and P. W. W.Hunter, *J. Org. Chem.* **1975**, *40*, 2880-2883.

[45] G. M. Sanders, M. van Dijk and H. C. van der Plas, *J. Heterocycl. Chem.* **1982**, *19*, 797-800.

[46] G. M. Sanders, M. van Dijk and H. C. van der Plas, *J. Heterocycl. Chem.* **1983**, *20*, 407-414.

[47] D. Mörler and F. Kröhnke, *Liebigs Ann. Chem.* **1971**, *744*, 65-80.

[48] S. Miyadera, *Chem. Pharm. Bull.* **1964**, 1344.

[49] T. Miyadera, H. Kuwano, Y. Kawano and R. Tachikawa, *Chem. Pharm. Bull.* **1978**, *26*, 2334-2339.

[50] A. Gelléri and A. Messmer, *Tetrahedron Lett.* **1973**, 4295.

[51] A. Gelléri, A. Messmer, S. Nagy and L. Radics, *Tetrahedron Lett.* **1980**, *21*, 663-666.

[52] A. Messmer, Gy. Hajós and G. Timári, *Tetrahedron* **1992**, *48*, 8451-8458.

[53] Gy. Hajós and A. Messmer, *J. Heterocycl. Chem.* **1984**, *21*, 809-811.

[54] V. Boekelheide and W. G. Gall, *J. Am. Chem. Soc.* **1954**, *76*, 1832-1836.

[55] V. Boekelheide, H. Fritz, J. M. Ross and H. X. Kaempfen, *Tetrahedron* **1964**, *20*, 33-41.

[56] D. T. Manning and H. A. Coleman, *J. Org. Chem.* **1969**, *34*, 3248-3252.

[57] I. Yavari, S. Esfandiari, A. J. Mostashari and P. W. W. Hunter, *J. Org. Chem.* **1975**, *40*, 2880-2883.

[58] R. M. Acheson and D. A. Robinson, *J. Chem. Soc.* **1968**, 1629-1633.

[59] C. D. Campbell, C. W. Rees, M. R. Bryce, M. D. Cooke, P. Hanson and J. M. Vernon, *J. Chem. Soc.* **1978**, 1006-1011.

[60] M. Moreno-Manas, R. M. Ortuno, M. Prat and M. A. Galán, *Synth. Commun.* **1986**, *16*, 1003-1013.

[61] C. S. Runk, S. M. Haverty, D. A. Klein, W. R. McCrea, E. D. Strobel and H. W. Pinnick, *Tetrahedron Lett.* **1992**, *33*, 2665-2668.

[62] S. Schulz, M. Steffensky and Y. Roisin, *Liebigs Ann. Chem.* **1996**, 941-946.

[63] J. deJong, L. Brandsma and J. F. Arens, *Recl. Trav. Chim. Pays-Bas* **1974**, *93*, 15-16.

[64] G. Lavielle and G. Sturz, *Bull. Soc. Chim. Fr.* **1970**, 1369-1376.

[65] F. Babudri, V. Fiandanese, L. Mazzone and F. Naso, *Tetrahedron Lett.* **1994**, *35*, 8847-8850.

[66] E. E. Schweizer and K. K. Light , *J. Org. Chem.* **1966**, *31*, 2912-2915.

[67] V. Nair and C. S. Cooper, *J. Org. Chem.* **1981**, *46*, 4759-4765.

[68] E. Zbiral, E. Bauer and J. Stroh, *Monatsh. Chem.* **1971**, *102*, 168-179.

[69] R. H. Good, G. Jones and J. R. Phipps, *J. Chem. Soc.* **1972**, 2441-2445.

[70] A. Alberola, F. Alonso, P. Cuadrado and M. C. Sanudo, *J. Heterocycl. Chem.* **1988**, *25*, 235-240.

[71] R. M. Keenan, J. Weinstock, J. A. Finkelstein, R. G. Franz, D. E. Gaitanopoulos, G. R. Girard, D. T. Hill, T. M. Morgan, J. M. Samanen, J. Hempel, D. S. Eggleston, N. Aiyar, E. Griffin, E. H. Ohlstein, E. J. Stack, E. F. Weidley and R. Edwards, *J. Med. Chem.* **1992**, *35*, 3858-3872.

[72] M. Yokoyama, K. Tsuji and T. Imamoto, *Bull. Chem. Soc. Jpn.* **1984**, *57*, 2954-2956 .

[73] S. R. Buzilova, V. M. Shulgina, G. V. Sakovich and L. I. Vereshagin, *Khim. Geterosikl. Soedin.* **1981**, *17*, 1279-1282.

[74] V. Lee, M. K. Cheung, W-T. Wong and K-F. Cheng, *Tetrahedron* **1996**, *52*, 9455-9468.

[75] M. F. Bryce, C. D. Reynolds, P. Hanson and J. M. Vernon, *J. Chem. Soc., Perkin Trans. 1* **1981**, 607-613.

[76] E. R. Blout and V. W. Eager, *J. Am. Chem. Soc.* **1945**, *67*, 1315-1319.

[77] T. Miyadera and T. Kishida, *Tetrahedron Lett.* **1965**, *14* , 905-912.

[78] R. Bodalski, M. Pietrusicewicz, P. Majewski and J. Michalski, *Coll. Czech. Chem. Commun.* **1971**, *36*, 4079-4082.

[79] R. Church, R. Trust, J. D. Albright and D. W. Powell, *J. Org. Chem.* **1995**, *60*, 3750-3758.

[80] U. Horn, F. Mutterer and C. D. Weis, *Helv. Chim. Acta* **1976**, *59*, 190-211.

[81] M. Korach and W. Bergmann, *J. Org. Chem.* **1949**, 1118-1123.

[82] M. R. Kamal and R. Levine, *J. Org. Chem.* **1962**, *27*, 1360-1363.

[83] A. Kotschy, Gy. Hajós, G. Timári and A. Messmer, *J. Org. Chem.* **1996**, *61*, 423-4426.

[84] A. Messmer, Gy. Hajós, G. Timári and A. Gelléri, *Monatsh. Chem.* **1988**, *119*, 1121-1124.

[85] M. S. Manhas, J. W. Brown, U. K. Pandit and P. Houdewind, *Tetrahedron* **1975**, 1325.

[86] A. Messmer, Gy. Hajós and G. Timári, *Monatsh. Chem.* **1988**, *119*, 1113-1119.

[87] G. T. Gmitter and F. L. Benton, *J. Am. Chem. Soc.* **1950**, *72*, 4586-4589.

[88] W. Langenbeck, O. Gödde, L. Weschky and R. Schaller, *Chem. Ber.* **1942**, *75*, 232.

[89] A. Kotschy, G. Hajós, G. Timári, A. Messmer and Joachim G. Schantl, *Heterocycl. Commun.* **1997**, *3*, 449-452.

[90] R. Neidlein, V. Poignée, W. Kramer and C. Glück, *Angew. Chem.* **1986**, *98*, 735.

[91] J. Firl, *Chem. Ber.* **1968**, *101*, 218-225.

[92] S-J. Lee, S-J. Chien, S-J. Peng, I. Chao and T. Chou, *J. Org. Chem.* **1994**, *59*, 4367-4369.

[93] R. H. Wightman, T. M. Cresp and F. Sondheimer, *J. Am. Chem. Soc.* **1976**, 6052-6053.

[94] B. I. Rosen and W. P. Weber, *J. Org. Chem.* **1977**, *42*, 47-50.

[95] Y. Ishii, C. Gao, W-X. Xu, M. Iwasaki and M. Hidai, *J. Org. Chem.* **1993**, *58*, 6818-6825.

[96] A. Elgavi, B. S. Green, G. M. J. Schmidt, *J. Am. Chem. Soc.* **1973**, 2058-2059.

[97] M. M. Campbell, N. D. P. Cosford, D. R. Rae and M. Sainsbury, *J. Chem. Soc., Perkin Trans. 1* **1991**, 765-770.

[98] A. Kotschy, Gy. Hajós and A. Messmer, *J. Org. Chem.* **1995**, *60*, 4919.

[99] Z. Novák, Z. Vincze, A. Kotschy, Gy. Hajós and D. M. Smith, *manuscript in preparation.*

[100] A. Kotschy, A. Csámpai and D. M. Smith, *submitted for publication.*

[101] H. N. Borah, P. Devi, J. S. Sandhu and J. N. Baruah, *Tetrahedron* **1984**, *40*, 1617-1621.

[102] D. N. Reinhoudt, G. W. Visser, W. Verbbom, P. H. Benders and M. L. M. Pennings, *J. Am. Chem. Soc.* **1983**, *105*, 4775-4781.

[103] Y. Ishii, S. Gao, W-X. Xu, M. Iwasaki and M. Hidai, *J. Org. Chem.* **1993**, *58*, 6818-6825.

ACID-CATALYZED DEUTERIUM EXCHANGE IN HANTZSCH-TYPE DIHYDROPYRIDINES

Darko Kocjan

Lek d. d., R&D, Ljubljana, Slovenia

Abstract

An interesting case of the acid-catalyzed deuterium exchange in methanol-d_4 was found for 4-phenyl-1,4-dihydropyridine derivatives that belong to the class of Ca-channel antagonists. Deuterium exchange of the C_α-methyl protons indicates formation of an enamine carbocation that can be described by three mesomeric models.

Introduction

Carbocations produced by interaction of the acid with the carbon-carbon double bond were extensively investigated using experimental and theoretical methods [1]. Carbocations generated from cycloalkene compounds in concentrated acid or super acid solutions are stable species at low temperatures and their structures can be directly determined by NMR spectroscopy. The carbocation formation in addition reactions, when milder conditions are applicable, is generally believed to be the crucial reaction step as demonstrated indirectly by reaction products [2, p141]. Reactivity of enamine derivatives depends on protonation site preference i. e. amine N vs. C_β in many reaction mechanisms. Both protonation sites are implied in the hydrolysis reactions of enamines, the proton transfer to the C_β atom is the reaction rate-determining step [3, 4]. Proton affinity of enamines was also investigated in the gas phase by theoretical and

experimental methods and it was demonstrated that the protonation occured at the C_β atom, the imine ion being more stable than the enammonium ion [5,6]. 1,4-dihydropyridines generally function as enamines [7] and can undergo reaction with electrophiles. On reaction with proton acids the iminium salt is formed by protonation of the dihydropyridine ring at the 3- or 5-position. It can act as a highly eletrophilic species on reaction with another molecule of 1,4-dihydropyridine forming dimeric structures [7, p157, p160] and with nucleophiles such as water [7, p160]. Hantzsch-type dihydropyridines that belong to the Ca-channel antagonists, can also generate iminium species under acid conditions. The reactive intermediate was captured with carbon-carbon double bonds or other internal nucleophiles in sequential cycloaddition reactions producing conformationally rigid 4-phenyl-1,4-dihydropyridines analogues [8, 9, 10, 11].

I have recently observed that strong acids such as benzenesulfonic acid in methanol-d_4 solution trigger regio-specific deuterium exchange in 4-phenyl-1,4-dihydropyridine derivatives. Deuterium exchange of protons of the C_α-methyl group evidences reversible formation of an enamine carbocation. The example is given for amlodipine benzenesulphonate (2-[(2-aminoethoxy)methyl]-4-(2-chlorophenyl)-1,4-dihydro-6-methyl-3,5-pyridinedicarboxylic acid 3-ethyl 5-methyl ester).

Experimental Part

Samples of amlodipine benzenesulfonate for C-13 NMR mesurements were dissolved in methanol-d_4 and in methanol-d_4 solution containing 1 molar equivalent of benzenesulfonic acid. C-13 NMR spectra were measured immediately after preparation of the samples. Samples for H-1 NMR measurements were prepared by dissolving amlodipine benzenesulfonate in solutions having different ratio of methanol/methanol-d_4 solvents and 1 molar equivalent of benzenesulfonic acid. H-1 NMR measurements were run 24 hrs after preparation of the samples.

H-1 and C-13 NMR measurements were run on a Varian instrument Unity+ at 300 and 75 MHz, respectively. H-1 and C-13 chemical shifts were referenced with regard to internal TMS.
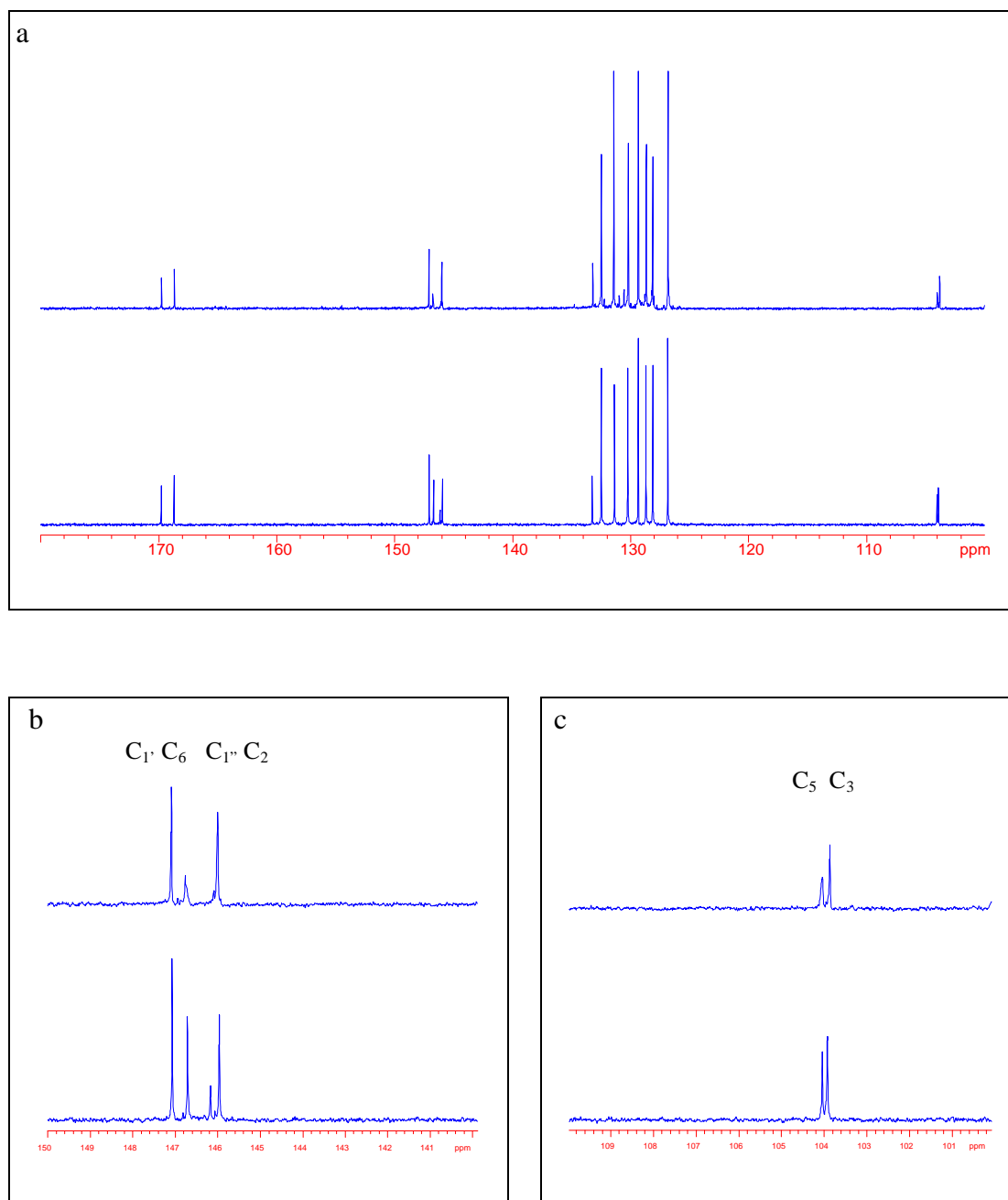
Results and Discussion

Figure 1. 75 MHz C-13 NMR spectra of amlodipine benzenesulfonate (lower trace) and amlodipine benzenesulfonate with the addition of 1 molar equivalent of benzenesulfonic acid (upper trace) in the range between 100 and 200 ppm (a) and expanded views (b and c).

C-13 NMR spectra of amlodipin benzenesufonate and amlodipin benzenesufonate with 1 molar equivalent of benzenesulfonic acid added demonstrate that the acid significantly alters the signal intensity of C_5 and C_6 (104.1 ppm and 146.7 ppm, respectively, Fig.1) reflecting additional relaxation mechanisms driven by the acid. The interaction of the acid with the double bond carbon atoms of the dihydropyridine ring might imply the formation of a π-complex prior to the proton transfer to the double bond. Such a mechanism is generally characteristic of a specific acid catalysis. General acid catalysis produces carbocations directly in a slow, reaction rate-determining step, without any intervening steps, and was found mostly in water solutions [2, p226].
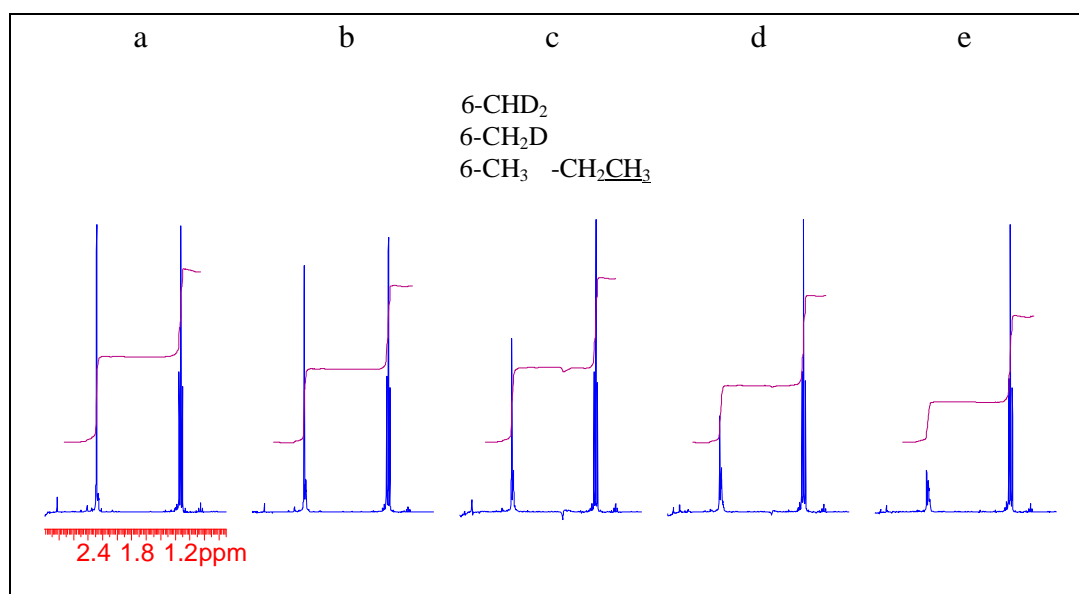

Figure 2. 300 MHz H-1 NMR spectra of amlodipine benzenesulfonate in mixtures of methanol-d_4 and methanol within the ratios: 0.2 (a), 0.5 (b), 1 (c), 2 (d) and 5 (e), with the addition of 1 molar equivalent of benzenesulfonic acid, in the range between 3.0 and 0.5 ppm.

H-1 NMR spectra presented in Figure 2 show variable intensity of the signal of the C_6-methyl group (2.3 ppm) with respect to the signal of the methyl group in the ethyl substituent (1.1 ppm). The intensity of the singlet line (C_6-CH$_3$) is reduced in direct proportion to the ratio of methanol/methanol-d$_4$ due to the partial (-CH$_2$D, -CHD$_2$) and complete H/D exchange (-CD$_3$) (Fig.2).
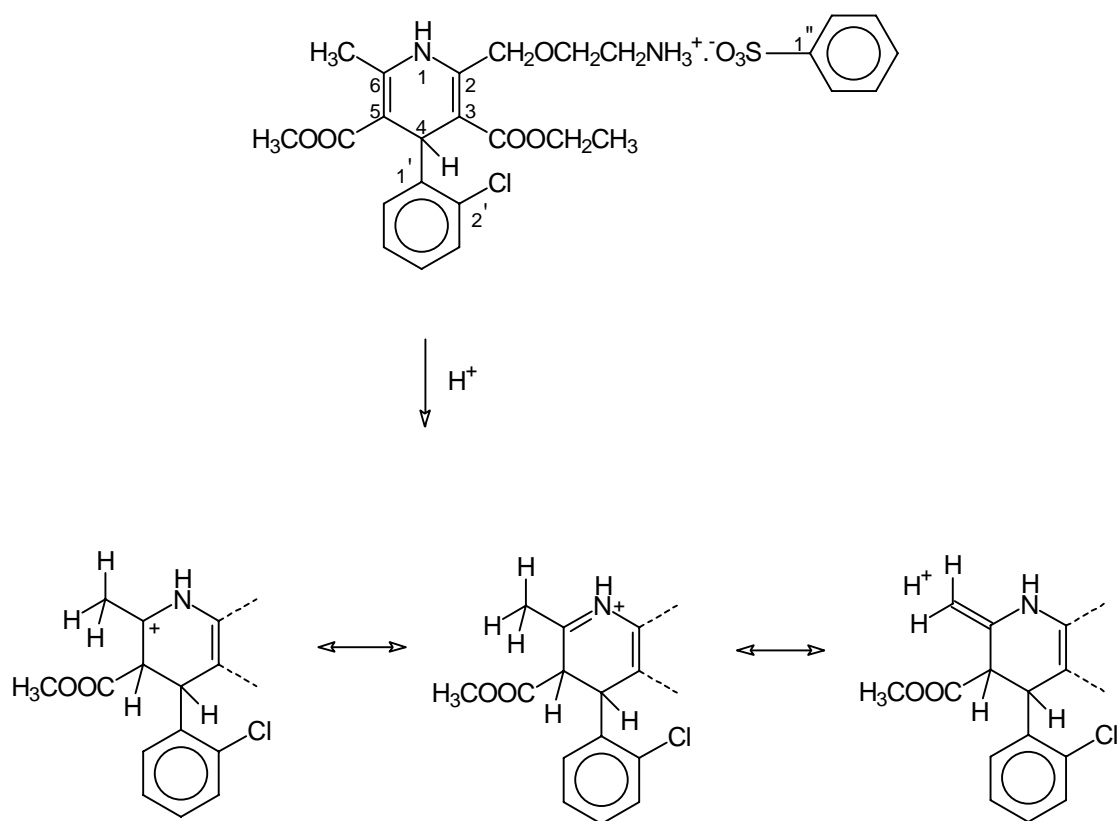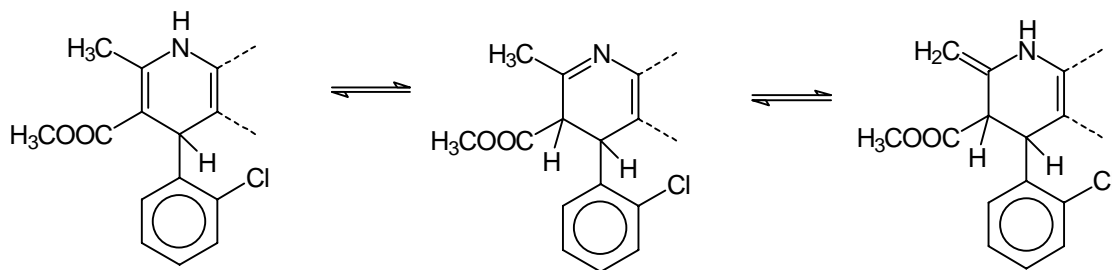

Scheme I

Thus, H-1 NMR spectra provide an indirect evidence for the proton transfer to the C_5 atom. It is transparent that the stabilization of the protonated enamine fragment of the 1,4-dihydropyridine ring brings about the destabilization of the C-H bonds of the methyl

group and, consequently, the isotopic exchange. The C_6-methyl group stabilization of the positive charge includes the hyperconjugative effect, too [1]. The C_β-protonated enamine fragment is normally described as a hybrid of two Lewis models, iminium and carbonium [5]. However, the acid-catalyzed H/D exchange in 1,4-dihydropyridines indicates that the enamine carbocation formed possesses significant contribution of the carbonium type model because of the positive charge delocalization to the C_α-methyl group, and it must be represented by a third model with the formal positive charge on the methyl group (Scheme I).

It is worthwhile to note that there exists a one-to-one correspondence between the three mesomeric models for the protonated enamine fragment and the possible tautomeric forms of the non-protonated enamine fragment (Scheme II).

Scheme II

In this preliminary report I have demonstrated that the enamine fragment of amlodipine benzensulphonate is very amenable toward protonation under an excess of the acid. The resulting enamine carbocation is extensively stabilized by the C_6 methyl group as evidenced by complete deuterium exchange of the methyl group protons. The effect is a general characteristic for 4-phenyl-1,4-dihydropyridine derivatives of the Ca-channel antagonist class [12].

References

[1]. G. K. Surya Prakash and P. v. R. Schleyer (Eds.), *Stable Carbocation Chemistry*, Wiley, New York, **1996**.
[2] J. March, *Advanced Organic Chemistry*, Wiley, New York, **1985**.
[3] E. J. Stamhuis and W. Maas, *J. Org. Chem*. **1965**, 30, 2156-60.
[4] P. Y. Sollenberger and R. B. Martin, *J. Am. Chem. Soc*. **1970**, 92, 4261-70.
[5] M. R. Ellenberger, D. A. Dixon and W. E. Farneth, *J. Am. Chem. Soc*. **1981**, 103, 5377-82.
[6] R. A. Eades, D. A. Weil, M. R. Ellenberger, W. E. Farneth, D. A. Dixon and C. H. Douglass*, J. Am. Chem. Soc*. **1981**, 103, 5372-77.
[7] R. E. Lyle, in *Pyridine and its Derivatives*, Supplement, Part One, (R. A. Abramovitch, Ed.), Wiley, New York, **1974**, p137-182, and the references cited therein .
[8] G. E. Hartman, B. T. Philips, and W. Halczenko, *J. Org. Chem*. **1985**, 50, 2423-27.
[9] G. T. Hartman, W. Halczenko, and B. T. Philips, *J. Org. Chem*. **1985**, 50, 2427-31.
[10] D. A. Claremone, J. Hirshfield, P. K. Lumma, D. E. McClure, and J. P. Springer, *Synthesis*, **1986**, 144-147.
[11] D. H. Kim, *J. Heterocyclic Chem*. **1986**, 23, 1471-74.
[12] D. Kocjan, *to be published*

Povzetek

Opisan je zanimiv primer kislinsko katalizirane devterijske izmenjave v metanolu-d4 pri 4-fenil-1,4-dihidropiridinski derivatih, ki sodijo v razred Ca antagonistov. Devterijska izmenjava protonov C_α-metilne skupine nakazuje nastanek enaminskega karbokationa, ki ga lahko opi{emo s tremi mezomerni strukturami.

Problemi pri pouku kemije v svetu in pri nas

Andrej Šmalc

Ljubljana, Vogelna 4

Kemije srednješolci na splošno nimajo preveč radi, seveda z izjemo tistih, ki se zanjo posebej zanimajo in so se zato morda odločili celo za visokošolski študij tega predmeta. O vzrokih za tako stanje in o tem, kaj bi bilo treba storiti, da bi se to izboljšalo, govori članek, objavljen v lanski majski številki *Journal of Chemical Education* (R. J. Gillespie, Reforming the General Chemistry Textbook, *J. Chem. Ed., 74, (1997) 484*), katerega prevod sledi v nadaljevanju. Avtor članka je svetovno znan raziskovalec na področju kemije fluora in superkislin ter profesor na univerzi v Hamiltonu (Ontario, Kanada).

Prepričan sem, da je članek zanimiv za vse, ki se kakor koli ukvarjajo s poukom kemije, saj se gotovo srečujejo s podobnimi problemi tudi v svojem okolju. V tem prepričanju me potrjujejo tudi lastne izkušnje, ki sem jih dobil v petnajstih letih, ko sem predaval kemijo na nekaterih oddelkih Biotehniške fakultete, torej študentom, ki so dojemali kemijo kot bolj ali manj stranski predmet. Upam le, da bo članek naletel na ugoden odziv, zlasti v današnjem času kurikularne prenove in tako pripomogel k izboljšanju pouka kemije na srednji šoli ter s tem njenega razumevanja. Predvsem pa naj bi dijaki dojemali kemijo ne kot nekakšno abstraktno znanost, ki je sama sebi namen, temveč kot predmet, ki obravnava pojave in dogajanja, s katerimi imamo opraviti v vsakdanjem življenju.

Reformiranje učbenikov splošne kemije

Ronald J. Gillespie

Večina nas, ki poučujemo kemijo, želi, da bi študenti *razumeli*, kar jih učimo. Vendar pa mnogi med njimi, nemara kar večina, tega niti ne poskušajo. Tudi če si to sprva prizadevajo, kaj kmalu pridejo do sklepa, da je kemija pretežka, da bi jo lahko razumeli, vsaj ne v času, ki jim je na voljo. Zato odnehajo in se, tako kot drugi, zatečejo k učenju snovi. Pri *učenju* imajo seveda v mislih *učenje na pamet* - imen spojin, formul, definicij oksidacije in redukcije, oblik orbital, načinov za določanje oksidacijskih števil, računanja pH itd. itd. Mnogi študenti niti nimajo nič proti temu, saj so to počeli tudi v srednji šoli in to pač pomeni učiti se. Mnogi bi nasprotovali, če bi od njih pričakovali, da bodo snov razumeli, saj se jim zdi laže snov naučiti se na pamet. Večina med njimi pa si tudi kaj dosti ne predstavlja, kaj pomeni snov razumeti. Kakor se nam že zdi to presenetljivo, imajo kemijo za zelo abstraktno, zelo težko in brez povezave z dejanskim življenjem. Vendar pa to ni tako presenetljivo, če pomislimo, da kemija za te dijake sestoji iz velike količine navidez nepovezane, nekoristne in neuporabne snovi, ki se jo morajo naučiti na pamet pa če jo razumejo ali ne. Njihov glavni cilj je prestati ta pouk, nato pa nadaljevati s čim drugim, po njihovem mnenju bolj zanimivim in bolj koristnim. Od predmeta kemije odnesejo zelo malo, najsibo v nadaljnji študij ali pa v kasnejše življenje, in zelo malo, če sploh kaj, vedo o tem, kaj kemija sploh je - razen golega prepričanja, da je ne bodo nikoli razumeli. V dolgih letih sem opazil, da so bili ljudje, ko sem prišel v družbo z njimi in jim zaupal, da sem profesor kemije, nad tem presenečeni. Kako more človek, ki je

> **Ne glede na to, kako imenitni se zdijo ti učbeniki učiteljem, ki se zanje odločijo, jim vendarle pri ogromni večini študentov ni uspelo vzbuditi zanimanja za kemijo ali pa pomagati, da bi jo razumeli...**

sicer videti povsem normalen, to reč razumeti. Često priznajo, nekako opravičujoče, da je bila kemija v srednji šoli ali na univerzi njihov najslabši predmet ali pa da je bil najtežji izmed vseh predmetov, ki so jih imeli. Zakaj le redko naletim na koga, ki se mu je kemija zdela ali

privlačna ali vznemirljiva ali pa vsaj zanimiva? Zakaj ne *razumejo* kemije, katero jih skušamo naučiti?

Kemija: odnos med makroskopskim in mikroskopskim

Mnogi izmed nas že dolgo občutimo, da mora biti s tem, kar učimo, nekaj narobe, nismo si pa edini v tem, kaj bi bilo treba spremeniti, da se kemija dijakom ne bi zdela tako težka, nekoristna in abstraktna. En problem predstavljajo težave, ki jih imajo dijaki pri povezovanju makrokozmosa opažanj z mikrokozmosom atomov in molekul. In vendar je ravno to tisti vidik, po katerem se kemija loči od drugih znanosti. Če dijaki te povezave ne najdejo, ne morejo videti koristnosti in pomembnosti kemije v resničnem svetu. Razumevanje te povezave je najbrž najpomembnejša stvar, ki jo lahko dijaki dobijo na začetku pouka kemije.

Zakaj se je tako malo spremenilo v pouku in v učnih knjigah kemije?

O splošni kemiji se je diskutiralo na neštetih konferencah in simpozijih, v strokovnih skupinah in odborih ter seminarjih, vendar se je le malo spremenilo. Splošna kemija je ostala v glavnem takšna, kot je bila pred dvajsetimi ali štiridesetimi leti. Zakaj? Eden od razlogov bi lahko bil ta, da se niso spremenile učne knjige. Do kakšne večje spremembe pa ne more priti vse dotlej, dokler ne bo izšla učna knjiga nove vrste, ki bo splošno sprejeta. Obstajajo mnogi dobro napisani in bogato ilustrirani učbeniki, vendar pa skoraj vsi med njimi obravnavajo enako konvencionalno tvarino na bolj ali manj enak konvencionalen način. Ne glede na to, kako imenitni se zdijo ti učbeniki učiteljem, ki se zanje odločijo, jim vendarle pri ogromni večini študentov ni uspelo vzbuditi zanimanja za kemijo ali pa jim pomagati, da bi jo razumeli ali vsaj dobili iz njih informacije, ki bi si jih zapomnili in jih uporabljali v kasnejšem življenju.

Zakaj je tako malo učbenikov poskusilo obravnavati tvarino na nov način? Založniki se upirajo investirati v nekonvencionalne knjige in staviti vse zgolj na možnost, da bo taka knjiga uspela in v temeljih spremenila pouk splošne kemije. Celo avtorji, ki so prepričani o potrebnosti sprememb, se upirajo pisati knjige, ki bi bile preveč nekonvencionalne, prav zaradi težav, kako najti založnika in ga pridobiti za to. Zakaj nobena izmed nekaj nekonvencionalnih knjig, ki so izšle, ni bila splošno sprejeta, da bi vodila v širšo reformo pouka splošne kemije? Zato, ker večina učiteljev bodisi ne vidi potrebe po spremembi ali pa nima časa, da bi se prilagodila novemu učbeniku in si delala nove zapiske za pouk? Ali zato, ker nobenemu avtorju doslej ni uspelo najti obrazca, ki bi dal spodbudo za to, več kot potrebno spremembo?

Kdo bo začel in podprl reformo?

Zdi se mi, da je bilo diskusije dovolj. Najbrž ne bomo nikoli dosegli popolnega soglasja o tem, kako reformirati pouk kemije, dokler ne bo izšel povsem nov učbenik, ki bo vplival na dovolj veliko število učiteljev, da bodo sprejeli novi način pouka. Da bi take knjige izhajale in bile sprejete, bo potrebna podpora organizacij, kot sta državni raziskovalni sklad (National Science Foundation) in ameriško kemijsko društvo (American Chemical Society) in ena ali več velikih kemijskih industrij. Njihova podpora in finančna pomoč pa ne bo potrebna samo za subvencioniranje pisanja in izdajanja takih knjig, temveč tudi za prirejanje seminarjev za prekvalifikacijo učiteljev. Omenjene organizacije ne bi mogle z ničimer bolje prispevati k bodočnosti kemije kot ravno s takšno podporo.

Nekaj napotkov avtorjem bodočih učbenikov

V upanju, da bom s tem spodbudil diskusijo, navajam nekaj predlogov avtorjem bodočih učbenikov v preudarek

.

1. *Pozabite na potrebe tistih, ki bodo šli študirat kemijo.* Le malo dijakov si bo v nadaljnjem študiju izbralo kemijo za glavni predmet in le maloštevilni bodo imeli več kot en kurz pouka kemije. Čeprav to ni glavni namen reforme pouka kemije, upamo, da nam bo na ta način tudi uspelo prepričati več dijakov, da se bodo odločili za študij kemije kot glavnega predmeta. Seveda pa to ne pomeni, da bi morali v učbenike vključevati določeno učno snov zgolj zato, ker jo bodo slednji potrebovali pri nadaljnjem študiju kemije. Če se bodo dijaki ogreli za kemijo, bodo to snov zlahka in z vnemo obvladali pri študiju kemije na univerzi.

2. *Neprestano je treba poudarjati odnos med makrokozmosom zapažanj in mikrokozmosom atomov in molekul.* Ta odnos je edinstven vidik kemije in ko ga razumemo, se pokaže, da je kemija življenjska in koristna. Bistvenega pomena je, da prikažemo lastnosti snovi in njihovo zvezo z vlogo teh snovi v svetu okrog nas, temu pa naj sledi razlaga opažanj na nivoju atomov in molekul, iz katerih sestoji snov. Iz tega, da so opažanja na prvem mestu, dijaki vidijo, da so teorije in načela, ki predstavljajo velik del splošne kemije, ne za to, da se jih samo naučimo, temveč zato, da nam pomagajo ta opažanja razumeti.

3. *Izločiti je treba vse nepotrebne podrobnosti in odvečno delo ter se osredotočiti na tisto, kar je potrebno za razumevanje kemije.* Zakaj začenjati učbenik s podrobnostmi o imenih in formulah snovi? To je vendar dolgočasno. Dijakom je treba pokazati resnično kemijo. Vse, kar je potrebno v zvezi s poimenovanjem snovi in pisanjem njihovih formul pa naj se navaja samo tedaj, ko se te snovi obravnavajo. Koliko kemikov pa se sploh kdaj ubada z urejanjem enačb, še posebno zapletenih redoks enačb, ki so v učbenikih tako pogoste? Nekaj študentov bo sicer uživalo v tem izzivu, toda ali se učijo kemije? Čeprav je princip pomemben, bi čas, ki ga porabimo za urejanje takih enačb, z izjemo najenostavnejših, bolje uporabili za obravnavanje drugih tem. Ali je res pomembno, da dijaki znajo izračunati pH raztopine, ko pa jim nikoli več v življenju ne bo treba računati česa takega? Pa tudi če bi v prihodnosti morali poznati pH neke raztopine, ga bodo pač izmerili s pH-metrom. Ta jim bo dal natančnejšo vrednost (v nekaterih primerih celo veliko natančnejšo) kot pa poenostavljeno računanje, ki so se ga naučili pri pouku kemije (in ga verjetno pozabili). Ali se morajo dijaki res učiti oblik orbital? Teh oblik na tej stopnji dijaki še ne morejo dojeti. Ali ni dovolj, če vedo, da atome držijo skupaj elektrostatske sile med elektroni in jedri? Podrobnosti teorije vezi naj ostanejo prihranjene za kasnejši študij kemije.

4. *Prikazati je treba širši pogled na kemijo.* Dijake pri pouku splošne kemije zanima cela vrsta stvari. Zakaj jim ne bi pokazali, da je kemija dejansko osrednja znanost, na kateri temelji razumevanje vseh materialov, najsibo organskih ali anorganskih, sintetičnih ali naravnih. Zakaj jim ne bi pokazali, da je kemija pomembna za geologe, biologe, tehnike, astronome, zdravnike kakor tudi za strokovnjake, ki se ukvarjajo z okoljem - dejansko za slehernega? Naj bo splošna kemija res splošna, ne pa elementarna fizikalna kemija, kar je sedaj.

5. *Učbeniki naj bodo krajši,* da bo hitrost podajanja učne snovi puščala dovolj časa za njeno razumevanje. Mnogi dijaki so zasuti tako s količino učne snovi kot tudi s podrobnostmi v njenem večjem delu.

Mogoče bodo te misli spodbudile nekatere avtorje k pisanju, nekatere založnike k izdajanju in nekatere organizacije k podpori revolucionarnih učbenikov, kakršne potrebujemo. Morda bo kakšen tak učbenik privzel le nekatere mojih idej (ali pa nobene), upam pa, da bodo vprašanja,

ki sem jih postavil, izzvala nekatere potencialne pisce, da bodo predlagali svoje lastne rešitve. Bližajoče se leto 2000 navdihuje mnoge k razmišljanju o spremembi. Upajmo, da bodo kemiki lahko vstopili v novo tisočletje z novim, spodbudnejšim načinom pouka splošne kemije.

Predstavitev knjige

"Exploring Aspects of Computational Chemistry, Concepts and Exercises" (J.-M. Andre, D.H. Mosley, M.-C. Andre, B. Champagne, E. Clementi, J.G. Fripiat, L. Leherte, L. Pisani, D.P. Vercauteren, M. Vračko), Presses universitaires de Namur, Namur 1997.

V začetku letošnjega leta je v Belgiji pri založbi *Presses universitaires de Namur* izšla knjiga v dveh delih z naslovom *"Exploring Aspects of Computational Chemistry, Concepts and Exercises"*. Knjigo, ki je plod dolgoletnega raziskovalnega in pedagoškega dela, so napisali sodelavci *Facultes universitaires Notre-Dame de la Paix* iz Namurja J.-M. Andre, D.H. Mosley, M.-C. Andre, B. Champagne, J.G. Fripiat, L. Leherte in D.P. Vercauteren. Pri delu so sodelovali tudi trije zunanji sodelavci: E. Clementi in L. Pisani, sodelavca *Universitaires Luis Pasteur* in M. Vračko, sodelavec *Kemijskega inštituta* iz Ljubljane. Prvi del s podnaslovom *"Concepts"* vsebuje sedem poglavij, ki podajajo pregled osnovnih načel računalniške kvantne kemije, vendar brez formalnih matematičnih izpeljav, saj je na koncu dodan še izčrpen pregled temeljnih del s tega področja, kjer lahko bralec najde vse podrobnosti, ki ga utegnejo zanimati. Drugi del *"Exercises"* sistematično podaja k vsakemu poglavju zbirko računskih nalog različnih težavnostnih stopenj. Nekatere naloge se dajo rešiti s svinčnikom in papirjem s pomočjo kalkulatorja, medtem ko spet druge zaradi numerične zapletenosti zahtevajo uporabo računalnika. Na koncu drugega dela je podan še seznam in krajši opis nekaterih poznanih najbolj uporabljanih kvantnokemijskih računalniških programov.

Začetki kvantne kemije segajo v prva desetletja tega stoletja, ko so bili postavljeni temelji kvantne mehanike. Lahko rečemo, da se je kvantna kemija začela s prvo uspešno razlago kemijske vezi. To je bila vez v molekuli vodika. V tej zgodnji dobi so

se morali znanstveniki omejevati na zelo majhne sisteme, ki so bili za kemijo manj zanimivi, ali pa uporabljati bolj grobe približke. Razvili so vse potrebne teoretične modele in postopke, za praktično uporabo le-teh pa je bilo treba čakati na pojav hitrih in vse zmogljivejših računalnikov v zadnjih tridesetih letih. Pa še potem je precej časa prevladovalo mnenje, da je kvantna kemija (še posebno njen računalniški del) področje, s katerim se praviloma ukvarjajo samo za to usposobljeni znanstveniki, vsekakor pa ne študenti na dodiplomskem študiju. Hitri razvoj računalništva je te trditve postavil na glavo. Danes skoraj povsod v svetu vključujejo osnove računalniške kvantne kemije v dodiplomski študij. Na ljubljanski univerzi poslušajo študenti kemije o tem v četrtem letniku študija v okviru predmeta Struktura atomov in molekul. Računalniška kvantna kemija je interdisciplinarna veda, ki združuje teoretično fiziko, kemijo, matematiko in računalništvo. Z razvojem teoretičnega ozadja in numeričnih algoritmov ter pisanjem računalniških programov se sicer še vedno ukvarjajo specialisti, uporaba programov in vrednotenje rezultatov pa postaja vse bolj potreba velikega dela populacije kemikov. Gre predvsem za seznanjanje z osnovnimi principi, ki so v ozadju računov, znanje o tem, kaj lahko s pomočjo kvantne kemije računamo in kje so njene meje. Prav to pa je področje, ki ga poskuša zapolniti predstavljena knjiga. Osnovno vodilo avtorjev je bilo, da mora biti študij na vsakem nivoju zaključena celota. Program mora vsebovati ustrezno prilagojen pouk o osnovnih načelih in vaje, ki prikazujejo praktično uporabo kvantne kemije. Prav vajam so avtorji posvetili posebno pozornost, saj naj bi študentom posredovale občutek za kritično presojo dobljenih rezultatov.

Jože Koller
FKKT